Universidad de Granada
Facultad de Farmacia
Departamento de Química Inorgánica

# Molecular Recognition between Copper(II)-iminodiacetates and purine-like ligands or synthetic nucleosides

# Reconocimiento Molecular entre Iminodiacetatos de Cobre(II) y Ligandos derivados de Purina o Nucleósidos de síntesis

ALICIA DOMÍNGUEZ MARTÍN

PROGRAMA DE DOCTORADO EN QUÍMICA
TESIS DOCTORAL CON MENCIÓN INTERNACIONAL

Granada, diciembre de 2012

Editor: Editorial de la Universidad de Granada
Autor: Alicia Domínguez Martín
D.L.: GR 1715-2013
ISBN: 978-84-9028-577-0

# Molecular Recognition between Copper(II)-iminodiacetates and purine-like ligands or synthetic nucleosides



# Reconocimiento Molecular entre Iminodiacetatos de Cobre(II) y Ligandos derivados de Purina o Nucleósidos de síntesis

Memoria de Tesis Doctoral presentada por

**Dña. ALICIA DOMÍNGUEZ MARTÍN** para aspirar al grado de Doctor

por la Universidad de Granada

Granada, diciembre de 2012.

Fdo. Alicia Domínguez Martín

LOS DIRECTORES DE LA MEMORIA


Dr. Juan Niclós Gutiérrez

Catedrático de Química Inorgánica
de la Universidad de Granada

Dra. Josefa María González Pérez

Catedrática de Química Inorgánica
de la Universidad de Granada

Dr. Duane Choquesillo Lazarte

Investigador contratado en el Laboratorio de Estudios Cristalográficos,
Instituto Andaluz de Ciencias de la Tierra – Consejo Superior de Investigaciones Científicas

El doctorando ALICIA DOMÍNGUEZ MARTÍN y los directores de la tesis JUAN NICLÓS GUTIÉRREZ, JOSEFA MARÍA GONZÁLEZ PÉREZ y DUANE CHOQUESILLO LAZARTE, garantizamos, al firmar esta tesis doctoral, que el trabajo ha sido realizado por el doctorando bajo la dirección de los directores de la tesis y hasta donde nuestro conocimiento alcanza, en la realización del trabajo, se han respetado los derechos de otros autores a ser citados, cuando se han utilizado sus resultados o publicaciones.

Granada, 15 de diciembre de 2012

DIRECTOR/ES DE LA TESIS

DOCTORANDO

Fdo.: Juan Niclós Gutiérrez

Fdo.: Alicia Domínguez Martín

Fdo.: Josefa María González Pérez

Fdo.: Duane Choquesillo Lazarte

*A mi abuelo Escolástico,*

*A mis padres.*

.

*Siempre ten presente que la piel se arruga,*
*el pelo se vuelve blanco, los días se convierten en años…*
*Pero lo importante no cambia,*
*tu fuerza y tu convicción no tienen edad.*
*Tu espíritu es el plumero de cualquier telaraña.*
*Detrás de cada línea de llegada, hay una de partida.*
*Detrás de cada logro, hay otro desafío.*
*Mientras estés viva, siéntete viva.*
*(…)*
*¡Nunca te detengas!*

Madre Teresa de Calcuta

# AGRADECIMIENTOS

Debería comenzar agradeciendo a Dios el haberme puesto en este camino, que empezó incluso antes de embarcarme en esta Tesis Doctoral. Ahora, echando una mirada a estos últimos cinco años, no encuentro una forma mejor de iniciar este trabajo que dando las gracias a todas aquellas personas que han formado parte de él.

En primer lugar, agradezco enormemente al Prof. Juan Niclós Gutiérrez y a la Prof. Josefa María González Pérez la confianza que han depositado en mí. Gracias por las horas, meses, años de generosa y entera dedicación a este Proyecto y a mi formación. Gracias también por vuestro cariño, respaldo y amistad. Sin vosotros no habría sido posible.

Al Dr. Duane Choquesillo Lazarte por brindarme la oportunidad de ampliar mi formación en el campo de la Cristalografía. Por su dedicación y estímulo, y por las discusiones que han enriquecido este trabajo.

Al Prof. Alfonso Castiñeiras, cuya indispensable colaboración ha permitido la elaboración de esta Tesis doctoral. Por su disponibilidad, apoyo constante, buenos consejos e inestimable ayuda. Gracias.

A todos los miembros del Departamento de Química Inorgánica de la Universidad de Granada, por su cálida acogida. Especialmente, me gustaría expresar mi agradecimiento a aquellos que se encuentran en la Facultad de Farmacia, con quienes he compartido el día a día de este Proyecto. Por su apoyo constante y hacerme sentir en familia durante todos estos años. Gracias a Nono, por su cercanía, continua disposición y ayuda siempre que la he necesitado. A Almudena por dar vida al departamento, por su contagiosa alegría y, por supuesto, por los maravillosos desayunos. A mis compañeros de laboratorio: a todos los que están, a los que ya se fueron y a las nuevas incorporaciones, por crear tan buen ambiente de trabajo y por todos los momentos compartidos, dentro y fuera del departamento. En especial a Hanan y a Inma, por las risas y confidencias durante estos últimos años. Ricardo, Manolo, D. Antonio, Pilar, Queca, Alejandro... Todos formáis parte, de una u otra forma, de este trabajo; no sólo desde el punto de vista científico, sino también desde lo personal.

My most sincere thanks to Prof. Dr. Roland K. O. Sigel for believing in my capabilities and giving me the opportunity to work on the 'Bio' side, for his personal and scientific support during my stay in Zürich.

Thanks to all the members of the SF-Lab for their warm welcome and friendship atmosphere, for the moments shared in and outside the Lab. Special thanks to the girls in the NMR subgroup of Sigel's Lab for all the technical advices and great support: Maria, Miriam, Daniela and particularly Silke, for her generous help, patience, as well as her dedication and good discussions. To Joachim for being 'next seat' in my 'NMR-sudoku' adventure and fun during the breaks and after them. I was very lucky to work with all of you. Finally, thanks to Jens and Anja for opening the doors of their apartment and their kindness.

Special thanks to Prof. Dr. Helmut Sigel for his huge support in the evaluation of the p$K_a$ measurements, his generous dedication and valuable discussions. I have learned a lot from your rigorous way of working. Likewise, thanks to Astrid Sigel for her help and patience, including weekends on the phone.

Al Prof. Jose Antonio Dobado, del Departamento de Química Orgánica de la Universidad de Granada, por su generosa disposición y su valiosa aportación en los cálculos de DFT que se incluyen en esta Tesis.

Al Prof. Luis Lezama, del Departamento de Química Inorgánica de la Universidad del País Vasco por su cercanía y su experta contribución en las medidas de EPR y susceptibilidad magnéticas recogidas en esta Tesis.

Al Prof. Ángel García Raso, del Departamento de Química Orgánica de la Universidad de las Islas Baleares, por su apoyo desinteresado y su colaboración en la síntesis de nuevos ligandos usados en este trabajo. A la Prof. Catalina Cabot por la realización de los bioensayos de actividad citoquinina y ayudarme con su interpretación.

Al Centro de Instrumentaciones Científicas de la Universidad de Granada. En especial a D. Alfredo Molina Quesada, al Dr. Miguel Ángel Salas Pelegrín y a D. José Romero Garzón, cuya contribución ha hecho posible este trabajo de investigación. Por su profesionalidad y sobre todo por su amabilidad, gracias.

A mis compañeras de carrera que hacen la Tesis en otros Departamentos de la Facultad de Farmacia, por compartir ilusiones y proyectos y mostrarme las preocupaciones con nuevos ojos.

A todo el personal de la Facultad de Farmacia que con tanto afecto me han tratado durante estos años; en particular a Marina, por echarme con tanto cariño por las noches.

Al Ministerio de Educación por la concesión de mi beca predoctoral FPU, al Ministerio de Ciencia e Innovación por la financiación del Proyecto MAT2010-15594 y a la Junta de Andalucía por la financiación al grupo "Complejos de metales de transición con interés bioinorganico y/o terapéutico" (FQM-283). La investigación realizada en este trabajo habría sido imposible sin esta ayuda económica.

Reservo el agradecimiento más sincero para mi familia y amigos. Gracias a mis padres por su cariño, confianza y apoyo incondicional durante todos estos años. Ellos me han enseñado que la perseverancia, el esfuerzo y la humildad son el camino para lograr cualquier objetivo que me proponga. Gracias a mi hermana Miriam, a mi abuela María y a mi tía Manuela, por animarme en este Proyecto y estar siempre atentas a mi próximo destino en el globo. Gracias a todos mis amigos por su silencioso pero notable apoyo. Espero poder responderles ahora a la eterna pregunta de: ¿esto para qué sirve?. En particular, quiero agradecerle a Jose su apoyo sincero en este tramo final de la Tesis, por estar ahí cuando vuelvo a casa, por las confidencias y sobre todo por su amistad. Por último, pero no por ello menos importante, me gustaría agradecerle a mi marido su amor y su fe en mí. Gracias por compartir tu tiempo con este Proyecto. Gracias por los desayunos en la cama, por calmar mis inquietudes, pero sobre todo, por tu compresión y apoyo sin límites.

Sin todos vosotros esta Tesis no habría sido posible, por eso, es también vuestra.

# CONTENTS

| | | |
|---|---|---|
| A | | Adenine |
| acv | | Acyclovir |
| C | | Cytosine |
| CD | | Circular Dichroism |
| CSD | | Cambridge Structural Database |
| DFT | | Density Functional Theory |
| DMF | | Dimethylformamide |
| DMSO | | Dimethylsulfoxide |
| DNA | | Deoxyribonucleic acid |
| DOSY | | Diffusion ordered spectroscopy |
| EPR | | Electron paramagnetic resonance |
| FT-IR | | Fourier-Transformed Infrared spectra |
| G | | Guanine |
| Hade | | Adenine |
| | $H_2ade^+$ | Adeninium(1+) cation |
| | $ade^-$ | Adeninate(1-) anion |
| | $[ade\text{-}H]^{2-}$ | Adeninate(2-) anion |
| | $[ade\text{-}2H]^{3-}$ | Adeninate(2-) anion |
| H2AP | | 2-Aminopurine |
| H4app | | 4-Aminopyrazolo[3,4-d]pyrimidine or 7-deaza-8-aza-adenine |
| H4abim | | 4-Azabenzimidazole |
| H5abim | | 5-Azabencimidazol / 5-azabenzimidazole |
| H7azain | | 7-Azaindole |
| H7deaA | | 7-Deaza-adenine |
| HBAP | | 6-Benzyladenine |
| HCy5ade | | 6-Cyclopentyladenine |
| HCy6ade | | 6-Cyclohexyladenine |
| Hcyt | | cytosine |
| HdimAP | | 6,6-Dimethyladenine |
| Hhyp | | Hypoxanthine |

| | |
|---|---|
| HThy | Thymine |
| $(HNPP)^{5-}$ | d(ApGpGpCpCpT) or hexa-2'-deoxynucleoside pentaphosphate |
| Hxan | Xanthine |
| $H_2$CBIDA | N-(*p*-chloro-benzyl)iminodiacetic acid |
| $H_2$EIDA | N-ethyliminodiacetic acid |
| $H_2$FBIDA | N-(*p*-fluoro-benzyl)iminodiacetic acid |
| $H_2$glygly | Glycylglycine |
| $H_2$IDA | Iminodiacetic acid |
| $H_2$MEBIDA | N-(*p*-methyl-benzyl)iminodiacetic acid |
| $H_2$MIDA | N-methyliminodiacetic acid |
| $H_2$NBzIDA | N-benzyliminodiacetic acid |
| $H_2$TEBIDA | N-terc-buthyliminodiacetic acid |
| $H_4$EDTA | Etilendiaminotetraacetic acid |
| IUPAC | *International Union of Pure and Applied Chemistry* |
| 1MeAde | 1-Methyladenine |
| 3MeAde | 3-Methyladenine |
| 7MeAde | 7-Methyladenine |
| 9MeAde | 9-Methyladenine |
| NMR | Nuclear Magnetic Resonance |
| NOESY | Nuclear Overhauser Effect Spectroscopy |
| ppm | parts per million |
| RNA | Ribonucleic acid |
| SQUID | Superconducting Quantum Interferente Device |
| T | Thymine |
| TG | Thermo-gravimetry |
| UV-Vis | Ultraviolet-visible spectroscopy |
| XRD | X-Ray Diffraction |

| | | |
|---|---|---|
| A | | Adenina |
| acv | | Aciclovir |
| C | | Citosina |
| CD | | Dicroismo circular |
| CSD | | *Cambridge Structural Database* |
| DFT | | Teoría del funcional de densidad |
| DMF | | Dimetilformamida |
| DMSO | | Dimetilsulfóxido |
| DNA | | Ácido desoxirribonucleico |
| DOSY | | Espectroscopía de Resonancia Magnética de experimentos de difusión |
| EPR | | Resonancia paramagnética electrónica |
| FT-IR | | Espectro infrarrojo por transformada de Fourier |
| G | | Guanina |
| Hade | | Adenina |
| | $H_2ade^+$ | Catión adeninio(1+) |
| | $ade^-$ | Anión adeninato(1-) |
| | $[ade\text{-}H]^{2-}$ | Anión adeninato(2-) |
| | $[ade\text{-}2H]^{3-}$ | Anión adeninato(3-) |
| H2AP | | 2-Aminopurina |
| H4app | | 4-Aminopirazolo[3,4-d]pirimidina o 7-deaza-8-aza-adenina |
| H4abim | | 4-Azabencimidazol |
| H5abim | | 5-Azabencimidazol |
| H7azain | | 7-Azaindol |
| H7deaA | | 7-Deaza-adenina |
| HBAP | | 6-Benciladenina |
| HCy5ade | | 6-Ciclopentiladenina |
| HCy6ade | | 6-Ciclohexiladenina |
| Hcyt | | citosina |

| | |
|---|---|
| HdimAP | 6,6-Dimetiladenina |
| Hhyp | Hipoxantina |
| HThy | Timina |
| $(HNPP)^{5-}$ | d(ApGpGpCpCpT) o hexa-2'-desoxinucleosido pentafosfato |
| Hxan | Xantina |
| $H_2$CBIDA | Ácido N-(*p*-cloruro-bencil)iminodiacético |
| $H_2$EIDA | Ácido N-etiliminodiacético |
| $H_2$FBIDA | Ácido N-(*p*-floruro-bencil)iminodiacético |
| $H_2$glygly | Glicil-glicina |
| $H_2$IDA | Ácido iminodiacético |
| $H_2$MEBIDA | Ácido N-(*p*-metil-bencil)iminodiacético |
| $H_2$MIDA | Ácido N-metiliminodiacético |
| $H_2$NBzIDA | Ácido N-beciliminodiacético |
| $H_2$TEBIDA | Ácido terc-butiliminodiacético |
| $H_4$EDTA | Ácido etilendiaminotetraacético |
| IUPAC | *International Union of Pure and Applied Chemistry* |
| 1MeAde | 1-Metiladenina |
| 3MeAde | 3-Metiladenina |
| 7MeAde | 7-Metiladenina |
| 9MeAde | 9-Metiladenina |
| NMR | Resonancia Magnética Nuclear |
| NOESY | Espectroscopía de Resonancia Magnética de efecto nuclear Overhauser |
| ppm | Partes por millón |
| RNA | Ácido ribonucleico |
| SQUID | Dispositivo superconductor de interferencia cuántica |
| T | Timina |
| TG | Termogravimetría |
| UV-Vis | Espectroscopía ultravioleta-visible |
| XRD | Difracción de Rayos-X |

## ABSTRACT

This Ph.D. dissertation essentially bears on the study of the molecular recognition patterns between Cu(II)-iminodiacetate chelates and different nucleobases derived from adenine: deaza-adenines, adenine isomers and N-substituted adenines. Likewise, as an attempt of doinf an approach to the Bio side, this dissertation also includes two studies regarding synthetic nucleosides. The obtained experimental results as well as their discussion are presented herein as five sections. All of them include contributions in high-level journals, included in the Inorganic Chemistry field:

The INTRODUCTION of this Ph.D. dissertation encompasses two parts. The first includes a general approach to this work and points out the objectives of the dissertation. Alternatively, the second part includes two *review articles* which analyse: (1) the current knowledge about the metal binding patterns of adenine, used as reference nucleobase, and (2) the available structural information about diverse N-ligands derived from adenine, in particular deaza-adenines, adenine isomers and aza-adenines. The two aforementioned reviews are based on the most rigorous structural support and are mainly devoted to the rationalization of the molecular recognition patterns of the just referred ligands. No restrictions about the metal ions or the different ionic (cationic or anionic) or neutral species of the N-ligands have been done.

CHAPTER 1 comprises the analysis of the molecular recognition patterns between different Cu(II)-iminodiacetate chelates and *deaza-adenine ligands*. The selected ligands (7-azaindole, 4-azabenzimidazole, 5-azabenzimidazole and 7-deaza-adenine) have in common the fact that, at least, all have one N-heterocyclic donor per aromatic moiety within the bicyclic skeleton of adenine. This chapter includes three original contributions, which are essentially focused on how the addition of N-donors in the heterocycle, from 7-azaindole to 7-deaza-adenine, favours tautomerism phenomena and the coordination abilities of these ligands.

CHAPTER 2 studies the molecular recognition patterns between different Cu(II)-iminodiacetate chelates and two *adenine isomers*. The two selected ligands (2-aminopurine and 4-aminopyrazolo[3,4-d]pirimidine) have in common the presence of the

tautomerizable/dissociable proton within the adenine skeleton. However, their nature is fairly different. While 2-aminopurine implies the shift of the exocyclic amino group, 4-aminopyrazolo[3,4-d]pirimidine involves the shift of two N-heterocyclic donors. This chapter has two original contributions where the metal binding patterns of these ligands are analysed, as well as relevant aspects of the supramolecular chemistry observed in the corresponding crystals.

CHAPTER 3 is about the molecular recognition patterns between different Cu(II)-iminodiacetate chelates and some *N-substituted adenines*. The selected ligands, and therefore the contributions included herein, are divided in two: (1) ligands with N-substitutions on the exocyclic amino group, and (2) ligands with N-substitutions on the heterocyclic donors. The first group comprises the natural cytokinin 6-benzyladenine as well as some derivatives (two 6-alkyladenines and 6,6-dimethyladenine). The second consists of the ligands 1-methyladenine, 3-methyladenine, 7-methyladenine y 9-methyladenine. The introduction of the referred substituents is rationalized according to the different metal binding modes obtained in the experimental part.

CHAPTER 4 addresses a more ambitious challenge and initiate studies with synthetic nucleosides. This chapter includes two original contributions. (1) One study about the molecular recognition between the well-known antiviral agent acyclovir and copper(II) iminodiacetates. In this work, it is remarked the relevance of the chelating ligand in the formation of appropriate intra- or inter-molecular interactions. (2) One study about the intrinsic acid-base properties of a hexa-2'-dexynucleoside. Therein, it was also evaluated the neighbouring effects and the isomeric equilibria. This latter study was performed during a pre-doctoral research stay at the Institute of Inorganic Chemistry at University of Zurich.

This dissertation ends with the appropriate CONCLUSIONS extracted from the careful analysis of the results presented in the aforementioned works.

# RESUMEN

Esta Tesis Doctoral versa, fundamentalmente, sobre el estudio de patrones de reconocimiento molecular entre iminodiacetatos de cobre(II) y nucleobases derivadas de adenina: deaza-adeninas, isómeros de adenina y derivados N-sustituidos de adenina. Asimismo, esta Memoria comprende el estudio de nucleósidos sintéticos, como una aproximación hacia un aspecto más biológico. Los resultados experimentales obtenidos, así como la discusión de los mismos, se presentan divididos en cinco apartados, todos ellos con aportaciones en revistas de primer nivel dentro del Campo de la Química Inorgánica:

La INTRODUCCIÓN de esta Tesis Doctoral consta de dos partes. La primera enmarca el planteamiento general de esta Memoria e indica los Objetivos de la presente Tesis. Por otro lado, la segunda parte recoge dos *artículos de revisión* que analizan: (1) el estado actual de conocimiento sobre los modos de coordinación de adenina, nucleobase de referencia, y (2) la información estructural disponible sobre distintos ligados nitrogenados derivados de adenina, en particular deaza-adeninas, isómeros de adenina y aza-adeninas. Ambas revisiones se basan en el más riguroso soporte estructural y están principalmente dirigidas hacia la racionalización de los modos de coordinación de los ligandos anteriormente mencionados. En dichas revisiones, no se han marcado restricciones en cuanto al metal o a las formas neutras o iónicas de los ligandos.

En el CAPÍTULO 1 se analizan los modos de reconocimiento molecular entre diferentes iminodiacetatos de cobre(II) y ligandos tipo *deaza-adenina*. Los ligandos seleccionados (7-azaindol, 4-azabencimidazol, 5-azabencimidazol y 7-deaza-adenina) cumplen el criterio común de poseer, al menos, un nitrógeno heterocíclico en cada uno de los anillos del esqueleto bicíclico de adenina. El capítulo se compone de tres aportaciones las cuales se centran, esencialmente, en el análisis de cómo la progresiva introducción de dadores nitrogenados en el heterociclo, desde 7-azaindol hasta 7-deaza-adenina, favorece los fenómenos de tautomería y la versatilidad coordinante de estos ligandos.

En el CAPÍTULO 2 se estudian los modos de reconocimiento molecular entre diferentes iminodiacetatos de cobre(II) y dos *isómeros de adenina*. Los ligandos seleccionados (2-aminopurina y 4-aminopirazolo[3,4-d]pirimidina) cumplen el criterio

común de mantener el protón tautomerizable en el esqueleto de adenina. Sin embargo, su naturaleza es diversa pues 2-aminopurina se debe a una transposición de grupo amino exocíclico mientras que 4-aminopirazolo[3,4-d]pirimidina se debe a la translocación de dos átomos de nitrógeno heterocíclicos. En este capítulo comprende dos artículos originales donde se analizan las propiedades coordinantes de los ligandos referidos, así como aspectos relevantes de la química supramolecular en los cristales de los correspondientes compuestos ternarios.

El CAPÍTULO 3 aborda el estudio de los modos de reconocimiento molecular entre diferentes iminodiacetatos de cobre(II) y *derivados N-sustituidos de adenina*. Los ligandos seleccionados, y por tanto las contribuciones dentro del capítulo, se dividen en dos clases: (1) ligandos sustituidos en el grupo amino exocíclico, y (2) ligandos sustituídos en un nitrógeno heterocíclico. El primer grupo incluye a la citoquinina natural 6-benciladenina y a tres derivados de la misma (dos 6-cicloalquiladeninas y la 6,6-dimetiladenina). El segundo grupo encierra a los ligandos 1-metiladenina, 3-metiladenina, 7-metiladenina y 9-metiladenina. La introducción de cada uno de los sustituyentes se relaciona con la expresión de los diversos modos de reconocimiento molecular obtenidos experimentalmente.

El CAPÍTULO 4 aborda un reto más ambicioso e inicia estudios con *nucleósidos de síntesis*. El capítulo incluye dos aportaciones originales. (1) Un estudio de reconocimiento molecular entre con el conocido agente antivirásico aciclovir e iminodiacetatos de cobre(II). En él se revela la importancia del agente quelante como partícicpe de interacciones intra y/o intermoleculares. (2) Un estudio sobre las propiedades ácido-base intrínsecas de un hexa-2'-desoxinucleósido. Además, se evalúan tanto la influencia que ejercen los monómeros vecinos entre sí como los fenómenos de tautomería e isomería dentro del hexanucleósidos. Este último estudio es fruto de una estancia predoctoral en el Instituto de Química Inorgánica de la Universidad de Zurich.

Esta Memoria termina con un apartado donde se resumen las CONCLUSIONES obtenidas del amplio trabajo de investigación que compone esta Tesis Doctoral.

# INTRODUCTION / INTRODUCCIÓN

# I. General Approach and Aim of the work

DNA and ARN are, probably, the most fascinating molecules in nature. In biological systems, nucleic acids and their building blocks interact with metal ions in a different but similar way. This fact turns nucleic acids into the largest and more interesting target ligands. Over the past decade, the Research Group FQM-283 *'Transition metal complexes with bioinorganic and/or therapeutic interest'* (http://biomec.ugr.es), has been devoted to the study of molecular recognition patterns between natural nucleobases (adenine, hypoxanthine, cytosine, etc.) and metal chelates. This research has been mainly based on a rigorous structural (crystallographic) support that usually reveals the formation of a Metal-N(purine-like) coordination bond, with or without the cooperation of intra-molecular interligand H-bonds. Moreover, in the studied ternary complexes, it is frequently observed other sort of intra- or inter-molecular interactions, among which should be remarked π,π-stacking interactions. Thus, the current knowledge in this area reveals an attractive panorama regarding its potential and also its diversity.

Among others, two recent reviews included in this Ph.D. dissertation show extremely versatile binding modes for adenine, which is able to coordinate metal ions in its different cationic, neutral and anion forms. However, these metal binding patterns are not fully understood. With the aim to shed light on the behaviour of adenine as ligand, novel strategies can be addressed that could provide valuable complementary information. Adenine ($C_5H_5N_5$, 6-aminopurine) is a byciclic ligand, rich in nitrogen atoms, that has four N-heterocyclic donors and one exocyclic primary amino group. The two fused rings within the adenine skeleton are quite different. One is a 6-membered ring and the other is a 5-membered ring, with pyrimidine or imidazole nature, respectively. These features should be taken into account when considering N-ligands analogues to adenine. Thus, the study of N-heterocycles that behave in a similar way to adenine could provide valuable additional information about the metal binding patterns of this nucleobase. In particular, these strategies include the use of four different N-ligands, analogues of adenine:

1. Deaza-adenines.
2. Adenine isomers.
3. N-substituted adenines.
4. Aza-adenines.

In the present Ph.D. dissertation there are included relevant results concerning the N-ligands of groups 1, 2 and 3. Such results are detailed in chapters 1 to 3. In addition, chapter 4 involves two contributions that have in common the study of synthetic nucleosides. One consists of a study about the metal binding properties of the antiviral agent acyclovir and copper(II) chelates. The other study addresses the intrinsic acid-base properties of a hexa-2'-deoxinucloside pentaphosphate.

Scheme 1 shows the formulas of the N-ligands included in this Ph.D. dissertation. All the N-ligands are numbered according to purine conventional notation for comparative reasons, irrespective of the corresponding IUPAC notation. The selection of deaza-adenine ligands has been done considering the appropriate bicyclic skeleton and the fact that all the ligands have, at least, one N-heterocyclic donor per ring moiety. Consequently, this group of N-ligands exhibit one tautomerizable/ dissociable proton that is tentatively tied to N9. Besides, adenine isomers also have an exocyclic amino group in positions 2 or 6. The N-substituted adenines used in the present work can be categorised as (a) $N^6$-substituted derivatives, (b) N-(heterocyclic)-methylated derivatives. Note that in this latter case, the substitution in N1, N3, N7 or N9 (N-heterocyclic atoms) leads to the absence of a tautomerizable/dissociable proton in the adenine moiety. The synthetic nucleoside acyclovir is a N9-substituted guanine derivative. This particular nucleoside was selected because of its interesting antiviral properties, its chemical stability (overall concerning the N9-C(exocyclic) bond) and its ability to act as H-donor (via the exocyclic amino group in C2) and H-acceptor (via the oxo group in C6). It should be also considered the absence of an easily dissociable proton, apart from that tied to N1 in the most stable tautomer.

Since adenine and its corresponding derivatives have N-H groups as potential H-dnors or H-acceptors, we considered convenient to use as chelating ligands the iminodiacetate(2-) anion (IDA) and seven N-substituted Ida derivatives with non-coordinating N-arms, alkyl- or benzyl- (see scheme 2). These tridentate chelators were selected due to their ability to satisfy three of the four closest sites around the copper(II) centre, what leaves one free basal position for the formation of the coordination bond Metal-N(adenine-like). Both, Cu(II)-IDA chelate and their derivatives are know to recognizes adenine in very different ways. This fact, may help to make a more comprehensive comparison between the results obtained in this dissertation and that previously described for adenine. In particular (a) the Cu(II)-IDA chelate binds Hade via N3 in cooperation with an intra-molecular interligand

interaction N9-H···O(carboxy). In the crystal [Cu(IDA)(Hade)($H_2O$)$_2$] no π,π-stacking interactions are observed. (b) the copper(II) chelates of MIDA and EIDA bind Hade by menas of the Cu-N7 bond, assisted by the intramolecular N6-H···O(carboxy) H-bond. In the corresponding crystals, pairs of molecules associate antiparallel Hade ligands by relevant π,π-stacking interactions. (c) Cu(II) chelates with NBzIDA and MEBIDA recognizes Hade by the Cu-N3 bond which is reinforced by the N9-H··3O(carboxy) intra-molecular interligand interaction. In the crystals, multi-stacked chains are built thanks to π,π-interactions between Hade and the aromatic moiety on benzyl-IDA ligands of an adjacent molecule. In the present study, the diprotonated species of ethylendiaminotetracetic acid ($H_2EDTA^{2-}$) and the divalent anion glycylglycinate(2-) ($glygly^{2-}$) are also included. The first ($H_2EDTA^{2-}$) can be considered as two IDA moieties linked by the ethylene spacer and is used in a ternary complex with 4-azabenzymidale. The second ($glygly^{2-}$) was used because of its ability to work as a tridentate chelating ligand offering one H-acceptor (carboxy) and one H-donor (amino) in its terminal endings. This feature was particularly interesting for the metal binding properties of acyclovir.

Therefore, according to all the above-mentioned, the OBJECTIVES of this dissertation can be summarised as follows:

1. To study the molecular recognition patterns between different deaza-adenines or adenine isomers and Cu(II) iminodiacetates.

2. To unravel the influence of the substitution on the exocyclic amino group of adenine over the molecular recognition patterns with Cu(II) iminodiacetates.

3. To rationalize the influence of the methylation on the N-heterocyclic donors of adenine over the molecular recognition patterns with Cu(II) iminodiacetates.

4. To study the molecular recognition Cu(II)chelate-nucleoside in two ternary complexes with acyclovir and the chelates IDA or glygly, that offers only O-acceptors in its terminal endings or one O-acceptor and one N-H donor group as terminal endings,

respectively. These features are relevant regarding the possibility of cooperation of coordination bonds with appropriate intra- or inter-molecular H-bonds.

5. From the very first moment that a Project of a Ph.D. Thesis is raised, both Ph.D. advisors and the Ph.D. student are expectant of additional objectives that could turn into a new start for future works after the Ph.D. defence. Hence, it was an ambitious challenge to move further on the 'Bio side' and start to study analogue molecules with bigger size. In this context, a pre-doctoral research stay at the Institute of Inorganic Chemistry, University of Zurich, allow the study of the intrinsic acid-base properties of a hexa-2'-deoxynucleoside pentaphosphate.

SCHEME 1. ADENINE-LIKE LIGANDS USED IN THE PH.D. THESIS

*i. Deaza-adenine ligands*

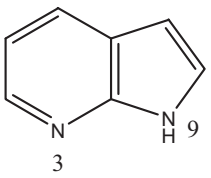

7-Azaindole
1,6,7-trideaza-adenine
(H7azain)

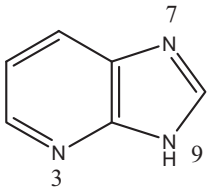

4-Azabenzimidazole
1,6-dideaza-adenine
(H4abim)

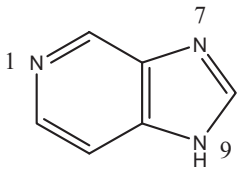

5-Azabenzimidazole
3,6-dideaza-adenine
(H5abim)

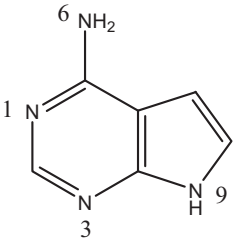

7-Deaza-adenine
(H7deaA)

*ii. Adenine isomers*

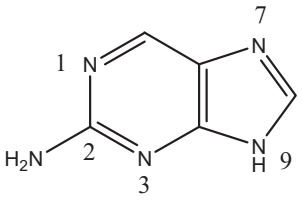

2-Aminopurine
(H2AP)

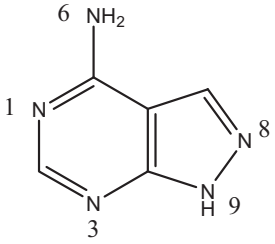

4-Aminopyrazole[3,4-d]pyrimidine
7-deaza-8-aza-adenine
(H4app)

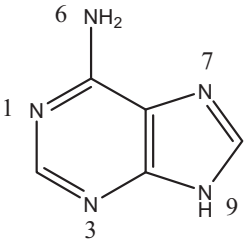

Adenine
(Hade)

*iii. $N^6$-substituted adenines*

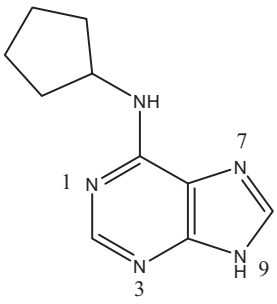

6-Cyclopentyladenine
(HCy5ade)

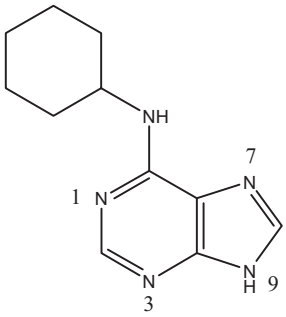

6-Cyclohexyladenine
(HCy6ade)

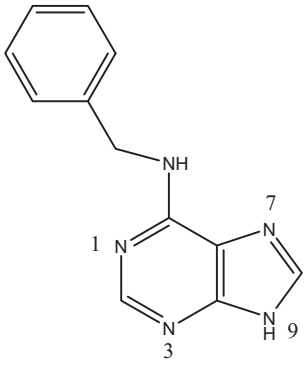

6-Benzyladenine
(HBAP)

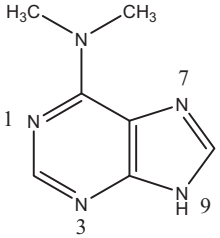

6,6-Dimethyladenine
(HdiMAP)

*iv. N-(heterocyclic) methylated adenines*

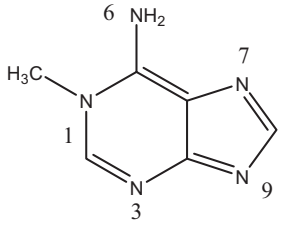

1-Methyladenine
(1Meade)

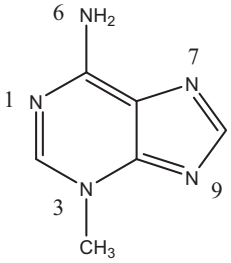

3-Methyladenine
(3Meade)

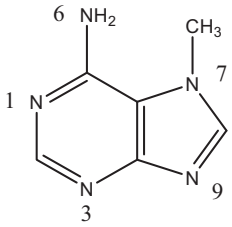

7-Methyladenine
(7Meade)

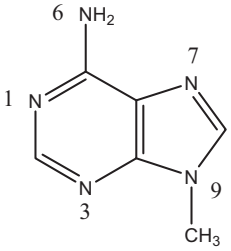

9-Methyladenine
(9Meade)

*v. Synthetic nucleosides*

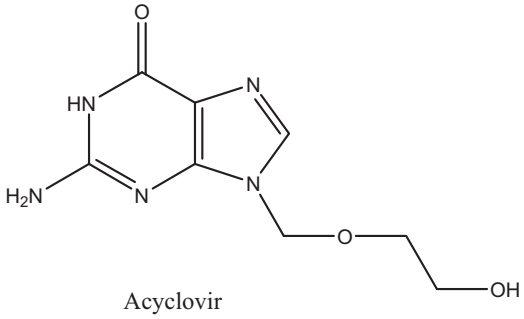

Acyclovir
(acv)

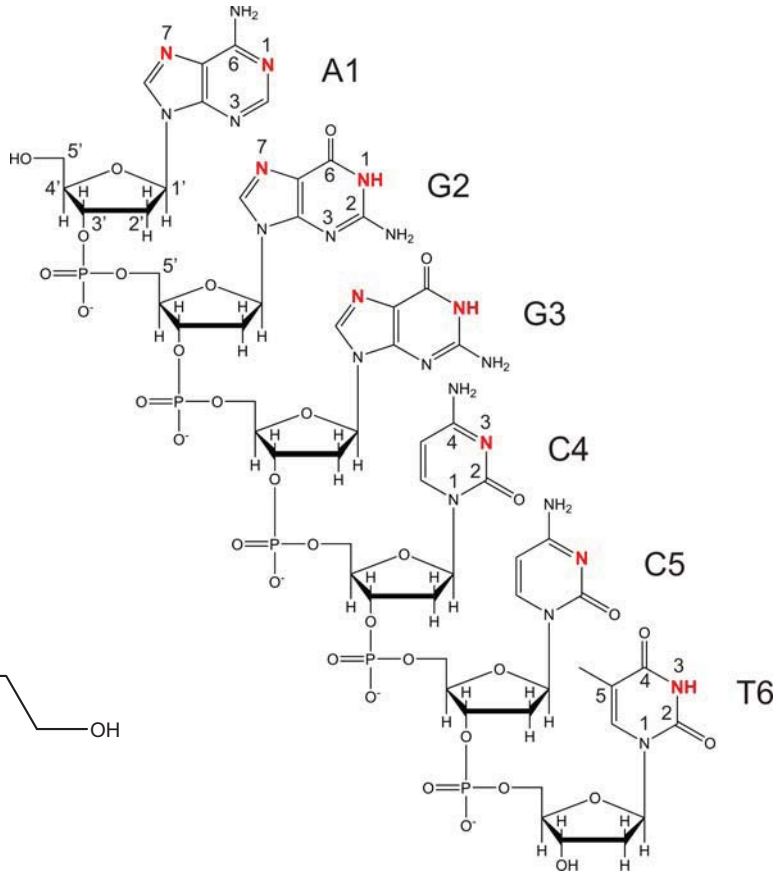


hexa-2'-deoxinucloside pentaphosphate

SCHEME 2. CHELATING LIGANDS USED IN THE PH.D. THESIS

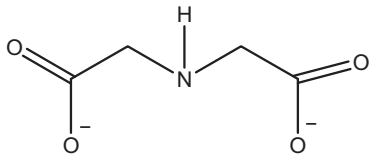

Iminodiacetate(2-) anion
(IDA)

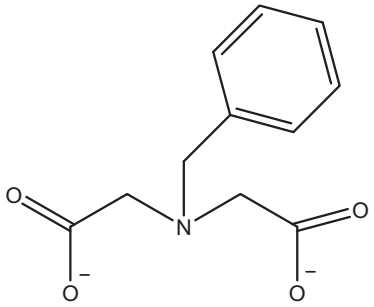

N-Benzyliminodiacetate(2-) anion
(NBzIDA)

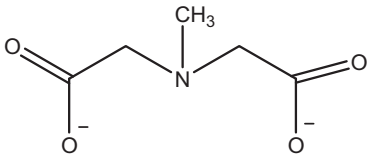

N-Methyliminodiacetate(2-) anion
(MIDA)

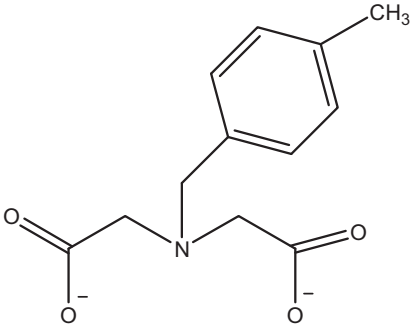

N-p(Methyl)benzyliminodiacetate(2-) anion
(MEBIDA)

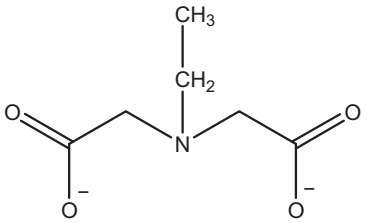

N-Ethyliminodiacetate(2-) anion
(EIDA)

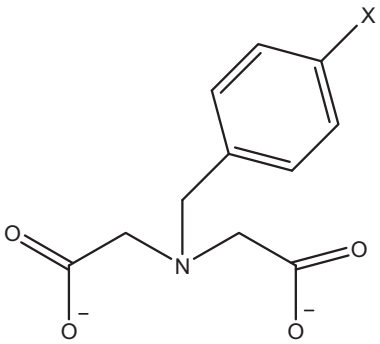

N-p(X)benzyliminodiacetate(2-) anion
X = F (FBIDA)
X = Cl (CBIDA)

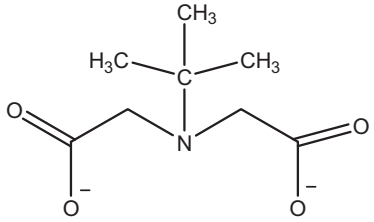

N-Terc-buthyliminodiacetate(2-) anion
(TEBIDA)

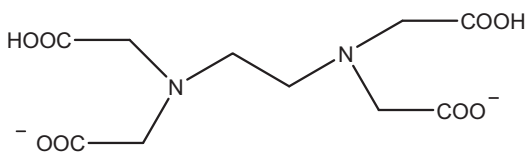

Ethylendiaminotetraacetate(2-) anion
($H_2$EDTA)

# I. PLANTEAMIENTO GENERAL Y OBJETIVOS

El ADN y el ARN son, probablemente, las moléculas más fascinantes de la naturaleza. En los sistemas biológicos, los ácidos nucleicos y sus constituyentes interaccionan con iones metálicos de manera diferente, aunque con aspectos relacionados. Este hecho, los convierte, por tanto, en ligandos naturales de gran tamaño y gran interés. Durante algo más de una década, el grupo de investigación FQM-283 "*Complejos de metales de transición con interés bioinorganico y/o terapéutico"* (http://biomec.ugr.es), viene realizando estudios sobre el reconocimiento molecular de bases nucleicas naturales (adenina, hipoxantina, citosina, etc.) con quelatos metálicos. Estas investigaciones se llevan a cabo en base al más riguroso soporte estructural (cristalográfico) que revela con frecuencia la formación de enlaces coordinados (metal-N), con o sin la cooperación de enlaces de hidrógeno intramoleculares interligandos. Además, en los complejos ternarios investigados, se observa con frecuencia otro tipo de interacciones intra o intermoleculares, entre las que son frecuentes los apilamientos-π,π entre anillos aromáticos. El estado actual de conocimiento, en este contexto, refleja un panorama atractivo por su diversidad y por su potencialidad.

Entre otras, dos recientes revisiones incluidas en esta Tesis Doctoral revelan un comportamiento extremadamente versátil de la adenina, que es capaz de coordinarse a iones metálicos en sus distintas formas (catiónica, neutra o aniónica). Sin embargo, a pesar de la abrumadora información estructural disponible sobre adenina, la química de coordinación de esta nucleobase no es del todo comprendida. Con objeto de contribuir al esclarecimiento de la versatilidad de la adenina como ligando, pueden plantearse nuevas estrategias de investigación de las que cabe esperar una valiosa información complementaria. La adenina ($C_5H_5N_5$, 6-aminopurina) es un ligando bicíclico, rico en nitrógeno, que contiene cuatro átomos N-heterocíclicos y un grupo amino primario exocíclico. Los anillos condensados en su esqueleto molecular son de 6 ó 5 átomos, con naturaleza pirimidínica o imidazólica respectivamente. Estas características han de ser tenidas en cuenta a la hora de considerar compuestos nitrogenados análogos a la adenina, cuyo comportamiento como ligandos pueda complementar la información que hoy en día se posee sobre esta nucleobase. Así pues, teniendo en cuenta estas características, podemos pensar, *a priori*, en cuatro grupos diferentes de ligandos nitrogenados, análogos de adenina:

1. Deaza-adeninas
2. Isómeros de adenina
3. Derivados N-sustituídos de adenina
4. Aza-adeninas

En esta Memoria se incluyen aportaciones sustanciales que se corresponden con los ligandos nitrogenados de los grupos 1, 2 y 3. Dichas aportaciones se reúnen en los capítulos 1 a 3 de este trabajo. Además, el capítulo 4 recoge dos contribuciones que tienen en común la utilización de nucleósidos de síntesis. En particular, se incluye (i) un estudio del reconocimiento molecular entre el agente antivirásico aciclovir y quelatos de cobre(II) y (ii) un estudio sobre las propiedades ácido-base intrínsecas de un hexa-2'-desoxirribonucleósido pentafosfato.

El esquema 1 (vide supra, *Scheme 1*) muestra las formulas de los ligandos nitrogenados incluidos en el presente estudio. Los heterociclos nitrogenados se numeran, con fines comparativos, de acuerdo con la notación convencional de purinas, independientemente de su correspondiente numeración IUPAC. La selección de *deaza-adeninas* se ha hecho considerando el esqueleto bicíclico de adenina y la condición de que contengan al menos un nitrógeno heterocíclico en cada uno de sus anillos. En consecuencia, este grupo de bases nitrogenadas contiene un protón disociable/tautomerizable que, en las fórmulas, aparece unido al nitrógeno 9. Los *isómeros de adenina* incluidos en este trabajo poseen también un grupo amino exocíclico sobre los carbonos 2 ó 6. Los *N-derivados de adenina* pueden agruparse, desde un punto de vista práctico, como (a) derivados $N^6$-sustituidos, que conservan un protón disociable/tautomerizable; (b) derivados metilados en cada uno de los cuatro nitrógenos heterocíclicos de la adenina. Nótese que estas bases nitrogenadas contienen el grupo amino exocíclico (-$^6NH_2$) pero carecen del protón disociable/tauromerizable. El *nucleósido sintético aciclovir* se trata de un derivado N9-sustituído de guanina. Su selección se ha hecho en base a sus atractivas propiedades antivirásicas, su considerable estabilidad química (sobre todo la que corresponde al enlace N9-C(exocíclico)) y por la función aceptora de hidrógenos del grupo oxo en el carbono 6, que contrasta con la función dadora de hidrógeno del grupo amino exocíclico de adenina. Asimismo, el grupo amino exocíclico sobre el carbono 2 tiene, en potencia, funciones dadoras para la formación de enlaces de hidrógeno, que no tienen por qué descartarse. Ha de considerarse igualmente la ausencia de

un protón fácilmente disociable, aunque sin ignorar el hidrógeno unido a N1, en su tautómero más estable.

Dado que la adenina y sus análogos contienen grupos N-H como potenciales dadores o aceptores de enlaces de hidrógeno, se estimó conveniente utilizar como ligandos quelantes el iminodiacetato(2-) (IDA) y siete derivados N-sustituidos de IDA, con sustituyentes no coordinantes de tipo alquílico o bencílico (vide supra, *Scheme 2*). Estos quelantes tridentados fueron seleccionados por su capacidad de unirse al cobre(II) ocupando tres de las cuatro posiciones más próximas de su entorno de coordinación, lo que deja una cuarta posición basal libre para la formación de un enlace Cu-N(base nitrogenada). Además, se conocen con anterioridad los diferentes modos de reconocimiento molecular entre dichos quelatos de cobre(II) y adenina. Este hecho permite una más exhaustiva comparación de los resultados obtenidos en la presente Memoria respecto al comportamiento de la nucleobase natural. En concreto, (a) el quelato Cu(IDA) se coordina a la adenina por N3 en cooperación con el enlace de hidrógeno intramolecular interligandos N9-H···O(carboxilato). En el cristal de $[Cu(IDA)(Hade)(H_2O)_2]$ no existen interacciones-π,π. (b) los quelatos de Cu(II) con MIDA o EIDA se reconocen con Hade por el enlace Cu-N7 reforzado por la interacción intramolecular interligandos N6-H···O(carboxilato). En los correspondientes cristales, pares de moléculas asocian sus ligandos Hade de forma antiparalela, mediante un relevante apilamiento-π,π. (c) los quelatos de Cu(II) con NBzIDA y MEBIDA, se reconocen con Hade mediante el enlace Cu-N3 y la interacción intramolecular interligandos N9-H···O(carboxylato). En sus cristales existen cadenas de moléculas cohesionadas por una interacción-π,π entre cada ligando Hade y el anillo aromático del sustituyente bencilo perteneciente a la molécula adyacente. En este estudio se incluyen también, como quelantes, la especie diprotonada del ácido etilendiaminotetraacético ($H_2EDTA^{2-}$) y el anión divalente glicilglicinato(2-) ($glygly^{2-}$). El primero se puede considerar como dos agrupaciones IDA unidas por un espaciador etileno. Con este ligando quelante se ha obtenido un compuesto conteniendo como ligando nitrogenado 4-azabencimidazol. El segundo, se ha utilizado por comportarse como un quelante tridentado que ofrece en sus extremos un grupo aceptor de hidrógeno (carboxilato) y otro grupo dador de hidrógeno (amino). Esta circunstancia resultaba particularmente atractiva para investigar el reconocimiento molecular de su quelato de cobre (II) con aciclovir.

Por todo lo anteriormente expuesto, los OBJETIVOS de este Proyecto de Tesis Doctoral se resumen en los siguientes puntos:

1. Estudiar el reconocimiento molecular entre diversas deaza-adeninas o isómeros de adenina con complejos de cobre(II) conteniendo, en general, quelantes tridentados tipo iminodiacetato.

2. Investigar la influencia de la sustitución en el nitrógeno N6-exocíclico de adenina sobre el reconocimiento molecular con diversos iminodiacetatos de cobre(II).

3. Investigar la influencia de la metilación en los átomos de nitrógeno heterocíclico de adenina sobre el reconocimiento molecular establecido entre adenina y diversos iminodiacetatos de cobre(II).

4. Estudiar los modos de reconocimiento molecular quelato de cobre(II)-nucleósido, en base a la formación de complejos ternarios de cobre(II) con aciclovir y quelantes de distinta naturaleza: sólo aceptores de hidrógeno (IDA) o con grupos terminales que pueden actuar como aceptores o como dadores de hidrógenos (glygly) para la cooperación entre un enlace coordinado y un enlace de hidrógeno apropiado tipo intramolecular interligandos.

5. Desde el momento en que se plantea un proyecto de Tesis Doctoral, tanto los directores como quien la realiza, quedan expectantes hacia objetivos adicionales, que en definitiva, puedan marcar futuras directrices después del punto y seguido que siempre se encuentra al final de la Tesis Doctoral. Así pues, constituía un reto adicional avanzar, desde un punto de vista biológico, en el estudio de moléculas análogas con mayor envergadura. En este contexto, una estancia predoctoral en el Instituto de Química Inorgánica de la Universidad de Zurich, permitió el estudio de las propiedades ácido base de un hexa-2'-desoxinucleósido pentafosfato.

## II.i. Metal ion binding modes of hypoxanthine and xanthine versus the versatile behaviour of adenine

Review article published in *Coord. Chem. Rev.* 256 (2012) 193-211

### RESEARCH HIGHLIGHTS

- Adenine is the most versatile purine-like ligand.
- Oxo-group restricts versatility for hydroxy-purines.
- Softness of metal ions favours anionic purine forms.
- Cationic, neutral and anionic purines bind metals.
- Metal binding patterns of purines involve tautomerisms.

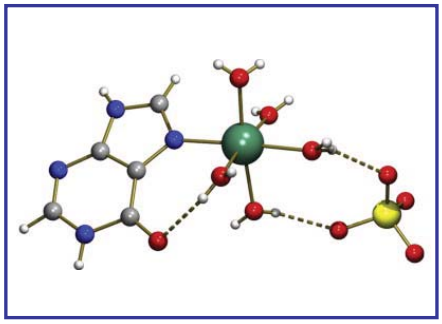

### RESUMEN

En este trabajo se revisan los modos de reconocimiento molecular de las nucleobases hipoxantina, xantina y oxo-purinas relacionadas, basándose en la información estructural disponible en la base de datos *Cambridge Structural Database* e incluyendo aquellas aportaciones recientes encontradas en *Scifinder*. Se dedica especial atención a los modos de unión a metales y a las interacciones interligandos en complejos con mezcla de ligandos, así como a las posibilidades de coordinación del átomo de O exocíclico. La correspondiente información ha sido también revisada para adenina en sus formas aniónica, neutra y catiónica, y para cualquier metal. En contra de la escasa información estructural disponible para hipoxantina y complejos relacionados, existe una amplia información estructural para complejos de adenina con una gran variedad de metales, lo que revela algunas correlaciones entre las propiedades del cristal y las propiedades químicas de los metales. Tres aspectos fundamentales han sido estudiados en profundidad: (i) los modos de coordinación, (ii) las interacciones interligando que influencian los modos de reconocimiento molecular en complejos metálicos con mezcla de ligandos y (iii) la

conectividad entre metales y diferentes especies de adenina, apoyando su gran versatilidad como ligando. Cuando ha sido posible, el conjunto del comportamiento mostrado por los complejos de adenina se ha discutido de acuerdo con el criterio HSAB de Pearson y con el comportamiento del tautómero observado para cada especie protonada de adenina. Asimismo, se han destacado las diferencias entre modos de coordinación de adenina y las referidos ligandos oxopurina.

Coordination Chemistry Reviews 256 (2012) 193–211

Contents lists available at ScienceDirect

Coordination Chemistry Reviews

journal homepage: www.elsevier.com/locate/ccr

Review

# Metal ion binding modes of hypoxanthine and xanthine versus the versatile behaviour of adenine

Dheerendra Kumar Patel [a], Alicia Domínguez-Martín [a], María del Pilar Brandi-Blanco [a], Duane Choquesillo-Lazarte [b], Valeria Marina Nurchi [c], J. Niclós-Gutiérrez [a,*]

[a] Department of Inorganic Chemistry, Faculty of Pharmacy, University of Granada, 18071 Granada, Spain
[b] Laboratorio de Estudios Cristalográficos, IACT-CSIC, Avda. del Conocimiento s/n, 18100 Armilla, Granada, Spain
[c] Dipartimento di Science Chimiche, Università di Cagliary, Cittadela Universitaria, 09042 Monserrato, CA, Italy

**Contents**



*Abbreviations:* Hade, adenine; $H_2ade^+$, adeninium(1+) cation; $ade^-$, adeninate(1−) anion; ade-$H^{2-}$, adeninate(2−) anion; ade-$2H^{3-}$, adeninate(3−) anion; bpdc, biphenyl-4,4′-dicarboxylate(2−) anion; btec, benzene-1,2,4,5-tetracarboxylate(4−) anion; CSD, Cambridge Structural Database; cyclen, 1,4,7,10-tetraazacyclododecane; DFT, density functional theory; 7,9-DM-$hyp^+$, 7,9-dimethyl-hypoxanthinium(1+) cation; 7,9-DM-hyp-$H^{\pm}$, 7,9-dimethyl-hypoxanthine zwitterion; DMF, dimethyl-formamide; dmso, dimethyl-sulfoxide; HEDTA, hydrogen-ethylenetetraminetetraacetate(2−) anion; Hhyp, hypoxanthine; $H_2hyp^+$, hypoxanthinium(1+) cation; $hyp^-$, hypoxanthinate(1−) anion; IDA, iminodiacetate(2−) anion; IDA-like, N-R-substituted iminodiacetate(2−) anions; mal, malonate(2−) anion; MEBIDA, N-(p-methyl-benzyl)-iminodiacetate(2−) anion; 7-Me-hyp, 7-methyl-hypoxanthine; 9-Me-hyp, 9-methyl-hypoxanthine; 9-Me-hyp-$H^-$, 9-methyl-hypoxanthinate(1−) anion; 2Memal, 2-methyl-malonate(2−) anion; $Me_5$-cp, pentamethylcyclopentanienyl(1−) anion; $CH_3$-Hg, methyl-mercury group; MIDA, N-methyl-iminodiacetate(2−) anion; MOF, metal–organic frameworks; NTA, nitrilotriacetate(3−) anion; ox, oxalate(2−) anion; 2,6-pdc, pyridine-2,6-dicarboxylate(2−) anion; 2,3-pdc, pyridine-2,3-dicarboxylate(2−) anion; pheida, N-phenetyl-iminodiacetate(2−) anion; pzdc, 2,5-pyrazoledicarboxylate(2−) anion; tda, thiodiacetate(2−) anion; tren, tris-(2-aminomethyl)amine; Hxan, xanthine; $xan^-$, xanthinate(1−) anion; xan-$H^{2-}$, xanthinate(2−) anion.

* Corresponding author. Tel.: +34 958243855; fax: +34 958246219.
*E-mail address:* jniclos@ugr.es (J. Niclós-Gutiérrez).


doi:10.1016/j.ccr.2011.05.014

ARTICLE INFO

*Article history:*
Received 31 March 2011
Accepted 20 May 2011
Available online 12 June 2011

Dedicated to all Senior and Young researchers that improve the European Group of Thermodynamic of Metal Complexes.

*Keywords:*
Metal binding pattern
Interligand interactions
Crystal structure
Adenine
Hypoxanthine
Xanthine

ABSTRACT

The metal coordination patterns of hypoxanthine, xanthine and related oxy-purines have been reviewed on the basis of the structural information available in the Cambridge Structural Database (CSD), including also the most recent reports founded in SciFinder. Attention is paid to the metal ion binding modes and interligand interactions in mixed-ligand metal complexes, as well as the possibilities of metal binding of the exocyclic-O atoms. The information in CSD is also reviewed for the complexes of adenine in cationic, neutral and anionic forms with every metal ion. In contrast to the scarce structural information about hypoxanthine and related complexes, large structural information is available for adenine complexes with a variety of metals that reveals some correlations between the crystal–chemical properties of metal ions. Three aspects are studied in deep: the coordination patterns, the interligand interactions influencing the molecular recognition in mixed-ligand metal complexes and the connectivity between metals for different adenine species, thus supporting its unique versatility as ligand. When possible, the overall behaviour showed by adenine metal complexes is discussed according to the HSAB Pearson criteria and the tautomeric behaviour observed for each protonated species of adenine. The differences between the roles of adenine and the referred oxypurines ligands are underlined.



## 1. Introduction

The interaction between nucleic acids and metal ions constitutes a field with multidisciplinary character such as the Bioinorganic Chemistry or Inorganic Biochemistry. Undoubtedly, DNA molecules are the biggest ligands of biological systems. However the relevance of these molecules is related to the information they codify and express rather than their dimension. At the present time, studies in this field are really broad, including research on native DNA but also studies with single to multi-stranded oligonucleotides or their more elemental constituents (nucleotides, nucleosides, nucleobases). For many years [1], the interaction between metal ions and constituents of nucleic acids has been of increasing interest. Such interactions depend on multiple factors that become further understood due to solution and/or solid state studies. In this kind of research, natural nucleic acid bases are used as well as designed synthetic bases. Both types of bases can be considered as nucleobases from a broad point of view. In fact, some synthetic nucleobases have recently been of interest per se or as constituents of drugs or pro-drugs.

During the last decade, some reviews have appeared that deal with different aspects of the behaviour of nucleobases as ligands [2–9]. These reviews bear on the multiplicity of metal ion binding patterns of nucleobases [2,4,8], the alterations of acidity constants promoted by metal coordination [3] or those aspects related to the molecular recognition that are tied to the interactions between nucleobases and metal complexes to generate mixed-ligand metal complexes [4,5,7]. This type of mixed-ligand metal complex can be molecular or polymeric [4–7]. In both cases, crystallographic studies reveal interesting aspects of supramolecular chemistry [4–7]. In this context, molecular recognition [4–6] always exhibits the formation of coordination bonds that are usually aided by inter-ligand interactions of diverse nature. Special attention should be paid to hydrogen bonding interactions but also to other interactions such as π,π-stacking or C–H/π interactions [5–7]. The role of crystallography in the progress of this field is significant because it quantifies the strength of the coordination bonds and the diverse intermolecular interactions. Indeed, crystallographic studies, in molecular mixed-ligand complexes, bring accurate data of molecular structure and also reliable information about the intermolecular interactions involved in the crystal packing [4–9]. Both aspects should be taken into account in considering the information gathered in the Crystallographic Database (CSD).

The initial studies about the metal binding pattern of nucleobases [2–8] began with those compounds that result from the reaction between the aforementioned nucleobases and simple inorganic salts (chloride, nitrate, sulfate, perchlorate) or complexes having organic ligands (carboxylates, amino acids, peptides). These studies have been of interest to numerous research groups for fifteen years. An important part of this research has been driven by the discovery of the antitumoral properties of cisplatin or the antiviral properties of other related compounds [2]. Parallel research has also been carried out just for the intrinsic interest of some particular nucleobases as ligands and the potential applications of their complexes. In this sense, studies carried out with purine ligands stand out [4–9] with adenine noted as a very singular versatile ligand [2,4–9].

The main aim of this review is to exhaustively display and compare the metal ion binding patterns of adenine (Hade), hypoxanthine (Hhyp) and closely related ligands (see Scheme 1). The information reviewed in CSD (version 5.32-updated to February 2011) does not introduce any constraint concerning metals. The available structural information is far more abundant for adenine complexes than for hypoxanthine ones. For this reason, data related to xanthine (Hxan) as well as xanthine and hypoxanthine derivatives are also provided. The scope of this review excludes other purine ligands, in particular amino-oxo-purines such as guanine. Information about guanine complexes and derivatives can be found in Refs. [2–8].

## 2. Adenine metal complexes

The structure of free adenine has been determined three times (FUSVAQ [10] or FUSVAQ01 [10] for Hade·3$H_2O$ and KOBFUD [11] for Hade) and corresponds to its most stable tautomer H(N9)ade. A recent study reports the stabilization of the unusual H(N7)ade tautomer in the lattice of the compound [Mn(ox)($H_2O$)$_2$]·Hade·$H_2O$ (SEGCOX [12]).

The H(N9)ade tautomer is also observed in twelve different adenine solvate compounds. They are adducts of organic molecules (see ADRBFT10 [13] with riboflavin or WUPGOE [14] and WUPGUK [14] having thymine), adeninium(1+) salts (see EVIFIY [15] with adeninium perchlorate) or different metal complexes (see NILNUS [16] having a ternary $Ni^{II}$ complex with adeninate(1−) and tren as ligands). In addition, there is a wide assortment of complexes known to contain the adeninium(1+) and adeninium(2+) cations,

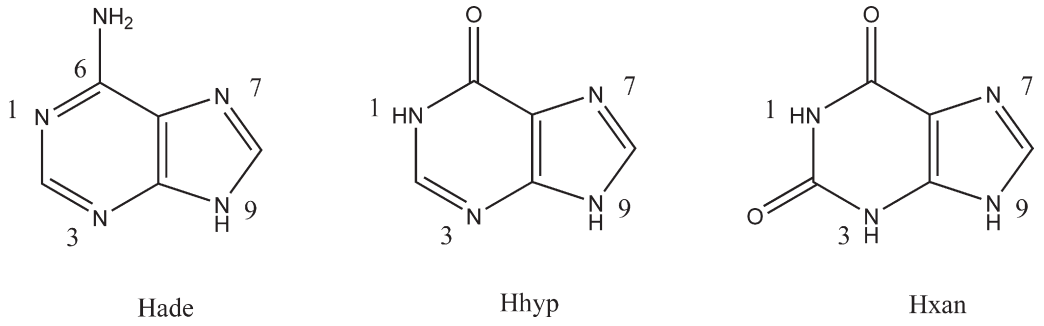


**Scheme 1.** Formulae of adenine (Hade), hypoxanthine (Hhyp) and xanthine (Hxan) with purine-like conventional numbering.

neutral adenine and the three anionic forms ($ade^-$, $[ade\text{-}H]^{2-}$ and $[ade\text{-}2H]^{3-}$).

### 2.1. Adeninium complexes

#### 2.1.1. Outer-sphere adeninium(2+) or adeninium(1+) complexes

The adeninium cations give rise to diverse salts containing a wide variety of counter-anions. Some of these salts have anionic coordination complexes that are monomers or polymers and can be considered as 'outer-sphere' complexes.

The $H_3ade^{2+}$ ion is found in the compounds $(H_3ade)_2[Sn^{IV}Cl_6]Cl_2{\cdot}6H_2O$ (FOMXUB [17]) and $(H_3ade)_n[Sb^{III}Cl_4(\mu_2\text{-}Cl)]_n{\cdot}nH_2O$ (ZETGIO [18]). In these complexes, the adeninium(2+) cation exists as the tautomeric form $H_3(N1,N7,N9)ade^{2+}$. The same cationic species is described in crystals of a variety of salts. However, there are no known complexes where the adeninium(2+) cation is directly bounded to a metal ion (Scheme 2).

The structures of adeninium(1+) salts are described for a wide variety of anions. The salt $(H_2ade)_n[Hg^{II}Cl_2(\mu_2\text{-}Cl)]_n{\cdot}1.5nH_2O$ (ADNCHG10 [19]) has been known for a long time ago. Nevertheless, the vast majority of outer-sphere metal complexes of the adeninium(1+) cation have been reported during the last decades, including a variety of anionic complexes having organic ligands. To this group belongs the compound $H_2(N1,N9)ade[Cu(HEDTA)(H_2O)]{\cdot}2H_2O$ (EGOWIG [5,20]). The crystal of this compound reveals anion–cation links by means of two hydrogen bonding interactions, where the $H_2(N1,N9)ade^+$ cation acts twice as H-donor and two oxygen atoms from the same coordinated carboxylate group of the ligand $HEDTA^{3-}$ act as acceptors. Moreover, in the crystal, pairs of such ion-pairs are associated by π,π-stacking between adeninium cations. More recently, the structure of $(H_2(N1,N9)ade)_2[Cu(ox)_2(H_2O)]$ (UDIJEX [21], Fig. 1) was reported as well as that of two iso-structural compounds with formula $(H_2(N3,N7)ade)_2[M(ox)_2(H_2O)_2]{\cdot}2H_2O$ (M = Co (UDIJIB [21], Fig. 2) or Zn (UDIJOH [21])). The crystals of these compounds show a supramolecular architecture that consists of anionic sheets of metal–oxalate–water complexes and ribbons of adeninium cations building lamellar inorganic–organic hybrid materials. This study is particularly interesting because it exhibits the first example where the adeninium(1+) cation is found as the rare tautomer $H_2(N3,N7)ade^+$. Furthermore, the coordination of the anion $[Cu(ox)_2(H_2O)]^{2-}$ is type 4 + 1 whereas the anions $[M(ox)_2(H_2O)_2]^{2-}$ (M = Co, Zn) are typically octahedral. Analysis of the crystal architecture establishes a correlation between the tautomer of the adeninium cation and the inorganic frameworks.

The tautomer $H_2(N1,N9)ade^+$ has been also described in similar inorganic–organic frameworks as $(H_2ade)_{2n}[Cu(\mu_2\text{-}mal)_2]_n{\cdot}2nH_2O$ (SOLDAZ [22], SOLDAZ01 [23]) and $(H_2ade)_2[Cu(2Memal)_2(H_2O)]$ (SOLCOM [22], SOLCOM01 [23]). This latter adeninium cation is also reported in the crystal $(H_2ade)_2[Sb^{III}Cl_5]$ (ZETGOU [18]). A very recent study reports the structure of two salts with formula $(H_2ade)_2[M^{II}(2,6\text{-}pdc)_2]{\cdot}3H_2O$ with $M^{II}$ = Mn (QUTJEV [24]) or Cu (QUTJAR [24]) and 2,6-pdc = bis-dipicolinate(2−) anion. These crystals exhibit pairs of the tautomeric cations $H_2(N1,N9)ade^+$ and $H_2(N3,N7)ade^+$ associated with two hydrogen bonds affording infinite zig–zag ribbons. These ribbons interact with the bis-dipycolinate-metal(II) anions and with water molecules generating a 3D structure stabilized by many hydrogen bonds. The presence of the tautomer $H_2(N3,N7)ade^+$ associated with $H_2(N1,N9)ade^+$ is an unprecedented feature, where the stabilization is tied to the structure of the inorganic–organic hybrid framework and/or the stabilization of the infinite zig–zag ribbons. The above mentioned crystals, where both tautomers of adeninium(1+) cation exist, are a singular case since only the tautomer $H_2(N1,N9)ade^+$ exists in $(H_2ade)_2[Mn(2,3\text{-}pdc)_2]{\cdot}4H_2O$ [25]. Indeed the tautomer $H_2(N1,N9)ade^+$ cation is assumed to be the most stable tautomer with respect to the N-basicities in Hade. The tautomerism of the adeninium(1+) cation in outer-sphere complexes is not influenced by a direct metal binding. In this context, the knowledge of protonation sites in neutral H(N9)ade (as the most stable tautomer), as well as in the $H_2(N1,N9)ade^+$ and $H_3(N1,N7,N9)ade^{2+}$ cations, support the basicity order (N9 > N1 > N7 > N3 > N6) generally assumed for adenine.

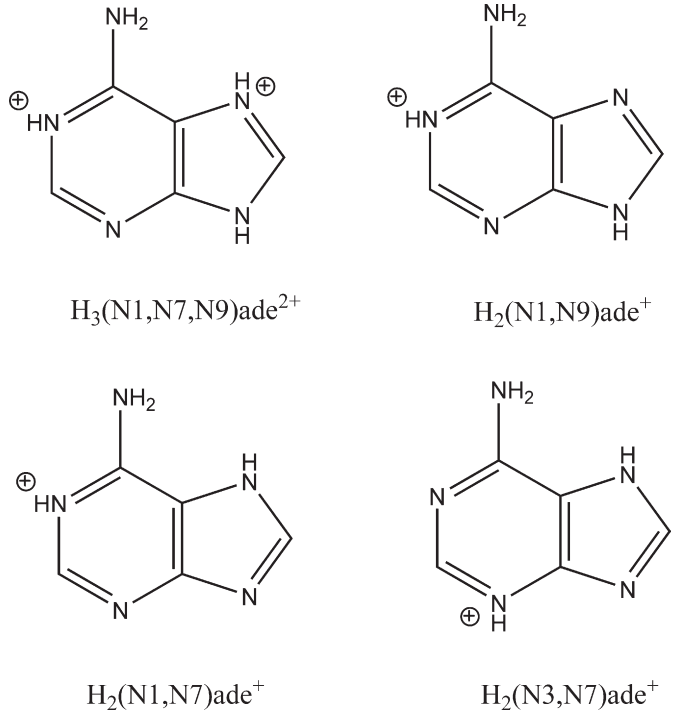


**Scheme 2.** Formulae of adeninium(2+) and adeninium(1+) cations. Different tautomers are reported for the adeninium(1+) cation.

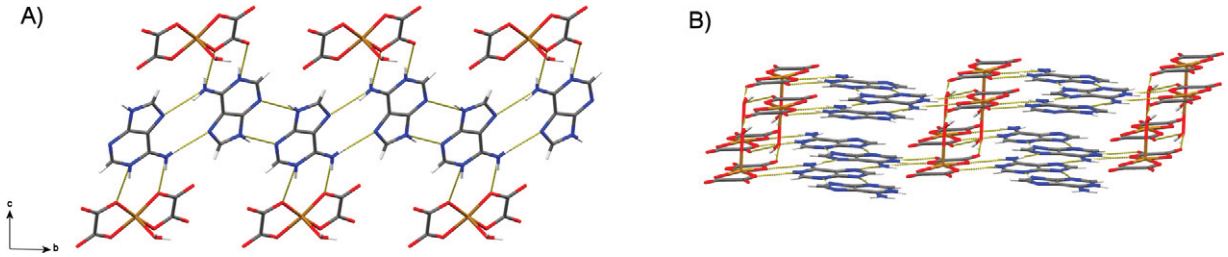


**Fig. 1.** Structure of the outer-sphere complex $(H_2(N1,N9)ade)_2[Cu(ox)_2(H_2O)]$ (UDIJEX [21]). (A) A ribbon of $H_2ade^+$ cations linked by pairs of symmetry related N6–H···N7 H-bonds. $H_2ade^+$ cations are further connected to Cu-oxalate frameworks by N6–H···O(aqua) and N1···O(ox) interactions. (B) 2D frameworks built by anionic sheets of $[Cu(ox)_2(H_2O)]^{2-}$ anions and H-bonding ribbons of adeninium(1+) cations.

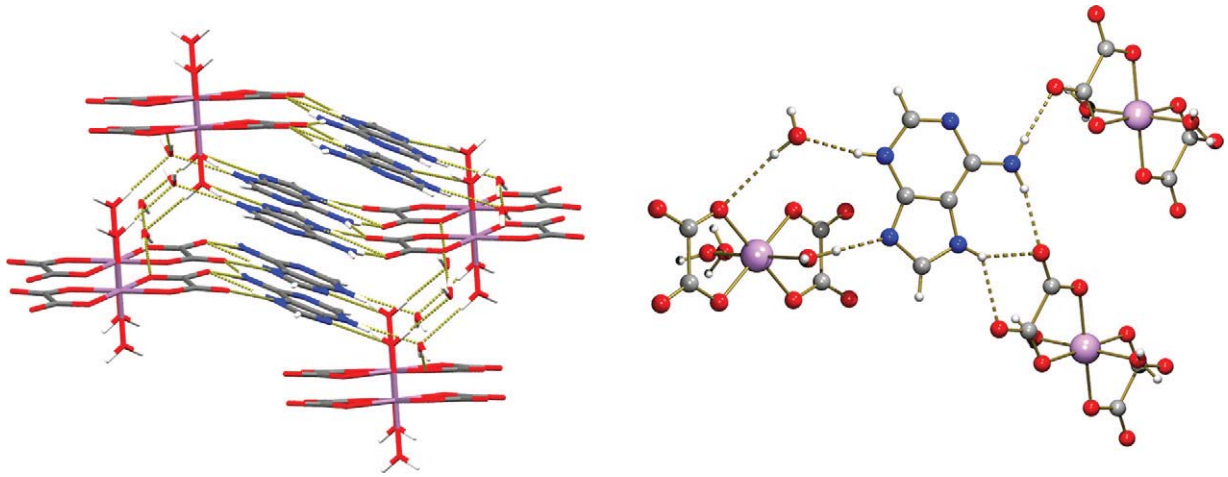

**Fig. 2.** Structure of $(H_2(N3,N7)ade)_2[Co^{II}(ox)_2(H_2O)_2]\cdot 2H_2O$ (M = Co (UDIJIB) [21]) with the rare tautomer $H_2(N3,N7)ade^+$ for the adeninium(1+) cation. (Left) In this compound (and in the isotype analogue UDIJOH) the octahedral anions with apical aqua ligands, water molecules and adeninium(1+) anions build a 3D H-bonded array, where there are no ribbons of $Hade^+$ cations. (Right) Adeninium(1+) cations are involved in N3–H···O(water), N9···H-O(aqua), bifurcated N7–H···$[O(ox)]_2$ and two N6–H···O(ox) H-bonding interactions connecting each complex unit.

### 2.1.2. Inner-sphere adeninium(1+) complexes

The roles of adeninium(1+) cation as ligand are summarized in Table 1. Two tautomers of the adeninium(1+) cation exist, acting as a ligand. The $H_2(N1,N7)ade^+$ cation can act as unidentate, coordinating by N9, or as bridging-bidentate ligand, binding two metal centres through its N3 and N9 donor atoms. There are some structures known for both coordination modes of the tautomer $H_2(N1,N7)ade^+$. All the referred cases have in common the presence of a bond metal–N9, which should determine the protonation of N7. The unidentate role of this tautomer is reported in examples where the metal ion is a hard ($Co^{III}$), borderline ($Cu^{II}$) or soft ($Pt^{II}$) Pearson acid whereas the bidentate bridging role is reported for borderline ($Cu^{II}$) or soft ($Ag^{I}$, $Cd^{II}$, $Pd^{II}$) Pearson acids.

**Table 1**
Metal binding patterns (MBP) of adeninium(1+) cations in inner-sphere complexes.

| MBP | CSD code | Metal | Ref. |
|---|---|---|---|
| M–N7[$H_2$(N1,N9)ade] | ADENZN | $Zn^{II}$ | [26] |
| | CADENZ02 | $Zn^{II}$ | [27] |
| | CADENZ10 | $Zn^{II}$ | [28] |
| | CADENZ20 | $Zn^{II}$ | [29] |
| | QOCTIL | $Ni^{II}$ | [30] |
| M–N9[$H_2$(N1,N7)ade] | BRADCU | $Cu^{II}$ | [31] |
| | CADENC | $Cu^{II}$ | [32] |
| | GIKTIE | $Pt^{II}$ | [33] |
| | ICIDEE | $Co^{III}$ | [34] |
| $M_2(\mu_2$-N3,N9)[$H_2$(N1,N7)ade] | ADAGPC | $Ag^{I}$ | [35] |
| | ADCDNO | $Cd^{II}$ | [36] |
| | ADCDNO10 | $Cd^{II}$ | [37] |
| | ADEHCU10 | $Cu^{II}$ | [38] |
| | WERKAG | $Pd^{II}$ | [39] |

The most stable tautomer $H_2(N1,N9)ade^+$ acts as a ligand in three different compounds. The crystal structure $Cl_3Zn$-N7[$H_2$(N1,N9)ade]·($H_2$(N1,N7)ade)Cl·$H_2O$ (ADENZN [26]) was reported, a long time ago, by Taylor and Westphalen [26]. This compound seems to be a co-crystallization of a zinc complex $Cl_3Zn$-N7[$H_2$(N1,N9)ade] with adeninium(1+) chloride and water but the corresponding cif file is not deposited in the CSD. Hence the presence of the rare tautomer $H_2(N1,N7)ade^+$ cannot be assessed. However, the crystal structure of compound $Cl_3Zn$-N7[$H_2$(N1,N9)ade] has been determined on three occasions (CADENZ02 [27], CADENZ10 [28] and CADENZ20 [29]). The $Zn^{II}$ atom exhibits a tetrahedral coordination, where the Zn–N7 bond cooperates with a N6–H···Cl inter-ligand interaction (3.186 Å, 169.46° in CADENZ02 [27]). The crystal of $[Ni(NTA)(H_2(N1,N9)ade)(H_2O)]\cdot 2.5H_2O$ (QOCTIL [30], Fig. 3) has two non-equivalent complex molecules in its asymmetric unit. Such molecules have the bond Ni–N7 in common but differ in their N6–H···O inter-ligand interactions, which are single (2.755 Å, 169.64°) or bifurcated (2.974 Å, 136.95°; 3.190 Å, 143.45°). The single H-bond is shortest and shows a more open angle than the bifurcated interaction.

## 2.2. Neutral adenine complexes

Neutral adenine can bind metals in unidentate as well as bridging bidentate modes.

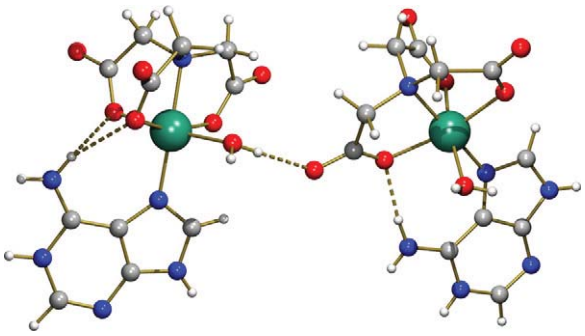

**Fig. 3.** Structure of [Ni(NTA)($H_2$(N1,N9)ade)($H_2O$)]·2.5$H_2O$ (QOCTIL [30]): two non-equivalent complex molecules of the asymmetric unit are depicted with single N6–H···O(carboxylate) (right) or bifurcated N6–H···[O(carboxylate)]$_2$ (left) intra-molecular interactions, further connected by an (aqua)O···O(carboxylate) intermolecular H-bonds.

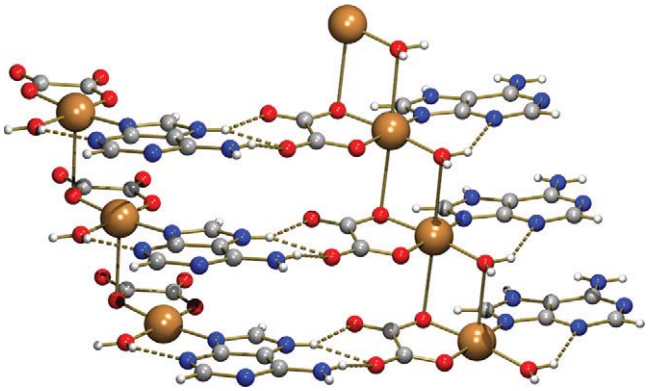

**Fig. 4.** Structure of [Cu($\mu_2$-ox)(Hade)($H_2O$)]$_n$[Cu($\mu_2$-ox)(Hade)($\mu_2$-$H_2O$)]$_n$·3.33$n$$H_2O$ (SEGCUD [12]). The tautomer H(N7)ade acts as ligand for two non-equivalent complex chains. Each Hade ligand is bound to a copper(II) centre by the Cu–N9 bond in cooperation with an intra-molecular (aqua)O–H···N3 interaction (2.635 Å and 134.36° for the 4 + 1 Cu(II) centre; 2.639 Å and 139.86° for the 4 + 2 Cu(II) centre). In addition, each H(N7)ade ligand involves the N7–H and the exocyclic-N6$H_2$ group in intermolecular H-bonds connecting both polymeric complex chains.

### 2.2.1. Unidentate adenine ligand

Table 2 summarizes the structural information regarding the metal binding patterns for unidentate adenine. The available information is very comprehensive and refers to complexes with some hard ($Co^{III}$ and $Mn^{II}$), borderline ($Cu^{II}$, $Co^{II}$ or $Zn^{II}$) and soft ($Pd^{II}$, $Pt^{II}$) Pearson acids. Noteworthy, none of the compounds referred in Table 2 exhibits the tautomer H(N1)ade, despite the stronger basicity of N1 rather than those of N7 or N3. The tautomer H(N7)ade is tied to the M–N9 bond whereas the tautomer H(N9)ade is related to the M–N7 or M–N3 bonds.

The coordination of adenine by its most basic donor N9 occurs with hard or borderline metal centres (Table 2). An interesting example, a coordination polymer with copper(II) and adenine, and oxalate and water as co-ligands (SEGCUD [12]) is shown in Fig. 4. In the crystal two polymers coexist that essentially differ in the coordination number of their metal centres. Moreover, in both polymers, each metal centre coordinates an adenine ligand by its N9 donor atom. One polymeric chain has metal centres with 4 + 1 coordination. The four closest donors to the copper(II) centre are two oxalate (ox) O-carboxylate atoms, the N9 atom of adenine and an aqua ligand. These square-planar units connect to each other through large and weak Cu–O(adjacent oxalate) bonds (2.848 Å). The other polymeric chain presents an elongated octahedral coordination close to 4 + 2. In this latter polymer, the copper(II) atom is also connected to an apical aqua ligand (Cu–OW 2.712 Å) and the successive complex units connect through adjacent O-carboxylate atoms (Cu–O 2.844 Å). An interesting detail, common to both polymers, is that the bridging role of oxalate ligands is made by means of one of the oxalate oxygen atoms involved in the chelation, hence the apical distances Cu–O(carboxylate oxalate) in both chains are nearly identical. Another remarkable feature is that Hade ligands are oriented on the same side throughout the chains encouraging multiple π,π-stacking. The parallel disposition of Hade ligands in the crystal is determined by the contribution of at least three factors: (1) first, each coordination bond Cu–N9 acts in cooperation with the inter-ligand interaction (equatorial aqua)O–H···N3 (2.635 Å and 143.36° or 2.696 Å and 139.86°); (2) H-bonding interactions N6–H···O(ox) and N7–H···O(ox) among chains, have a bifurcated nature. The O-oxalate atoms involved in these hydrogen bonds are not bonded to copper(II) atoms; (3) π,π-stacking within each polymeric chain seems to contribute to its stabilization. DFT calculations [12] for the individual ternary compound agree with the coordination bond distances but support a $Cu^{II}$ coordination with a significant distortion with respect to the four closest donor set of the metal environment.

**Table 2**
Metal binding patterns (MBP) of neutral unidentate adenine ligand.

| MBP | CSD code | Metal | Ref. |
|---|---|---|---|
| M–N9[H(N7)ade] | ADHCOS10 | $Co^{II}$ | [40] |
| | ICIDAA | $Co^{III}$ | [34] |
| | ICIDII | $Co^{III}$ | [34] |
| | SEGCIR | $Mn^{II}$ | [12] |
| | SOLCEC | $Co^{III}$ | [22] |
| | SOLCUS | $Cu^{II}$ | [22] |
| | SEGCUD | $Cu^{II}$ | [12] |
| | YIDPEH | $Cu^{II}$ | [41] |
| M–N7[H(N9)ade] | CUHFUH | $Cu^{II}$ | [42] |
| | CUHFOB | $Cu^{II}$ | [42] |
| | UHECUF | $Cu^{II}$ | [43] |
| | UHEDIU | $Cu^{II}$ | [43] |
| | FEZJEA | $Pt^{II}$ | [44] |
| M–N3[H(N9)ade] | EGUXUZ | $Cu^{II}$ | [45] |
| | LAFTAO | $Zn^{II}$ | [46] |
| | LAFSUH | $Co^{II}$ | [46] |
| | RIWYUR | $Pd^{II}$ | [47] |
| | RIWZAY | $Pd^{II}$ | [47] |
| | UHEDAM | $Cu^{II}$ | [43] |
| | UHEDOA | $Cu^{II}$ | [43] |

The M–N7[H(N9)ade] coordination mode is known for a compound of $Pt^{II}$ and four compounds of $Cu^{II}$. Two compounds have the general formula [Cu(N-alkyl-iminodiacetate)(Hade)($H_2O$)]·$H_2O$ (UHECUF [5,43], UHEDIU [5,43]). In these cases, the Cu–N7 coordination bond is reinforced by the intra-molecular inter-ligand H-bonding interaction N6–H···O(coord. iminodiacetate). The Hade ligand occupies one of the four closest sites of the 4 + 1 environment of the metal ion. The other copper(II) complexes (CUHFUH [42], CUHFOB [42], Fig. 5) have two chelating-type acetyl-acetonate ligands that satisfy the four closest sites around the metal ion and the adenine ligand moves to the apical coordination site (Cu–N7 2.287 Å in CUHFUF and 2.328 Å in CUHFOB). The stability of these molecules, as well as the association among molecules, seems favoured by weak bifurcated H-bonds between each N6–H and two O donor atoms from both acetylacetonate ligands (within the own molecule or with one adjacent molecule). The role of adenine as apical/distal ligand in a distorted copper(II) coordination polyhedron is not usual since all its N-donor atoms are typical borderline Pearson bases, and therefore, with a predominant affinity for $Cu^{II}$ atoms, a typical borderline Pearson acid. These compounds suggest that the use of appropriate rigid chelating ligands (that efficiently block the equatorial sites in the copper(II) surrounding)

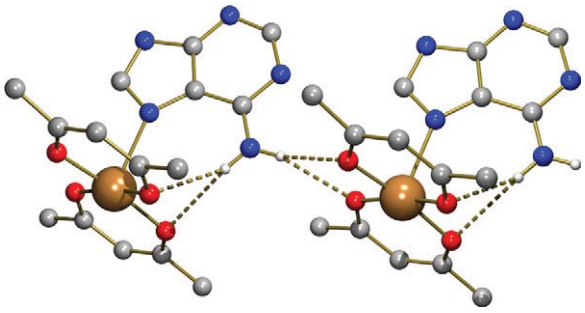

**Fig. 5.** Structure of [Cu(acetylacetonate)$_2$(H(N9)ade)]·EtOH (CUHFOB [42]). For clarity reasons only those H atoms involved in H-bonds are depicted. The Cu–N7(apical) bond (2.328 Å) is supported by asymmetric H-bonding interactions (N6–H···[O(acac)]$_2$, N···O 3.154 or 3.421 Å) that are extremely weak because of the implication of this group in additional intermolecular H-bonds.

can force the coordination of a unidentate ligand such as adenine to an apical site.

Some compounds are also known where adenine acts as a unidentate ligand by its less basic N-heterocyclic donor atom, N3. For this purpose, Hade exhibits its more stable tautomer H(N9)ade. The examples include some mixed-ligand metal complexes where the formation of the bond M–N3 is assisted by a type N9–H···O ($M^{II}$ = Co, Cu or Zn inter-ligand interaction). Two organometallic $Pd^{II}$ compounds also belong to this group where the metal ion is partially coordinated by a $CS_2$-macrocycle that acts as receptor of one adenine (RIWYUR [47], RIWZAY [47], Fig. 6). In these palladium complexes adenine coordinates by N3, which seems to be encouraged by the formation of a weak type N6–H···O(macrocycle) (3.157 Å and 159.11° in RIWYUR; 3.000 Å and 134.36° in RIWZAY) intra-molecular inter-ligand H-bond.

### 2.2.2. Bridging bidentate adenine ligand

Table 3 summarizes the structural information for the bridging role of the Hade ligand. The compounds reported are derivatives of divalent cations of first-row transition metal ions (Co–Zn) or ruthenium(II). These are borderline Pearson acids except for the $Ru^{II}$ derivative.

The coordination mode $\mu_2$-N7,N9[Hade] is described for two different tautomers of neutral adenine. The tautomer H(N3)ade is found in a dinuclear $Cu^{II}$ complex (MUNXUO [5,48]) obtained by reaction of the N-benzyl-iminodiacetate-$Cu^{II}$ chelate and the complementary base pair adenine:thymine. In this particular case, the tautomer H(N3)ade is favoured in order to reinforce the Cu–N9 bond by an intra-molecular inter-ligand H-bonding interaction N3–H···O (2.651 Å, 122.25°). Furthermore, in the molecule, the bond Cu–N7 is also supported by the N6–H···O H-bond (2.674 Å, 147.89°). This latter compound does not exhibit π,π-stacking. The organometallic $Ru^{II}$ compound [$Ru^{II}$($\mu_2$-N7,N9-H(N1)ade)($\eta_6$-benzene)Cl]$_4$·10$H_2$O is tetranuclear (SULYON [49], Fig. 7). The Ru–N7 bond is assisted by the N6–H···Cl intra-molecular inter-ligand interaction (N6···Cl 3.148 Å) whereas the Ru–N9 bond is not reinforced. The bridging $\mu_2$-N7,N9 mode of adenine involves two rare tautomers, H(N3)ade in MUNXUO and H(N1)ade in SULYON.

The coordination of adenine in the mode $\mu_2$-N3,N9 is well-documented for the adeninium(1+) cation – see Table 1, neutral adenine (H(N7)ade) – see Table 3 – and the adeninate(1−) anion – see Table 5. This coordination role favours the formation of dinuclear units, having four (ADAQCU [50], CADCUC [51], FUDQUR [52]) or two (SOLCIG [22], SOLCIG01 [23], SOLDED [22], TUMLEX [23], TUMLIX [23]) bridging $\mu_2$-N3,N9[H(N7)ade] ligands. Fig. 8 shows two closely related examples of ternary compounds having very similar dinuclear cores of cobalt(II) (TUMLET, TUMLIX [23]). They are two different hydrates. Each core has two bridging adenines, two bridging malonates and two aqua ligands. The role of the bridging adenines is the same in both compounds. The crystal packing of these compounds determine that the dinuclear core of TUMLET is reinforced by two intra-molecular (aqua)O–H···O(non-coord. malonate) interactions (2.797 Å, 170.00°) whereas in TUMLIX the aqua ligands are involved

**Table 3**
Metal binding patterns (MBP) of neutral bridging $\mu_2$-adenine ligand.

| MBP | CSD code | Metal | Ref. |
|---|---|---|---|
| $M_2$($\mu_2$-N7,N9)[H(N3)ade] | MUNXUO | $Cu^{II}$ | [48] |
| $M_2$($\mu_2$-N7,N9)[H(N1)ade] | SULYON | $Ru^{II}$ | [49] |
| $M_2$($\mu_2$-N3,N9)[H(N7)ade] | ADAQCU | $Cu^{II}$ | [50] |
| | CADCUC | $Cu^{II}$ | [51] |
| | FUDQUR | $Cu^{II}$ | [52] |
| | SOLCIG | $Ni^{II}$ | [22] |
| | SOLCIG01 | $Ni^{II}$ | [23] |
| | SOLDED | $Zn^{II}$ | [22] |
| | TUMLET | $Co^{II}$ | [23] |
| | TUMLIX | $Co^{II}$ | [23] |
| $M_2$($\mu_2$-N1,N9)[H(N7)ade] | CARCEE | $Cu^{II}$ | [53] |
| $M_2$($\mu_2$-N3,N7)[H(N9)ade] | UHEDEQ | $Cu^{II}$ | [43] |

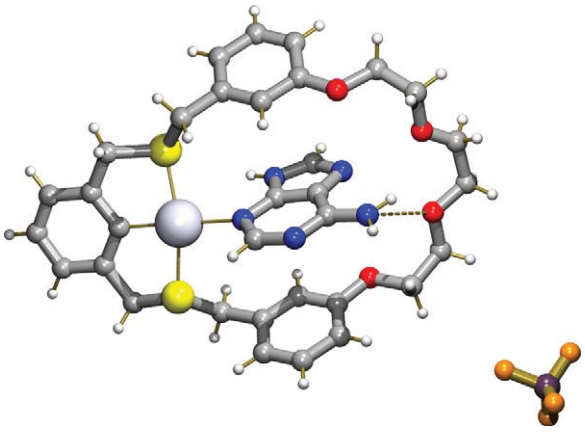

**Fig. 6.** Structure of the cationic organometallic macrocyclic complex [Pd($CS_2$-macrocycle)(H(N9)ade)]$BF_4$ (RIWZAY [47]) having neutral adenine. The $Pd^{II}$–N3 bond is reinforced by the intra-molecular interaction N6–H···O(ether, 3.000 Å, 134.36°).

**Table 4**
Metal binding pattern (MBP) of unidentate adeninate(1−) anion.

| MBP | CSD code | Metal | Ref. |
|---|---|---|---|
| M–N9[ade] | ADBPPD | $Pd^{II}$ | [54] |
| | ADDNCU | $Cu^{II}$ | [55] |
| | ADENCO10 | $Co^{II}$ | [56] |
| | ADMEHH | $Hg^{II}$ | [57] |
| | CUYCUY | $Hg^{II}$ | [58] |
| | DARGAE | $Au^{I}$ | [59] |
| | FASWIG | $Au^{I}$ | [60] |
| | ICICUT | $Co^{III}$ | [34] |
| | ICIDOO | $Co^{III}$ | [34] |
| | MIQVOX | $Cu^{II}$ | [61] |
| | NILNUS | $Ni^{II}$ | [16] |
| | PUNRAS | $Cu^{II}$ | [62] |
| | VEHPUT | $Au^{I}$ | [63] |
| | WULXAC | $Zn^{II}$ | [64] |
| | XOQZEJ | $Zn^{II}$ | [65] |
| | XOQZIN | $Cd^{II}$ | [65] |
| | XOQZOT | $Ni^{II}$ | [65] |
| | YAYWEB | $Pd^{II}$ | [66] |
| | YURWOX | $Cu^{II}$ | [67] |

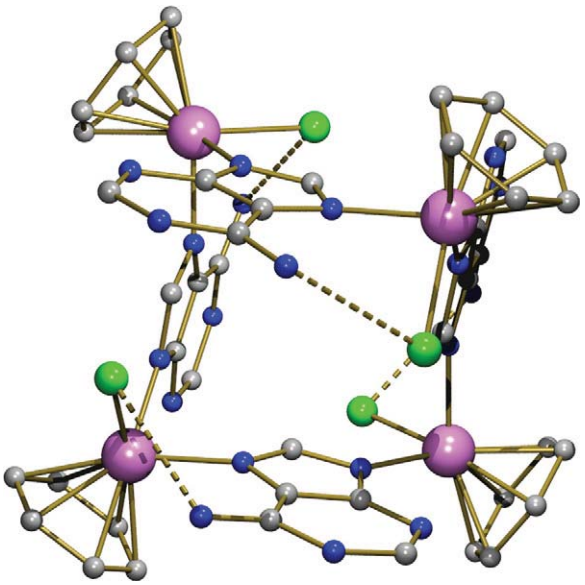

**Fig. 7.** Structure of the tetranuclear cation in the salt $[Ru^{II}(\mu_2\text{-N7,N9-H(N1)ade})(\eta_6\text{-benzene})Cl]_4\cdot 10H_2O$ (SULYON [49]). H atoms omitted for clarity. The rare tautomer H(N1)ade ligand assists the Ru-N7 bond (2.108 Å) with an intra-molecular N6–H···Cl interaction (N···Cl 3.148 Å) whereas the longest Ru–N9 bond (2.117 Å) has no such reinforcement. Each N1–H forms a hydrogen bond (not shown) with a free chloride(1−) anion (2.797 Å, 170.00°).

**Table 5**
Metal binding patterns (MBP) of bridging adeninate anions.

| MBP | CSD code | Metal | Ref. |
|---|---|---|---|
| $M_2(\mu_2\text{-N3,N9})$[ade] | FUDQOL | $Cu^{II}$ | [52] |
| | PUDZOE | $Pd^{II}$ | [68] |
| | SUFHAC | $Pd^{II}$ | [69] |
| | TIMCOI | $Cu^{II}$ | [70] |
| | VAZTEW | $Mn^{II}$ | [71] |
| | VILLUY | $Mn^{II}$ | [72] |
| $M_2(\mu_2\text{-N7,N9})$[ade] | ADHGND | $Hg^{II}$ | [73] |
| | ADEHGND10 | $Hg^{II}$ | [74] |
| | DUXDIJ | $Hg^{II}$ | [75] |
| | NUDKON | $Zn^{II}$ | [76] |
| $M_2(\mu_2\text{-N6,N7,N9})$[ade] | TIWQEV | $Ru^{II}$ | [77] |
| | XEDMEY | $Ir^{II}$ | [78] |
| $M_3(\mu_3\text{-N3,N7,N9})$[ade] | ADHGNO | $Hg^{II}$ | [79] |
| | ADMEHG | $Hg^{II}$ | [80] |
| | DUXDIJ | $Hg^{II}$ | [75] |
| | DUXDOP | $Hg^{II}$ | [75] |
| | PECNUH | $Cu^{II}$ | [71] |
| | SIRGEG | $Cd^{II}$ | [81] |
| | XACZEH | $Cu^{II}$ | [82] |
| $M_4(\mu_4\text{-N1,N3,N7,N9})$[ade] | NUDLAA | $Zn^{II}$ | [83] |
| | PUCFEZ | $Cu^{II}$ | [84] |

in intermolecular H-bonds (aqua)O–H···O(non-coord. malonate; 2.708 Å, 163.63°).

The structure of the polymer CARCEE [53] (Fig. 9) reveals the presence of the bridging $\mu_2$-N1,N9[H(N7)ade] mode. No other compound involving adenine (in its cationic, neutral o anionic form) shows the metal coordination via its N1 donor atom. In CARCEE the bonds Cu–N1 and Cu–N9 are aided by N6–H···O(aqua; 2.899 Å, 154.62°) and (aqua)O–H···N3 (2.777 Å, 150.00°) inter-ligand interactions, respectively. The coordination mode $\mu_2$-N3,N7[H(N9)ade] is reported only in a tetranuclear complex of $Cu^{II}$ (UHEDQ [43], Fig. 10). In this compound, the bonds Cu–N3 and Cu–N7 are reinforced by two intra-molecular inter-ligand H-bonding N9–H···O (2.798 Å, 135.72°; 2.701 Å, 133.92°) and N6–H···O (2.742 Å, 169.19°; 2.800 Å, 165.22°), respectively. This compound does not show π,π-stacking. The tetranuclear nature is determined by the bridging roles of adenine and the N-phenetyl-iminodiacetate(2−) chelator.

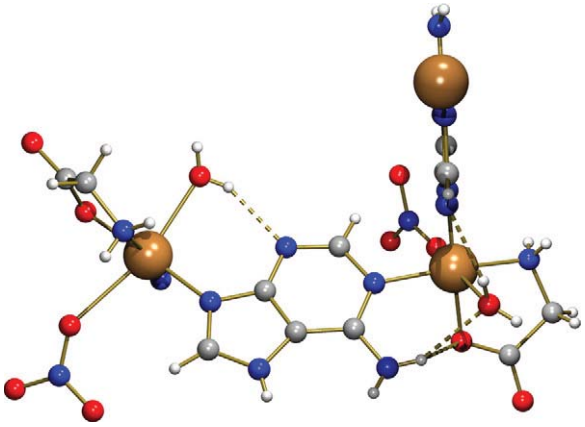

**Fig. 9.** A fragment of the polymeric chain of $[Cu(\mu_2\text{-N1,N9-H(N7)ade})(H_2O)(gly)(NO_3)]_n$ (CARCEE [53]). The Cu–N9 bond is reinforced by an intra-chain (aqua)O–H···N3 interaction (2.777 Å, 154.62°). The unusual Cu–N1 bond is reinforced by a 'bifurcated' intra-chain H-bond [N6–H···O(aqua),O(coord. gly)] (2.899 Å and 150.00° or 2.970 Å and 116.09°, respectively).

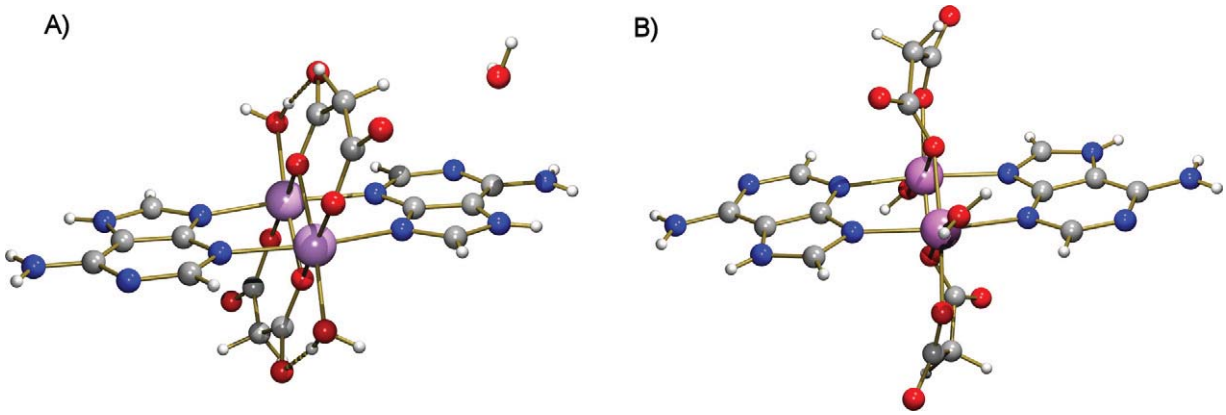


**Fig. 8.** Two closely related binuclear Co(II) compounds with $\mu_2$-N3,N9-H(N7)ade ligands [23]. (A) In $[Co(\mu_2\text{-mal})(\mu_2\text{-H(N7)ade})(H_2O)]_2\cdot 2H_2O$ (TUMLET) there are intra-molecular (aqua)O–H···O(non-coord. mal) H-bonds (3.063 Å, 114.12°). (B) $[Co(\mu_2\text{-mal})(\mu_2\text{-H(N7)ade})(H_2O)]_2$ (TUMLIX) does not show the corresponding intra-molecular H-bonds.

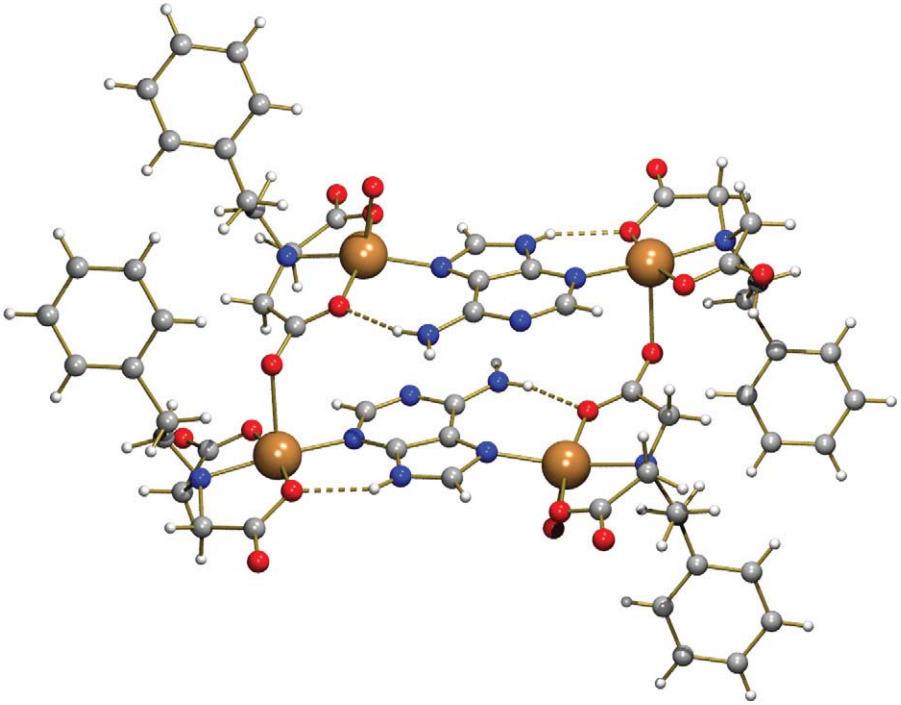

**Fig. 10.** In the tetranuclear compound $[Cu_4(\mu_2\text{-N3,N7-H(N9)ade})_2(\mu_2\text{-pheida})_2(\text{pheida})_2(H_2O)_2]\cdot 4H_2O$ (UHEDEQ [43]), the Cu–N7 and Cu-N3 bonds are assisted by appropriate N–H···O(coord. pheida) interactions. Only one of two independent molecules within the asymmetric unit is shown.

### 2.3. Adeninate(1−) complexes

The dissociation of the proton on N9 from neutral adenine seems to be rather easy. The formation of the adeninate(1−) anion has various consequences. Firstly, it increases the basicity and the metal binding possibilities on its most basic N9 atom. Secondly, it restricts the possibilities of proton tautomeries. Finally, it promotes the denticity of the adeninate(1−) anion. While neutral adenine (Hade) acts as unidentate (Table 2) or as $\mu_2$-bridging bidentate (Table 3) ligand (in both cases using different tautomeric forms) the anionic adeninate(1−) ion ($ade^-$) acts as N9-unidentate ligand (Table 4) but also plays a variety of bridging roles (Table 5).

#### 2.3.1. Unidentate adeninate(1−) ligand

There are reported nineteen structures with the unidentate adeninate(1−) ligand (Table 4). In these compounds the metal ions are hard ($Co^{III}$), borderline ($Ni^{II}$, $Cu^{II}$, $Zn^{II}$) or soft ($Au^{I}$, $Cd^{II}$, $Pd^{II}$, $Hg^{II}$) Pearson acids.

The common feature of all these compounds is the formation of the metal–N9($ade^-$) coordination bond. This bond can be assisted by an H-bonding inter-ligand interaction if the N3($ade^-$) atom acts as acceptor. That occurs, for example, in the following ternary cationic complexes with $M^{II}$, tren and $ade^-$ [$M^{II}$ = Ni (XOQZOT, 3.088 Å, 139.36° [65]), Zn (XOQZEJ, 2.991 Å, 120.14° [65], Fig. 11) or Cd (XOQZIN, 3.206 Å, 117.59° [65])]. In the crystals, the ternary complexes are associated with pairs of symmetry related hydrogen bonds between adjacent adeninate(1−) ligands, involving the exocyclic N6-amino group as donor and the N7 atom as acceptor, giving rise to adeninate(1−) ribbons.

#### 2.3.2. Bridging $\mu_2$-bidentate adeninate(1−) ligand

The bridging $\mu_2$-bidentate modes of the adeninate(1−) ligand include $\mu_2$-N3,N9 and $\mu_2$-N7,N9 (Table 5). These two bidentate modes have been also reported for neutral adenine. A good example of a $\mu_2$-N3,N9[ade] derivative is depicted in Fig. 12 (TIMCOI [70]). In this compound, the adeninate bridges contribute to build dinuclear complex units where each $Cu^{II}$ atom also has a phenantroline and a p-toluene-sulfonate ligand. This latter ligand acts as apical O-unidentate. In the crystal, the adeninate ligands are involved in the formation of symmetry-related pairs of H-bonding interactions type N6–H···N7 (3.049 Å, 156.12°), building infinite chains. The $\mu_2$-N3,N9[ade] bridge is also described in other compounds such as $[Cu_2(\mu_2\text{-N3,N9-ade})_4(H_2O)_2]\cdot 7H_2O$ (VAZTEW [5,71]). This core has the aqua ligands placed in apical sites and offers possibilities for expansion through the N7 donor atoms (vide infra PECNUH).

The bridging mode $\mu_2$-N7,N9[ade] is found in some $Hg^{II}$ derivatives and an interesting hexanuclear mixed-ligand $Zn^{II}$ compound (NUDKON [76], Fig. 13). In this compound, the Zn–N7 bond is supported by an H-bonding inter-ligand interaction type N6–H···O(coord. dimethyl-carbamate, 2.889 Å, 161.19°) whereas the Zn–N9 bond is not reinforced. The hexanuclear molecules are linked to neighbouring units by pairs of N6–H···N1 hydrogen bonds (3.002 Å, 175.58°), a role that is played by every adeninate ligand.

#### 2.3.3. Chelating + $\mu_2$-bridging tridentate adeninate(1−) ligand

A unique bridging mode of the adeninate(1−) ligand (Table 5) occurs in two tetranuclear organometallic compounds with $Ru^{II}$ (TIWQEV [77], Fig. 14) and $Ir^{II}$ (XEDMEY [78]). In both compounds, each adeninate ligand plays two cooperative roles, acting as N7,N6-chelating ligand for a soft metal centre and as $\mu_2$-N6,N7,N9 bridging ligand between two soft Pearson metal centres. In these compounds, the adeninate(1−) ligand displays the rather unusual tautomer $[H(N1)ade\text{-}H(N6)]^-$. This represents the migration of one H atom from the exocyclic N6-amino group to the N1 atom, a feature that seems to be only tied to soft Pearson acids ($Ru^{II}$ and $Ir^{II}$).

#### 2.3.4. Bridging $\mu_3$-tridentate adeninate(1−) ligand

The adeninate(1−) ligand plays the $\mu_3$-N3,N7,N9 bridging role in compounds with soft ($Cd^{II}$ or $Hg^{II}$ – this latter as methyl-mercury) or borderline ($Cu^{II}$) metal ions (Table 5). The DUXDIJ crystal [75] has two types of adeninate ligands, the $\mu_2$-N7,N9 and $\mu_3$-N3,N7,N9[ade], and is therefore placed twice in Table 5. The compound PECNUH [5,71] is a hexanuclear derivative obtained by controlled expansion of the binuclear

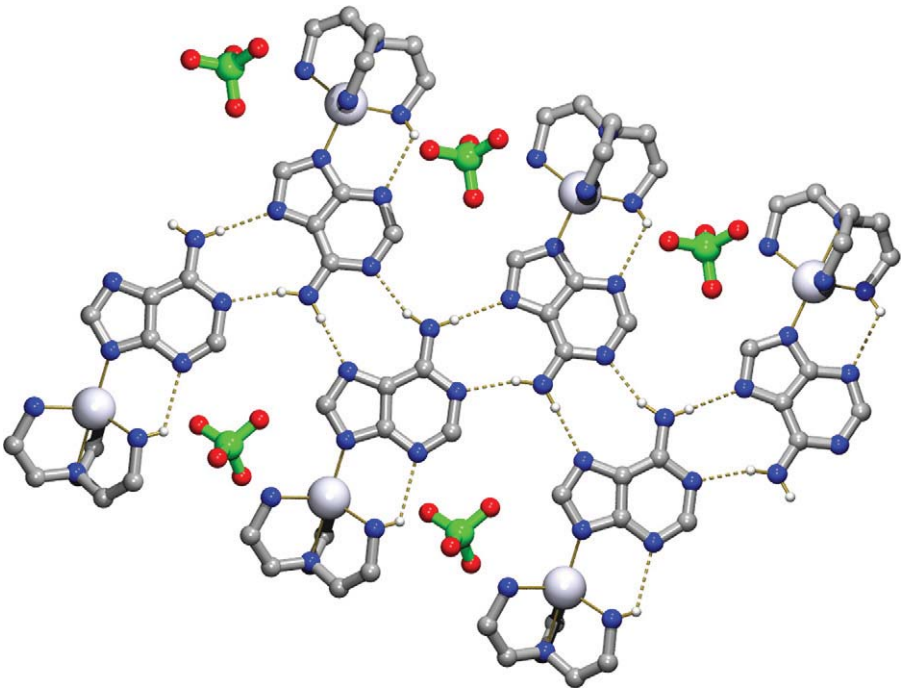

**Fig. 11.** Graphic showing the H-bonded adeninate(1−) ribbons in the crystal of [Zn(ade)(tren)]$ClO_2$ (XOQZEJ [65]). Only those H-bonds involving the adeninate(1−) ligand are depicted due to clarity reasons. The Zn–N9 bond (2.043 Å) acts in cooperation with the intra-molecular inter-ligand H-bond (tren)N–H··N3(ade) interaction (2.991 Å, 120.14°). Each perchlorate anion is H-bonded to a tren ligand (not shown) in the ribbons of complex molecules which extend along the b axis.

complex VAZTEW [5,71] (vide supra). The controlled expansion is made by addition of four $Cu^{II}$(oxydiacetate)(aqua) moieties that bind the central core by means of Cu–N7(ade) bonds reinforced by N6–H···O(coord. oxydiacetate) interactions (2.876 Å, 153.08°; 2.791 Å, 168.31°). In this compound, the tridentate chelating oxydiacetate ligand and the N7(ade) atom supply the four closest donor atoms to the peripheral $Cu^{II}$ centres blocking further expansion. On the other hand, in XACZEH [82] the use of bidentate oxalate groups as chelating ligands favours the formation of the 3D polymer $\{[Cu_2(\mu_3\text{-N3,N7,N9-ade})_4(H_2O)_2][Cu(\mu_2\text{-ox})(H_2O)]_2\cdot\sim 14H_2O\}_n$ (Fig. 15). This polymer is built by addition of four $Cu^{II}$(oxalate)(aqua) moieties to the dinuclear core $Cu_2(\mu_3\text{-N3,N7,N9-ade})(H_2O)_2$. Furthermore, each Cu(ox)(aqua) moiety connects neighbouring cores binding the N7 atom of two different adeninate ligands. The amino exocyclic group of adeninate(1−) ligands is involved in two H-bonds. One of these interactions (N6–H···O(aqua), N6···O 2.855 Å) is intra-molecular whereas the other (N6–H···O(coord. oxalate), N6···O 3.035 Å) is intermolecular. This latter intermolecular interaction acts in cooperation with the other, namely (aqua)O–H···N1(ade) (N1···OW 2.870 Å). The self-assembly of this 3D polymer builds nanotubular channels of about 13 Å diameter where non-coordinated water

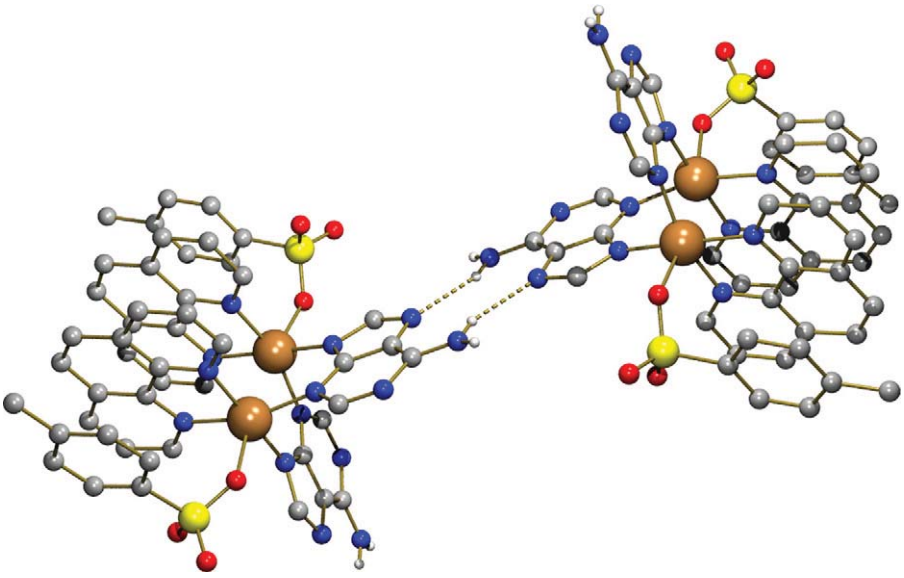

**Fig. 12.** Structure of the dinuclear compound $[Cu_2(\mu_2\text{-N3,N9-ade})_2(phen)_2(p\text{-toluenesulfonate})_2]\cdot 2H_2O$ (TIMCOI [70]). In the molecule the two bridges $\mu_2$-N3,N9-ade efficiently contribute to the formation of pairs of dinuclear units linked by two symmetry related N6–H···N7 interactions (3.049 Å, 156.12°). For clarity reasons only those H atoms involved in H-bonds are depicted.

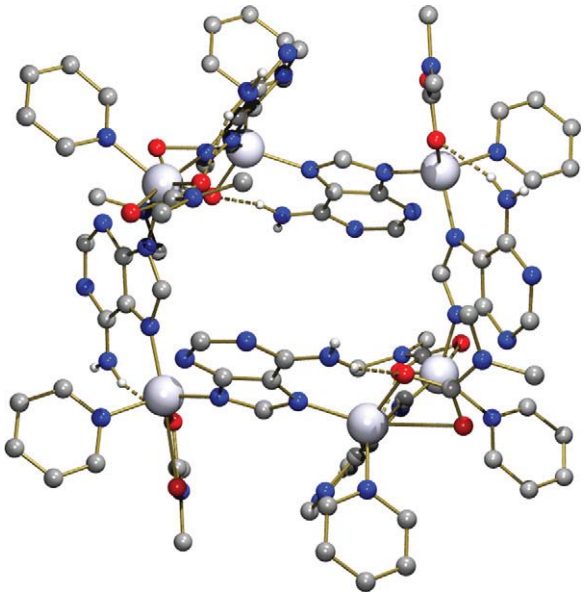

**Fig. 13.** Structure of the hexanuclear complex molecule of [Zn($\mu_2$-N7,N9-ade)(N,N-dimethyl-carbamate)(pyridine)]·10.5 DMF (NUDKON [76]). The internal stability of the molecule is reinforced by each Zn–N7 bond with an intra-molecular inter-ligand H-bond N6–H···O(coord. carbamate, 2.889 Å, 161.19°). For clarity reasons only those H atoms involved in H-bonds are depicted. In the crystal, neighbouring molecules are linked by a pair of symmetry related N6–H···N1 bonds (3.002 Å and 175.58° – not shown).

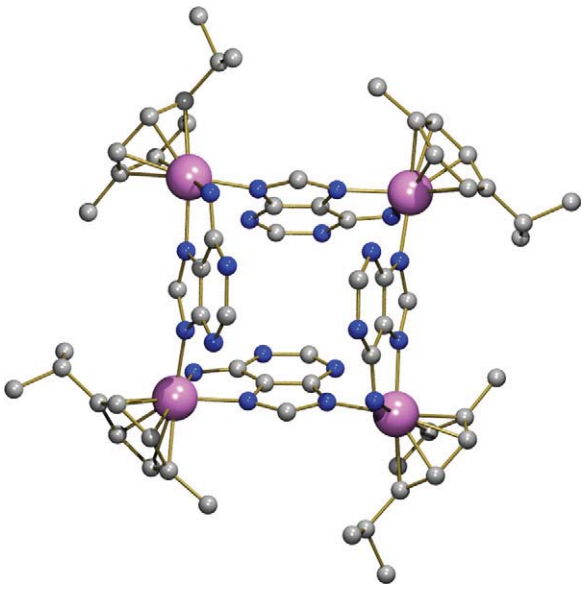

**Fig. 14.** Structure of the tetranuclear organometallic cation in the crystal of [$Ru^{II}_4$($\mu_2$-N6,N7,N9-H(N1)ade)$_4$($\eta_6$(p-cymene))$_4$]($F_3CSO_3$)$_4$ (TIWQEV [77]). H-atoms are omitted. This structure is remarkable for the chelating + bridging role of adeninate(1−) ligand but also for the presence of the rare tautomer [H(N1)ade$^-$] that enables this dual role around the soft acid Ru(II). Such features can also be applied to the $Ir^{II}$ derivative XEDMEY [78].

molecules are guest. The stability of the polymer is enough to enable the water loss (40–95 °C) without modifying the external morphology of the crystal.

### 2.3.5. Bridging $\mu_4$-tetradentate adeninate (1−)

Two recent independent studies have reported novel compounds where the adeninate(1−) anion acts as a bridge among four metal centres, involving, in this role, its four N-heterocyclic donor atoms (Table 5). The compound PUCFEZ [84] [$Cu_4$(DMF)$_6$($\mu_4$-N1,N3,N7,N9-ade)$_2$($\mu_2$-Cl)$_2$Cl$_4$]$_n$ is a 2D polymer where two types of metal centres coexist. One metal centre exhibits a trigonal bipyramidal coordination, where the trans-apical donor atoms are N3 and N9 from two adeninate ligands. The equatorial donor atoms are three chloride ligands: one unidentate and two $\mu_2$-bridging ligands. The other metal centre has a distorted octahedral coordination built by the N1 and N7 donor atoms of two different adeninates, three O(DMF) donor atoms and one chloride ligand. In this coordination polyhedron, the three shortest distances correspond to Cu–N1, Cu–N7 and one Cu–O(DMF) bond. Interestingly, the internal cohesion of the 2D framework is assisted by H-bonds involving the N6-exocyclic amino group as donor and O(DMF) as acceptor. There are bifurcated (2.800 Å, 147.54°; 2.943 Å, 104.02°) and single (2.903 Å, 170.37°) H-bonding interactions (Fig. 16). The same $\mu_4$-N1,N3,N7,N9-ade bridging mode is reported in a metal–organic framework with $Zn^{II}$ (NUDLAA [83]). This compound can be formulated as {($CH_3NH_3$)$_2$[$Zn_8$($\mu_4$-ade)$_4$($\mu_2$-bpdc)$_2$($\mu_4$-O)]·8DMF 11$H_2O$}$_n$. The MOF builds columns of Zn–O–adeninate interconnected by bridging $\mu_2$-bpdc ligands. In the polymer, the exocyclic amino group of each adeninate ligand is involved in two single N6–H···O(carboxylate) interactions (2.873 Å, 170.37°; 2.841 Å, 144.64°). The connectivity pattern of this MOF yields large channels that run along the c axis. The MOF is anionic and the channels hold dimethyl-ammonium cations and solvent molecules (DMF and water). The $\mu_4$-N1,N3,N7,N9 metal binding

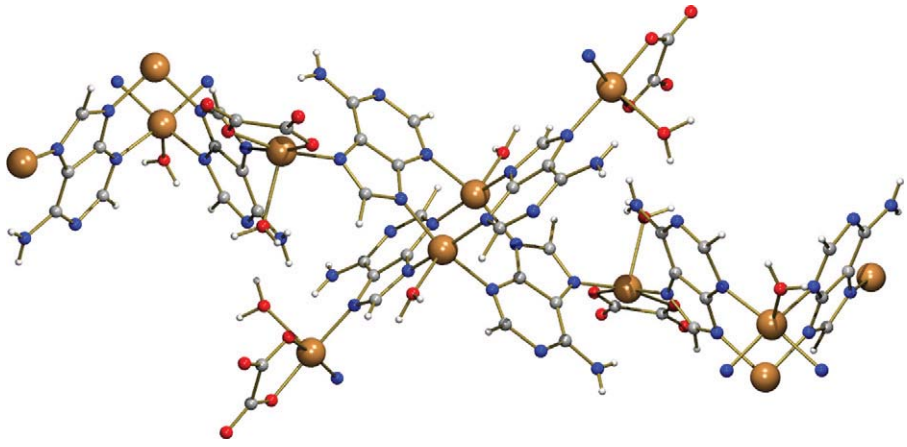

**Fig. 15.** Fragment of the 3D polymer {[$Cu_2$($\mu_3$-N3,N7,N9-ade)$_4$($H_2O$)$_2$]·[Cu($\mu_2$-ox)($H_2O$)]$_2$·∼14$H_2O$}$_n$ (XACZEH [82]). The use of bridging $\mu_2$-[Cu(ox)($H_2O$)] moieties promotes the 3D-expansion of the core [$Cu_2$($\mu_3$-N3,N9-ade)$_4$($H_2O$)$_2$].

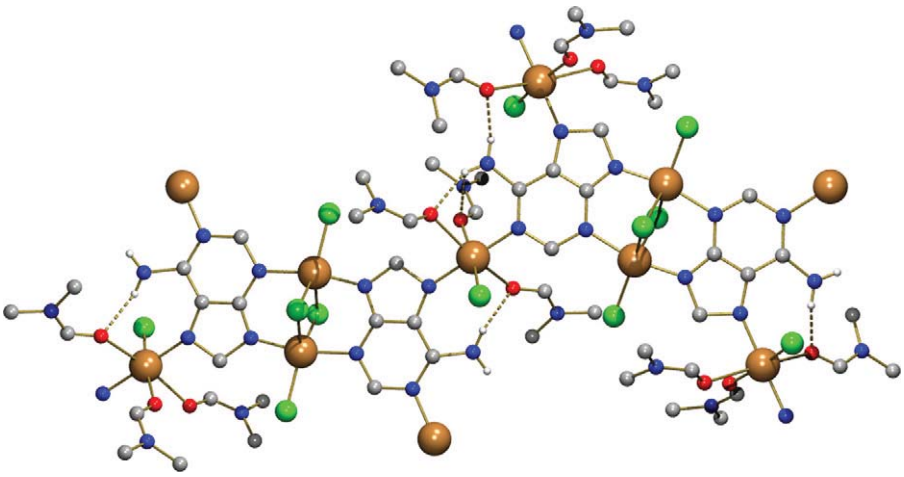

**Fig. 16.** Fragment of the 2D polymeric compound $[Cu_4(DMF)_6(\mu_4\text{-N1,N3,N7,N9-ade})_2(\mu_2\text{-Cl})_2Cl_4]_n$ (PUCFEZ [84]). For clarity reasons only those H atoms involved in H-bonds are depicted. The adeninate anion acts as a bridging-tetradentate ligand binding four borderline metallic centres by means of all its N-heterocyclic donor atoms. Since borderline Pearson acids are not expected to promote the dissociation of the primary exocyclic group, this represents the highest denticity for the adeninate(1−) anion.

**Table 6**
Metal binding patterns (MBP) of $[ade\text{-}H(N6)]^{2-}$ and $[ade\text{-}2H(N6)]^{3-}$ anions.

| MBP | CSD code | Metal | Ref. |
|---|---|---|---|
| $M_2(\mu_2\text{-N6,N9})[ade\text{-}H(N6)]^{2-}$ | FEDCOG | $Hg^{II}$ | [85] |
| $M_3(\mu_3\text{-N6,N6,N9})[ade\text{-}2H(N6)]^{3-}$ | CAVHIQ | $Hg^{II}$ | [86] |
| | CAVHIQ10 | $Hg^{II}$ | [87] |
| $M_4(\mu_4\text{-N3,N6,N6,N9})[ade\text{-}2H(N6)]^{3-}$ | FAKNAG | $Hg^{II}$ | [87] |

pattern which is the highest denticity for an $ade^-$ ligand is only reported for two typical borderline Pearson acids ($Cu^{II}$ and $Zn^{II}$).

### 2.4. Adeninate(2−) and adeninate(3−) complexes

Table 6 includes three reported examples of compounds that have methyl-mercury(1+) coordinated to bridging adeninate ligands. These compounds exhibit two common features. First, at least one of the two H atoms from the exocyclic amino group is replaced by a $CH_3$-Hg moiety. Second, the N9(ade) atom is always metalated by one $CH_3$-$Hg^+$ fragment. Each of these compounds represents a distinct metal binding pattern. In FEDCOG [85] the divalent anion $[ade\text{-}H(N6)]^{2-}$ bridge two methyl-mercury moieties, yielding a molecular compound (ethanol solvate). CAVHIQ [86] (also reported as CAVHIQ10 [87], Fig. 17) is a molecular compound (hemihydrate) where three $CH_3$-$Hg^+$ moieties link the bridging $[ade\text{-}2H(N6)]^{3-}$ anion. In the crystal, each water molecule is H-bonded to the N3 atom of two neighbouring complex molecules. In the nitrate salt FAKNAG [87] one additional metalation occurs on N3, hence the referred trivalent adeninate anion bridges four methyl-mercury moieties.

**Table 7**
Metal binding patterns (MBP) of neutral hypoxanthine (Hhyp).

| MBP | CSD code | Metal | Ref. |
|---|---|---|---|
| M–N7[H(H9)hyp] | BAKDOG | $Ru^{III}$ | [94] |
| | FIZHUR | $Co^{II}$ | [95] |
| | FIZJAZ | $Ni^{II}$ | [95] |
| | FIZJAZ10 | $Ni^{II}$ | [96] |
| $M_2(\mu_2\text{-N3,N7})[H(N9)hyp]$ | FIZHOL | $Cu^{II}$ | [95] |
| $M_2(\mu_2\text{-N3,N9})[H(N7)hyp]$ | HPURCU | $Cu^{II}$ | [98] |
| | JESLAU | $Cu^{II}$ | [99] |
| | JESLEY | $Cd^{II}$ | [99] |
| | JESLIC | $Zn^{II}$ | [99] |
| | KOXPOC | $Co^{II}$ | [100] |

**Table 8**
Metal binding patterns (MBP) of hypoxanthinium(1+) cation and hypoxanthinate(1−) anions.

| MBP | CSD code | Metal | Ref. |
|---|---|---|---|
| M–N3[$H_2$(N7,N9)hyp] | NAVSIN | $Ru^{III}$ | [101] |
| M–N9[hyp] | NILPII | $Ni^{II}$ | [16] |
| | WULXIK | $Zn^{II}$ | [64] |
| | XOQZUZ | $Zn^{II}$ | [65] |
| $M_2(\mu_2\text{-N7,N9})[hyp]$ | MIQWAK | $Cu^{II}$ | [61] |
| | NILPEE | $Ni^{II}$ | [16] |
| | NILPOO | $Ni^{II}$ | [16] |
| | PUNREW | $Cu^{II}$ | [62] |
| | XEDMUO | $Ru^{II}$ | [78] |
| | XORBAI | $Cd^{II}$ | [65] |

According to the suggestion of Lippert [8], the coordination of the N6-exocyclic amino atom is only possible with the deprotonation of its primary amino group. In practice, this only happens when N6 binds a rather soft Pearson acid, such as methyl-mercury(I). In addition, single or double metalation of N6 atom of adenine is always concomitant with the metalation on N9.

## 3. Hypoxanthine complexes

Hypoxanthine (Hhyp) is a 6-hydroxy-purine. However, crystallographic studies regarding this nucleobase agree with the lactam

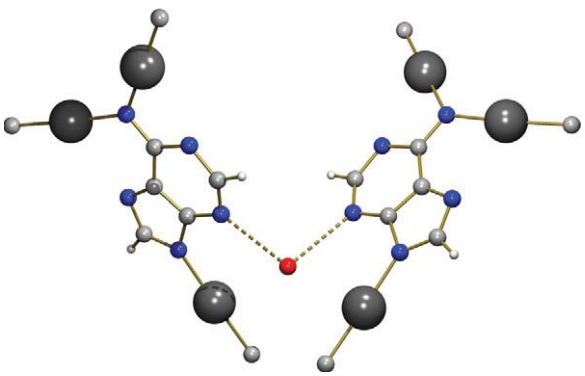

**Fig. 17.** Two complex molecules of $[(CH_3Hg)_3(\mu_3\text{-N6,N6,N9-ade-2H(N6)})]\cdot 0.5H_2O$ (CAVHIQ10 [87]). The full-deprotonation of adenine is shown in its anionic form $[ade\text{-}2H(N6)]^{3-}$ and its connection in the crystal by two (water)O–H···N3 interactions (O···N3 2.758 Å).

**Table 9**
Metal binding patterns (MBP) of 9-methyl-hypoxanthine (9-Me-hyp).

| MBP | CSD code | Metal | Ref. |
|---|---|---|---|
| M–N7[9-Me-hyp] | DALXIX | $Pt^{II}$ | [102] |
| | EQIYEI | $Pt^{II}$ | [103] |
| | MHPCHG | $Hg^{II}$ | [104] |
| | OHABUV | $Pt^{II}$ | [105] |
| | PAGQAQ | $Pt^{II}$ | [106] |
| | PEWSEP | $Os^{III}$ | [107] |
| | TUWTOU | $Pt^{II}$ | [108] |
| | TUWTUA | $Pt^{II}$ | [108] |
| | WERYOH | $Pt^{II}$ | [109] |
| | WERZEY | $Pt^{II}$ | [109] |
| | WERZIC | $Pt^{II}$ | [109] |
| | XINRAN | $Pt^{II}$ | [110] |
| M–N7[9-Me-hyp]$_2$ | BOTHAT | $Pt^{II}$ | [111] |
| | CEZBUE | $Ag^{I}$ | [112] |
| | CUHYPX10 | $Cu^{II}$ | [113] |
| | MHPXAG | $Ag^{I}$ | [114] |
| | TAHYPC | $Cu^{II}$ | [115] |
| | TUWTIO | $Pt^{II}$ | [108] |
| M–N7[9-Me-hyp]$_4$ | TAMVUZ | $Pt^{II}$ | [116] |
| M–N1[9-Me-hyp] | OHABOP | $Pt^{II}$ | [105] |
| $M_2(\mu_2$-N7,N9)[9Me-hyp] | TYMHGE | $Ag^{I}$ | [117] |
| $M_2$-($\mu_2$-[O6($Cu^{II}$),N7($Pt^{II}$)])[9Me-hyp] | TAMWAG | $Cu^{II}$, $Pt^{II}$ | [116] |

(keto) form. For this reason either Hhyp or its analogues are referred to as 6-oxo-purines. Two polymorphs of Hhyp, are reported GEBTUC [88] (triclinic system, space group P-1) and GEBTUC01 [89] (monoclinic system, space group $P2_1/c$). The keto form of Hhyp is tied to the presence of a proton bonded to N1. Henceforth, we will refer to the most stable tautomer of hypoxanthine as H(N9)hyp. The high stability of this tautomer means that the hydrogen of N1 does not dissociate in any of the hypoxanthine complexes. Nevertheless, this cannot be applied to 9-methyl-hypoxanthine (see OHABOP in Table 9). This circumstance strongly suggests a restriction in the tautomeric possibilities, which are limited to the shift of the proton associated with N9 in the free nucleobase.

Structures of simple salts of the hypoxanthinium(1+) cation are known, that have as counter-anion nitrate (BONKOE [90], BONKOE01 [91]), chloride (HYPXCL [92]) or tetrachloroaurate(1−) (HYPXAM [93]). These salts have in common the $H_2$(N7,N9)$hyp^+$ cation. On this basis, the basicity order of the N-donor atoms for hypoxanthine agrees with N9 > N7 > N3.

### 3.1. Neutral hypoxanthine complexes

The currently available information in CSD reveals the crystalline structure of complexes having unidentate and bridging bidentate hypoxanthine (Table 7) with soft ($Cd^{II}$) or borderline (first-row $M^{II}$ ions or $Ru^{III}$) Pearson acids.

The unidentate role of hypoxanthine is known for $[Ru^{III}(NH_3)_5$(H(N9)hyp)]$Cl_3\cdot 3H_2O$ (BAKDOG [94]). In this compound, hypoxanthine binds the metal by its N7 atom. The coordination bond Ru–N7 cooperates with two amine ligands by means of two symmetry related intra-molecular N–H···O6 interactions (2.882 Å). The structure of two compounds $[M^{II}(H_2O)_5$(H(N9)hyp)]$SO_4$ ($M^{II}$ = Co (FIZHUR [95]) or Ni (FIZJAZ [95], FIZJAZ10 [96]), Fig. 18) reveals the coordination of the nucleobase via N7 with an intra-molecular H-bond (aqua)O–H···O6 (2.758 Å and 145.68° in FIZJAZ10).

The compounds here referred to, reveal a common molecular recognition: the M–N7 coordination bond reinforced by an intra-molecular H-bonding interaction. Keeping that in mind, we have carried out a broad structural study concerning ternary complexes synthesized by reaction of metal(II)–iminodiacetate-like ligands and Hhyp [97]. The main contribution of this study comprises four groups of compounds:

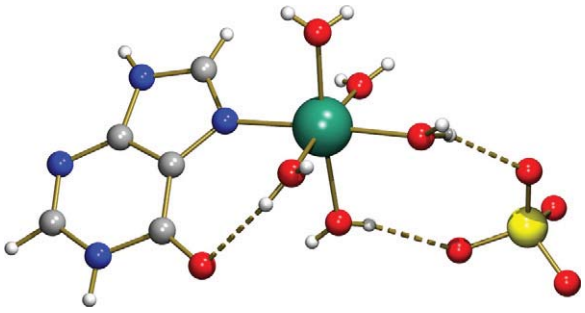

**Fig. 18.** Structure of $[Ni(H_2O)_5$(H(N9)hyp)]$SO_4$ (FIZJAZ10 [96]). One aqua ligand cooperates with the Ni–N7 bond through an inter-ligand H-bond (2.758 Å, 145.68°). Two other cis-aqua ligands are connected with the sulfate anion by two unequal (aqua)O–H···O(sulfate) cation–anion interactions (2.696 Å, 155.26°; 2.772 Å, 165.72°).

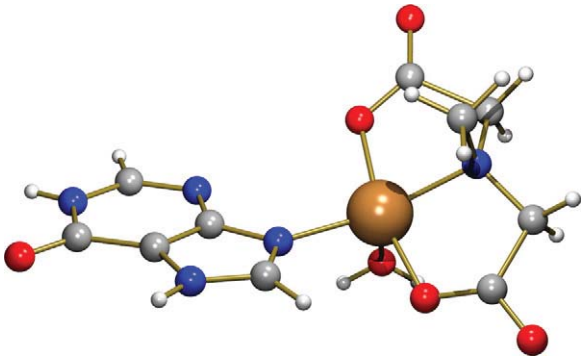

**Fig. 19.** Structure of the complex molecule in [Cu(MIDA)(H(N7)hyp)($H_2O$)]·$H_2O$ [97] where the Cu–N9 bond is not H-bonding reinforced. The Cu–N9(H(N7)hyp) metal binding pattern seems related to the mer-$NO_2$ conformation in the iminiodiacetate moiety of the MIDA chelator.

(1) Eight compounds contain Cu(II) having iminodiacetate (IDA) or N-R-IDA-like chelating ligands and hypoxanthine. These compounds have molecular or polymeric structures. A good example is shown in Fig. 19. All exhibit the Cu–N9 bond and the tautomer H(N7)hyp. Consequently, the coordination bond Cu–N9 is not reinforced by any intra-molecular inter-ligand H-bonding interaction. In these compounds, the chelating ligand exhibits a mer-$NO_2$ conformation in a five-coordination polyhedron type 4 + 1. The Cu–N9 bond is *trans* to the Cu–N(IDA-like) bond. The apical donor atom is supplied by an aqua ligand or an O-carboxylate atom (in polymers).
(2) Eight compounds have the general formula $[M^{II}$(N-benzyl-IDA-like)(H(N9)hyp)($H_2O)_2$]·$H_2O$ ($M^{II}$ = Co or Ni). The common structural features of these compounds are depicted in Fig. 20.

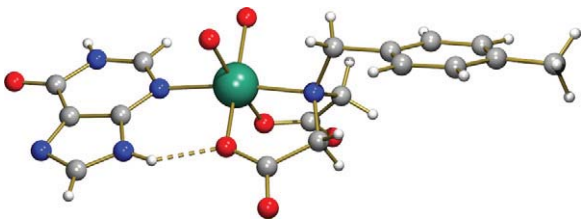

**Fig. 20.** Structure of the complex molecule in [Ni(NBzIDA)(H(N9)hyp)($H_2O)_2$]·$H_2O$ [97] where the Cu-N3 bond is assisted by the intra-molecular inter-ligand N9–H···O(coord. carboxylate) interaction. This (coordination + H-bond) metal binding pattern seems related to the fac-$NO_2$ conformation in the iminodiacetate moiety of NBzIDA-like chelators.

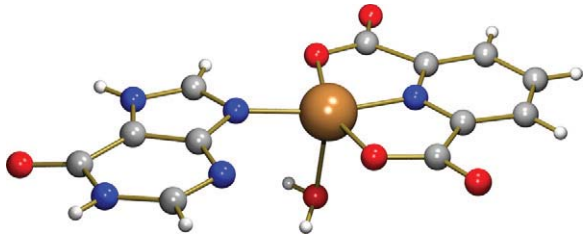

**Fig. 21.** Structure of the complex molecule [Cu(2,6-pdc)(H(N7)hyp)($H_2O$)] [97]. In this case, the rigid 2,6-pdc chelating ligand imposes the mer-$NO_2$ conformation. Hence, the single Cu–N9(H(N7)hyp) metal binding pattern is observed.

In these compounds, hypoxanthine exists as its most stable tautomer and the M–N3 bond is assisted by an intra-molecular inter-ligand H-bond N9–H···O(coord. IDA-like). All these compounds exhibit the expected octahedral coordination and the IDA moiety of the chelating ligand adopts a fac-$NO_2$ conformation. Again, the M–N3 bond is *trans* to the M–N(IDA-like) bond.

(3) In order to clarify if there is a correlation between the metal binding pattern of Hhyp and the IDA moiety conformation, four ternary compounds were synthesized using the rigid planar chelating ligand pyridine-2,6-dicarboxylate(2−) (2,6-pdc): [Cu(2,6-pdc)(H(N7)hyp)($H_2O$)] (Fig. 21), [Co(2,6-pdc)(H(N7)hyp)($H_2O$)$_2$]·$H_2O$, [$M^{II}$(2,6-pdc)(H(N7)hyp)($H_2O$)$_2$] ($M^{II}$ = Ni or Zn, Fig. 22). The rigid planar 2,6-pdc chelating ligand imposes a mer-$NO_2$ conformation, hence all compounds display a $M^{II}$–N9 binding pattern. The copper(II) compound exhibits a 4 + 1 coordination whereas the other compounds show an octahedral coordination. Thus the molecular recognition M–N9(H(N7)hyp) should be related to the mer-$NO_2$ IDA-like chelating conformation whereas a fac-$NO_2$ chelating conformation would promote the coordination of Hhyp by its less basic N3 donor atom assisted by an intra-molecular H-bonding interaction.

(4) In order to discern if the referred pathway is restricted to the use of IDA-like ligands, the compound [Cu(tda)(H(N7)hyp)($H_2O$)]·2$H_2O$ (Fig. 23) was synthesized. In this compound, the Cu(II) exhibits a 4 + 1 coordination. The thiodiacetate ligand (tda) adopts a fac-SO + O(apical) conformation whereas hypoxanthine and the aqua ligand act as unidentate basal ligands. Thus, the presence of the fac-SO + O(apical) conformation in tda does not lead to the Cu–N3(Hhyp) bond (supported by an H-bond). This fact addresses the idea that the behaviour of tda is far from the correlation established by the ternary complexes having IDA or IDA-like chelating ligands.

The polymeric compound [Cu($\mu_2$-N3,N7[H(N9)hyp])($H_2O$)($\mu_2$-$SO_4$)]$_n$ (FIZHOL [95]) is a unique example with neutral hypoxanthine as a bridging ligand using its most stable tautomer (Table 7). Alternatively, the tautomer H(N7)hyp has also been described for the bridging $\mu_2$-N3,N9 role. Four bridges of this latter type are found in the compound [Cu($\mu_2$-N3,N9[H(N7)hyp])$_4$$Cl_2$]·6$H_2O$ (HPURCU [98]). In this compound, the Cu···Cu distance is 3.024 Å, a bit longer than the corresponding inter-metallic distance in related dinuclear cores with adenine ligands. Moreover, four isotype crystals have the general formula [$M^{II}$($\mu_2$-N3,N9[H(N7)hyp])$_2$($\mu_2$-$H_2O$)$_2$($H_2O$)$_2$($SO_4$)$_2$] ($M^{II}$ = Cu (JESLAU [99]), Zn (JESLIC [99]), Cd (JESLEY [99]) or Co (KOXPOC [100]), Fig. 24).

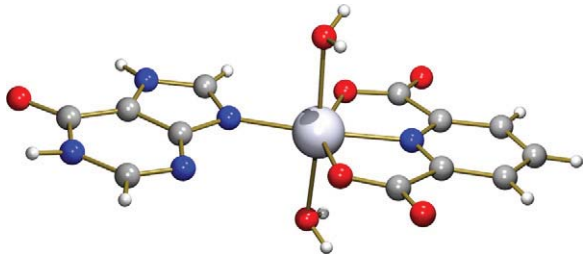

**Fig. 22.** Structure of the complex molecule [Zn(2,6-pdc)(H(N9)hyp)($H_2O$)$_2$] [97]. In this octahedral complex, where once more the rigid pdc chelating ligand imposes the mer-$NO_2$ conformation, the single Cu–N(H(N9)hyp) metal binding pattern is observed.

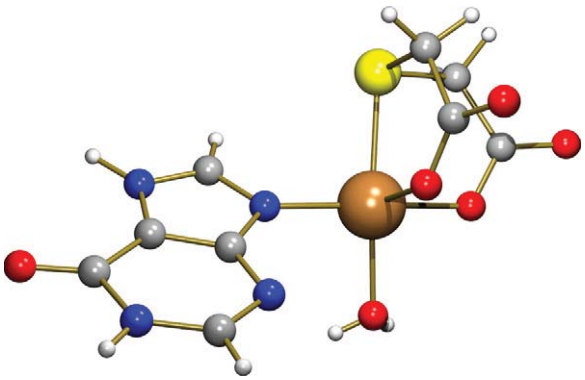

**Fig. 23.** Molecular structure of the complex in [Cu(tda)(H(N7)hyp)($H_2O$)]·2$H_2O$ [97]. The thiodiacetate ligand (tda) exhibits the unusual fac-SO + O(apical) conformation. The metal binding pattern of H(N7)hyp employs the Cu–N9 bond. The correlation 'chelating IDA-like ligand conformation/metal binding pattern of hypoxanthine' cannot be applied to this compound.

### 3.2. *Hypoxanthinium(1+) or hypoxanthinate(1−) complexes*

Besides the compound ($H_2$(N7,N9)hyp)[$AuCl_4$]·2$H_2O$ (HYPXAM [93]), that can be considered an outer-sphere hypoxanthinium(1+) complex, the structure of the mixed–ligand complex [$Ru^{III}$($H_2$(N7,N9)hyp)$Cl_4$(S-dmso)]·1.72$H_2O$ (NAVSIN [101]), Fig. 25, has been described (Table 8). In this complex, the Ru–N3 bond is reinforced by a symmetrical bifurcated H-bonding interaction, involving N9–H and two chloride ligands (3.190 Å, 117.59°).

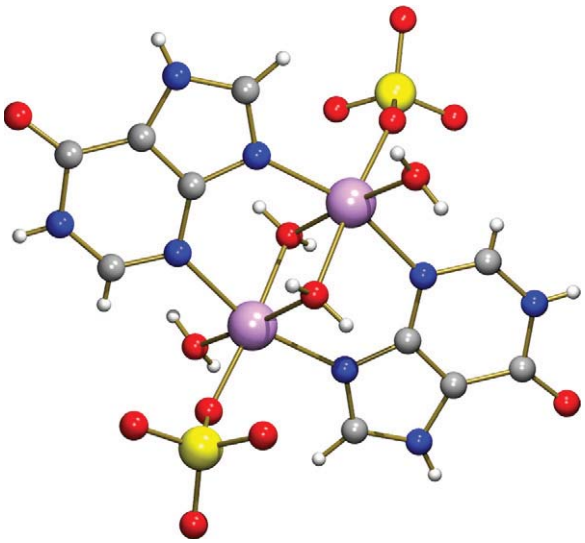

**Fig. 24.** Structure of the binuclear complex molecule [$Co_2$($\mu_2$-N3,N9-H(N7)hyp)$_2$($\mu_2$-$H_2O$)$_2$($H_2O$)$_2$($SO_4$)$_2$] (KOXPOC [100]). The $Co^{II}$···$Co^{II}$ distance in this compound is 3.124 Å.

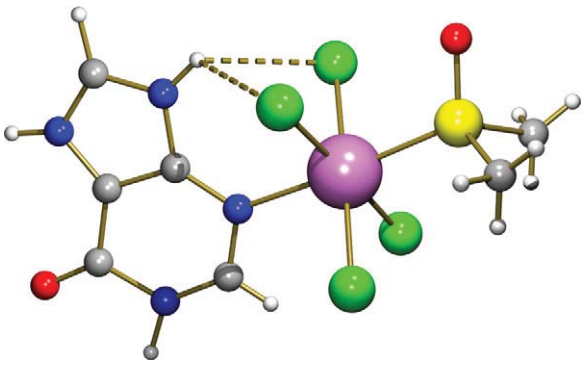

**Fig. 25.** Structure of the complex $[Ru^{III}(H_2(N7,N9)hyp)Cl_4(S\text{-}dmso)]\cdot 1.72H_2O$ (NAVSIN [101]) where the Ru–N3 bond cooperates with a symmetrical bifurcated H-bonding interaction, N9–H···$(Cl)_2$ (3.190 Å, 117.59°).

Examples are also reported where the hypoxanthinante(1−) anion acts as an unidentate, M–N9, or bridging $M_2(\mu_2$-N7,N9) ligand (Table 8). The metal centres of these compounds are borderline Pearson acids ($Ru^{III}$ or $M^{II}$ first-row transition metal ion) or the soft $Cd^{II}$ atom (XORBAI [65]). The unidentate coordination of the hypoxanthinate(1−) ligand is accomplished by its most basic donor N9. In the ternary compound WULXIK [64], the bond Zn–N9(hyp) cannot be assisted by any hydrogen bond whereas in the compounds NILPII [16] or XOQZUZ [65], where the metal is chelated by the tripodal tetradentate amine tren, a terminal amino group reinforces the coordination M–N9 with a H-bond N–H···N3. The distance N···N3 is 3.086 Å (XOQZUZ) or 3.167 Å (NILPII). The bridging mode $\mu_2$-N7,N9-hyp has been determined for a $Ru^{III}$ compound (XEDMUO [78]) and for ternary complexes of first-row transition metal ions having the amine tren (MIQWAK [61], NILPEE [16], NILPOO [16]) or cyclen (PUNREW [62], Fig. 26). In this latter compound, the bonds Cu–N7 and Cu–N9 are supported by inter-ligand H-bonding interactions with O6 and N3 atoms of Hhyp acting as acceptors (N–H···O6 3.01 Å and N–H···N3 3.16 Å). An interesting feature of this compound is that each cyclen ligand satisfies the four closest coordination sites to the metal (2.014–2.041 or 2.004–2.042 Å). Thus the bond Cu–N7 (2.111 Å) and Cu–N9 (2.096 Å) corresponds to the apical/distal coordination site of the corresponding Cu(II) centres. Nevertheless, the bonds Cu–N7 and Cu–N9 are relatively short which can be attributed to the anionic nature of the hypoxanthinate(1−) ligand.

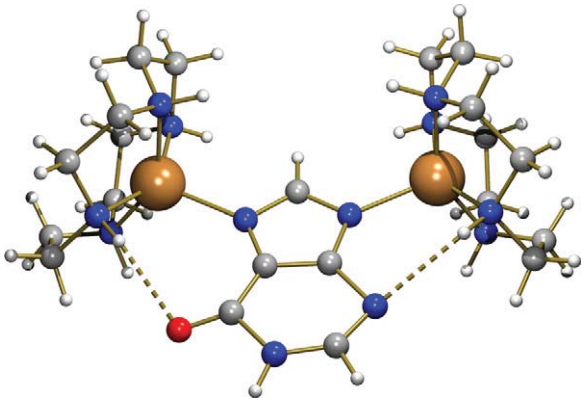

**Fig. 26.** Structure of the binuclear complex cation of $[Cu_2(\mu_2$-N7,N9-hyp)$(cyclen)_2](ClO_4)_3$ (PUNREW [62]). N-donors of hyp ligand occupy apical sites in the 4+1 copper(II) coordination polyhedron. The Cu–N7 (2.111 Å) and Cu–N9 (2.096 Å) bonds cooperate with intra-molecular inter-ligand interactions (aqua)O–H···O6 and (aqua)O–H···N3, respectively.

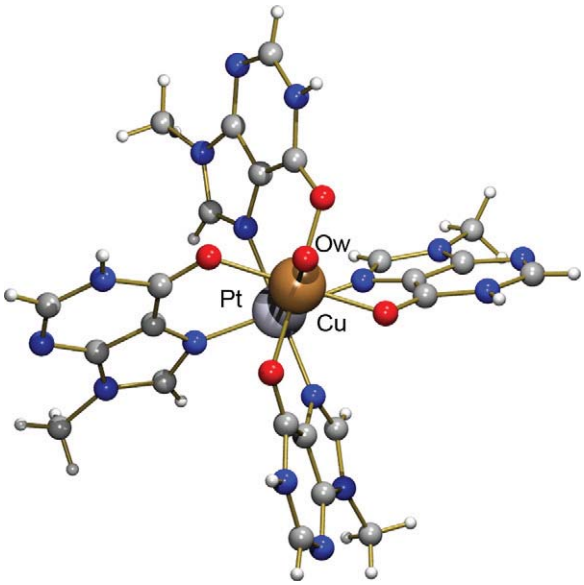


**Fig. 27.** Structure of the hetero-bimetallic complex cation of $[Pt^{II}(\mu_2$-O6,N7-(9-Me-hyp))$_4Cu^{II}(H_2O)][Cu(ClO_4)_4](NO_3)(ClO_4)\cdot 12H_2O$ (TAMWAG [116]). The $Pt^{II}$ atom has a square planar coordination (Pt–N7) 2.002–2.020 Å. The borderline $Cu^{II}$ atom displays a 4+1 coordination (with four Cu–O6 bonds (1.958–1.980 Å)) and one apical Cu–OW bond (2.290 Å). The rather short inter-metallic Pt···Cu distance is 2.792 Å.

## 4. Metal complexes with different N-methyl-hypoxanthines

In contrast to the scarce information about hypoxanthine, numerous complexes concerning 9-methyl-hypoxanthine (9-Me-hyp) are known. The use of 9-substituted purine ligands has been promoted by their relative similarity with 9-substituted-purine bioligands.

### 4.1. 9-Methyl-hypoxanthine complexes

Table 9 includes examples with one, two or four 9-Me-hyp ligands per metal centre. Some of these complexes are bimetallic (WERYOH [109], TAMWAG [116]). Some other compounds present different purine ligands (WERZEY [109], WERZIC [109], WERYOH [109], XINRAN [110]) or pyrimidine ligands (TUWTIO [108]) besides 9-Me-hyp. The metal centres are usually soft Pearson acids although some complexes have Cu(II), a typical borderline Pearson acid.

Among the complexes shown in Table 9 there is the crystal OHABOP [105], an organometallic complex having a bidentate chelating N,C-(dimethyl-benzyl)-amine as well as a triphenylphosphine and one 9-Me-hyp linked to the metal by the Pt–N1 bond. A particularly interesting bimetallic compound is TAMWAG [116], which contains the $[Pt^{II}(\mu_2$-O6,N7-(9-Me-hyp))$_4Cu^{II}(H_2O)]^{4+}$ cation (Fig. 27) and $NO_3^-$, $ClO_4^-$ and $[Cu(ClO_4)_4]^-$ as counter-anions according to the formula $[Pt^{II}(\mu_2$-O6,N7-(9-Me-hyp))$_4Cu^{II}(H_2O)]_2[Cu(ClO_4)](NO_3)_4(ClO_4)\cdot 12H_2O$. In the complex cation, the soft $Pt^{II}$ atom exhibits a square planar coordination built by the N7 donor atoms of four 9-Me-hyp ligands (Pt–N7(9-Me-hyp) 2.002–2.020 Å), whereas the borderline $Cu^{II}$ atom displays a 4+1 coordination where the O6 donor of the four referred 9-Me-hyp ligands are the four closest donors (Cu–O6(9-Me-hyp) 1.958–1.980 Å) and one aqua ligand is moved to the apical/distal coordination site (Cu–OW 2.290 Å). The inter-metallic Pt···Cu distance is 2.792 Å.

In addition to those compounds summarized in Table 9, with neutral 9-Me-hyp as ligand, the structures for two interesting compounds (ZAPROX [118] and XINRER [110]) are known where the anion 9-methyl-hypoxanthinate(1−) (9-Me-hyp-$H^-$) is bonded

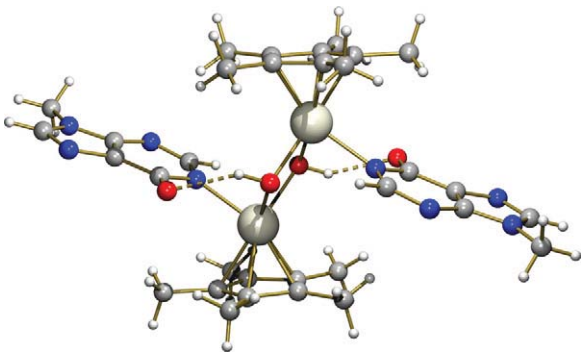

**Fig. 28.** Structure of the binuclear complex $[Rh^{III}(\mu_2\text{-OH})(9\text{-Me-hyp})(\eta_5\text{-Me}_5\text{-cp})]_2\cdot 8H_2O$ (ZAPROX [118]). The Rh–N1 bond distance is 2.148 Å. The Rh–N1 bond cooperates with intra-molecular inter-ligand interactions O–H···O6 (2.759 Å, 140.37°). The Rh···Rh separation is 3.309 Å.

to a metal ion. ZAPROX [118] is a binuclear $Rh^{III}$ organometallic compound with the 9-Me-hyp-H(N1)$^-$ anion bonded to the metal via N1 (Fig. 28). The centro-symmetric dinuclear entity is built up by a central moiety $Rh_2(\mu_2\text{-OH})_2$, with Rh–O distances of 2.120 and 2.136 Å. The Rh–N1 bond distance is 2.148 Å. Noteworthy, the Rh–N1 bond cooperates with intra-molecular inter-ligand interactions O–H···O6 (2.759 Å, 140.37°) in the metal binding pattern displayed in this compound. On the other hand, XINRER [110] is a bimetallic polymer where the anion 9-Me-hyp-H(N1)$^-$ acts as a $\mu_3$-bridge between two $Ag^I$ atoms and one $Pt^{II}$ atom (Fig. 29). The bridging ligand displays the metal binding pattern $\mu_3$-[N1(Ag),N3(Ag),N7(Pt)]. This compound has also 9-methyl-adenine as ligand. Each $Ag^+$ ion is coordinated by a pair of N1 atoms (one from 9-Me-hyp-H(N1)$^-$ anion, the other from 9-Me-ade) or a pair of N3 atoms from two 9-Me-hyp-H(N1)$^-$ anions. The $Pt^{II}$ atom exhibits a *trans*-square planar coordination built by two amino ligands and two N7 atoms from two different 9-Me-hyp-H(N1)$^-$ anions. ZAPROX and XINRER have in common the presence of the metal-N1 bond, a feature that has been not determined for neutral Hhyp ligands. The formation of the metal–N1 bond has been also reported for a trinuclear organometallic Rh(III) compound (ZAPRIR [118]) where the [9-ethyl-hypoxantinate-H(N1)](1−) anion acts in the 'chelating + bridging' mode $\mu_2$-[N7 + O6,N1]. Compounds such as XINRER or ZAPRIR demonstrate that a borderline metal ion (as Rh(III) [119]) can promote the ionization of the N1–H bond in 9-alkyl-hypoxanthines.

### 4.2. Other N-methyl-hypoxanthine complexes

Apart from the structural information referred to in complexes with neutral 9-Me-hyp or anionic 9-Me-hyp-H(N1)$^-$, relevant complementary data about other N-methyl-hypoxanthine complexes are also reported. The structure of only one compound having 7-methyl-hypoxanthine (7-Me-hyp), has been determined, which has the formula $[Ru^{III}(7\text{-Me-hyp})(NH_3)_5]Cl_3$ (BAKDUM [94]). This structure reveals the formation of a coordination bond Ru–N9. The N3 atom of 7-Me-hyp is equidistant (3.112 Å) from two N-amino ligands, however the existence of reinforcement by an intra-molecular inter-ligand interaction is quite unclear. Structural information is also available for the zwitterionic form of the 7,9-dimethyl-hypoxanthinium(1+) cation, the structure of the salt (7,9-DM-hyp)I (KATGUI [120]) having been reported The dissociation of the proton on N1 yields to the zwitterionic species $[(7,9\text{-DM-hyp})\text{-H(N1)}]^{\pm}$. Four more complexes are described in the literature with the aforementioned zwitterionic species with the soft $Pt^{II}$ metal ion (BOBJOR [121], ENXPTA10 [122] and ENX-

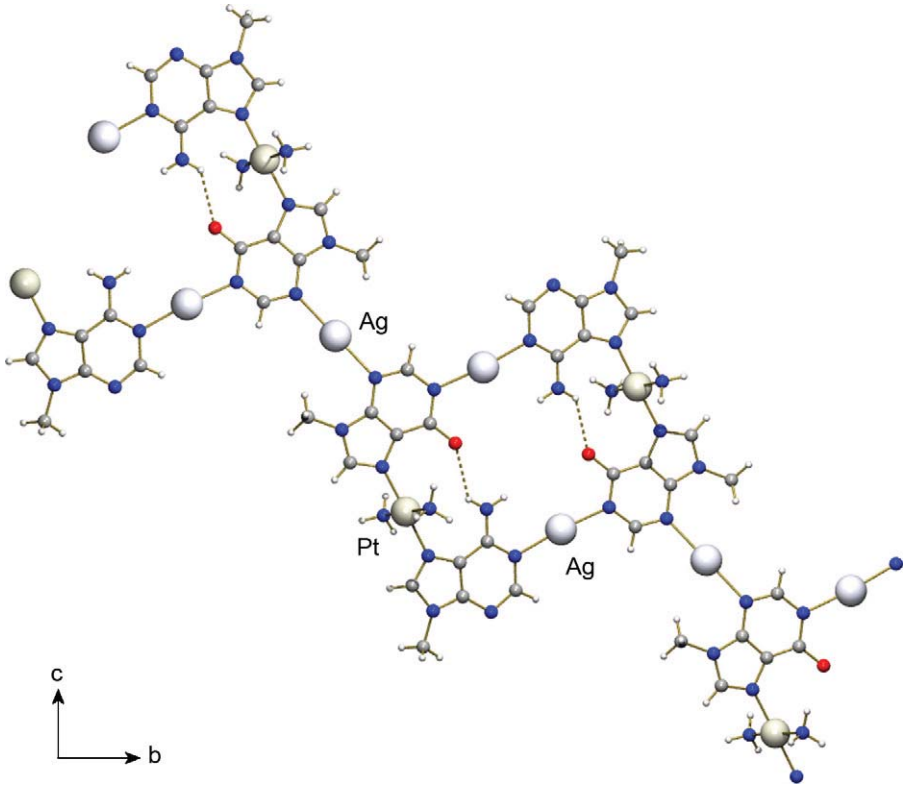


**Fig. 29.** Fragment of the bimetallic polymer $\{[Pt^{II}_2Ag^{I}_3(\mu_3\text{-N1(Ag),N3(Ag),N7(Pt)-Me-hyp-H(N1)})_2(\mu_2\text{-N1(Ag),N7(Pt)-9-Me-ade})_2](NO_3)_5\cdot 7H_2O\}$ (XINRER [110]). Nitrate ions and water molecules omitted for clarity. Each *trans*-$Pt(NH_3)_2$ moiety is linked to two N7 donors of both purine ligands. Each Ag atom is bonded to two N1 of such purine ligands or two N3 atoms of two adjacent 9-Me-hyp ligands. The purine ligands linked to the same Pt atom are further connected by an intra-molecular inter-ligand H-bond (3.036 Å, 134.11°).

**Table 10**
Metal binding patterns (MBP) of xanthine (Hxan) and two different xanthinate anions.

| MBP | CSD code | Metal | Ref. |
|---|---|---|---|
| M–N9[H(N7)xan] | YAHRUU | $Cu^{II}$ | [127] |
| | YAHSAB | $Cu^{II}$ | [127] |
| | YAHSEF | $Zn^{II}$ | [127] |
| M–N9[xan] | MGXABC | $Co^{III}$ | [128] |
| M–N7[xan] | RAGDAE | $Zn^{II}$ | [129] |
| | SOPNOB | $Zn^{II}$ | [130] |
| | SOPNUH | $Cd^{II}$ | [130] |
| | SOPPAP | $Ni^{II}$ | [130] |
| | WULYAD | $Zn^{II}$ | [131] |
| | PUNROG | $Cu^{II}$ | [62] |
| $M_2(\mu_2$-N3,N9)[xan-H]$^{2-}$ | TEZLUF | $Au^{I}$ | [132] |
| $M_3(\mu_3$-N3,N7,N9)[xan-H]$^{2-}$ | CUMJAV | $Hg^{II}$ | [133] |
| $M_2(\mu_2$-N3,N9) + $M_3(\mu_3$-N3,N7,N9)[xan-H]$^{2-}$ | SOPPET | $Cu^{II}$ | [130] |
| $M_4(\mu_4$-N1,N3,N7,N9)[xan-2H]$^{3-}$ | CUMJEZ | $Hg^{II}$ | [133] |

PTB10 [123]) or the borderline $Cu^{II}$ Pearson acid (GLHXCU10 [124]). These compounds are all mixed-ligand metal complexes with one (GLHXCU10) or two (others) [(7,9-DM-hyp)-H(N1)]$^{\pm}$ ligands per metal ion. As expected, all these compounds have the M–N1 coordination bond. In ENXPTA10 [122] and ENXPTB10 [123] there is a cooperative effect of these coordination bonds and one (amino)N–H···O6 inter-ligand interaction (2.946 Å, 128.20° for ENXPTA10; N···O6 2.893 Å in ENXPTB10).

## 5. Xanthine metal complexes

There is no information about the crystalline structure of xanthine (Hxan). Two structures of its salts are known with $Li^{I}$ (XEGDOC [125]) and $Na^{I}$ (NAXATI [126]). Some structural information is available about complexes having neutral Hxan or two anionic xanthinate forms as ligands (Table 10).

### 5.1. Neutral xanthine complexes

Structural data are available for compounds having $Cu^{II}$ or $Zn^{II}$ and Hxan. In YAHSAB [127] and YAHSEF [127] the xanthine is coordinated by its most basic donor atom (N9) as the tautomer H(N7)xan. The centro-symmetric compound *trans*-[$Cu(H(N7)xan)_2(H_2O)_2(NO_3)_2$] (YAHRUU [127], Fig. 30) shows the cooperation of each Cu–N9(Hxan) bond with inter-ligand interactions N3–H···O(nitrate, apical; 2.741 Å, 149.09°). The reason why neutral xanthine coordinates only by N9 remains still unclear.

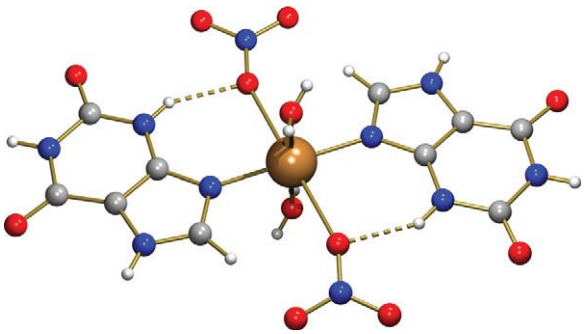

**Fig. 30.** Structure of the centro-symmetric complex molecule *trans*-[$Cu(H(N7)xan)_2(H_2O)_2(NO_3)_2$] (YAHRUU [127]) where each Cu–N9(Hxan) bond is assisted by an intra-molecular inter-ligand interaction N3–H···O(nitrate, apical; 2.741 Å, 149.09°).

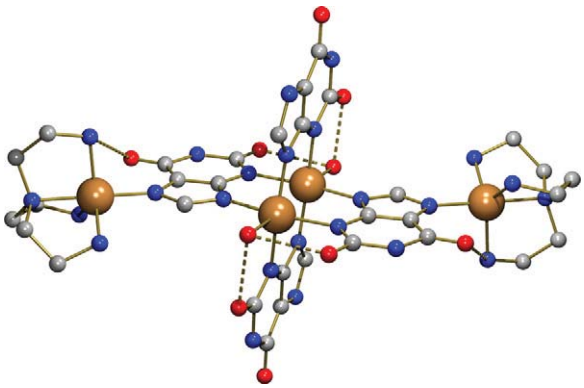

**Fig. 31.** Structure of the trinuclear complex molecule in [{Cu(tren)}$_2$Cu$_2$($\mu_2$-N3,N9-xan-H)$_2$($\mu_3$-N3,N7,N9-xan-H)$_2$($H_2O$)$_2$]·10$H_2O$ (SOPPET [130]) where the anion [xan-H(N3)]$^{2-}$ displays two different bridging modes. H-atoms omitted for clarity. The molecule can be looked upon as the expansion of a central core [Cu$_2$($\mu_2$-N3,N9-xan-H(N3))$_4$($H_2O$)$_2$] linked to two Cu(tren) moieties via N7 atoms of two *trans*-xanthinate(2−) anions. This latter coordination bond is reinforced by an intra-molecular inter-ligand interaction (tren)N···O6 (2.874 Å). Additional inter-ligand H-bonds in the central core are also depicted OW···O6 (2.648 Å and 2.644 Å).

### 5.2. Xanthinate(1−) or xanthinate(2−) complexes

The dissociation of the proton (supposed on N9 for neutral xanthine) yields the anion xanthinate(1−). This anion acts as N9 donor atom in a $Co^{III}$ complex (MGXABC [128]). There are six compounds known with borderline ($Zn^{II}$, $Ni^{II}$ or $Cu^{II}$) or soft ($Cd^{II}$) Pearson acids. In PUNROG [62] [Cu(cyclen)(xan)]$ClO_4$·4.5$H_2O$, the metal exhibits a rather common 4 + 1 coordination. The four closest donor atoms are supplied by cyclen whereas the Cu–N7(xan) is the longest bond (2.156 Å) which cooperates in the metal binding pattern with an intra-molecular H-bonding interaction (2.893 Å). Table 10 shows three compounds where the divalent anion [xan-H(N3)]$^{2-}$ acts as bridging ligand between two or three metal centres. These compounds have soft ($Au^{I}$, $Hg^{II}$) or borderline ($Cu^{II}$) metal ions. The tridentate and tetradentate bridging modes are known only for methyl-mercury(II) derivatives. In the Cu(II) complex SOPPET [130] (Fig. 31), bidentate and tridentate bridging modes are shown according to the formula [{Cu(tren)}$_2$Cu$_2$($\mu_2$-N3,N9-xan-H)$_2$($\mu_3$-N3,N7,N9-xan-H)$_2$($H_2O$)$_2$]·10$H_2O$. The centro-symmetric tetranuclear molecule can be understood as a consequence of the controlled expansion of the central core [Cu$_2$($\mu_2$-N3,N9-xan-H)$_2$($\mu_3$-N3,N7,N9-xan-H)$_2$($H_2O$)$_2$] by addition of two $Cu^{II}$(tren) moieties via N7(xan-H) atom. All $Cu^{II}$-N(xan-H) bonds are close to 2 Å. The internal stability of the core is reinforced by four H-bonding interactions assisted by the apical aqua ligands and the O2 atom of two xan-H ligands (OW···O2 2.648 Å or 2.644 Å). The expansion of the core shows that each Cu–N7 bond cooperates with an inter-ligand H-bonding interaction (tren)N···O6 (2.874 Å). This tetranuclear molecule defines a half-way expansion with respect to what was previously described for the hexanuclear molecule PECNUH [5,71].

## 6. Latest developments

During the review process of this work, some developments have been published [134–141]. The essential contribution of these papers is summarized in the following. The outer-sphere complex ($H_2$ade)$_3$[$AlF_6$]·6.5$H_2O$ [134] exhibits the tautomers $H_2$(N1,N9)ade$^+$ and $H_2$(N3,N7)ade$^+$ in the same crystal as previously reported in two related compounds [23]. In the polymer {[Cd($\mu_2$-ox)($H_2O$)(H(N7)ade)]·$H_2O$}$_n$ [135], the Cd–N3 bond is assisted by the (aqua)O–H···N9 interaction. The formation of the metal–N3[H(N9)ade] bond has been previously described in

Table 2 for divalent metal ions (Co, Cu, Zn, Pd); however, the novel compound stabilises the H(N7)ade tautomer. The presence of this tautomer seems to be tied to the H-bond that involves N9 as acceptor. The complex $[Ag_2(\mu_2\text{-N3,N9-H}_2\text{(N1,N7)ade})_2(NO_3)_4]$ [136] represents a novel example of inner-compounds with the adeninium(1+) cation, as referred to in Table 1. Three porous MOFs based on adenine have been reported [137–139]. The compounds $\{[Co_2(\mu_2\text{-N3,N7,N9-ade})_2(\mu_2\text{-acetate})_2]\cdot 2DMF\cdot H_2O\}_n$ [137] and $[Ni_3(\mu_2\text{-pzdc})_2(\mu_2\text{-N3,N9-H(N7)ade})_2(H_2O)_4]\cdot 2.18H_2O$ [138] demonstrate good and selective $CO_2$ uptake. The MOF $[Cu_2(\mu_2\text{-N3,N9-H(N7)ade})_4Cl_2]Cl_2\cdot\sim 2CH_3OH$ [139] is able to host different guest molecules within 1D channels of ~ 6 Å diameter. Recently, a MOF based on hypoxanthine has been proposed, with formula $\{[Cu_4(\mu_2\text{-N7,O6-H(N9)hyp})(H_2O)(btec)_2]\cdot 3H_2O\}_n$. This compound is a 3D polymer that displays long range ferromagnetic ordering at long temperatures and exhibits a novel bridging mode of hypoxanthine involving the exocyclic O6-atom [140]. The synthesis and applicability of this MOF has been recorded in a patent (Bibliographic Espacenet data: CN 101857604 (A)). The crystal structure of the salt $H_2$(N7,N9)xan $[ClO_4]$ has also been reported [141].

## 7. Concluding remarks and perspectives for future studies

A detailed analysis of the metal binding patterns of adenine (in cationic, neutral and anionic forms) reveals its unique versatility as a ligand. In addition, a detailed review has been carried out about the ligand behaviour of oxo-purines, mainly hypoxanthine, various methyl-hypoxanthine derivatives and xanthine. The structural information has been reviewed without restrictions of metal ions. This fact enables us to discuss some aspects regarding the hard, borderline or soft nature of diverse metal ions and donor atoms of the involved ligands. For each ligand, the metal binding pattern is addressed according to its connectivity within metallic centres and the implication of intra- and/or inter-molecular inter-ligand interaction. Furthermore, proton shift processes and tautomerism are considered. The overall available information reveals that:

(1) The oxo-purines have a restricted behaviour versus the unique versatility of adenine. This can be related to restrictions in the tautomeric possibilities of the N1–H bond of Hhyp or N1–H and N3–H bonds in Hxan.
(2) Proton tautomerism is a relevant and versatile phenomenon. For instance, the unusual H(N7)adenine tautomer acts as ligand or as solvate in coordination polymers or MOFs. More frequently, rare tautomers of adenine are encouraged to reach the most advantageous metal-binding patterns. These latter cases are observed in proton migrations from N(heterocyclic)-H and N(exocyclic)-H moieties.
(3) The anionic forms of these purine-like bioligands promote bridging roles and therefore tend to increase their connectivity. Currently, a large variety of bridging modes is described, including 'bidentate chelating + bridging' modes.
(4) In appropriate cases, the N–H bonds build N–H···A(acceptor) interactions. In addition, hydrogen-free N-heterocyclic or O-exocyclic atoms can play H-acceptor roles in inter-ligand H-bonding interactions. Frequently, such H-bonds cooperate with coordination bonds in the molecular recognition patterns observed for mixed-ligand metal complexes.
(5) π,π-Stacking is often observed in outer- and inner-sphere purine-metal complexes. Nevertheless, such interactions are missing in some cases, mostly in oligonuclear complexes where the metal–N(purine) bonds actively cooperate with inter-ligand H-bonds.
(6) According to the borderline behaviour of the heterocyclic N-donor atoms in purine ligands, most of the structures reviewed correspond to borderline or soft metal centres. Only a few complexes are reported with the hard Co(III) ion with Hade or $ade^-$ ligands.
(7) The softness of the metal centre favours the deprotonation of these purine-like ligands, in particular on the exocyclic N6-amino group of Hade or the N1–H group of 9-Me-hyp. Moreover, the deprotonation of the N3–H group has been demonstrated for a Cu(II)-xanthinate tetranuclear derivative.
(8) The N-heterocyclic purine-like donor atom usually binds the borderline Cu(II) atom occupying any of the four closest sites of the distorted coordination polyhedron. However, the use of rigid planar chelating ligands (such as two bidentate acetylacetonate ligands) or macrocycles (as cyclen) is able to move the N-heterocyclic donor atom of adenine or xanthinate ligands to apical/distal coordination sites.
(9) A relevant difference between adenine and the oxo-purines considered (with lactam nature) is that the exocyclic primary N6-amino group only binds soft metal centres after the appropriate proton migration or, more frequently, deprotonation. The O-exocyclic atom of oxo-purines is a rather hard Pearson base. Indeed, the O2–$Li^I$ ionic bond has been described in a $Li^I$–xanthinate(1−) salt. In absence of hard metal ions, a borderline Pearson acid is able to bind O-exocyclic donor atoms of oxo-purines. For instance, the O6 exocyclic atom binds a copper(II) centre without the dissociation of its N1–H in a complex of 9-methyl-hypoxanthine.

More recently, a family of coordination polymers $[Cu_2(\mu_3\text{-N3,N7,N9-ade})_2(\mu_2\text{-}CH_3(CH_2)_nCOO)_2]\cdot xH_2O$ (n = 0–5) has been reported containing micro-channels tailored by carboxylate ligands [142]. Only the crystal structures for n = 0 and n = 2 are described. The tunable permanent porosity of these guest-free MOFs is proved by N2 adsorption measurements.

## Acknowledgements

Financial support from Research Group FQM-283 (Junta de Andalucía) and MICINN-Spain (Project MAT2010-15594) is acknowledged. Structural support from the project "Factoría Española de Cristalización" **CONSOLIDER INGENIO-2010** is also acknowledged. D.K.P. thanks the University of Granada for his stay in Prof. Niclós-Gutiérrez's Research Group. ADM thanks ME-Spain for a FPU Ph.D. fellowship.

## References

[1] L.G. Marzilli, T.J. Kistenmacher, Acc. Chem. Res. 10 (1977) 146.
[2] B. Lippert, Coord. Chem. Rev. 200–202 (2000) 487.
[3] B. Lippert, in: K.D. Karlin (Ed.), Progress in Inorganic Chemistry, vol. 54, Wiley, 2005 (Chapter 6).
[4] A. Terrón, J.J. Fiol, A. García-Raso, M. Barceló-Oliver, V. Moreno, Coord. Chem. Rev. 251 (2007) 1973.
[5] D. Choquesillo-Lazarte, M.P. Brandi-Blanco, I. García-Santos, J.M. González-Pérez, A. Castiñeiras, J. Niclós-Gutiérrez, Coord. Chem. Rev. 252 (2008) 1241.
[6] P.J. Sanz Miguel, P. Amo-Ochoa, O. Castillo, A. Houlton, F. Zamora, in: N. Hadjiliadis, E. Sletten (Eds.), Metal Complex–DNA Interactions, Blackwell-Wiley, 2009 (Chapter 4).
[7] O. Castillo, A. Luque, J.P. García-Terán, P. Amo-Ochoa, in: A.S. Abd-El-Aziz, Ch.E. Carraher, Ch.U. Pittman, M. Zeldin (Eds.), Macromolecules Containing Metal and Metal-like Elements, vol. 9, Wiley, 2009 (Chapter 9).
[8] B. Lippert, N.V. Hud (Eds.), Nucleic Acid–Metal Ion Interactions, RSC Publishing, 2009 (Chapter 2).
[9] S. Verma, A.K. Mishra, J. Kumar, Acc. Chem. Res. 43 (2010) 79.
[10] S.M. Tret'yak, V.V. Mitkevich, L.F. Sukhodub, Kristallografiya 32 (1987) 1268 (in Russian).
[11] S. Mahapatra, S.K. Nayak, S.J. Prathapa, T.N.G. Row, Cryst. Growth Des. 8 (2008) 1223.
[12] J.P. García-Terán, O. Castillo, A. Luque, U. García-Couceiro, G. Beobide, P. Román, Dalton Trans. (2006) 902.

[13] S. Fujii, K. Kawasaki, A. Sato, T. Fujiwara, K.-I. Tomita, Arch. Biochem. Biophys. 181 (1977) 363.
[14] S. Chandrasekhar, T.R.R. Naik, S.K. Nayak, T.N.G. Row, Bioorg. Med. Chem. Lett. 20 (2010) 3530.
[15] V. Zelenak, Z. Vargova, I. Cisarova, Acta Crystallogr. E: Struct. Rep. Online 60 (2004) o742.
[16] K. Aoki, Md.A. Salam, C. Munakata, I. Fujisawa, Inorg. Chim. Acta 360 (2007) 3658.
[17] S. Bouacida, M. Hocine, A. Beghidja, C. Beghidja, Acta Crystallogr. E: Struct. Rep. Online E61 (2005) m1153.
[18] L. Zhi-Xian, T. Lian-Dong, H. Sheng-Zhi, J. Huaxue, Chin. J. Struct. Chem. 14 (1995) 423.
[19] M. Authier-Martin, A.L. Beauchamp, Can. J. Chem. 53 (1975) 2345.
[20] E. Serrano-Padial, D. Choquesillo-Lazarte, E. Bugella-Altamirano, A. Castiñeiras, R. Carballo, J. Niclós-Gutiérrez, Polyhedron 21 (2002) 1451.
[21] J.P. García-Terán, O. Castillo, A. Luque, U. García-Couceiro, G. Beobide, P. Roman, Inorg. Chem. 46 (2007) 3593.
[22] A. Castiñeiras, I. García-Santos, J.M. González-Pérez, J. Niclós-Gutiérrez, 9th European Biological Inorganic Chemistry Conference (EUROBIC 9) Medimond-International Proceedings, Bologna, Italia, 2008, pp. 135–140 (also available as private communication in CSD).
[23] S. Pérez-Yánez, O. Castillo, J. Cepeda, J.P. García-Terán, A. Luque, P. Roman, Eur. J. Inorg. Chem. (2009) 3889.
[24] B. Das, J.B. Baruah, Cryst. Growth Des. 10 (2010) 3242.
[25] B. Das, A.K. Boudalis, J.B. Baruah, Inorg. Chem. Commun. 13 (2010) 1244.
[26] M.R. Taylor, J.A. Westphalen, Acta Crystallogr. A: Cryst. Phys. Diffr. Theor. Crystallogr. 37 (1981) C63.
[27] P.T. Muthiah, S.K. Mazumdar, S. Chaudhuri, J. Inorg. Biochem. 19 (1983) 237.
[28] M.R. Taylor, Acta Crystallogr. B: Struct. Crystallogr. Cryst. Chem. B29 (1973) 884.
[29] M.R. Taylor, L.M. Vilkins, M.J. McCall, Acta Crystallogr. C: Cryst. Struct. Commun. C45 (1989) 1625.
[30] M.A. Salam, K. Aoki, Inorg. Chim. Acta 311 (2000) 15.
[31] P.d. Meester, A.C. Skapski, Dalton Trans. (1973) 424.
[32] D.B. Brown, J.W. Hall, H.M. Helis, E.G. Walton, D.J. Hodgson, W.E. Hatfield, Inorg. Chem. 16 (1977) 2675.
[33] K.D. Klika, H. Kivela, V.V. Ovcharenko, V. Nieminen, R. Sillanpaa, J. Arpalahti, Dalton Trans. (2007) 3966.
[34] T. Suzuki, Y. Hirai, H. Monjushiro, S. Kaizaki, Inorg. Chem. 43 (2004) 6435.
[35] C. Gagnon, J. Hubert, R. Rivest, A.L. Beauchamp, Inorg. Chem. 16 (1977) 2469.
[36] C.H. Wei, K.B. Jacobson, ACA Ser. 2 (7) (1980) 14.
[37] C.H. Wei, K.B. Jacobson, Inorg. Chem. 20 (1981) 356.
[38] P.d. Meester, A.C. Skapski, Dalton Trans. (1972) 2400.
[39] E.-J. Gao, Q.-T. Liu, Huaxue Xuebao 63 (2005) 725.
[40] P.d. Meester, A.C. Skapski, J. Chem. Soc. Dalton Trans. (1973) 1596.
[41] M.P. Brandi-Blanco, B. Dumet-Fernandes, J.M. González-Pérez, D. Choquesillo-Lazarte, Acta Crystallogr. E: Struct. Rep. Online E63 (2007) m1598.
[42] M.J. Zaworotko, H.H. Hammud, A.T. Kabbani, G. Mc-Manus, A. Ghannoum, M.S. Masoud, J. Chem. Crystallogr. 39 (2009) 853.
[43] E. Bugella-Altamirano, D. Choquesillo-Lazarte, J.M. González-Pérez, M.J. Sánchez-Moreno, R. Marín-Sánchez, J.D. Martín-Ramos, B. Covelo, R. Carballo, A. Castiñeiras, J. Niclós-Gutiérrez, Inorg. Chim. Acta 339 (2002) 160.
[44] C.G. Barry, C.S. Day, U. Bierbach, J. Am. Chem. Soc. 127 (2005) 1160.
[45] M.J. Sánchez-Moreno, D. Choquesillo-Lazarte, J.M. González-Pérez, R. Carballo, A. Castiñeiras, J. Niclós-Gutiérrez, Inorg. Chem. Commun. 5 (2002) 800.
[46] J.P. García-Terán, O. Castillo, A. Luque, U. García-Couceiro, P. Roman, F. Lloret, Inorg. Chem. 43 (2004) 5761.
[47] J.E. Kickham, S.J. Loeb, S.L. Murphy, Chem. Eur. J. 3 (1997) 1203.
[48] P.X. Rojas-González, A. Castiñeiras, J.M. González-Pérez, D. Choquesillo-Lazarte, J. Niclós-Gutiérrez, Inorg. Chem. 41 (2002) 6190.
[49] W.S. Sheldrick, H.S. Hagen-Eckhard, S. Heeb, Inorg. Chim. Acta 206 (1993) 15.
[50] A. Terzis, A.L. Beauchamp, R. Rivest, Inorg. Chem. 12 (1973) 1166.
[51] P.d. Meester, A.C. Skapski, J. Chem. Soc. A (1971) 2167.
[52] J. Cepeda, O. Castillo, J.P. García-Terán, A. Luque, S. Pérez-Yánez, P. Román, Eur. J. Inorg. Chem. (2009) 2344.
[53] S. Das, C. Madhavaiah, S. Verma, P.K. Bharadwaj, Inorg. Chim. Acta 358 (2005) 3236.
[54] W.M. Beck, J.C. Calabrese, N.D. Kottmair, Inorg. Chem. 18 (1979) 176.
[55] H. Sakaguchi, H. Anzai, K. Furuhata, H. Ogura, Y. Iitaka, T. Fujita, T. Sakaguchi, Chem. Pharm. Bull. 26 (1978) 2465.
[56] T.J. Kistenmacher, Acta Crystallogr. B: Struct. Crystallogr. Cryst. Chem. B30 (1974) 1610.
[57] L. Prizant, M.J. Olivier, R. Rivest, A.L. Beauchamp, Can. J. Chem. 59 (1981) 1311.
[58] J.-P. Charland, A.L. Beauchamp, Croat. Chem. Acta 57 (1984) 679.
[59] Y. Rosopulos, U. Nagel, W. Beck, Chem. Ber. 118 (1985) 931.
[60] U.E.I. Horvath, S. Cronje, J.M. McKenzie, L.J. Barbour, H.G. Raubenheimer, Z. Naturforsch. 59 (2004) 1605.
[61] Md.A. Salam, K. Aoki, Inorg. Chim. Acta 314 (2001) 71.
[62] Md.S. Rahman, H.Q. Yuan, T. Kikuchi, I. Fujisawa, K. Aoki, J. Mol. Struct. 966 (2010) 92.
[63] E.R.T. Tiekink, T. Kurucsev, B.F. Hoskins, J. Crystallogr. Spectrosc. Res. 19 (1989) 823.
[64] D. Badura, H. Vahrenkamp, Inorg. Chem. 41 (2002) 6013.
[65] Md.A. Salam, H.Q. Yuan, T. Kikuchi, N.A. Prasad, I. Fujisawa, K. Aoki, Inorg. Chim. Acta 362 (2009) 1158.
[66] M. Odoko, N. Okabe, Acta Crystallogr. E: Struct. Rep. Online E61 (2005) m2670.
[67] A. Marzotto, A. Ciccarese, D.A. Clemente, G. Valle, Dalton Trans. (1995) 1461.
[68] E.J. Gao, H.X. Yin, M.C. Zhu, Y.G. Sun, X.F. Gu, Q. Wu, L.X. Ren, J. Struct. Chem. 49 (2008) 1048.
[69] J.W. Suggs, M.J. Dube, M. Nichols, Chem. Commun. (1993) 307.
[70] J.L. García-Giménez, G. Alzuet, M. González-Álvarez, A. Castiñeiras, M. Liu-González, J. Borras, Inorg. Chem. 46 (2007) 7178.
[71] J.M. González-Pérez, C. Alarcon-Payer, A. Castiñeiras, T. Pivetta, L. Lezama, D. Choquesillo-Lazarte, G. Crisponi, J. Niclós-Gutiérrez, Inorg. Chem. 45 (2006) 877.
[72] T.F. Mastropietro, D. Armentano, N. Marino, G.D. Munno, Polyhedron 26 (2007) 4945.
[73] L. Prizant, M.J. Olivier, R. Rivest, A.L. Beauchamp, J. Am. Chem. Soc. 101 (1979) 2765.
[74] L. Prizant, M.J. Olivier, R. Rivest, A.L. Beauchamp, Acta Crystallogr. B: Struct. Crystallogr. Cryst. Chem. B38 (1982) 88.
[75] J.-P. Charland, J.F. Britten, A.L. Beauchamp, Inorg. Chim. Acta 124 (1986) 161.
[76] J. An, R.P. Fiorella, S.J. Geib, N.L. Rosi, J. Am. Chem. Soc. 131 (2009) 8401.
[77] S. Korn, W.S. Sheldrick, Inorg. Chim. Acta 254 (1997) 85.
[78] P. Annen, S. Schildberg, W.S. Sheldrick, Inorg. Chim. Acta 307 (2000) 115.
[79] J. Hubert, A.L. Beauchamp, Acta Crystallogr. B: Struct. Crystallogr. Cryst. Chem. B36 (1980) 2613.
[80] J. Hubert, A.L. Beauchamp, Can. J. Chem. 58 (1980) 1439.
[81] E.-C. Yang, H.-K. Zhao, B. Ding, X.-G. Wang, X.-J. Zhao, New J. Chem. 31 (2007) 1887.
[82] J.P. García-Terán, O. Castillo, A. Luque, U. García-Couceiro, P. Román, L. Lezama, Inorg. Chem. 43 (2004) 4549.
[83] J. An, S.J. Geib, N.L. Rosi, J. Am. Chem. Soc. 131 (2009) 8376.
[84] E.-C. Yang, H.-K. Zhao, Y. Feng, X.-J. Zhao, Inorg. Chem. 48 (2009) 3511.
[85] J.-P. Charland, Inorg. Chim. Acta 135 (1987) 191.
[86] J.-P. Charland, M. Simard, A.L. Beauchamp, Inorg. Chim. Acta 80 (1983) L57.
[87] J.-P. Charland, A.L. Beauchamp, Inorg. Chem. 25 (1986) 4870.
[88] H.W. Schmalle, G. Hanggi, E. Dubler, Acta Crystallogr. C: Cryst. Struct. Commun. C44 (1988) 732.
[89] R.-Q. Yang, Y.-R. Xie, Acta Crystallogr. E: Struct. Rep. Online E63 (2007) o3309.
[90] R.D. Rosenstein, M. Oberding, J.R. Hyde, J. Zubieta, K.D. Karlin, N.C. Seeman, Cryst. Struct. Commun. 11 (1982) 1507.
[91] H.W. Schmalle, G. Hanggi, E. Dubler, Acta Crystallogr. C: Cryst. Struct. Commun. C46 (1990) 340.
[92] J. Sletten, L.H. Jensen, Acta Crystallogr. B: Struct. Crystallogr. Cryst. Chem. B25 (1969) 1608.
[93] M.R. Caira, L.R. Nassimbeni, A.L. Rodgers, Acta Crystallogr. B: Struct. Crystallogr. Cryst. Chem. B31 (1975) 1112.
[94] M.E. Kastner, K.F. Coffey, M.J. Clarke, S.E. Edmonds, K. Eriks, J. Am. Chem. Soc. 103 (1981) 5747.
[95] E. Dubler, G. Hanggi, W. Bensch, J. Inorg. Biochem. 29 (1987) 269.
[96] E. Dubler, G. Hanggi, H. Schmalle, Acta Crystallogr. C: Cryst. Struct. Commun. C43 (1987) 1872.
[97] D.K. Patel, M.P. Brandi-Blanco, A. Domínguez-Martín, D. Choquesillo-Lazarte, J.M. González-Pérez, A. Castiñeiras, J. Niclós-Gutiérrez, under review.
[98] E. Sletten, Acta Crystallogr. B: Struct. Crystallogr. Cryst. Chem. B26 (1970) 1609.
[99] E. Dubler, G. Hanggi, H. Schmalle, Inorg. Chem. 29 (1990) 2518.
[100] G. Hanggi, H. Schmalle, E. Dubler, Acta Crystallogr. C: Cryst. Struct. Commun. C48 (1992) 1008.
[101] A. García-Raso, J.J. Fiol, A. Tasada, M.J. Prieto, V. Moreno, I. Mata, E. Molins, T. Bunic, A. Golobic, I. Turel, Inorg. Chem. Commun. 8 (2005) 800.
[102] J. Arpalahti, E. Niskanen, R. Sillanpaa, Chem. Eur. J. 5 (1999) 2306.
[103] J. Arpalahti, K.D. Klika, Eur. J. Inorg. Chem. (2003) 4195.
[104] N.B. Behrens, B.A. Cartwright, D.M.L. Goodgame, A.C. Skapski, Inorg. Chim. Acta 31 (1978) L471.
[105] J. Ruiz, N. Cutillas, M.D. Villa, G. López, A. Espinosa, D. Bautista, Dalton Trans. (2009) 9637–9644.
[106] M. Roitzsch, B. Lippert, Inorg. Chem. 43 (2004) 5483.
[107] A. Johnson, L.A. O'Connell, M.J. Clarke, Inorg. Chim. Acta 210 (1993) 151.
[108] E. Freisinger, I.B. Rother, M.S. Luth, B. Lippert, Proc. Natl. Acad. Sci. U.S.A. 100 (2003) 3748.
[109] I.B. Rother, E. Freisinger, A. Erxleben, B. Lippert, Inorg. Chim. Acta 300 (2000) 339.
[110] I.B. Rother, M. Willermann, B. Lippert, Supramol. Chem. 14 (2002) 189.
[111] A.T.M. Marcelis, H.-J. Korte, B. Krebs, J. Reedijk, Inorg. Chem. 21 (1982) 4059–4063.
[112] K. Aoki, W. Saenger, Acta Crystallogr. C: Cryst. Struct. Commun. C40 (1984) 772.
[113] E. Sletten, Acta Crystallogr. B: Struct. Crystallogr. Cryst. Chem. B30 (1974) 1961.
[114] F. Belanger-Gariepy, A.L. Beauchamp, J. Am. Chem. Soc. 102 (1980) 3461.
[115] E. Sletten, R. Kaale, Acta Crystallogr. B: Struct. Crystallogr. Cryst. Chem. B33 (1977) 158.
[116] P.J.S. Miguel, B. Lippert, Dalton Trans. (2005) 1679.
[117] A.L. Beauchamp, F. Belanger-Gariepy, J.-P. Charland, F. Guay, M. Simard, Acta Crystallogr. A: Cryst. Phys. Diffr. Theor. Crystallogr. A37 (1981) C64.

[118] H. Chen, M.M. Olmstead, D.P. Smith, M.F. Maestre, R.H. Fish, Angew. Chem. 34 (1995) 1514.
[119] M. Calligaris, P. Faleschini, E. Alessio, Acta Crystallogr. C: Cryst. Struct. Commun. C47 (1991) 747.
[120] H.R. Nasiri, H. Schwalbe, M. Bolte, J. Wohnert, Acta Crystallogr. E: Struct. Rep. Online E61 (2005) o3353.
[121] J.D. Orbell, K. Wilkowski, L.G. Marzilli, T.J. Kistenmacher, Inorg. Chem. 21 (1982) 3478.
[122] B.D. Castro, C.C. Chiang, K. Wilkowski, L.G. Marzilli, T.J. Kistenmacher, Inorg. Chem. 20 (1981) 1835.
[123] T.J. Kistenmacher, B.D. Castro, K. Wilkowski, L.G. Marzilli, J. Inorg. Biochem. 16 (1982) 33.
[124] L.G. Marzilli, K. Wilkowski, C.C. Chiang, T.J. Kistenmacher, J. Am. Chem. Soc. 101 (1979) 7504.
[125] N. Okabe, M. Tsujita, Acta Crystallogr. C: Cryst. Struct. Commun. C56 (2000) 1418.
[126] H. Mizuno, T. Fujiwara, K. Tomita, Bull. Chem. Soc. Jpn. 42 (1969) 3099.
[127] E. Dubler, G. Hanggi, H. Schmalle, Inorg. Chem. 31 (1992) 3728.
[128] L.G. Marzilli, L.A. Epps, T. Sorrell, T.J. Kistenmacher, J. Am. Chem. Soc. 97 (1975) 3351.
[129] M. Ruf, K. Weis, H. Vahrenkamp, Inorg. Chem. 36 (1997) 2130.
[130] H.Q. Yuan, K. Aoki, I. Fujisawa, Inorg. Chim. Acta 362 (2009) 975.
[131] D. Badura, H. Vahrenkamp, Inorg. Chem. 41 (2002) 6020.
[132] E. Colacio, R. Cuesta, J.M. Gutiérrez-Zorrilla, A. Luque, P. Román, T. Giraldi, M.R. Taylor, Inorg. Chem. 35 (1996) 4232.
[133] F. Allaire, A.L. Beauchamp, Can. J. Chem. 62 (1984) 2249.
[134] A. Cadiau, K. Adil, A. Hemon-Ribaud, M. Leblanc, A. Jouanneaux, A.M.Z. Slawin, P. Lightfoot, V. Maisonneuve, Solid State Sci. 13 (2011) 151.
[135] S. Pérez-Yáñez, O. Castillo, J. Cepeda, J.P. García-Terán, A. Luque, P. Román, Inorg. Chim. Acta 365 (2011) 211.
[136] A.K. Mishra, R.K. Prajapati, S. Verma, Dalton Trans. (2010) 10034.
[137] J. An, S.J. Geib, N.L. Rosi, J. Am. Chem. Soc. 132 (2010) 38.
[138] K.C. Stylianou, J.E. Warren, S.Y. Chong, J. Rabone, J. Bacsa, D. Bradshaw, M.J. Rosseinsky, Chem. Commun. 47 (2011) 3389.
[139] J. Thomas-Gipson, G. Beobide, O. Castillo, J. Cepeda, A. Luque, S. Pérez-Yánez, A.T. Aguayo, P. Román, CrystEngComm 13 (2011) 3301.
[140] E.-C. Yang, Z.-Y. Liu, Z.-Y. Liu, L.-N. Zhao, X.-J. Zhao, Dalton Trans. (2010) 8868.
[141] K. Biradha, S. Samai, A.C. Maity, S. Goswami, Cryst. Growth Des. 10 (2010) 937.
[142] S. Pérez-Yánez, G. Beobide, O. Castillo, J. Cepeda, A. Luque, A.T. Aguayo, P. Román, Inorg. Chem. 50 (2011) 5330.

## II.ii. Unravelling the versatile metal binding modes of adenine: Looking at the recognition roles of deaza- and aza-adenines in mixed-ligand metal complexes.

Review article submitted to *Coord. Chem. Rev.*

### RESEARCH HIGHLIGHTS

- The reasons of the extreme versatile behaviour of adenine are studied.
- One N-heterocyclic donor atom per ring moiety, within adenine skeleton, is required.
- Deaza-adenines, adenine isomers and aza-adenines are considered.
- The structures of metal complexes with N-ligands related to adenine are discussed.

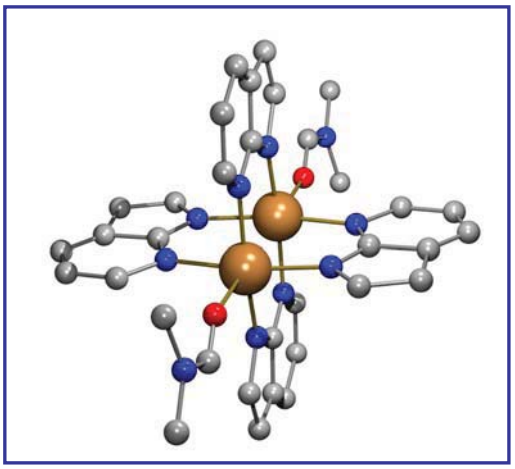

### RESUMEN

Con el objeto de contribuir el esclarecimiento de la versatilidad de la adenina como ligando, se han revisado, bajo el punto de vista estructural, los patrones de reconocimiento molecular de diversos ligandos tipo deaza-adenina, isómeros de adenina y aza-adeninas. Esta revisión no incluye restricciones en cuanto a la carga de los ligandos nitrogenados, es decir, se incluyen formas catiónica, neutra y aniónica, ni respecto a los iones metálicos presentes en los diferentes modos de coordinación.

# Unravelling the versatile metal binding modes of adenine: Looking at the recognition roles of deaza- and aza-adenines in mixed-ligand metal complexes

Alicia Domínguez Martín[a*], María del Pilar Brandi-Blanco[a] ,Antonio Matilla-Hernández[a], Hanan El Bakkali[a], Valeria Marina Nurchi[b], Josefa María González-Pérez[a], Alfonso Castiñeiras[c], Juan Niclós-Gutiérrez[a]

[a] Department of Inorganic Chemistry, Faculty of Pharmacy, University of Granada, 18071 Granada, Spain

[b] Dipartimento di Science Chimiche, Università di Cagliary, Cittadela Universitaria, 09042 Monserrato (CA), Italy

[c] Department of Inorganic Chemistry, Faculty of Pharmacy, University of Santiago de Compostela, 15782 Santiago de Compostela, Spain

CONTENTS



* Corresponding author: Department of Inorganic Chemistry, Faculty of Pharmacy, Campus Cartuja, University of Granada, E-18071 Granada, Spain. Phone: +34958243853, Fax: +34958246219.
E-mail address: adominguez@ugr.es

*Abbreviations:* A, acceptor; AcO, acetate; adp, adipate(2-); 7atp, 7-amino[1,2,4]triazolo[1,5-a]pyrimidine; BF4, tetrafluoroborate; btec, benzene-1,2,4,5-tetracarboxylate(4-); btrc, benzene-1,2,3-tricarboxylate(3-); CBIDA, N-(p-chloro)benzyliminodiacetate(2-) anion; $CH_3$-$Hg^+$, methyl-mercury; Cp, cyclopentadienilate(1-) ion; 2-(cPh)AcO, 2-(carboxyphenyl)acetate(2-); CSD, Cambridge Structural Database; cyclen, 1,4,7,10-tetraazacyclododecane; D, donor; DCE, dichloroethane; DCM, dichloromethane; DFT, Density Functional Theory; 6,9-diMeAde-H, 6,9-dimethyladeninate(1-); DMBA-H, N,N-dimethyl-benzylaminate(1-) ion; DMF, dimethylformamide, DMOet, dimethoxyethane; DMSO, dimethylsulfoxide; 5,7-dtt, 5,7-diamino[1,2,4]triazolo[1,5-a][1,3,5]triazine; EIDA, N-ethyliminodiacetate(2-) anion; EtAcO, ethylacetate; EtO, etoxide; FBIDA, N-(p-fluoro)benzyliminodiacetate(2-) anion; H4abim, 4-azabenzimidazole; H5abim, 5-azabenzimidazole; Hade, adenine; H4app, 4-aminopyrazolo[3,4-d]pyrimidine; H2AP, 2-aminopurine; H8aA, 8-aza-adenine; H7azain, 7-azaindole; $H_2$EDTA, ethylendiaminotetraacetate(2-) anion; H7deaA, 7-deaza-adenine; Hdap, 2,6-diaminopurine; HFP, 1,3-hexafluoro-2-propionate; Hpur, purine; IDA, iminodiacetate(2-) anion; mal, malonate(2-) anion; MEBIDA, N-(p-methyl)benzyliminodiacetate(2-) anion; MeO, metoxide; MeOH, methanol; NBu4, tetrabuthylamonia; NBzIDA, N-benzyliminodiacetate(2-) anion; ox, oxalate(2-) anion; $PBu_3$, tributhylphosphine; $PiPr_3$, trisopropylphosphine; 1,3-pn, 1,3-propanediamine; $PPh_3$, triphenilphosphine; Suc, succinate(2-) anion; TEBIDA, N-terc-buthyliminodiacetate(2-) anion; Terpy, terpyridine; TFPy, 2,3,5,6-tetrafluoro-4-pyridyl; THF, tetrahydrofurane; tm, trimesate(3-); tol, toluene; tp, terephtalate(2-); ZIF, zeolitic imidazolate frameworks.

---

ABSTRACT

For a better understanding of the extreme versatility of adenine as a ligand, the metal binding patterns of various deaza-adenines, isomers of adenine and aza-adenine are reviewed from a structural point of view, without restrictions on the neutral or charged species of these N-ligands and the metal ions involved in coordination.

---

## 1. Introduction

During the past decades, the number of papers concerning metal complexes with purine ligands and derivatives has been increasing rapidly [1-9]. In this context, the structures having adenine, in its anionic, neutral or cationic forms, are noticeable; raising the idea that adenine is an extremely versatile ligand [4,8,9]. Without taking into consideration adenine derivatives, among which are included nucleosides, nucleotides and closely related ligands, the versatile behaviour of this nucleobase seems to be related to the tautomerism phenomena of its dissociable proton, to its denticity and the strategic disposition of their N-donor atoms. These former issues were the aim of an initial revision dedicated to copper(II) complexes with adenine [4]. More recently, our research group has published a new updated revision in which oxo-purine and adenine complexes, with any metal ion, were also considered [9]. The conclusions reached under this global viewpoint encourage further researches in this fascinating area of Coordination Chemistry. In this context, two additional strategies can be considered:

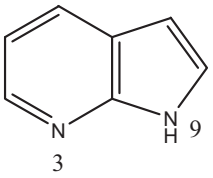

7-Azaindole

1,6,7-trideaza-adenine

(H7azain)

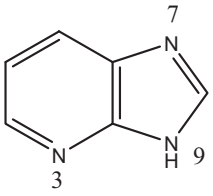

4-Azabenzimidazole

1,6-dideaza-adenine

(H4abim)

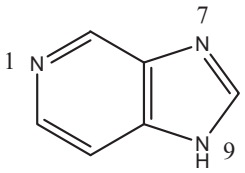

5-Azabenzimidazole

3,6-dideaza-adenine

(H5abim)

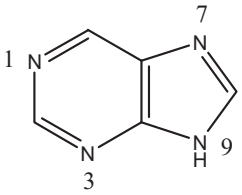

Purine

6-deaza-adenine

(Hpur)

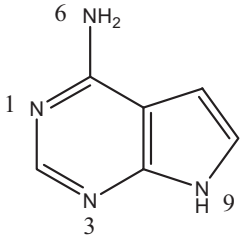

7-Deaza-adenine

(7deaA)

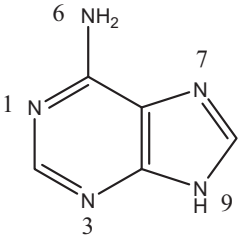

Adenine

(Hade)

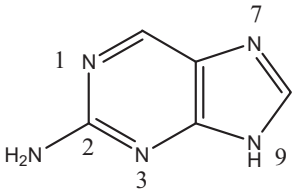

2-Aminopurine

(H2AP)

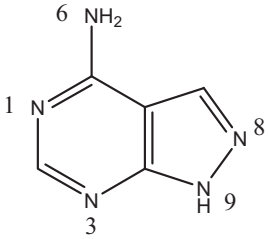

4-Aminopyrazole[3,4-d]pyrimidine

7-deaza-8-aza-adenine

(H4app)

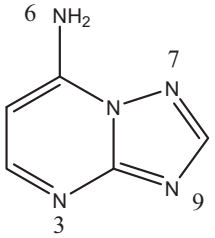

7-Amino-[1,2,4]triazolo[1,5a]pyrimidine

1-deaza-5-aza-adenine

(7atp)

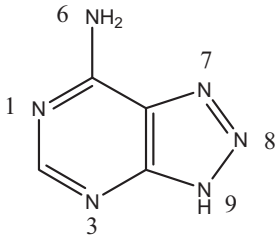

8-Aza-adenine

(H8aA)

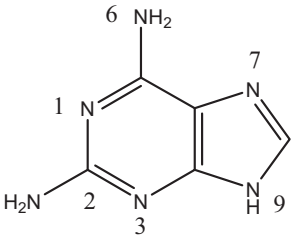

2,6-Diaminopurine

(Hdap)

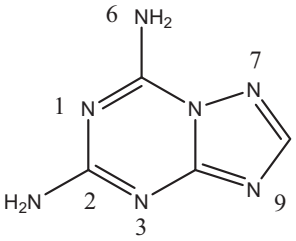

5,7-Diamino[1,2,4]triazolo[1,5-a][1,3,5]triazine

5-aza-2,6-diaminopurine

(5,7-dtt)

**Scheme 1.** Formulas of the N-ligands included in the present work

(i) to study metal complexes with N-heterocyclic ligands related to adenine; (ii) to work on metal complexes with N-substituted adenine ligands. In this work, it is revised all the structural contributions related to N-heterocyclic adenine-like ligands, in particular deaza-adenines, isomers of adenine and aza-adenine ligands. The formulas of the considered ligands are included in Scheme 1, accompanied by the corresponding abbreviation. Moreover, with the aim of easing the comparison between adenine and the studied ligands, the purine conventional notation will be adopted for the referred ligands, irrespective of the IUPAC numbering notation. Thus, i.e. the N-donor atoms of 7-azaindole will be numbered as N3 (pyrimidine moiety) and N9 (pyrrol moiety) instead of N7 and N1, respectively. In all the cases, the tautomer included for each ligand is that directly related to the most stable tautomer of adenine, that is H(N9)ade. Note that the considered ligands have at least one N-heterocyclic donor atom per cycle. Nonetheless, this restrain still allows the tautomerism of the dissociable proton in most of them. It is noteworthy that in those ligands that have a primary exocyclic amino group, at least one is located in position 6, with the sole exception of 2-aminopurine.

**2. Deaza-adenine metal complexes.**

2.1. Metal complexes with 7-azaindole (H7azain, 1,6,7-trideaza-adenine).

With the aforementioned criteria, there are only four possible di-nitrogenated heterocycles, included in Scheme 2.

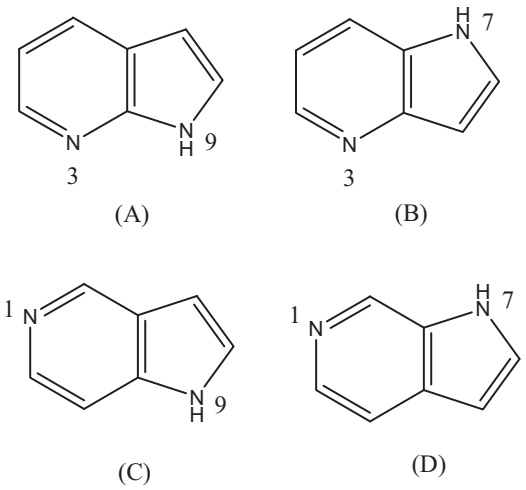


**Scheme 2.** Formulas of the four possible trideaza-adenine ligands: (A) 7azaindole; (B) 1H-pyrrolo[3,2-b]pyridine; (C) 1H-pyrrolo[3,2-c]pyridine; (D) 1H-pyrrolo[2,3-c]pyridine.

Among these N-ligands, the Cambridge Structural Database (CSD) only reports structures of 7azaindole (JESPAY, [10]) as well as its numerous metal complexes. In the crystal of the ligand, there are two non-equivalent molecular groups of four H7azain per each. Therein, four ligands are associated by symmetry related H-bonds (Fig. 1). It is interesting to note that H7azain is disordered in only one of the groups. A recent review was also published devoted to the lumiscence and reactivity of metal complexes with H7azain or its derivatives [11].

*2.1.1. 'Outer sphere' complexes with $H_27azain^+$ cation.*

It has been reported four structures of anionic metal complexes with $H_27azain^+$ as counter anion. In $(H_27azain)_2[ZnCl_4]$ (Fig. 2) (BIFXET, [12]) there are two non-equivalent cations.

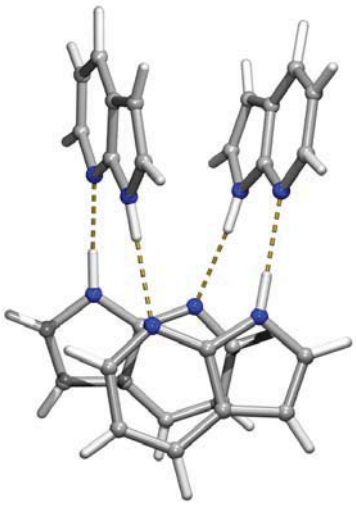

**Fig. 1**. Group of four non-disordered H7azain free ligands in JESPAY [10], showing the symmetry related N9-H···N3 intra-molecular interactions.

Thus, one is associated to the same chloro ligand by the N3-H···Cl (3.112 Å, 147.7º) and N9-H···Cl (2.779 Å, 130.56º) interactions whereas the other cation is related with two different chloro ligands by two H-bonds N3-H···Cl (3.189 Å, 167.9º) and N9-H···Cl (3.275 Å, 169.9º).The structure of this compound suggests that the N3-H group (formally displaying a positive change) has more tendencies to be associated by hydrogen bonds. The compounds HAGNOS y HAGNIM [13] contains 1D-polymeric anions plus aqua and unidentate or $\mu_2$-bridging chloro ligands that interact with the $H_27azain^+$ cation. In the former structures, the organic cations are delocalized. In PEGCUA [14], with formula $(H_27azain)[B(C_6F_5)_3OH]$, anion and cation interact by means of a H-bond N3-H···O (2.732 Å, 143.04º).

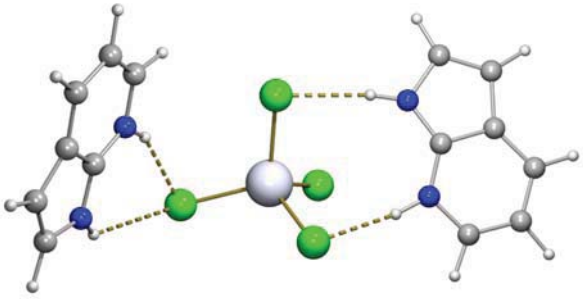

**Fig. 2.** Asymmetric unit in the crystal $(H_27azain)_2[ZnCl_4]$ (BIFXET, [12]). The complex anion is associated to two 7-azaindazolium(1+) ligand by means of H-bonding interactions that involve both N3-H and N9-H groups.

*2.1.2. Metal complexes with neutral H7azain.*

It has been reported structures of ternary complexes having different H7azain ligand:metal ratios, from 1:1 until 4:1.

a) With H7azain:metal ratio 1:1.

It has been reported four ternary complexes containing 7-azaindole and iminodiacetate (IDA) or an N-substituted iminodiacetate. Two of these compounds with formulas $[Cu(IDA)(H7azain)]_n$ [15] and $\{[Cu(FBIDA)(H7azain)]\cdot H_2O\}_n$ [16] are polymers where H7azain recognizes the Cu(II)-chelate by the bond Cu-N3 and the N9-H···O(coord.) interaction. The molecular compounds $[Cu(TEBIDA)(H7azain)(H_2O)]\cdot 3H_2O$ [16], $[Cu(EIDA)(H7azain)(H_2O)]$ (BUNZIU, [17]) and $[Cu(NBzIDA)(H7azain)(H_2O)]$ (BUNZOA, [17]) also display the Cu-N3 bond but the molecular recognition pattern H7azain/metal-chelate present in their crystal structures is different. In the two first former complexes, the coordination bond is reinforced by the interaction N9-H···O(coord. carboxy)

[2.883 Å, 123.2º in [Cu(TEBIDA)(H7azain)($H_2O$)]·3$H_2O$ and 2.765 Å, 133.8º in BUNZIU] whereas in BUNZOA the referred coordination bond is assisted by a bifurcated interaction that involve the N9-H group and one carboxy O-atom of NBzIDA (2.996 Å, 108.9º) and the apical O-aqua (2.874 Å, 163.5º). It has been also reported the structure of a $Nb^V$ derivative (YESNUF, [18]) that contains the cation $[NbO(H7azain)(Cl)_4]^+$ and one univalent organic anion derived from H7azain. In the cation, H7azain exhibits the bond Nb-N3 (2.533 Å) assisted by the intra-molecular interligand interaction N9-H··Cl (3.185 Å, 121.8º).

In KOQDID, $[Cu_2(\mu_2\text{-}AcO)_4(H7azain)_2]$, the binuclear core recognizes two H7azain ligands by the Cu-N3 bond (1.78 Å) and the N9-H···O(coord., 2.822 Å, 141.0º) H-bond [19]. This structure is interesting because proves that the referred metal binding pattern enable the coordination of neutral H7azain to the apical site of a 4+1 surrounding for a metal ion. In this context, a recent paper of K. Aoki et al. [20] has reported the apical coordination of adeninate(1-) anion to the [Cu(cyclen)] complex. The copper(II) compound KOQDID is similar to $[Rh_2(\mu_2\text{-}AcO)_4(H7azain)_2]$ (PRNRHB, [21]) and to the mixed-valence compound $[Ru^{II},Ru^{III}(\mu_2\text{-}AcO)_4(H7azain)_2]$ [PF6]·DCE (TAVWOP, [22]). In this latter compound the bonds Ru-N3 (2.288 Å) are reinforced by the appropriate intra-molecular N9-H···O(coord., 3.048 Å, 119.7º) H-bonds. Other related compounds are WAJROO $[Cu_4(\mu_4\text{-}O)(\mu_2\text{-}Cl)_6(H7azain)_4]$·0.5EtAcO [23]; WERLEK trans-$[Re^V(O)(H7azain)(Cl_2)(EtO)(PPh_3)]$ [24] and JESPIG $[CH_3\text{-}Hg(H7azain)(\mu_2\text{-}NO_3)]_2$ [10] where the Hg-N3 bond (2.127 Å) cooperates with a nearly linear N9-H···O(non-coordinated, nitrate) interaction (2.862 Å, 178.9º).

b) With H7azain:metal ratio 2:1.

This group of compounds includes the coordination polymer trans-$\{[Cu(\mu_2\text{-}SO_4)(H7azain)_2(H_2O)_2]\cdot H_2O\}_n$ (BUNZUG, [17]) in which the bridging sulphate anion occupies the apical positions of two adjacent 4+2 copper(II) centres (Cu-O 2.478 Å) and the ligands H7azain and aqua occupy cis-positions. Herein, each H7azain ligand is involved in a Cu-N3 (2.012 Å) bond and one interaction N9-H···O(coord. sulphate, 2.817 Å, 153.7º). There is reported a family of compounds with general formula $[Cu(H7azain)_2(\mu_2\text{-}N,N\text{-}N3)(\mu_2\text{-}O,O'\text{-}A)]_2$ that display two cis-H7azain ligands (A is nitrate (ULUZEH), perchlorate (ULUZOR) or trifluromethyl-sulphonate (ULUZIL) [25]). In these compounds, the molecular recognition pattern consists of a Cu-N3 bond and intra-molecular N9-H···O(A) H-bonding interactions. It has also been described a family of closely related compounds with general formula $[Cu(H7azain)_2(\mu_2\text{-}MeO)(\mu_2\text{-}O,O'\text{-}A)]_2$ (A is nitrate (IVECOC), perchlorate (IVECES) or trifluromethyl-sulphonate (IVECIW) [26]). One again, in these compounds the Cu-N3 bond is in cooperation with the N9-H···O(A) interaction.

An interesting square planar complex of copper(II) (RIVQET, [27]) with formula $[Cu(H7azain)_2Cl_2]$ has been reported. In the crystal, the complex molecules build chains that extend along the b axis as a consequence of inter-molecular N9-H···Cl (3.215 Å, 141.0º) H-bonds that involve one chlorido ligand of one adjacent unit. It is noticeable that in this compound the Cu-N3 is not assisted by intra-molecular interaction, as reported for all the previous complexes. In the compound cis-

$[Pt(H7azain)_2Cl_2]\cdot DMF$ (FAMRIW, [28]), both H7azain ligands reinforce the Pt-N3 bonds with the intra-molecular N9-H···O(DMF) interaction. Thus, the O-DMF atom plays a double H-accepting role. However, in the crystal of the related compound cis-$[Pt(H7azain)_2(ox)]$ (FAMROC, [28]), the Pt-N3 bond is not reinforced and the N9-H group is involved in inter-molecular N9-H···O(ox) H-bonding interactions (single or bifurcated) leading to the formation of pairs of complex molecules (Fig. 3).

In the tetrahedral compound $[Zn(H7azain)_2Cl_2]$ (BIFXAP, [12]), the Zn-N3 bonds act in cooperation with two N9-H···Cl interactions sharing the same Cl-acceptor. In the crystal of the related compound $[Zn(H7azain)_2(AcO)_2]$ (UCEDEL, [29]) the two H7azain ligands play different roles: one H7azain reinforces the Zn-N3 bond with a single N9-H···O(non-coord. AcO) H-bonding interaction while the other H7azain is involved in a bifurcated interaction type N9-H···O(non-coord. AcO). Therein, the O-acceptor atoms appertain to the same complex molecule (intra-molecular), so that cooperating with the corresponding Zn-N3 bond, or to an adjacent complex molecule (inter-molecular), associating pairs of complex molecules. Bifurcated H-bonds are also present in the molecular complex $[ReOCl_2(EtO)(H7azain)_2]$ (LENYEI, [30]). Nevertheless, in LENYEI the two H7azain ligands show a similar behaviour where the reported bifurcated interactions are intra-molecular comprising the N9-H···Cl (3.290 Å, 117.3º) and N9-H···O (2.915 Å, 118.0º) H-bonds. Note that in this latter interactions the two H7azain share the same oxo ligand as acceptor.

c) With H7azain:metal ratio 4:1.

The structures of two compounds have been reported where the metal surrounding is partially satisfied with four H7azain ligands.

In the salt $[Cu(H7azain)_4F]BF_4\cdot H_2O$ (HIVLEE, [31]), the metal adopts a 4+1 coordination (Fig. 4) where the fluoro ligand occupies the apical position (Cu-F 2.190 Å) and four H7azain ligands are coordinated by their N3 donor atoms (Cu-N3 2.038 Å). The referred coordination bonds act in cooperation with the corresponding N9-H···F (2.692 Å, 147.5º) interactions, involving the apical fluoro ligand.

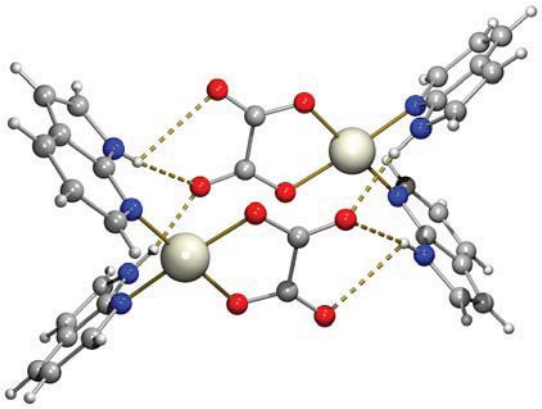

**Fig. 3**. Pairs of complex molecules in the crystal of cis-$[Pt(H7azain)_2(ox)]$ (FAMROC, [28]). These units are connected by two different inter-molecular N9-H···O interactions: single (2.858 Å, 168.36º) or weak bifurcated (3.067 Å, 174.44º and 3.035 Å, 105.94º).

Alternatively, in the molecular complex trans-$[Re(O)_2(H7azain)_4]Cl\cdot 0.5HCl_3\cdot 4H_2O$ (LENYIM, [19]), the heterocyclic ligands are delocalised over two positions and their coordination represents the formation of the bond Re-N3 which is assisted by the interaction N9-H···O.

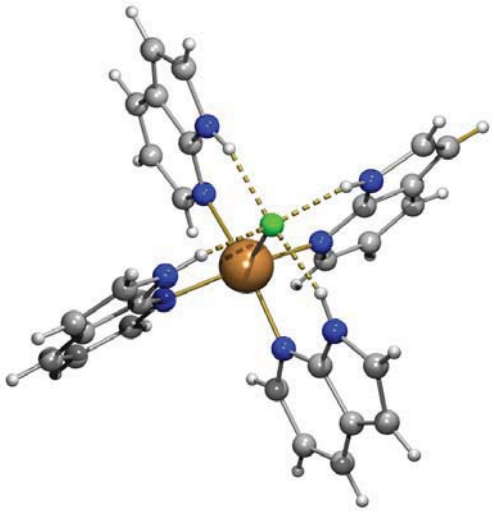

**Fig. 4**. Complex cation in $[Cu(H7azain)_4F]BF_4 \cdot H_2O$ (HIVLEE, [31]). The four Cu-N3(H7azain) bonds act in cooperation with intra-molecular H-bonds N9-H···F, involving the same H-acceptor .

d) With two different H7azain/metal ratios

The compound ULUZUX [25] is a 1D polymer where alternating binuclear units are linked by $\mu_2$-N,N'-N3 bridges. One metal centre has two H7azain ligands and satisfies the 4+1 coordination with three N-atoms from azide ligands whereas the other metal centre has only one H7azain ligand plus three N-azide donors and one O-perchlorate atom. Likewise, in $[Cu(H7azain)_4Cl][Cu(H7azain)_2Cl_3]$ (WAJRII01, [31]) two different H7azain/metal ratios are observed. In the complex cation, four H7azain ligands are coordinated to the Cu(II) centre via N3. Two of such heterocyclic ligands are involved in intra-molecular H-bonds N9-H···Cl (3.133 Å, 148.8º) reinforcing the coordination bond while the other two H7azain participates in very weak inter-molecular interactions with the apical chloro ligand of the complex anion associating both the complex anion and cation. In the former anion, only two H7azain ligands are coordinated by the N3-donor atom and assisted by intra-molecular interaction N9-H···Cl (3.136 Å, 114.5º).

*2.1.3. Metal complexes with H7azain and 7azain(1-) ligands*

The crystal of the binuclear complex JAVRUT [32], with formula $[Cu_2(\mu_2\text{-}AcO)_2(\mu_2\text{-}7azain)_2(H7azain)_2]$, is closely related with the structure of $[Cu_2(\mu_2\text{-}AcO)_4(H_2O)_2]$ (CUAQAC22, [33]). The difference between both structures consists of the substitution in JAVRUT of two AcO bridges by two 7-azaindolate bridges and the two water molecules by two H7azain ligands. Given the conformational rigidity of the N-heterocyclic ligand, the inter-atomic distance Cu··Cu (2.747 Å) in JAVRUT is longer than the corresponding in CUAQAC22 (2.616 Å). The H7azain ligands occupy the apical site of the copper(II) atoms in JAVRUT with a Cu-N3 distance of 2.229 Å. The Cu-N3 bond is in cooperation with an intra-molecular interaction N9-H···O(coord., 2.789 Å). One intermediate situation between the CUAQAC22 and JAVRUT, is that shown in the compound $[Cu_2(AcO)_4(H7azain)_2]$ (previously described as KOQDID) where the inter-metallic distance is 2.651 Å. From this comparison it follows that the increase of the inter-metallic distance is due to the contribution of two main factors: (1) the rigidity of $\mu_2$-7azain bridges and (2) the contribution of the apical H7azain ligands.

The coexistence of the neutral and anionic forms of 7-azaindole is also described in the square planar complexes within the salts $(NBu_4)$cis-$[M(H7azain)(7azain)(C_6F_5)_2]$ ·H7azain [34] [M = Pd(II) (HUWJAL) or Pt(II) (HUWJEP)]. Note that again the neutral H7azain exhibits its most stable tautomer

H(N9)7azain, thus coordination is driven through N3. In contrast, the 7azain(1-) anion behaves as a unidentate ligand binding the metal centre via N9. It is remarkable that the cis-geometry of these complexes favours the formation of intra-molecular interligand N9-H···N3 interactions. A similar behaviour is observed in the family of compounds [Al(H7azain)(7azain)($(F_3C)_2CHO$)] (QIDJOC, [35]), [Al(H7azain)(7azain)$_2$($CH_3$)] (QIDJES, [35] – Fig. 5) and [Al(H7azain)(7azain)$_3$] ·0.5DCM (QIDJIW, [35]). Herein the coordination to aluminium of H7azain and 7azain is unidentate via N9 what means that the neutral ligand adopts the unusual tautomer H(N3)7azain. In these three compounds, an intra-molecular N3-H···N3 H-bond is observed.

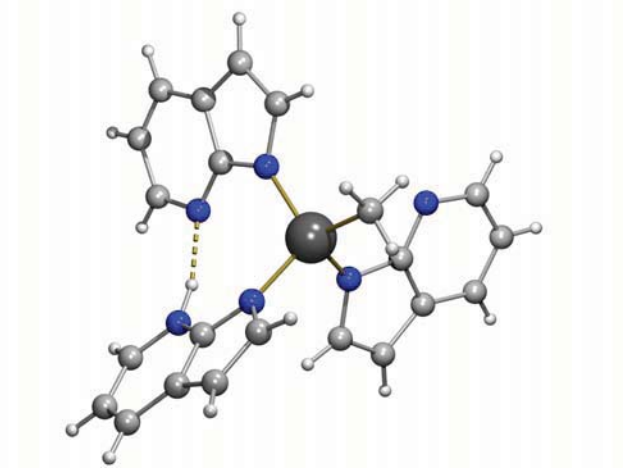

**Fig. 5**. Complex molecule of [Al(H7azain)(7azain)$_2$($CH_3$)] (QIDJES, [35]). Neutral 7-azaindole exhibits the rare tautomer H(N3)7azain. In the crystals, two Al-N9 bonds cooperates with the intra-molecular H-bond N3-H···N3 (2.697 Å, 165.27º).

*2.1.4. Metal complexes with 7azain(1-) ligand*

The dissociation of the proton, placed on N9 in the most stable tautomer, drives to the formation of the 7-azaindolate(1-) anion. This anionic form does not have any tautomeric possibilities. This fact increases the basicity of the ligand and furthermore encourages diverse metal binding patterns among which should be remarked the bridging modes.

2.1.4.1. Unidentate 7azain(1-) ligand.

A total of three structures are available in which 7azain acts as unidentate ligand: [Au(7azain)($PPh_3$)] (YIRLIU, [36]), [$CH_3$-Hg(7azain)] (JESPEC, [10]) and [Pt(7azain)(DMBA-H)(S-DMSO)]·0.5$H_2O$·0.25tol (HUWJOZ, [34]). These three compounds have in common that 7azain coordinates via N9. In the crystal of HUWJOZ, the water molecule forms O-H···N3 interactions associating pairs of complex molecules.

2.1.4.2. 7azain(1-) as bidentate chelating ligand.

There is known the structure of two ytterbium complexes where 7azain acts only as bidentate chelating ligand. In trans-[Yb(7azain)$_2$(DMOet)$_2$] (GORJEC, [37]), the cation Yb(II) adopts an octa-coordinated surrounding where the two disordered 7azain ligands act as bidentate chelators. The crystal of [Yb(7azain)($\eta^5$-Cp)$_2$] (LIZZID, [38]), has two crystallographically independent molecules which mainly differs in the delocalization of the 7azain ligands. In this compound, the chelating $\eta^2$-N,N role of 7azain defines the Yb-N9 (2.279 Å) and Yb-N3 (2.362 Å) coordination bonds.

2.1.4.3. 7azain(1-) with unidentate and bridging bidentate roles.

Probably the most surprising metal binding pattern described for 7azain is that reported by L.A. Oro et al. (GERRIE, [39]) according to

the formula $[Ru_3(\mu_2\text{-H})(\mu_3\text{-7azain})(CO)_9]$ (Fig. 6). In this trinuclear complex, each metal centre has three unidentate carbonyl ligands. Alternatively, H and 7azain play bridging modes: (i) the ligand H is coordinated to two metal centres; (ii) the 7azain ligand is coordinated to three metal centres. The unequivocally tridentate role of 7azain represents that its N9-donor is a quaternary nitrogen. Thus, the metal binding role of 7azain in this compound can be described as the as the bridging bidentate role $\mu_2$-N3,N9 in cooperation with the unidentate function of N9 or as the unidentate coordination via N3 in cooperation with the bidentate $\mu_2$-N9 role.

2.1.4.4. 7azain(1-) as bridging ligand.

a) One bridging 7azain(1-) ligand between two metal centres.

In general, the anion 7-azaindolate(1-) has been always attractive due to its possibility to act as a bridging ligand between two metal centres.

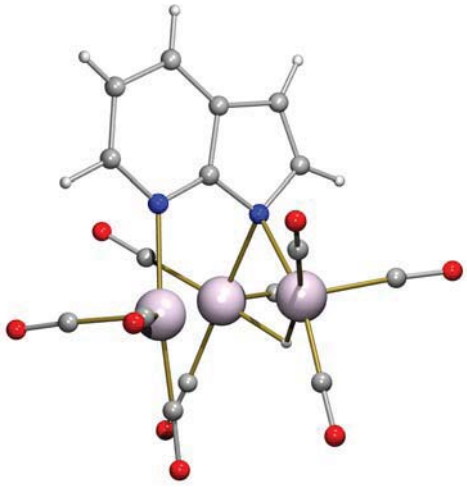

**Fig. 6**. Structure of $[Ru_3(\mu_2\text{-H})(\mu_3\text{-7azain})(CO)_9]$ (GERRIE, [39]) where the 7-azaindolate(1-) anion displays the unique tridentate role. The Ru···Ru distances are close to 2.76 Å.

To the best of our knowledge, this role highlights the similarities between the 7azain(1-) and purinate(1-) ligands. Hence, at least in this sense, 7azain(1-) should be considered as a bioisoster of purine, or particularly, as a deaza-adenine ligand.

A relevant number of complexes that exhibit the $\mu_2$-N3,N9-7azain role have been reported with different metal ions: Co(II) (FASHOW, [40]), Ni(II) (QACNUD, [41]), Cu(II) (AYEYOS, [42] - Fig. 7; AYEYUY, [42]; HAWBAK, [43]), Zn(II) (SUFBIE, [44]), Pt(II) (HUWJIT, [34]; LABPEJ, [45]), Os (RONBAX, [46]; RONBIF, [46]); as well as one bimetallic compound with Ag(I) and Pt(II) (HUNLIL, [47]).

The copper(II) compounds have in common their binuclear nature and the presence of a pentadentate dinucleating chelating ligand. The stabilization of the binuclear entity essentially deals with the $\mu_2$-O-alcoholate and the $\mu_2$-N3,N9-7azain bridges. This structural feature generates a metal-organic 6-membered ring that leads to a Cu···Cu separation between 3.117 Å (HAWBAK) and 3.239 Å (AYEYOS). The lowest inter-metallic distance in HAWBAK is related to the additional contribution of the mono-atomic bridge $\mu_2$-(O-DMSO). In this context, while AYEYOS and AYEYUY exhibit a bit distorted square planar coordination, HAWBAK is penta-coordinated, type 4+1, where the O-DMSO donor occupies the apical position. In the three referred compounds, the two metal centres are non-equivalent what is reflected, among other features, in the different distortions of the mean basal coordination plane and different coordination distances; i.e. Cu···O apical

distances in HAWBAK are 2.370 Å and 2.460 Å. Likewise, it should be remarked the hetero-metallic compound HUNLIL. In this compound, 7azain coordinates its N-donor atoms to two different metal ions (the N3 donor to a Pt(II) centre and the N9 donor to a Ag(I) ion) with very similar M-N(7azain) distances (~ 2.1 Å), showing an inter-metallic distance of 3.004 Å.

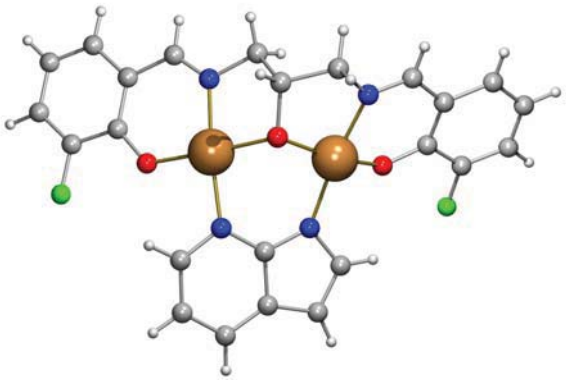

**Fig. 7.** Structure of $[Cu_2(\mu_2\text{-}7azain)(\mu_2\text{-}1,3\text{-}bis(3\text{-}fluorosalicylideneamino)propan\text{-}2\text{-}olato)]$ (AYEYOS, [42]) showing the rather common $\mu_2$-bridging role of 7azain(1-) anion (Cu-N3 1.971 Å, Cu-N9 1.947 Å).

Moreover, it has been reported three multinuclear complexes in which the ligand 7azain acts as a $\mu_2$-bridge. The compounds $[Zn_4(\mu_4\text{-}O)(\mu_2\text{-}7azain)_6]\cdot H_2O\cdot DCM$ (SUFBIE) and $[Co_4(\mu_4\text{-}O)(\mu_2\text{-}7azain)_6]\cdot HCCl_3$ (FASHOW) are very similar (Fig. 8). They have four tetrahedral cores of metallic atoms linked by one oxo donor in its centre and six peripheral $\mu_2$-7azain ligands bridging two adjacent metallic centres related by the edges of the above-referred tetrahedron. A related heptanuclear compound $[Cu_7(\mu_2\text{-}7azain)_6(OH)_6(H_2O)_2(MeOH)_4](AcO)_2\cdot tol\cdot 3MeOH$ [48] has also been characterised. In the disk-shaped cation, the central copper(II) atom is surrounded by O-donor atoms from six bridging $\mu_3$-OH ligands in an octahedral environment. Besides, six non-equivalent peripheral Cu(II) ions exhibit similar octahedral coordination. The peripheral Cu centres are coordinated to the six 7azain ligands via N3 from one 7azain and via N9 from a second 7azain. The coordination spheres of the Cu centres are completed by bridging methanol and bridging aqua ligands, with two of the Cu(II) ions bonded to two $\mu_2$-O-methoxo ligands and four Cu(II) ions each bonded to one $\mu_2$-O-methoxo and one $\mu_2$-O-aqua.

b) Two bridging 7azain(1-) ligand between two metal centres.

It has been reported structures with two $\mu_2$-7azain bridges of aluminium (GALLUA and GALPAK, [49]), molybdenum (CEPMPZ, [50], JADDOH, [51]), rhodium (CESWUS10) and DEDRUZ, [52]) and silver (REGNOG, [53]).

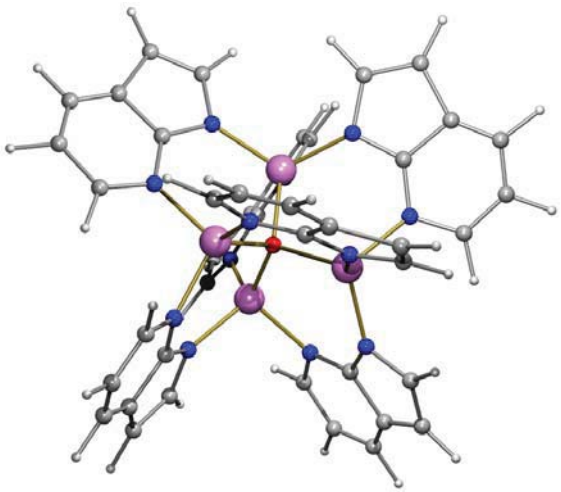

**Fig. 8**. Complex molecule of $[Co_4(\mu_4\text{-}O)(\mu_2\text{-}7azain)_6]\cdot HCCl_3$ (FASHOW, [40]). The four tetrahedral metal centres are coordinated by three $\mu_2$-7azain and one $\mu_4$-O ligand. In particular, three cobalt(II) ions are coordinated by two N9 and one N3(7azain) donors whereas the last Co(II) centre is chelated by three N3 donors.

The inter-metallic distances within the Al complexes (GALLUA, ~3.8 Å, GALPAK 3.372 Å) are significantly different. This is in contrast to that observed in the Mo complexes where the distances are very similar and noticeably shorter (CEPMPZ, 2.125 Å and JADDOH, 2.112 Å). The silver complex (REGNOG) is fairly simple since only involves the $\mu_2$-7azain ligands thus leading to a nearly planar molecule.

It has been also described one centro-symmetric tetranuclear copper(II) complex that exhibits pairs of $\mu_2$-7azain bridges between pairs of metal centres (FASHIQ, [40]). In addition, four metoxide(1-) ligands and two DMF molecules play bridging roles. Hence, two types of metal surroundings can be observed in this curious tetranuclear molecule: (i) two square-planar centres that have as cis-donors two O-(MeO) atoms and two N9(7azain) donor atoms; (ii) two centres with 4+1 coordination that display in cis two O-(MeO) donors and two N3(7azain) donors plus one apical O-DMF donor. The inter-metallic distance between two MeO bridges (3.014 Å) or two 7azain bridges (2.999 Å) are surprisingly similar.

c) Four bridging 7azain(1-) ligand between two metal centres.

There have been described compounds with four $\mu_2$-7azain bridges between two metal centres for aluminium (GALNUC and NOMVAM01, [49]) and different divalent metal ions (Cr (SEZVIC, [54], XAFFIT, [55]), Ni (JAVSAA, [32]), Cu (FASHEM, [40]), Nb (ADEKUP, [56], HOYRAO, [57], PAWFEY, [58]) or Mo (MEHCAD and MEHCEH [59]) or W (NIQJEC, [60]).

The compound $[Al_2(CH_3)_2(\mu_2\text{-7azain})_4]$ [49] consists of a centro-symmetric molecule with an inter-metallic distance of 3.40 Å. In the related trinuclear compound $[Al_3(CH_3)(\mu_2\text{-7azain})_4(\mu_3\text{-O})(HFP)_2]\cdot THF$ [49], 7azain exhibits two different bridging modes for two types of Al ions. The coordination of the methyl group to one Al centre determines its tetrahedral surrounding which is also satisfied by the $\mu_3$-oxo ligand and two N9(7azain) bonds from two different $\mu_2$-7azain ligands, thus associating the three Al centres. The remaining Al centres adopt a bipyramidal trigonal coordination where each aluminium centre is coordinated by two O-donors in trans configuration ($\mu_3$-oxo and one O-HFP) and three N-atoms of three different $\mu_2$-7azain ligands. Hence, the two latter Al centres display four bridging 7azain where as the tetrahedral Al ion only shows to two 7azain bridges.

The compound $[Cr_2(\mu_2\text{-7azain})_4(O\text{-DMF})_2]2DMF$ (SEZVIC, [54]) was prepared with the aim of studying the interaction between metal centres, in this case separated by 2.60 Å. However, the magnitude of this inter-metallic distance, as well as the nature of the metallic properties of the referred compound, can not be interpreted as the existence of a “super-long” Cr-Cr quadruple bond. Something similar occurs in XAFFIT where the Cr-Cr distance is 2.688 Å. The structure of the compound $[Cu_2(\mu_2\text{-7azain})_4(O\text{-DMF})_2]$ (FASHEM, [40] – Fig. 9) is rather similar to that of chromium(II) SEZVIC, but in the copper(II) derivative the inter-metallic distance is 2.781 Å and the metal surrounding is type 4+1. It is interesting to note that in $[Ni_2(\mu_2\text{-7azain})_4]_2DMF$ [32] the 3d8 electronic configuration of niquel(II) favours the square planar conformation, thus showing a Ni-Ni

separation of 2.594 Å. This difference in distance can be explained due to the absence of a fifth donor atom per each metal centre. In the compound $Li_2[Nb_2(7azain)_4Cl_2]\cdot 4THF$ [58], the binuclear core has four $\mu_2$-7azain bridges, with Nb···Nb distance of 2.278 Å. Note that the chloro ligands are loosely coordinated to the Nb atoms (Nb-Cl 2.849 Å).

d) Other singular bridging compounds

In the structure of the tetranuclear bimetallic compound $[Cu_2^{I}Au_2^{I}(\mu_2\text{-}7azain)_4(PPh_3)_2$ (YIRLAM, [36] - Fig. 10), the copper(I) atoms adopt a distorted trigonal conformation, with the metal centres located nearly in the N,N,N-plane.

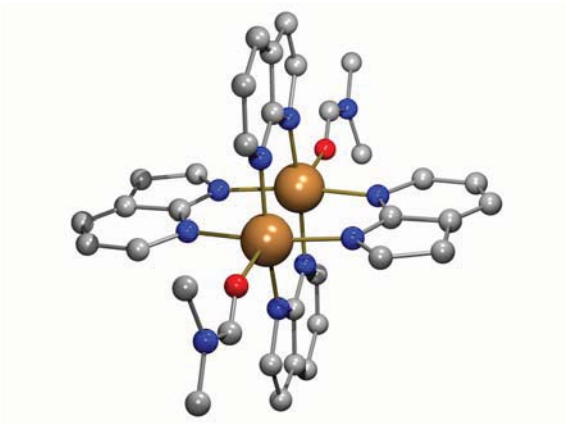

**Fig. 9.** Structure of the centrosymmetric compound $[Cu_2(\mu_2\text{-}7azain)_4(O\text{-}DMF)_2]$ (FASHEM, [40]. H-atoms are omitted for clarity. The apical site is occupied by the DMF ligands (Cu-O 2.326 Å) whereas the basal positions are occupied by the μ2-7azain ligands (Cu-N3 ~ 2.01 Å, Cu-N9 ~ 1.99 Å).

Hence, the two Cu(I) centres exhibit two bridging 7azain(1-) ligands plus one $\mu_2$-7azain that associate the Cu(I) and Au(I) ions. On the other hand, the Au(I) centres adopt an almost linear coordination (<N9-Au-P 171.8º). Another interesting bridging role is observed in the compound $[Al_4(\mu_3\text{-}O)_2(\mu_2\text{-}7azain)_6(HFP)2]\cdot 2tol$ (GALQEP, [49]). In GALQEP, each oxo atom is coordinated to three metal centres so that results two types of aluminium ions: two central and two terminal. Both metal centres adopt a five-coordinated environment which differs in the nature of the donors that satisfies the aluminium coordination. Thus the peripheral Al ions are coordinated by two N3 and one N9 donor of three different $\mu_2$-7azain ligands while the central Al ions are coordinated by two N9 and one N3($\mu_2$-7azain) atoms. Likewise, the two O-donor atoms within the peripheral Al ions are one O-HFP and one $\mu_3$-O whereas in central Al ion the two O-donors are provided by the $\mu_3$-oxo ligand.

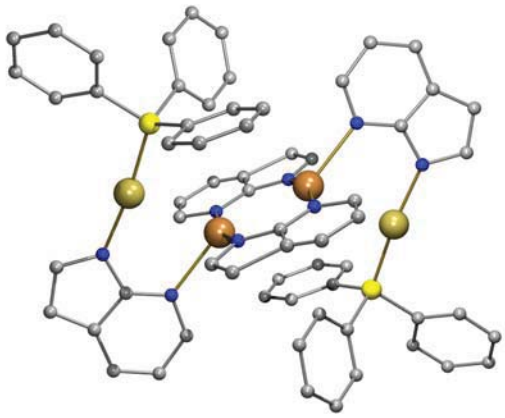

**Fig. 10**. Structure of the bimetallic compound $[Cu_2^{I}Au_2^{I}(\mu_2\text{-}7azain)_4(PPh_3)_2$ (YIRLAM, [36]). H-atoms omitted for clarity. Inter-metallic distance Cu(I)···Au(I) 3.010 Å.

*2.2. Metal complexes with 4-azabenzimidazole (H4abim, 1,6,-dideaza-adenine).*

In clear contrast to that reported for 7-azaindole, the available structural information for 4-azabenzimidazole is very scarce. For instance, the molecular and/or crystal structure

of H4abim ligand has not been reported. However, two DFT studies have been carried out [16, 61] that suggest that H(N9)4abim is the most stable tautomer. Nevertheless, it is remarkable that when solvent effect (water) is included in the DFT calculations, the difference in terms of energy between the H(N9)4abim and N(7)4abim is significantly reduced [16]. Indeed, this is consistent with that found in the crystals of two octanuclear $Ga^{III}$ complexes (UWUWIT and UWUWOZ, [62]).where the H(N7)4abim tautomer has been observed playing a solvate role. Moreover, there is reported the structures of two synthetic nucleosides derived from H4abim which have the sugar moiety linked to N7 or N9 (PITWAR or PITWEB, respectively, [63]).

There is not known any salt containing the 4-azabenzimidazolium(1+ or 2+) cations. By comparison, several crystal structures are available regarding metal complexes. In particular, three crystal structures are available for mixed-ligand complexes with neutral unidentate H4abim. Two of these compounds have a Cu(II)-iminodiacetate chelate and the tautomer H(N9)4abim: $[Cu(NBzIDA)\ (H4abim)]_n$ (BUNZEK, [17] and $\{[Cu(CBIDA)(H4abim)]\cdot 2H_2O\}_n$ [18]. In both ternary complexes the metal coordination is type 4+1 and molecular recognition represents only the formation of the Cu-N7 bond, thus preventing the formation of an intra-molecular interligand H-bond. The Cu-N7 distance is ~ 1.95 Å and, in the two former cases, the N9-H group is involved inter-molecular H-bonding interactions that play a key role in the crystal packing. The third reported compound with neutral H4abim is $[Cu(H_2EDTA)(H4abim)]\ \cdot 0.5H_2O$ [18]. Herein, the copper(II) centre exhibit an octahedral polyhedron where the longest coordination bond corresponds to a coordinated carboxylic group. Particularly noteworthy is the presence of the H(N7)4abim tautomer what drives coordination via N9. Note that this molecular recognition pattern is just the opposite to that above-referred, hence the cooperation of the Cu-N9 bond with any intra-molecular interaction is not possible. It is also noticeable the absence of protonation in H4abim by the chelating ligand $H_2EDTA(2-)$. This fact is in clear contrast to that described for an analogous compound where adenine exists as non-coordinated to the metal adeninium(1+) cation [64]. Therefore, these latter compounds reveal the real possibilities of tautomerism in this ligand according to the small energetic difference reported for the tautomers H(N9) and H(N7) in the aforementioned theoretical results.

There is also available the crystal structures of three binuclear copper(II) complexes where H4abim acts as bidentate $\mu_2$-N3,N9 bridging ligand: $[Cu_2(\mu_2\text{-N3,N9-H4abim})_4Cl_2]Cl_2\cdot 3MeOH$ (TETGIJ, [65]; $[Cu_2(\mu_2\text{-N3,N9-H4abim})_4Br_2]Br_2\cdot 0.5\ H_2O$ (TETGOP, [65] - Fig.11) and $[Cu_2(\mu_2\text{-N3,N9-H4abim})_4(SO_4)_2]\cdot 12H_2O$ (COSVIQ, [66]). In these compounds, the metal centres are linked by four bridging deaza-adenine ligands coordinated by its N3 and N9 donor atoms, thus they exhibit the tautomer H(N7)4abim. The influence of the apical ligands on the inter-metallic Cu···Cu distance bears correspondence to the slightly longer distances within the halide(1-) derivatives (3.055 Å average in TETGIG, 3.039 Å in TETGOP) compared to that reported for the $SO_4(2-)$ derivative (2.960 Å in COSVIQ). Furthermore, the structures of two 3D polymers containing the 4abim(1-)

anion, with formula $[M_2(\mu_2\text{-N7,N9})_2]_n$ (M = Fe (XASGON, [67]) or Zn (MIHOB, [68])), have been reported. The Fe complex is iso-structural with its analogue of cobalt(II) [67]. In these latter compounds each metal ion is coordinated to two N7 donors and two N9 of four bridging $\mu_2$-4abim ligands. Note that this metal binding patterns is different from the $\mu_2$-bridging role above-described for neutral H4abim.

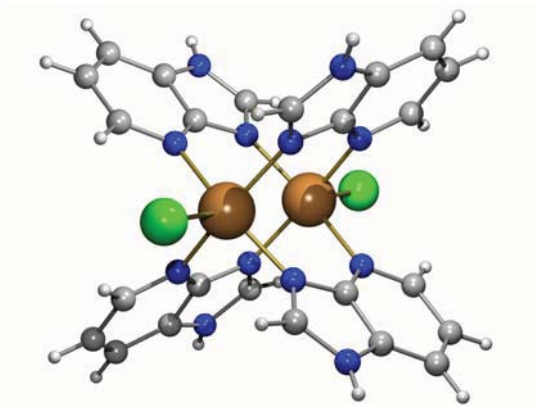

**Fig. 11**. Binuclear core in the compound $[Cu_2(\mu_2\text{-N3,N9-H4abim})_4Br_2]Br_2{\cdot}0.5\ H_2O$ (TETGOP, [65]). Neutral H4abim ligand shows the bidentate $\mu_2$-N3,N9 bridging mode. The Cu-N distances are fairly similar (Cu-N3 2.036 Å, Cu-N9 2.039 Å).

*2.3. Metal complexes with 5-azabenzimidazole (H5abim, 3,6,-dideaza-adenine).*

Analogously to that described for 4-azabenzimidazole, the crystal structure of the isolated ligand H5abim has not been reported. DFT calculations, including solvent effect (water), have been also performed for this ligand that suggest H(N9)5abim as the most stable tautomer, closely followed in terms of energy by the H(N7)tautomer. Likewise, there are not available structures where H5abim is involved as solvate or as a part of synthetic nucleosides/nucleotides. Indeed, only two structures of ternary compounds have been reported for H5abim having Cu(II)-iminodiacetate chelates: $\{[Cu_2(IDA)_2(\mu_2\text{-N7,N9-H5abim})]\cdot H_2O\}_n$ and $[Cu_2(NBzIDA)_2(\mu_2\text{-N7,N9-H5abim})(H_2O)_2]\cdot H_2O$ [16] (Fig. 12). The main difference between these two complexes is their molecular or polymeric nature which is directly related to the different coordination environments 4+2 or 4+1, respectively. The most noticeable feature of

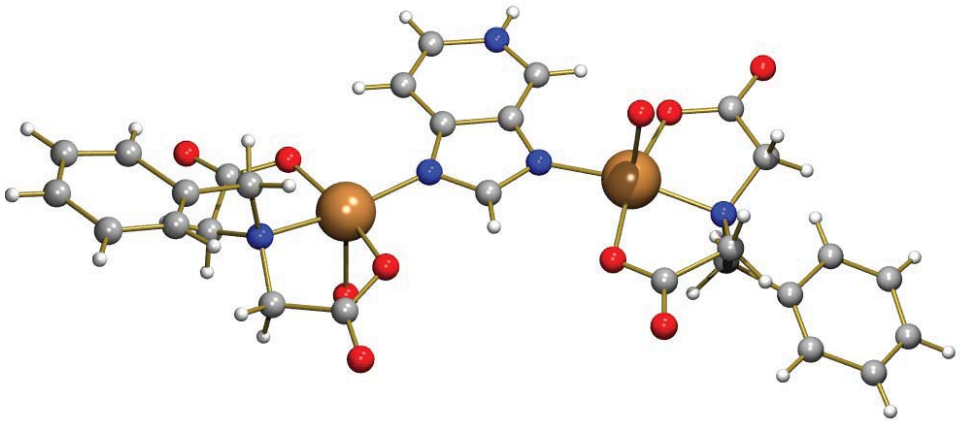

**Fig. 12**. Complex molecule of the compound $[Cu_2(NBzIDA)_2(\mu_2\text{-H5abim})(H_2O)_2]\cdot H_2O$ [16]. Only one of the two disordered positions is depicted for clarity (average Cu-N distance 1.960 Å). The bridging mode $\mu_2$-N7,N9 is the only metal binding pattern reported for this ligand, either in neutral or anionic form.

these compounds is the $\mu_2$-N7,N9 bridge mode of the heterocyclic ligand that represents the use of the tautomer H(N1)5abim. This means the formation of the coordinated bonds Cu-N7 and Cu-N9 can not be reinforced by intra-molecular N-H···O interactions although the N1-H group is actively involved in inter-molecular H-bonds within crystal packing. The structures of these latter compounds are closely related to that of compound $[Cu_2(NBzIDA)_2(\mu_2\text{-N7,N9-Hade})(H_2O)_2]\cdot 3H_2O$ [69]. Note that, in this complex, adenine shows the rare tautomer H(N3) which make possible the cooperation of the Cu-N7 and Cu-N9 bonds with the corresponding intra-molecular N6-H···O and N3-H···O interactions. Alternatively, the sole structure reported for the 5abim(1-) anion is $[Zn(\mu_2\text{-N7,N9-5abim})_2]_n$, a 3D polymer closely related to its analogue having $\mu_2$-4abim (vide supra, section 2.2.). Both compounds have been investigated because of their zeolitic imidazolate frameworks structures (ZIFs) regarding their gas-adsorbent properties and because of their selective adsorbent preferences. It is noteworthy that for 5-azabenzimidazole only the $\mu_2$-N7,N9 bridging role has been reported regardless of its neutral or anionic form.

*2.4. Metal complexes with 7-deaza-adenine (H7deaA).*

According to its pharmaceutical interest, the structure of tubercidine (7-deazaadenosine, TUBERC01, [70]) and closely related synthetic nucleosides have been reported [71-74]. However, no structural information is available about the free ligand H7deaA or its anions or cations.

Very recently, the structures of three ternary copper(II) complexes with neutral unidentate H7deaA and iminodiacetate chelators have been reported: $[Cu(IDA)(H7deaA)(H_2O)]\cdot 2H_2O$, $[Cu(NBzIDA)(H7deaA)]_n$ and $[Cu(MEBIDA)(H7deaA)]_n$ [16]. In all the former complexes, the Cu(II) centres exhibit a 4+1 coordination and the H7deaA shows its most stable tautomer H(N9)7deaA. Irrespective of their molecular or polymeric nature, H7deaA coordinates the metal ion via N3 and this bond is assisted by an intra-molecular interligand interaction. Note that this molecular recognition pattern is the same previously described for H7azain (vide supra, section 2.1). In addition, the compound $[Cu_2(MIDA)_2(\mu_2\text{-N1,N3-H7deaA})(H_2O)_2]\cdot 5H_2O$ [16] was reported in which the neutral H(N9)7deaA plays the unprecedented $\mu_2$-N1,N3-bidentate role. Surprisingly, the N9-H group is not cooperating with the Cu-N3 bond (1.986 Å) and only the Cu-N1 bond (1.993 Å) is assisted by an intra-molecular H-bond (N6-H···O 2.853 Å, 132.3º). Thus, the N9-H group is involved in inter-molecular interactions determined by the crystal packing. This latter compound is especially interesting because of the presence of the Cu-N1 bond. Indeed, only one compound has been reported where Hade involves its N1 donor in coordination [75].

*2.5. Metal complexes with purine (Hpur, 6-deaza-adenine).*

The structure of this N-heterocyclic ligand is known for a long time (PURINE01, [76]) and exhibits the tautomer H(N7)pur. Nevertheless, in the crystal of urea·2Hpur (PURURE, [77]), the purine solvate is present as the H(N9)pur tautomer. Moreover, the co-existence the two aforementioned tautomers

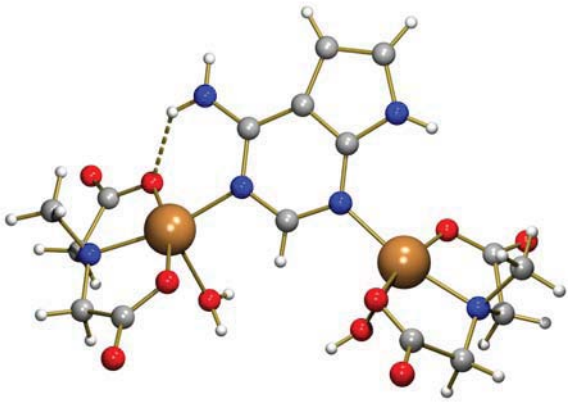

**Fig. 13**. Molecular struture of $[Cu_2(MIDA)_2(\mu_2\text{-}H7deaA)(H_2O)_2]\cdot 5H_2O$ [16] showing the unique bidentate role $\mu_2$-N1,N3 (Cu-N1 1.993 Å, Cu-N3 1.993 Å).

(H(N7)pur and H(N9)pur) has been reported in trans-$[Sn(CH_3)_2Cl_2(H_2O)_2]\cdot 4Hpur$ (DABLUN, [78]). In this latter compound, the trans-complex molecule is associated to four Hpur ligands by means of inter-molecular interactions that involve the aqua ligands, showing two O-H···N1(H(N9)pur and two O-H···N3(H(N7)pur H-bonds. Besides, adjacent purine ligands are associated by N-H···N interactions generating a 3D framework. It has also been reported the structures of two nucleosides derived from Hpur (NEDULR [79] and NISVIU [80]).

The purinium(1+) cation exists as $H_2(N1,N9)pur^+$ in the crystal structure of WIVFIQ [81]. This latter compound can be understood as one purinium(1+) perchlorate co-crystallized with an crown ether and acetonitrile and water solvents. The $H_2(N1,N9)pur^+$ cation is also reported in the out-sphere complex $(H_2pur)[AlF_4(\mu_2\text{-}F)]$ (ELEGEI, [82]). In this case, the anion is based on a coordination polymer that extends along the c axis leading to lineal chains. Adjacent chains are further associated via the purinium(1+) ligands by means of N1-H···F (2.597 Å, 166.64º) and N9-H···F (2.637 Å, 165.68º) H-bonds. The 1D polymer $[Cu_2(\mu_2\text{-}Cl)_4Cl_2(H_3pur)]_n$ (GOJGOB, [83]), consists of alternating penta-coordinated complex units where the Cu(II) centres are surrounded by five chloro ligands or by four chloro ligands and one purinium(2+) cation as the $H_3(N1,N7,N9)pur^{2+}$ tautomer. The metal surroundings are type 4+1 and the apical positions are occupied by a chloro ligand (2.754 Å) or by the N3 donor of the nitrogenated cation (2.561 Å), respectively. The $H_3(N1,N7,N9)pur^{2+}$ cation is significantly involved in H-bonding interactions: one simple (N7-H···Cl, 3.055 Å, 164.29º) and two bifurcated (N1-H···$Cl_2$, 3.163 Å, 127.27º and 3.238 Å, 142.43º, and N9-H···$Cl_2$, 3.217 Å, 138.04º and 3.168 Å, 126.05º). In the crystal of the closely related compound CLPRCV [84], the purinium(1+) cation exits as $H_2(N1,N9)pur^+$, which is bonded to the corresponding Cu(II) ion via N3 in an apical site (2.563 Å). Again, the N1-H and N9-H bonds are involved in bifurcated H-bonding interactions with chloride acceptors. In the tetrahedral molecular compound $[Zn(H_2pur)Cl_3]$ (BIFWUI, [12]), the tautomer $H_2(N1,N9)pur^+$ gives the Zn-N7 bond (2.054 Å). In the crystal, pairs of complex molecules are associated by symmetry related H-bonds N1-H···Cl (3.197 Å, 146.67º) which are further linked to adjacent pairs by the N9-H···Cl interactions (3.169 Å, 161.82º).

Neutral purine is able to act both as unidentate or bridging ligand. Concerning unidentate purine, the crystal structures of a family of four polymers with general formula $[M^{II}(\mu_2\text{-}ox)_4(Hpur)(H_2O)]_n$, M = Mn (SEGCIR, [85]), Co (LAFSAN, [86], Fig. 14), Cu (LAFRUG, [86] or Zn (LAFSER, [86]) have been reported. In these polymers, the oxalate

ligand acts as bridging-tetradentate between two metal centres. Hence, the former compounds lead to linear polymers where the metal centres exhibit octahedral surroundings built by two $\mu_2$-oxalate ligands, in perpendicular to each other, one aqua ligand and one neutral purine via N9, thus showing the tautomer H(N7)pur. One interesting feature in this isomorphic series is the variation of the coordination M-N9(Hpur) distance: Mn (2.253 Å) < Co (2.125 Å) ~ Zn (2.117 Å) < Cu (2.009 Å). The longest M-N distance corresponds to the manganese(II) compound, metal ion placed in the border between hard and borderline Pearson acids. In contrast, the shortest M-N bond corresponds to the Cu(II) compound, being Cu(II) the softest among the above-mentioned borderline Pearson acids. It is interesting to note that the M-N distances in these compounds tend to decrease according to the Irving-Williams series (Mn > Fe < Co < Cu > Zn, with Co ~ Zn), established from stability constants of complexes with these divalent cations and ligands with N- or O-donors. A closely related compound has been reported with purine and adenine ligands. The hybrid polymer agrees to the formula $[M^{II}(\mu_2\text{-ox})(Hpur)_{0.76}(Hade)_{0.24}(H_2O)]_n$ (LAFSAN01, [86]), in which the average Co-N9 bond distance is 2.121 Å. The tautomer H(N9)pur has also been observed in the tetrahedral molecular complex $[Zn(Hpur)_2Cl_2]$ (ZAYDAE, [87]). Herein, the Zn-N7 bond distances (2.027 Å or 2.033 Å) are shorter than those referred for the octahedral compound LAFSER (2.117 Å) as a logical consequence of the bond order. Furthermore, the tautomer H(N9)pur act as bridging $\mu_2$-N1,N7-Hpur in the tetranuclear compound $[Hg(CF_3)_2(\mu_2\text{-Hpur})]_4$ (YAKREI, [88]). This latter metal binding pattern is unknown for adenine, particularly as regards to the N1 donor atom [9].

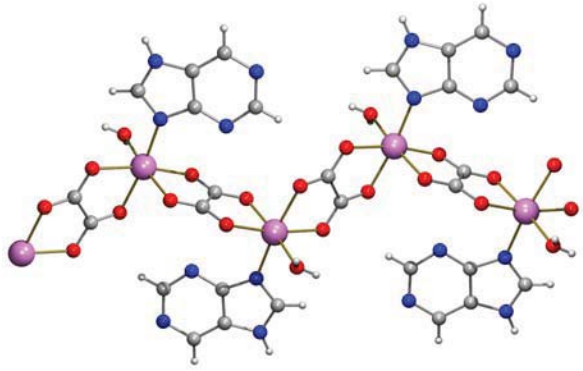

**Fig. 14**. Fragment of the linear polymer $[Co(\mu_2\text{-ox})(Hpur)(H_2O)]_n$ (LAFSAN, [86]). This compound appertains to an isostructural series of polymers with transition metal ions.

Alternatively, both adenine and purine are able to build $\mu_2$-N7,N9 bridges. This metal binding mode is shown in the 1D polymer $\{[Cu(\mu_2\text{-N7,N9-Hpur})(H_2O)_4]\ SO_4{\cdot}2H_2O\}_n$ (BIKJIO, [89]), where neutral purine uses the tautomer H(N1)pur.

The deprotonation of purine only produces the univalent anion purinate(1-). This is in clear contrast to that established for adenine, which is also able to dissociate the protons from the exocyclic amino group when it is coordinated to metal centres with marked soft Pearson acid character. All the coordination modes reported for the purinate(1-) anion involve its N9donor atom. Consequently, this is the N-donor coordinated to the metal centre in the tetrahedral molecular complex $[Ti(Cp)_2(pur)Cl]$ (CUGHAN, [90]) as well as in two Au(I) mononuclear $[Au(pur)(PPh_3)]{\cdot}2MeOH$ (FASWOM) and $[Au(pur)(PBu_3)]$ (FASWUS) or two binuclear $[Au_2(\mu_2\text{-}Ph_2PC_2H_4PPh_2)(pur)_2]$ (FASWAY) and $[Au_2(\mu_2\text{-}Ph_2PC_3H_6PPh_2)(pur)_2]$ (FASWEC) derivatives [91]. Note that in all the former

compounds the metal surrounding is almost linear.

It has been reported the crystals of two hydrated ZIF structures closely related to the aforementioned 4- and 5-benzymidazolate ligands [68], according to the general formula $\{[M(\mu_2\text{-N7,N9-pur})_2]\cdot nH_2O$ with n = 4.4 and M = Co (MIHHER) or Zn (MIHHAN). Very recently, it has been described the synthesis of the anhydrous ZIF $[Zn(\mu_2\text{-N7,N9-pur})_2]_n$ (YAVMIT, [92]). It is remarkable that in this 3D polymer, each metal centre exhibits a nearly non-distorted tetrahedral coordination. Likewise, the same bridging mode has been described for the trinuclear compound $[Pd_3(\mu_2\text{-N7,N9-pur})_3(PiPr_3)_3(TFPy)_3]$ (VIRNAM, [93], Fig. 15). It is noteworthy that in this cyclic molecule, the purinate rings lay on the same side of the plane defined by the three Pd atoms. Lately, the major denticity established for the purinate(1-) anion has been found in the ZIF polymers $[Zn(\mu_3\text{-N1,N7,N9-pur})(AcO)]_n$ and $\{[Zn(\mu_3\text{-N1,N7,N9-pur})(Br)]\cdot 0.25DMF\}_n$ (XEDPON and XEDPIH, respectively [94]). Consider that the $\mu_3$-N1,N7,N9 bridging role uses the three more basic N-donor atoms within the purinate(1-) anion. This molecular recognition pattern has never been observed for the adeninate(1-). In contrast, the $\mu_4$-tetradentate role has been described for the adeninate(1-) but not for the purinate(1-) anion.

## 3. Metal complexes with adenine isomers.

One of the approaches that can help to better understand the fascinating versatility of adenine concerns the research on the metal binding properties of isomers of this nucleobase.

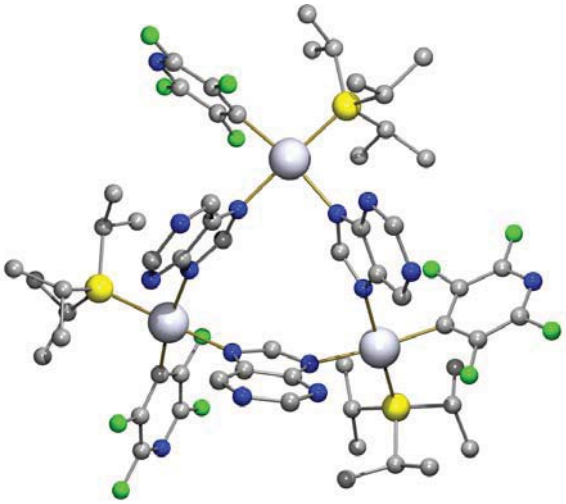

**Fig. 15**. Molecular complex molecule in the trinuclear compound $[Pd_3(\mu_2\text{-N7,N9-pur})_3(PiPr_3)_3(TFPy)_3]$ (VIRNAM, [93]). H-atoms are omitted for clarity. The three palladium ions are not equivalent, thus Pd-N7 and Pd-N9 bond distances are slightly different, approx. 2.09 Å and 2.08 Å, respectively.

Herein, two possibilities can be addressed: (i) shifting the 6-exocyclic amino group to carbons 2 or 8 of adenine or (ii) shifting one N-heterocyclic donor atom in the adenine skeleton. Up-to-date, there is not available structural information regarding 8-aminopurine and that about 2-aminopurine is very limited. Furthermore, despite the large possible combinations derived from the translocation of N-heterocyclic donors in adenine, only two isomers are described in literature: 4-aminopyrazolo[3,4-*d*]pyrimidine and 7-amino-[1,2,4]triazolo[1,5-*a*]pyrimidine.

### *3.1. Metal complexes with 2-aminopurine (H2AP)*

The structure of 2-aminopurine monohydrate (MIMWAH01, [95]) places the dissociable proton in N9, thus showing the tautomer H(N9)2AP, according to other

theoretical studies about H2AP tautomerism [96]. It has been also reported the structure of the antiviral first-line commercial drug famcyclovir, which is chemically defined as a synthetic nucleoside derived from H2AP (Famciclovir·$H_2O$, YACHAL, [97]).

Concerning metal complexes, the structural information of H2AP is fairly scarce. One recent paper [98] reports the structures of four ternary complexes with copper(II)-iminodiacetate-like chelates and H2AP. The referred chelating ligands include the own iminodiacetate(2-) anion as well as three N-derivatives with a non-coordinating N-arm (methyl, benzyl or p-tolyl): [Cu(IDA)(H2AP)($H_2O$)]·$H_2O$ (OSOGUZ) – Fig. 16, [Cu(MIDA)(H2AP)($H_2O$)]·3$H_2O$ (OSOHAG), {[Cu(NBzIDA)(H2AP)] ·1.5$H_2O$}$_n$ (OSOHEK), [Cu(MEBIDA)(H2AP)($H_2O$)] ·3.5$H_2O$ (OSOHIO). Regardless of their molecular or polymeric nature, in all the former compounds the Cu(II) centre adopts a square-base pyramidal coordination, with the O-aqua or O-carboxylate donors as apical atoms. In all the cases, H2AP exhibits the tautomer H(N9)2AP and binds the metal via N7.

Obviously the bond Cu-N7 can not cooperate with any intra-molecular interligand interaction type N-H···O. This behaviour is in clear contrast to that observed for the corresponding compounds with Hade instead of H2AP [4, 99]. Therein, the chelates Cu(IDA), Cu(NBzIDA) and Cu(MEBIDA) recognizes H(N9)ade by the Cu-N3 bond plus the intra-molecular N9-H···O interaction. In contrast, the chelate Cu(MIDA) exhibit a different molecular recognition pattern and coordinates H(N9)ade through the Cu-N7 bond, assisted by the intra-molecular N6-H···O interaction. The invariable metal binding behaviour of H2AP has been rationalized based on the influence of the 2-amino exocyclic group over the relative basicity of its N-heterocyclic atoms, as well as the hindrances that the amino group imposes over N1 and N3. Particularly noteworthy is the role of the N2-H group in the reported compounds, building chains via inter-molecular Watson-Crick like H-bonding interactions.

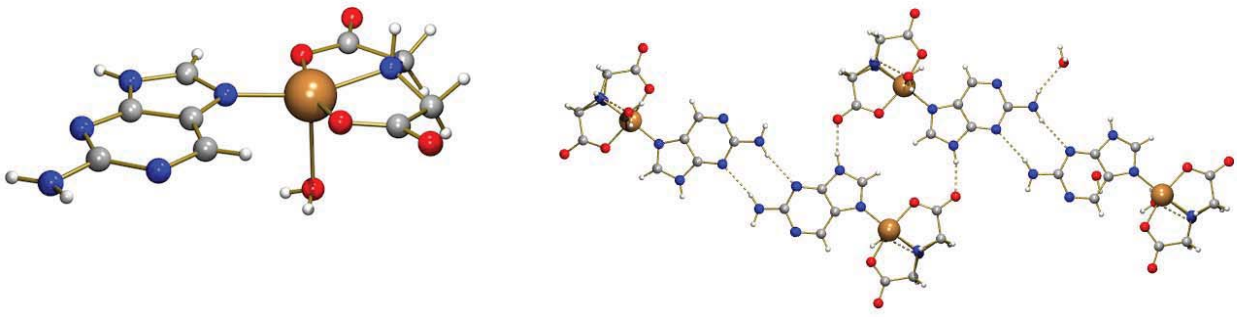

**Fig. 16**. Left: Molecular complex of [Cu(IDA)(H2AP)($H_2O$)]·$H_2O$ (OSOGUZ, [98]). Cu-N7 bond distance: 1.955 Å. Right: Detail of 1D chains built by N2-H···N1 H-bonds.

*3.2. Metal complexes with 4-aminopyrazolo[3,4-d]pyrimidine (H4app, 7-deaza-8-aza-adenine)*

The formula of H4app represents the translocation of the N7 and C8 atoms within the adenine skeleton. It is not available the crystal structure of the free ligand. Nevertheless, solution studies concerning H4app suggest an N-basicity order similar to adenine, with a remarkable small difference in basicity between the N8 and N9 donor atoms [100]. It has been described the structures of, at least, four nucleosides that include 8-azatubercidine monohydrate (AZTUBC, [101]) and two polymorphs of 2'-desoxi-8-azatubercidine (BOQLIC and BOQLOI [102]).

Long time ago, the crystal structure of one compound derived from H4app and methyl-mercury was reported: $Hg_2(H4app)](NO_3)_2$ (VEWTIA, [103]). In VEWTIA, this N-ligand acts as the H(N1)4app tautomer showing the coordination mode $\mu_2$-N8,N9. Lately, this metal binding mode has also been established for one non-linear, acyclic tetranuclear compound with formula $[Cu_4(FBIDA)_4(\mu_2\text{-}N8,N9\text{-}H4app)_2(H_2O)]\cdot 3.5H_2O$ [104]. The molecular topology of this compound is particularly influenced by the intra-molecular H-bonds established between the apical aqua ligand from the Cu4 unit and the O-carboxylate atoms from the chelating ligand FBIDA corresponding to the Cu1 (2.905 Å, 140º) and Cu3 (2.757 Å, 165º) units. A different bidentate bridging role has been reported for H4app in the binuclear complex $[Cu_2(MEBIDA)_2(\mu_2\text{-}N1,N8\text{-}H4app)(H_2O)_2]\cdot 4H_2O$ [104] (Fig. 17). Hence, the N-heterocyclic ligand exhibits the H(N9)4app tautomer. It is noticeable that in this compound the bonds Cu-N1 and Cu-N8 are assisted by the correponding

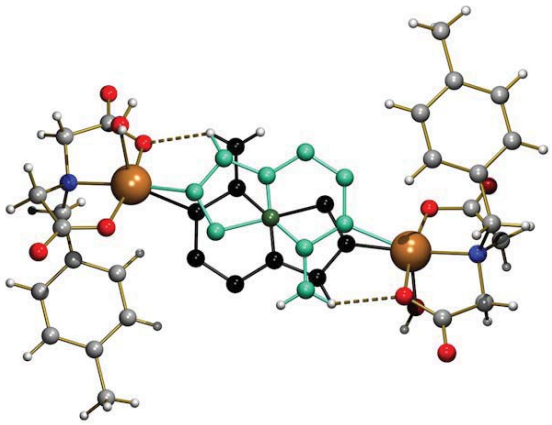

**Fig. 17**. Complex molecule of $[Cu_2(MEBIDA)_2(\mu_2\text{-}N1,N8\text{-}H4app)(H_2O)_2]\cdot 4H_2O$ [104]. The two disordered positions of H4app ligand are plotted in black and turquoise, respectively. The carbon atom shared by the two disordered position is depicted in dark green. Solvent molecules omitted for clarity.

intra-molecular interligand interactions N6-H···O and N9-H···O, respectively. Moreover, this structure has the complexity of presenting the ligand H4app disordered over two positions, with an occupancy factor of 0.5.It is also known a group of several $CH_3\text{-}Hg^+$ derivatives of 4app(1-) and 4app-H(2-) anions [103]. In the compound $[CH_3\text{-}Hg(4app)]$ (VEWTAS), methyl-mercury is coordinated to the N9 donor of the 4app(1-) anion that acts as unidentate ligand.

Furthermore, the 4app(1-) anion is able to accept three or four $CH_3\text{-}Hg^+$ groups in the compounds $[(CH_3\text{-}Hg)_3(\mu_3\text{-}4app)](NO_3)_2\cdot H_2O$ (VEWPOG) or $[(CH_3\text{-}Hg)_4(\mu_4\text{-}4app)](NO_3)_3\cdot H_2O$ (VEWVAU), leading to the bridging modes $\mu_3$-N1,N8,N9 or $\mu_4$-N1,N3,N8,N9, respectively. Note that in these three latter compounds, the N9 atom is always involved in coordination what highlights this N-atom as the most basic donor in the heterocycle. They also have in common the

absence of the N6-atom as metal binding donor. However, the involvement of the N6 exocyclic amino group in coordination has been reported for the 4app-H(2-) anion in the structure of the salt $[(CH_3\text{-}Hg)_4(\mu_4\text{-}4app\text{-}H)](NO_3)_2\cdot 2H_2O$ (VEWTUM). In VEWTUM, the tetradentate $\mu_4$-N3,N6,N8,N9 bridging mode of 4app-H(2-) anion implies the metallation of N6 accompanied by the dissociation of one of its H-atoms. Although it does not have any structural support, it is noteworthy that NMR studies, in DMSO, of this former compound evidences the shift of one $CH_3$-$Hg^+$ moiety from N3 to N1 leading to the tetradentate bridging mode $\mu_4$-N1,N6,N8,N9. This and other results obtained through the study of metal complexes with H4app derivatives reveal that the N6 metallation, and subsequent deprotonation, increases the basicity of the N1 donor.

The apparent difference in the metal binding behaviour between H2AP and H4app should be analysed carefully, taking into account the lack of structural support for methyl-mercury complexes with H2AP. Nevertheless, the available data about ternary complexes having Cu(II)-iminodiacetate chelates and H2AP or H4app reveal a significant difference between the consequences derived from the translocation of the exocyclic amino group (from C6 to C2) or the N-heterocyclic donor (from N7 to N8) within the adenine moiety.

### *3.3. Metal complexes with 7-amino-[1,2,4]triazolo[1,5-a]pyrimidine (7atp, 1-deaza-5-aza-adenine)*

The ligand 7atp is an isomer of adenine resulting from the translocation of the N1 donor of adenine to the bridging carbon placed between C6 and N7. Such translocation means that 7atp has three aromatic C-H groups, instead of two present in adenine. Therefore, it can not be expected proton tautomerism phenomena in neutral 7atp. Indeed, this is shown in the crystal structure of the ligand (VANVUD, [105]).

It is known several metal complexes where the 7atp ligand is present either in its cationic, neutral or anionic forms. The ligand 7atp is protonated in the outer-sphere complex $(H7atp)_2[Cu(ox)_2]\cdot 2H_2O$ (YADWIL, [106]). Surprisingly, the $H7atp^+$ cation is protonated at the N3 position. This fact is probably related to the role of the N3-H group in the crystal packing, being largely involved in inter-molecular H-bonds using the O-ox or O-water as acceptors. Moreover, it has been described the molecular and/or crystal structures of four complexes where neutral 7atp is coordinated via the N9 donor. The most simple structure corresponds to the molecular complex $[Cu(mal)(7atp)(H_2O)_2]\cdot H_2O$ (VANWAK, [105]). In this latter compound, the copper(II) coordination is type 4+1 and the two aqua ligands satisfy one basal and one apical sites. The Cu-N9 bond (2.009 Å) is reinforced by the intra-molecular interaction (w)O-H···N3 (2.703 Å, 150.93º), involving the basal aqua and the 7atp ligands. Note that, herein, the 7atp:Cu(II) ratio is 1:1. It has also been reported the crystal structures of two polymeric compounds in which the 7atp:Cu(II) ratio is 2:1. In $\{[Cu(\mu_2\text{-}ox)(7atp)_2]\cdot 3H_2O\}_n$ (VANWIS, [105]), the oxalate ligand acts as a syn-anti bridging carboxylate between two copper(II) ions and as a chelating ligand for one of these metal centres. Alternatively, in the compound $\{[Cu(\mu_2\text{-}suc)(7atp)_2]\cdot 2H_2O\}_n$ (VANWOY, [105]) the copper(II) ion is six-coordinated and

the suc(2-) anion acts as bridging ligand coordinating the two O-atoms of each carboxylate group to the same metal centre, thus building a 1D chain that extend along the a axis. In these two former compounds the Cu-N9 bond distances [1.977 or 1.989 Å (in VANWIS) or 1.984 Å (in VANWOY)] are slight shorter than in the related complex VANWAK. In the binuclear compound $[Zn_2(7atp)_4(\mu_2\text{-}2,2'\text{-bipy})(H_2O)_4]\cdot 7atp$ (FAJZAT, [107]), each metal centre is coordinated by two equatorial aqua ligands, two N-donors from the bridging $\mu_2$-2,2'-bipy and two 7atp ligands via N9, occupying the distal positions (Cu-N9 2.176 or 2.203 Å). Furthermore, the neutral form 7atp is also able to exhibit the bidentate $\mu_2$-N3,N9-bridging mode in two binuclear complexes: $[Ag_2(\mu_2\text{-}7atp)_2(ClO_4)_2]$ (OCIYEG, [108]) and $[Cu_2(\mu_2\text{-}7atp)_4(H_2O)_2](ClO_4)_2$ (VANWEO, [105], Fig. 18), in which the inter-metallic distances are very similar and show a value close to 3 Å. Note that this kind of molecular recognition pattern is also well-known for adenine, as well as other adenine-like ligands.

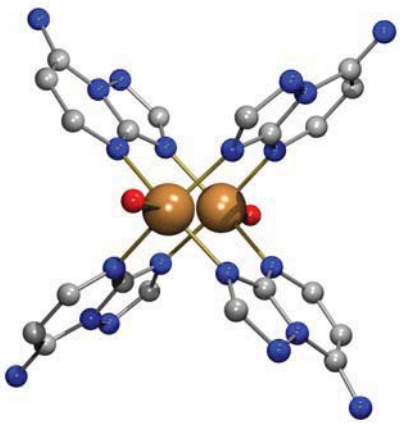

**Fig. 18**. Complex molecule in $[Cu_2(\mu_2\text{-}7atp)_4(H_2O)_2](ClO_4)_2$ (VANWEO, [105]). Note that this metal binding pattern has also been reported previously for deaza-adenine ligands, as well as the own adenine.

As commented before, the 7atp does not have one tautomerizable proton bonded to the N-heterocyclic atoms. However, this N-ligand is able to dissociate protons from the N6-exocyclic amino group leading to different anionic forms.The dissociation of such N6-protons is generally related to the N6 coordination of a metal ion with marked soft Pearson acid character. Very recently, it has been reported the structure of a Zn(II) complex (VARZEV, [109]) where the ligand 7atp acts in the monoanionic form 7atp-H(1-). This compound, of formula $\{[Zn(\mu_3\text{-}7atp\text{-}H)(1,3\text{-}pn)]ClO_4\}_n$ has two crystallographically the b axis. Two aspects are particularly noteworthy in this compound: (i) it shows the deprotonation of the exocyclic amino group tied to a Zn(II) ion, which is unequivocally considered as a borderline Pearson acid; (ii) it displays the chelating + bridging $\mu_2$-N3,N6,N7 metal binding pattern. Curiously, the mode $\mu_2$-N3,N6,N7 has been also established for one Li(I) derivative with $[6,9\text{-diMeAde-H}]^-$ (NIYDUV, [110]). There are barely reported a few compounds that the show the chelating-N6,N7(adenine-like) role [9]. This pattern is only possible when one of the protons of the exocyclic amino group is dissociated or when one of the protons of the exocyclic amino group shifts to a closer N-heterocyclic donor in the adenine moiety, usually the N1 atom. However, note that 7atp does not have N1 donor. Thus, to ensure the minimum charge separation (negative in N6 and positive in N1), dissociation will be the preferred option rather than shifting such proton to a remote N-acceptor, such as N3 or N9.

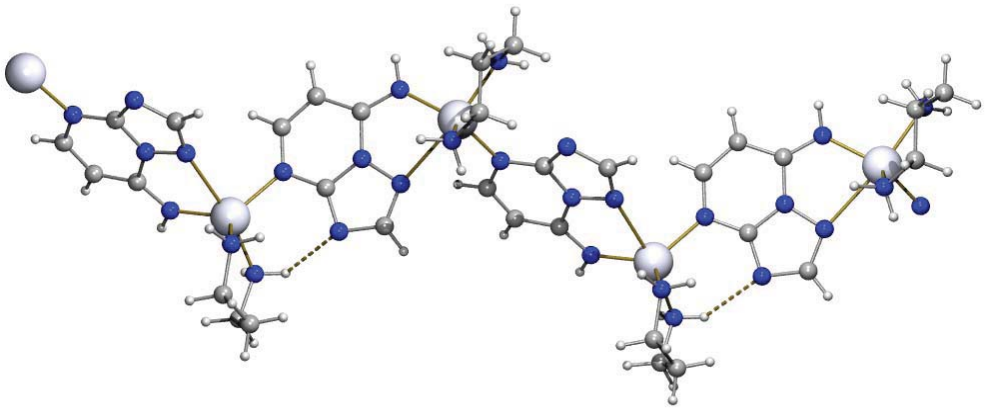

**Fig. 19.** Fragment of the polymer $\{[Zn(\mu_3\text{-}7atp\text{-}H)(1,3\text{-}pn)]ClO_4\}_n$ (VARZEV, [109]). Herein, the rare chelating + bridging $\mu_2$-N3,N6,N7 role is reported. Note that the stability of the polymer is reinforced by the cooperation of the Zn-N3 bond with a weak H-bond (3.075 Å, 129.70º)

**4. Metal complexes with aza-adenine ligands.**

It can be considered as aza-adenine ligands those adenine derivatives that exhibit additional N-exocyclic amino groups (at C2 and/or C8) or N-heterocyclic atoms (at C2, C4 and/or C5) or any combination of the aforementioned possibilities. A wide search in the CSD only reveals large structural information for two of these N-ligands: 2,6-diaminopurine and 8-aza-adenine. Nevertheless, three additional crystal structures are reported for other aza-adenine ligands. First, it has been found the crystal structure of the salt 8-aza-2,6-diaminopurinium(1+) sulphate monohydrate (AZADMS10, [111]). Second, it is described a synthetic nucleoside derived from 2-aza-adenine (ZADENH10, [112]). Finally, it has been reported one copper(II) complex with the ligand 5,7-diamino[1,2,4]triazolo[1,5-a][1,3,5]triazine.

In the centro-symmetrical octahedral compound $[Cu(5,7\text{-}dtt)_2(H_2O)_4]Cl_2$ (LAQBOV, [113]), the aza-adenine ligand shows a Cu-N9 bond (1.983 Å) that is assisted by an intra-molecular interligand (basal aqua)O-H···N3(5,7-dtt) interaction (2.761 Å, 148.72º). In the crystal, the ligand 5,7-dtt is largely involved in H-bonding interactions. Thus, pairs of complex molecules are associated by symmetrically related H-bonds N2-H···N1 building chains which are further connected by symmetrically related N6-H···N7 interactions. The 3D network is accomplished thanks to the chloride and aqua ligands.

*4.1. Metal complexes with 2,6-diaminopurine (Hdap)*

Recently, it has been established the crystal structure of the free ligand Hdap monohydrate (WUZROZ, [114]) which shows the tautomer H(N9)dap. In the crystal, adjacent Hdap units build zig-zag ribbons by means of two pairs of symmetrically related H-bonds: N2-H···N1 and N9-H···N3. In addition, non-coordinated water molecules connect the referred ribbons leading to 2D layers. The 3D network is accomplished by pi,pi-stacking interactions between adjacent anti-parallel Hdap ligands. Surprisingly, the N6-exocyclic amino group is not involved in H-bonds. Moreover, it has been reported the structures of three complexes with carboxylate ligands and Nd (AYOKUV, [115]), Dy (DUKPIJ, [116]) or

Ho( DUKPOP, [116]) and H(N9)dap solvate. It is also known the structure of several nucleosides derived from Hdap, among which should be remarked the well-known antiretroviral agent Abacavir (CUHGAO, [117]).

Two salts of the cationic species $H_2$(N1,N9)dap$^+$ have been reported. The first contains one organic anion (WUZRUF, [114]) while the second has one dodecafluoro-closo-dodecaborato anion (OYUZOY, [118]). It is also known the structure of one outer-sphere complex (AKEHOO, [119]) which has one Nd(III) binuclear anion and the $H_2$(N3,N7)dap(1+) cation. In the crystal structure of this latter compound, adjacent binuclear complex anions connect each other by inter-molecular interactions generating cages where the cations $H_2$dap$^+$ are hosted; thus, leading to a rather stable H-bonded 3D framework. Furthermore, the $H_2$dap$^+$ cation has been found coordinated to several metal centres. For instance, two iso-structural compounds with Co(II) (OQUMUJ, [120]) or Ni(II) (OQUMOD, [120]) have been reported. Herein, the metal centres exhibit trans-octahedral surroundings generated by pairs of carboxylate, aqua and $H_2$dap(1+) ligands. In these compounds, the coordination of the N-cation is via N9 using the tautomer $H_2$(N1,N7)dap$^+$. The coordination bond M-N9 (2.147 Å in OQUMUJ) is reinforced by an intra-molecular interligand (aqua)O-H···N3 interaction (2.741 Å, 160.41º in OQUMUJ). In addition, further intra-molecular interactions contribute to the greater stability of the complex molecule. It has also been described the structure of the salt trans-[Co($H_2$dap)$_2$($H_2O$)$_4$]btec·4$H_2O$ (AWICUF, [121]). In this case, the complex cation is non-centrosymmetrical and the N-ligand exists as the $H_2$(N3,N7)dap$^+$ tautomer, thus showing Co-N9 bonds (2.144 or 2.149 Å), which are not assisted by intra-molecular H-bonds.

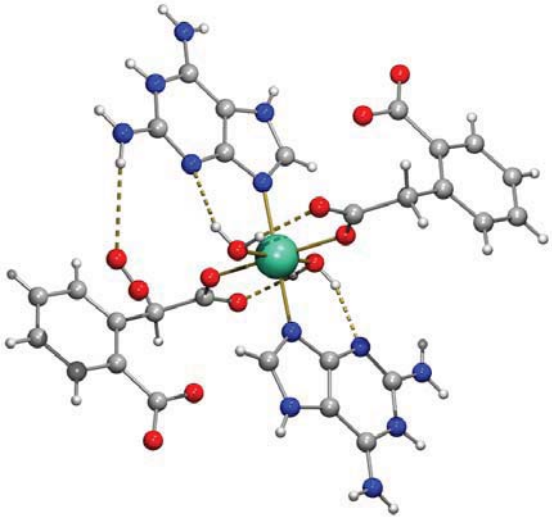

**Fig. 20.** Complex molecule in the centro-symmetrical compound [Ni($H_2$(N1,N7)dap)$_2$(2-(cPh)AcO)$_2$ ($H_2O$)$_2$]·4$H_2O$ (OQUMOD, [120]). Molecular recognition consists of a Ni-N9 bond (2.101 Å) plus an intra-molecular O-H···N3 interaction (2.733 Å, 154.77º).

Lately, it has been published a comprehensive structural study where 2,6-diaminopurine is coordinated either in its cationic, neutral or anionic forms [122]. The $H_2$(N3,N7)dap$^+$ cation is coordinated via N9 in the polymeric complex {[Zn($H_2$dap)(btrc)($H_2O$)]·3$H_2O$}$_n$ (QUDKOQ). In this polymer, the Zn(II) ion is pentadentate and adopts a bipyramidal trigonal geometry. The Zn-N9 bond is not reinforced by an intra-molecular H-bonding interaction despite the presence of one proton in the N3 donor atom. Alternatively, the $H_2$(N1,N9)dap$^+$ cation is coordinated via N7 in one Cd(II) polymer {[Cd($H_2$dap)(tp)($H_2O$)$_2$]·0.5tp·$H_2O$}$_n$ (QUDLAD). In this case, the Cd(II) atom adopts a slightly distorted octahedral geometry in which the aza-adenine

ligand occupies an equatorial position. The Cd-N7 bond is reinforced by an intra-molecular interaction N6-H···O(coord.) (2.924 Å, 146.62 Å). In the crystal, 1D Z-shaped chains are built by the bridging role of tp(2-) anions, and the N-H groups of $H_2dap^+$ are involved, as H-donors, in the supramolecular structure.

In addition, it has been described three Zn(II) polymers built by aromatic polycarboxylates and neutral 2,6-diaminopurine. In the three related compounds, Hdap always displays a $\mu_2$-bidentate bridging role although two different tautomers and metal bindings are shown. In one of these compounds, Hdap acts as $\mu_2$-N3,N9-H(N7)dap (QUDKAC). The Zn-N3 bond cooperates with a N2-H···O(coord.) interligand interaction whereas the Zn-N9 bond can not be assisted by an intra-molecular H-bond. The crystal of $\{[Zn_4(\mu_2\text{-Hdap})_2(\mu_3\text{-OH})_2]\cdot 2H_2O\}_n$ (QUDKAC) is built by 2D covalent layers in which the metal centres exhibit a pyramidal square based coordination. In contrast, in the two other polymers: $[Zn_2(\mu_2\text{-Hdap})(tp)_2]_n$ (QUDKEG) and $\{[Zn_2(\mu_2\text{-Hdap})(\mu_2\text{-OH})(tm)]\cdot H_2O\}_n$ (QUDKIK), the N-ligand plays the $\mu_2$-N7,N9-H(N3)dap role. In these compounds, the Zn-N7 and Zn-N9 coordination bonds are both reinforced by the N6-H··O(coord.) and N3-H··O(non-coord.) intra-molecular interactions, respectively. The Zn(II) ions exhibit a tetrahedral coordination generating a supra-molecular 2D polymeric structure. Finally, the dap(1-) anion is reported in the Cd(II) polymer $\{[Cd_3(\mu_3\text{-dap})_2(H_2O)_2(adp)_2]\cdot H_2O\}_n$ (QUDKUW). Herein, the anionic $dap^-$ ligand plays the $\mu_3$-N3,N7,N9-bridging role, generating a 2D framework. This tridentate role imposes a Cd-Cd separation of 3.582 Å between the metal centres linked to N3 and N9. Only the Cd-N7 bond (2.298 Å) is assisted by an intra-molecular H-bond N6-H···O(coord.) (2.779 Å, 161.94º).

It is also known that the dap(1-) anion displays the N9 unidentate role in a mixed-ligand Zn(II) complex with a tris-pyrazolyl-borate chelator (WULXEG, [123]). The M-N9 bond is expected for unidentate coordination since N9 is the most basic N-donor in the heterocycle. In the crystal, the dap(1-) is largely involved in inter-molecular interactions linking adjacent complex molecules through Watson-crick like H-bonds.

*4.2. Metal complexes with 8-aza-adenine (H8aA)*

The ligand 8-aza-adenine implies an additional N-atom within the imidazole moiety of adenine. To date, the crystal structure of the neutral ligand is not available. It is known, for quite a long time, several nucleosides derived from H8aA that have biological activity, in particular antitumoral properties. Consequently, some 8-aza-adenine nucleosides have been structurally characterize such as 8-aza-adenosine hydrochloride (VASVAM, [124]), one related nucleoside containing a rest of homocysteine in the 5'carbon (SAHCYB10, [125]) or one analogue that has the sugar moiety linked to N7 (WUZSIU, [126]).

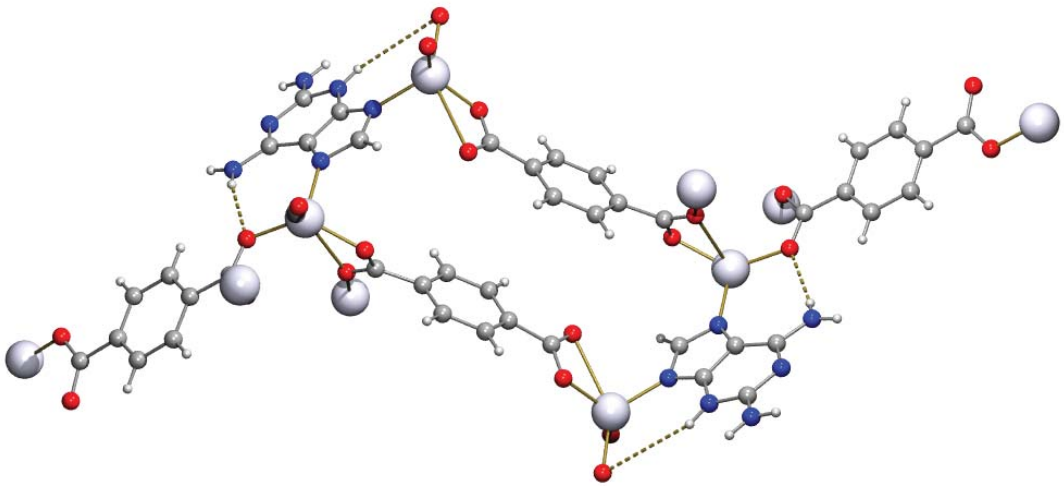

**Fig. 21**. Fragment of the polymer in $[Zn_2(\mu_2\text{-Hdap})(tp)_2]_n$ (QUDKEG). Both coordination bonds (Zn-N7 2.003 Å and Zn-N9 1.984 Å) are assisted by H-bonding interactions stabilizing the 2D supramolecular framework (N6-H···O 2.912 Å, 155.29º and N3-H···O 2.739 Å, 172.74º, respectively).

Likewise, there are known the crystal structures of the salts $(H_2 8aA)Cl$ (AZADNC, [127]), with the protons located at N1 and N9, and $(H_2 8aA)NO_3 \cdot H_2O$ (FAXFOZ, [128]), with the protons localised in N8 and N9. The structures of these latter cationic forms reflect the similarity between H8aA and Hade but also with the previously revised ligand H4app, which shows a similar basicity between its N8 and N9 atoms (vide supra). Note that in the referred ligands the most basic N-donor is any case N9. It is available only crystal structure in which the $H_2 8aA^+$ cation is coordinated to a metal centre. In the tetrahedral compound $[Zn(H_2 8aA)Cl_3]$ (AZADZN10, [129]) the N-ligand shows the $H_2$(N1,N8)8aA(1+) tautomer and is coordinated to the Zn(II) centre via N3 (2.073 Å). It has been suggested that the metallation in N3 promotes the shift of one proton from N9 to N8.

It has been reported the crystal structure of three compounds having the neutral form H8aA. In the polymer $[Hg(H8aA)_2(\mu_2\text{-Cl})Cl]_n$ (BABZUZ, [130]), H8aA exists as the tautomer H(N9)8aA. The structure of this polymer consists of alternating units of $\mu_2$-Cl ligands where each metal centre coordinates two H8aA ligands through the N3 donor atom. Unexpectedly, the N9-H group is not involved in intra-molecular interactions type N9-H···Cl. In the compounds $[CH_3\text{-}Hg(H8aA)]NO_3$ (DOCDAA, [131]) and trans-$[Cu(H8aA)_2(H_2O)_4](NO_3)_2$ (FAXDOX, [127]) the tautomer H(N1)8aA exhibits the bond M-N9. The former copper(II) complex has aqua ligands in basal and trans-apical positions which make possible the reinforcement of the Cu-N9 bond by an intra-molecular interaction (inter-atomic distance (basal aqua)O···N3 2.754 Å). In the crystal, adjacent complex molecules are linked by symmetry related Hoogstein-like H-bonds (N6-H···N7) building chains which are further associated by means of inter-molecular N1-H···O(apical aqua) interactions (inter-atomic distance 2.761 Å) (Fig. 22).

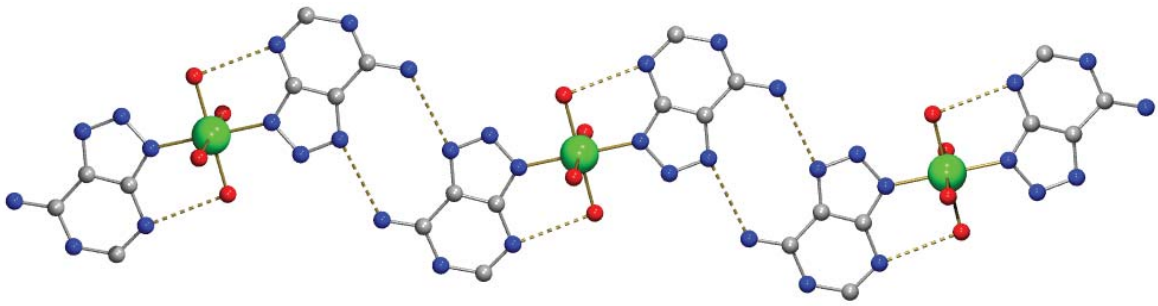

**Fig. 22.** Detail of the molecular complexes in trans-$[Cu(H8aA)_2(H_2O)_4](NO_3)_2$ (FAXDOX, [127]) building 1D chains by symmetry related H-bonding interactions (interatomic distance N6···N7 2.887 Å). No H-atoms are depicted due to the absence of real coordinates available in CDS.

The 3D network is accomplished thanks to the nitrate anions. It has also been reported the structure of two compounds derived from methyl-mercury and the univalent anion 8aA(1-). In the crystal of the molecular complex $[CH_3$-$Hg(8aA)]\cdot 4H_2O$ (DOCDEE, [132]), the $8aA^-$ anion is coordinated by means of the Hg-N9 bond (2.088 Å). Moreover, pairs of Hg···N8 interactions (2.804 Å) associate neighbouring molecules in dimmers. In the crystal of the salt $[(CH_3\text{-}Hg)_2(\mu_2\text{-}8aA)]NO_3\cdot H_2O$ (DOCDII, [132]) the $8aA^-$anion displays the $\mu_2$-N3,N9 role (Hg-N3 2.133 Å and Hg-N9 2.093 Å). In this bridging mode, the steric hindrance caused by the relative high volume of the mercury ions leads to a Hg···Hg inter-metallic distance of 3.478 Å, noticeably higher than twice the Van der Waals radium of mercury (1.50 Å). It has been discussed that the insertion of the N8 atom in the skeleton of adenine reduces the electronic density in the triazole ring, thus reducing the coordination abilities of the N7 donor atom and increasing the basicity of N3. Furthermore, it is available the crystal structure of the compound $[(CH_3\text{-}Hg)_3(\mu_3$-N1,N6,N9-8aA-H)]$NO_3$ (DOCDOO, [131]). Their presence of the 8aA-H(2-) anion is tied to the metallation of N6 that is accompanied by the dissociation of one H atom from the exocyclic amino group. This fact noticeably increases the basicity of the N1 donor atom, leading to the bridging mode $\mu_3$-N1,N6,N9. Note that in the referred 8-aza-adeninate(1-) or (2-) anions, the N9 atom is always involved in coordination what points out N9 as the most basic donor.

## 5. Overall Remarks.

*5.1. Tautomerism phenomena.*

7-azaindole exists, both in the crystal of the free ligand and in metal complexes, as its most stable tautomer H(N9)7azain expect for three Al complexes where the H(N3)7azain tautomer is present. This latter unusual tautomer seems to be favoured by the coexistence, in the crystals, of the neutral and anion forms of 7-azaindole, thus making possible intra-molecular H3-H···N3 interactions. The successive addition of N-heterocyclic atoms to the H7azain moiety leads to an increasing tautomerism phenomena that affects not only to the isolated ligands but also to the corresponding metal complexes. This general trend turns into particular cases depending on the position of the referred N-heterocyclic donor atoms within the molecular bicylic skeleton. Thus, 4-aza- and

5azabenzimidazole can easily shift their tautomerizable proton between the N9 and N7 donors. However, while in H4abim the N3 donor is never involved in tautomerism phenomena, in H5abim the H(N1) tautomer has been reported in the bidentate bridging mode $\mu_2$-N7,N9.

The presence of the -$^6NH_2$ exocyclic amino group and the absence of the N7 donor in 7-deaza-adenine lead to a singular situation that favours the existence of the most stable tautomer H(N9)7deaA. Noticeably, this feature also drives the coordination through the pyrimidine moiety and, in particular, enhances the involvement of the N1 donor in metal complexes where the M-N1 bond acts in cooperation with the N6-H···A intra-molecular interaction. Indeed, this fact has been also observed for one adenine isomer (H4app) that shows the above-mention feature. In contrast, the absence of the -$^6NH_2$ exocyclic amino group and the presence of the N7 donor in purine encourage tautomerism phenomena, either in the crystal of purine as in the crystals of different solvates or metal complexes, where H(N9)pur, H(N7)pur and H(N1)pur are found. Moreover, these data are in general agreement with the basicity order N9 > N1 >N7 >N3, generally accepted for the N-heterocyclic donors of Hade and Hpur.

The shift of the exocyclic amino group from C6 (in Hade) to C2 (in H2AP) reduces significantly the tautomerism of 2-aminopurine. Indeed, only the H(N9)2AP tautomer has been found. However, the translocation of N-heterocyclic donors in 4-aminopyrazolo[3,4-d]pyrimidine does not affect to the tautomeric possibilities of this ligand that shows two different tautomers in the two single compounds reported for this ligands: H(N9)4app and H(N1)4app.

Regarding aza-adenine ligands, neutral 2,6-diaminopurine always shows the H(N9)dap tautomer. Nevertheless, the univalent cation $H_2dap^+$ exhibits in different simple salts, outer- or inner-sphere complexes three different tautomers: $H_2$(N1,N9), $H_2$(N1,N7) or $H_2$(N3,N7), thus involving the four N-heterocyclic donors. Moreover, these modes act frequently in cooperation with H-bonds. The molecular structure of H8aA has not been established by crystallographic methods although it has been suggested that the dissociable/tautomerizable proton should be over N9 or N8. In the salts with chloride or nitrate anions it has been identified the tautomers $H_2$(N1,N9)8a$A^+$ and $H_2$(N8,N9)8a$A^+$, what suggest that the N9 donor should be considered as the most basic donor. Moreover, it supports the idea that the basicity between N9 and N8, and maybe between N8 and N1, should not be such differerent. In addition, the $H_2$8a$A^+$ cation involves the N1, N8 and N9 atoms in tautomerism phenomena but H(N3) or H(N7) have never been reported.

*5.2. Metal binding patterns.*

This review provides relevant structural support about the molecular recognition patterns of different N-ligands derived from adenine. For practical reasons, it seems more appropriate to stand back about the behaviour of deaza-aadenine, adenine isomers and aza-adenine ligands independently.

5.2.1. Metal binding patterns of deaza-adenine ligands.

With overwhelming difference, the more investigated deaza-adenine ligand is H7azain,

followed from a distance by Hpur. 7-Azaindole gathers the minimum requisites addressed in the present review, thus being considered as a 1,6,7-trideaza-adenine. It has been reported a varied coordination chemistry for H7azain. There are known outer-sphere metal complexes with the $H_2$7azain$^+$ cation, as well as metal complexes having either the molecule H7azain or its anion 7azain(1-), or even both forms in the same complex. All the available information for metal complexes with neutral 7-azaindole, with different ligand to metal ratios (1:1, 2:1 and 4:1 or combinations), reveal the most stable tautomer H(N9)7azain. In this complexes, the M-N3 bond is usually reinforced by an intra-molecular interligand N9-H···A interaction, with acceptors A = O, F, Cl. The maximum expression of this collaboration is found in the cation $[(H7azain)_4F]^+$ where the four short bonds Cu-N3 cooperates with four intra-molecular interactions N9-H···F. The metal binding patterns of the 7azain(1-) anion is fairly rich. Thus, it can act as unidentate ligand via N9, as bidentate chelating $\eta^2$-N3-N9, as bridging $\mu_2$-N3,N9 and even with an very unusual coordination role unidentate + $\mu_2$-bridge. Nevertheless, the most frequent coordination role corresponds to $\mu_2$ N3,N9(7azain). This pattern has been reported for one, two or four bridges between two metal centres. In this kind of complexes, the bite angle N3-C-N9 of 7azain (~125º) and the relevant structural rigidity of the ligand, are responsible of intermetallic distances that limit the interaction between metal centres and the bond order in the interaction metal-metal, which is also affected by the coordination of other co-ligands.

In clear contrast, the metal binding patterns of the tri-nitrogenated heterocycles (H4abim or H5abim and their corresponding anions) are very limited. The available information suggests reduced differences in basicity between the N7 and N9 donor atoms, more pronounced for H5abim. In the crystals, H4abim acts as unidentate ligand via N7 or N9 or as bridging ligand in the modes $\mu_2$-N3,N9 or $\mu_2$-N7,N9. To date, only the $\mu_2$-N7,N9 role has been reported either for H5abim or its anion 5abim(1-).

7-deaza-adenine has four nitrogen atoms, among which is included the exocyclic amino group (-$^6NH_2$), absent in the former deaza-adenine ligands. The scarce structural support shows the molecular form coordinated as unidentate via N3, in cooperation with an intra-molecular interaction N9-H···O, or as bridging $\mu_2$-N1,N3. The latter bridging mode occurs in a complex where Cu-N1 cooperates with the intra-molecular interaction N6-H···O whereas the bond Cu-N3 is not assisted by H-bonding interactions. This fact is related to the driving forces within the crystal that involve the N9-H group in inter-molecular H-bonds. There are not known complexes with cationic or anionic forms of this interesting ligand.

It is remarkable the relative limited structural information regarding purine complexes. This fact is in clear contrast to the broad and varied information about adenine. In purine, there is not exocyclic amino group in 6 and therefore the possibility to reinforce the bond M-N1 or M-N7 with a N6-H···A interaction is missing. However, the absence of the referred N6 exocyclic amino group also leads to the absence of a steric hindrance over the N1 donor. The metal binding patterns of the molecular form Hpur reveal the relevance of tautomerism phenomena (vide supra). This fact can be related to its versatility as ligand;

for instance, H(N7)pur acts as unidentate via N9, H(N9)pur coordinates by N7 or as $\mu_2$-N1,N7 and H(N1)pur plays the role $\mu_2$-N7,N9. Alternatively, the anion pur(1-) acts as N9-unidentate or the bridging modes $\mu_2$-N7,N9 and $\mu_3$-N1,N7,N9. Nonetheless, there are not known any complexes where the pur(1-) anion behaves as tetradentate. Note that no examples are where Hpur or its cationic or anions involve the N3 atom in coordination.

5.2.2. Metal binding patterns of adenine isomers

Among the adenine isomers studied in the present work, only two of them have tautomeric possibilities: H2AP and H4app. Likewise, only two of the N-ligands considered herein exhibit the exocyclic amino group over the carbon 6: H4app and 7atp. In contrast, H2AP has the amino group shifted to carbon 2. The scarce available information about this latter N-ligand is limited to four mixed-ligand copper(II) complex where the tautomer H(N9)2AP coordinates in all the cases via N7. Note that no possibility of intra-molecular interaction N-H···A is possible. It seems clear that both electronic and steric hindrances, associated to the $-^2NH_2$ group, come together favouring metallation in N7.

Alternatively, the translocation of N7 and C8 atoms in Hade generates the isomer H4app for which only bidentate roles have been established: $\mu_2$-N8,N9-H(N1)4app and $\mu_2$-N1,N8-H(N9)4app. This latter mode cooperates with intra-molecular N6-H···O and N9-H···O interactions. As commented previously in 5.1. Section, the absence of N7 atom favours somehow the implication of N1 as donor atom. It has been described several derivatives of methyl-mercury and 4app(1-) with the coordination modes N9-unidentate or bridging $\mu_2$-N3,N9, $\mu_3$-N1,N3,N9 or $\mu_4$-N1,N3,N8,N9. Besides, one complex has been described for the divalent anion 4app-H(2-) with the mode $\mu_4$-N3,N6,N8,N9.

The shift of the N1 donor of adenine to the bridging position in between C6 and N7 yields the ligand 7atp. The molecular form of this N-liagnd does not have tauromerizable proton and usually plays the roles N3-unidentate or bridging $\mu_2$-N3,N9. For the univalent anion 7atp-H(1-), it has been also established the $\mu_2$-N3,N6,N7 role. Noticeably, in this latter compound, the N6 donor is deprotonated and coordinated to a Zn(II) ion, defined as a borderline Pearson acid. This tridentate mode supposes the cooperation of the chelating mode N6,N7 and the additional bridging mode using N3. No protonated forms are reported for H4app or H2AP. In contrast, 7atp exists as H(N3)7atp(1+) in an outer-sphere metal complex with the anion bis-(oxalate)copper(II).

5.2.3. Metal binding with aza-adenine ligands.

The contributions regarding metal complexes of aza-adenines are mainly focused on 2,6-diaminopurine, with two exocyclic amino group, and on 8-aza-adenine, with one additional N-heterocyclic atom, respect to adenine.

The tautomers $H_2$(N1,N7)dap$^+$ and $H_2$(N3,N7)dap$^+$ correspond to metal complexes where the N-ligand coordinates as unidentate via N9, whereas the tautomer $H_2$(N1,N9)dap$^+$ is shown the M-N7 bond assisted by a N6-H···O interaction. Alternatively, the neutral form Hdap acts as bidentate ligands $\mu_2$-N3,N9 or $\mu_2$-N7,N9 using the tautomers H(N7)dap or H(N3)dap, respectively. Note that these metal binding

patters have been also established by complexes with neutral adenine. The dap(1-) anion behaves a unidentate ligand via N9 or as bidentate bridge $\mu_3$-N3,N7,N9. This latter coordination role does not imply the N1 coordination, which should be hindered by the relevant steric factor of the exocyclic amino groups in C2 and C6.

The tautomeric possibilities of 8aza-adenine seem to be remarkable, especially if we consider the reported cations (vide supra). This fact is also shown in the molecular form where H8aA can coordinate via N9, using the tautomer H(N1)8aA, or via M-N3, in one complex with the H(N9)8aA tautomer. This latter M-N3 bond is in cooperation with an intra-molecular H-bonding interaction N9-H···Cl. The 8aA(1-) anion can display N9-unidentate or $\mu_2$-N3,N9 bridging roles, whereas the 8aA-H(2-) anion is able to build the $\mu_3$-N1,N6,N9 mode in a methyl-mercury derivative, involving the exocyclic amino group in coordination. The deprotonation and coordination of the exocyclic amino group of adenine is well-known for metal ions, or related species, considered as soft Pearson acids.

## 6. Conclusions and Outlook.

The current available structural information about deaza-adenines, adenine isomers or aza-adenine ligands and, in particular, about their metal complexes, offers a very unbalanced and limited panorama. Nevertheless, from the gathered information, some general ideas can be derived. Thus, the increase of N-heterocyclic donors and their distribution within the bicyclic skeleton, as well as the presence or absence of exocyclic amino groups, are a group of factors that highly influence tautomerism phenomena but also the coordination abilities of the referred N-ligands. It bears noting that, in mixed-ligand complexes, those molecular recognition patterns that exhibit a coordination bond M-N(N-ligand) reinforced by an intra-molecular interligand interaction (N-H···A or D-H···N) are noticeably favoured. This is possible when the other coligands are/have appropriate H-acceptors and/or H-donors.

Lately, further developments on this subject are encouraged by the potential biological and/or therapeutical activity of these adenine-like ligands, their synthetic nucleosides or even some of their metal complexes. Moreover, the study of the molecular recognition patterns of deaza-adenines, adenine isomers or aza-adenines ligands is closely tied to the development of new biomaterials with promising physico-chemical applications. In particular, the use of the N-ligands as building blocks in Metal Organic Frameworks, such as ZIFs, is currently investigated with the aim of hosting or separating different guest molecules with certain selectivity.

## Acknowledgements

Financial support from Research Group FQM-283 (Junta de Andalucía) and MICINN-Spain (Project MAT2010-15594) is acknowledged. ADM gratefully acknowledges ME-Spain for a FPU Ph.D Contract.

## References

[1] B. Lippert, Coord. Chem. Rev. 200-202 (2000) 487.

[2] B. Lippert, in K.D. Karlin (Ed.), Progress in Inorganic Chemistry, vol. 54, Wiley, 2005 (Chapter 6).

[3] A. Terrón, J.J. Fiol, A. García-Raso, M. Barceló-Oliver, V. Moreno, Coord. Chem. Rev. 251 (2007) 1973.

[4] D. Choquesillo-Lazarte, M.P. Brandi-Blanco, I. García-Santos, J.M. González-Pérez, A. Castiñeiras, J. Niclós-Gutiérrez, Coord. Chem. Rev. 252 (2008) 1241.

[5] P.J. Sanz Miguel, P. Amo-Ochoa, O. Castillo, A. Houlton, F. Zamora, in N. Hadjiliadis y E. Sletten (Eds.), Metal complex-DNA interactions, Blackwell-Wiley, 2009 (Chapter 4).

[6] O. Castillo, A. Luque, J. P. García-Terán, P. Amo-Ochoa, in A.S. Abd-El-Aziz, Ch.E. Carraher, Ch.U. Pittman y M. Zeldin (Eds.), Macromolecules Containing Metal and Metal-Like Elements, vol. 9, Wiley, 2009 (Chapter 9).

[7] B. Lippert, in N.V. Hud (Ed.), Nucleic acid-metal ion interactions, RSC Publishing, 2009 (Chapter 2).

[8] S. Verma, A.K. Mishra, J. Kumar, Acc. Chem. Res. 43 (2010) 79.

[9] D.K. Patel, A. Domínguez-Martín, M.P. Brandi-Blanco, D. Choquesillo-Lazarte, V.M. Nurchi, J. Niclós-Gutiérrez, Coord. Chem. Rev. 256 (2012) 193.

[10] P. Dufour, Y. Dastiguenave, M. Dartiguenave, N. Dufour, A.M. Lebuis, F. Belanger-Gariepy, A.L. Beauchamp, Can. J. Chem. 68 (1990) 193.

[11] S.-B. Zhao, S. Wang, Chem. Soc. Rev. 39 (2010) 3142.

[12] W.S. Sheldrick, Z. Naturforsch. 37b (1982) 653.

[13] J. Poitras, M. Leduc, A.L. Beauchamp, Can. J. Chem. 71 (1993) 549.

[14] F. Focante, I. Camurati, L. Resconi, s. Guidotti, T. Beringhelli, G.D'Alonso, D. Dongui, D. Maggioni, P. Mercandelli, A. Sironi, Inorg. Chem. 45 (2006) 1683.

[15] A. Domínguez-Martín, D. Choquesillo-Lazarte, C. Sánchez de Medina-Revilla, J.M. González-Pérez, A. Castiñeiras, J. Niclós-Gutiérrez, in H. Kozlowski (Ed.), Proceeding of the 9th European Biological Inorganic Chemistry Conference (EUROBIC9), Medimond, 2008, pp. 105-108.

[16] A. Domínguez-Martín, D. Choquesillo-Lazarte, J.A. Dobado, I. Vidal, L. Lezama, J.M. González-Pérez, A. Castiñeiras, J. Niclós-Gutiérrez, Dalton Trans. (2012) *submitted*.

[17] D. Choquesillo-Lazarte, A. Domínguez-Martín, A. Matilla-Hernández, C. Sánchez de Medina-Revilla, J.M. González-Pérez, A. Castiñeiras, J. Niclós-Gutiérrez, Polyhedron 29 (2010) 170.

[18] J. Poitras, A.L. Beauchamp, Can. J. Chem. 72 (1994) 1675.

[19] Y. Kani, M. Tsuchimoto, S. Ohba, Acta Crystallogr. C56 (2000) e193.

[20] Md.S. Rahman, H.Q. Yuan, T. Kikuchi, I. Fujisawa, K. Aoki, J. Mol. Struct. 966 (2010) 92.

[21] F.A. Cotton, T.R. Felthouse, Inorg. Chem. 20 (1981) 600.

[22] B.R.A. Bland, H.J. Gilfoy, G. Vamvounis, K.N. Robertson, T.S. Cameron, M.A.S. Aquino, Inorg. Chim. Acta 358 (2005) 3927.

[23] J. Poitras, A.L. Beauchamp, Can. J. Chem. 70 (1992) 2846.

[24] A.M. Lebuis, A.L. Beauchamp, Acta Crystallogr. C50 (1994) 882.

[25] G.A. Van Albada, M.G. Van der Horst, I. Mutikainen, U. Turpeinen, J. Reedijk, Inorg. Chim. Acta 367 (2011) 15.

[26] G.A. Van Albada, M.G. Van der Horst, I. Mutikainen, U. Turpeinen, J. Reedijk, J. Mol. Struct. 995 (2011) 130.

[27] G.A. Van Albada, S. Tanase, I. Mutikainen, U. Turpeinen, J. Reedijk, Inorg. Chim. Acta 361 (2008) 1463.

[28] P. Starha, J. Marek, Z. Travnicek, Polyhedron 33 (2012) 404.

[29] Q. Wu, J.A. Lavigne, Y. Tao, M. D'lorio, S. Wang, Inorg. Chem. 39 (2000) 5248.

[30] A.M. Lebuis, A.L. Beauchamp, Can. J. Chem. 71 (1993) 2060.

[31] G.A. Van Albada, S. Nur, M.G. Van der Horst, I. Mutikainen, U. Turpeinen, J. Reedijk, J. Mol. Struct. 874 (2008) 41.

[32] S.-M. Peng, C.-H. Lai, J. Chin. Chem. Soc. 35 (1988) 325.

[33] G. Ferguson, C. Glidewell, Acta Crystallogr. E59 (2003) m710.

[34] J. Ruiz, V. Rodríguez, C. de Haro, A. Espinosa, J. Pérez, C. Janiak, Dalton Trans. 39 (2010) 3290.

[35] J. Ashenhurst, G. Wu, S. Wang, J. Am. Chem. Soc. 122 (2000) 2541.

[36] C.-K. Chan, C.-X. Guo, K.-K. Cheung, J. Chem. Soc., Dalton Trans. (1994) 3677.
[37] G.B. Deacon, E.E. Delbridge, B.W. Skelton, A.H. White, Eur. J. Inorg. Chem. (1999) 751.
[38] G.B. Deacon, E.E. Delbridge, G.D. Fallon, C. Jones, D.E. Hibbs, M.B. Hursthouse, B.W. Skelton, A.H. White, Organometallics 19 (2000) 1713.
[39] J.A. Cabeza, L.A. Oro, A. Tiripicchio, M. Tiripicchio-Camellini, J. Chem. Soc., Dalton Trans. (1988) 1437.
[40] S.-M. Peng, Y.-N. Lin, Acta Crystallogr. C42 (1986) 1725.
[41] G. Sánchez, F. Ruiz, J. García, M.C. Ramirez de Arellano, G. López, Helv. Chim. Acta 80 (1997) 2477.
[42] Y.-C. Chou, S.-F. Huang, R. Koner, G.-H. Lee, Y. Wang, S. Mohanta, H.-H. Wei, Inorg. Chem. 43 (2004) 2759.
[43] L.D. Popov, S.I. Levchenkov, I.N. Shcherbakov, V.V. Lukov, K.Y: Suponitsky, V.A. Kogan, Inorg. Chem. Commun. 17 (2012) 1.
[44] C.-F. Lee, K.-F. Chin, S.-M. Peng, C.-M. Che, J. Chem. Soc., Dalton Trans. (1993) 467.
[45] J.A. Bailey, V.M. Miskowski, H.B. Gray, Acta Crystallogr. C49 (1993) 793.
[46] F.-S. Kong, W.-T. Wong, J. Chem. Soc., Dalton Trans. (1997) 1237.
[47] J.M. Casas, J. Fornies, A. Martín, A.J. Rueda, Organometallics 21 (2002) 4560.
[48] J. A. Przyojski, N. N. Myers, H. D. Arman, M. Natarajan, A. Prosvirin, K. Dunbar, J. A. Walmsley J. Inorg. Biochem. (2013) in press.
[49] J. Ashenhurst, L. Brancaleon, A. Hassan, W. Liu, H. Schmider, S. Wang, Q. Wu, Organometallics 17 (1998) 3186.
[50] F.A. Cotton, D.G. Lay, M. Millar, Inorg. Chem.. 17 (1978) 186.
[51] F. Allaire, A.L. Beauchamp, Inorg. Chim. Acta 156 (1989) 241.
[52] L.A. Oro, M.A. Ciriano, B.E. Villarroya, A. Tiripicchio, F.J. Lahoz, J. Chem. Soc., Dalton Trans. (1985) 1891.
[53] J. Beck, M. Reitz, Z. Naturforsch. 52b (1997) 604.
[54] J.J.H. Edema, S. Gambarotta, A. Meetsma, F. Van Bolhuis, A.L. Spek, W.J.J. Smeets, Inorg. Chem. 29 (1990) 2147.
[55] F.A. Cotton, C.A. Murillo, H.-C. Zhou, Inorg. Chem. 39 (2000) 3728.
[56] M. Tayebani, K. Feghali, S. Gambarotta, G:P:A: Yap, Inorg. Chem. 40 (2001) 1399.
[57] M. Tayebani, K. Feghali, S. Gambarotta, G:P:A: Yap, L.K. Thompson, Angew. Chem., Int. Ed. 38 (1999) 3659.
[58] F.A. Cotton, J.H. Matonic, C.A. Murillo, J. Am. Chem. Soc. 120 (1998) 6047.
[59] F.A. Cotton, L.M. Daniels, C.A. Murillo, H.-C. Zhou, Inorg. Chim. Acta 300 (2000) 319.
[60] F.A. Cotton, L.R. Falvello, W. Wang, Inorg. Chim. Acta 261 (1997) 77.
[61] S. Yurdakul, S. Badoglu, Spectrochim. Acta A 89 (2012) 252.
[62] W. Uhl, M. Voss, J. Muler, K. Seubert, Chem.-Eur. J. 17 (2011) 7582.
[63] J. Muller, F.-A. Polonius, E. Freisinger, E.G. Bardaji, Carbohydr. Res. 343 (2008) 397.
[64] E. Serrano-Padial, D. Choquesillo-Lazarte, E. Bugella-Altamirano, A. Castiñeiras, R. Carballo and J. Niclós-Gutiérrez, Polyhedron 21 (2002) 1451.
[65] G.A. Van Albada, I. Mutikainen, U. Turpeinen, J. Reedijk, Polyhedron 25 (2006) 3278.
[66] C. Sánchez de Medina-Revilla, D. Choquesillo-Lazarte, A. Domínguez-Martín J.M. González-Pérez, A. Castiñeiras, J. Niclós-Gutiérrez, in H. Kozlowski (Ed.), Proceeding of the 9th European Biological Inorganic Chemistry Conference (EUROBIC9), Medimond, 2008, pp. 101-104.
[67] S.J. Rettig, V. Sánchez, A. Storr, R.C. Thompson, J. Trotter, J. Chem. Soc., Dalton Trans. (2000) 3931.
[68] H. Hayashi, A.P. Cote, H. Furukawa, M. O'Keeffe, O.M. Yagui, Nat. Mater. 6 (2007) 501.
[69] P. X. Rojas-González, A. Castiñeiras, J. M. González-Pérez, D. Choquesillo-Lazarte, J. Niclós-Gutiérrez, Inorg. Chem. 41 (2002) 6190.

[70] J. Abola, M. Sundaralingam, Acta Crystallogr. B29 (1973) 697.
[71] V. Zabel, W. Saenger, F. Seela, Acta Crystallogr. C43 (1987) 131.
[72] R. McKenna, R. Kuroda, S. Neidle, P. Serafinowski, Acta Crystallogr. C43 (1987) 1790.
[73] G. J. Gainsford, R. F. G. Frohlich, G. B. Evans, Acta Crystallogr. E66 (2010) o1688.
[74] A.B. Eldrup, M. Prhavc, J. Brooks, B. Bhat, T.P. Prakash, Q. Song, S. Bera, N. Bhat, P. Dande, P.D. Cook, C.F. Bennett, S.S. Carroll, R.G. Ball, M. Bosserman, C. Burlein, L.F. Colwell, J.F. Fay, O.A. Flores, K. Getty, R.L. LaFemina, J. Leone, M. MacCoss, D.R. McMasters, J.E. Tomassini, D. Von Languen, B. Wolanski, D.B. Olsen, J. Med. Chem. 41 (2004) 5284.
[75] S. Das, C. Madhavaiah, S. Verma, P.K. Bharadwaj, Inorg. Chim. Acta 358 (2005) 3236.
[76] D.G. Watson, R.M. Sweet, R.E. Marsh, Acta Crystallogr. 19 (1965) 573.
[77] A. Itai, H. Yamada, T. Okamoto, Y. Iitaka, Acta Crystallogr. B33 (1977) 1816.
[78] G. Valle, G. Plazzogna, R. Ettorre, J. Chem. Soc., Dalton Trans. (1985) 1271.
[79] T. Takeda, Y. Ohashi, y. Sasada, Acta Crystallogr. B30 (1974) 825.
[80] T. Ma, J.-S. Lin, M.G. Newton, Y.-C. Cheng, C.K. Chu, J. Med. Chem. 40 (1997) 2750.
[81] M. Nissinen, S. Kiviniemi, K. Rissanen, J. Pursiainen, CrystEngComm 2 (2000) 102.
[82] A. Cadiau, K. Adil, A. Hemon-Ribaud, M. Leblanc, A. Jouanneaux, A.M.Z. Slawin, P. Lightfoot, V. Maisonneuve, Solid State Sci. 13 (2011) 151.
[83] E. Sletten, J. Sletten, N.A. Froystein, Acta Chem. Scand. A 42 (1988) 413.
[84] W.S. Sheldrick, Acta Crystallogr. B37 (1981) 945.
[85] J.P. García-Terán, O. Castillo, A. Luque, U. García-Couceiro, G. Beobide, P. Román, Dalton Trans. (2006) 902.
[86] J.P. García-Terán, O. Castillo, A. Luque, U. García-Couceiro, P. Román, F. Lloret, Inorg. Chem. 43 (2004) 5761.
[87] H.L. Laity, M.R. Taylor, Acta Crystallogr. C51 (1995) 1791.
[88] P. Nockemann, F. Schulz, D. Naumann, G. Meyer, Z. Anorg. Allg. Chem. 631 (2005) 649.
[89] P.I. Vestues, E. Sletten, Inorg. Chim. Acta 52 (1981) 269.
[90] A.L. Beauchamp, D. Cozak, A. Mardhy, Inorg. Chim. Acta 92 (1984) 191.
[91] U.E.I. Horvath, S. Cronje, J.M. McKenzie, L.J. Barbour, H.G. Raubenheimer, Z. Naturforsch. 59 (2004) 1605.
[92] A. Cadiau, K. Adil, Acta Crystallogr. E68 (2012) m449.
[93] A. Steffen, T. Braun, B. Neumann, H.-G. Stammler, Angew. Chem., Int. Ed. 46 (2007) 8674.
[94] J. Kahr, J.P.S. Mowat, A.M.Z. Slawin, R.E. Morris, D. Fairen-Jimenez, P.A. Wright, Chem. Commun. 48 (2012) 6690.
[95] R.K. Neely, S.W. Magennis, S. Parsons, A.C. Jones, ChemPhysChem 8 (2007) 1095.
[96] R. Ramaekers, L. Adamowicz, G. Maes, Eur. Phys. J. D. 20 (2002) 375.
[97] M.R. Harnden, R.L. Jarvest, A.M.Z. Slawin, D.J. Williams, Nucleos. Nucleot. 9 (1990) 499.
[98] A. Domínguez-Martín, D. Choquesillo-Lazarte, J.M. González-Pérez, A. Castiñeiras, J. Niclós-Gutiérrez, J. Inorg. Biochem. 105 (2011) 1073.
[99] E. Bugella-Altamirano, D. Choquesillo-Lazarte, J.M. González-Pérez, M.J. Sánchez-Moreno, R. Marín-Sánchez, J.D. Martín-Ramos, B. Covelo, R. Carballo, A. Castiñeiras, J. Niclós-Gutiérrez, Inorg. Chim. Acta 399 (2002) 160.
[100] G. Dodin, M. Dreyfus, O. Bensaude, J.-E. Dubois, J. Am. Chem. Soc. 99 (1977) 7257.
[101] S. Sprang, R. Scheller, D. Rohrer, M. Sundaralingam, J. Am. Chem. Soc. 100 (1978) 2867.
[102] F. Seela, M. Zulauf, H. Reuter, G. Kastner, Acta Crystallogr. C55 (1999) 1947.
[103] W.S. Sheldrick, P. Bell, H.-J. Hausler, Inorg. Chim. Acta 163 (1989) 181.
[104] A. Domínguez-Martín, D. Choquesillo-Lazarte, J.A. Dobado, H. Martínez-García, L.

# CHAPTER 1:

Copper(II) complexes with deaza-adenine ligands

## 1.1. Looking 7-azaindole as 1,6,7-trideazaadenine for Metal-complex Formation: Structure of [Cu(IDA)(H7azain)]n

Published in *Proceedings of the 9th European Biological Inorganic Chemistry Conference*, (EUROBIC9), Ed. Henryk Kozlowski - Medimond, Wroclaw, 2008, pp. 105-108.

SYNOPSIS

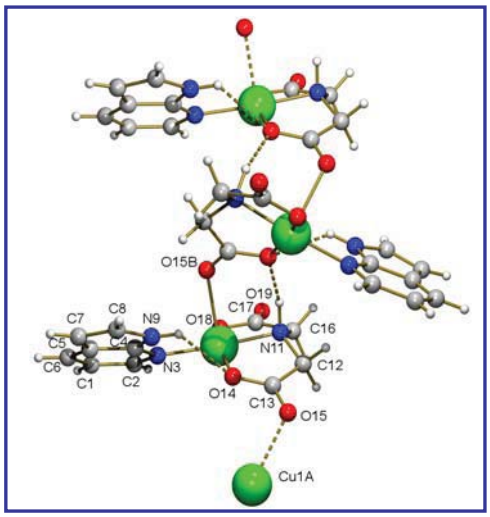


7-azaindole (H7azain) can be looked as 1,6,7-trideaza-adenine. The crystal structures reveal that H7azain always binds the copper(II) centre via Cu-N3 bonds. We report the structure of $[Cu(IDA)(H7azain)]_n$, where the Cu-N3(HL) bond is reinforced by an intra-molecular H-bonding interaction. The new compound grows as a polymer due to a syn-anti carboxylate bridge also reinforced by (IDA)N-H····O(IDA) intra-chain interactions along the b axis.

RESUMEN

7-azaindol (H7azain or HL) puede considerarse como una 1,6,7-trideaza-adenina. Las estructuras cristalinas disponibles revelan que uno, dos o cuatro HL pueden coordinarse al mismo centro de cobre ocupando posiciones tanto ecuatoriales como apicales, en todos los casos formando el enlace Cu-N3. En este trabajo se presenta la estructura $[Cu(IDA)(HL)]_n$ (293 K, monoclinic system, space group $P2_1$, $R_1$ 0.026), donde el enlace Cu-N3(HL, 1.992(2) Å) está reforzado por un enlace de hidrógeno intra-molecular (HL)N9-H···O(IDA, 2.88 Å, 120.7º). Un modo de reconocimiento molecular similar (Cu-N3 + refuerzo por enlace de hidrógeno) se ha observado en complejos ternarios Cu(II)-acetato-HL. El compuesto reportado es un polímero cuyas cadenas crecen a lo largo del eje b debido a la función puente 'syn-anti' de los grupos carboxilato. Además, la cadena esta intra-estabilizada por interacciones NH(IDA)····O(IDA vecino, 2.92 Å, 155.5º).

# Looking 7-azaindole as 1,6,7-trideazaadenine for Metal-complex Formation: Structure of $[Cu(IDA)(H7azain)]_n$

**A. Domínguez-Martín[1], D. Choquesillo-Lazarte[2], C. Sánchez de Medina-Revilla[1], J.M. González-Pérez[1], A. Castiñeiras[3] and J. Niclós-Gutiérrez[1]**

*[1]Department of Inorganic Chemistry, Faculty of Pharmacy, University of Granada, E-18071 Granada, Spain. E-mail: jmgp@ugr.es, jniclos@ugr.es*
*[2]IACT-CSIC, Laboratorio de Estudios Cristalográficos, Edif. Inst. Lopez-Neyra, PTCS. Avda. del Conocimiento, s/n. E-18100 Armilla (Granada), Spain. E-mail: duanec@ugr.es*
*[3]Department of Inorganic Chemistry, Faculty of Pharmacy, University of Santiago de Compostela, E-15782 Santiago de Compostela, Spain. E-mail: qiac01@usc.es*

## Summary

7-azaindole (H7azain or HL) can be looked as 1,6,7-trideaza-adenine. The crystal structures reveal that one, two or four HL can be coordinated to the same Cu(II) centre occupying equatorial or apical sites, in all cases forming Cu-N3 bonds. We report the structure of $[Cu(IDA)(HL)]_n$ (293 K, monoclinic system, space group $P2_1$, final $R_1$ 0.026), where the Cu-N3(HL) bond (1.992(2) Å) is reinforced by one intra-molecular L-H···O(IDA) interaction (2.88 Å, 120.7º). A similar recognition mode Cu-N3 + H-bonding interaction exist in ternary Cu(II)-acetate-HL complexes. The new compound grows as a polymer due to a *syn,anti*-carboxylate bridge, which is also reinforced by a N-H(IDA)···O(adjacent IDA) interaction (2.92 Å, 155.5º) between adjacent complex units in the chain, extending along the *b* axis.

## Introduction

7-azaindole is a $N_2$-heterocycle that is able to form salts of its $H_2L^+$ cation or complexes of HL or $L^-$ species. More than 150 structures concerning this ligand are deposited in the CSD data-base. It can be looked as a 1,6,7-trideaza-adenine where, according to the conventional numbering of Hade, the N-pyridine and the N-pyrrole donors should by re-numbered as N3 and N9,

 

respectively. The anionic form has been broadly used as binucleating $\mu_2$-N3,N9-L ligand, in some cases to promote metal-metal bonds. The neutral molecule HL only acts as unidentate. In a variety of compounds, $Cu^{II}$, $Zn^{II}$, $Rh^{II}$, $Hg^{II}$, $Rh^{II,III}$, $B^{III}$, $Nb^{V}$ and $Re^{v}$ bind towards M-N3(HL) bond to the tautomer H(N9)azain, which is also recognized in the crystal of free HL. In contrast, a derivative of $CH_3Hg^+$ and three $Al^{III}$ complexes have the H(N3)azain tautomer and M-N9(HL) coordination bond.

The aim of this work is to study the recognition mode between the Cu(II) iminodiacetate chelate, Cu(IDA), and H7azain. We can expect two possibilities (Fig. 1): A) the coordination mode involving the (IDA)Cu-N3 bond with one N9-H···O(IDA) interaction. B) the formation of a (IDA)Cu-N9 bond with one N3-H···O(IDA) interaction.

## Materials, methods and supplementary structural information

H7azain, $H_2IDA$ and bluish $Cu_2(CO_3)(OH)_2$ were purchased to Aldrich or Probus, and used as received. The Cu(IDA) chelate was obtained in solution by reaction of the $Cu^{II}$ salt (0.5 mmol) and $H_2IDA$ (1mmol) in water (100 ml) with heating, stirring and vacuum to remove $CO_2$ (by-product). To this solution H7azain (1 mmol) was added, with stirring until a blue solution was obtained. By slow evaporation, many suitable single crystals were obtained. The structural data were taken on a Bruker 8 Proteum diffractometer: 293(2) K, l 1.54178 Å, monoclinic system, space group $P2_1$, final $R_1$ 0.026; results deposited at the Cambridge Crystallographic Data Centre with CCDC No. 695578. The infrared spectra (KBr pellet, Jasco FT–IR 410 spectrophotometer) and TG analysis in air-dried flow (Shimadzu Thermobalance TGA–DTG–50H coupled to a FT-IR Nicolet Magma 550 spectrometer) are available.

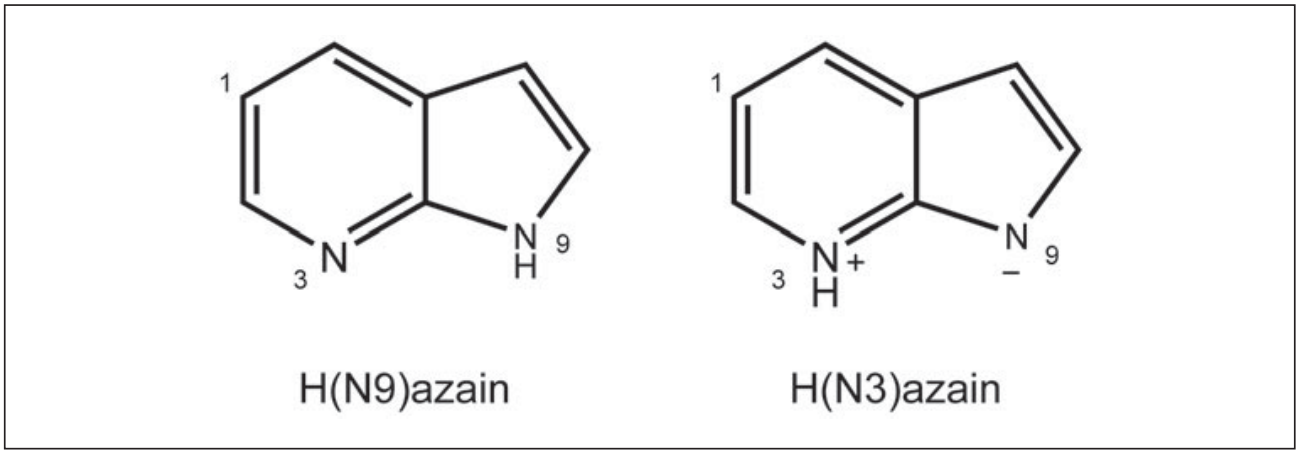


*Figure 1. The two tautomers of neutral 7-azaindole (H7azain) re-numbered as a 1,6,7-trideaza-adenine, supposedly able to bind the Cu(IDA) chelate by means of a Cu-N(3 or 9) coordination bond plus a possible N(9 or 3)-H···A(acceptor) interligand interaction, respectively.*

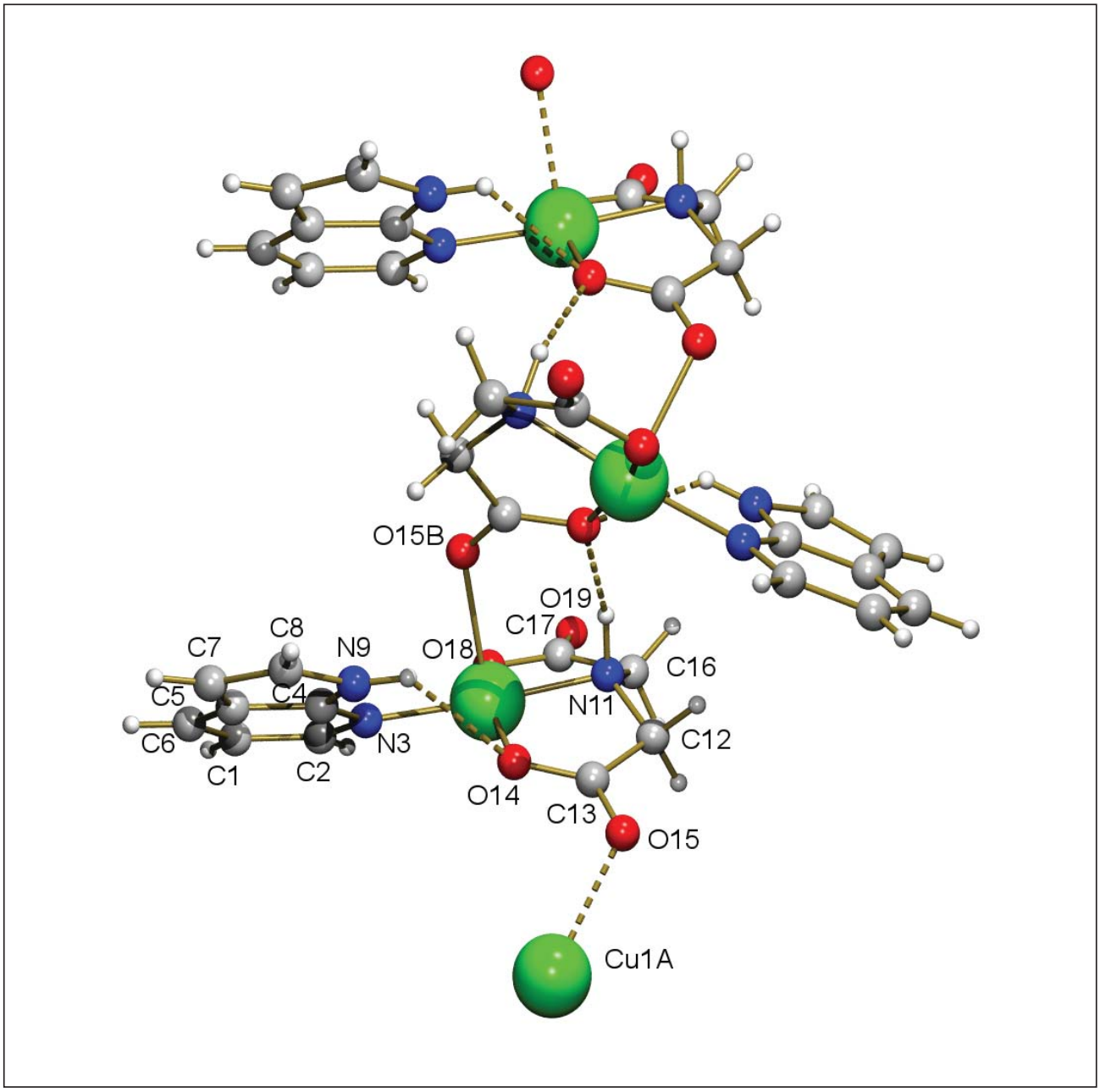


*Figure 2. Fragment of the polymer [Cu(IDA)(H(N9)-azain)]$_n$ . Bond lengths (‘),* trans-*coordination angles (°) and* $\tau = (\theta-\psi)/60$ *value: Cu1-O18 1.951(2), Cu1-O14 1.955(2), Cu1-N11 1.979(2), Cu1-N3 1.992(2), Cu1-O15 2.410(2),* $\theta$ *= N11-Cu1-N3 175.4(1),* $\psi$ *= O18-Cu1-O14 162.1(1);* $\tau$ *0.22. Relevant H-bonding interactions: N9-H9···O14 (2.884(3) Å 120.7°), N11-H11···O14B (2.924(3) Å, 155.5°). Cu$_A$···Cu = Cu···Cu$_B$ 5.270(1) Å. Symmetry tranformations: A = -x+1,y-1/2,-z+1; B = -x+1, y+1/2, -z+1.*

## Results and discussion

The crystal structure solution revealed that the studied compound is a polymer and consist of chains $[Cu(IDA)(H(N9)\text{-azain})]_n$ (Fig. 2) extending along the b axis. Each $Cu^{II}$ atom exhibits a distorted square base pyramidal coordination, type 4+1. The four closest donor atoms are supplied by the tridentate chelating IDA, in the expectable *mer*-$NO_2$ conformation, and the

N3 atom of the most stable tautomer H(N9)-azain. The polymeric nature of the compound in the crystal is due to the bridging role of one carboxylate group oh IDA, which adopts a *syn*,*anti*-conformation. Thus, one O donor of the bridging carboxylate group not involved in chelation occupies the fifth apical/distal coordination site in the $Cu^{II}$ surrounding.

In the novel compound, two H-bonding interactions are of special relevance (see Fig. 2). One is the intra-molecular interligand interaction, (H7azain) N9-H9···O14(chelating, IDA), which reinforces the Cu-H3(H(N9)azain) coordination bond. The other one, (IDA)N11-H11···O14B(adjacent IDA), cooperates with the bridging carboxylate group to the stability of the polymeric complex chain. Thus each O14 acts twice as acceptor atom to H-bonding interactions.

The FT-IR spectrum shows two broad and medium intensity bands (3300 and 2200 $cm^{-1}$) of ν(N-H) modes. The corresponding bending bands, δ(N-H), appear near to 1550 and 1515 $cm^{-1}$, as two typically weak peaks, but with a remarkable diagnostic value. The $\nu_{as}$ and $\nu_{s}$ bands (1624 and 1382 $cm^{-1}$) do not distinguish the two kinds ($\mu_2$-*syn,anti*-bridging and monodentate) of carboxylate chromophores. The aromaticity is evidenced in series of weak peaks in the 2000-1800 $cm^{-1}$ as well as a defined and intense band at 730 $cm^{-1}$ due to the out-of-plane aromatic C-H deformation. In air-dry flow, the non-hydrated polymer is stable below 200 ºC. It decomposes in two pyrolytic steps. The first one (200 to 315ºC) produces $CO_2$, $H_2O$, CO and $N_2O$; and the latter step (315-475ºC) gives $H_2O$, $CO_2$ and three nitrogen oxides ($N_2O$, NO and $NO_2$). Finally, about 475ºC, a residue of CuO should be formed (exp. 27.029%; calc. 25.433%).

## Concluding remark

We can conclude that H7azain recognized the Cu(IDA) chelate as the free adenine recognize a family of Cu(N-benzyl-IDA-like) chelates (with the formation of a $Cu^{II}$-N3 coordination bond and a N9-H···O(coordinated) interaction [1], but without developing inter-molecular π,π-staking interactions.

## References

[1] D. CHOQUESILLO-LAZARTE, M.P. BRANDI-BLANCO, I. GARCÍA-SANTOS, J. M. GONZÁLEZ PÉREZ, A. CASTIÑEIRAS, J. NICLÓS-GUTIÉRREZ, Interligand interactions involved in the molecular recognition between copper(II) complexes and adenine or related purines, Coord. Chem. Rev., 252, 1241-1256, 2008, and references therein.

## Acknowledgements

Financial support: Project CTQ2006-15329-C02/BQU (ERDF-EC, MEC-Spain). ADM thanks to the MEC for a Collaboration grant. CSMR thanks to the CACOF for a research grant. DChL thanks CSIC-EU for an I3P postdoctoral research contract. The "Factoría de Cristalización, CONSOLIDER INGENIO-2010" provided X-ray diffraction facilities.

## 1.2. Restricting the versatile metal-binding behaviour of adenine by using deaza-purine ligands in mixed-ligand copper(II) complexes

Article published in *Polyhedron* 29 (2010) 170-177

SYNOPSIS

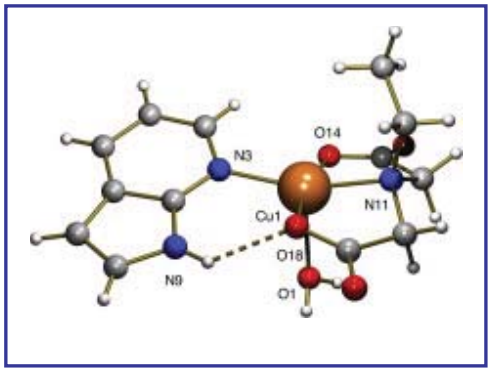


The crystal structures of four novel ternary copper(II) compounds having 4-aza-benzimidazole or 7-azaindole (as N1,N6-dideaza-adenine or N1,N6,N7-trideaza-adenine, respectively) are reported. Both deaza-adenines partially simulate the role of adenine in related complexes but the crystal packing of one of these compounds influences the binding mode of the purine-like ligand.

RESUMEN

Con el objeto de ampliar nuestro conocimiento sobre las razones que hacen de adenina (Hade) un ligando de gran versatilidad coordinante, se han sintetizado cuatro nuevos compuestos ternarios de cobre(II) conteniendo dos ligandos tipo deaza-adenina: 4-azabencimidazol (H4abim) o 7-azaindol (H7azain), entendidos como N1,N6-dideaza-adenina o N1,N6,N7-trideaza-adenina respectivamente. Dichos compuestos han sido estudiados mediante métodos térmicos, espectrales y cristalografía de Rayos-X. En $[Cu(NBzIDA)(H4abim)]_n$ (**1**), el reconocimiento entre H4abim y el quelato de N-benciliminodiacetato de cobre(II) sólo muestra la formación de un enlace Cu–N7(tipo purina), en contra de de lo observado para Hade en $[Cu(NBzIDA)(Hade)(H_2O)]\cdot H_2O$, donde el enlace Cu–N3(Hade) está reforzado mediante el enlace de hidrógeno N9–H···O(NBzIDA). Por otro lado, en $[Cu(EIDA)(H7azain)(H_2O)]$ (**2**, EIDA = N-etiliminodiacetato), $[Cu(NBzIDA)(H7azain)(H_2O)]$ (**3**) y $[Cu(\mu_2\text{-}SO_4)(H7azain)_2(H_2O)_2]_n$ (**4**), H7azain se une al centro de cobre(II) mediante el enlace Cu–N3(tipo purina), reforzado por una interacción intra-molecular interligandos N9–H···O(tipo IDA o sulfato).

Polyhedron 29 (2010) 170–177

Contents lists available at ScienceDirect

Polyhedron

journal homepage: www.elsevier.com/locate/poly

# Restricting the versatile metal-binding behaviour of adenine by using deaza-purine ligands in mixed-ligand copper(II) complexes

Duane Choquesillo-Lazarte [a,*], Alicia Domínguez-Martín [b], Antonio Matilla-Hernández [b], Celia Sánchez de Medina-Revilla [b], Josefa María González-Pérez [b], Alfonso Castiñeiras [c], Juan Niclós-Gutiérrez [b]

[a] Laboratorio de Estudios Cristalográficos, IACT-CSIC, Avda. del Conocimiento s/n, E-18100 Armilla (Granada), Spain
[b] Department of Inorganic Chemistry, Faculty of Pharmacy, University of Granada, E-18071 Granada, Spain
[c] Department of Inorganic Chemistry, Faculty of Pharmacy, University of Santiago de Compostela, E-15782 Santiago de Compostela, Spain

ARTICLE INFO

*Article history:*
Available online 27 June 2009

*Keywords:*
Copper(II)
Mixed-ligand
Iminodiacetate
Deaza-purines
Crystal structure
H-bonding interactions

ABSTRACT

In order to deepen our understanding of the versatile behaviour of adenine (Hade) as ligand, we have synthesized four novel ternary copper(II) complexes having two deazaadenine ligands, namely 4-azabenzimidazole (H4abim) or 7-azaindole (H7azain) as N1,N6-dideazaadenine or N1,N6,N7-trideazaadenine, respectively. The related compounds were studied by thermal, spectral and single crystal X-ray diffraction methods. In $[Cu(NBzIDA)(H4abim)]_n$ (**1**) the recognition between H4abim and the (*N*-benzyliminodiacetate)-copper(II) chelate only displays the formation of the Cu–N7(purine-like) bond, in contrast to Hade behaviour in $[Cu(NBzIDA\text{-like})(Hade)(H_2O)]\cdot H_2O$ (Cu–N3(Hade) bond reinforced by N9–H···O(IDA-like) interaction). In $[Cu(EIDA)(H7azain)(H_2O)]$ (**2**, EIDA = *N*-ethyliminodiacetate ligand), $[Cu(NBzIDA)(H7azain)(H_2O)]$ (**3**) and $[Cu(\mu_2\text{-}SO_4)(H7azain)_2(H_2O)_2]_n$ (**4**), H7azain binds Cu(II) centre by the Cu–N3(purine-like) bond, reinforced by a N9–H···O(IDA-like or sulfate) intra-molecular interligand interaction.



## 1. Introduction

In recent years, much effort has been made to rationalize the metal-binding modes of nucleobases and their derivatives [1]. In this context, adenine (Hade) has proved to display a remarkable versatile behaviour in ternary copper(II) complexes having iminodiacetate (IDA) or *N*-substituted-IDA ligands [2–6], as well as glycyl–glycinate and other dipeptide ligands [7,8]. In these complexes, the molecular recognition between Hade and different copper(II) chelates are featured by a Cu–N(Hade) bond and an intra-molecular interligand (Hade)N–H···O(coordinated, IDA-like or glygly) interaction. For example, Cu(N-alkyl-IDA) chelates bind Hade by the Cu–N7 bond reinforced by a N6–H···O interaction; in these crystals, pairs of complex molecules stack Hade bases by a π,π-interaction [2,3]. On the other hand, Cu(N-benzylIDA) chelates and Hade exhibits a Cu–N3 bond and a N9–H···O interaction. In this time, crystals build multi-stacked chains by means of benzyl-(adjacent Hade) π,π-stacking [2,4]. Curiously, the reaction of Cu(NBzIDA) chelate and the adenine:thymine base-pair yields the binuclear compound $[Cu_2(NBzIDA)_2(H_2O)_2(\mu\text{-N7,N9-Hade})]$ with the unusual tautomer H(N3)ade acting as a $\mu_2$-bridging ligand, with Cu–N7 and Cu–N9 bonds, reinforced by N6–H···O and N3–H···O interactions. No π,π-stacking interactions are observed [6]. A recent paper [9] has reported a unique compound where the adeninate(1−) anion plays a $\mu_4$-N1,N3,N7,N9-ade role as bridging ligand between four Cu(II) centres.

As a part of our research, we have been working on ternary Cu(II) complexes having deaza-adenines as ligands (see Fig. 1). In this regard, we have reported our results on $[Cu_2(\mu\text{-N3,N9-H4abim})_4(SO_4)_2]\cdot 11H_2O$ [10] (a molecular compound closely related to the salts $[Cu_2(\mu\text{-N3,N9-H4abim})_4X_2]\cdot X_2$ (X = Cl, Br) [11]) and $[Cu(IDA)(H7azain)]_n$ [12], a polymer where the Cu–N3 bond is reinforced by the N9–H···O(coordinated, IDA) interaction.

The information about H4abim is rather limited but clearly reveals that it is able to bind dinuclear Cu(II) complexes with four bridging μ-N3,N9-(H4abim) moieties, very similar to μ-N3,N9-(Hade) role in $[Cu_2(\mu\text{-Hade})_4(H_2O)_2](ClO_4)_4\cdot H_2O$ [13] or μ-N3,N9-ade in $[Cu_2(\mu_2\text{-ade})_4(H_2O)_2]\cdot 7H_2O$ [14,15] and a related hexa-copper(II) derivative [15]. However, $\mu_2$-N7,N9-abim(1−) role is known in polymers of Fe(II) [16] and Zn(II) [17]. We have not found structural information of metal complexes with monodentate H4abim ligands.

It has been referred plenty of Cu(II) complexes with $Cu_2$(μ-N3,N9-7azain) bridges [18–20] and also with Cu–N3(H7azain) bonds [21,22] or only having Cu–N3(H7azain) bonds [23–25]

* Corresponding author.
*E-mail address:* duanec@ugr.es (D. Choquesillo-Lazarte).

0277-5387/$ - see front matter © 2009 Elsevier Ltd. All rights reserved.
doi:10.1016/j.poly.2009.06.054

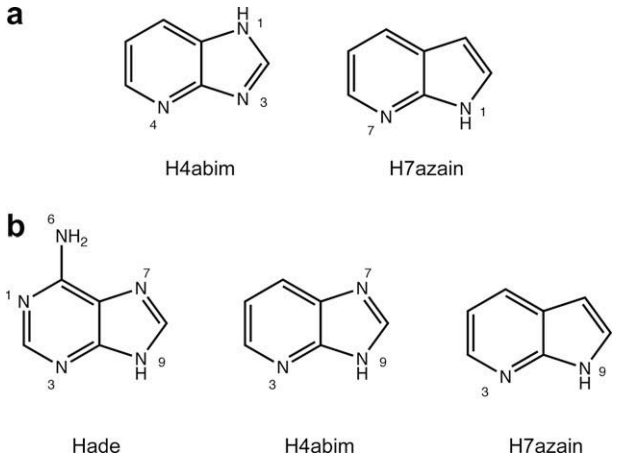


**Fig. 1.** Deaza-adenines used in this work, with the notation (a) as 4-azabenzimidazole or 7-azaindole and (b) as purine-like conventional numbering related to the adenine.

reinforced by N9–H···X(acceptor) interactions (X = O [21,22], F [24] or Cl [23–25]). A noticeable and recent example of this latter behaviour is found in $[Cu(H7azain)_4F]BF_4{\cdot}H_2O$ [24], where all four H7azain ligands reinforce the Cu–N3 bond with a intra-molecular N9–H···F interactions (2.69 Å, 147.5°).

Biological and therapeutic activities of a large variety of purine ligands or some purine-like metal complexes are well known and extensively documented. Most of them are as metallo-enzyme inhibitors as well as anti-viral and/or anti-cancer drugs or pre-drugs [1]. In recent years, biological activities of some deaza-purines have focused a lot of attention, among them, 4-azabenzimidazole derivatives [26] as well as 7-azaindole derivatives [27,28]. For example, some 7-azaindole-nucleosides have anti-viral properties [27] and other ones have been studied as synthetic cytokinin analogues [28].

## 2. Experimental

### 2.1. Materials

All reagents are commercially available and were purchased from Sigma–Aldrich.

**Table 2**
Selected interatomic bonds lengths (A) and *trans* angles (°) in compounds **1**–**4**.

| Lengths | Angles | Lengths | Angles |
|---|---|---|---|
| ***1*** | | | |
| Cu1–O11 | 1.9537(14) | O11–Cu1–O21 | 168.11(6) |
| Cu1–O21 | 1.9601(14) | N7–Cu1–N10 | 168.00(7) |
| Cu1–N7 | 1.9624(17) | | |
| Cu1–N10 | 2.0060(16) | | |
| Cu1–O22#1 | 2.2798(14) | | |
| #1 $-x+1, y+1/2, -z+1/2$ | | | |
| ***2*** | | | |
| Cu1–O14 | 1.9447(16) | N3–Cu1–N11 | 160.43(7) |
| Cu1–O18 | 1.9680(15) | O14–Cu1–O18 | 167.49(6) |
| Cu1–N3 | 1.9945(19) | | |
| Cu1–N11 | 2.0124(16) | | |
| Cu1–O1 | 2.2805(15) | | |
| ***3*** | | | |
| Cu1–O18 | 1.9403(16) | O18–Cu1–O14 | 168.54(7) |
| Cu1–O14 | 1.9663(16) | N3–Cu1–N11 | 157.05(8) |
| Cu1–N3 | 1.996(2) | | |
| Cu1–N11 | 2.0194(19) | | |
| Cu1–O1 | 2.2748(17) | | |
| ***4*** | | | |
| Cu1–O10 | 1.985(2) | O10#1–Cu1–N3 | 173.49(11) |
| Cu1–O10#1 | 1.985(2) | O10–Cu1–N3#1 | 173.49(11) |
| Cu1–N3 | 2.009(3) | O1–Cu1–O1#1 | 166.00(8) |
| Cu1–N3#1 | 2.009(3) | | |
| Cu1–O1 | 2.478(2) | | |
| Cu1–O1#1 | 2.478(2) | | |
| #1 $-x, y, -z+3/2$ | | | |

### 2.2. Synthesis of compounds

$[Cu(NBzIDA)(H4abim)]_n$ (**1**), [Cu(EIDA)(H7azain)($H_2O$)] (**2**) and [Cu(NBzIDA)(H7azain)($H_2O$)] (**3**) were prepared following a general procedure which could be described as: $Cu_2CO_3(OH)_2$ (0.25 mmol, 0.0553 g) was reacted in 80 mL of distilled water with the appropriate N-substituted iminodiacetic acid (0.5 mmol) in a Kitasato flask, by heating (50 °C) and stirring under vacuum (water pump) in order to remove $CO_2$, a by-product of the reaction. Once obtain a clear blue solution, H4abim (0.5 mmol, 0.06 g) (**1**) or H7azain (0.5 mmol, 0.059 g) (**2** and **3**) were added, respectively. The reacting mixtures were stirred until the ligands were completely dissolved, approximately half an hour in case of

**Table 1**
Crystal and structure refinement data.

| Compound | **1** | **2** | **3** | **4** |
|---|---|---|---|---|
| Empirical formula | $C_{17}H_{16}CuN_4O_4$ | $C_{13}H_{17}CuN_3O_5$ | $C_{18}H_{19}CuN_3O_5$ | $C_{14}H_{16}CuN_4O_6S$ |
| Formula weight | 403.88 | 358.84 | 420.90 | 431.91 |
| Crystal system | monoclinic | orthorhombic | monoclinic | orthorhombic |
| Space group | $P2_1/c$ | *Pbca* | $P2_1/c$ | *Pbcn* |
| *Unit cell dimensions* | | | | |
| $a$ (Å) | 12.8288(4) | 10.44350(10) | 11.503(2) | 17.4233(4) |
| $b$ (Å) | 8.1099(3) | 10.64250(10) | 8.2259(16) | 14.7918(4) |
| $c$ (Å) | 18.0022(7) | 27.1157(3) | 18.337(4) | 6.8851(2) |
| $\alpha$ (°) | 90 | 90 | 90 | 90 |
| $\beta$ (°) | 103.4870(10) | 90 | 94.484(3) | 90 |
| $\gamma$ (°) | 90 | 90 | 90 | 90 |
| $V$ (Å$^3$) | 1821.30(11) | 3013.74(5) | 1729.8(6) | 1774.44(8) |
| $Z$ | 4 | 8 | 4 | 4 |
| $\rho_{calc}$ (g cm$^{-3}$) | 1.473 | 1.582 | 1.616 | 1.617 |
| $F$(0 0 0) | 828 | 1480 | 868 | 884 |
| Crystal size (mm) | 0.34 × 0.20 × 0.04 | 0.42 × 0.40 × 0.08 | 0.36 × 0.18 × 0.10 | 0.10 × 0.06 × 0.04 |
| θ Range (°) | 1.63–26.02 | 8.49–66.24 | 1.78–26.37 | 7.86–66.25 |
| Reflections collected | 24 542 | 36 778 | 3535 | 21 722 |
| Independent reflections | 3585 | 2448 | 3535 | 1544 |
| Maximum/minimum transmission | 0.9525–0.6801 | 0.8370–0.4442 | 0.8810–0.6519 | 0.8824–0.7398 |
| Goodness-of-fit (GOF) on $F^2$ | 1.068 | 1.028 | 1.057 | 1.058 |
| Final $R$ indices [$I > 2\sigma(I)$] | $R_1$ = 0.0290 | $R_1$ = 0.0369 | $R_1$ = 0.0314 | $R_1$ = 0.0464 |
| | $wR_2$ = 0.699 | $wR_2$ = 0.1057 | $wR_2$ = 0.0748 | $wR_2$ = 0.1193 |

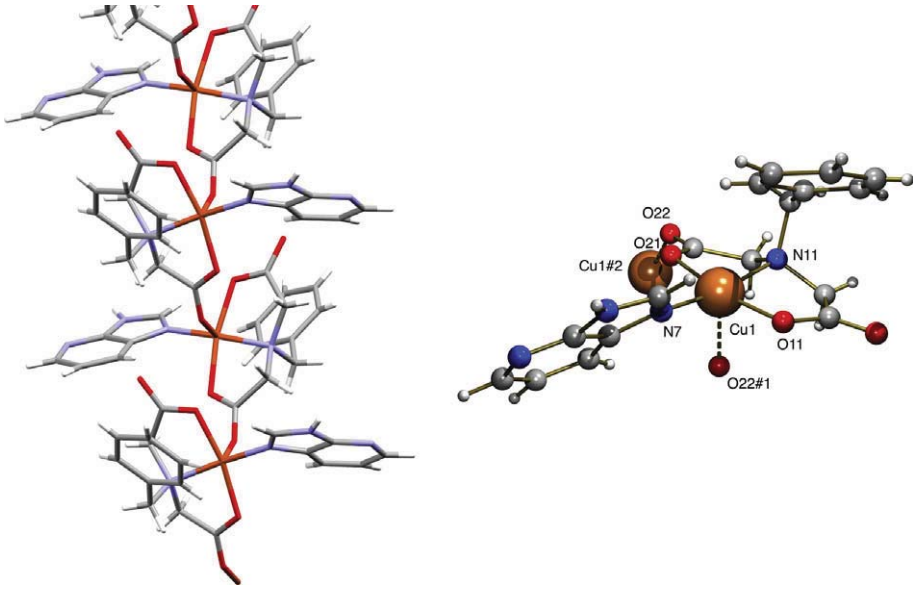


**Fig. 2.** Structure of $[Cu(NBzIDA)(H4abim)]_n$ (**1**). Left: coordination polymer running along the *b* axis. Right: detail of the numeration scheme of the coordination environment in **1**.

H4abim while H7azain needed nearly an hour. Only with H4abim, an intensification of the colour was observed when the ligand was added. Then, the blue solutions were filtered, without vacuum, on a crystallization device. These solutions were allowed to stand at room temperature covered with a plastic film to control the evaporation. After two weeks, blue crystals appeared. Typical yields in these syntheses are *ca.* 60–75%. *Anal.* Calc. for $C_{17}H_{16}CuN_4O_4$ (**1**): C, 50.56; H, 3.99; N, 13.87. Found: C, 50.26; H, 4.05; N, 13.67%. *Anal.* Calc. for $C_{13}H_{17}CuN_3O_5$ (**2**): C, 43.51; H, 4.78; N, 11.71. Found: C, 43.48; H, 4.35; N, 11.66%. *Anal.* Calc. for $C_{18}H_{19}CuN_4O_5$ (**3**): C, 51.36; H, 4.55; N, 9.98. Found: C, 51.10; H, 4.99; N, 10.28%.

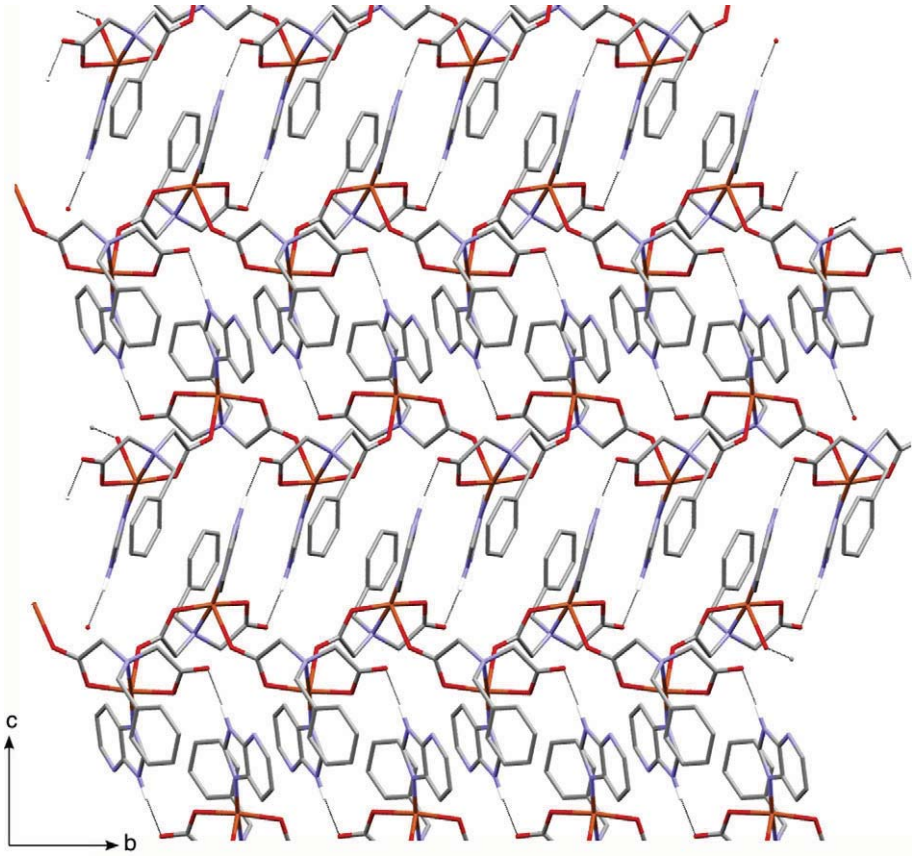


**Fig. 3.** View in the *bc* plane of the 2D layer in **1** obtained by hydrogen bonding interactions.

Compound **4** was synthesized adding a water solution of 10 mL of $CuSO_4{\cdot}5H_2O$ (0.25 mmol, 0.0624 g) to 40 mL of another solution of H7azain (0.5 mmol, 0.059 g) in distilled water. The reaction did not carry out properly and after 1 h stirring and heating (50 °C), the reacting mixture was not a completely clear solution. Therefore the solution was filtered on a crystallization device obtaining a very pale greenish solution. The residue retained on the filtration device was eliminated. The solution was left evaporating at room temperature till the presence of green crystals one month later. Yield was 65%. *Anal.* Calc. for $C_{14}H_{16}CuN_4O_6S$ (**4**): C, 38.93; H, 3.73; N, 12.97, S, 7.42. Found: C, 38.79; H, 3.79; N, 12.82; S, 7.22%.

### 2.3. Physical methods

Analytical data were obtained in a Fisons–Carlo Erba EA 1108 elemental micro-analyser. TG analysis (pyrolysis) of the studied compounds (295–800 °C) were carried out in air flow (100 mL/min) by a Shimadzu Thermobalance TGA–DTG–50H instrument, and a series of FT-IR spectra (20–30 per sample) of evolved gasses were recorded for the studied compounds, using a coupled FT-IR Nicolet Magma 550 spectrometer. Infrared spectra were recorded by using KBr pellets on a Jasco FT-IR 410 spectrometer. Electronic (diffuse reflectance) spectra were obtained in a Varian Cary-5E spectrophotometer. Electron spin resonance spectra were recorded in X band at room temperature in a Bruker ERP 300E spectrometer.

### 2.4. X-ray crystallography

Suitable crystals were mounted on glass fibers and these samples were used for data collection. Data were collected with Bruker SMART CCD 1000 (**1** and **3**, 100 K) or Bruker X8 Proteum (**2** and **4**, 293 K) diffractometers. The data were processed with SAINT (**1** and **3**) [29] or APEX2 (**2** and **4**) [30] and corrected for absorption using SADABS [31]. These structures were solved by direct methods [32], which revealed the position of all non-hydrogen atoms. These atoms were refined on $F^2$ by a full-matrix least-squares procedure using anisotropic displacement parameters [33]. All hydrogen atoms were located in difference Fourier maps and included as fixed contributions riding on attached atoms with isotropic thermal displacement parameters 1.2 times those of the respective atom. Geometric calculations were carried out with PLATON [34] and drawings were produced with PLATON [34] and MERCURY [35].

## 3. Results and discussion

Crystal data for compounds $[Cu(NBzIDA)(H4abim)]_n$ (**1**), [Cu(EIDA)(H7azain)($H_2O$)] (**2**), [Cu(NBzIDA)(H7azain)($H_2O$)] (**3**) and $[Cu(_2\text{-}SO_4)(H7azain)_2(H_2O)_2]_n$ (**4**) (NBzIDA and EIDA are N-benzyl- and N-ethyl-iminodiacetate ligands, respectively) are shown in Table 1.

### 3.1. Crystal structure and properties of *1*

Selected interatomic distances and angles are listed in Table 2. The coordination environment of the copper atom is shown in Fig. 2, together with the atom-numbering scheme used.

The crystal structure of **1** is based on a coordination polymer built by means of the *syn–anti* bridging role of a carboxylate group of the NBzIDA ligand. The copper(II) atom exhibits a square-base pyramidal coordination, type 4+1, with a rather planar base (Addison parameter $\tau = 0.002$). The tridentate *mer*-$NO_2$-NBzIDA chelating agent and the N7 atom from the H4abim ligand are the closest Cu donors. The apical/distal donor is the O#1 (carboxyl) from the bridging carboxylate group of an adjacent NBzIDA (#1 = $-x+1$, $y+1/2$, $-z+1/2$) and the Cu(II) atom is moved

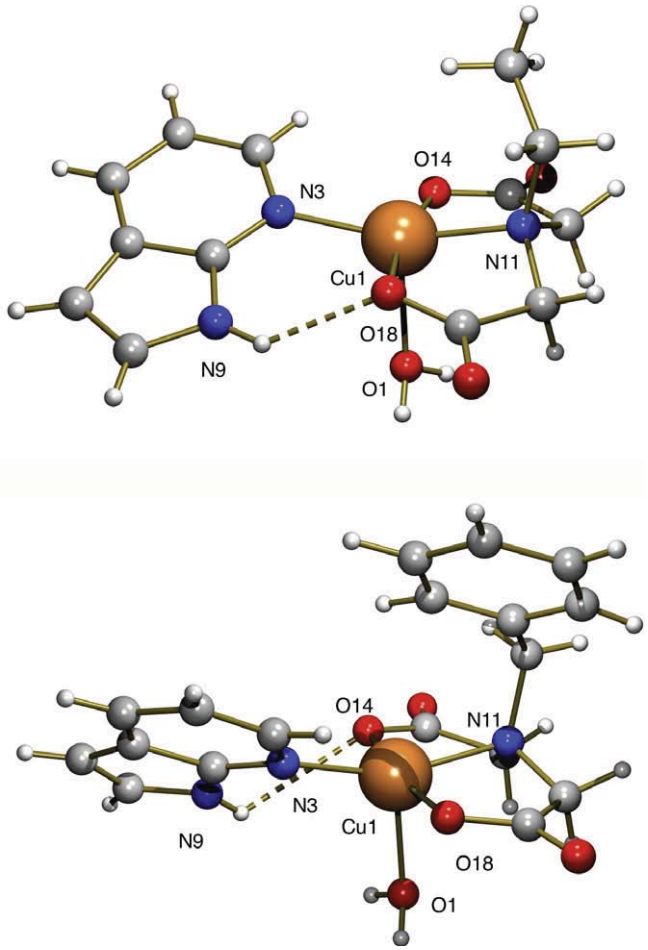


**Fig. 4.** Molecular structure of [Cu(EIDA)(H7azain)($H_2O$)] (**2**, top) and [Cu(NBzIDA)(H7azain)($H_2O$)] (**3**, bottom).

0.13 Å out of the basal plane towards the apex. A close similar low distortion towards the bi-pyramidal coordination (with $\tau = 1.00$) occurs in the binuclear compound $[Cu_2(\mu\text{-N3,N9-H4bim})_4(SO_4)_2]{\cdot}11H_2O$ [10] and the salts $[Cu_2(\mu\text{-N3,N9-H4bim})_4X_2]{\cdot}X_2$ (X = Cl, Br) [11], where the μ-N3,N9-H4abim bridging role of H4abim approaches to $\mu_2$-N3,N9-Hade [13] or $\mu_2$-N3,N9-ade [14,15] modes. The formation of the Cu–N7(H4abim) bond in **1** is according to the basicity order (N7 > N3) in purines. However, it should be noted that such coordination cannot be reinforced by an intra-molecular N–H···O interaction. Consider that the H(*N*9)4abim tautomer has the dissociable hydrogen atom on N9. A reason of this finding can be related to the crystal packing, with polymeric chains extending along $2_1$ screw axis (intra-chain shortest Cu···Cu separations are 5.699(1) Å). The chains connect to each other by means of symmetry related H-bonding interactions, N9–H9···O12#3 (2.73 Å, 173.6°) with O-acceptors from the non-bridging carboxylate group of a neighbouring NBzIDA ligands (#3 = $-x+1$, $-y+1$, $-z+1$), building a 2D layer (Fig. 3) parallel to the *bc* plane. No π,π-stacking interactions between aromatic rings were observed in **1**. Hydrophobic contacts contribute to the crystal structure connecting layers along the *a* axis resulting in a 3D architecture. It seems clear that the crystal packing in the coordination polymer **1** strongly influences the observed recognition patterns between the Cu(NBzIDA) chelate and the H4abim (N1,N6-dideazaadenine) base.

Compound **1** is stable until 180 °C and decomposes in dry-air (three steps between 180 and 435 °C, with production of $H_2O$,

$CO_2$, CO, $H_2CO$ and three N-oxides) to give a residue of ~CuO·Cu$(NO_3)_3$ (Found 22.99%, Calc. 21.72%). The FT-IR spectrum ($cm^{-1}$) shows typical bands of carboxylate groups ($\nu_{as}$ 1600, $\nu_s$ 1387), N–H ($\nu$ 3134, $\delta$ 1500) and C–$H_{(arom)}$ ($\pi$ 750 and 707) chromophores. A large series of peaks are observed in this spectrum between 2500 and 3250 $cm^{-1}$, including N–H and C–H bands (and overtones and/or combination bands). The electronic (diffuse reflectance) spectrum exhibits an asymmetric d–d band ($\nu_{max}$ 14 560 $cm^{-1}$) whereas the ESR spectrum has a typical axial shape ($g_{//}$ 2.23 and $g_{\perp}$ 2.05) corresponding to Cu(II) centres in $d_{x^2-y^2}$ ground state and misaligned $CuN_2O_2$ + O chromophores.

### 3.2. Molecular and crystal structure and properties of **2** and **3**

Compounds **2** and **3** have the same type of formula, [Cu(IDA-like)(H7azain)($H_2O$)] and consist of ternary complex molecules, with the Cu(II) atom in a distorted square-base pyramidal coordination. Drawings of the asymmetric units **2** and **3** are shown in Fig. 4, together with the atom-numbering schemes. The basal plane of the four closest donors is defined by the *mer*-$NO_2$(IDA-like) ligand and N3-purine-like donor of H7azain. The coordination bond Cu–N3(H7azain) is reinforced by the intra-molecular interligand N9–H···O(coordinated, IDA-like) interaction (2.77 Å and 133.7° in **2**, 2.99 Å and 108.8° in **3**). The weakness of the intra-molecular H-bond in **3** is due to the implication of its H7azain ligand in one additional inter-molecular N9–H···O(12)#2 interaction (2.87 Å, 163.5°; #2 = $-x+1$, $-y+1$, $-z$). In this regard, the dihedral angle between the basal coordination plane and H7azain plane is 25.45° in **2** and 41.29° in **3**. In both compounds, apical aqua ligands uses their H atoms to build inter-molecular O–H···O(noncoordinated) interactions with O-carboxylate acceptor of two adjacent molecules forming chains running along the *b* axis (Fig. 5). π,π-Stacking interactions between H7azain ligands (**2**) or between H7azain and the aryl ring of NBzIDA ligands (**3**) from adjacent chains contribute to the formation of 2D layers. In **2**, five-member rings from H7azain ligands are involved in the π,π-stacking (centroid to centroid distance of 3.46 Å and an interplanar dihedral angle of 0.0°, Fig. 6) meanwhile in **3**, $C_6$-ring from NBzIDA ligands and both five- and six-member rings from H7azain ligands are involved (centroid to centroid distances of 3.57/3.52 Å and an interplanar dihedral angle of 1.1°, Fig. 7). Thus, π,π-stacking results in a face-to-face mode with a parallel disposition of the aromatic rings. Hydrophobic interactions connect 2D layers in a 3D architecture of crystals **2** and **3**.

Unlike the molecular nature of **2** and **3**, the closely related compound $[Cu(IDA)(H7azain)]_n$ [12] is a coordination polymer. However, it is interesting to note that these three ternary complexes exhibit the same Cu(IDA-like) chelate-H7azain recognition pattern, with the Cu–N3(purine-like) coordination bond reinforced by an intra-molecular N9–H···O(coordinated IDA-like) interaction. It

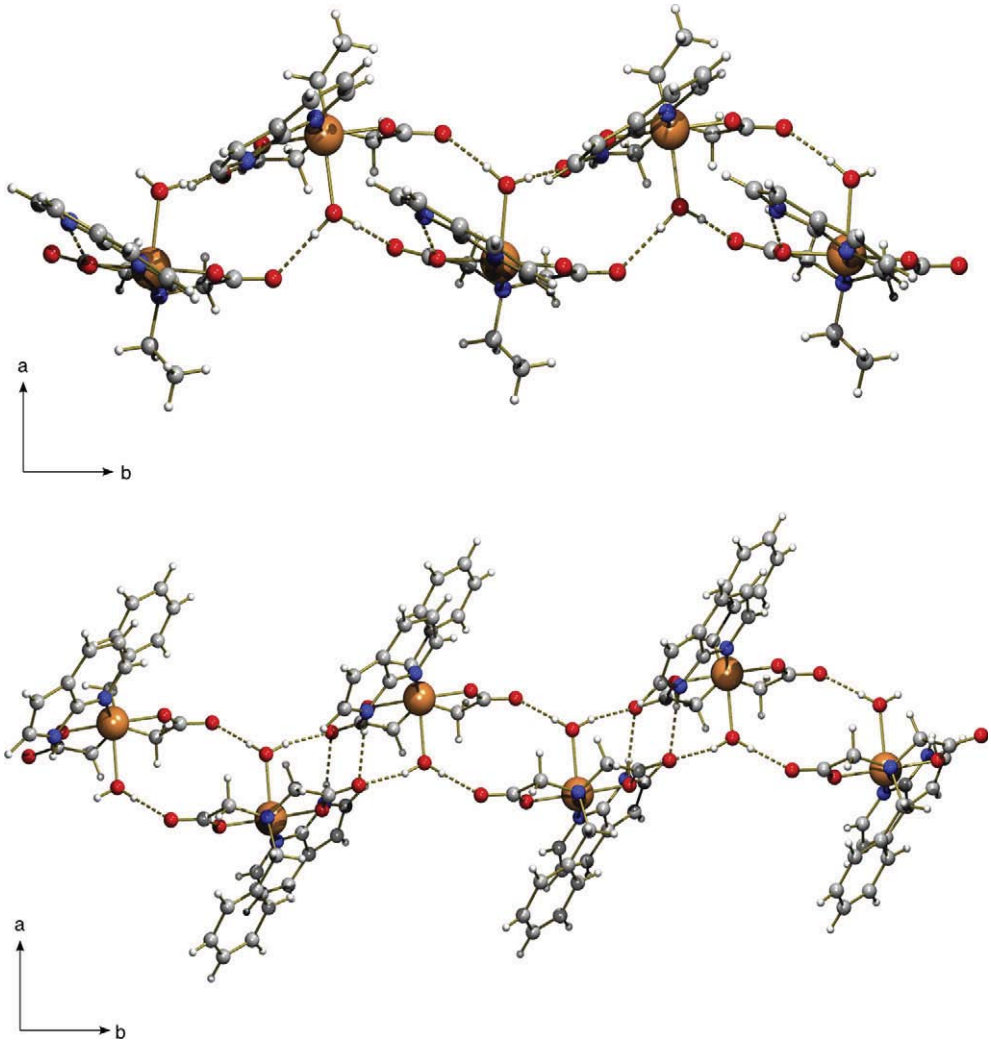


**Fig. 5.** View in the *ab* plane of chains obtained from hydrogen bonding interactions, running along the *b* axis in **2** (top) and **3** (bottom).

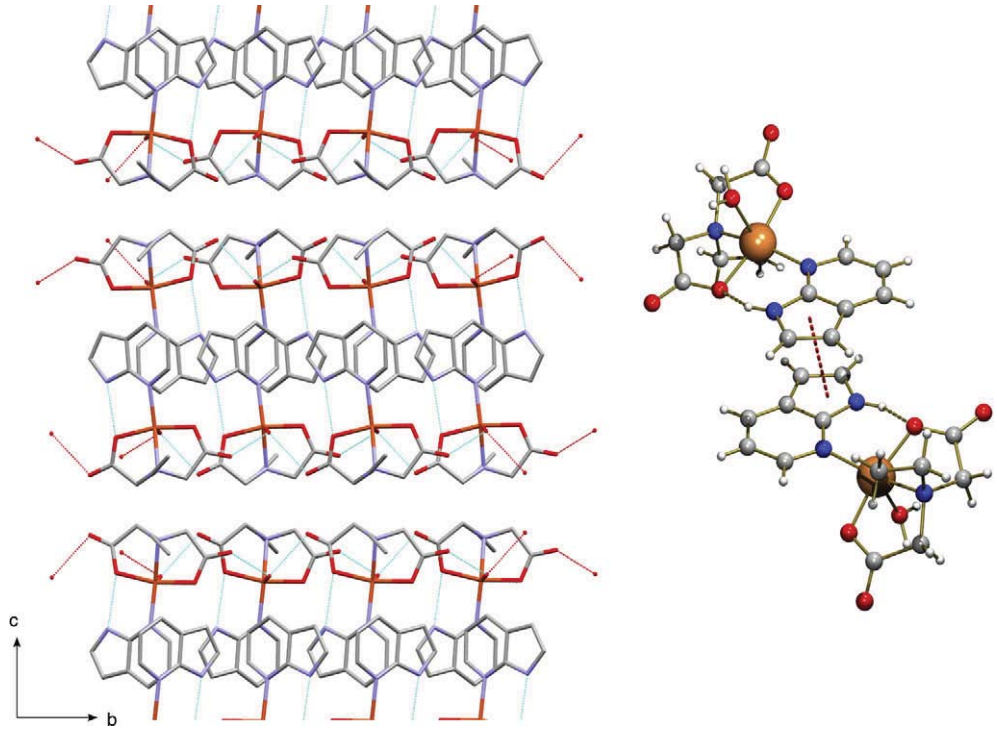


**Fig. 6.** View in the *ab* plane of the 3D architecture in **2**, showing hydrogen bonding and π,π-stacking interactions. Right: detail of the π,π-stacking between H7azain ligands.

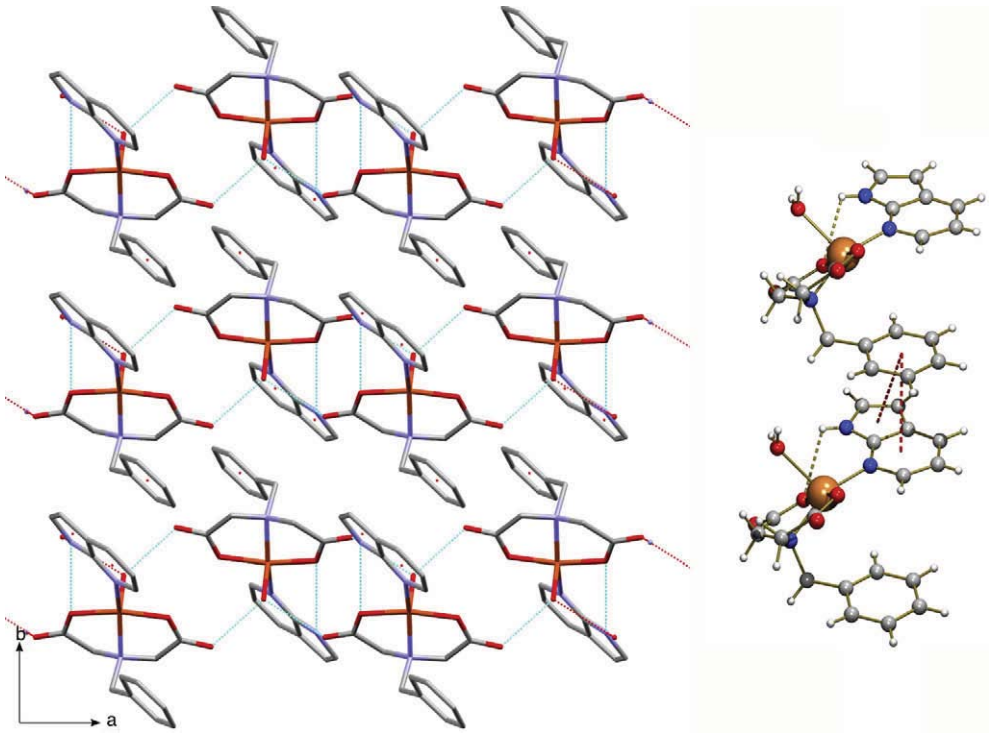


**Fig. 7.** View in the *ab* plane of the 3D architecture in **3**, showing hydrogen bonding and π,π-stacking interactions. Right: detail of the π,π-stacking between NBzIDA and H7azain ligands.

seems clear that the absence or presence of an alkyl or benzyl N-arm in the IDA-like chelating ligand does not alter the chelate-H7azain recognition pattern in the three referred complexes. That is in clear contrast to the different recognition patterns reported for ternary Cu(IDA-like)-Hade complexes [3,4,6].

Compounds **2** and **3** also have very similar properties. The FT-IR spectra show bands of the aqua ligand, carboxylate, chromophores of IDA-like ligands and N–H bond of H7azain. In the spectrum of **3,** two deformation out-of-plane $\pi(C–H)_{arom}$ are easily recognised, as well defined absorptions, at 754 and 738 $cm^{-1}$. On the other hand,

the spectrum of **2** only shows a $\pi(C–H)_{arom}$ band at 723 $cm^{-1}$, as 'the most intense and defined absorption among 800–700 $cm^{-1}$ spectral range'. It is also interesting to point out the wave-number ($cm^{-1}$) of the stretching mode $\nu$(N–H) band, observed at 3322 for **2** (with a single N–H···O interaction) and 3160 for **3** (with a 'bifurcated' H-bonding interaction).

The thermal behaviour of these molecular complexes exhibits two closely related features. The first step corresponds to the loss weight of $H_2O + CO_2$ (these gasses are identified in the corresponding FT-IR spectra). Pyrolytic steps yield a residue of CuO (Found 19.65% and Calc. 18.90% for **2**; Found 23.00% and Calc. 22.17% for **3**). The electronic spectrum of **3** shows an asymmetric d–d band with $\nu_{max}$ at 14560 $cm^{-1}$, with an intensity barycentre near 13 000 $cm^{-1}$.

### 3.3. Crystal structure and properties of **4**

The stoichiometric reaction of copper(II) sulfate and H7azain afforded green crystals. The structure of **4** is based on a coordination polymer extending along the *c* axis (Fig. 8). The copper(II) atom exhibits an elongated octahedral coordination, type 4+2. The four closest donors are two sets of symmetry related donors (#1 = $-x$, $y$, $-z + 3/2$), *cis*-O10(aqua), O10#1 and *cis*-N3(H7azain), N3#1 atoms. Apical donors belong to two *trans*-$\mu_2$-sulfate bridges, resulting polymeric chains. The internal stability of these chains is reinforced by two kind of H-bonding interactions: N9–H9···O(1)#1(coordinated sulfate; 2.82 Å, 153.61°) and O10–H10A···O2(noncoordinated sulfate; 2.65 Å, 174.3°). Pairs of chains are linked by H-bonding interactions O10–H10B···O(2)#3(noncoordinated sulfate; 2.72 Å, 172.1°; #3 = $x$, $-y$, $z + 1/2$), giving double-stranded chains with H7azain ligands on the outer positions and a paddle–wheel shape (Fig. 9). The *cis*-coordination of pairs of aqua and H7azain ligands seems to enable the referred H-bonding stabilization of pairs of polymeric chains. In the crystal, each double-stranded chain is interconnected to other four through symmetrical C–H···π interactions, involving the –C8–H8 bond and the five-member ring of H7azain, allowing a 3D network (Fig. 9). The C–H···centroid distance is 2.74 Å and the C–H···centroid angle is 146.0°.

The structure of compound $[Cu(\mu_2\text{-}SO_4)(H7azain)_2(H_2O)_2]_n$ (**4**) strongly differs from that reported to $[Cu_2(\mu_2\text{-}N3,N9\text{-}H4bim)_4$

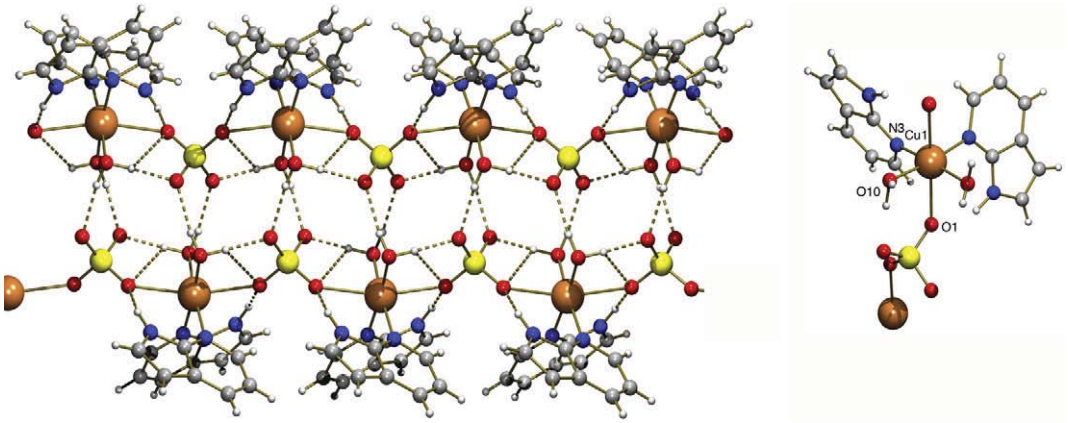


**Fig. 8.** Structure of $[Cu(\mu_2\text{-}SO_4)(H7azain)_2(H_2O)_2]_n$ (**4**). Left: double-stranded chain obtained by hydrogen bonding, running along the *c* axis. Right: detail of the numeration scheme of the coordination environment in **4**.

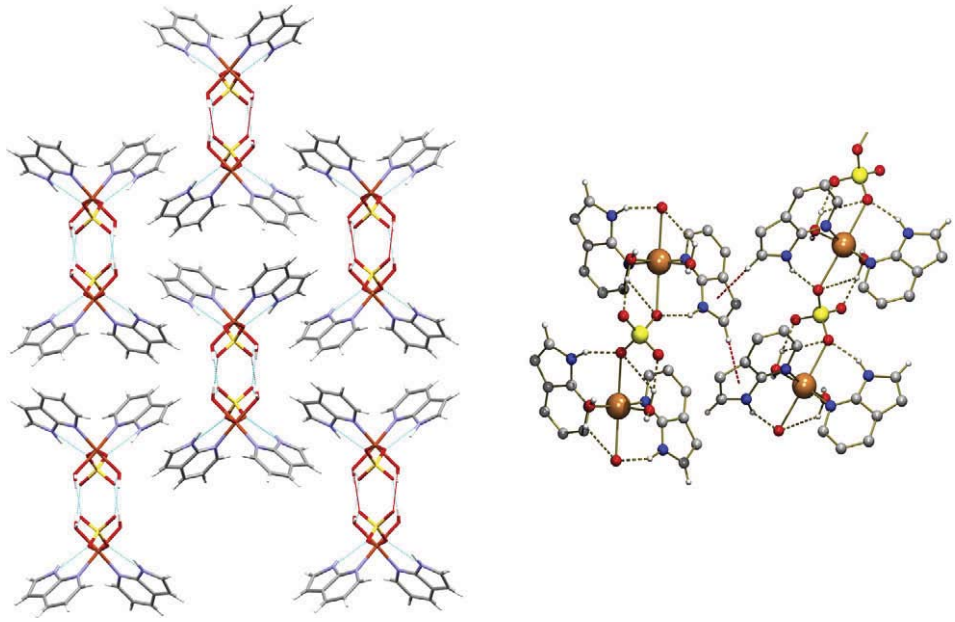

**Fig. 9.** View of the 3D architecture in **4** (left). Right: retail of CH···π interactions involving H7azain ligand.

$(SO_4)_2]\cdot 11H_2O$ [11]. This feature will be rationalized on the basis of the impossibility of neutral H7azain to use both N-atoms for metal-binding. It is well proved that the 7azain anion build $\mu_2$-N3,N9-bridges. The bridging $\mu_2$-N3,N9-H4abim role uses the H(*N*7)4abim tautomer.

Compound **4** has normal spectral and thermal properties. Its FT-IR spectrum ($cm^{-1}$) shows bands of the N9–H ($\nu$ 3145, $\delta$ 1507 and/or 1490) and C–$H_{arom}$ ($\pi$ 750) chromophores. Once more, the region 2500–3250 exhibits a series of weak peaks. The bridging $\mu_2$-sulfate [36] can be indentified as the three intense (s) bands expected for the $\nu_3$ mode (1092s, 1108s, 1125s) as well as three weak (w) absorptions (572w, 601w, 616w) related to the $\nu_4$ mode, and very weak (vw) peaks due to the modes $\nu_2$ (445vw) and $\nu_1$ (983vw). The electronic spectrum shows an unsymmetrical d–d band, with $\nu_{max}$ at $\sim$15 500 $cm^{-1}$ and a shoulder near 10 500 $cm^{-1}$. The thermogravimetric behaviour of this compound, under dry-air flow shows a first steep for the loss of two aqua ligands (100–175 °C, Found 8.208%, Calc. 8.242%) followed by three pyrolytic steps with production of $CO_2$, $H_2O$, CO, $SO_2$ and three N-oxides, to lead CuO.

## 4. Concluding remarks

In contrast to Hade-like behaviour and the one reported to H4abim in $[Cu_2(\mu\text{-N3,N9-H4abim})_4(SO_4)_2]\cdot 11H_2O$ and related salts, having the tautomer H(*N*7)4abim, this 1,6-dideazaadenine binds the Cu(N-benzyliminodiacetate) chelate by the N7-donor, using the H(*N*9)4abim tautomer, without intra-molecular interligand H-bonding reinforce. This latter seems to be promoted by the crystal packing in **1**.

Compounds **2**–**4** have N1,N6,N7-trideazaadenine as H(*N*9)7azain tautomer and, as previously reported for $[Cu(IDA)(H7azain)]_n$, this $N_2$-heterocyclic compound binds the Cu(II) centre by the Cu–N3(purine-like) bond, reinforced by a N9–H···O(coordinated, IDA-like or sulfate) interaction. This metal-H7azain coordination mode is also supported by structures of a variety of complexes [26,27,37–41]. However, the hypothetical formation of a Cu–N9(H7azain) bond, reinforced by the N3–H···O(IDA-like or sulfate), has been never observed, meanwhile the formation of metal–N9 coordination bond with the anionic 7azain$^-$ form, in mononuclear $CH_3$–$Hg^+$ [41] and $Au^+$ [18] or in a large series of compounds with metal–($\mu_2$-7azain)–metal bridges [18,19,21,42–45] have been reported. Thus, it seems clear that neutral H7azain only can simulate Hade role in ternary Cu-(IDA-like)-Hade compounds by the formation of a Cu–N3(purine-like) coordination bond, which is reinforced by the intra-molecular interligand N9–H···O(coordinated) interaction. The remarkable variety of Hade–Cu coordination modes needs the N-rich purine moiety, enabling several tautomeric forms.

## 5. Supplementary data

CCDC 730725, 730726, 730727 and 730728 contain contains the supplementary crystallographic data for **1**, **2**, **3** and **4**, respectively. These data can be obtained free of charge via http://www.ccdc.cam.ac.uk/conts/retrieving.html, or from the Cambridge Crystallographic Data Centre, 12 Union Road, Cambridge CB2 1EZ, UK; fax: (+44) 1223-336-033; or e-mail: deposit@ccdc.cam.ac.uk.

## Acknowledgements

Financial support from ERDF-EC, MEC-Spain (Project CTQ2006-15329-C02/BQU) is acknowledged. ADM thanks MICINN-Spain for a FPU Grant. DChL thanks CSIC-EU for a I3P postdoctoral research contract. The project "Factoría de Cristalización, CONSOLIDER INGENIO-2010" provided X-ray structural facilities for this work.

## References

[1] B. Lippert, Coord. Chem. Rev. 200–202 (2000) 487.
[2] D. Choquesillo-Lazarte, M.P. Brandi-Blanco, I. García-Santos, J.M. González-Pérez, A. Castiñeiras, J. Niclós-Gutiérrez, Coord. Chem. Rev. 252 (2008) 1241.
[3] E. Bugella-Altamirano, D. Choquesillo-Lazarte, J.M. González-Pérez, M.J. Sánchez-Moreno, R. Marín-Sánchez, J.D. Martín-Ramos, B. Covelo, R. Carballo, A. Castiñeiras, J. Niclós-Gutiérrez, Inorg. Chim. Acta 339 (2002) 160.
[4] M.J. Sánchez-Moreno, D. Choquesillo-Lazarte, J.M. González-Pérez, R. Carballo, A. Castiñeiras, J. Niclós-Gutiérrez, Inorg. Chem. Commun. 5 (2002) 800.
[5] A.C. Morel, D. Choquesillo Lazarte, J.M. González Pérez, A. Castiñeiras, J. Niclós Gutiérrez, Inorg. Chem. Commun. 6 (2003) 1354.
[6] P.X. Rojas-González, A. Castiñeiras, J.M. González-Pérez, D. Choquesillo-Lazarte, J. Niclós-Gutiérrez, Inorg. Chem. 41 (2002) 6190.
[7] M.P. Brandi-Blanco, B. Dumet-Fernandes, J.M. González-Pérez, D. Choquesillo-Lazarte, Acta Crystallogr., Sect. E 63 (2007) m1598.
[8] A. Terrón, J.J. Fiol, A. García-Raso, M. Barceló-Oliver, V. Moreno, Coord. Chem. Rev. 251 (2007) 1973.
[9] E.-C. Yang, H.-K. Zhao, X.J. Zhao, Inorg. Chem. 48 (2009) 3511.
[10] C. Sánchez de Medina-Revilla, D. Choquesillo-Lazarte, A. Domínguez-Martín, L. Lezama, J.M. González-Pérez, A. Castiñeiras, J. Niclós-Gutiérrez, in: Ninth European Biological Inorganic Chemistry Conference (EUROBIC 9), Medimond, S.r.l., Wroclaw, 2008, p 101.
[11] G.A. van Albada, I. Mutikanien, U. Turpeinen, J. Reedijk, Inorg. Chim. Acta 25 (2006) 3278.
[12] A. Domínguez-Martín, D. Choquesillo-Lazarte, C. Sánchez de Medina-Revilla, J.M. González-Pérez, A. Castiñeiras, J. Niclós-Gutiérrez, in: Ninth European Biological Inorganic Chemistry Conference (EUROBIC 9), Medimond, S.r.l., Wroclaw, 2008, p. 105.
[13] A. Terzis, A.L. Beachamp, R. Rivest, Inorg. Chem. 12 (1973) 1166.
[14] E. Sletten, Acta Crystallogr., Sect. B 25 (1969) 1480.
[15] J.M. González-Pérez, C. Alarcón-Payer, A. Castiñeiras, T. Pivetta, L. Lezama, D. Choquesillo-Lazarte, G. Crisponi, J. Niclós-Gutiérrez, Inorg. Chem. 45 (2006) 877.
[16] S.J. Retting, V. Sánchez, A. Storr, R.C. Thompson, J. Trotter, Dalton. Trans. (2000) 3931.
[17] H. Hayashi, A.P. Cote, H. Furukawa, M. O'Keeffe, O.M. Yaghi, Nat. Mater. 6 (2007) 501.
[18] Chi-Keung, Chun-Xiao Guo, Kung-Kai Cherung, Dan Li, Chi-Ming Che, J. Chem. Soc., Dalton Trans. (1994) 3677.
[19] Shie-Ming Pen, Yi-Nan Li, Acta Crystallogr., Sect. C 42 (1986) 1725.
[20] Yi-Chian Chou, Shu-Fei Huang, R. Koner, Gene-Hsiang Lee, Yu Wang, S. Mohanta, Ho-Hsiang Wei, Inorg. Chem. 43 (2004) 1759.
[21] Shie-Ming Pen, Chien-Hsien Lai, J. Chin. Chem. Soc. (Taipei) 35 (1988) 325.
[22] Y. Kani, M. Tsucimito, S. Ohba, Acta Crystallogr., Sect. C 56 (2000) e193.
[23] J. Poitras, A.L. Beauchamp, Can. J. Chem. 70 (1992) 2846.
[24] G.A. van Albada, S. Nur, M.G. van der Horst, I. Mutikanien, U. Turpeinen, J. Reedijk, J. Mol. Struct. 874 (2008) 41.
[25] G.A. van Albada, S. Tanase, I. Mutikanien, U. Turpeinen, J. Reedijk, Inorg. Chim. Acta 361 (2008) 1467.
[26] P.K. Dubey, K.V. Kumar, A. Naidu, S.M. Kulkarni, Asian J. Chem. 14 (2002) 1129.
[27] S. Vittori, D. Dal Ben, C. Lambertucci, G. Marucci, R. Volpini, G. Cristalli, Curr. Med. Chem. 13 (2006) 3529.
[28] J. Guillard, M. Decorp, N. Gallay, C. Espanel, E. Boissier, O. Herault, M.-C. Vidaud-Massuard, Bioorg. Med. Chem. Lett. 17 (2007) 1943.
[29] Bruker, SMART and SAINT. Area Detector Control Integration Software, Bruker.
[30] Bruker, APEX2 Software, Bruker AXS Inc. V2008.1, Madison, Wisconsin, USA, 2008.
[31] G.M. Sheldrick, SADABS, Program for Empirical Absorption Correction of Area Detector Data, University of Göttingen, Germany, 1997.
[32] G.M. Sheldrick, Acta Crystallogr., Sect. A 46 (1990) 467.
[33] G.M. Sheldrick, SHELXL-97. Program for the Refinement of Crystal Structures, University of Göttingen, Germany, 1997.
[34] A.L. Spek, PLATON. A Multipurpose Crystallographic Tool, Utrecht University, Utrecht, The Netherlands, 2003.
[35] C.F. Macrae, I.J. Bruno, J.A. Chisholm, P.R. Edgington, P. McCabe, E. Pidcock, L. Rodriguez-Monge, R. Taylor, J. van de Streek, P.A. Wood, J. Appl. Cryst. 41 (2008) 466.
[36] K. Nakamoto, Infrared Spectra of Inorganic and Coordination Compounds, 2nd ed., Willey and Sons, New York, 1970. p. 173.
[37] A.-M. Lebuis, A.L. Beauchamp, Can. J. Chem. 71 (1993) 2060.
[38] B.R.A. Bland, H.J. Gilfoy, G. Vamvounis, K.N. Robertson, T.S. Cameron, M.A.S. Aquino, Inorg. Chim. Acta 358 (2005) 3927.
[39] F.A. Cotton, T.R. Felthouse, Inorg. Chem. 20 (1981) 600.
[40] Qingguo Wu, J.A. Lavigne, Ye Tao, M. D'Iorio, Suning Wang, Inorg. Chem. 39 (2000) 5248.
[41] P. Dufour, Y. Dartiguenave, M. Dartiguenave, N. Dufour, A.-M. Lebuis, F. Belanger-Gariepy, A.L. Beauchamp, Can. J. Chem. 68 (1990) 193.
[42] F.A. Cotton, L.R. Falvello, Wenning Wang, Inorg. Chim. Acta 261 (1997) 77.
[43] F.A. Cotton, J.H. Matonic, C.A. Murillo, J. Am. Chem. Soc. 120 (1998) 6047.
[44] J. Beck, M. Reitz, Z. Naturforsch., B: Chem. Sci. 52 (1997) 604.
[45] F.A. Cotton, C.A. Murillo, Hong-Cai Zhou, Inorg. Chem. 39 (2000) 3728.

## 1.3. From 7-azaindole to adenine: molecular recognition aspects on mixed-ligand Cu(II) complexes with deaza-adenine ligands

Article submitted to *Dalton Trans.* (2012)

SYNOPSIS

Crystal structures and DFT calculations of ternary copper(II) complexes are used to better understand the versatility of adenine as ligand.

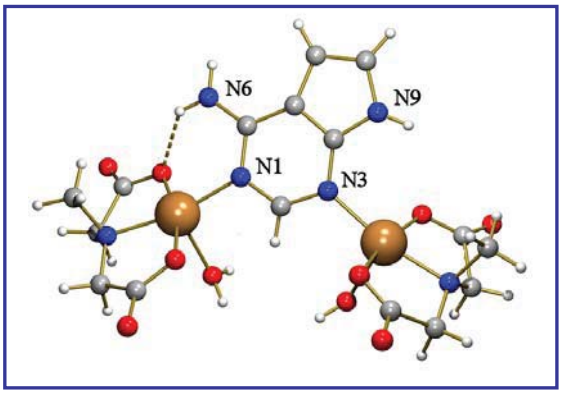


RESUMEN

Con el fin de comprender mejor el versátil comportamiento de adenina como ligando, se han sintetizado y caracterizado mediante difracción de Rayos-X una serie de diez complejos ternarios de cobre(II) con ligandos tipo deaza-adenina [7-azaindol (1,6,7-trideaza-adenina, H7azain), 4-azabencimidazol (1,6-dideaza-adenina, H4abim), 5-azabencimidazol (3,6-dideaza-adenina, H5abim) y 7-deaza-adenina (H7deaA)]. Asimismo, todos los compuestos estudiados han sido analizados mediante técnicas espectroscópicas y termogravimetría. Los tautómeros y las capacidades dadoras de los ligando deaza-adenina descritos anteriormente han sido calculadas mediante estudios de DFT. Se concluye que el número creciente de dadores nitrogenados en los ligandos tipo deaza-adenina favorece el fenómenos de tautomería y su versatilidad como ligandos. Cabe destacar que H7azain siempre usa el mismo tautómero mientras que H4abim usa dos tautómeros diferentes, pero no es protonado por el ligando pentadentado $H_2$EDTA(2-). H(N1)5abim muestra el modo puente $\mu_2$-N7,N9 y H(N9)7deaA se une al cobre(II) vía N3, cooperando con una interacción intra-molecular tipo N9-H···O, o usando el singular modo bidentado $\mu_2$-N1,N3 puente.

# From 7-azaindole to adenine: molecular recognition aspects on mixed-ligand Cu(II) complexes with deaza-adenine ligands

| | |
|---|---|
| Journal: | *Dalton Transactions* |
| Manuscript ID: | Draft under Revision |
| Manuscript Type: | Paper |
| Date Submitted by the Author: | 20/09/2012 |
| Complete List of Authors: | Dominguez-Martin, Alicia;<br>University of Granada, Department of Inorganic Chemistry, Faculty of Pharmacy.<br>Choquesillo-Lazarte, Duane; CSIC, LEC.<br>Dobado, Jose; Universidad de Granada, Química Orgánica.<br>Vidal, Isaac; Universidad de Granada, Química Orgánica.<br>Lezama, Luis; University of Basque Country, Faculty of Science and Technology.<br>González-Pérez, Josefa; Universidad de Granada, Química Inorgánica.<br>Castiñeiras, Alfonso; University of Santiago de Compostela, Department of Inorganic Chemistry.<br>Niclós-Gutiérrez, Juan; University of Granada, Department of Inorganic Chemistry, Faculty of Pharmacy. |
| | |

Dalton Transactions

www.rsc.org/xxxxxx

ARTICLE

# From 7-azaindole to adenine: molecular recognition aspects on mixed-ligand Cu(II) complexes with deaza-adenine ligands

**Alicia Domínguez-Martín,*[a] Duane Choquesillo-Lazarte,[b] Jose A. Dobado,[c] Isaac Vidal,[c] Luis Lezama,[d] Josefa María González-Pérez,[a] Alfonso Castiñeiras[e] and Juan Niclós-Gutiérrez[a]**

***Received (in XXX, XXX) Xth XXXXXXXXX 200X, Accepted Xth XXXXXXXXX 200X***
**DOI: 10.1039/b000000x**

For a better understanding of the versatile behaviour of adenine as a ligand, a series of 10 ternary copper(II) complexes with deaza-adenine ligands [7-azaindole (1,6,7-trideaza-adenine, H7azain), 4-azabenzimidazole (1,6-dideaza-adenine, H4abim), 5-azabenzimidazole (3,6-dideaza-adenine, H5abim), and 7-deaza-adenine (H7deaA)] have been synthesised and characterised by X-ray diffraction. Likewise, all the compounds studied have been analysed by spectral and thermal methods. The proton tautomers and donor capabilities of the above-mentioned deaza-adenine ligands have been calculated by DFT. We conclude that the increasing presence of N-donors in deaza-adenine ligands favours the proton tautomerism and their versatility as co-ligands. Notably, H7azain consistently uses the same tautomer, H4abim uses two different tautomers but is not protonated by the pentadentate $H_2EDTA^{2-}$ ligand, and H(N1)5abim displays the $\mu_2$-N7,N9 mode, whereas H(N9)7deaA binds Cu(II) by N3 in cooperation with an intra-molecular N9-H···O interaction or using the unprecedented bidentate $\mu_2$-N1,N3 bridging mode.

## Introduction

Over recent decades, supramolecular chemistry has become a matter of current interest. The design and development of new bio-materials as well as molecular frameworks has increased rapidly, addressing the coordination chemistry of biologically related ligands.[1] In this sense, nucleic acids and especially purine-like ligands such as adenine, are outstanding because of their rich, versatile behaviour.[2] The in-depth understanding of the molecular recognition patterns of different nucleobases and their derivatives and/or analogues has been devoted to rationalizing biochemical processes, leading to promising physico-chemical developments, i.e. molecular probes or sensors, or further pharmaceutical approaches. Indeed, therapeutical and biotechnological applications are extensively documented for a large variety of purine-like ligands and/or purine-like metal complexes.[3] For instance, regarding deaza-adenine ligands, Jose Ruiz et al.[3b] have reported two ternary Pt(II) complexes with 7azaindolate, according to the formula [Pt(dmba)(7azain)(L')] (dmba is N,N-dimethylbenzylamine-kN,kC, 7azain is 7-azaindolate and L' is DMSO or $PPh_3$), which are able to form adducts with DNA showing *in vitro* cytotoxicity. These latter compounds are active in the sub-micromolar range towards the cis-platin resistant human breast-cancer cell line T47D and the epithelial ovarian carcinoma cells A2780 and A2780cisR. Likewise, research has been fruitful in the synthesis and characterization of zeolitic imidazolate frameworks, involving purine-like ligands.[3e] The complexes $\{[Zn(\mu_2\text{-}5azabenzimidazolate)_2]\cdot DMF_{0.75}\cdot(H_2O)_2\}_n$ and $\{[Zn(\mu_2\text{-}4azabenzimidazolate)_2]\cdot(H_2O)_{0.25}\}_n$ have proved useful as gas adsorbents for $H_2$, $CH_4$, $CO_2$ or Ar. A notable property of these materials is also their selective gas adsorption within some gas mixtures which could be used for gas storage or catalysis.[4] Alternatively, it is known that 7-deazapurine ligands are electrochemically

oxidizable at carbon electrodes at less positive potentials compared to any natural building block of DNA. Thus, 7-deaza-adenine, incorporated into DNA, could be useful as an electro-active label for easily monitoring PCR amplification.[3c]

As part of our research, we have been working on ternary Cu(II) complexes having deaza-adenine ligands. The relevance of deaza-adenine ligands is related to fact that 7-azaindole (H7azain = 1,6,7-trideaza-adenine), 4- and 5-azabenzimidazole (H4abim = 1,6-dideaza-adenine and H5abim = 3,6-dideaza-adenine, respectively) or 7-deaza-adenine (H7deaA), among others, can be considered as bioisosteres of the purine moiety (Scheme 1). Note that all the ligands mentioned herein have at least one N-heterocyclic donor atom in each cycle. Hence, the study of ternary complexes involving deaza-adenine ligands is challenging, since it could provide new insights into how restrictions on the N-heterocyclic donor atoms affect the relative basicity order of the N-donors in the purine moiety and therefore the coordination abilities of such ligands. In this context, it should be remarked that, in the study of molecular recognition, work on mixed-ligand complexes, single-crystal X-ray diffraction (XRD), and density functional theory (DFT) calculations offers useful tools by providing reliable information on the metal-binding pattern as well as on the non-covalent interligand interactions (H-bonds, pi,pi-stacking, C-H/pi-interactions, etc).

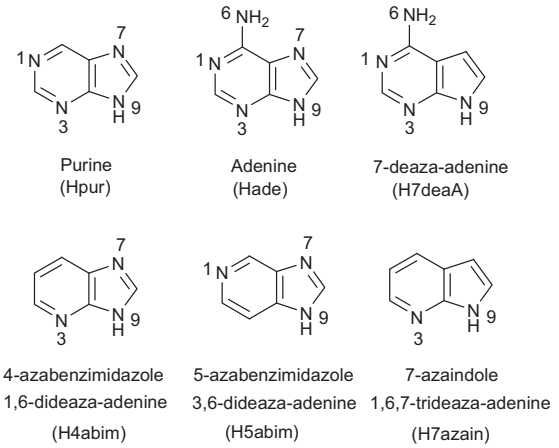


Scheme 1. Adenine and related deaza-adenine ligands (with purine conventional notation).

## Results and discussion

### 1. DFT Calculations

#### Tautomers for the isolated deaza-adenine ligands

To explore the relative stability of the corresponding hydrogen tautomers of the above-mentioned deaza-adenine ligands, we calculated the gas phase and solvent-effect Gibbs energies, these being summarized in Table 1. As expected, the H(N9) tautomers are the most stable ones in the gas phase and also when the solvent effect is included. Note that H5abim, in the gas phase, shows a small difference of only 0.3 kcal·mol$^{-1}$ with respect to the next stable tautomer, H(N7), which remains almost the same once the solvent effect (0.6 kcal·mol$^{-1}$) is considered. For H7azain and H7deaA ligands, the second tautomer in terms of energy is the H(N3), with values close to 12 kcal·mol$^{-1}$.

Only one study is available on the experimental and theoretical tautomers of H4abim.[5] In accordance with our results, the most stable tautomer is reportedly the H(N9) form among the four possible tautomers. In that study, the electronic relative energies ($E_r$) were reported, yielding values of 4.14 and 4.19 kcal·mol$^{-1}$ for the H(N7) tautomer, at very accurate B3LYP/6-311++G**//B3LYP/6-311++G** and QCISD/cc-pVDZ//B3LYP/6-311++G** theoretical levels, respectively. Our results are in good agreement with those previously reported, although in the present study we report $\Delta G_r$ values of 3.9 kcal·mol$^{-1}$. However, it bears mentioning that when the solvent effect is included in the calculations, this difference is reduced significantly to 0.2 kcal·mol$^{-1}$. Therefore, although the most stable tautomer for H4abim and H5abim is the H(N9), the next tautomer in energy is the H(N7) within a narrow range of approx. 0.5 kcal·mol$^{-1}$.

#### Mononuclear copper(II) complexes

To estimate the coordination abilities of the N-heterocyclic donors of H7azain, H4abim, H5abim, and H7deaA, we selected different model systems which consist of ternary copper(II) complexes having the chelating ligand N-methyl-

Table 1: DFT Gas phase and solvent (water) relative Gibbs energies (ΔGrel) for the different tautomers of deaza-adenine ligands, calculated at the B3LYP/6-31+G**//B3LYP/6-31+G** and PCM-B3LYP/6-31+G**//PCM-B3LYP/6-31+G** theoretical levels, respectively.

| Compound [a] | Tautomer-H9 $\Delta G_{rel}$ (Kcal/mol) | Tautomer-H7 $\Delta G_{rel}$ (Kcal/mol) | Tautomer-H3 $\Delta G_{rel}$ (Kcal/mol) | Tautomer-H1 $\Delta G_{rel}$ (Kcal/mol) |
|---|---|---|---|---|
| I-p9 / I-p3 (H7azain) | 0.0 | - | 12.5 (9.7) | - |
| II-p9 / II-p7 / II-p1 (H5abim) | 0.0 | 0.3 (0.6) | - | 7.8 (3.8) |
| III-p9 / III-p7 / III-p3 (H4abim) | 0.0 | 3.9 (0.2) | 9.6 (6.1) | - |
| IV-p9 / III-p3 / III-p1 (H7deaA) | 0.0 | - | 11.2 (8.5) | 22.6 (12.5) |

[a]. The Latin numbers refer to the deaza-adenine ligand (i.e. I is 7-azaindole; II is 4-azabenzimidazole; III is 5-azabenzimidazole and IV is 7-deaza-adenine). Values in parentheses correspond to the solvent effect PCM (water). The number after the 'p' indicates where the tautomerizable proton is located, i.e. p9.

iminodiacetate(2-) (MIDA). The Cu(II)/MIDA chelate was tested for all the purine-like ligands. Calculations were also extended to other iminodiacetate-like ligands such as N-benzyl- and N-(p-chlorobenzyl)-iminodiacetate(2-) or ethylendiaminotetraacetate(2-) anions (NBzIDA, CBIDA or $H_2$EDTA, respectively).

As discussed above, the free nucleobases here presented exhibit the tautomer H(N9) in neutral form (see Table 1). However, for the model systems, we also calculated all the protonation alternatives for the mononuclear Cu(II) complexes since the presence of copper could alter these tautomeric preferences. Figure 1 depicts the structures of the most stable mononuclear Cu(II) complexes calculated at the B3LYP/6-31+G**//B3LYP/6-31+G** theoretical level. Besides, Table S2 (see Supporting Material) summarizes the relative Gibbs energy ($\Delta G_r$) for the different coordination and proton tautomer complexes, together with some selected geometrical parameters.

For the Cu(II)/MIDA chelate, H7azain shows a coordination preference via N3, with a $\Delta G_r$ difference of 3.5 kcal·mol$^{-1}$ respect to the 9p3 metal-binding mode.[§]. In addition, this difference is also observed for the complex Cu(II)/NBzIDA/H7azain. Structurally, the most significant features of these mononuclear complexes are the following: (i) the chelating ligands MIDA and NBzIDA display a mer-$NO_2$ conformation and the distances of the coordination bonds N···Cu and O···Cu are close to 2.0 and 1.9 Å, respectively. The latter bond becomes slightly larger (increasing in 0.2 Å) when the oxygen atom is involved in H-bonds (see Figure 1 and Table S2); (ii) they show an intra-molecular interaction with values of approx. 1.79 Å and 140º for the N···O distance and <N-H···O angle, respectively. Moreover, the chelating ligand and the deaza-adenine are coplanar (dihedral angle close to 2º). As we will discuss in the crystallographic section, the theoretical results agreed well with the experimental ones.

The structures of H4abim with the chelates Cu(II)/MIDA and Cu(II)/CBIDA also adopt a mer-$NO_2$ coplanar conformation, yielding similar geometrical data (see Table S2). However, the $H_2$EDTA ligand has different coordination preferences. A restricted search for EDTA(4-) and Cu(II) in the Cambridge Structural Database (CSD) reported mostly pentadentate coordination of this former ligand. Hence, we performed theoretical models for the Cu(II)/$H_2$EDTA complex behaving as tetra- or pentadentate ligand, resulting in the calculations the tetradentate form the most stable due to the existence of two intra-molecular H-bonds.

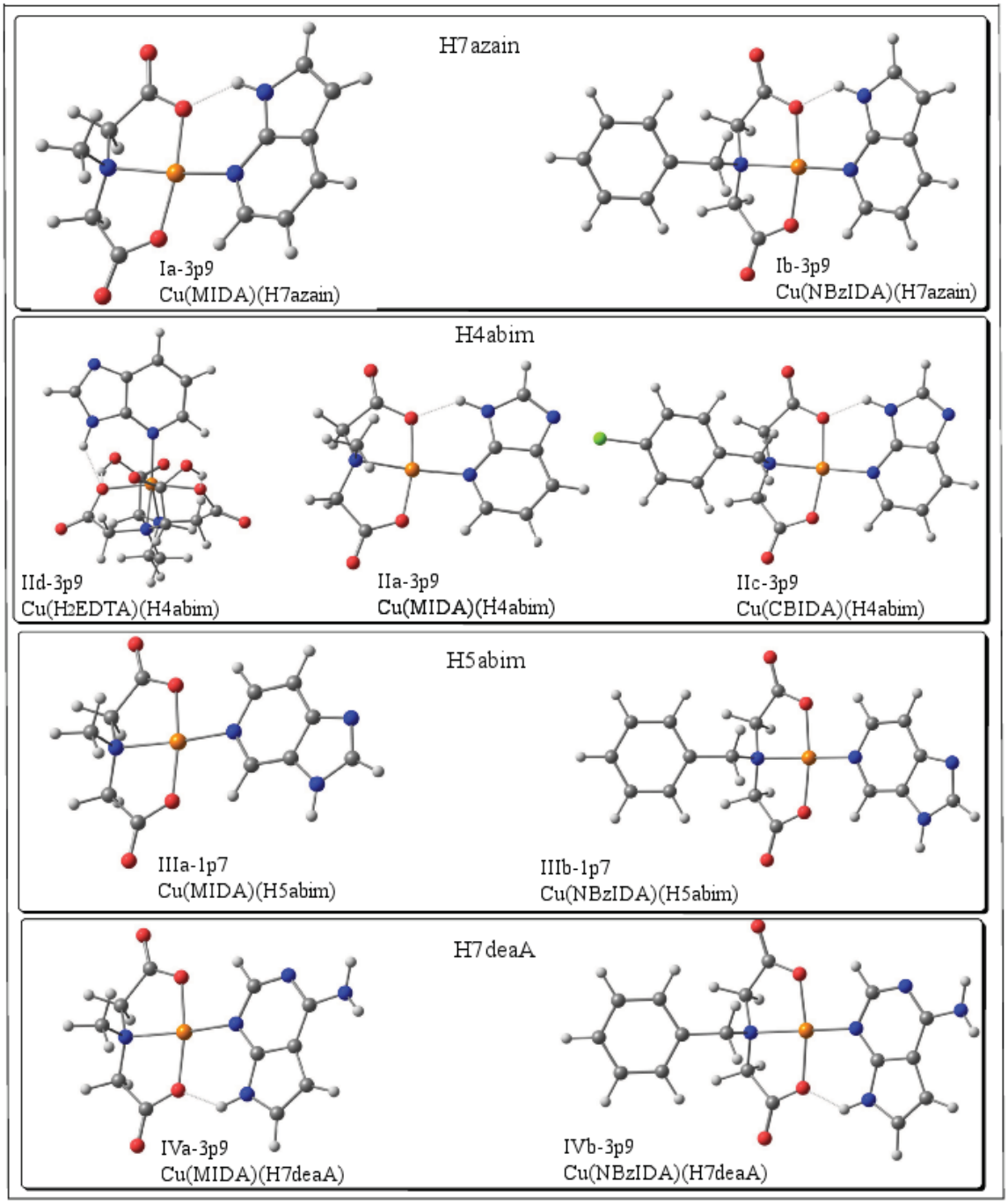


Figure 1. DFT (B3LYP/6-31+G**//B3LYP/6-31+G**) most stable coordination modes and proton tautomers for the mononuclear copper(II) complexes with nucleobases (H7azain, H4abim, H5abim and H7deaA) and the chelating ligands (MIDA, CBIDA, NBzIDA and $H_2EDTA$).

In this former complex, H4abim was not coplanar with $H_2$EDTA but formed a dihedral angle close to 10º. However, in the presence of a deprotonated N-atom (i.e. in the 3p7 or 9p7 forms) this dihedral angle significantly increases to approx. 60º. In energy terms, the most stable complexes of H4abim are the 3p9 species, similar to H7azain. The following in terms of energy are the 9p3 for MIDA and CBIDA in approx. 3.0 kcal·mol$^{-1}$. This situation changes significantly when we consider the $H_2$EDTA ligand. In this case, the next stable structure is the 3p7 within 1.1 kcal·mol$^{-1}$. It is remarkable that for MIDA and CBIDA ligands the $\Delta G_r$ of the 3p7 conformation were approx. 10.0 kcal·mol$^{-1}$. This means that the $H_2$EDTA chelating ligand allows more coordination versatility due to a significant decrease of the protonation barrier (p7 and p9).

Cu(II)/MIDA/H5abim and Cu(II)/NBzIDA/H5abim complexes also show similar geometries compared to the above-mentioned H7azain and H4abim complexes. Nevertheless, the energetics and theoretical coordination preferences differ. In the present study, the 1p7 mode is the most stable one but, as opposed to aforementioned cases, we can also find the 1p9, 9p7 or 7p9 modes within a narrow range of 1.5 kcal·mol$^{-1}$ (see Table S2). This indicates that such coordination alternatives are plausible as well as a bidentate role (vide infra - dinuclear copper(II) complexes section).

The geometrical DFT results of those complexes concerning the Cu(II)/MIDA and Cu(II)/NBzIDA chelates and H7deaA are very similar to those previously reported for H7azain and H4abim. Thus, the energy again favours the 3p9 mode. Nevertheless, the second most stable mode is the 1p9,with $\Delta G_r$ values of 2.8 and 2.3 kcal·mol$^{-1}$ for MIDA and NBzIDA, respectively.

**Dinuclear copper(II) complexes**

In the previous section, we discussed that the H5abim complexes presented energy in a range of approx. 1.5 kcal·mol$^{-1}$ for the different coordination modes. Moreover, we also synthesised and crystallized Cu(II) complexes where H5abim coordinate as a bidentate ligand.

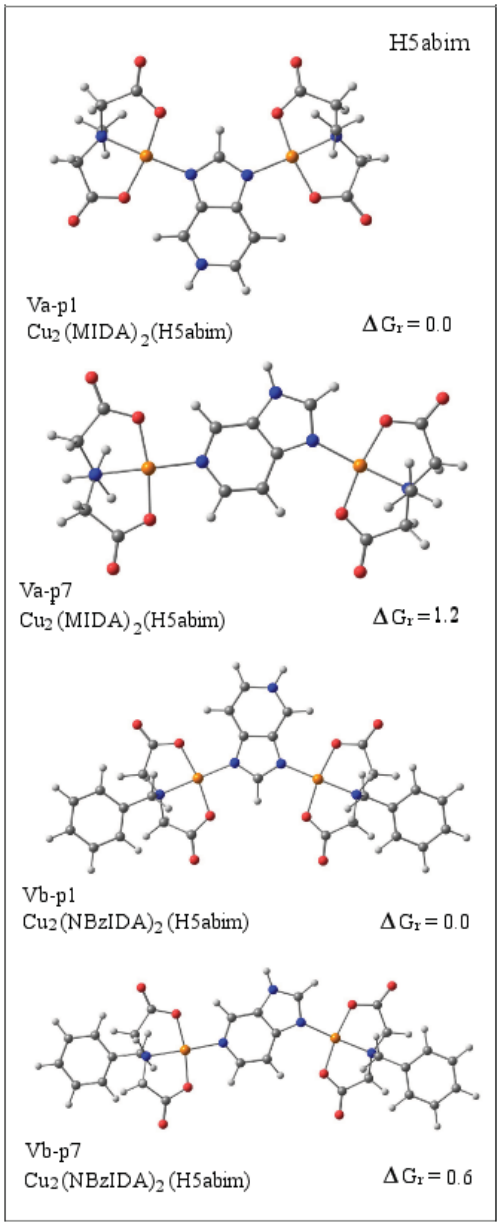


Figure 2. DFT (B3LYP/6-31+G**//B3LYP/6-31+G**) two most stable coordination modes and proton tautomers of the dinuclear copper(II) complexes with H5abim and the chelating ligands MIDA and NBzIDA

Consequently, we carried out DFT calculations of different dinuclear Cu(II) model system with H5abim, which are depicted in Figure 2. It is notable that the preferred protonation site changed to p1, as opposed to the mononuclear models, which pointed out p7 (see Figure 1).‡ Nonetheless, these results are not contradictory, since the energy range for these proton tautomers is very small, approx. 1.2 and 0.6 kcal·mol$^{-1}$, for MIDA and NBzIDA, respectively. Therefore, the theoretical results support the experimental findings of a bidentate coordination mode. In terms of geometries, the dinuclear complexes yielded geometrical parameters similar to the mononuclear ones (see Table S2).

## 2. X-Ray-diffraction Studies

### Compounds with 7-azaindole

The ligand 7-azaindole is structurally rich. The structure of the neutral ligand, H(N9)7azain, has been reported,[6] as well as several metal complexes where H7azain shows the M-N3 bond, usually reinforced by an intra-molecular H-bonding interaction N9-H···A.[7] Alternatively, metal complexes with the 7-azaindolate anion typically display the monodentate M-N9 or the bridging $\mu_2$-N3,N9 modes;[8] although $\eta_2$-N3,N9 and $\mu$-N3,$\eta_2$-N9 roles are also known.[9]

Compound **1** [Cu(TEBIDA)(H7azain)($H_2O$)] ·3$H_2O$ consists of a complex molecule and water molecules. The copper(II) atom exhibits a 4+1 coordination polyhedron where the four closest donor atoms correspond to the tridentate IDA-like chelating ligand (N10, O11, O21) and the N3(purine-like) donor of H7azain. Thus, the TEBIDA ligand adopts a mer-$NO_2$ conformation. One aqua ligand occupies the apical position. In this complex, the Cu(II) coordination environment is close to a square-based pyramidal coordination, according to the Addison parameter,[10] $\tau$ = 0.21. It bears noting that the ligands TEBIDA and H7azain are not coplanar as expected (dihedral angle <O-Cu-N-C is 46.88º), considering the previous theoretical information. Hence, the H-bonding interaction N9-H···O21(coord. carboxy) is weakened, this being related essentially to those packing forces present within the crystal (see Table S4.3 and Figure and comments in S4.4).

The crystal of **2**, {[Cu(FBIDA)(H7azain)] ·2$H_2O$}$_n$, is based on a coordination polymer built by the syn-anti-bridging carboxylate group of FBIDA ligand. The two copper(II) atoms are not crystallographically equivalent. They both exhibit a square-based pyramidal coordination, type 4+1, with a slight basal distortion ($\tau$ = 0.10 for Cu(1) and $\tau$ = 0.12 for Cu(2)). The N10, O11, and O21 donors of the tridentate mer-$NO_2$ FBIDA chelator and the N3 atom from H7azain satisfy the basal coordination plane. It seems that the tautomerizable proton, placed on N9, could be involved in a weak bifurcated H-bonding interaction: one intra-molecular and the other inter-molecular (see Table S5.3). The apical donor is the O12 atom from the bridging carboxylate group of an adjacent FBIDA ligand (Fig. 3). Again, the dihedral angle is higher than expected [49.76º for Cu(1) and 47.33º for Cu(2)]. Note that despite the molecular (**1**) and polymeric (**2**) nature of the two novel compounds, the dihedral angles are quite similar. Furthermore, it is noteworthy that, among the 26 first-row transition metal complexes containing H7azain referred to in the CSD, only three have a polymeric structure.

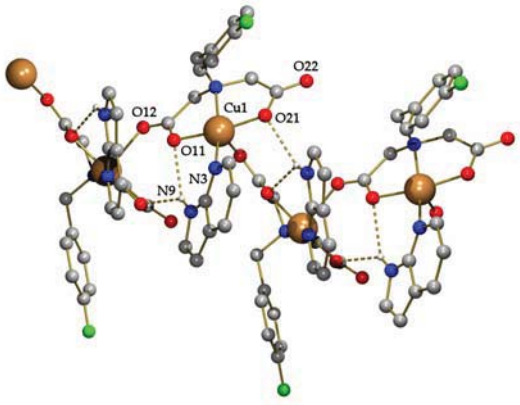


Figure 3. Structure of {[Cu(FBIDA)(H7azain)]·2$H_2O$}$_n$ (**2**): Fragment of the coordination polymer and numbering of the coordination environment.

The results from theoretical and crystallographic methods support the general molecular recognition

pattern described for monodentate neutral 7-azaindole, which consists of an M-N3 bond in cooperation with an intra-molecular interligand interaction involving the N9-H group. Indeed, previous results from our group support the aforementioned molecular recognition pattern.[11] The stability of the H(N9) tautomer appears to be related with the large difference in basicity between the two N-donor atoms in H7azain. There is a known exception that is found in three aluminium complexes where H7azain and 7azain are involved in metal binding. In these complexes, H7azain shows the rare tautomer H(N3)7azain and coordinates via N9 in cooperation with an intra-molecular N3-H···N3 H-bond.[12]

**Compounds with 4-azabenzimidazole**

The structural information concerning H4abim is rather limited; indeed the crystal structure of the ligand remains unknown. Concerning metal complexes, H4abim is found in three different Cu(II) paddlewheel-like compounds in which a $\mu_2$-N3,N9 mode is displayed.[13] Alternatively, the 4abim(1-) anion is present in two compounds serving as a $\mu_2$-N7,N9 bridge.[4,14]

The crystal of compound **3**, $\{[Cu(CBIDA)(H4abim)]\cdot 2H_2O\}_n$, consists of polymeric chains that extend parallel to b axis and water molecules. The metal exhibits a 4+1 coordination polyhedron where the four closest donor atoms are supplied by the tridentate-chelating CBIDA ligand (N10, O11 and O21) and H4abim via N7. Hence, the tautomer H(N9)4abim cannot reinforce the Cu-N7 bond with an intra-molecular H-bond. However, the N9-H group is involved in inter-molecular interactions of building 2D layers (see Table S6.3 and Figure and comments in S6.4). This fact may contribute to the value of the dihedral angle (<O-Cu-N-C 49.86º). In addition, the CBIDA ligand, in mer-$NO_2$ conformation, displays a $\mu_2$-bridging role by means of a syn-anti-carboxylate group, occupying the apical position in the Cu(II) surrounding. In this compound, the Addison parameter $\tau = 0.007$ reveals a nearly regular square-based pyramidal coordination.

Compound **4** agrees with the formula $[Cu(H_2EDTA)(H4abim)]\cdot 0.5H_2O$. The asymmetric unit consists of a complex molecule (Fig. 4) and half water molecule. The copper(II) atom shows a 4+1+1 coordination polyhedron. The $H_2EDTA$ chelator acts as a pentadentate ligand, occupying three of the four closest sites around the metal centre (N10, O11, O21) plus the two apical positions (N20 and O16). Note that the longest coordination bond corresponds to a coordinated carboxylic group (see Table S7.2). This is worth mentioning because it means that the carboxylic group has not been able to transfer its proton to H4abim, which is coordinated via N9 as the tautomer H(N7)4abim. Thus, no intra-molecular H-bond is possible in this configuration. However, the N7-H group is involved in inter-molecular interactions that help to stabilise the multi-stacked 1D chains within the crystal (see Table S14.2 and Figure and comments in S7.4).

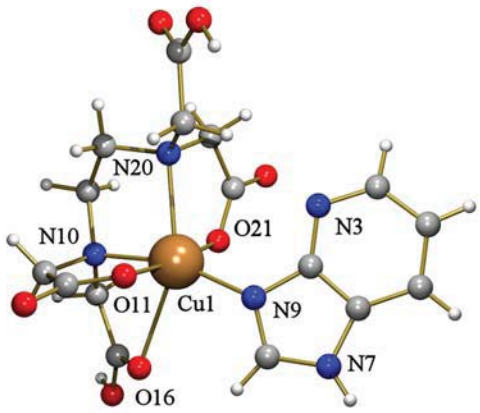


Figure 4. Structure of $[Cu(H_2EDTA)(H4abim)]\cdot 0.5H_2O$ (**4**): Molecular structure and numbering of the coordination environment.

In compound **3**, H4abim acts as a monodentate ligand through N7. This molecular recognition pattern has previously been reported by our group, referring to a close polymer with the chelating ligand N-benzyl-iminodiacetate.[11] In both compounds, the proton is tightly bonded to N9 (the most basic N-heterocyclic donor atom), and thus coordination takes place via the second-most basic

N-donor. Alternatively, compound **4** reveals a new monodentate coordination role for neutral H4abim. Herein, the tautomer H(N7)4abim is first reported and this implies that N9 is now available for coordination. These patterns are not the same as those observed as 'preferred' in the theoretical results (see 'Mononuclear copper(II) complexes' section). However, the discrepancy is acceptable, taking into account the driving forces of the crystal packing and the small protonation barrier between the p9 and p7 tautomers (see Table 1). Moreover, if we consider H4abim as a 1,6-dideaza-adenine, the formation of a Cu-N7 bond is according to the assumed sequence of basicity of adenine (N9 > N1 > N7 > N3 >> $6NH_2$). Indeed, these former molecular recognition patterns have previously been reported for mononuclear metal complexes with neutral Hade and iminodiacetate-like ligands,[15] as well as other related chelating ligands.[16] The use of the chelating ligand $H_2$EDTA(2-) in compound **4** was based on the idea of synthesising compounds containing the $H_2$4abim(1+) cation. In fact, the transfer of the proton from a carboxylic group of $H_2$EDTA(2-) to adenine has formerly been described.[17] The reason why H4abim remained in its neutral form could be related to the crystal packing or the relative acidity of the protons.

Furthermore, irrespective of the vagaries of compounds **3** and **4**, it should be noted that the coordination versatility of H4abim has increased noticeably with respect to H7azain. This fact may be related to the addition of one N-heterocyclic donor atom. Thus, the difference of basicity between the N-donors in the heterocycle is shorter, this promoting tautomerism phenomena.

**Compounds with 5-azabenzimidazole**

A recent search in the CSD reveals that, to date, there is no structure reported for neutral H5abim. However, one Zn(II) polymeric compound has been reported for 5abim(1-), displaying the bridging $\mu_2$-N7,N9 mode.[4]

Compound **5** $\{[Cu_2(IDA)_2(\mu_2\text{-N7,N9-H5abim})]\cdot H_2O\}_n$ consists of a coordination polymer built by dinuclear units. Such units extend, leading to a 3D network by means of the syn-anti-bridging role of two carboxylate groups from the IDA moiety (see Figure and comments in S8.4). The copper(II) centres are equivalent and exhibit a 4+2 coordination. Three donor atoms from the tridentate mer-$NO_2$ IDA chelator and the N7 or N9 atom from H5abim are the closest Cu(II) donors. The apical donors are the O12 and O22 from the bridging carboxylate groups of adjacent IDA ligands. The $\mu_2$-N7,N9 role forces the tautomerizable proton to shift to N1, thus no intra-molecular H-bonds are involved in the metal-binding pattern. The dihedral angle is higher than expected (<O-Cu-N-C 52.68º). It should be noted that a mirror plane is located in the middle of H5abim ligand, and then the ligand is delocalised over two positions, with an occupancy factor of 0.5.

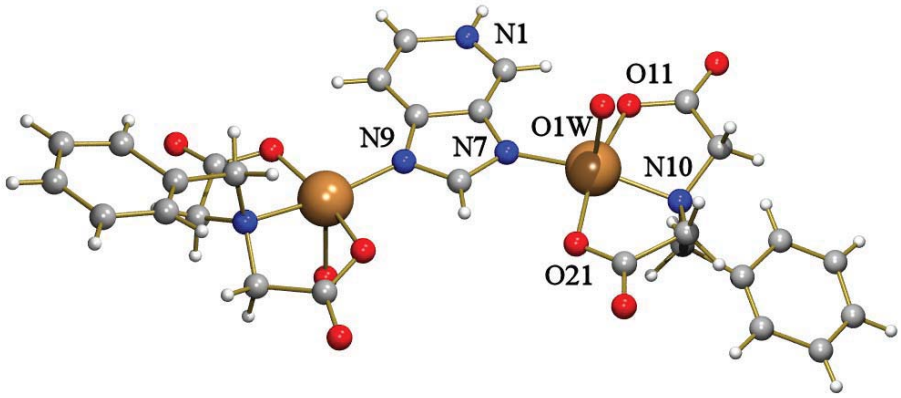


Figure 5. Structure of $[Cu_2(NBzIDA)_2(\mu_2\text{-N7,N9-H5abim})(H_2O)_2]\cdot H_2O$ (**6**): Molecular structure and numbering of the coordination environment.

The crystal of **6**, $[Cu_2(NBzIDA)_2(\mu_2\text{-}N7,N9\text{-}H5abim)(H_2O)_2]\cdot H_2O$, consists of a centro-symmetric dinuclear complex molecule plus non-coordinated water. The metal exhibits a square-based pyramidal coordination, type 4+1 (Addison parameter $\tau$ = 0.003), built by the N10, O11, and O21 donors of the tridentate NBzIDA chelator (mer-$NO_2$ conformation) and the N7 or N9 atom of H5abim. The apical position is occupied by one aqua ligand. Again, H5abim acts as a bridging ligand, between the two metal centres, displaying a $\mu_2$-N7,N9 role (Fig. 5) and showing the H(N1) tautomer. Likewise, a binary axe is located in the middle of H5abim ligand, so that it is again delocalized at 50%. The two N-benzyl moieties of the NBzIDA ligand and the water molecule are also disordered over two alternative positions with an occupancy factor of 0.52/0.48 and 0.69/0.31, respectively. This fact should be considered in the analysis of inter-molecular interactions and crystal packing (see Figure and comments in S9.4). Within the dinuclear units, a bifurcated non-classical H-bond is observed between H5abim and the O-carboxy atoms from the two NBzIDA moieties (see Table S9.3). This probably influences the rather close shape of the dinuclear motifs and might contribute to the low value of the dihedral angle according to the theoretical model (<O-Cu-N-C 11.16º).

It bears remarking that, regardless of the molecular or polymeric nature of the compounds (**6** and **5**, respectively), both display the same molecular recognition pattern: $\mu_2$-N7,N9. This latter role has previously been mentioned regarding the 4abim and 5abim anions.[4] Moreover, this metal binding has also been described for Hade and ade ligands[18-19]. For instance, our group reported the dinuclear complex $[Cu_2(NBzIDA)_2(\mu_2\text{-}N7,N9\text{-}H(N3)ade)(H_2O)_2]H_2O$.[18] Therein, both coordination bonds were assisted by the corresponding N6-H···O and N3-H···O H-bonds, respectively. By contrast, the reported complexes show the H(N1)5abim tautomer and therefore reinforcement is not possible. The fact that both N-ligands are able to display the same molecular recognition pattern, despite their N-restrictions, supports the idea of using these kinds of deaza-adenine ligands as models to study the versatility and metal-binding patterns of purine ligands. The reason why N1 is not involved in coordination in these sorts of complexes remains unknown. Note that the absence of the exocyclic amino group could have encouraged the coordination abilities of N1. However, no coordination was observed. It is remarkable that this recognition pattern is clearly favoured in terms of energy (vide supra – dinuclear copper(II) complexes section). In addition, crystal-packing features should also be considered, since the N1-H group appears to play a relevant role regarding intermolecular H-bonding interactions (see Figure and comments in S8.4 and S9.4).

**Compounds with 7-deazaadenine**

In accordance to their pharmaceutical interest, the structures of tubercidine (7-deazaadenosine) and closely related synthetic nucleosides have been reported.[20] Nevertheless, no other structural information is available on 7-deaza-adenine.

Compound **7** $[Cu(IDA)(H7deaA)(H_2O)]\cdot 2H_2O$ consists of a complex molecule and two water molecules. The copper(II) atom exhibits a 4+1 coordination polyhedron, where the four closest donor atoms correspond to the tridentate IDA chelating ligand (N10, O11, O21) and the N3 donor of H7deaA. Thus, IDA ligand adopts a mer-$NO_2$ conformation. One aqua ligand occupies the apical position. The stability of the ternary complex is reinforced by the intra-molecular interligand H-bonding interaction N9-H···O21(coord. carboxy – see Table S10.3). The dihedral angle (<O-Cu-N-C) is nearly 40º, probably because of the influence of pi,pi-stacking interactions between adjacent H7deaA ligands within the crystal (see Figure and comments in S10.4). In this complex, the Cu(II) coordination environment is fairly close to a regular square-based pyramidal coordination, according to the Addison parameter $\tau$ = 0.02.

Compound **8** $[Cu_2(MIDA)_2(\mu_2\text{-}N1\text{-}N3\text{-}H7deaA)(H_2O)_2]\cdot 5H_2O$ is an asymmetrical dinuclear complex having the unique $\mu_2$-N1,N3 bridging mode (Fig. 6). The copper(II) atoms exhibit a square-based pyramidal coordination, type 4+1, built by three

donor atoms from the MIDA chelator in a mer-$NO_2$ conformation, one N-donor from H7deaA and one apical aqua ligand. There is a small difference in the distortion of the two Cu(II) centres: $\tau$ = 0.021 for Cu(1) and $\tau$ = 0.008 for Cu(2) as well as in the dihedral angles <O-Cu-N-C 40.06º and 54.39º for Cu1 and Cu2, respectively. To the best of our knowledge, the $\mu_2$-N1,N3 bridging mode has never been reported for any metal complex having purine-like bases. This pattern uses the most stable tautomer H(N9)7deaA. Although, *a priori*, both coordination bonds have the possibility of being reinforced by an intra-molecular H-bond, experimental data indicate that only the Cu-N1 bond is assisted with the intra-molecular N6-H6A···O21(coord. carboxy - see Table S11.3) H-bond whereas the Cu-N3 bond is not reinforced since the N9-H group is involved in inter-molecular N9-H···O interactions, highly influenced by the crystal packing (see Figure and comments in S11.4).

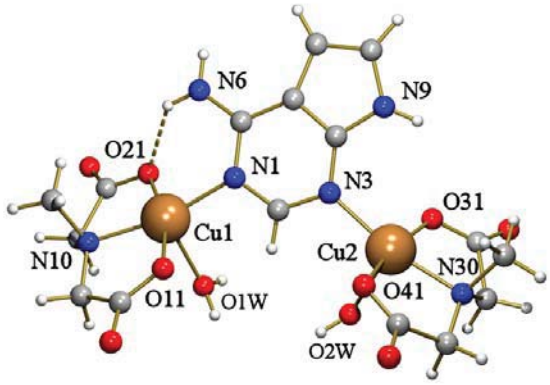


Figure 6. Structure of $[Cu_2(MIDA)_2(\mu_2\text{-N1,N3-H7deaA})(H_2O)_2]\cdot 5H_2O$ (**8**): Molecular structure and numbering of the coordination environment.

The polymeric compounds **9** $[Cu(NBzIDA)(H7deaA)]_n$ and **10** $[Cu(MEBIDA)(H7deaA)]_n$ give very similar crystals. These 1D polymers extend throughout the c axis by means of the syn-anti-bridging carboxylate group of NBzIDA or MEBIDA ligands, respectively. The metal exhibits a 4+1 coordination polyhedron, with a slight basal distortion ($\tau$ = 0.052 in **9** and $\tau$ = 0.075 in **10**). The four closest Cu(II) donor atoms are supplied by the tridentate-chelating IDA-like ligands (N10, O11 and O21) and the N3 donor atom of H(N9)7deaA ligand. The apical position is occupied by one O-carboxylate bridging atom. The dihedral angles (<O-Cu-N-C) are 36.12º in **9** or 41.49º in **10**. This fact could be related to the bifurcated character of the H-bond tied to the tautomerizable proton. Thus, N9-H would be involved both in the reinforcement of the Cu-N3 bond [N9-H···O21(coord. carboxy)] and in an inter-molecular interligand H-bond [N9-H···O11(coord. carboxy)] (Fig. 7). In the crystal, the exocyclic amino group plays a key role connecting adjacent polymeric chains (see Figure and comments in S12.4 and S13.4).

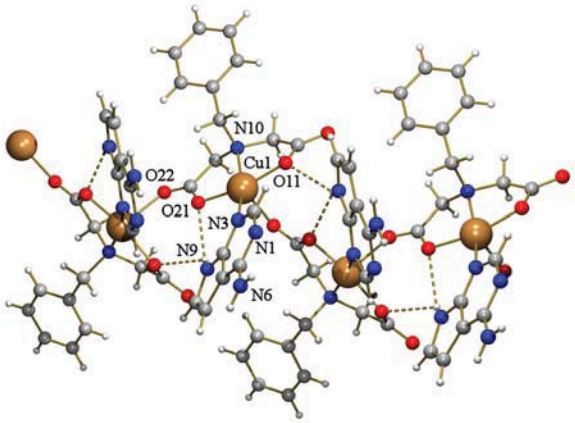


Figure 7. Structure of $[Cu(NBzIDA)(H7deaA)]_n$ (**9**): Fragment of the coordination polymer and numbering of the coordination environment.

In all the described 7-deaza-adenine derivatives, the N-heterocyclic ligand exists as its most stable tautomer H(N9)7deaA. This is consistent with the theoretical results and the basicity order of adenine, which highlights N9 as the most basic N-donor atom. In three of the four compounds studied, H7deaA shows a similar molecular recognition pattern to H7azain, despite that H7deaA offers more N-heterocyclic donors available for coordination. Why N3 is preferred over N1 for a monodentated coordination seems to be related to the possibility of establishing the M-N3 bond assisted by an intra-molecular interligand H-bond N9-H···O. This reinforcement would form a six-membered ring with an angle close to 136º. In

principle, the N1 donor is also able to assist the Cu-N1 bond with an intra-molecular interaction N6-H···O. However, this reinforcement has a much lower angle, close to 119º. Moreover, the Cu-N1 coordination is partially hindered due to the negative contribution of the electronic and steric effects of the exocyclic amino group. It should be noted that, according to solutions studies made by H. Sigel, B. Lippert et al. with adenine-like ligands,[21] the N3-metalation significantly alters the basicity of N1, thus turning it into a poorer metal-binding site. Nonetheless, these former hindrances *per se* are not enough to avoid coordination via N1. Indeed, in compound **8**, H(N9)7deaA exhibits an unique $\mu_2$-N1,N3 coordination role. The relevance of this new coordination mode is tied not only to its novelty but to the metal-binding pattern consequences of the absence of N7. Thus, the restriction on the N7(purine) donor enhances mostly the coordination abilities of the six-membered ring in the purine moiety and drives the coordination through N3 and, furthermore, promotes the coordination role of N1. In this context, the N7 vs. N1 dichotomy can also be analysed in terms of geometry. Although both N1 and N7 coordination can be assisted by an H-bonding interaction N6-H···A, the N7 reinforcement forms a seven-membered ring with an angle of close to 130º, in contrast to the above-mentioned six-membered ring with an angle of close to 119º. Also, no relevant hindrances could be expected for the N7 donor atom. Therefore, in the presence of N7, this latter donor constitutes a richer metal-binding site compared to N1, regardless of their difference of basicity. Nevertheless, when N7 is removed, N1 turns into a more competitive metal-binding site; this tendency has also been observed, for instance, with other purine-like ligands.[22]

## Experimental section

### Materials

Bluish $Cu_2CO_3(OH)_2$ was purchased from Probus. Iminodiacetic acid ($H_2$IDA) was supplied by Alfa-Aesar and N-methyl-iminodiacetic acid ($H_2$MIDA) was supplied by Across. Ethylendiaminotetraacetic acid ($H_4$EDTA), 7-azaindole, 4-azabenzimidazole, 5-azabenzimidazole and 7-deazaadenine were purchased from sigma-Aldrich. All the above reagents were used without further purification. N-(p-tBu)-, N-benzyl-, N-(p-methylbenzyl)-, N-(p-fluorobenzyl)- and N-(p-chlorobenzyl)-iminodiacetic acids ($H_2$TEBIDA, $H_2$NBzIDA, $H_2$MEBIDA, $H_2$FBIDA and $H_2$CBIDA, respectively) were synthesised in their acid form as reported in refs. 14a and 22.

### Syntheses of the complexes

**[Cu(TEBIDA)(H7azain)($H_2O$)]·3$H_2O$ (1)**

$Cu_2CO_3(OH)_2$ (0.25 mmol, 0.055 g) was reacted in 80 mL of distilled water with $H_2$TEBIDA acid (0.5 mmol, 0.095 g) in a Kitasato flask, heating (50ºC ) and stirring under moderate vacuum. Once a clear blue solution was obtained, H7azain was added (0.5 mmol, 0.059 g). The reacting mixture was stirred for 1 h until the ligand was completely dissolved. Afterwards, the resulting blue solution was filtered, without a vacuum, in a crystallization device and allowed to stand at room temperature, covered with a plastic film to control the evaporation. After several weeks, parallelepiped crystals suitable for XRD purposes were collected. The yield was ca. 70-75%. Elemental analysis (%): Calc. for $C_{15}H_{27}CuN_3O_8$: C 40.86, H 6.17, N 9.53; Found: C 40.73, H 6.32, N 9.59. FT-IR (KBr, $cm^{-1}$) $\nu_{as}(H_2O)$ 3456, $\nu_s(H_2O)$ 3250, $\nu$(N-H) 3163, $\nu_{as}(CH_3)$ 2985, $\nu_s(CH_3)$ 2854, $\nu_{as}(CH_2)$ 2964, $\nu_s(CH_2)$ 2825, $\delta(H_2O)$ 1633, $\nu_{as}$(COO) 1608, $\delta$(N-H) 1507, $\nu_s$(COO) 1384, $\pi(C\text{-}H)_{ar}$ 725. The UV/Vis spectrum showed an asymmetric d-d band with $\lambda_{max}$ at 677 nm ($\nu_{max}$ 14770 $cm^{-1}$). Under air-dry flow, the sample lost the non-coordinated water molecules, and thus the TG experiment started with an average formula [Cu(TEBIDA)(H7azain)($H_2O$)]. The thermo-gravimetric curve shows three steps. The first step corresponds to the loss weight of the apical aqua ligand (Calc. 4.66%; Found 4.56%). Indeed, only $H_2O$ was found in the evolved gasses during the first step. The following pyrolytic steps yielded a final residue of CuO (425ºC , Calc. 20.56%; Found 21.45%). The evolved gasses during the pyrolysis

involved $H_2O$, $CO_2$, CO and two N-oxide gasses ($N_2O$ and NO).

**{[Cu(FBIDA)(H7azain)]·$H_2O$}$_n$ (2)**

A synthetic procedure similar to that of compound (**1**) was followed, using $H_2$FBIDA acid (0.5 mmol, 0.120 g) instead of $H_2$TEBIDA acid. In two days, needle-like crystals were obtained. The reaction yielded 65%. Elemental analysis (%): Calc. for $C_{18}H_{21}CuFN_3O_9$: C 49.15, H 4.35, N 9.55; Found: C 49.33, H 6.28, N 9.48. FT-IR (KBr, $cm^{-1}$) $\nu_{as}(H_2O)$ 3434, $\nu_s(H_2O)$ shoulder 3257, $\nu$(N-H) overshadowed, $\nu_{as}(CH_2)$ 2927, $\nu_s(CH_2)$ 2852, $\delta(H_2O)$ overlapped 1620, $\nu_{as}$(COO) 1620, $\delta$(N-H) 1512, $\nu_s$(COO) 1384, $\pi(C\text{-}H)_{ar}$ 731 (H7azain), $\pi(C\text{-}H)_{ar}$ 793 (FBIDA). The UV/Vis spectrum shows an asymmetric d-d band with $\lambda_{max}$ at 681 nm ($\nu_{max}$ 14680 $cm^{-1}$). Under air-dry flow, the sample lost part of the non-coordinated water molecule. Hence, the sample started the TG experiment with formula {[Cu(FBIDA)(H7azain)]· 0.55$H_2O$}. The thermal behaviour was divided into four steps. The sample lost the former 0.55 $H_2O$ molecules during the first step (Calc. 2.30%; Found 2.60%), according to the evolved gasses. Three additional pyrolytic steps produced $H_2O$, $CO_2$, CO, and N-oxide gasses ($N_2O$, NO, $NO_2$) to reach a final CuO residue (480ºC, Calc. 18.42%; Found 19.45%).

**{[Cu(CBIDA)(H4abim)]·2$H_2O$}$_n$ (3)**

A synthetic procedure similar to that of compound (**1**) was followed, using $Cu_2CO_3(OH)_2$ (0.25 mmol, 0.055 g), $H_2$CBIDA acid (0.5 mmol, 0.128 g), and H4abim (0.5 mmol, 0.060 g). In approximately three weeks, needle-like crystals were collected. The reaction yielded 81%. Elemental analysis (%): Calc. for $C_{17}H_{19}ClCuN_4O_6$: C 43.04, H 4.04, N 11.81; Found: C 42.85, H 3.98, N 11.93. FT-IR (KBr, $cm^{-1}$) $\nu_{as}(H_2O)$ 3418, $\nu_s(H_2O)$ 3258, $\nu$(N-H) 3132, two different $\nu_{as}(CH_2)$ 2971 and 2927, two different $\nu_s(CH_2)$ 2872 and 2818, $\delta(H_2O)$ shoulder 1625, $\nu_{as}(COO)_{bridging}$ 1614, $\nu_{as}(COO)_{monodentate}$ 1600, $\delta$(N-H) 1539, $\nu_s(COO)_{bridging}$ 1399, $\nu_s(COO)_{monodentate}$ 1388, $\pi(C\text{-}H)_{ar}$ 780 (H4abim), $\pi(C\text{-}H)_{ar}$ 677 (CBIDA). The UV/Vis spectrum shows an asymmetric d-d band with $\lambda_{max}$ at 677 nm ($\nu_{max}$ 14770 $cm^{-1}$). The ESR spectrum shows a typical axial shape ($g_{II}$ 2.24 and $g_{\perp}$ 2.04) corresponding to a Cu(II) centre in $d_{x2-y2}$ ground state. Under air-dry flow, the sample lost 1.5 non-coordinated water molecules, and hence the TG experiment started with an average formula {[Cu(CBIDA)(H4abim)]·0.5$H_2O$}. The thermo-gravimetric curve was divided into four steps. The first step corresponded only to the loss of 0.5 $H_2O$ molecules (Calc. 2.01%; Found 1.94%). Pyrolysis of the organic ligands was conducted in three consecutive steps, in which $H_2O$, $CO_2$, CO, $N_2O$, NO, and $NO_2$(t) were evolved. At the end, a CuO residue was obtained (530ºC, Calc. 17.78%; Found 17.88%).

**[Cu($H_2$EDTA)(H4abim)]·0.5$H_2O$ (4)**

A synthetic procedure similar to that of compound (**3**) was followed, using $H_4$EDTA acid (0.5 mmol, 0.146 g) instead of $H_2$CBIDA acid. Four weeks later, suitable crystals for XRD purposes were collected. Yield is ca. 75-80%. Elemental analysis (%): Calc. for $C_{16}H_{20}CuN_5O_{8.5}$: C 39.88, H 4.18, N 14.53; Found: C 40.01, H 4.23, N 14.26. FT-IR (KBr, $cm^{-1}$) $\nu_{as}(H_2O)$ 3435, $\nu_s(H_2O)$ shoulder 3259, $\nu$(N-H) 3136, two different $\nu_{as}(CH_2)$ 2929 and 2919, two different $\nu_s(CH_2)$ 2879 and 2857, $\nu(C{=}O)_{free\ -COOH}$ 1727, $\delta(H_2O)$ 1617, $\nu_{as}$(COO) 1568, $\delta$(N-H) overshadowed, combined mode $\nu$(C-O)+$\delta$(O-H) shoulder 1412, $\nu_s$(COO) 1384, $\delta$(O-H) 1116, $\pi$(O-H) 733, $\pi(C\text{-}H)_{ar}$ 783. The UV/Vis spectrum shows an asymmetric d-d band with $\lambda_{max}$ at 675 nm ($\nu_{max}$ 14810 $cm^{-1}$) and a shoulder at $\lambda$ 1050 nm ($\nu_{sh}$ 9480 $cm^{-1}$). Under air-dry flow, the sample lost all the non-coordinated water molecule. The thermo-gravimetric curve was divided into three steps. In the TG experiment, the sample directly underwent pyrolysis, from 170ºC to 525ºC, when the CuO residue was measured (Calc. 16.82%; Found 18.29%). The pyrolysis of [Cu($H_2$EDTA)(H4abim)] produced $H_2O$, $CO_2$, CO, and N-oxide gasses ($N_2O$, NO, and $NO_2$).

**{[$Cu_2$(IDA)$_2$($\mu_2$-N7,N9-H5abim)]·$H_2O$}$_n$ (5)**

A synthetic procedure similar to that of compound (**1**) was followed, using $Cu_2CO_3(OH)_2$ (0.25 mmol,

0.055 g), $H_2IDA$ acid (0.5 mmol, 0.067 g), and H5abim (0.5 mmol, 0.060 g). However, only extremely thin needle-like crystals, useless for XRD purposes, resulted. Hence, the synthesis was redesigned. $Cu_2CO_3(OH)_2$ (0.06 mmol, 0.013 g) was reacted in 5 mL of distilled water with $H_2IDA$ acid (0.125 mmol, 0.016 g) in a small Erlenmeyer flask, heating (50ºC) and stirring. Once the reaction was completed, an aliquot (3 mL) of such blue solution was moved to a vial. Separately, H5abim (0.125 mmol, 0.017 g) was dissolved in 5 mL of DMF and slowly added to the aforementioned blue solution. The vial was properly capped and the solution left to evaporate at 120ºC. After two days, good parallelepiped crystals were obtained. The reaction yielded 65%. Elemental analysis (%): Calc. for $C_{14}H_{17}Cu_2N_5O_9$: C 31.94, H 3.26, N 13.30; Found: C 32.09, H 3.46, N 13.21. FT-IR (KBr, $cm^{-1}$) $\nu_{as}(H_2O)$ 3478, $\nu_s(H_2O)$ 3205, ν(N-H) 3131 (H5abim), ν(N-H) 3100 (IDA), $\nu_{as}(CH_2)$ 2925, $\nu_s(CH_2)$ 2829, $\delta(H_2O)$ overlapped 1618, $\nu_{as}(COO)$ 1618, δ(N-H) 1547, $\nu_s(COO)$ 1382, $\pi(C\text{-}H)_{ar}$ 641. The UV/Vis spectrum shows an asymmetric d-d band with $\lambda_{max}$ at 687 nm ($\nu_{max}$ 14555 $cm^{-1}$). The absence of enough high-quality samples allowed us to analyse the TG experiment only in a qualitative way. The TG curve was divided into four steps. In the first step (to 230ºC), only the water content was lost according to the evolved gasses. Successive pyrolytic steps produced $H_2O$, $CO_2$, CO, $NO_2$, and NO gasses, yielding a possible CuO residue (440ºC).

**$[Cu_2(NBzIDA)_2(\mu_2\text{-}N7,N9\text{-}H5abim)(H_2O)_2]\cdot H_2O$ (6)**

A synthetic procedure similar to that of compound (**1**) was followed, using $Cu_2CO_3(OH)_2$ (0.25 mmol, 0.055 g), $H_2NBzIDA$ acid (0.5 mmol, 0.112 g), and H5abim (0.5 mmol, 0.060 g). Six weeks later, parallelepiped crystals suitable for XRD purposes were collected. Yield is ca. 65-70%. Elemental analysis (%): Calc. for $C_{28}H_{33}Cu_2N_5O_{11}$: C 45.28, H 4.48, N 9.43; Found: C 45.06, H 4.31, N 9.57. FT-IR (KBr, $cm^{-1}$) $\nu_{as}(H_2O)$ 3427, $\nu_s(H_2O)$ 3269, ν(N-H) 3126, two different $\nu_{as}(CH_2)$ 2983 and 2937, two different $\nu_s(CH_2)$ 2872 and 2835, $\delta(H_2O)$ overlapped 1629, $\nu_{as}(COO)$ 1629, δ(N-H) 1538, $\nu_s(COO)$ 1384, $\pi(C\text{-}H)_{ar}$ 644 (H5abim), $\pi(C\text{-}H)_{ar}$ 708 (NBzIDA). The UV/Vis spectrum shows an asymmetric d-d band with $\lambda_{max}$ at 675 nm ($\nu_{max}$ 14815 $cm^{-1}$). Under air-dry flow, the sample lost all the water content. The thermal behaviour was divided into two steps. The TG experiment started at 190ºC when the sample directly underwent pyrolysis up to 455ºC , when the CuO residue was measured (Calc. 20.16%; Found 21.42%). The pyrolysis of $[Cu_2(NBzIDA)_2(H5abim)]$ produced $H_2O$, $CO_2$, CO, $N_2O$, NO and $NO_2$(t).

**$[Cu(IDA)(H7deaA)(H_2O)]\cdot 2H_2O$ (7)**

A synthetic procedure similar to that of compound (**1**) was followed, using $Cu_2CO_3(OH)_2$ (0.25 mmol, 0.055 g), $H_2IDA$ acid (0.5 mmol, 0.067 g), and H7deaA (0.5 mmol, 0.067 g). In two weeks, greenish needle-like crystals were collected. The reaction yielded 75%. However, the easy ageing of the crystals prevented the successful X-ray data collection. To avoid this problem, we grew the crystals in a gel medium to preserve their integrity, as described here. H7deaA (0.02 mmol, 0.0027 g) was added as a solid powder to a vial. Afterwards, 2 mL of an 0.5% agar solution of $[Cu(IDA)(H_2O)_2]$ 0.01M was added to the same vial, stirring the solution in a water bath (gentle heating) until the reaction took place. Then, the solution, properly capped, was left gel at room temperature. The vial stood at room temperature where better crystals appeared within four weeks. One of these crystals was removed and successfully used for XRD purposes. Elemental analysis (%): Calc. for $C_{10}H_{17}CuN_5O_7$: C 31.37, H 4.48, N 18.29; Found: C 31.49, H 4.53, N 18.15. FT-IR (KBr, $cm^{-1}$) $\nu_{as}(H_2O)$ 3421, $\nu_{as}(NH_2)$ 3346, $\nu_s(NH_2)$ 3272, $\nu_s(H_2O)$ 3228, ν(N-H) 3134 (H7deaA and IDA overlapped), $\nu_{as}(CH_2)$ 2943, $\nu_s(CH_2)$ overshadowed, $\delta(H_2O)$ 1652, $\delta(NH_2)$ 1604, $\nu_{as}(COO)$ 1586, δ(N-H) 1514, $\nu_s(COO)$ 1392, $\pi(C\text{-}H)_{ar}$ 734. The UV/Vis spectrum shows an asymmetric d-d band with $\lambda_{max}$ at 726 nm ($\nu_{max}$ 13755 $cm^{-1}$). Under air-dry flow, the sample lost only part of the non-coordinated water molecule. Hence, the sample started with a TG formula $[Cu(IDA)(H7deaA)(H_2O)]\cdot 1.5H_2O$. The thermal behaviour was divided into four steps. The entire water content was lost during the first step (Calc. 12.05%; Found 12.16%), according to the

evolved gasses – only $H_2O$. Three additional pyrolytic steps produce $H_2O$, $CO_2$, CO, $NH_3$, and N-oxide gasses ($N_2O$, NO, $NO_2$) to reach a final CuO residue (550ºC , Calc. 21.27%; Found 21.39%).

**$[Cu_2(MIDA)_2(\mu_2\text{-N1,N3-H7deaA})(H_2O)_2]\cdot 5H_2O$ (8)**

A synthetic procedure similar to that of compound (**1**) was followed, using $Cu_2CO_3(OH)_2$ (0.25 mmol, 0.055 g), $H_2$MIDA acid (0.5 mmol, 0.073 g), and H7deaA (0.5 mmol, 0.067 g). After two months, very thin needle-like crystals were collected. Yield was ca. 70-75%. Elemental analysis (%): Calc. for $C_{16}H_{34}Cu_2N_6O_{15}$: C 28.36, H 5.06, N 12.40; Found: C 28.26, H 4.88, N 12.56. FT-IR (KBr, $cm^{-1}$) $\nu_{as}(H_2O)$ 3470, $\nu_{as}(NH_2)$ 3401, $\nu_s(NH_2)$ 3236, $\nu_s(H_2O)$ overlapped 3236, $\nu$(N-H) shoulder 3120, $\nu_{as}(CH_3)$ 2975, $\nu_{as}(CH_2)$ 2934, $\nu_s(CH_3)$ 2858, $\nu_s(CH_2)$ 2859, $\delta(H_2O)$ 1639, $\delta(NH_2)$ overlapped 1614, $\nu_{as}$(COO) 1614, $\delta$(N-H) 1512, $\nu_s$(COO) 1391, $\pi(C\text{-}H)_{ar}$ 738. The UV/Vis spectrum shows an asymmetric d-d band with $\lambda_{max}$ at 696 nm ($\nu_{max}$ 14370 $cm^{-1}$). Under air-dry flow, the sample lost part of the non-coordinated water molecules. The TG experiment started with an average formula $[Cu_2(MIDA)_2(H7deaA)(H_2O)_2]\cdot 2.3H_2O$. The thermo-gravimetric curve was divided into four steps. The first step agreed with the loss of 4.3 $H_2O$ molecules, which corresponded to 2.3 non-coordinated plus two apical aqua ligands (Calc. 12.32%; Found 12.42%). Pyrolysis of the organic ligands was conducted in three consecutive steps, in which $H_2O$, $CO_2$, CO, $NH_3$, trimethyl-amine, $N_2O$, and NO were evolved. Note that trimethyl-amine is a typical gas present in the pyrolysis of MIDA ligand. In the end, a CuO residue was obtained (450ºC, Calc. 23.48%; Found 23.78%).

**$[Cu(NBzIDA)(H7deaA)]_n$ (9)**

A synthetic procedure similar to that of compound (**8**) was followed, using $H_2$NBzIDA acid (0.5 mmol, 0.112 g) instead of $H_2$MIDA acid. The day after, micro-crystals covered the crystallization device and the solution was filtered with the aim of obtaining larger crystals. Two weeks later, crystals reached an appropriate size but X-ray data collection was not successful. The reaction yielded 65%. Hence, crystallization on gel medium was performed to improve the size and the quality of the crystals: H7deaA (0.01 mmol, 0.0013 g) was added as a solid powder into a vial. Afterwards, 2 mL of an 0.5% agar solution of $[Cu(NBzIDA)(H_2O)_2]$ 2.5 mM was added to the same vial, stirring the solution in a water bath (gentle heating) until the reaction took place. Then, the solution was left to gel at room temperature. Once the solution was a proper gel, 200 µL of MeOH was added as an anti-solvent and the vial was capped. The vial stood at room temperature, and suitable crystals appeared within four weeks. One of these crystals was removed and successfully used for XRD purposes. Elemental analysis (%): Calc. for $C_{17}H_{17}CuN_5O_4$: C 48.74, H 4.09, N 16.72; Found: C 48.79, H 4.09, N 16.69. FT-IR (KBr, $cm^{-1}$) $\nu_{as}(NH_2)$ 3304, $\nu_s(NH_2)$ 3270, $\nu$(N-H) 3190, two different $\nu_{as}(CH_2)$ 2959 and 2928, two different $\nu_s(CH_2)$ 2888 and 2863, $\delta(NH_2)$ shoulder 1605, $\nu_{as}$(COO) 1593, $\delta$(N-H) 1509, $\nu_s$(COO) 1399, $\pi(C\text{-}H)_{ar}$ 746 (H7deaA), $\pi(C\text{-}H)_{ar}$ 710 (NBzIDA). The UV/Vis spectrum shows an asymmetric d-d band with $\lambda_{max}$ at 731 nm ($\nu_{max}$ 13680 $cm^{-1}$). The thermal behaviour was divided into three steps. Since the sample did not have any water content, the compound directly followed three pyrolytic steps, producing $H_2O$, $CO_2$, CO, and N-oxide gasses ($N_2O$, NO, $NO_2$) to reach a final CuO residue (, 440ºC Calc. 18.99%; Found 20.81%).

**$[Cu(MEBIDA)(H7deaA)]_n$ (10)**

A synthetic procedure similar to that of compound (**8**) was followed using $H_2$MEBIDA acid (0.5 mmol, 0.120 g) instead of $H_2$MIDA acid. Two weeks later, suitable parallelepiped crystals were collected. Yield is ca. 70-75%. Elemental analysis (%): Calc. for $C_{18}H_{19}CuN_5O_4$: C 49.94, H 4.42, N 16.18; Found: C 49.82, H 4.26, N 16.14. FT-IR (KBr, $cm^{-1}$) $\nu_{as}(NH_2)$ 3365, $\nu_s(NH_2)$ 3280, $\nu$(N-H) 3195, $\nu_{as}(CH_3)$ 2942, $\nu_{as}(CH_2)$ 2922, $\nu_s(CH_3)$ 2859, $\nu_s(CH_2)$ 2822, $\delta(NH_2)$ 1637, $\nu_{as}$(COO) 1596, $\delta$(N-H) 1513, $\nu_s$(COO) 1390, $\pi(C\text{-}H)_{ar}$ 739 (H7deaA), $\pi(C\text{-}H)_{ar}$ 808 (MEBIDA). The UV/Vis spectrum shows an asymmetric d-d band with $\lambda_{max}$ at 710 nm ($\nu_{max}$ 14085 $cm^{-1}$). The thermal behaviour was divided into three steps. Since the sample had no water content, the

compound directly followed three pyrolytic steps, producing $H_2O$, $CO_2$, CO, and N-oxide gasses ($N_2O$, NO, $NO_2$) to form a final CuO residue (470ºC, Calc. 18.33%; Found 18.04%).

## Conclusions

In the ternary iminodiacetate-copper(II) complexes studied in this work, we found a general trend to use different tautomers and to diversify the metal-binding patterns of the deaza-adenines studied. It was notable that, although H(N9) was the most stable tautomer of all the purine-like ligands, tautomerism phenomena are possible within the metal complexes, i.e. H4abim and H5abim, where the tautomers H(N9) and H(N7) were very close in terms of energy. We found that the absence of N7 in H(N9)7deaA encouraged the formation of the rare Cu-N1 bond in cooperation with an intra-molecular interligand N6-H···O H-bond. Overall, a remarkable and broad agreement was observed between the molecular structures and the reported DFT calculations.

## Acknowledgements

Financial support from Research Groups FQM-283 and FQM-174 (Junta de Andalucía) and MICINN-Spain (Project MAT2010-15594) is gratefully acknowledged. The project 'Factoría de Cristalización, CONSOLIDER INGENIO-2010' provided X-ray structural facilities for this work. We thank the "Centro de Servicios de Informática y Redes de Comunicaciones" (CSIRC), Universidad de Granada, for providing computing time. Financial support from ERDF Funds and Junta de Andalucía to acquire the FT-IR spectrophotometer Jasco 6300 is gratefully acknowledged. ADM thanks ME-Spain for a FPU Ph.D contract.

## Notes and references

[a] *Department of Inorganic Chemistry, Faculty of Pharmacy, University of Granada, Campus Cartuja s/n, 18071 Granada, Spain. Fax: +34 958 246219; Tel: +34 958 243853; E-mail: adominguez@ugr.es*

[b] *Laboratorio de Estudios Cristalográficos, IACT, CSIC-University of Granada, Avenida de las Palmeras 4, 18100 Armilla (Granada), Spain.*

[c] *Grupo de Modelización y Diseño Molecular, Department of Organic Chemistry, University of Granada, Severo Ochoa s/n, 18071 Granada, Spain.*

[d] *Department of Inorganic Chemistry, Faculty of Science and Technology, University of Basque Country, E-48080 Bilbao, Spain.*

[e] *Department of Inorganic Chemistry, Faculty of Pharmacy, University of Santiago de Compostela, 15782 Santiago de Compostela, Spain.*

† Electronic Supplementary Information (ESI) available: Experimental details are provided in S1. Additional crystal data, formula and structural plots of all the compounds reported in this work are included in the supporting information (S4 to S13). CCDC 881136 - 881145. As an example, relevant spectral properties and thermal stability information of compound 8 are also provided in S14. See DOI: 10.1039/b000000x/.

Additional spectroscopic (FT-IR and UV-Vis) and thermal (TGA) analyses have been carried out for all the reported compounds. For further information, please contact the corresponding author.

**§** Notation for the N-atom coordinated to Cu(II) and the N atom protonated, i.e. 9p3 means coordination via N9 and the dissociable proton bound to N3 of the deaza-adenine ligand.

‡ There is another possibility of dinuclear coordination: 1,7p9. This former conformation has been intentionally discarded due to the distortions arising from the proximity of both chelating ligands (see, for example, the dihedral angles in Table S2).

1 (a) P.J. Sanz Miguel, P. Amo-Ochoa, O. Castillo, A. Houlton and F. Zamora, in Metal complex-DNA interactions, ed. N. Hadjiliadis and E. Sletten, Blackwell-Wiley, UK, 2009, ch. 4; (b) B. Lippert, in Nucleic acid-metal ion interactions, ed. N.V. Hu, RSC Publishing, UK, 2009, ch.2; (c) A. Terrón, J.J. Fiol, A. García-Raso, M. Barceló-Oliver and V. Moreno, *Coord. Chem. Rev.*, 2007, **251**, 1973.

2 (a) D. K. Patel, A. Domínguez-Martín, M. P. Brandi-Blanco, D. Choquesillo-Lazarte, V. M. Nurchi, J. Niclós-Gutiérrez, *Coord. Chem. Rev.*,

2012, **256**, 193; (b) S. Verma, A. K. Mishra and J. Kumar, *Acc. Chem. Res.*, 2010, **43**, 79.
3 (a) P. Starha, J. Marek, and Z. Trávnícek, *Polyhedron*, 2012, **33**, 404; (b) J. Ruiz, V. Rodríguez, C. de Haro, A. Espinosa, J. Pérez and C. Janiak, *Dalton Trans.*, 2010, **39**, 3301; (c) H. Pivoňková, P. Horáková, M. Fojtová and M. Fojta, *Anal. Chem.*, 2010, **82**, 6807; (d) I. Lakomska, H. Kooijman, A. L. Spek, W. Shen and J. Reedijk, *J. Chem. Soc., Dalton Trans.*, 2009, 10736; (e) O.M. Yagui, H. Furukawa and B. Wang, International Patent B01J29/06, 2009; (f) K.B. Hall, *Methods Enzymol*, 2003, **469**, 269; (g) P. K. Dubey, K. V. Kumar, A. Naidu, S. M. Kulkarni, *Asian J. Chem.*, 2002, **14**, 1129.
4 H. Hayashi, A. P. Côté, H. Furukawa, M. O'Keeffe and O. M. Yagui, *Nat. Mater.*, 2007, **6**, 501.
5 S. Yurdakul and S. Badoglu, *Spectrochimica Acta Part A*, 2012, **89**, 252.
6 P. Dufour, Y. Dartiguenave, N. Dufour, A.-M. Lebuis, F. Belanger-Gariepy and A. L. Beauchamp, Can. J. Chem., 1990, 68, 193.
7 (a) G. A. Van Albada, S. Nur, M. G. Van der Horst, I. Multikainen, U. Turpeinen, J. Reedijk, *J. Mol. Struct.*, 2008, **874**, 41; (b) B. R. A. Bland, H. J. Gilfoy, G. Vamvounis, K. N. Robertson, T. S. Cameron and M. A. S. Aquino, *Inorg. Chim. Acta*, 2005, **358**, 3927; (c) J. Poitras and A. L. Beauchamp, *Can. J. Chem.*, 1992, **70**, 2846.
8 (a) N. Tsoureas, M. F. Haddow, A. Hamilton, G. R. Owen, *Chem. Commun.*, 2009, 2538; (b) T. Saito, S. Kuwata and T. Ikariya, *Chem. Lett.*, 2006, **35**, 1224; (c) S.-M. Peng and Y.-N. Lin, *Acta Crystallogr.*, 1986, **C42**, 1725.
9 (a) G. B. Deacon, E. E. Delbridge, B. W. Skelton and A. H. White, *Eur. J. Inorg. Chem.*, 1999, 751; (b) J. A. Cabeza, L. A. Oro and M. Tiripicchio Camellini, *J. Chem. Soc., Dalton Trans.*, 1988, 1437.
10 A. W. Addison, T. N. Rao, J. Reedijk, J. Van Rijn and G. C. Verschoor, *J. Chem. Soc., Dalton Trans.*, 1984, 1349.
11 D. Choquesillo-Lazarte, A. Domínguez-Martín, A. Matilla-Hernández, Celia Sánchez de Medina-Revilla, J. M. González-Pérez, A. Castiñeiras and J. Niclós-Gutiérrez, *Polyhedron*, 2009, **29**, 170.
12 J. Ashenhurst, G. Wu and S. Wang, *J. Am. Chem. Soc.*, 2000, **122**, 2541.
13 (a) C. Sánchez de Medina-Revilla, D. Choquesillo-Lazarte, A. Domínguez-Martín, J. M. González-Pérez, A. Castiñeiras, J. Niclós-Gutiérrez, Proceedings of the 9th European Biological Inorganic Chemistry Conference, Wroclaw, 2008; (b) G. A. Van Albada, I. Multikainen, U. Turpeinen and J. Reedijk, *Polyhedron*, 2006, **25**, 3278.
14 S.J. Rettig, V. Sánchez, A. Storr, R.C. Thompson, J. Trotter, J. Chem. Soc., Dalton Trans. 2000, 3931.
15 (a) E. Bugella-Altamirano, D. Choquesillo-Lazarte, J.M. González-Pérez, M. J. Sánchez-Moreno, R. Marín-Sánchez, J.D. Martín-Ramos, B. Covelo, R. Carballo, A. Castiñeiras and J. Niclós-Gutiérrez, *Inorg. Chim. Acta*, 2002, **339**, 160; (b) A. C. Morel, D. Choquesillo-Lazarte, C. Alarcon-Payer, J. M. González-Perez, A. Castiñeiras, J. Niclós-Gutiérrez, *Inorg. Chem. Commun*., 2003, **6**, 1354; (c) M. P. Brandi-Blanco, B. Dumet-Fernandes, J. M. González-Perez, D. Choquesillo-Lazarte, *Acta Crystallogr.*, 2007, *E63*, m1598.
16 (a) M. J. Zaworotko, H. H. Hammud, A. Kabbani, G. J. McManus, A. M. Ghannoum, M. S. Masoud, *J. Chem. Cryst.*, 2009, **39**, 853; (b) J. P. García-Terán, O. Castillo, A. Luque, U. García-Couceiro, G. Beobide, P. Román, Dalton Trans., 2006, 902.
17 E. Serrano-Padial, D. Choquesillo-Lazarte, E. Bugella-Altamirano, A. Castiñeiras, R. Carballo and J. Niclós-Gutiérrez, Polyhedron, 2002, 21, 1451.
18 P. X. Rojas-González, A. Castiñeiras, J. M. González-Pérez, D. Choquesillo-Lazarte, J. Niclós-Gutiérrez, *Inorg. Chem.*, 2002, **41**, 6190.
19 J. An, R.P. Fiorella, S.J. Geib and N.L. Rosi, *J. Am. Chem. Soc.*, 2009, **131**, 8401.
20 (a) R. M. Stroud, *Acta Crystallogr.*, 1973, **B29**, 690; (b) J. Abola and M. Sundaralingam, *Acta Crystallogr.*, 1973, **B29**, 697; (c) V. Zabel, W. Saenger and F. Seela, *Acta Crystallogr.*, 1987, **C43**, 131; (d) R. McKenna, R. Kuroda, S. Neidle and P. Serafinowski, *Acta Crystallogr.*, 1987, **C43**, 1790; (d) G. J. Gainsford, R. F. G. Frohlich, G. B. Evans, *Acta Crystallogr.*, 2010, **E66**, o1688.
21 C. Meiser, B. Song, E. Freisinger, M. Peilert, H. Sigel, B. Lippert, *Eur. Chem. J.*, 1997, **3**, 388.
22 A. Domínguez-Martín, D. Choquesillo-Lazarte, L. Lezama, J.M. González-Pérez, A. Castiñeiras, J. Niclós-Gutiérrez, *Inorg. Chem. Submitted.*

# CHAPTER 2:

Copper(II) complexes with adenine isomers

## 2.1. Molecular recognition patterns of 2-aminopurine versus adenine: A view through ternary copper(II) complexes

Article published in *J. Inorg. Biochem*. 105 (2011) 1073-1080

SYNOPSIS

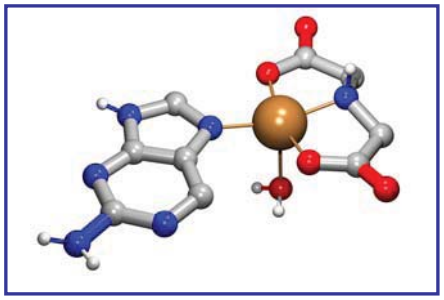

Iminodiacetate-like-Cu(II) chelates and 2-aminopurine recognize each other by the Cu-N7(purine-like) bond with no possibility of intra-molecular H-bonding reinforcement. This is in contrast to the versatile coordination behavior of its isomer adenine and a consequence of the shift of the amino group from C6(adenine) to C2(2-aminopurine).

RESUMEN

En contra de la extensa información disponible sobre complejos metálicos con adenina, la información relativa a su isómero 2-aminopurina (H2AP) es extremadamente pobre. Con el objeto de racionalizar los patrones de unión a metales de H2AP, se presentan las estructuras molecular y/o cristalina de cuatro nuevos compuestos con diferentes quelatos de iminodiacetato de cobre(II): $[Cu(IDA)(H2AP)(H_2O)]\cdot H_2O$ (**1**), $[Cu(MIDA)(H2AP)(H_2O)]\cdot 3H_2O$ (**2**), $\{[Cu(NBzIDA)(H2AP)]\cdot 1.5H_2O\}_n$ (**3**) y $[Cu(MEBIDA)(H2AP)(H_2O)]\cdot 3.5\ H_2O$ (**4**), donde IDA, MIDA, NBzIDA y MEBIDA son R=H, $CH_3$, bencil- y p-tolil- en los ligandos R-N-$(CH_2\text{-}COO^-)_2$, respectivamente. Las estrategias de síntesis incluyen reacciones directas de los quelatos de cobre(II) con H2AP (para **1** y **3**) y/o con los pares de bases H2AP:timina (**1**-**4**) o H2AP:citosina (**3**). Además, los compuestos también han sido investigados por métodos espectrales y térmicos. Con independencia del N-derivado del quelante tipo IDA, el reconocimiento molecular entre H2AP y los referidos quelatos de cobre(II) sólo muestran la formación de un enlace Cu-N7(tipo purina). Este hecho difiere notablemente de lo descrito en la bibliografía para adenina. El patrón de

reconocimiento molecular de 2-aminopurina se discute en base a los efectos electrónicos y los impedimentos estéricos del grupo amino exocíclico.

Journal of Inorganic Biochemistry 105 (2011) 1073–1080

Contents lists available at ScienceDirect

Journal of Inorganic Biochemistry

journal homepage: www.elsevier.com/locate/jinorgbio

# Molecular recognition patterns of 2-aminopurine versus adenine: A view through ternary copper(II) complexes

Alicia Domínguez-Martín [a,*], Duane Choquesillo-Lazarte [b], Josefa María González-Pérez [a], Alfonso Castiñeiras [c], Juan Niclós-Gutiérrez [a]

[a] Department of Inorganic Chemistry, Faculty of Pharmacy, Campus Cartuja, University of Granada, E-18071 Granada, Spain
[b] Laboratorio de Estudios Cristalográficos, IACT-CSIC, Avda. del Conocimiento s/n, E-18100 Armilla (Granada), Spain
[c] Department of Inorganic Chemistry, Faculty of Pharmacy, University of Santiago de Compostela, E-15782 Santiago de Compostela, Spain

ARTICLE INFO

*Article history:*
Received 18 February 2011
Received in revised form 11 May 2011
Accepted 18 May 2011
Available online xxxx

*Keywords:*
Molecular recognition
Mixed-ligand copper(II) complexes
2-aminopurine
Iminodiacetate
Metal binding pattern
Interligand interactions

ABSTRACT

In contrast to the comprehensive structural information about metal complexes with adenine, the corresponding to its isomer 2-aminopurine (H2AP) is extremely poor. With the aim to rationalize the metal binding pattern of H2AP, we report the molecular and/or crystal structure of four novel compounds with various iminodiacetate-like (IDA-like) copper(II) chelates: [Cu(IDA)(H2AP)(H2O)]·H2O (1), [Cu(MIDA)(H2AP)(H2O)]·3H2O (2), {[Cu(NBzIDA)(H2AP)]·1.5H2O}n (3) and [Cu(MEBIDA)(H2AP)(H2O)]·3.5 H2O (4), where IDA, MIDA, NBzIDA and MEBIDA are R = H, CH3, benzyl- and p-tolyl- in R-N-(CH2-COO-)2 ligands, respectively. Synthesis strategies include direct reactions of copper(II) chelates with H2AP (alone, for 1 and 3) and/or with the base pairs H2AP:thymine (1–4) or H2AP:cytosine (3). Moreover, these compounds have been also investigated by spectral and thermal methods. Regardless of the N-derivative of the IDA chelator, molecular recognition between H2AP and the referred Cu(II)-chelates only displays the formation of the Cu–N7(purine-like) bond what is clearly in contrast to what was previously reported for adenine. The metal binding pattern of 2-aminopurine is discussed on the basis of the electronic effects and steric hindrance of the 2-amino exocyclic group.



## 1. Introduction

The study of ternary complexes involving first-row transition metal ions and nucleobases and/or derivatives is a very high topic because of their presence in biological systems. Therefore, during the last decade, a comprehensive number of contributions focused on rationalize the metal binding modes of nucleic acids, nucleosides and nucleotides have appeared paying special attention to non-covalent interligand interactions (hydrogen bonds, π,π-stacking and C–H/π interactions, hydrophobic forces, etc.) since they play a very important role in molecular recognition phenomena [1–7]. In particular, our research group has been devoted to study the molecular recognition pattern between M(II)-iminodiacetate chelates (M(II) = first-row transition metal ions) and purine-like ligands, specially adenine (Hade) due to its remarkable versatility [3]. In these latter complexes, molecular recognition is given by a coordination bond Cu–N(purine-like) plus a reinforcement by an intra-molecular interligand H-bonding interaction type N–H···O(carboxy), which nature depends on the N-substituent of the iminodiacetate (IDA) chelator. For example, Cu(N-alkyl-IDA) chelates bind Hade by the Cu–N7 bond reinforced by a N6–H···O interaction whereas the Cu(IDA) chelate or Cu(N-benzyl-IDA) chelates and Hade exhibit a Cu–N3 bond and a N9–H···O interaction [6]. It should be remarked that in the research of metal binding patterns, especially if we are working on mixed-ligand complexes, as for example the system metal-chelate + nucleobase, X-ray diffraction (XRD) becomes a really useful tool because it gives us very reliable information about molecular recognition.

2-Aminopurine (H2AP) is a structural isomer of Hade in which the amino group is shifted from C6 to C2 (Scheme 1). Despite this fact, H2AP is able to form stable Watson–Crick-like base pairs with thymine, with only slightly reduced thermal and thermodynamics stability [8] but also can form 'mismatched' base pairs with cytosine much more readily than Hade does [9]. This implies A:T → G:C transition mutations during replication which is the cause of its mutagenicity [10].

For several decades, H2AP has been well-known due to its efficient fluorescence properties [11,12]. Its red-shifted absorption, relative to that of typical nucleic acids and proteins, as well as the extreme sensibility of fluorescence to local environmental factors, has enhanced the use of 2-aminopurine as molecular probe to investigate problems in structural biology, biochemistry and biophysics. It should be highlighted the researches on reaction mechanisms of different RNA and DNA enzymes [13], probing of conformational transitions and dynamics of nucleic acids [14] and studies about the interactions between nucleic acids and proteins or small molecules [15,16].

* Corresponding author: Tel.: +34 958243853; fax: +34 958246219.
*E-mail address:* adominguez@ugr.es (A. Domínguez-Martín).

0162-0134/$ – see front matter © 2011 Elsevier Inc. All rights reserved.
doi:10.1016/j.jinorgbio.2011.05.009

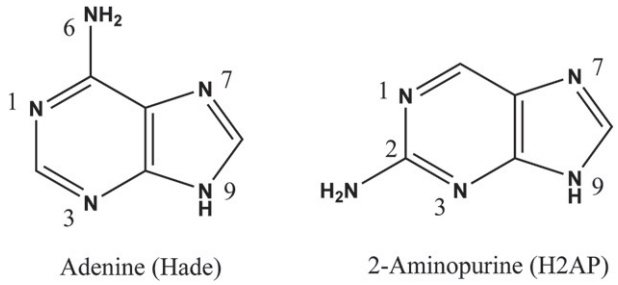


**Scheme 1.** Purine-like N-numbering system in adenine (Hade) and 2-aminopurine (H2AP).

Likewise, antiviral activity has been described for different synthetic nucleosides or nucleotides derived from H2AP. These derivatives normally act as pro-drugs and *in vivo* become into the active species mediated by a xanthine oxidase [17]. A good example is Famciclovir, a commercial first-line option drug with demonstrated antiviral activity against viruses of the alpha sub-family of Herpesviridae as well as hepatitis B virus [18]. The development of new antiviral drugs is still needed. Hence, promising research on this field is being done in the recent years about some synthetic nucleosides [19] or acyclic nucleoside phosphonates [20,21] involving H2AP.

Although there are a large number of papers about H2AP, the available structural information is very scarce. In fact, only four related structures have been reported in the Cambridge Structural Database [11,22,23]. The crystalline structure of H2AP locates the dissociable proton on N9 [11], according to other theoretical studies about H2AP tautomerism [24]. In the crystal, adjacent H2AP molecules are connected through N9–H···N1 H-bonds (2.811 Å, 166.77º). This interaction, besides other hydrogen bonds involving water molecules, generates an H-bonded architecture that would mimic what H2AP experiences once incorporated to the DNA duplex [11].

According to this panorama, we have synthesized and structurally characterized four novel ternary Cu(II) complexes with iminodiacetate-like chelators and H2AP with the aim to rationalize the metal binding pattern of this aminopurine ligand.

## 2. Experimental

### 2.1. Materials

Bluish $Cu_2CO_3(OH)_2$ was purchased from Probus. Iminodiacetic acid ($H_2IDA$) was supplied by alfa-Aesar and N-methyl-iminodiacetic acid ($H_2MIDA$) and 2-aminopurine were supplied by Sigma-Aldrich. All reagents were used as received. N-benzyl- and N-tolyl- (so-called N-(p-methylbenzyl))-iminodiacetic acids ($H_2NBzIDA$, $H_2MEBIDA$) were synthesized in the acid form as reported in [6].

### 2.2. Physical measurements

Analytical data were obtained in a Fisons-Carlo Erba EA 1108 elemental micro-analyser. Infrared spectra were recorded by using KBr pellets on a Jasco FT-IR 410 or a Jasco FT-IR 6300 spectrometer. TG analyses of the studied compounds (water loss plus pyrolysis; 295–800 °C) were carried out in air-dry flow (100 mL/min) by a Shimadzu Thermogravimetric analyzer (TGA)-50 H instrument, coupled with a FT-IR Nicolet Magma 550 spectrometer. A series of FT-IR spectra (20–30 per sample) of evolved gasses were time-spaced recorded during the thermogravimetric (TG) experiment. For each analysis, the TG experiment only starts after the stabilization of the balance (once reached a stable weight of the sample). It should be noted that, under air-dry flow, compounds lose a variable quantity of water before the TG experiment starts. The fitting of the referred formula and the starting material is assumed to be right if calculated and experimental data for the final residue (non-pure CuO in our compounds) have an agreement within the experimental error (≤1%). Electronic (diffuse reflectance) spectra were obtained in a Varian Cary-5E spectrophotometer.

### 2.3. Crystallography

Suitable crystals were mounted on glass fibers and these samples were used for data collection. Data were collected with Bruker X8 KappaAPEXII (1 and 4, 100 K), Bruker X8 Proteum (2, 293 K) or Bruker SMART APEX (3, 293 K) diffractometers. The data were processed with SAINT (3) [25] or APEX2 (1, 2 and 4) [26] and corrected for absorption using SADABS [27]. The structures were solved by direct methods [28], which revealed the position of all non-hydrogen atoms. These atoms were refined on F2 by a full-matrix least-squares procedure using anisotropic displacement parameters [28]. All hydrogen atoms were located in difference Fourier maps and included as fixed contributions riding on attached atoms with isotropic thermal displacement parameters 1.2 times those of the respective atom. Geometric calculations were carried out with PLATON [29] and drawings were produced with PLATON [29] and MERCURY [30]. One of the non-coordinated water molecules in the structure of compound **3** is highly disordered and the SQUEEZE procedure (PLATON) [29] was then applied to subtract the contribution of the disordered solvent from the diffraction data, which were subsequently used in the final refinement. Additional crystal data and more information about the X-ray structural analyses are shown in Supplementary material S1 to S4. Crystallographic data for the structural analysis have been deposited with the Cambridge Crystallographic Data Centre, CCDC No. CCDC 804482–804485 from **1** to **4** respectively. Copies of this information may be obtained free of charge on application to CCDC, 12 Union Road, Cambridge CB2 1EZ, UK (fax: 44 1223 336 033; e-mail: deposit@ccdc.cam.ac.uk or www: http://www.ccdc.cam.ac.uk).

### 2.4. Synthesis of compounds

#### 2.4.1. Synthesis of $[Cu(IDA)(H2AP)(H_2O)]\cdot H_2O$ (**1**) and $\{[Cu(NBzIDA)(H2AP)]\cdot 1.5H_2O\}_n$ (**3**)

Blue solutions of iminodiacetate or N-benzyl-iminodiacetate copper(II) chelates were prepared by reaction of $Cu_2CO_3(OH)_2$ (0.25 mmol, 0.055 g) and $H_2IDA$ (0.5 mmol, 0.066 g, **1**) or $H_2NBzIDA$ (0.5 mmol, 0.111 g, **3**) in 90 mL of water, heating (50 °C) and stirring under moderate vacuum. Such solutions were cooled at room temperature and then H2AP (0.5 mmol, 0.068 g) was added. One hour later, only part of H2AP was dissolved. However, we decided to filter the corresponding solutions on a crystallization device at the expense of lower yields. Mother solutions were allowed to stand at room temperature covered with a plastic film to control the evaporation of the solvent. One month later, blue crystals suitable for X-ray diffraction appeared. Yield of these synthesis are ca. 30–40%.

Alternatively, in order to favour the reaction of H2AP with the aforementioned copper(II) chelates, additional experiments were carried out replacing this aminopurine ligand by the corresponding base pairs with thymine (H2AP:Hthy, compounds **1** and **3**) [8] or cytosine (H2AP:Hcyt, compound **3**) [9]. The general procedure consists of the reaction between $Cu_2CO_3(OH)_2$ (0.25 mmol, 0.055 g) and the appropriate iminodiacetic-like acid ($H_2IDA$ or $H_2NBzIDA$, 0.5 mmol) in 70 mL of water, in a Kitasato flask, heating (50 °C) and stirring under moderate vacuum. Once clear blue solutions were obtained, they were left to cool at room temperature. Then, a solution of 30 mL of water of H2AP:Hthy (**1**,**3**) and/or H2AP:Hcyt (**3**) base pairs (0.5 mmol:0.5 mmol) was added. Afterwards, solutions were filtered on the corresponding crystallization devices. Evaporation of the solvent was controlled with the aid of a plastic film in every case. Approximately two weeks later, well-shaped crystals of **1** and **3** were formed, many of them suitable for XRD purposes. Typical yields of these syntheses are ca. 70–75%. Elemental analysis (%): Calc. for $C_9H_{14}CuN_6O_6$ (**1**): C 29.78, H 3.80, N 23.01; Found: C 29.55, H 3.66, N 22.88. FT-IR [KBr, $cm^{-1}$, m = medium, s = strong, vs = very strong, w = weak] (**1**): $\nu_{as}(NH_2)$ 3367(s), $\nu_s(NH_2)$

and $\nu$(N–H) overlapped 3190(w), $\nu_{as}(CH_2)$ 2933(w), $\nu_s(CH_2)$ 2845(w), $\delta(NH_2)$ and $\nu_{as}$(COO) overlapped 1598(vs), $\delta$(N–H) 1516(vs), $\nu_s$(COO) 1384(s), $\pi(C–H)_{ar}$ 798(m). The UV/visible (UV/Vis) spectrum of **1** shows an asymmetric d–d band with $\lambda_{max}$ at 669 nm ($\nu_{max}$14,950 $cm^{-1}$). Elemental analysis (%): Calc. for $C_{32}H_{38}Cu_2N_{12}O_{11}$ (**3**): C 43.00, H 4.29, N 18.80; Found C 43.14, H 4.23, N 18.72. FT-IR [KBr, $cm^{-1}$] (**3**): $\nu_{as}(NH_2)$ 3329(s), $\nu_s(NH_2)$ and $\nu$(N–H) overlapped 3197(w), $\nu_{as}(CH_2)$ 2921(w), $\nu_s(CH_2)$ 2852(w), $\delta(NH_2)$ and $\nu_{as}$(COO) overlapped 1593(vs), $\delta$(N–H) 1516(vs), $\nu_s$(COO) 1385(s), $\pi(C–H)_{ar}$(H2AP) 797(m), $\pi(C–H)_{ar}$ (NBzIDA) 755(m). The UV/Vis spectrum of **3** shows an asymmetric d–d band with $\lambda_{max}$ at 665 nm ($\nu_{max}$ 15,040 $cm^{-1}$).

#### 2.4.2. Synthesis of [Cu(MIDA)(H2AP)($H_2O$)]·3$H_2O$ (**2**), and [Cu(MEBIDA)(H2AP)($H_2O$)]·3.5$H_2O$ (**4**)

These compounds were prepared by reaction of the appropriate Cu(II) chelates ($H_2$MIDA or $H_2$MEBIDA) and the H2AP:Hthy base pair as previously reported for compounds **1** and **3**. In these cases, the direct reaction with the Cu(II) chelates and the free H2AP ligand were not carried out. Typical yields in these syntheses were also ca. 70–75%. Elemental analysis (%): Calc. for $C_{10}H_{20}CuN_6O_8$ (**2**): C 29.02, H 4.64, N 20.45; Found C 28.88, H 4.85, N 20.21. FT-IR [KBr, $cm^{-1}$] (**2**): $\nu_{as}(NH_2)$ overshadowed, $\nu_s(NH_2)$ and $\nu$(N–H) overlapped 3194(w), $\nu_{as}(CH_2)$ 2934(w), $\nu(CH_3–N)$ 2800(w), $\nu_s(CH_2)$ 2847(w), $\delta(NH_2)$ and $\nu_{as}$(COO) overlapped 1607(vs), $\delta$(N–H) 1517(vs), $\nu_s$(COO) 1396(s), $\pi(C–H)_{ar}$ 796(m). The UV/Vis spectrum of **2** shows an asymmetric d–d band with $\lambda_{max}$ at 673 nm ($\nu_{max}$ 14,860 $cm^{-1}$). Elemental analysis (%): Calc. for $C_{17}H_{27}CuN_6O_{8.5}$ (**4**): C 39.82, H 5.06, N 16.35; Found C 39.65, H 5.28, N 16.32. FT-IR [KBr, $cm^{-1}$] (**4**): $\nu_{as}(NH_2)$ 3329(s), $\nu_s(NH_2)$ and $\nu$(N–H) overlapped 3194(w), $\nu_{as}(CH_2)$ 2939(w), $\nu_{as}(CH_3)$ 2979(w), $\nu_s(CH_2)$ 2840(w), $\delta(NH_2)$ and $\nu_{as}$(COO) overlapped 1602(vs), $\delta$(N–H) 1517(vs), $\nu_s$(COO) 1384(s), $\pi(C–H)_{ar}$(H2AP) 796(m), $\pi(C–H)_{ar}$ (MEBIDA) 805(m). UV/Vis analysis was not performed to compound **4** since it was not possible to have enough pure samples due to thymine co-crystallization.

#### 2.4.3. Synthesis of ternary compounds from quaternary systems using the Hade:Hthy and H2AP:Hthy base pairs

Syntheses of quaternary systems were carried out using equimolar quantities of (Cu/MIDA or NBzIDA/Hade/H2AP). The purine ligands were introduced as their corresponding base pairs with Hthy. The use of these base pairs is founded in the previous syntheses (see Section 2.4.1) and in the belief that thymine is not a candidate for metal binding.

Blue solutions of IDA-like copper(II) chelates were prepared by reaction of $Cu_2CO_3(OH)_2$ (0.25 mmol, 0.055 g) and $H_2$MIDA (0.5 mmol, 0.073 g) or $H_2$NBzIDA (0.5 mmol, 0.111 g) in 70 mL of water, heating (50 °C) and stirring under moderate vacuum. Besides, two solutions of 20 mL of both base pairs (Hade:Hthy and H2AP:Hthy) (0.5 mmol:0.5 mmol) were prepared. These latter solutions were added to both IDA-like copper(II) chelates at room temperature and well-stirred during 20 minutes. In the described experimental conditions, we obtained blue clear solutions that were filtered on appropriate crystallization devices and covered with a plastic film.

In the solution containing MIDA as chelating ligand, approximately in one month, two different plate blue crystals appeared nearly at the same time. A mixture of both types of crystals was placed in a clock glass and separated by hand according to differences in colour and habit with the aid of a magnifying glass. One part of the sample was identified as compound **2** whereas the other type of plate-like crystals were identified as [Cu(MIDA)(Hade)($H_2O$)]·$H_2O$ [6]. Identification was confirmed by FT-IR spectroscopy and X-ray Powder Diffraction, comparing diffractograms of both separated samples of plate-like crystals with the corresponding ternary compounds (see S6). Then, co-crystallization of colourless crystals of the free purine and/or pyrimidine ligands occurs.

On the other hand, the evaporation of the quaternary solution containing NBzIDA yields needle-like blue crystals identified as compound **3** by FT-IR. This compound was removed twice by filtration and the remaining solution was placed in a new crystallization device. Additional evaporation of solvent yielded needle-like blue crystals of compound **3** and plate blue crystals which were identified as [Cu(NBzIDA)(Hade)($H_2O$)]·$H_2O$ [6] by FT-IR. When these complexes were removed by filtration, the solution evaporates yielding additional amount of both Cu(II) compounds and colourless crystals.

## 3. Results and discussion

### 3.1. Synthesis

Current knowledge on molecular recognition field points out the possibility of preparing metal chelates that are able to selectively recognize nucleobases and/or related synthetic ligands. In fact, this seems to be the main axis of research of recent papers of K. Aoki et al. [31–34]. In this context, the main aim of this paper is to achieve molecular recognition information about H2AP through the study of ternary copper(II) complexes where the metal is chelated by IDA or N-substituted IDA ligands. In the syntheses, in order to avoid the presence of undesired by-products (as alkaline inorganic salts) the formation of the metal chelate is systematically carried out by reaction of Cu(II) hydroxy-carbonate and the chelating agent in its acid form (see Refs. [5–7]). This reaction yields the metal chelate in solution and $CO_2$ as by-product, easily removable [7]. Then the binary compound reacts with the purine-like ligand (alone) and/or with an appropriate base pair (see Sections 2.4.1 and 2.4.2). The use of complementary base pairs in this kind of syntheses with ternary complexes was first introduced by us [5]. Our observations suggest that the use of appropriate base pairs, instead of the purine-like base alone, yields to more efficient incorporation of such latter ligand. This is because the base pair increases the global solubility of the system and, in some way, dosages the quantity of free purine-like ligand able to bind the metal chelate. According to literature [8,9], H2AP is able to build complementary base pairs with Hthy or Hcyt. Our results do not show any advantage of using one base pair or another, except for the fact that Hthy, in neutral form, is unable to bind metal ions whereas H(N1)cyt, the most stable tautomer of cytosine, could *a priori* coordinate via N3.

The syntheses described in Section 2.4.3 aim to discuss to what extent metal chelates, such as Cu(MIDA) or Cu(NBzIDA), could selectively prefer to bind Hade or H2AP. We carefully chose the latter Cu(II)-chelates considering that Cu(MIDA) and Cu(NBzIDA) chelates recognize adenine through different Cu–N(purine) bonds (Cu–N7 and Cu–N3 bonds respectively) which are cooperatively reinforced by appropriate interligand H-bonds [6]. It is also important to keep in mind that the Cu(NBzIDA) chelate reacts in a different way with the Hade:Hthy base pair or with the nucleobase Hade alone, giving rise, in the first case, to a dinuclear ternary compound with $\mu_2$-N7,N9–H(N3)ade [5]. With this purpose, we carried out syntheses of equimolar quaternary systems Cu/MIDA or NBzIDA/ Hade/H2AP where, due to solubility reasons, the purine-like bases were introduced as their corresponding complementary base pairs with thymine. Removal of appreciable quantities of unreacted products was not needed. Evaporation of these solutions led to crystallization of the corresponding ternary complexes with H2AP and Hade, with slight differences in time that could be attributed to relative solubility of the formed complexes and/or favourable crystal packing. Two main aspects should be pointed out regarding this experience: (i) when the reaction-mixture starts to evaporate, the metal chelates (Cu(MIDA) or Cu(NBzIDA)) are faced to equimolar quantities of both purine-like ligands. This means that crystallization of one of the possible ternary complexes, for example the H2AP one, increases the relative proportion of the other ligand in the solution (in this example: adenine); (ii) Other item to consider is that, in contrast to our

previous results [5,6], evaporation of these quaternary systems has led to the same reported ternary complexes that were obtained by evaporation of the mixed-ligand solutions. Nevertheless, it can be explained since the quaternary system does not behave like the ternary one, the relative concentration and solubility of the ligands is changing throughout the experience. To the best of our knowledge these quaternary experiences are now first carried out. Indeed, these results raise more questions than answers.

### 3.2. Molecular and crystal structure of [Cu(IDA)(H2AP)($H_2O$)]·$H_2O$ (**1**)

The crystal of compound **1** consists of a complex molecule and water (Fig. 1 left). The copper(II) atom exhibits a 4 + 1 coordination polyhedron where the four closest donor atoms corresponds to the tridentate IDA chelating ligand (N10, O21, O11) and the N7(purine-like) donor of H2AP. Thus IDA ligand adopts a *mer*-$NO_2$ conformation. One aqua ligand occupies the apical position. It should be noted that such coordination cannot be reinforced by an intra-molecular interligand H-bonding interaction. The N10(IDA) atom is disordered over two positions with a very close occupancy factor: 0.54(1) for N10 (A) and 0.46(1) for N10(B). In contrast to the N10(A) atom, with a τ value of 0.06, nearly a true square-base pyramidal coordination (τ = 0) according to Addison parameter [35], the N10(B) atom represents a bigger distortion in the mean basal plane of the copper (II) with a τ value of 0.145.

In the crystal, pairs of adjacent H2AP are H-bonded by inter-molecular symmetric interactions N2–H(2A)···N3 (3.087 Å, 168.0°). Likewise adjacent units are connected by intermolecular N9–H···O12 (non coord., IDA) (2.847 Å, 153.5°) symmetric hydrogen bonds. The association of both interactions gives rise to zigzag ribbons (Fig. 1 right). Although the hydrogen bond that involves the amino group of H2AP is rather large, it should be considered since it is essential for the crystal packing. Indeed, this kind of interaction will be observed in all the complexes hereafter reported with some little differences. These ribbons are further connected by H-bonding interactions that involve the water molecule as H-donor and H-acceptor building 2D layers. Finally, π,π-stacking and hydrogen bonds cooperate to reach the 3D structure (Fig. 2). π,π-Stacking is observed between the five-membered rings of anti-parallel neighbouring H2AP ligands (α = 0°, β = γ = 21.94°; $d_{Cg-Cg}$ = 3.52 Å, $d_{π-π}$ = 3.26 Å). The apical aqua ligand acts twice as H-donor. Only one of the disordered positions of N10 (IDA) participates in H-bonding interactions involving the water molecule as H-acceptor. A plot explaining the meaning of stacking parameters and the analyses of π,π-stacking interactions are shown in S5. Table of hydrogen bonds is given in S1.3.

The thermogravimetric curve of **1** is divided in three steps. Under air-dry flow, the sample loses a little amount of water. Hence, the TG experiment starts with an average formula [Cu(IDA)(H2AP)($H_2O$)]·0.93$H_2O$. Since non-coordinated water and the apical aqua ligand of the 4 + 1 surrounding of Cu(II) are lost overlapped, the loss weight of the first step agrees with the loss of 1.93 water molecules. (Calc. 9.54%; Found 9.53%). Then, consecutive steps (II and III) are assigned to the pyrolysis of the organic ligands (190–310 and 310–430 °C). FT-IR spectra of the evolved gasses show $H_2O$, $CO_2$, $NH_3$ and CO(t) in (II) plus several nitrogen-oxide gases as $N_2O$, NO and $NO_2$(t) in (III). Finally it yields to a CuO residue (Calc. 21.82%; Found 22.84%).

### 3.3. Molecular and crystal structure of [Cu(MIDA)(H2AP)($H_2O$)]·3 $H_2O$ (**2**)

The crystal of compound **2** consists of ternary complex molecules and water (Fig. 3 left). The copper(II) atom shows a 4 + 1 configuration. The Cu(II) mean basal plane is built by the three donors of the tridentate MIDA chelating ligand, adopting a *mer*-$NO_2$ conformation, and the N7 atom of H2AP. The apical site is occupied by an aqua ligand. As compound **1**, there is no chance of intra-molecular reinforcement through the purine moiety. There are two intermolecular H-bonding interactions involving the apical aqua ligand and different water molecules. In this complex, the Cu(II) coordination environment is very close to a square pyramidal coordination, according to the Addison geometric criterion (τ = 0.02) [35].

In a similar but not equivalent way of **1**, the crystal of **2** build zigzag ribbons stabilized by intermolecular symmetric H-bonding interactions between pairs of adjacent H2AP by N2–H(2B)···N1 interactions (3.094 Å, 174.2°) and pairs of complex molecules by N9–H···O22(non coord., MIDA) interactions (2.715 Å, 173.4°) (Fig. 3 right). The H2AP base pairs shown in this complex reveal the –$NH_2$ amino group as H-donor and N1 as H-acceptor. These 1D chains are associated by multi-stacked π,π interactions. In this system, each H2AP ligand stacks its five- and six-membered rings with the five- and six-membered rings of two adjacent H2AP ligands respectively. Stacking parameters are: (i) for pairs of 5-membered rings (α = 0°, β = γ = 18.78°; $d_{Cg-Cg}$ = 3.62 Å, $d_{π-π}$ = 3.43 Å) and (ii) pairs of 6-membered rings (α = 0°, β = γ = 25.49°; $d_{Cg-Cg}$ = 3.76 Å, $d_{π-π}$ = 3.40 Å) (see S5.2). H2AP ligands, in each multi-stacked system, fall in parallel since dihedral angle between stacked rings are α = 0°. Water molecules and the apical aqua ligand, as well as the amino group, are involved in intermolecular hydrogen bonding interactions (see Table S2.3) to build the 3D network as shown in Fig. 4.

The thermal behaviour of **2** is divided in four steps. In air-dry flow compound **2** loses the non-coordinated water. Afterwards, the sample [Cu(MIDA)(H2AP)($H_2O$)] experiments the loss of weight of the apical aqua ligand (25–155 °C; Calc. 5.21%; Found: 5.43%). Three additional pyrolytic steps (155–250 (II), 250–350 (III) and 350–440 °C (IV)) produce, besides $H_2O$ and $CO_2$ in (II), CO, $NH_3$ and $N(CH_3)_3$ in (III). This latter gas is typically observed from pyrolysis of MIDA chelating

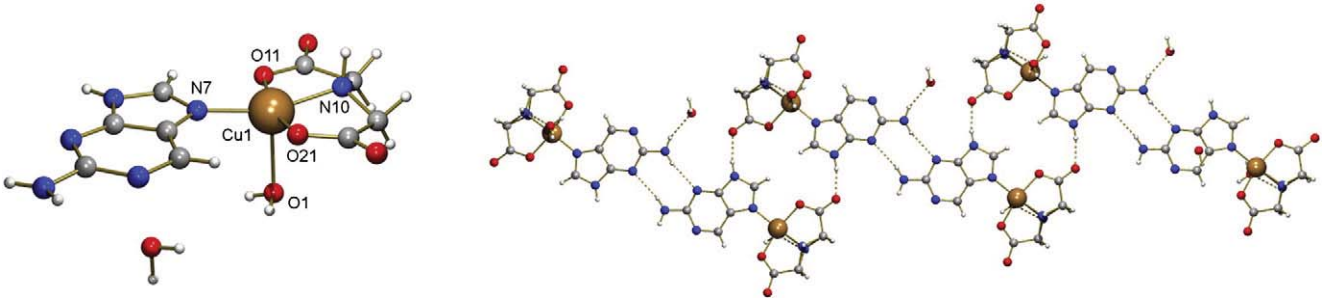


**Fig. 1.** Structure of [Cu(IDA)(H2AP)($H_2O$)]·$H_2O$ (**1**). Left: Asymmetric unit of **1** where only the N10A–H10A possibility is plotted. Bond distances (Å): Cu1–N7 1.955(3), Cu1–N10A 1.950(6), Cu1–N10B 2.059(8), Cu1–O11 1.989(3), Cu1–O21 1.988(3), Cu1–O1 2.289(4). Right: Fragment of a 1D ribbon built by base pairing through N2–H···N3 and N9–H···O (carboxy) interactions (water molecules omitted for clarity).

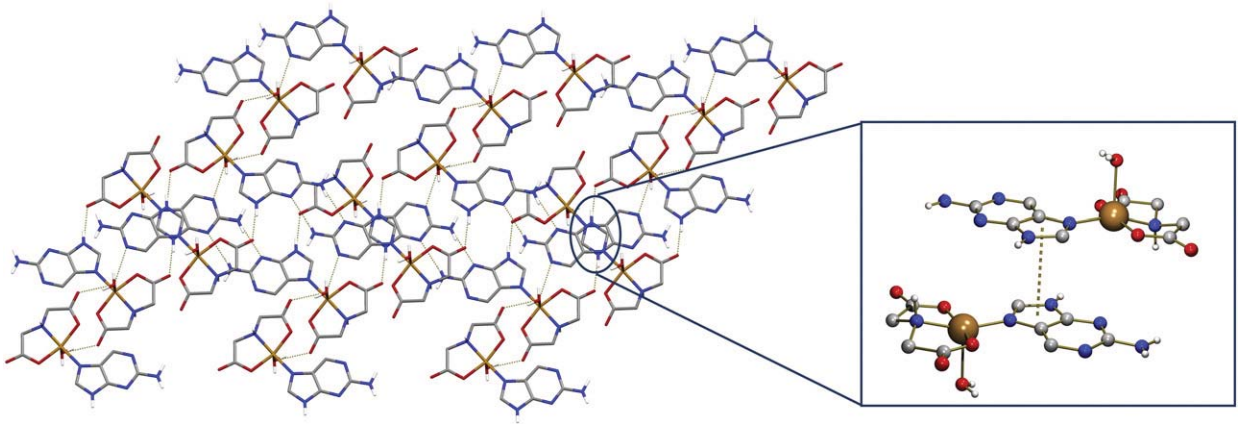

**Fig. 2.** 3D network of compound **1** with a detail of π,π-stacking interaction between H2AP ligands (water molecules and those hydrogens that do not participate in H-bonded interactions are omitted for clarity).

ligand. $H_2O$, $CO_2$ CO, $NH_3$, $N_2O$, NO and trace amounts of $NO_2$ are released in (IV). A CuO residue was expected at the end of the experiment (Calc. 23.02%; Found 23.99%).

### 3.4. Crystal structure of compound {[Cu(NBzIDA)(H2AP)·1.5$H_2O$}$_n$ (**3**)

The crystal structure of **3** is based on a coordination polymer built by means of the syn-anti bridging role of a carboxylate group of the NBzIDA ligand (Fig. 5 left). The copper(II) atom exhibits a square-base pyramidal coordination, type 4 + 1, with only a slight distortion through a trigonal bypyramide according to the Addison parameter $\tau = 0.015$ [35]. The tridentate *mer*-$NO_2$ NBzIDA chelating ligand and the N7 atom from the H2AP ligand are the closest Cu(II) donors. As described for the previous complexes, no intra-molecular H-bonding interactions can reinforce the Cu–N(H2AP) coordination bond. The 1.5-hydrated formula is related with the presence of a water molecule in a special crystallographic position.

1D chain extends through the b axis orientating adjacent H2AP ligands towards opposite sites. These 1D chains are associated by base pairing symmetry related N2-H(2A)···N3 (3.039 Å, 170.9º) hydrogen bonding interactions giving rise to two-dimensional frameworks parallel to the ab plane (Fig. 5 right). Such base pairing it is also found for compound **1**. The 3D array is completed thanks to additional H-bonding interactions involving the water molecules and the rest of N-donors (see Table S3.3). Despite both the chelating ligand and H2AP have aromatic parts, there are no π,π-stacking interactions in this crystal.

Compound **3** loses approximately 2/3 of its water content under air-dry flow. Therefore, the starting sample for the TG experiment agree to a formula {[Cu(NBzIDA)(H2AP)·0.44$H_2O$}$_n$. The remaining non-coordinated water is lost during the first step (80–180 °C; Calc. 1.85%; Found 1.84%). The second and the third weight loss take place between 180–320 and 320–450 °C respectively, leading to a CuO residue (Calc. 18.59%; Found 19.30%). FT-IR spectra during the pyrolysis reveal $H_2O$, $CO_2$, CO and $CH_3OH$ in (II). The aforementioned gasses, except for methanol, are also released in (III) plus N-oxide gasses ($N_2O$, NO and $NO_2$). It should be noted that irrespective of the chelating ligands (**1**–**3**) and the molecular or polymeric nature of these compounds, the formation of the CuO residue is completed at similar temperatures (430–450 °C).

### 3.5. Molecular and crystal structure of [Cu(MEBIDA)(H2AP)($H_2O$)]·3.5 $H_2O$ (**4**)

The asymmetric unit of compound **4** contains two crystallographic independent but chemically very similar molecules and seven water molecules, according to the simplified chemical formula [Cu(MEBIDA)(H2AP)($H_2O$)]·3.5$H_2O$ (Fig. 6 left). Both complex molecules have copper(II) atoms in a more distorted square-base pyramidal coordination mode in comparison with the other three reported structures (Addison parameters: $\tau Cu1 = 0.11$, $\tau Cu2 = 0.23$) [35]. The more pronounced deviation from the mean basal plane of the copper centres is related to the N atom of MEBIDA ligands (N10 and N20). No cation-aromatic ring interactions are present but non equivalent π,π-stacking interactions within the molecules (see below) act as main force of these latter unequal distortions. The tridentate *mer*-$NO_2$-MEBIDA chelating ligand and the N7 atom from the H2AP ligand are the closest donors in both Cu centres. The apical/distal position is occupied by aqua ligands.

In the crystal of **4**, π,π-stacking interactions build infinite chains that extend along the c axis, involving the C6 aromatic moiety of MEBIDA ligands and the six-membered ring of H2AP ligands of two crystallographic independent complex units (two types of interactions with $\alpha = 2.38°$, $\beta = 11.79°$, $\gamma = 13.34°$, $d_{Cg-Cg} = 3.38$ Å, $d_{\pi-\pi} = 3.29$ Å and

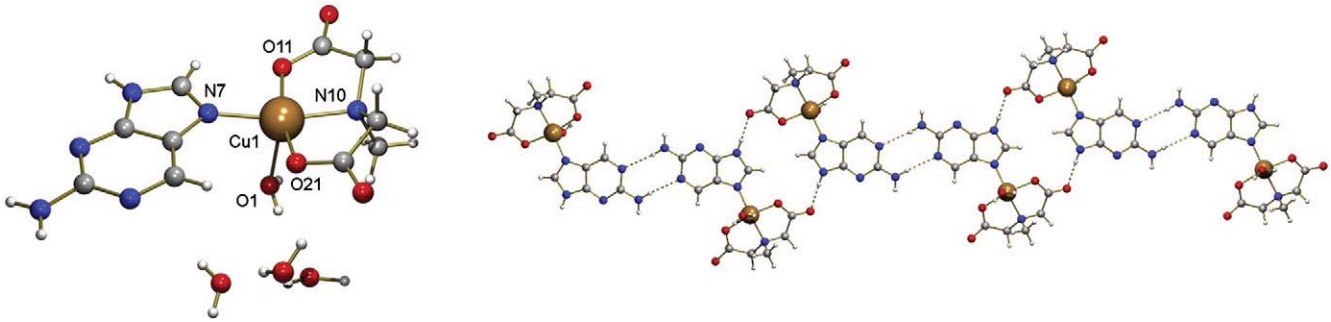


**Fig. 3.** Structure of [Cu(MIDA)(H2AP)($H_2O$)]·3$H_2O$ (**2**). Left: Asymmetric unit of **2**. Bond distances (Å): Cu1–N7 1.989(2), Cu1–N10 2.021(2), Cu1–O11 1.944(2), Cu1–O21 1.965(2), Cu1–O1 2.318(2). Right: Fragment of a 1D ribbon built by base pairing through N2–H···N1 and N9–H···O(carboxy) interactions (water molecules omitted for clarity).

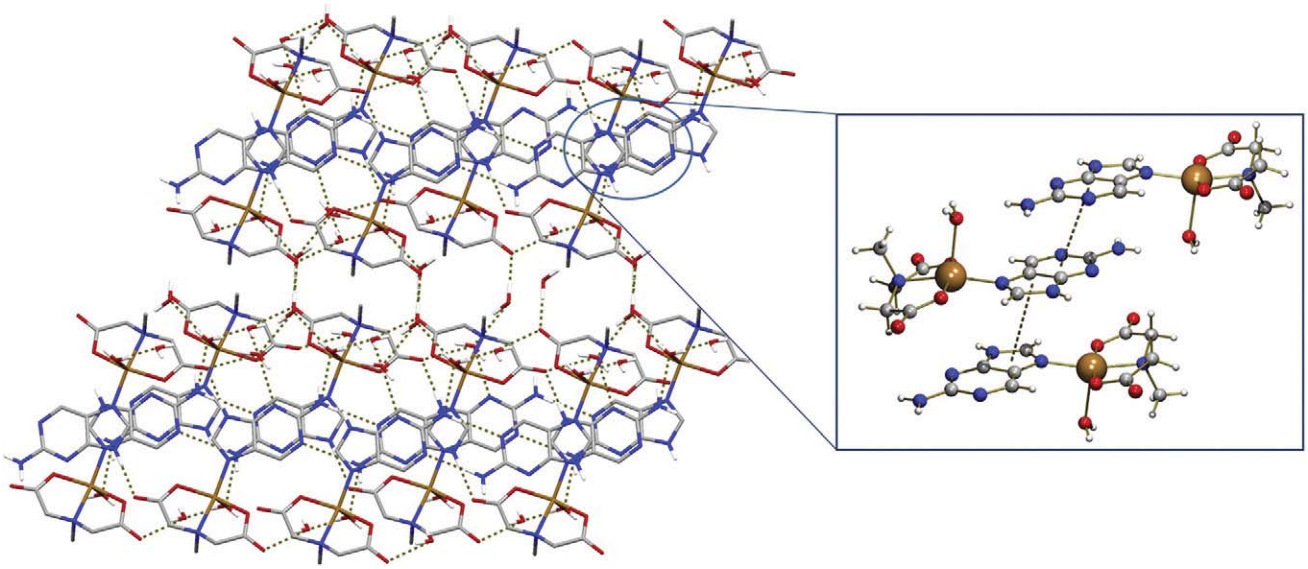

**Fig. 4.** 3D network of compound **2** with a detail of π,π-stacking interaction between H2AP ligands (those hydrogens that do not participate in H-bonded interactions are omitted for clarity).

α = 4.60°, β = 26.73°, γ = 30.09°, $d_{Cg-Cg}$ = 3.84 Å, $d_{\pi-\pi}$ = 3.38 Å). Pairs of H2AP ligands adopt a symmetrical H-bonding motif with N2–H and N3 acting as donor and acceptor respectively (2.994 Å, 171.6°) and pairs of complex molecules are further connected by N9–H···O12(non coord., MEBIDA) interactions (2.785 Å, 176.7°) (Fig. 6 right), thus connecting π,π-chains to form 2D layers running parallel to the bc plane of the crystal. Besides, an 1D infinite water chain made of 11-membered water clusters is found in compound **4**, and connects the 2D-networks into the 3D upper framework (Fig. 7) by hydrogen bonding interactions between water molecules and the oxygen atom from carboxylate groups from complex units and the aqua ligand respectively (see S4.3). The undecameric water cluster is associated by hydrogen bonding interactions and consists of a water chair hexamer (Fig. 7), a water cyclic tetramer and one lattice water molecule that connects both cyclic structures. The average O···O distance in the hexamer is 2.73 Å. This distance is shorter than those observed in liquid water (2.85 Å) [36] and comparable to the corresponding value in hexagonal ice (Ih) (2.76 Å) [37].

Thermogravimetric analysis was not performed to compound **4** since it was not possible to have enough pure samples due to thymine co-crystallization.

### *3.6. Metal binding patterns of H2AP and molecular recognition consequences*

Our crystallographic results reveal that metal binding pattern of H2AP is opposed to what was previously reported for its natural isomer adenine. The four ternary complexes with H2AP reveal the formation of a Cu–N7(purine-like) bond, irrespective of the N-substituent of the IDA-like ligand. Keeping that in mind, it is possible to make some considerations about the consequences that lead the shift of the exocyclic amino group from C6 (in Hade) to C2 (in H2AP).

Firstly, it is important to note that there is a wide consensus regarding the basicity of the nitrogen atoms in adenine (N9>N1>N7>N3>N6). This basicity order finds only partial support in solution studies. Indeed only two data of dissociation constants are known for the adeninium(1+) cation ($pK_1$ = 4.20; $pK_2$ = 9.65; 298 K, 0.1 M $NaNO_3$) [38]. They are attributable to successive and independent ($\Delta pK_a$>4) dissociations of protons placed on N1 and N9 respectively. Alternatively, the N-basicity order of Hade can be deduced from a large number of crystal structures available in CSD database. These data concern the structure of neutral adenine (H(N9)ade tautomer) as well as a variety of salts for adeninium (1+) ($H_2$(N1,N9)ade$^+$) and adeninium(2+) (as $H_3$(N7,N1,N9)ade$^{2+}$)

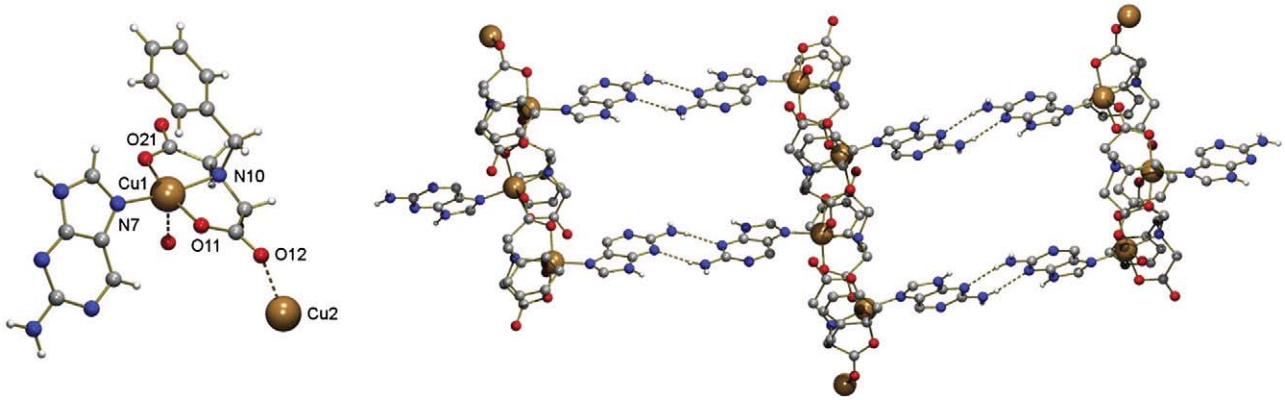


**Fig. 5.** Structure of {[Cu(NBzIDA)(H2AP)]·1.5$H_2O$}$_n$ (**3**). Left: A complex unit of the polymeric chain. Bond distances (Å): Cu1–N7 1.959(4), Cu1–N10 2.001(4), Cu1–O11 1.952(3), Cu1–O21 1.945(3), Cu1–O12#1 2.256(3) [#1 = −x + 1/2, y + 1/2, −z + 1/2]. Right: Fragment of the 2D framework built by base pairing through N2–H···N3 interactions (water molecules and those hydrogens that do not participate in H-bonded interactions are omitted for clarity).

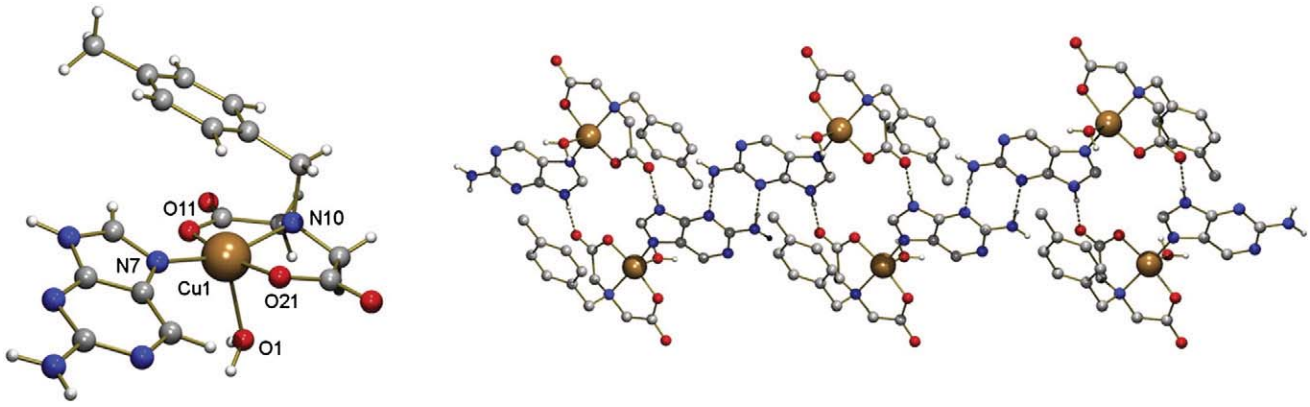


**Fig. 6.** Structure of [Cu(MEBIDA)(H2AP)($H_2O$)]·3.5$H_2O$ (**4**). Left: The complex molecule 1 of the asymmetric unit (water molecules omitted for clarity). Bond distances (Å): Cu1–N7 1.962(2), Cu1–N10 2.007(2), Cu1–O11 1.959(2), Cu1–O21 1.951(2), Cu1–O1 2.289(2), Cu2–N77 1.954(2), Cu2–N20 2.003(2), Cu2–O41 1.963(2), Cu2–O51 1.975(2), Cu2–O2 2.240(2). Right: Fragment of one layer built by base pairing through N2–H···N3 and N9–H···O(carboxy) interactions (water molecules and those hydrogens that do not participate in H-bonded interactions are omitted for clarity).

cations (see details in ref. 3). In clear contrast, for 2-aminopurine, only structural information about the neutral form H(N9)2AP is available [11]. Tentatively, we can guess the basicity order of the N-atoms for H2AP considering the electronic and steric effects that the exocyclic –$NH_2$ group displays in Hade and H2AP. An exocyclic amino group displays both an electron withdrawing effect (−I) and an electron donating mesomeric effect (+M). These two effects act in opposite sense with a dominant influence of the electron withdrawing effect (since the lonely electron pair on its N atom is not involved in the aromaticity of the purine moiety). In addition, the exocyclic amino group also displays a steric hindrance that mainly affect to the adjacent donor atoms. Hence the electronic and steric effects of the exocyclic amino group are noticeably focused on N1 in Hade or N1 and N3 in H2AP [39]. In this sense, there are no reported structures where neutral Hade coordinates by N1. If we compare the N-basicity order of H2AP and Hade, we can also expect a slight increase of the N7-basicity and a significant decrease of the N3-basicity for H2AP. In addition, no relevant steric hindrance could be expected for N7 donor atom of H2AP [40]. Consequently, the N-basicity order in 2-aminopurine should be similar to that of adenine but with a higher difference of basicity for its N7 and N3 donor atoms.

Scheme 2 shows four tautomers of H2AP, two molecular (A and B) and two zwiterionic (C and D) ones. Similar tautomers can be formulated for its natural isomer adenine. In case of adenine, the tautomer H(N3)ade has been found in a dinuclear copper(II) complex, with bridging $\mu_2$-N7,N9-Hade [5]. The tautomer H(N7)ade is also well-known [3] but the H(N1)ade tautomer does not have structural support. A theoretical and experimental study about the H2AP tautomerism strongly suggests that neutral H(N9)2AP and H(N7)2AP are the most important tautomers [24]. By now, zwiterionic tautomers of H2AP as well as the molecular tautomer H(N7)2AP have no structural support.

Therefore, we can assume that N1 and N3 atoms of H2AP are poor metal binding sites because the negative contribution of the aforementioned electronic and steric effects. In practice our results point out N7 as the most suitable metal binding site in H2AP using its most stable tautomer H(N9)2AP. That is in accordance with solution studies recently carried out by H. Sigel and cols. [21] and structural results for transition metal complexes of 2-aminopurine-like ligands such as the antiviral acyclovir [7].

## 4. Concluding remarks

Our results in solid state, as well as other solution studies reported by H. Sigel [21], point out that the shift of the exocyclic amino group

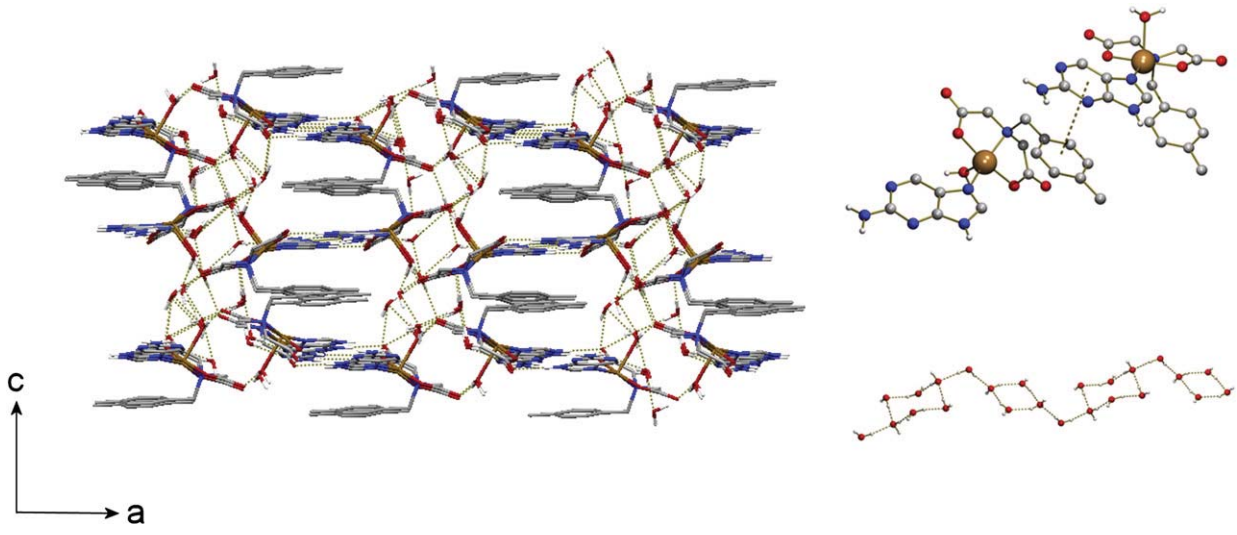


**Fig. 7.** 3D network of compound 4 with details of π,π-stacking interaction (between the aromatic rings of MEBIDA and H2AP) and clusters of water molecules (those hydrogens that do not participate in H-bonded interactions are omitted for clarity).

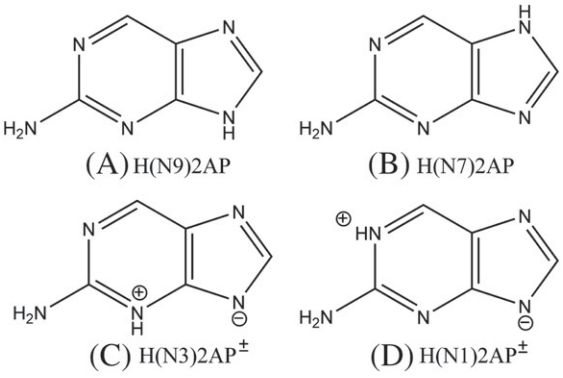


**Scheme 2.** Possible tautomers of H2AP.

from C6 in Hade to C2 in H2AP favours N7 as the most suitable metal binding site of 2-aminopurine.

## Acknowledgements

Financial support from Research Group FQM-283 (Junta de Andalucía) is acknowledged. Financial support from MICINN-Spain (Project MAT2010-15594) is also acknowledged. The project "Factoría de Cristalización, CONSOLIDER INGENIO-2010" provided X-ray structural facilities for this work. Financial support from ERDF Funds and Junta de Andalucía to acquire the FT-IR spectrophotometer Jasco 6300 is acknowledged. ADM thanks ME-Spain for a FPU Ph.D. fellowship.

## Appendix A. Supplementary data

Additional crystal data and structural information for 1, 2, 3 and 4 (S1–S4), analysis of π,π-stacking interactions in 1, 2 and 4 (S5), X-ray Power Diffractograms (S6), FT-IR and electronic spectra (S7) and thermal analyses with FT-IR identification of evolved gases (S8) are provided. Supplementary data to this article can be found online at doi:10.1016/j.jinorgbio.2011.05.009.

## References

[1] B. Lippert, in: K.D. Karlin (Ed.), Progress in Inorganic Chemistry, Vol. 54, Wiley, 2005, Chap. 6.
[2] A. Terrón, J.J. Fiol, A. García-Raso, M. Barceló-Oliver, V. Moreno, Coord. Chem. Rev. 251 (2007) 1973–1986.
[3] D. Choquesillo-Lazarte, M.P. Brandi-Blanco, I. García-Santos, J.M. González-Pérez, A. Castiñeiras, J. Niclós-Gutiérrez, Coord. Chem. Rev. 252 (2008) 1241–1256.
[4] P.J. Sanz Miguel, P. Amo-Ochoa, O. Castillo, A. Houlton, F. Zamora, in: N. Hadjiliadis, E. Sletten (Eds.), Metal Complex–DNA Interactions, Blackwell-Wiley, 2009, Chap. 4.
[5] P.X. Rojas-González, A. Castiñeiras, J.M. González-Pérez, D. Choquesillo-Lazarte, J. Niclós-Gutiérrez, Inorg. Chem. 41 (2002) 6190–6192.
[6] E. Bugella-Altamirano, D. Choquesillo-Lazarte, J.M. González-Pérez, M.J. Sánchez-Moreno, R. Marín-Sánchez, J.D. Martín-Ramos, B. Covelo, R. Carballo, A. Castiñeiras, J. Niclós-Gutiérrez, Inorg. Chim. Acta 339 (2002) 160–170.
[7] M.P. Brandi-Blanco, D. Choquesillo-Lazarte, A. Domínguez-Martín, J.M. González-Pérez, A. Castiñeiras, J. Niclós-Gutiérrez, J. Inorg. Biochem. 105 (2011) 616–623.
[8] A. Dallmann, L. Dehmel, T. Peters, C. Muegge, C. Griesinger, J. Tuma, N.P. Ernsting, Angew. Chem. 49 (2010) 5989–5992.
[9] S.M. Watanabe, M.F. Goodman, Proc. Natl. Acad. Sci. U.S.A. 78 (1981) 2864–2868.
[10] L.C. Sowers, Y. Boulard, G.V. Fazakerley, Biochemistry 39 (2000) 7613–7620.
[11] R.K. Neely, S.W. Magennis, S. Parsons, A.C. Jones, Chemphyschem 8 (2007) 1095–1102.
[12] E.Y.M. Bonnist, A.C. Jones, Chemphyschem 9 (2008) 1121–1129.
[13] M. Wang, H.R. Lee, W. Konigsberg, Biochemistry 48 (2009) 2075–2086.
[14] K.B. Hall, Methods Enzymol. 469 (2009) 269–285.
[15] M. Li, Y. Sato, S. Nishizawa, T. Seino, K. Nakamura, N. Teramae, J. Am. Chem. Soc. 131 (2009) 2448–2449.
[16] S.V. Avilov, J. Godet, E. Piemont, Y. Mely, Biochemistry 48 (2009) 2422–2430.
[17] K.K. Manouilov, L.S. Manouilova, F.D. Boudinot, R.F. Schinazi, C.K. Chu, Antiviral Res. 35 (1997) 187–193.
[18] S. Mubareka, V. Leung, Y. Aoki Fred, C. Vinh Donald, Expert Opin. Drug Saf. 9 (2010) 643–658.
[19] S. Menne, G. Asif, J. Narayanasamy, S.D. Butler, A.L. George, S.J. Hurwitz, R.F. Schinazi, C.K. Chu, P.J. Cote, J.L. Gerin, B.C. Tennant, Antimicrob. Agents Chemother. 51 (2007) 3177–3184.
[20] A. Fernández-Botello, A. Holy, V. Moreno, P.B. Opperschall, H. Sigel, Inorg. Chim. Acta 362 (2009) 799–810.
[21] A. Fernández-Botello, P.B. Opperschall Bert, A. Holy, V. Moreno, H. Sigel, Dalton Trans. 39 (2010) 6344–6354.
[22] F. Mazza, H.M. Sobell, G. Kartha, J. Mol. Biol. 43 (1969) 407–422.
[23] M.R. Harnden, R.L. Jarvest, A.M.Z. Slawin, D.J. Williams, Nucleos. Nucleot. Nucl. 9 (1990) 499–513.
[24] R. Ramaekers, L. Adamowicz, G. Maes, Eur. Phys. J. D. 20 (2002) 375–388.
[25] Bruker, SMART, SAINT, Area Detector Control Integration Software, Bruker Analytical X-ray Instruments, Inc, Madison, Wisconsin, 1999.
[26] BRUKER, APEX2 Software, Bruker AXS Inc, Madison, Wisconsin, USA, 2010 V2010.11.
[27] G.M. Sheldrick, SADABS, Program for Empirical Absorption Correction of Area Detector Data, University of Göttingen, Germany, 2009.
[28] G.M. Sheldrick, Acta Cryst. A64 (2008) 112–122.
[29] A.L. Spek, PLATON, A Multipurpose Crystallographic Tool, Utrecht University, Utrecht, The Netherlands, 2010.
[30] C.F. Macrae, J.A. Chisholm, P.R. Edgington, P. McCabe, E. Pidcock, L. Rodríguez-Monge, R. Taylor, J. Van de Streek, P.A. Wood, J. Appl. Cryst. 41 (2008) 466.
[31] K. Aoki, M.A. Salam, C. Munakata, I. Fujisawa, Inorg. Chim. Acta 360 (2007) 3658–3670.
[32] H.Q. Yuan, K. Aoki, I. Fujisawa, Inorg. Chim. Acta 362 (2009) 975–984.
[33] M.A. Salam, H.Q. Yuan, T. Kikuchi, N.A. Prasad, I. Fujisawa, K. Aoki, Inorg. Chim. Acta 362 (2009) 1158–1168.
[34] M.S. Rahman, H.Q. Yuan, T. Kikuchi, I. Fujisawa, K. Aoki, J. Mol. Struct. 966 (2010) 92–101.
[35] D.S. Marlin, M.M. Olmstead, P.K. Mascharak, Inorg. Chem. 40 (2001) 7003–7008.
[36] J.K. Gregory, D.C. Clary, K. Liu, M.G. Brown, R.J. Saykally, Science 275 (1997) 814–817.
[37] M. Matsumoto, S. Saito, I. Ohmine, Nature 416 (2002) 409–413.
[38] M.M.A. Mohamed, M.R. Shehata, M.M. Shoukry, J. Coord. Chem. 53 (2001) 125–142.
[39] L.E. Kapinos, H. Sigel, Inorg. Chim. Acta 337 (2002) 131–142.
[40] L.E. Kapinos, A. Holy, J. Guenter, H. Sigel, Inorg. Chem. 40 (2001) 2500–2508.

## 2.2. Structural consequences of the N7 and C8 translocation on the metal binding behavior of adenine

Article submitted to *Inorg. Chem.* (2012)

SYNOPSIS

X-Ray crystallography and DFT calculations concerning two novel oligo-nuclear ternary Cu(II)-complexes with 7-deaza-8-azaadenine reveal new insights into the coordination abilities and protonation roles of this purine-like ligand.

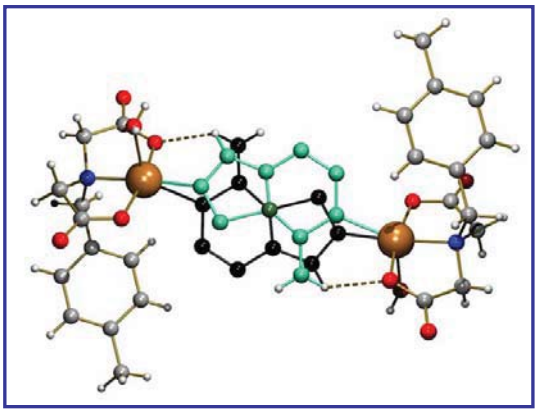

RESUMEN

7-Deaza-8-aza-adenina, también nombrada 4-aminopirazolo[3,4-d]pirimidina (H4app), es un bio-isómero de adenina (Hade) que resulta de la translocación de los átomos N7 y C8 en el anillo de purina. Con el propósito de estudiar la influencia de esta translocación en las capacidades de unión a metales de H4app, se han preparado y caracterizado estructuralmente dos complejos ternarios de cobre(II) conteniendo H4app y un quelante tipo N-bencil-iminodiacetato (MEBIDA o FBIDA, con un grupo metilo o fluor en *para*- al anillo bencilo respectivamente): $[Cu_2(MEBIDA)_2(\mu_2\text{-}N1,N8\text{-}H4app)(H_2O)_2]\cdot 4H_2O$ (**1**) y $[Cu_4(FBIDA)_4(\mu_2\text{-}N8,N9\text{-}H4app)_2(H_2O)]\cdot 3.5H_2O$ (**2**). Además, se han investigado las propiedades térmicas, espectrales y magnéticas de los compuestos descritos. Nótese que los dos compuestos estudiados tienen en común el enlace Cu-N8. En **1**, H(N9)4app está desordenado al 50% en dos posiciones y el modo de coordinación $\mu_2$-N1,N8 está débilmente asistido por sendas interacciones intra-moleculares N6-H···O y N9-H···O, respectivamente. La topología acíclica, no linear, del compuesto **2** está fuertemente influenciada por dos enlaces de hidrógeno intra-moleculares (O-H···O-carboxylato), involucrando al agua apical de un centro de cobre(II) en posición terminal. Para comprender mejor la limitada información estructural disponible, también se han llevado a

cabo cálculos de DFT para los tautómeros individuales de H4app así como cálculos más complejos sobre sistemas modelos mononucleares de cobre(II). De acuerdo con resultados anteriores, se concluye que H(N9)4app es el tautómero más estable seguido de H(N8)4app. Cuando N9 y N8 están unidos a metales, el tautómero H(N1)4app puede entrar en juego como se observa en el compuesto **2**. Asimismo, los resultados relativos al compuesto **1** sugieren que la formación de un enlace Cu-N1 en H4app resulta favorecido respecto a Hade, para quien sólo un caso ha sido descrito con dicha coordinación a pesar de la gran información estructural disponible en la bibliografía sobre compuestos relacionados conteniendo Cu(II) y adenina neutra.

**Structural consequences of the N7 and C8 translocation on the metal binding behavior of adenine**

| | |
|---|---|
| Journal: | *Inorganic Chemistry* |
| Manuscript ID: | Draft – Accepted with minor revisions |
| Manuscript Type: | Article |
| Date Submitted by the Author: | 02/10/2012 |
| Complete List of Authors: | Dominguez-Martin, Alicia;<br>University of Granada, Department of Inorganic Chemistry, Faculty of Pharmacy.<br>Choquesillo-Lazarte, Duane; CSIC, LEC.<br>Dobado, Jose; Universidad de Granada, Química Orgánica.<br>Martínez-García, Henar; Universidad de Valladolid, Departamento de Química Orgánica.<br>Lezama, Luis; University of Basque Country, Faculty of Science and Technology.<br>González-Pérez, Josefa; Universidad de Granada, Química Inorgánica.<br>Castiñeiras, Alfonso; University of Santiago de Compostela, Department of Inorganic Chemistry.<br>Niclós-Gutiérrez, Juan; University of Granada, Department of Inorganic Chemistry, Faculty of Pharmacy. |
| | |

# Structural consequences of the N7 and C8 translocation on the metal binding behavior of adenine

Alicia Domínguez-Martín,[*†] Duane Choquesillo-Lazarte,[‡] Jose A. Dobado,[¤] Henar Martínez-García,[¶] Luis Lezama,[§] Josefa M. González-Pérez,[†] Alfonso Castiñeiras,[¥] Juan Niclós-Gutiérrez[†]

[†] Department of Inorganic Chemistry, Faculty of Pharmacy, University of Granada, E-18071 Granada, Spain.

‡ Laboratorio de Estudios Cristalográficos, IACT, CSIC-Universidad de Granada, Av. de las Palmeras 4, E-18100 Armilla, Granada, Spain.

[¤] Grupo de Modelización y Diseño Molecular, Departamento de Química Orgánica, Facultad de Ciencias, Universidad de Granada, E-18071 Granada, Spain.

[¶] Departamento de Química Orgánica, Escuela de Ingenierías Industriales, Universidad de Valladolid, E-47071 Valladolid, Spain.

[§] Department of Inorganic Chemistry, Faculty of Science and Technology, University of Basque Country, E-48080 Bilbao, Spain.

[¥] Department of Inorganic Chemistry, Faculty of Pharmacy, University of Santiago de Compostela, E-15782 Santiago de Compostela, Spain.

Supporting Information

**ABSTRACT:** 7-Deaza-8-aza-adenine, namely 4-aminopyrazolo[3,4-d]pyrimidine (H4app), is a bioisoster of adenine (Hade) resulting from the translocation of N7 and C8 atoms on the purine moiety. With the aim of studying the influence of this translocation on the metal binding abilities of H4app, we have prepared and structurally characterized two ternary copper(II) complexes having H4app and one N-benzyl-iminodiacetate chelator (MEBIDA or FBIDA, with a methyl or fluoro group in para- of the benzyl aromatic ring): $[Cu_2(MEBIDA)_2(\mu_2\text{-}N1,N8\text{-}H4app)(H_2O)_2]\cdot 4H_2O$ (**1**) and $[Cu_4(FBIDA)_4(\mu_2\text{-}N8,N9\text{-}H4app)_2(H_2O)]\cdot 3.5H_2O$ (**2**). Furthermore, thermal, spectral and magnetic properties have been also investigated. In **1**, H(N9)4app is disordered over two equally pondered positions and the $\mu_2$-N1,N8 coordination mode is weakly assisted by N6-H···O and N9-H···O intra-molecular interactions, respectively. The acyclic non-linear molecular topology of **2** is strongly influenced by two intra-molecular H-bonding interactions (O-H···O-carboxylate) involving the apical aqua ligand of a terminal Cu(II) atom. Thus, both compounds have in common the Cu-N8 bond. In order to better understand our limited structural information, DFT calculations for the individual tautomers of H4app as well as mononuclear Cu(II) model systems have been carried out. According to previous results, we conclude that H(N9)4app is the most stable tautomer followed by H(N8)4app. When N9 and N8 are metallated, then the tautomer H(N1)4app can come into play as observed in compound **2**. Likewise, the findings concerning compound 1 suggest that the formation of a Cu-N1 bond in H4app results favored compared to neutral adenine, for which only one case has been reported with such coordination despite the large variety of related Cu(II)-Hade described in literature.

## INTRODUCTION

In the last decades, a large number of papers has addressed the metal binding patterns of natural nucleobases as well as closely related ligands.[1] In this sense, our research group has been devoted to the study of adenine, which has proved to be a fairly rich versatile ligand.[2] Moreover, in order to extend the reach of our results, we have also studied several oxo-, amino-, aza- and/or deaza-purine derivatives.[3] The better understanding of the metal binding patterns of these purine analogues is challenging because it could reveal new insights into the behavior of nucleic acids in living beings. 7-Deaza-8-aza-adenine (4-aminopyrazolo[3,4-

d]pyrimidine, H4app) is an structural analogue of adenine (Hade) that has a fused pyrazole ring instead of an imidazole ring. Thus, it represents the translocation of the N7 and C8 atoms in Hade, according to purine conventional notation (see scheme 1). This fact should perturb the proton tautomerism and the metal binding abilities of this former nucleobase. Indeed, the absence of the N7 residue in H4app, which is believed to be the most relevant metal binding site in natural purines (exposed at the major groove of DNA), has raised high and broad interest regarding its potential applications. In this context, several pharmacological properties have been already described for pyrazolo[3,4-d]pyrimidine ligands such as antibacterial and antifungal,[4] antiparasite,[5] or antiproliferative agents.[6] Likewise, they have been reported as adenosine antagonists[7] and inhibitors some enzymes.[8] However, further than these applications, the rationalization of the metal binding patterns in this kind of ligands is still necessary to better understand more complex processes concerning nucleic acids such as the role of metal ions in the molecular crowding and their structural, functional and stability consequences within biomolecules, for example concerning ribozymes.[9]

Under the structural point of view, the roles of H4app as ligand are rather unexplored. Some synthetic nucleosides derived from H4app have been isolated and characterized crystallographically.[10] Nevertheless, the existing data about H4app is mainly focused on two papers. According to data from solution studies, Dubois et al.[11] proposed the basicity order N9≥N8>N1>N3>>N6 for the N-donors of H4app (see scheme 1). Alternatively, by increasing metallation with $CH_3Hg(I)$, Sheldrick et al.[12] reported structural support about four metal binding patterns of H4app or its 4app- and 4app-H2- anionic forms, in good agreement to the N-basicity order of this ligand. Therefore, in order to deepen our knowledge on the molecular recognition patterns of the nucleobase H4app, we have synthesized and characterized two novel mixed-ligand ternary copper(II) complexes with iminodiacetate-like chelators and H4app.

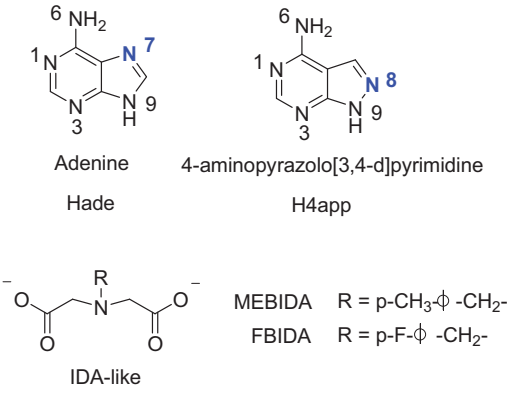


Scheme 1. Top: Adenine and 4-aminopyrazolo[3,4-d]pyrimidine with the conventional notation of purines. Bottom: Formulas of the chelating ligands used in this work: N-(p-methylbenzyl)-iminodiacetate(2-) and N-(p-fluorobenzyl)-iminodiacetate(2-) anions (MEBIDA and FBIDA, respectively).

## EXPERIMENTAL SECTION

Materials. Bluish $Cu_2CO_3(OH)_2$ was purchased from Probus. 4-Aminopyrazolo[3,4-d]pyrimidine (H4app) was purchased from Sigma-Aldrich. All the former reagents were used without further purification. N-(p-methylbenzyl)- and N-(p-fluorobenzyl)-iminodiacetic acids ($H_2$MEBIDA and $H_2$FBIDA, respectively) were synthesized in their acid form as previously reported for N-benzyl-iminodiacetic acid[13] using 4-methyl-benzylamine (p-xylylamine) or 4-fluorobenzylamine instead of benzylamine, respectively.

Syntheses of the complexes.

$[Cu_2(MEBIDA)_2(\mu_2\text{-}N1,N8\text{-}H4app)(H_2O)_2]\cdot 4H_2O$ (**1**): $Cu_2CO_3(OH)_2$ (0.25 mmol, 0.055 g) was reacted in 50 mL of distilled water with $H_2$MEBIDA acid (0.5 mmol, 0.119 g) in a Kitasato flask, heating (50 °C) and stirring under moderate vacuum until a clear blue solution of the binary chelate is obtained. Alternatively, a suspension of H4app (0.5 mmol, 0.068 g) in 40 mL of isopropanol was prepared at r.t. Afterwards, the suspension of H4app was added to the binary chelate solution and the reacting mixture was stirred for 1 hour until the reactants were completely dissolved. The resulting blue solution was filtered, without vacuum, on a crystallyzation device and allowed to stand at room temperature, covered with a plastic film to control the

evaporation. After six weeks, needle-like crystals suitable for XRD purposes were collected. Yield is ca. 70-75%. Elemental analysis (%): Calc. for $C_{29}H_{43}Cu_2N_7O_{14}$: C 41.43, H 5.15, N 11.66; Found: C 41.83, H 4.24, N 11.77. FT-IR (KBr, $cm^{-1}$) $\nu_{as}(H_2O)$ 3398, $\nu_{as}(NH_2)$ overshadowed, $\nu_s(NH_2)$ overlapped with $\nu_s(H_2O)$ 3247, $\nu$(N-H) 3184, $\nu_{as}(CH_2)$ 2924, $\nu_s(CH_2)$ 2852, $\delta(H_2O)$ and $\delta(NH_2)$ overlapped with $\nu_{as}$(COO) 1611, $\delta$(N-H) 1517, $\nu_s$(COO) 1384, $\pi(C\text{-}H)_{ar}$ 809 (MEBIDA), $\pi(C\text{-}H)_{ar}$ 788 (H4app). Under air-dry flow, the sample loses only 0.5 non-coordinated water molecule, thus the TG experiment starts with an average formula $[Cu_2(MEBIDA)_2(\mu_2\text{-}N1,N8\text{-}H4app)(H_2O)_2]\cdot 3.5H_2O$ The thermogravimetric curve shows five steps. The first step corresponds to the loss weight of the rest of water content (n = 5.5 $H_2O$; Calc. 12.03%; Found 12.07%). Indeed only $H_2O$ and trace amounts of $CO_2$ are identified as evolved gasses during this first step. The following pyrolitic steps yield a final residue of 2 CuO (470 °C, Calc. 19.31%; Found 20.77%). The evolved gasses during the pyrolysis involve $H_2O$, $CO_2$, CO and three N-oxide gasses ($N_2O$, $NO_2$ and NO). See S-6 in Supporting Information.

$[Cu_4(FBIDA)_4(\mu_2\text{-}N8,N9\text{-}H4app)_2(H_2O)]\cdot 3.5H_2O$ (**2**): A synthetic procedure similar to that of compound 1 was followed, using $H_2$FBIDA acid (0.5 mmol, 0.120 g) instead of $H_2$MEBIDA acid. The addition of isopropanol to the mother liquors is again needed to reach the complete solution of the ternary system. In two months, needle-like crystals were obtained. The reaction yielded 65%. Elemental analysis (%): Calc. for $C_{54}H_{59}Cu_4F_4N_{14}O_{20.5}$: C 41.51, H 3.81, N 12.55; Found: C 41.08, H 3.90, N 12.65. FT-IR (KBr, $cm^{-1}$) $\nu_{as}(H_2O)$ 3433, $\nu_{as}(NH_2)$ overshadowed, $\nu_s(NH_2)$ overlapped with $\nu_s(H_2O)$ 3232 $\nu$(N-H) 3131 (sh), $\nu_{as}(CH_2)$ 2930, $\nu_s(CH_2)$ 2860, $\delta(H_2O)$ 1629, $\delta(NH_2)$ overlapped with $\nu_{as}$(COO) 1606, $\delta$(N-H) 1512, $\nu_s$(COO) 1384, $\nu$(C-F) 1005, $\pi(C\text{-}H)_{ar}$ 736 (FBIDA), $\pi(C\text{-}H)_{ar}$ 782 (H4app). The UV/Vis spectrum shows an asymmetric d-d band with $\lambda_{max}$ at 670 nm ($\nu_{max}$ 15000 cm-1). Under air-dry flow, the sample loses part of the non-coordinated water molecule. Hence, the sample starts the TG experiment with formula $[Cu_4(FBIDA)_4(\mu_2\text{-}N8,N9\text{-}H4app)_2(H_2O)]\cdot 2.6H_2O$. The thermal behavior is divided in six steps. The sample loses all the water content during the first step (n = 3.60 $H_2O$; Calc. 4.21%; Found 4.20%), according to the evolved gasses. Five additional pyrolitic steps produce $H_2O$, $CO_2$, CO and N-oxide gasses ($N_2O$, NO, $NO_2$) to finally reach an impure CuO residue (480 °C, Calc. 20.58%; Found 20.80%). See S-7 in Supporting Information.

X-Ray Structure Determinations. Measured crystals were prepared under inert conditions immersed in perfluoropolyether as protecting oil for manipulation. Suitable crystals were mounted on MiTeGen MicromountsTM and these samples were used for data collection. Data were collected with Bruker X8 Proteum (compound 1, 293 K) or Bruker SMART CCD 1000 (compound 2, 110 K) diffractometers. The data were processed with SAINT[14] (**1**) or APEX2[15] (**2**) programs and corrected for absorption using SADABS.[16] The structures were solved by direct methods,[17] which revealed the position of all non-hydrogen atoms. These atoms were refined on F2 by a full-matrix least-squares procedure using anisotropic displacement parameters.[17] All hydrogen atoms were located in difference Fourier maps and included as fixed contributions riding on attached atoms with isotropic thermal displacement parameters 1.2 times those of the respective atom. Geometric calculations were carried out with PLATON[18] and drawings were produced with PLATON[18] and MERCURY.[19] Additional crystal data and more information about the X-ray structural analyses are shown in Supporting Information S3 to S5. Crystallographic data for the structural analysis have been deposited with the Cambridge Crystallographic Data Centre, CCDC No. 881146 – 881147 for 1 and 2 respectively. Copies of this information may be obtained free of charge on application to CCDC, 12 Union Road, Cambridge CB2 1EZ, UK (fax: 44 1223 336 033; e-mail: deposit@ccdc.cam.ac.uk or http://www.ccdc.cam.ac.uk).

Computational methods. DFT calculations, at the B3LYP[20] and unrestricted M06-L/6-31G* theoretical levels for the isolated H4app ligand and mononuclear copper complexes, respectively, have been performed with the Gaussian09 program,[21] using the 6-31+G** basis set, for the isolated ligands and the 6-31G* one for the copper complexes.[22] These methods have proven to be a reliable theoretical levels for the study of similar compound.[23] All structures were fully optimized at the following theoretical levels: B3LYP/6-31+G**//B3LYP/6-31+G** for the isolated ligands, and M06-L/6-31G*//M06-L/6-31G* for the

copper(II) complexes. The most stable spin multiplicities for the mononuclear copper complexes studied were doublet. The local stability of all structures was checked through the eigenvalues of the matrix of second derivatives (Hessian); all energetic minima presented no imaginary frequencies. Solvent effect was taken into account by means of the self consistent reaction field (SCRF) method, selecting PCM algorithm with water as solvent.[24] Additional information about DFT calculations is provided in Supporting Information S1 to S2.

Other Physical methods. Analytical data were obtained in a Thermo-Scientific (Flash 2000) elemental micro-analyzer. Infrared spectra were recorded by using KBr pellets on a Jasco FT-IR 6300 spectrometer. TG analyses were carried out in air-dry flow (100 mL/min) with a Shimadzu thermobalance TGA-DTG-50H instrument, coupled with a FT-IR Nicolet Magma 550 spectrometer. A series of FT-IR spectra (20-30 per sample) of the evolved gasses were time-spaced recorded during the TG experiment. Diffuse reflectance (electronic) spectra were recorded in a Varian Cary-5E spectrophotometer. Variable temperature (2-300 K) magnetic susceptibility measurements on polycrystalline samples were carried out with a Quantum Design MPMS-7 SQUID magnetometer under a magnetic field of 0.1T. The experimental susceptibilities were corrected for the diamagnetism of the constituent atoms by using Pascal's tables. X-band EPR measurements were carried out on a Bruker ELEXSYS 500 spectrometer with a maximum available microwave power of 200 mW and equipped with a super-high-Q resonator ER-4123-SHQ. For Q-band studies, EPR spectra were recorded on a Bruker EMX system equipped with an ER-510-QT resonator and an ER-4112-HV liquid helium cryostat. The magnetic field was calibrated by a NMR probe and the frequency inside the cavity was determined with a Hewlett-Packard 5352B microwave frequency counter. Computer simulation: WINEPR-Simfonia, version 1.5, Bruker Analytische Messtechnik GmbH).

## RESULTS AND DISCUSSIONS

### DFT CALCULATIONS

Tautomers for 4-aminopyrazolo[3,4-d]pyrimidine. In order to explore the relative stability of the corresponding hydrogen tautomers of H4app, gas phase and solvent effect Gibbs energies have been calculated and summarized in Table 1. As should be expected, H(N9)4app is the most stable tautomer in gas phase and also when solvent effect is included. Moreover, according to previous solution studies,[11] H(N8)4app is the next stable tautomer, showing our calculations a difference of 3.26 kcal·mol$^{-1}$ in water compared to H(N9)4app. The H(N3)4app and H(N1)4app tautomers are higher in terms of $\Delta$Gr (9.59 and 11.99 kcal·mol$^{-1}$, respectively), although they are rather close to each other. Moreover, it is noteworthy that when solvent effect is taken into account in the calculations, all free Gibbs energy values are reduced significantly; i.e. the difference between the tautomer H(N1)4app in gas phase and H(N1)4app considering the solvent effect is 16.18 kcal·mol$^{-1}$.

Models for mononuclear copper(II) complexes. With the aim of estimating the coordination abilities of H4app, DFT calculations have been carried out for ternary copper(II) model systems having the chelating ligand N-methyl-iminodiacetate(2-) anion (MIDA) and H4app. For all the calculations, a mer-$NO_2$ conformation was chosen for the iminodiacetate moiety and the binary chelate and the H4app ligand were induced to be coplanar, according to related structural results.[13,23] Moreover, the Cu(II)/MIDA chelate was tested for all the possible tautomers of H4app (see Table S-1. and S-2. in Supporting Information) since the presence of copper could alter the tautomeric preferences shown in Table 1 (vide supra). The most stable structure for the discrete system CuII/MIDA/H4app is the one having the most stable tautomer H(N9)4app.

In this latter case, the Cu(II) atom is coordinated by N3(H4app) and assisted by an intra-molecular H-bond via N9 [3p9; N9-H···O(non-coord. carboxylate)]. Herein, the H4app and the MIDA chelating ligand remain coplanar, being the referred intra-molecular interligand H-bond of maximum strength. However, for the same tautomer H(N9)4app and speaking in terms of solvent effect, two other possibilities, 1p9 and 8p9, are rather close to the 3p9 form in terms of free Gibbs energy (Fig. 1).

Table 1. DFT Gas phase and solvent (water) relative free Gibbs energies (ΔGr) for 4-aminopyrazolo[3,4-d]pyrimidine, calculated at the B3LYP/6-31+G**//B3LYP/6-31+G** and PCM-B3LYP/6-31+G**//PCM-B3LYP/6-31+G** theoretical levels, respectively.

| Compound | Tautomer-H9 ΔGr (Kcal/mol) | Tautomer-H8 ΔGr (Kcal/mol) | Tautomer-H6 ΔGr (Kcal/mol) | Tautomer-H3 ΔGr (Kcal/mol) | Tautomer-H1 ΔGr (Kcal/mol) |
|---|---|---|---|---|---|
| Gas Phase (II-p9 / II-p8 / II-p6/ II-p3 / II-p1)a | 0.0 | 8.37 | 57.59 | 16.39 | 28.17 |
| Solvent(water) (IIs-p9 / IIs-p8 / IIs-p6 / IIs-p3 / IIs-p1) | 0.0 | 3.26 | 33.0 | 9.59 | 11.99 |

[a] The latin number 'II' refers to H4app ligand and the number after the 'p' to the position where the tautomerizable proton is located. The letter 's' indicates when solvent effect is included in calculations.

This fact points out the possibility of two additional molecular recognition patterns for H(N9)4app (ΔGr = 2.18 and 2.86 kcal·mol-1 for the 1p9 and 8p9 forms, respectively- see Table S-1. in Supporting Information) Furthermore, the small difference between the two latter aforementioned patterns (0.68 kcal·mol$^{-1}$) suggests the possibility of the bidentate role $\mu_2$-N1,N8 for H(N9)4app, as is indeed observed in compound 1 (see Results and discussion).

If we extend the analysis of the CuII/MIDA/H4app model system to other H4app tautomers, different from H(N9)4app, then the lowest energetic value is 4 kcal·mol$^{-1}$. In particular, when we focus on the H(N1)4app tautomer, the three possible coordination modes are 3p1, 8p1 and 9p1. Among them, only the 8p1 and 9p1 forms are likely to occur (see Table S-1 in Supporting Information). Note that, although they show quite high ΔGr values (11.28 and 10.08 kcal·mol$^{-1}$, respectively), the difference between these two values is rather small what could be indicative of a bidentate role for H(N1)4app tautomer, provided it is favored in more complex systems. In fact, the bidentate $\mu_2$-N8,N9-H(N1)4app molecular recognition pattern has been proved by X-Ray crystallography, not only in compound **2** but also in a pyrazolo[3,4-d]pyrimidin-4-one complex.[25]

**MOLECULAR AND CRYSTAL STRUCTURES**

Compound **1**, with formula $[Cu_2(MEBIDA)_2(\mu_2\text{-}N1,N8\text{-}H4app)(H_2O)_2]\cdot 4H_2O$, consists of a centro-symmetric dinuclear complex molecule (Fig. 2) and solvent water. In the complex, the copper(II) atoms exhibit a 4+1 coordination polyhedron where the four closest donor atoms correspond to the tridentate IDA-like chelating ligand MEBIDA (N10, O11, O21) and one N-donor (N1 or N8) from H4app (see Table S-3.2 in Supporting Information). Thus, MEBIDA ligand adopts a mer-$NO_2$ conformation. The apical/distal coordination sites are occupied by aqua ligands which show rather short bond lengths [Cu1-O1 2.220(2) Å] in contrast to related apical distances which usually fall in the range of 2.3-2.6 Å.

According to previous results, H4app shows its most stable tautomer H(N9)4app. Moreover, it acts as a bridging ligand displaying the unprecedented $\mu_2$-N1,N8 mode. It is also remarkable that the coordination bond Cu-N1 is a bit longer than expected if we compare the present distance [Cu1-N1 2.109(2) Å] to those of Cu-N1(neutral purine) bonds available in literature [i.e. 1.993(4) Å in $\mu_2$-N1,N8-H7deaza-adenine in ref. 23 or 2.020(2) Å in $\mu_2$-N1,N9-Hade in ref. 26].

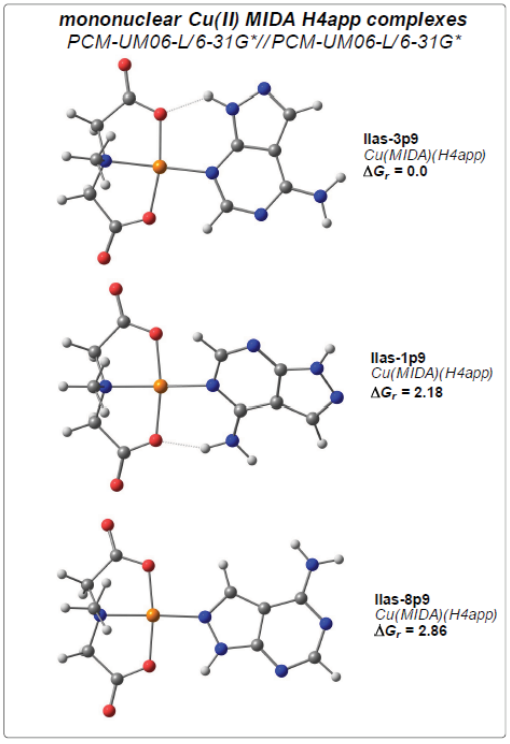


Figure 1. DFT (PCM-B3LYP/6-31G*//PCM-B3LYP/6-31G*) three most stable coordination modes for the mononuclear copper(II) complexes with the H(N9)4app tautomer and the chelating ligand MIDA. ΔGr values in kcal·mol$^{-1}$.

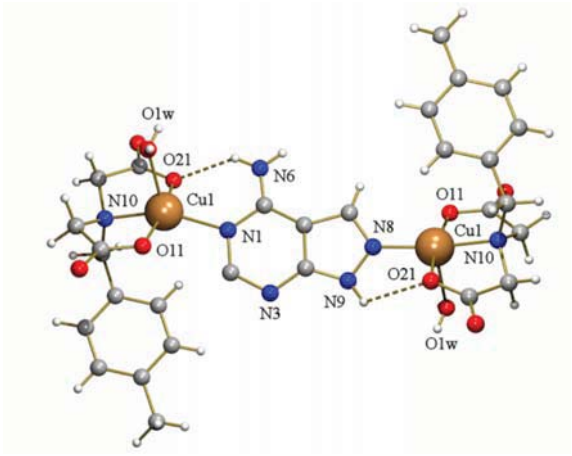


Figure 2. Complex molecule of $[Cu_2(MEBIDA)_2(\mu_2\text{-}N1,N8\text{-}H4app)(H_2O)_2]\cdot 4H_2O$ (**1**) with the numbering of the coordination environment. Only one of the two disordered positions is plotted for H4app. Solvent molecules omitted for clarity.

Furthermore, both Cu-N1 and Cu-N8 bonds are assisted by very weak intra-molecular interligand H-bonding interactions [N6-H6A···O21(carboxy coord., 3.091(7) Å, 136°) and N9-H···O21(carboxy coord., 2.975(3) Å, 119°)], respectively (see Fig. 2). The weakness of these H-bonding interactions seems to be related to the implication of N6-H and N9-H groups in bifurcated intermolecular H-bonds. This fact may also contribute to the loss of planarity between the H4app ligand and the mean basal CuII coordination planes, displaying an open dihedral angle close to 40°.Furthermore, it should be noticed that, in the crystal, the ligand H4app is disordered over two positions, related to each other by an inversion centre. This means that the H4app ligand is found in a special crystallographic position and therefore each CuII centre is 50 % bonded to N1 or N8 (see Fig. 3).

In the crystal of 1, inter-molecular pi,pi-stacking interactions between the aromatic ring of MEBIDA and the 5- and 6-membered rings of H4app build multi-stacked chains that extend along the b axis (Fig. 3, left) [Geometrical stacking parameters: (i) Cg···Cg 3.628(3) Å, α = 3.2(3)°, β = 18.57°, γ = 21.38° and (ii) Cg···Cg 3.564(3) Å, α = 2.3(2)°, β = 13.11°, γ = 15.41°, respectively – see S-5.1 in Supporting Information]. Adjacent chains connect to each other by inter-molecular H-bonds that involve the apical aqua ligands and non-coordinated carboxylate O-atoms leading to a 3D honeycomb-like network (Fig. 4, right - see also Table S-3.3 in Supporting Information).

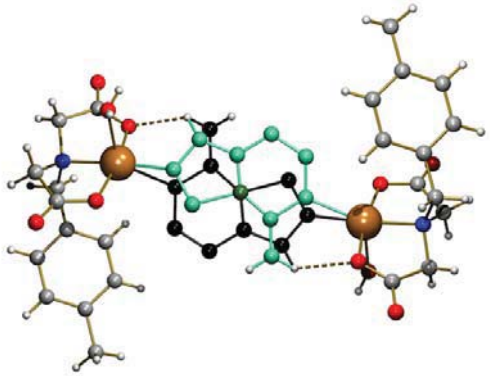

Figure 3. Complex molecule of $[Cu_2(MEBIDA)_2(\mu_2\text{-}N1,N8\text{-}H4app)(H_2O)_2]\cdot 4H_2O$ (**1**). The two disordered positions of H4app ligand are plotted in black and turquoise, respectively. The carbon atom shared by the two disordered position is depicted in dark green. Solvent molecules omitted for clarity.

Compound **2** consists of an asymmetric tetranuclear complex molecule (Fig. 5) and non-coordinated water molecules. The four copper(II) centers show a square-based pyramidal coordination, type 4+1. Cu1 and Cu3 metal surroundings are of the same type. The donor atoms of the basal plane are supplied by a tridentate FBIDA chelator and the N9 atom of an H4app whereas the apical sites are occupied by an O-monoatomic $\mu_2$-carboxylate atom. The Cu2 coordination is quite similar to those of Cu1 or Cu3, except for the apical O-atom that belongs to a syn,anti $\mu_2$-bridging carboxylate group. In contrast, the apical Cu4 site is remarkably occupied by one aqua ligand [Cu4-O(aqua) 2.463(3) Å]. Other selected bond lengths, interatomic distances and angles are provided in Table S-4.2 in Supporting Information. It should be noted that the FBIDA ligands play three different roles: (i) only as a tridentate chelator for Cu1; (ii) as tridentate chelator plus O-monoatomic $\mu_2$-carboxylate ligand for Cu4 and (iii) as tridentate chelator and as a syn,anti $\mu_2$-O-O'-carboxylate ligand for Cu2 and Cu3. Herein, both H4app show a $\mu_2$-N8,N9 bidentate role, using the H(N1)4app tautomer due to the transfer of the H(N9) atom to the N1 acceptor (the most basic N-donor atom available in the $\mu_2$-N8,N9 coordination mode). Note that using this tautomer, the Cu-N(heterocyclic) bonds can not cooperate with appropriate intra-molecular interligand H-bonding interactions. This bridging $\mu_2$-N8,N9 role was previously reported for methyl-Hg(II) derivatives of H4app, with formula $[(CH_3Hg)_2(\mu_2\text{-N8,N9-H(N1)4app})](NO_3)_2{\cdot}H_2O$.[12] Moreover, the H(N1) tautomer together with the $\mu_2$-N8,N9 coordination role has been also described for one zinc(2+) complex of allopurinol (pyrazolo[3,4-d]pyrimidin-4-one).[25] Interestingly, the complex molecule of **2** exhibits an unusual acyclic, non-linear asymmetric topology, in which the apical aqua ligand of Cu4 plays two relevant roles. First, it restricts the nuclearity of the complex to four (instead of yielding, for example, a 1D polymer). Second, it determines the non-linearity of the tetramer conformation by means of two intra-molecular interligand H-bonds (Fig. 5). In such interactions, the O(carboxylate) acceptors appertain to the FBIDA chelators of Cu1 [O4-H4A···O21(coord. carboxy), 2.905(4) Å, 140.5°] and Cu3 [O4-H4B···O16(non coord. carboxy), 2.757(4) Å, 165.1°]. This topology is in clear contrast to that of the cyclic-tetranuclear complex molecule found in $[Cu_4(pheida)_2(\mu_2\text{-O,O'-pheida})_2(\mu_2\text{-N3,N7-H(N9)ade})(H_2O)_2]{\cdot}4H_2O$ (pheida = N-phenethyl-iminodiacetate(2-) ligand).[13] In this case, the cyclic topology is tied to the cooperation of the Cu-N3 and Cu-N7 bonds with appropriate intra-molecular interligand N9-H···O(carboxy) and N6-H···O(carboxy) H-bonds and the $\mu_2$- bridging role of two pheida ligands.

Besides the above-mentioned H-bonds (vide supra), additional inter-molecular H-bond plus intra- and inter-molecular pi,pi-stacking, ring-metal, X-H···ring and X-Y···ring interactions are present in the crystal packing of compound **2**, contributing to the overall stabilization of the 3D network (Table 2 – see also Table S-4.3 and S-5.2 in Supporting Information).

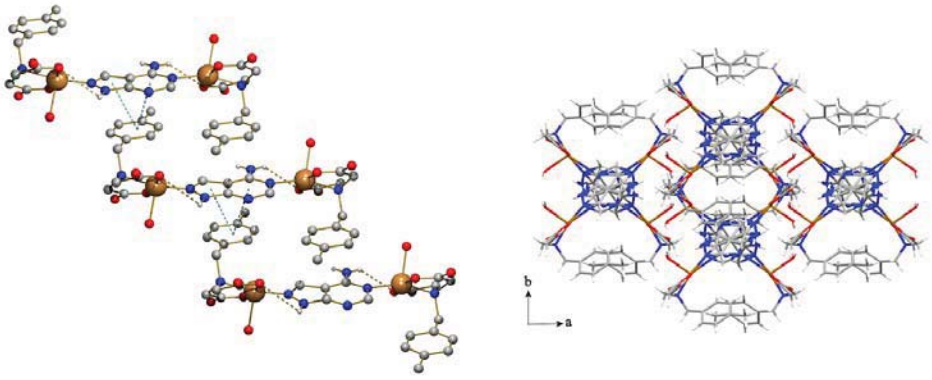


Figure 4. Left: detail of multi-stacked 1D chains in compound **1**. Only one of the two disordered positions for the H4app ligand is depicted for clarity. Right: View in the ba plane of the 3D honeycomb-like architecture in the crystal of **1**.

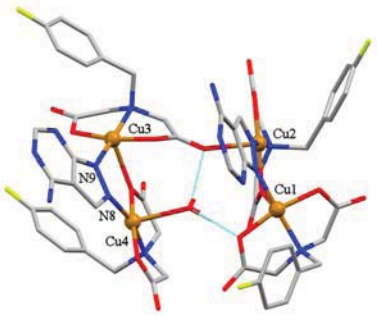


Figure 5. Complex molecule of $[Cu_4(FBIDA)_4(\mu_2\text{-}N8,N9\text{-}H4app)_2(H_2O)]\cdot 3.5H_2O$ (**2**). Solvent molecules and H-atoms not involved in intra-molecular H-bonding interactions are omitted for clarity.

Besides the above-mentioned H-bonds, additional inter-molecular H-bond plus intra- and inter-molecular pi,pi-stacking, ring-metal, X-H···ring and X-Y···ring interactions are present in the crystal packing of compound **2**, contributing to the overall stabilization of the 3D network (Table 2 – see also Table S-4.3 and S-5.2 in Supporting Information). Among those interactions, the most significant ones are: (i) the pi,pi-stacking between the 6-membered rings of two H4app ligands (bridging Cu1 and Cu2) of adjacent tetrameric units and that involving the aromatic moieties from FBIDA chelators of Cu3 and Cu4 (Figure 6 - left). In the former interactions, the Cg···Cg distances are 3.53(1) and 3.78(1) Å, respectively, and the dihedral angles (α) in the range of 0-4°, which are considered as rather intense pi,pi-stacking interactions (see S-5.2 in Support. Information).[27] (ii) Likewise, it is remarkable the intra-molecular ring-metal interaction observed between the aromatic moiety of the FBIDA(4) ligand and the related copper(II) centre (Figure 6 - right), with a Cu4···Cg distance of 3.62(1) Å. Moreover, the distance metal-to-plane of 2.77(1) Å (from the normal to the mean plane of the ring, passing through the copper(II) atom) also reveals its significance. Such interaction is the only one present among the four possible alternatives within the tetranuclear unit, what underline the conformational versatility of the FBIDA ligands inside the tetramer.

## MOLECULAR RECOGNITION CONSEQUENCES

Despite the broad structural information regarding adenine, in any of its forms, only 51 structures reported in the Cambridge Structural Database show the M-N1 coordination bond. The vast majority of them comprise soft metal ions (such as $Pt^{2+}$ or $Ag^{+}$) and N9-blocked adenine derivatives showing the bidentate $\mu_2$-N1,N7 role, see for example ref. 28. It is important to note that in 9-substistuted purine ligands all the remaining N-donors are potential coordination sites since there are no tautomerism phenomena. On the other hand, just five structures have been characterized displaying the Cu-N1 bond. Three of them correspond to one bridging $\mu_4$-N1,N3,N7,N9-tetradentate adeninate(1-) anion[29] and two N9-blocked adenines with the aforementioned bridging $\mu_2$-N1,N7 mode.[30] Interestingly, only two structures have neutral purine-like ligands: one is a mixed-ligand Cu-Hade complex[26] and the other is a Cu-H7deaza-adenine derivative recently characterized by our group.[23] Why the N1 donor is rarely involved in coordination in purine ligands still remains quite uncertain. Obviously the presence of the exocyclic amino group hinders the N1 atom, which is a poorer metal binding site in comparison to N7. However, equilibrium data published by Sigel et al.[31] concluded that purine residues may coordinate two metal ions simultaneously at N1 and N7 sites under physiological conditions.

The relevance of **1** lies in the formation of the Cu-N1 bond, as a part of the $\mu_2$-N1,N8 coordination mode displayed by H(N9)4app. Thus, molecular recognition studies with purine analogues without the N7 atom, such as the previously referred H7deaza-adenine or H4app, point out the relevance of the N1/N7 dichotomy. In these latter ligands, the absence of the N7 donor seems to encourage the coordination abilities of the N-purine six-membered ring and hence it turn N1 donor into a more attractive metal binding site. In compound **1** this is specially favored because: (i) the metallation of N9 and N8 increase the acidity of N3 and (ii) in this mixed-ligand metal complex the N6-H bond can be involved in intra-molecular interligand interaction that cooperates with the coordination bond. All this information may help us to better understand some processes in nature where purine ligands actively participate, especially larger oligonucleotides, but also to rationalize the molecular recognition processes in which this ligand, as part of new promising drugs, are involved.

Table 2. Inter- and intra-molecular interactions (A, º) present in $[Cu_4(FBIDA)_4(\mu_2\text{-N8,N9-H4app})_2(H_2O)]\cdot 3.5H_2O$ (**2**).

| π···π interactions | Cg(I)···Cg(J) | α |
|---|---|---|
| Cg(1)···Cg(1)i | 3.532 | 0.00 |
| Cg(2)···Cg(3)ii | 3.780 | 3.63 |
| Cg(3)···Cg(2)iii | 3.780 | 3.63 |
| **Ring-Metal interactions** | **Cg(I)···Cu** | **β** |
| Cg(3)···Cu(4) | 3.622 | 40.12 |
| **X–H···π interactions** | **H···Cg(I)** | **γ** |
| O(3)–H(3B)···Cg(4)iv | 2.83 | 21.95 |
| C(37)–H(37)···Cg(5)i | 2.83 | 7.65 |
| **X–Y···π interactions** | **Y···Cg(I)** | **γ** |
| C(45)–F(2)···Cg(6)v | 3.26 | 18.86 |
| C(22)–O(22)···Cg(7) | 3.76 | 27.34 |
| C(26)–O(26)···Cg(2) | 3.93 | 22.04 |

Cg(I)···Cg(J): Distance between ring centroids; α: Dihedral angle between planes I and J; β: angle between Cg(I)–Cu vector and normal to plane I; γ: angle between X–H vector and normal to plane I

Constitution of ring plane(number): Cg(1)-(N51/C52/N53/C54/C55/C56); Cg(2)-(C62/C63/C64/C65/C66/C67); Cg(3)-(C72/C73/C74/C75/C76/C77); Cg(4)-(N58/N59/C54/C55/C57); Cg(5)-(N81/C82/N83/C84/C85/C86); Cg(6)-(C42/C43/C44/C45/C46/C47); Cg(7)-(C32/C33/C34/C35/C36/C37).

Symmetry transformations: i = -x, 2-y, 1-z; ii = -1+x, y, z; iii = 1+x, y, z; iv = 1+x, -1+y, z; v = -1-x, 2-y, -z.

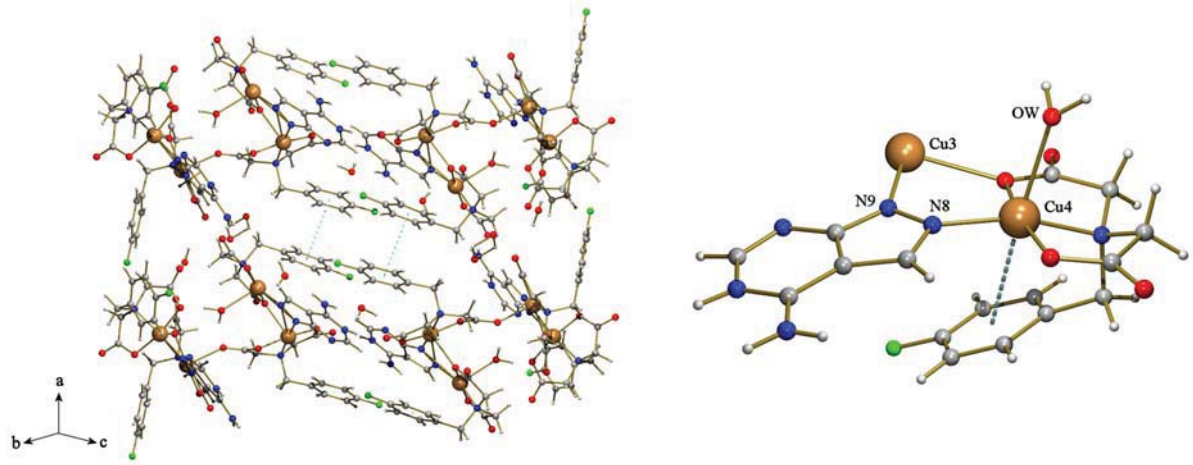


Figure 6. Left: view of unit cell of **2** showing pi,pi-stacking between phenyl groups of neighboring FBIDA ligands; Right: detail of metal-ring interaction within a fragment of the tetranuclear complex (**2**).

Alternatively, other molecular recognition pattern has been described in compound **2** for the H4app ligand. Herein, the ligand uses the H(N1)4app tautomer and display the $\mu_2$-N8,N9 coordination mode. As we have commented previously, this role has been previously reported for H4app and its hydroxo-derivative allopurinol. It should be noted that, although the DFT calculations carried out in this study consider the use of the latter bridging mode, ΔGr values were more favorable to the $\mu_2$-N1,N8 bidentate role. This can be explain considering the difference in energy between the H(N9)4app and H(N1)4app tautomers but the vagaries of compound **2**, i.e. $\mu_2$-N8,N9 can not cooperate with intra-molecular interligand H-bonding interactions. Anyhow, the molecular recognition patterns described for compounds 1 and 2 are in accordance with the assumed N-basicity order of H4app (N9≥N8>N1>N3>>N6), obtained from solution studies, and the previous theoretical calculations (vide supra – see DFT calculations section). Going further on compound **2**, it is noteworthy how non-covalent interactions mainly drive the acyclic non-linear topology of this tetranuclear complex molecule. In this compound, the unit corresponding to Cu4 plays an essential role controlling the nuclearity by means of intra-molecular H-bonds that involve the apical aqua ligand. Besides this, it seems that the topology is further influenced by an unusual contribution of different inter-molecular forces, from which it should be remarked the metal(Cu4)-ring interaction. This latter phenomenon is rather infrequent and of special relevance regarding the interaction of metal ions with biomolecules (i.e. blue copper proteins[32]).

## EPR AND MAGNETIC PROPERTIES

Since compounds **1** and **2** have relevant stacking interactions within their molecular and crystal structures, X and Q band EPR measurements were carried out on powdered samples at several temperatures in the range 5-300 K. In all cases, the spin hamiltonian parameters were estimated by comparison of the experimental spectra with those obtained by a computer simulation program working at the second order of the perturbation theory.

The X-band powder EPR spectrum of 1 has the characteristic shape of Cu(II) sites with rhombic symmetry (Fig. 7). The main g-values are $g_1$ = 2.205, $g_2$ = 2.135 and $g_3$ = 2.048 ($g_{iso}$= 2.129), remaining practically unchanged from room temperature down to 5 K. The calculated G parameter[33] is 2.3, which indicates that the g values obtained from the experiment are not equal to the molecular ones. This fact implies the averaging by exchange coupling of the signal corresponding to magnetically non-equivalent copper sites, as Cu1 and Cu1e (1/2-x, -1/2+y, 1/2-z), connected via hydrogen bonding and separated by 7.8 Å (see Figure S-8.1 in Supporting Information). The EPR line corresponds to a collective resonance when the exchange interaction (J) between copper ions in different lattice sites is larger than the difference between their Zeeman energies (0.3 $cm^{-1}$ at X-band). However, on the Q-band EPR spectrum an additional rhombic signal is observed, with $g'_1$ = 2.269, $g'_2$ = 2.070 and $g'_3$ = 2.048 ($g'_{iso}$= 2.128). Considering that these g-values are molecular (G = 4.7), while the average parameter is practically the same in both signals, it can be concluded that the Q-band spectrum shows the simultaneous presence of collapsed and independent resonances for Cu1 and Cu1e sites. This is a rather uncommon behavior and implies that the condition JCu1-Cu1e>|gCu1-gCu1e|μBH does not hold for any orientation of the magnetic field operating at Q-band.

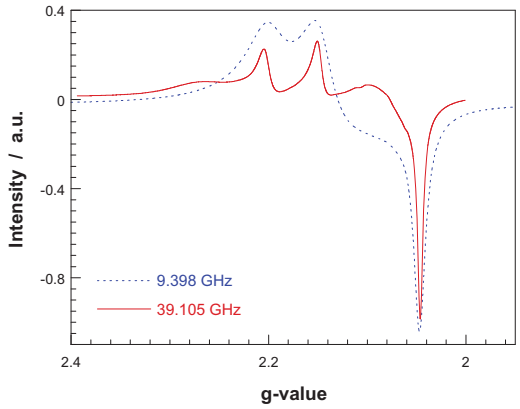


Figure 7. X and Q-band powder EPR spectra of compound 1 registered at r.t.

Only one quasi-isotropic line, with $g_{iso}$=2.13, is observed on the X and Q-band powder EPR spectra of compound **2** registered at room temperature (see

Figure S-8.2 in Supporting Information). The intensity of this signal increases with decreasing temperature, reaching a maximum about 14 K after which it rapidly decreases. Below 20 K, two new satellite bands are observed at about 270 and 375 mT. At the same time, the classical "half-field signal" (ΔMs=2) is also detected. These results indicates that at room temperature EPR spectra are dominated by the characteristics of an S=2 spin state, while a triplet state becomes more important below 20 K. Considering that the two satellite lines correspond to the perpendicular fine structure of the S=1 state, the splitting between them yields the zero-field splitting parameter |D|=52 mT. The g value associated with this doublet is g⊥=2.07. The zero-field interaction within the S=2 state is small and hidden within the experimental line width. It is noteworthy that the observation of a fine structure at low temperatures indicates the absence of appreciable magnetic exchange between tetrameric units.

The thermal variation of the inverse of the magnetic molar susceptibility ($\chi_m^{-1}$) and the $\chi_m$T product ($\mu eff^2 = 8\chi_m T$) for compound 1 is shown in Fig. 8. The effective magnetic moment exhibits a plateau from room temperature to 20 K having a value of 1.8 μB, decreasing to a value of 1.5 μB at 2 K. Above 10 K, the magnetic susceptibility follows a Curie–Weiss law with Cm=0.86 $cm^3Kmol^{-1}$ and θ = -0.7 K. Both, the negative temperature intercept and the decrease of the magnetic effective moment at low temperatures are in agreement with weak antiferromagnetic interactions in the compound. Taking into account the crystal structure the experimental data were fitted to the Bleaney-Bowers[34] expression [Equation 1] for an isotropically coupled pair of S=1/2 ions:

$$\chi m = \frac{Ng^2\beta^2}{kT(3+3\exp(-J/kT)} \qquad [1]$$

where the singlet-triplet energy gap (2J) is defined by the Hamiltonian H = −2J·S1·S2 (S1 = S2 = 1/2); g is the Lande's g factor; N, β and k are the Avogadro's number, the Bohr magneton, and Boltzmann's constant, respectively. The best-fit parameters obtained by minimizing the reliability factor $R = \Sigma[(\chi_m T)\exp - \chi_m T)\text{cal}]^2/\Sigma[(\chi_m T)\exp]^2$ are g = 2.13, J = -0.8 $cm^{-1}$ and R = 6.1x10-5. As shown in Figure 8, calculated curves reproduce satisfactorily the experimental data in the whole investigated temperature range. The low value of the calculated coupling parameter is in good agreement with the long exchange pathway via the H4app ligand.

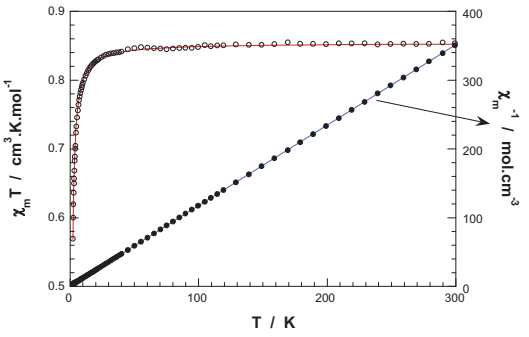


Figure 8. Thermal evolution of the reciprocal magnetic molar susceptibility $\chi_m^{-1}$ and the $\chi_m$T product for compound 1. The solid lines correspond to the best theoretical fits.

The thermal evolutions of both the magnetic molar susceptibility and $\chi_m$T values for compound **2** are shown in Fig. 9. At room temperature, $\chi_m$T is equal to 1.68 $cm^3mol^{-1}K$, a value that is only slightly lower than that expected for a set of four magnetically non-interacting copper(II) ions (ca. 1.70 $cm^3mol^{-1}K$ using the <g> = 2.13 value obtained from the EPR data). Upon cooling, $\chi_m$T continuously decreases, and it practically vanishes at very low temperatures. As the temperature is lowered the susceptibility increases until a maximum of 0.0535 $cm^3mol^{-1}$, which is reached at about 16 K, and then rapidly decreases (0.0035 $cm^3mol^{-1}$ at 3 K). The susceptibility increases below 3 K, probably due to the presence of a small paramagnetic impurity. At high temperature, T ≥ 100 K, the thermal evolution of $\chi_m$ follows the classical Curie−Weiss law, with Weiss temperature θ = −8.5 K and Curie constant Cm = 1.72 $cm^3mol^{-1}K$. These results confirm the prevalence of antiferromagnetic interactions in this compound.

To interpret quantitatively the magnetic data we had analyzed them in terms of the "dipolar coupling" approach for a Cu(II) tetrameric compound. With the numbering scheme used in Figure 2, the Heisenberg spin hamiltonian appropriate for the exchange interaction in this system can be written as:

$H=-2J_1(S1.S2+S3.S4)-2J_2(S2.S3)$

where $J_1$ describes the nearest neighbor interaction between the outer pairs of copper and $J_2$ the central exchange constant. Interactions between non-nearest neighbors or via hydrogen bonds have been neglected to avoid an excessive number of adjustable parameters. The eigenvalues derived from this Hamiltonian[35] were introduced in the van Vleck equation36 to obtain an analytical expression for the magnetic susceptibility. An additional term (ρ) which accounts for uncoupled Cu(II) ions following a simple Curie law, and having the same g factor has been also included [Equation 2]:

$$\chi_m = (1-\rho)\frac{Ng^2\beta^2}{3kT}\frac{\sum_i S_i(S_i+1)(2S_i+1)\exp\left(-\frac{E_i}{kT}\right)}{\sum_i (2S_i+1)\exp\left(-\frac{E_i}{kT}\right)} + 4\rho\frac{Ng^2\beta^2}{4kT} \qquad [2]$$

The best fit to the data where obtained with $J_1$ =-8.9 $cm^{-1}$, $J_2$ = -0.8 $cm^{-1}$, g = 2.14 and ρ=0.007 (R = $2.5x10^{-5}$). The calculated J values implies that the ground state of this cluster is S=0 but two S=1 triplet states are only a few Kelvin over the singlet, in good agreement with the spin triplet signals observed in the EPR spectra at low temperatures.

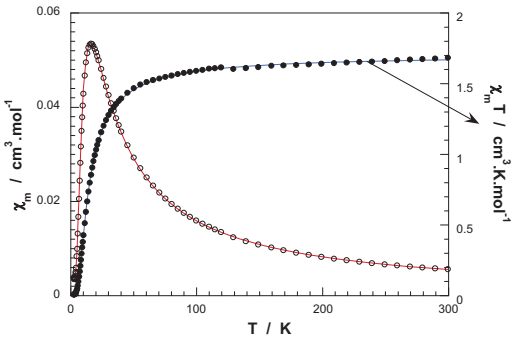


Figure 9. Plots of $\chi_m$ and $\chi_m$T for compound **2**. The solid lines correspond to the best fit to equation 2.

## CONCLUDING REMARKS

The crystallographic and DFT theoretical results presented herein are in good agreement and indicate that the N7/C8 translocation still allows a high versatility in the coordination abilities of H4app compared to adenine. In particular, H4app enables two bridging coordination modes, namely $\mu_2$-N1,N8 and $\mu_2$-N8,N9 for H(N9)4app and H(N1)4app, respectively. In contrast to the metal binding behavior of adenine, our findings suggest that the metal binding to the N1 donor in H4app is favored. In addition, the coordination ability of N8 in H4app should be also remarked. In conclusion, the study of the molecular recognition patterns of this kind of purine-like ligands can provide new insights into the metal binding behavior of larger oligonucleotides in biological systems and, in extend, help to rationalize the design of new promising drugs derived from pyrazolo[3,4-d]pyrimidines.

## ASSOCIATED CONTENT

Supporting Information Available: Additional structural information is provided in S1 to S3 (CCDC 881146 - 881147). Relevant spectral properties and thermal stability information as well as magnetic properties can be found in S4 and S5, respectively. This material is available free of charge via internet at http://pubs.acs.org.

## AUTHOR INFORMATION

### Corresponding Author

* Alicia Domínguez-Martín; e-mail: adominguez@ugr.es; telephone number: +34 958 24 38 53; fax: +34 958 24 62 19.

## ACKNOWLEDGMENT

Financial support from Research Group FQM-283 (Junta de Andalucía), MICINN-Spain (Project MAT2010-15594) and 'Factoría de Cristalización, CONSOLIDER INGENIO-2010' is acknowledged. ADM gratefully acknowledge ME-Spain for a FPU Ph.D contract.

## REFERENCES

(1) (a) Terrón, A.; Fiol, J. J.; García-Raso, A.; Barcelo-Oliver, M.; Moreno, V. *Coord. Chem. Rev.* **2007**, *251*, 1973. (b) Choquesillo-Lazarte, D.; Brandi-Blanco, M. P.; García-Santos, I.; González-Pérez, J. M.; Castiñeiras, A.; Niclós-Gutiérrez, J. *Coord. Chem. Rev.* **2008**, *252*, 1241. (c) Sanz Miguel, P. J.; Amo-Ochoa, P.; Castillo, O.; Houlton, A.; Zamora, F. Metal Complex - DNA interactions; Hadjiliadis, N., Sletten, E., Eds.; Wiley-Blackwell: Chichester, U.K., **2009**; Chapter 4. (d) Lippert, B. Nucleic Acid - Metal Ion Interactions; Hud, N. V., Ed.; RSC Publishing: London, **2009**; Chapter 2.

(2) Patel, D. K.; Domínguez-Martín, A.; Brandi-Blanco, M. P.; Choquesillo-Lazarte, D.; Nurchi, V. M.; Niclós-Gutiérrez, J. *Coord. Chem. Rev.* **2012**, *256*, 193.

(3) (a) Choquesillo-Lazarte, D.; Domínguez-Martín, A.; Matilla-Hernández, A.; Sánchez de Medina Revilla, C; González-Pérez, J. M.; Castiñeiras, A.; Niclós-Gutiérrez, J. *Polyhedron* **2010**, *29*, 170. (b) Patel, D. K.; Choquesillo-Lazarte, D.; Domínguez-Martín, A.; Brandi-Blanco, M.P.; González-Pérez, J. M.; Castiñeiras, A.; Niclós-Gutiérrez, J. *Inorg. Chem.* **2011**, *50*, 10549. (c) Domínguez-Martín, A.; Cho-quesillo-Lazarte, D.; González-Pérez, J. M.; Castiñeiras, A.; Niclós-Gutiérrez, J. *J. Inorg. Biochem.* **2011**, *105*, 1073.

(4) Holla, B. S.; Mahalinga, M.; Karthikeyan, M. S.; Akberali, P. M.; Shetty, N. S.
*Bioorg. Med. Chem.* **2006**, *14*, 2040.
(5) Hasan, A.; Satyanarayana, M.; Mishra, A.; Bhakuni, D. S.; Pratap, R.; Dube, A.; Guru, P. Y. *Nucleos Nucleot Nucleic Acids* **2006**, *25*, 55.
(6) (a) Carraro, F.; Naldini, A.; Pucci, A.; Locatelli, G. A.; Maga, G.; Schenone S.; Bruno, O.; Ranise, A.; Bondavalli, F.; Brullo, C.; Fossa, P.; Menozzi, G.; Mosti, L.; Modugno M.; Tintori, C.; Manetti, F.; Botta M. *J. Med. Chem.* **2006**, *49*, 1549-1561. (b) Franco, L.; Davide, D. F.; Stevens, M. R. PCT Int. Appl. WO2011014239 (A1) **2011**. (c) Indovina, P.; Giorgi, F.; Rizzo, V.; Khadang, B.; Schenone, S.; Di Marzo, D.; Forte, I.M.; Tomei, V.; Mattioli, E.; D'Urso, V.; Grilli, B.; Botta, M:; Giordano, A.; Pentimalli, F. *Oncogene* **2012**, *31*, 929.
(7) Davies, L. P.; Brown, D. J.; Chow, S. C.; Johnston, G. A. R. *Neurosci. Lett.*
**1983**, *41*, 189.
(8) (a) Da Settimo, F.; Primofiore, G.; La Motta, C.; Taliani, S.; Simorini, F.; Marini, A. M.; Mugnaini, L.; Lavecchia, A.; Novellino, E.; Tuscano, D.; Martini, C. *J. Med. Chem.* **2005**, *48*, 5162-5174. (b) Hsieh, J-F.; Wu, S.-H.; Yang, Y.-L.; Choong, K.-F.; Chen, S.-T. *Bioorg. Med. Chem.* **2007**, *15*, 3450-3456.
(9) Nakano, S.; Karimata, H.T.; Kitagawa, Y.; Sugimoto, N. *J. Am. Chem. Soc.* **2009**, *131*, 16881.
(10) (a) Sprang, S.; Scheller, R.; Rohrer, D.; Sundaralingam, M. *J. Am. Chem. Soc.* **1978**, *100*, 2867. (b) Seela, F.; Zulauf, M.; Reuter, H.; Kastner, G. *Acta Crystallogr.* **1999**, *C55*, 1947. (c) Zhang, X.; Budow, S.; Leonard, P.; Eickmeier, H.; Seela, F. *Acta Crystallogr.* **2006**, *C62*, o79. (d) Pasternak, A.; Kierzek, R.; Gdaniec, Z.; Gdaniec, M. *Acta Crystallogr.* **2008**, *C64*, o467.
(11) Dodin, G.; Dreyfus, M.; Bensaude, O.; Dubois J.-E. *J. Am. Chem. Soc.* **1977**, *99*, 7257.
(12) Sheldrick, W. S.; Bell, P.; Hausler, H.-J. *Inorg. Chim. Acta* **1989**, *163*, 181-192.
(13) Bugella-Altamirano, E.; Choquesillo-Lazarte, D.; González-Pérez, J.M.; Sánchez-Moreno, M. J.; Marín-Sánchez, R.; Martín-Ramos, J.D.; Covelo, B.; Carballo, R; . Castiñeiras A.; Niclós-Gutiérrez, J. *Inorg. Chim. Acta*, **2002**, *339*, 160.
(14) BRUKER, SMART and SAINT. Area Detector control and Integration Software, Bruker analytical X-ray instruments Inc., **1997**, Madison, Wisconsin, USA.
(15) BRUKER, APEX2 Software, Bruker AXS Inc., V.2010.11, Madison, Wisconsin, USA.
(16) G.M. Sheldrick, SADABS, Program for Empirical Absorption Correction of Area Detector Data, **2009**, University of Göttingen, Germany.
(17) G.M. Sheldrick, *Acta Crystallogr.*, **2008**, *A64*, 112.
(18) A.L. Spek, PLATON. A Multipurpose Crystallographic Tool, **2010**, Utrecht University, Utrecht, The Netherlands.
(19) C.F. Macrae, I.J. Bruno, J.A. Chisholm, P.R. Edgington, P. McCabe, E. Pidcock, L. Rodriguez-Monge, R. Taylor, J. van de Streek and P.A. Wood, *J. Appl. Cryst.*, **2008**, *41*, 466.
(20) Becke, A. D. *J. Chem. Phys.* **1993**, *98*, 5648.
(21) Gaussian 09, Revision B.01, M. J. Frisch, G. W. Trucks, H. B. Schlegel, G. E. Scuseria, M. A. Robb, J. R. Cheeseman, G. Scalmani, V. Barone, B. Mennucci, G. A. Petersson, H. Nakatsuji, M. Caricato, X. Li, H. P. Hratchian, A. F. Izmaylov, J. Bloino, G. Zheng, J. L. Sonnenberg, M. Hada, M. Ehara, K. Toyota, R. Fukuda, J. Hasegawa, M. Ishida, T. Nakajima, Y. Honda, O. Kitao, H. Nakai, T. Vreven, J. A. Montgomery, Jr., J. E. Peralta, F. Ogliaro, M. Bearpark, J. J. Heyd, E. Brothers, K. N. Kudin, V. N. Staroverov, T. Keith, R. Kobayashi, J. Normand, K. Raghavachari, A. Rendell, J. C. Burant, S. S. Iyengar, J. Tomasi, M. Cossi, N. Rega, J. M. Millam, M. Klene, J. E. Knox, J. B. Cross, V. Bakken, C. Adamo, J. Jaramillo, R. Gomperts, R. E. Stratmann, O. Yazyev, A. J. Austin, R. Cammi, C. Pomelli, J. W. Ochterski, R. L. Martin, K. Morokuma, V. G. Zakrzewski, G. A. Voth, P. Salvador, J. J. Dannenberg, S. Dapprich, A. D. Daniels, O. Farkas, J. B. Foresman, J. V. Ortiz, J. Cioslowski, and D. J. Fox, Gaussian, Inc., Wallingford CT, **2010**.
(22) Hehre, W.J.; Ditchfield R.; Pople, J.A. *J. Chem. Phys.* **1972**, *56*, 2257.
(23) Domínguez-Martín, A.; Choquesillo-Lazarte, D.; Dobado, J. A.; Vidal, I.; González-Pérez, J. M.; Castiñeiras A.; Niclós-Gutiérrez, J. *Dalton Trans.* **2012**, *submitted*.
(24) Miertuš, S.; Scrocco, E.; Tomasi, J.; *Chem. Phys.* **1981**, *55*, 117.
(25) Hänggi, G.; Schmalle, H.; Dubler, E. *J. Chem. Soc. Dalton Trans.* **1993**, 941.
(26) Das, S.; Madhavaiah, C.; Verma, S.; Bharadwaj, P. K. *Inorg. Chim. Acta* **2005**, *358*, 3236.
(27) Janiak, C. *J. Chem. Soc. Dalton Trans.*, **2000**, 3885.
(28) (a) Roitzsch, M.; Lippert, B. *Chem. Commun.* **2005**, 5991; (b) Roitzsch, M.; Lippert, B. *Inorg. Chem.* **2004**, *43*, 5483; (c) Purohit, C.S.; Verma, S. *J. Am. Chem. Soc.* **2007**, *129*, 3488.
(29) Yang, E.-C.; Zhao, H.-K.; Feng, Y.; Zhao, X.-J. *Inorg.Chem.* **2009**, *48*, 3511.
(30) (a) Srivatsan, S. G.; Parvez, M.; Verma, S. *Chem. Eur. J.* **2002**, *8*, 5184; (b) Prajapati, R. K.; Verma, S. *Inorg. Chem.* **2011**, *50*, 3180.
(31) Knobloch, B.; Sigel, R.K.O; Lippert, B.; Sigel, H. *Angew. Chem. Int. Ed.* **2004**, *43*, 3793.
(32) Abdelhamid, R. F.; Obara, Y.; Uchida, Y.; Kohzuma, T.; Dooley, D. M.; Brown, D. E.; Hori H. *J. Biol. Inorg.Chem.* **2007**, *12*, 165.
(33) Hathaway, B.J.; Billing, D. *Coord. Chem. Rev.* **1970**, *5*, 143
(34) Bleaney, B.; Bowers, K.D. *Proc. R. Soc. London, Ser. A*, **1952**, *214*, 451.
(35) Papadopoulos, A.N.; Tangoulis, V.; Raptopoulou, C.P.; Terzis, A.; Kessissoglou, D.P. *Inorg. Chem.* **1996**, *35*, 559.
(36) Van Vleck, J.H. *Theory of Electric and Magnetic Susceptibilities;* Oxford University Press, **19.**

# CHAPTER 3:

Copper(II) complexes with N-substituted adenines

## 3.1. Structural insights on the molecular recognition patterns between N6-substituted adenines and N-(aryl-methyl)iminodiacetate copper(II) chelates.

Article submitted to *J. Inorg.Biochem.*

SYNOPSIS

$N^6$-R-adenines recognize $Cu^{II}$-IDAs chelates by cooperation of the Cu-N3(purine) bond and one intra-molecular interligand N9-H···O(carboxy) interaction. In contrast, $N^6$,$N^6$-dimethyl-aminopurine shows the unprecedented rare tautomer H(N3)dimAP in the cooperation of the Cu-N9 bond with the N3-H···O(carboxy) interaction.

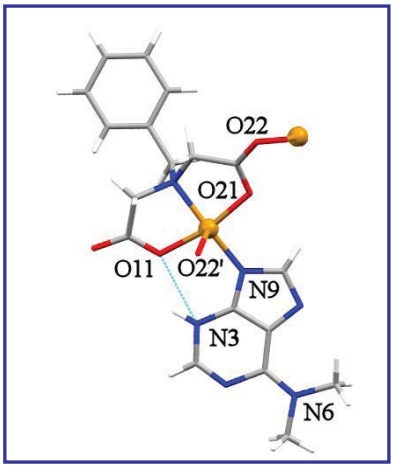


RESUMEN

Con el objetivo de estudiar en mayor profundidad los modos de reconocimiento molecular de adeninas $N^6$-sustituidas, se han sintetizado y caracterizado estructuralmente seis nuevos complejos ternarios de cobre(II): [Cu(NBzIDA)(HCy5ade) ($H_2O$)]·$H_2O$ (**1**), [Cu(NBzIDA)(HCy6ade)($H_2O$)]·$H_2O$ (**2**), [Cu(FurIDA)(HCy6ade)($H_2O$)] ·$H_2O$ (**3**), [Cu(MEBIDA)(HBAP)($H_2O$)]·$H_2O$ (**4**), $[Cu(FurIDA)(HBAP)]_n$ (**5**) y $\{[Cu(NBzIDA)(HdimAP)]\cdot H_2O\}_n$ (**6**). En estos compuestos: (i) los quelantes tipo IDA son iminodiacetatos N-sustituidos con un brazo aril-metil no coordinante (bencil en NBzIDA, p-tolil en MEBIDA y furfuril en FurIDA); (ii) los derivados de citoquininas tienen como sustituyentes un grupo bencilo (HBAP, es una citoquinina natural), cicloalquilo (HCy5ade o HCy6ade) o dos grupos metilos (HdimAP) en posición N6 de adenina. Con independencia de la naturaleza molecular (**1**-**4**) o polimérica (**5**-**6**) de los compuestos ternarios estudiados, el centro de cobre(II) exhibe un entorno tipo 4+1 donde la agrupación quelante tipo IDA adopta una conformación *mer*. En **1**-**5**, las $N^6$-R-adeninas usan su tautómero más estable H(N9) y el reconocimiento molecular consiste en la cooperación de

un enlace de coordinación Cu-N3(tipo purina) y un enlace de hidrógeno intra-molecular interligandos N9-H···O(carboxilato coordinado). Por el contrario, en el compuesto **6**, $N^6$,$N^6$-dimetil-adenina revela el raro tautómero H(N3)dimAP, de forma que el reconocimiento molecular con el quelato Cu(NBzIDA) consiste en el enlace Cu-N9 y una interacción intra-molecular interligandos N3-H···O(carboxilato coordinado). Por otra parte, en contra de la actividad citoquinina mostrada por los ligandos libres HBAP, HCy5ade y HCy6ade, los correspondientes compuestos ternarios investigados no presentan actividad citoquinina en el rango de concentraciones estudiadas.

**Structural consequences of the N7 and C8 translocation on the metal binding behavior of adenine**

| | |
|---|---|
| Journal: | *Inorganic Chemistry* |
| Manuscript ID: | Draft – Accepted with minor revisions |
| Manuscript Type: | Article |
| Date Submitted by the Author: | 02/10/2012 |
| Complete List of Authors: | Dominguez-Martin, Alicia;<br>University of Granada, Department of Inorganic Chemistry, Faculty of Pharmacy.<br>Choquesillo-Lazarte, Duane; CSIC, LEC.<br>Dobado, Jose; Universidad de Granada, Química Orgánica.<br>Martínez-García, Henar; Universidad de Valladolid, Departamento de Química Orgánica.<br>Lezama, Luis; University of Basque Country, Faculty of Science and Technology.<br>González-Pérez, Josefa; Universidad de Granada, Química Inorgánica.<br>Castiñeiras, Alfonso; University of Santiago de Compostela, Department of Inorganic Chemistry.<br>Niclós-Gutiérrez, Juan; University of Granada, Department of Inorganic Chemistry, Faculty of Pharmacy. |
| | |

# Structural consequences of the N7 and C8 translocation on the metal binding behavior of adenine

Alicia Domínguez-Martín,[*†] Duane Choquesillo-Lazarte,[‡] Jose A. Dobado,[¤] Henar Martínez-García,[¶] Luis Lezama,[§] Josefa M. González-Pérez,[†] Alfonso Castiñeiras,[¥] Juan Niclós-Gutiérrez[†]

[†] Department of Inorganic Chemistry, Faculty of Pharmacy, University of Granada, E-18071 Granada, Spain.

‡ Laboratorio de Estudios Cristalográficos, IACT, CSIC-Universidad de Granada, Av. de las Palmeras 4, E-18100 Armilla, Granada, Spain.

[¤] Grupo de Modelización y Diseño Molecular, Departamento de Química Orgánica, Facultad de Ciencias, Universidad de Granada, E-18071 Granada, Spain.

[¶] Departamento de Química Orgánica, Escuela de Ingenierías Industriales, Universidad de Valladolid, E-47071 Valladolid, Spain.

[§] Department of Inorganic Chemistry, Faculty of Science and Technology, University of Basque Country, E-48080 Bilbao, Spain.

[¥] Department of Inorganic Chemistry, Faculty of Pharmacy, University of Santiago de Compostela, E-15782 Santiago de Compostela, Spain.

Supporting Information

**ABSTRACT:** 7-Deaza-8-aza-adenine, namely 4-aminopyrazolo[3,4-d]pyrimidine (H4app), is a bioisoster of adenine (Hade) resulting from the translocation of N7 and C8 atoms on the purine moiety. With the aim of studying the influence of this translocation on the metal binding abilities of H4app, we have prepared and structurally characterized two ternary copper(II) complexes having H4app and one N-benzyl-iminodiacetate chelator (MEBIDA or FBIDA, with a methyl or fluoro group in para- of the benzyl aromatic ring): $[Cu_2(MEBIDA)_2(\mu_2\text{-}N1,N8\text{-}H4app)(H_2O)_2]\cdot 4H_2O$ (**1**) and $[Cu_4(FBIDA)_4(\mu_2\text{-}N8,N9\text{-}H4app)_2(H_2O)]\cdot 3.5H_2O$ (**2**). Furthermore, thermal, spectral and magnetic properties have been also investigated. In **1**, H(N9)4app is disordered over two equally pondered positions and the $\mu_2$-N1,N8 coordination mode is weakly assisted by N6-H···O and N9-H···O intra-molecular interactions, respectively. The acyclic non-linear molecular topology of **2** is strongly influenced by two intra-molecular H-bonding interactions (O-H···O-carboxylate) involving the apical aqua ligand of a terminal Cu(II) atom. Thus, both compounds have in common the Cu-N8 bond. In order to better understand our limited structural information, DFT calculations for the individual tautomers of H4app as well as mononuclear Cu(II) model systems have been carried out. According to previous results, we conclude that H(N9)4app is the most stable tautomer followed by H(N8)4app. When N9 and N8 are metallated, then the tautomer H(N1)4app can come into play as observed in compound **2**. Likewise, the findings concerning compound 1 suggest that the formation of a Cu-N1 bond in H4app results favored compared to neutral adenine, for which only one case has been reported with such coordination despite the large variety of related Cu(II)-Hade described in literature.

## INTRODUCTION

In the last decades, a large number of papers has addressed the metal binding patterns of natural nucleobases as well as closely related ligands.[1] In this sense, our research group has been devoted to the study of adenine, which has proved to be a fairly rich versatile ligand.[2] Moreover, in order to extend the reach of our results, we have also studied several oxo-, amino-, aza- and/or deaza-purine derivatives.[3] The better understanding of the metal binding patterns of these purine analogues is challenging because it could reveal new insights into the behavior of nucleic acids in living beings. 7-Deaza-8-aza-adenine (4-aminopyrazolo[3,4-

d]pyrimidine, H4app) is an structural analogue of adenine (Hade) that has a fused pyrazole ring instead of an imidazole ring. Thus, it represents the translocation of the N7 and C8 atoms in Hade, according to purine conventional notation (see scheme 1). This fact should perturb the proton tautomerism and the metal binding abilities of this former nucleobase. Indeed, the absence of the N7 residue in H4app, which is believed to be the most relevant metal binding site in natural purines (exposed at the major groove of DNA), has raised high and broad interest regarding its potential applications. In this context, several pharmacological properties have been already described for pyrazolo[3,4-d]pyrimidine ligands such as antibacterial and antifungal,[4] antiparasite,[5] or antiproliferative agents.[6] Likewise, they have been reported as adenosine antagonists[7] and inhibitors some enzymes.[8] However, further than these applications, the rationalization of the metal binding patterns in this kind of ligands is still necessary to better understand more complex processes concerning nucleic acids such as the role of metal ions in the molecular crowding and their structural, functional and stability consequences within biomolecules, for example concerning ribozymes.[9]

Under the structural point of view, the roles of H4app as ligand are rather unexplored. Some synthetic nucleosides derived from H4app have been isolated and characterized crystallographically.[10] Nevertheless, the existing data about H4app is mainly focused on two papers. According to data from solution studies, Dubois et al.[11] proposed the basicity order N9≥N8>N1>N3>>N6 for the N-donors of H4app (see scheme 1). Alternatively, by increasing metallation with $CH_3Hg(I)$, Sheldrick et al.[12] reported structural support about four metal binding patterns of H4app or its 4app- and 4app-H2- anionic forms, in good agreement to the N-basicity order of this ligand. Therefore, in order to deepen our knowledge on the molecular recognition patterns of the nucleobase H4app, we have synthesized and characterized two novel mixed-ligand ternary copper(II) complexes with iminodiacetate-like chelators and H4app.

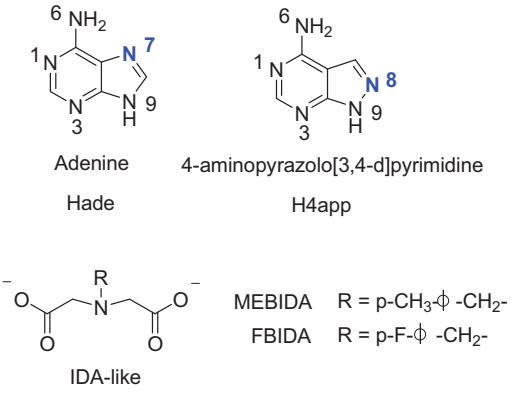


Scheme 1. Top: Adenine and 4-aminopyrazolo[3,4-d]pyrimidine with the conventional notation of purines. Bottom: Formulas of the chelating ligands used in this work: N-(p-methylbenzyl)-iminodiacetate(2-) and N-(p-fluorobenzyl)-iminodiacetate(2-) anions (MEBIDA and FBIDA, respectively).

## EXPERIMENTAL SECTION

Materials. Bluish $Cu_2CO_3(OH)_2$ was purchased from Probus. 4-Aminopyrazolo[3,4-d]pyrimidine (H4app) was purchased from Sigma-Aldrich. All the former reagents were used without further purification. N-(p-methylbenzyl)- and N-(p-fluorobenzyl)-iminodiacetic acids ($H_2$MEBIDA and $H_2$FBIDA, respectively) were synthesized in their acid form as previously reported for N-benzyl-iminodiacetic acid[13] using 4-methyl-benzylamine (p-xylylamine) or 4-fluorobenzylamine instead of benzylamine, respectively.

Syntheses of the complexes.

$[Cu_2(MEBIDA)_2(\mu_2\text{-}N1,N8\text{-}H4app)(H_2O)_2]\cdot 4H_2O$ (**1**): $Cu_2CO_3(OH)_2$ (0.25 mmol, 0.055 g) was reacted in 50 mL of distilled water with $H_2$MEBIDA acid (0.5 mmol, 0.119 g) in a Kitasato flask, heating (50 °C) and stirring under moderate vacuum until a clear blue solution of the binary chelate is obtained. Alternatively, a suspension of H4app (0.5 mmol, 0.068 g) in 40 mL of isopropanol was prepared at r.t. Afterwards, the suspension of H4app was added to the binary chelate solution and the reacting mixture was stirred for 1 hour until the reactants were completely dissolved. The resulting blue solution was filtered, without vacuum, on a crystallyzation device and allowed to stand at room temperature, covered with a plastic film to control the

evaporation. After six weeks, needle-like crystals suitable for XRD purposes were collected. Yield is ca. 70-75%. Elemental analysis (%): Calc. for $C_{29}H_{43}Cu_2N_7O_{14}$: C 41.43, H 5.15, N 11.66; Found: C 41.83, H 4.24, N 11.77. FT-IR (KBr, $cm^{-1}$) $\nu_{as}(H_2O)$ 3398, $\nu_{as}(NH_2)$ overshadowed, $\nu_s(NH_2)$ overlapped with $\nu_s(H_2O)$ 3247, $\nu$(N-H) 3184, $\nu_{as}(CH_2)$ 2924, $\nu_s(CH_2)$ 2852, $\delta(H_2O)$ and $\delta(NH_2)$ overlapped with $\nu_{as}$(COO) 1611, $\delta$(N-H) 1517, $\nu_s$(COO) 1384, $\pi(C\text{-}H)_{ar}$ 809 (MEBIDA), $\pi(C\text{-}H)_{ar}$ 788 (H4app). Under air-dry flow, the sample loses only 0.5 non-coordinated water molecule, thus the TG experiment starts with an average formula $[Cu_2(MEBIDA)_2(\mu_2\text{-}N1,N8\text{-}H4app)(H_2O)_2]\cdot 3.5H_2O$ The thermogravimetric curve shows five steps. The first step corresponds to the loss weight of the rest of water content (n = 5.5 $H_2O$; Calc. 12.03%; Found 12.07%). Indeed only $H_2O$ and trace amounts of $CO_2$ are identified as evolved gasses during this first step. The following pyrolitic steps yield a final residue of 2 CuO (470 °C, Calc. 19.31%; Found 20.77%). The evolved gasses during the pyrolysis involve $H_2O$, $CO_2$, CO and three N-oxide gasses ($N_2O$, $NO_2$ and NO). See S-6 in Supporting Information.

$[Cu_4(FBIDA)_4(\mu_2\text{-}N8,N9\text{-}H4app)_2(H_2O)]\cdot 3.5H_2O$ (**2**): A synthetic procedure similar to that of compound 1 was followed, using $H_2$FBIDA acid (0.5 mmol, 0.120 g) instead of $H_2$MEBIDA acid. The addition of isopropanol to the mother liquors is again needed to reach the complete solution of the ternary system. In two months, needle-like crystals were obtained. The reaction yielded 65%. Elemental analysis (%): Calc. for $C_{54}H_{59}Cu_4F_4N_{14}O_{20.5}$: C 41.51, H 3.81, N 12.55; Found: C 41.08, H 3.90, N 12.65. FT-IR (KBr, $cm^{-1}$) $\nu_{as}(H_2O)$ 3433, $\nu_{as}(NH_2)$ overshadowed, $\nu_s(NH_2)$ overlapped with $\nu_s(H_2O)$ 3232 $\nu$(N-H) 3131 (sh), $\nu_{as}(CH_2)$ 2930, $\nu_s(CH_2)$ 2860, $\delta(H_2O)$ 1629, $\delta(NH_2)$ overlapped with $\nu_{as}$(COO) 1606, $\delta$(N-H) 1512, $\nu_s$(COO) 1384, $\nu$(C-F) 1005, $\pi(C\text{-}H)_{ar}$ 736 (FBIDA), $\pi(C\text{-}H)_{ar}$ 782 (H4app). The UV/Vis spectrum shows an asymmetric d-d band with $\lambda_{max}$ at 670 nm ($\nu_{max}$ 15000 cm-1). Under air-dry flow, the sample loses part of the non-coordinated water molecule. Hence, the sample starts the TG experiment with formula $[Cu_4(FBIDA)_4(\mu_2\text{-}N8,N9\text{-}H4app)_2(H_2O)]\cdot 2.6H_2O$. The thermal behavior is divided in six steps. The sample loses all the water content during the first step (n = 3.60 $H_2O$; Calc. 4.21%; Found 4.20%), according to the evolved gasses. Five additional pyrolitic steps produce $H_2O$, $CO_2$, CO and N-oxide gasses ($N_2O$, NO, $NO_2$) to finally reach an impure CuO residue (480 °C, Calc. 20.58%; Found 20.80%). See S-7 in Supporting Information.

X-Ray Structure Determinations. Measured crystals were prepared under inert conditions immersed in perfluoropolyether as protecting oil for manipulation. Suitable crystals were mounted on MiTeGen MicromountsTM and these samples were used for data collection. Data were collected with Bruker X8 Proteum (compound 1, 293 K) or Bruker SMART CCD 1000 (compound 2, 110 K) diffractometers. The data were processed with SAINT[14] (**1**) or APEX2[15] (**2**) programs and corrected for absorption using SADABS.[16] The structures were solved by direct methods,[17] which revealed the position of all non-hydrogen atoms. These atoms were refined on F2 by a full-matrix least-squares procedure using anisotropic displacement parameters.[17] All hydrogen atoms were located in difference Fourier maps and included as fixed contributions riding on attached atoms with isotropic thermal displacement parameters 1.2 times those of the respective atom. Geometric calculations were carried out with PLATON[18] and drawings were produced with PLATON[18] and MERCURY.[19] Additional crystal data and more information about the X-ray structural analyses are shown in Supporting Information S3 to S5. Crystallographic data for the structural analysis have been deposited with the Cambridge Crystallographic Data Centre, CCDC No. 881146 – 881147 for 1 and 2 respectively. Copies of this information may be obtained free of charge on application to CCDC, 12 Union Road, Cambridge CB2 1EZ, UK (fax: 44 1223 336 033; e-mail: deposit@ccdc.cam.ac.uk or http://www.ccdc.cam.ac.uk).

Computational methods. DFT calculations, at the B3LYP[20] and unrestricted M06-L/6-31G* theoretical levels for the isolated H4app ligand and mononuclear copper complexes, respectively, have been performed with the Gaussian09 program,[21] using the 6-31+G** basis set, for the isolated ligands and the 6-31G* one for the copper complexes.[22] These methods have proven to be a reliable theoretical levels for the study of similar compound.[23] All structures were fully optimized at the following theoretical levels: B3LYP/6-31+G**//B3LYP/6-31+G** for the isolated ligands, and M06-L/6-31G*//M06-L/6-31G* for the

copper(II) complexes. The most stable spin multiplicities for the mononuclear copper complexes studied were doublet. The local stability of all structures was checked through the eigenvalues of the matrix of second derivatives (Hessian); all energetic minima presented no imaginary frequencies. Solvent effect was taken into account by means of the self consistent reaction field (SCRF) method, selecting PCM algorithm with water as solvent.[24] Additional information about DFT calculations is provided in Supporting Information S1 to S2.

Other Physical methods. Analytical data were obtained in a Thermo-Scientific (Flash 2000) elemental micro-analyzer. Infrared spectra were recorded by using KBr pellets on a Jasco FT-IR 6300 spectrometer. TG analyses were carried out in air-dry flow (100 mL/min) with a Shimadzu thermobalance TGA-DTG-50H instrument, coupled with a FT-IR Nicolet Magma 550 spectrometer. A series of FT-IR spectra (20-30 per sample) of the evolved gasses were time-spaced recorded during the TG experiment. Diffuse reflectance (electronic) spectra were recorded in a Varian Cary-5E spectrophotometer. Variable temperature (2-300 K) magnetic susceptibility measurements on polycrystalline samples were carried out with a Quantum Design MPMS-7 SQUID magnetometer under a magnetic field of 0.1T. The experimental susceptibilities were corrected for the diamagnetism of the constituent atoms by using Pascal's tables. X-band EPR measurements were carried out on a Bruker ELEXSYS 500 spectrometer with a maximum available microwave power of 200 mW and equipped with a super-high-Q resonator ER-4123-SHQ. For Q-band studies, EPR spectra were recorded on a Bruker EMX system equipped with an ER-510-QT resonator and an ER-4112-HV liquid helium cryostat. The magnetic field was calibrated by a NMR probe and the frequency inside the cavity was determined with a Hewlett-Packard 5352B microwave frequency counter. Computer simulation: WINEPR-Simfonia, version 1.5, Bruker Analytische Messtechnik GmbH).

## RESULTS AND DISCUSSIONS

### DFT CALCULATIONS

Tautomers for 4-aminopyrazolo[3,4-d]pyrimidine. In order to explore the relative stability of the corresponding hydrogen tautomers of H4app, gas phase and solvent effect Gibbs energies have been calculated and summarized in Table 1. As should be expected, H(N9)4app is the most stable tautomer in gas phase and also when solvent effect is included. Moreover, according to previous solution studies,[11] H(N8)4app is the next stable tautomer, showing our calculations a difference of 3.26 kcal·mol$^{-1}$ in water compared to H(N9)4app. The H(N3)4app and H(N1)4app tautomers are higher in terms of $\Delta$Gr (9.59 and 11.99 kcal·mol$^{-1}$, respectively), although they are rather close to each other. Moreover, it is noteworthy that when solvent effect is taken into account in the calculations, all free Gibbs energy values are reduced significantly; i.e. the difference between the tautomer H(N1)4app in gas phase and H(N1)4app considering the solvent effect is 16.18 kcal·mol$^{-1}$.

Models for mononuclear copper(II) complexes. With the aim of estimating the coordination abilities of H4app, DFT calculations have been carried out for ternary copper(II) model systems having the chelating ligand N-methyl-iminodiacetate(2-) anion (MIDA) and H4app. For all the calculations, a mer-$NO_2$ conformation was chosen for the iminodiacetate moiety and the binary chelate and the H4app ligand were induced to be coplanar, according to related structural results.[13,23] Moreover, the Cu(II)/MIDA chelate was tested for all the possible tautomers of H4app (see Table S-1. and S-2. in Supporting Information) since the presence of copper could alter the tautomeric preferences shown in Table 1 (vide supra). The most stable structure for the discrete system CuII/MIDA/H4app is the one having the most stable tautomer H(N9)4app.

In this latter case, the Cu(II) atom is coordinated by N3(H4app) and assisted by an intra-molecular H-bond via N9 [3p9; N9-H···O(non-coord. carboxylate)]. Herein, the H4app and the MIDA chelating ligand remain coplanar, being the referred intra-molecular interligand H-bond of maximum strength. However, for the same tautomer H(N9)4app and speaking in terms of solvent effect, two other possibilities, 1p9 and 8p9, are rather close to the 3p9 form in terms of free Gibbs energy (Fig. 1).

Table 1. DFT Gas phase and solvent (water) relative free Gibbs energies (ΔGr) for 4-aminopyrazolo[3,4-d]pyrimidine, calculated at the B3LYP/6-31+G**//B3LYP/6-31+G** and PCM-B3LYP/6-31+G**//PCM-B3LYP/6-31+G** theoretical levels, respectively.

| Compound | Tautomer-H9 ΔGr (Kcal/mol) | Tautomer-H8 ΔGr (Kcal/mol) | Tautomer-H6 ΔGr (Kcal/mol) | Tautomer-H3 ΔGr (Kcal/mol) | Tautomer-H1 ΔGr (Kcal/mol) |
|---|---|---|---|---|---|
| Gas Phase (II-p9 / II-p8 / II-p6/ II-p3 / II-p1)a | 0.0 | 8.37 | 57.59 | 16.39 | 28.17 |
| Solvent(water) (IIs-p9 / IIs-p8 / IIs-p6 / IIs-p3 / IIs-p1) | 0.0 | 3.26 | 33.0 | 9.59 | 11.99 |

[a] The latin number 'II' refers to H4app ligand and the number after the 'p' to the position where the tautomerizable proton is located. The letter 's' indicates when solvent effect is included in calculations.

This fact points out the possibility of two additional molecular recognition patterns for H(N9)4app (ΔGr = 2.18 and 2.86 kcal·mol-1 for the 1p9 and 8p9 forms, respectively- see Table S-1. in Supporting Information) Furthermore, the small difference between the two latter aforementioned patterns (0.68 kcal·mol$^{-1}$) suggests the possibility of the bidentate role $\mu_2$-N1,N8 for H(N9)4app, as is indeed observed in compound 1 (see Results and discussion).

If we extend the analysis of the CuII/MIDA/H4app model system to other H4app tautomers, different from H(N9)4app, then the lowest energetic value is 4 kcal·mol$^{-1}$. In particular, when we focus on the H(N1)4app tautomer, the three possible coordination modes are 3p1, 8p1 and 9p1. Among them, only the 8p1 and 9p1 forms are likely to occur (see Table S-1 in Supporting Information). Note that, although they show quite high ΔGr values (11.28 and 10.08 kcal·mol$^{-1}$, respectively), the difference between these two values is rather small what could be indicative of a bidentate role for H(N1)4app tautomer, provided it is favored in more complex systems. In fact, the bidentate $\mu_2$-N8,N9-H(N1)4app molecular recognition pattern has been proved by X-Ray crystallography, not only in compound **2** but also in a pyrazolo[3,4-d]pyrimidin-4-one complex.[25]

**MOLECULAR AND CRYSTAL STRUCTURES**

Compound **1**, with formula $[Cu_2(MEBIDA)_2(\mu_2\text{-}N1,N8\text{-}H4app)(H_2O)_2]\cdot 4H_2O$, consists of a centro-symmetric dinuclear complex molecule (Fig. 2) and solvent water. In the complex, the copper(II) atoms exhibit a 4+1 coordination polyhedron where the four closest donor atoms correspond to the tridentate IDA-like chelating ligand MEBIDA (N10, O11, O21) and one N-donor (N1 or N8) from H4app (see Table S-3.2 in Supporting Information). Thus, MEBIDA ligand adopts a mer-$NO_2$ conformation. The apical/distal coordination sites are occupied by aqua ligands which show rather short bond lengths [Cu1-O1 2.220(2) Å] in contrast to related apical distances which usually fall in the range of 2.3-2.6 Å.

According to previous results, H4app shows its most stable tautomer H(N9)4app. Moreover, it acts as a bridging ligand displaying the unprecedented $\mu_2$-N1,N8 mode. It is also remarkable that the coordination bond Cu-N1 is a bit longer than expected if we compare the present distance [Cu1-N1 2.109(2) Å] to those of Cu-N1(neutral purine) bonds available in literature [i.e. 1.993(4) Å in $\mu_2$-N1,N8-H7deaza-adenine in ref. 23 or 2.020(2) Å in $\mu_2$-N1,N9-Hade in ref. 26].

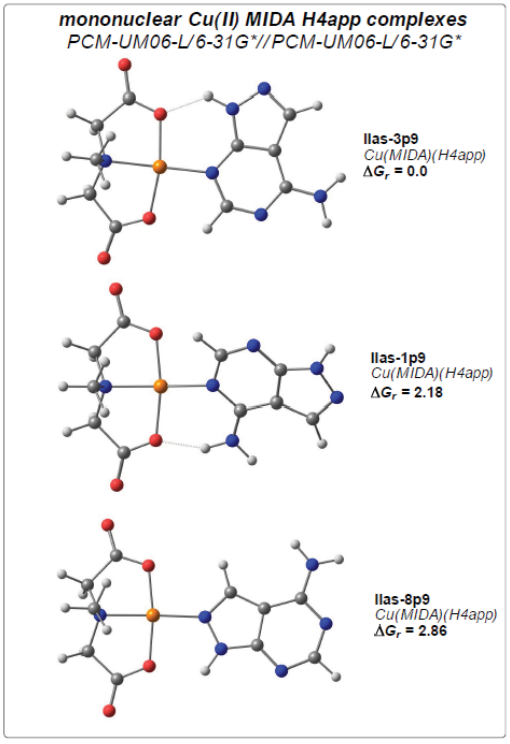


Figure 1. DFT (PCM-B3LYP/6-31G*//PCM-B3LYP/6-31G*) three most stable coordination modes for the mononuclear copper(II) complexes with the H(N9)4app tautomer and the chelating ligand MIDA. ΔGr values in kcal·mol$^{-1}$.

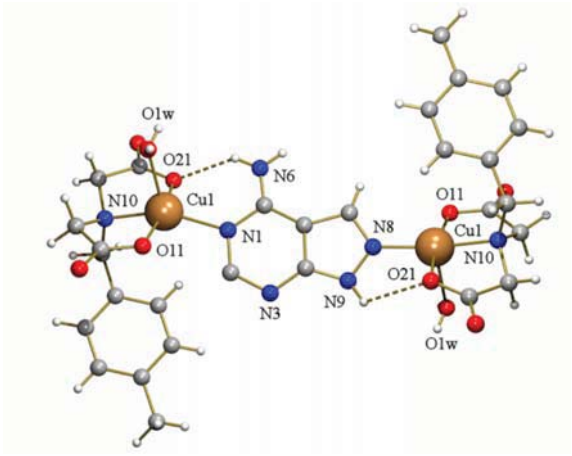


Figure 2. Complex molecule of $[Cu_2(MEBIDA)_2(\mu_2\text{-}N1,N8\text{-}H4app)(H_2O)_2]\cdot 4H_2O$ (**1**) with the numbering of the coordination environment. Only one of the two disordered positions is plotted for H4app. Solvent molecules omitted for clarity.

Furthermore, both Cu-N1 and Cu-N8 bonds are assisted by very weak intra-molecular interligand H-bonding interactions [N6-H6A···O21(carboxy coord., 3.091(7) Å, 136°) and N9-H···O21(carboxy coord., 2.975(3) Å, 119°)], respectively (see Fig. 2). The weakness of these H-bonding interactions seems to be related to the implication of N6-H and N9-H groups in bifurcated intermolecular H-bonds. This fact may also contribute to the loss of planarity between the H4app ligand and the mean basal CuII coordination planes, displaying an open dihedral angle close to 40°.Furthermore, it should be noticed that, in the crystal, the ligand H4app is disordered over two positions, related to each other by an inversion centre. This means that the H4app ligand is found in a special crystallographic position and therefore each CuII centre is 50 % bonded to N1 or N8 (see Fig. 3).

In the crystal of 1, inter-molecular pi,pi-stacking interactions between the aromatic ring of MEBIDA and the 5- and 6-membered rings of H4app build multi-stacked chains that extend along the b axis (Fig. 3, left) [Geometrical stacking parameters: (i) Cg···Cg 3.628(3) Å, α = 3.2(3)°, β = 18.57°, γ = 21.38° and (ii) Cg···Cg 3.564(3) Å, α = 2.3(2)°, β = 13.11°, γ = 15.41°, respectively – see S-5.1 in Supporting Information]. Adjacent chains connect to each other by inter-molecular H-bonds that involve the apical aqua ligands and non-coordinated carboxylate O-atoms leading to a 3D honeycomb-like network (Fig. 4, right - see also Table S-3.3 in Supporting Information).

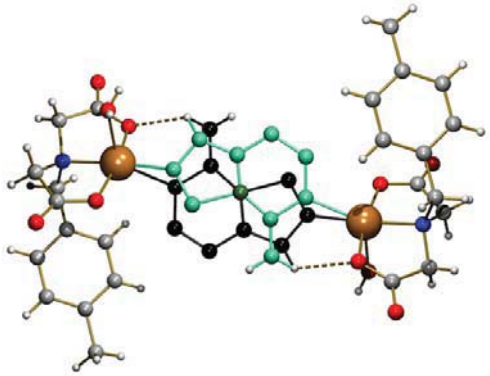

Figure 3. Complex molecule of $[Cu_2(MEBIDA)_2(\mu_2\text{-}N1,N8\text{-}H4app)(H_2O)_2]\cdot 4H_2O$ (**1**). The two disordered positions of H4app ligand are plotted in black and turquoise, respectively. The carbon atom shared by the two disordered position is depicted in dark green. Solvent molecules omitted for clarity.

Compound **2** consists of an asymmetric tetranuclear complex molecule (Fig. 5) and non-coordinated water molecules. The four copper(II) centers show a square-based pyramidal coordination, type 4+1. Cu1 and Cu3 metal surroundings are of the same type. The donor atoms of the basal plane are supplied by a tridentate FBIDA chelator and the N9 atom of an H4app whereas the apical sites are occupied by an O-monoatomic $\mu_2$-carboxylate atom. The Cu2 coordination is quite similar to those of Cu1 or Cu3, except for the apical O-atom that belongs to a syn,anti $\mu_2$-bridging carboxylate group. In contrast, the apical Cu4 site is remarkably occupied by one aqua ligand [Cu4-O(aqua) 2.463(3) Å]. Other selected bond lengths, interatomic distances and angles are provided in Table S-4.2 in Supporting Information. It should be noted that the FBIDA ligands play three different roles: (i) only as a tridentate chelator for Cu1; (ii) as tridentate chelator plus O-monoatomic $\mu_2$-carboxylate ligand for Cu4 and (iii) as tridentate chelator and as a syn,anti $\mu_2$-O-O'-carboxylate ligand for Cu2 and Cu3. Herein, both H4app show a $\mu_2$-N8,N9 bidentate role, using the H(N1)4app tautomer due to the transfer of the H(N9) atom to the N1 acceptor (the most basic N-donor atom available in the $\mu_2$-N8,N9 coordination mode). Note that using this tautomer, the Cu-N(heterocyclic) bonds can not cooperate with appropriate intra-molecular interligand H-bonding interactions. This bridging $\mu_2$-N8,N9 role was previously reported for methyl-Hg(II) derivatives of H4app, with formula $[(CH_3Hg)_2(\mu_2\text{-N8,N9-H(N1)4app})](NO_3)_2{\cdot}H_2O$.[12] Moreover, the H(N1) tautomer together with the $\mu_2$-N8,N9 coordination role has been also described for one zinc(2+) complex of allopurinol (pyrazolo[3,4-d]pyrimidin-4-one).[25] Interestingly, the complex molecule of **2** exhibits an unusual acyclic, non-linear asymmetric topology, in which the apical aqua ligand of Cu4 plays two relevant roles. First, it restricts the nuclearity of the complex to four (instead of yielding, for example, a 1D polymer). Second, it determines the non-linearity of the tetramer conformation by means of two intra-molecular interligand H-bonds (Fig. 5). In such interactions, the O(carboxylate) acceptors appertain to the FBIDA chelators of Cu1 [O4-H4A···O21(coord. carboxy), 2.905(4) Å, 140.5º] and Cu3 [O4-H4B···O16(non coord. carboxy), 2.757(4) Å, 165.1º]. This topology is in clear contrast to that of the cyclic-tetranuclear complex molecule found in $[Cu_4(pheida)_2(\mu_2\text{-O,O'-pheida})_2(\mu_2\text{-N3,N7-H(N9)ade})(H_2O)_2]{\cdot}4H_2O$ (pheida = N-phenethyl-iminodiacetate(2-) ligand).[13] In this case, the cyclic topology is tied to the cooperation of the Cu-N3 and Cu-N7 bonds with appropriate intra-molecular interligand N9-H···O(carboxy) and N6-H···O(carboxy) H-bonds and the $\mu_2$- bridging role of two pheida ligands.

Besides the above-mentioned H-bonds (vide supra), additional inter-molecular H-bond plus intra- and inter-molecular pi,pi-stacking, ring-metal, X-H···ring and X-Y···ring interactions are present in the crystal packing of compound **2**, contributing to the overall stabilization of the 3D network (Table 2 – see also Table S-4.3 and S-5.2 in Supporting Information).

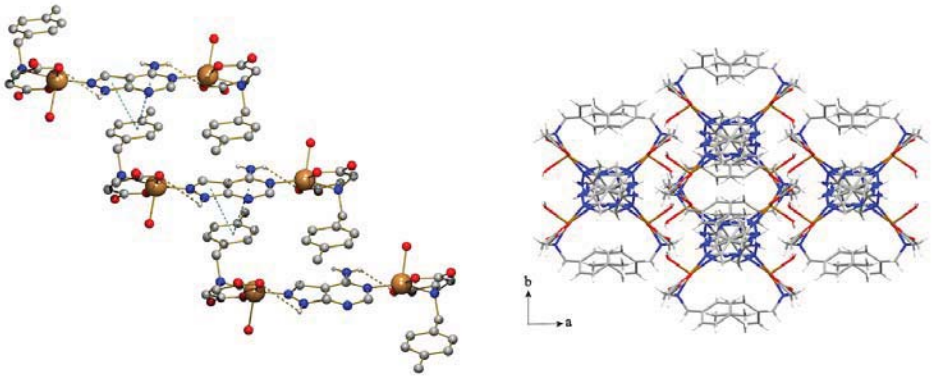


Figure 4. Left: detail of multi-stacked 1D chains in compound **1**. Only one of the two disordered positions for the H4app ligand is depicted for clarity. Right: View in the ba plane of the 3D honeycomb-like architecture in the crystal of **1**.

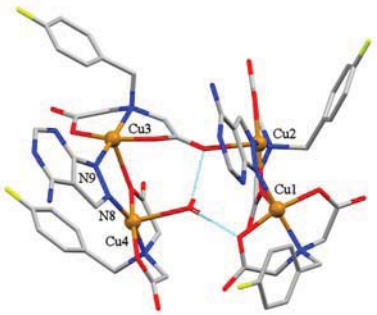


Figure 5. Complex molecule of $[Cu_4(FBIDA)_4(\mu_2\text{-}N8,N9\text{-}H4app)_2(H_2O)]\cdot 3.5H_2O$ (**2**). Solvent molecules and H-atoms not involved in intra-molecular H-bonding interactions are omitted for clarity.

Besides the above-mentioned H-bonds, additional inter-molecular H-bond plus intra- and inter-molecular pi,pi-stacking, ring-metal, X-H···ring and X-Y···ring interactions are present in the crystal packing of compound **2**, contributing to the overall stabilization of the 3D network (Table 2 – see also Table S-4.3 and S-5.2 in Supporting Information). Among those interactions, the most significant ones are: (i) the pi,pi-stacking between the 6-membered rings of two H4app ligands (bridging Cu1 and Cu2) of adjacent tetrameric units and that involving the aromatic moieties from FBIDA chelators of Cu3 and Cu4 (Figure 6 - left). In the former interactions, the Cg···Cg distances are 3.53(1) and 3.78(1) Å, respectively, and the dihedral angles (α) in the range of 0-4°, which are considered as rather intense pi,pi-stacking interactions (see S-5.2 in Support. Information).[27] (ii) Likewise, it is remarkable the intra-molecular ring-metal interaction observed between the aromatic moiety of the FBIDA(4) ligand and the related copper(II) centre (Figure 6 - right), with a Cu4···Cg distance of 3.62(1) Å. Moreover, the distance metal-to-plane of 2.77(1) Å (from the normal to the mean plane of the ring, passing through the copper(II) atom) also reveals its significance. Such interaction is the only one present among the four possible alternatives within the tetranuclear unit, what underline the conformational versatility of the FBIDA ligands inside the tetramer.

## MOLECULAR RECOGNITION CONSEQUENCES

Despite the broad structural information regarding adenine, in any of its forms, only 51 structures reported in the Cambridge Structural Database show the M-N1 coordination bond. The vast majority of them comprise soft metal ions (such as $Pt^{2+}$ or $Ag^{+}$) and N9-blocked adenine derivatives showing the bidentate $\mu_2$-N1,N7 role, see for example ref. 28. It is important to note that in 9-substistuted purine ligands all the remaining N-donors are potential coordination sites since there are no tautomerism phenomena. On the other hand, just five structures have been characterized displaying the Cu-N1 bond. Three of them correspond to one bridging $\mu_4$-N1,N3,N7,N9-tetradentate adeninate(1-) anion[29] and two N9-blocked adenines with the aforementioned bridging $\mu_2$-N1,N7 mode.[30] Interestingly, only two structures have neutral purine-like ligands: one is a mixed-ligand Cu-Hade complex[26] and the other is a Cu-H7deaza-adenine derivative recently characterized by our group.[23] Why the N1 donor is rarely involved in coordination in purine ligands still remains quite uncertain. Obviously the presence of the exocyclic amino group hinders the N1 atom, which is a poorer metal binding site in comparison to N7. However, equilibrium data published by Sigel et al.[31] concluded that purine residues may coordinate two metal ions simultaneously at N1 and N7 sites under physiological conditions.

The relevance of **1** lies in the formation of the Cu-N1 bond, as a part of the $\mu_2$-N1,N8 coordination mode displayed by H(N9)4app. Thus, molecular recognition studies with purine analogues without the N7 atom, such as the previously referred H7deaza-adenine or H4app, point out the relevance of the N1/N7 dichotomy. In these latter ligands, the absence of the N7 donor seems to encourage the coordination abilities of the N-purine six-membered ring and hence it turn N1 donor into a more attractive metal binding site. In compound **1** this is specially favored because: (i) the metallation of N9 and N8 increase the acidity of N3 and (ii) in this mixed-ligand metal complex the N6-H bond can be involved in intra-molecular interligand interaction that cooperates with the coordination bond. All this information may help us to better understand some processes in nature where purine ligands actively participate, especially larger oligonucleotides, but also to rationalize the molecular recognition processes in which this ligand, as part of new promising drugs, are involved.

Table 2. Inter- and intra-molecular interactions (A, º) present in $[Cu_4(FBIDA)_4(\mu_2\text{-}N8,N9\text{-}H4app)_2(H_2O)]\cdot 3.5H_2O$ (**2**).

| π···π interactions | | Cg(I)···Cg(J) | α |
|---|---|---|---|
| | Cg(1)···Cg(1)i | 3.532 | 0.00 |
| | Cg(2)···Cg(3)ii | 3.780 | 3.63 |
| | Cg(3)···Cg(2)iii | 3.780 | 3.63 |
| Ring-Metal interactions | | Cg(I)···Cu | β |
| | Cg(3)···Cu(4) | 3.622 | 40.12 |
| X–H···π interactions | | H···Cg(I) | γ |
| | O(3)–H(3B)···Cg(4)iv | 2.83 | 21.95 |
| | C(37)–H(37)···Cg(5)i | 2.83 | 7.65 |
| X–Y···π interactions | | Y···Cg(I) | γ |
| | C(45)–F(2)···Cg(6)v | 3.26 | 18.86 |
| | C(22)–O(22)···Cg(7) | 3.76 | 27.34 |
| | C(26)–O(26)···Cg(2) | 3.93 | 22.04 |

Cg(I)···Cg(J): Distance between ring centroids; α: Dihedral angle between planes I and J; β: angle between Cg(I)–Cu vector and normal to plane I; γ: angle between X–H vector and normal to plane I

Constitution of ring plane(number): Cg(1)-(N51/C52/N53/C54/C55/C56); Cg(2)-(C62/C63/C64/C65/C66/C67); Cg(3)-(C72/C73/C74/C75/C76/C77); Cg(4)-(N58/N59/C54/C55/C57); Cg(5)-(N81/C82/N83/C84/C85/C86); Cg(6)-(C42/C43/C44/C45/C46/C47); Cg(7)-(C32/C33/C34/C35/C36/C37).

Symmetry transformations: i = -x, 2-y, 1-z; ii = -1+x, y, z; iii = 1+x, y, z; iv = 1+x, -1+y, z; v = -1-x, 2-y, -z.

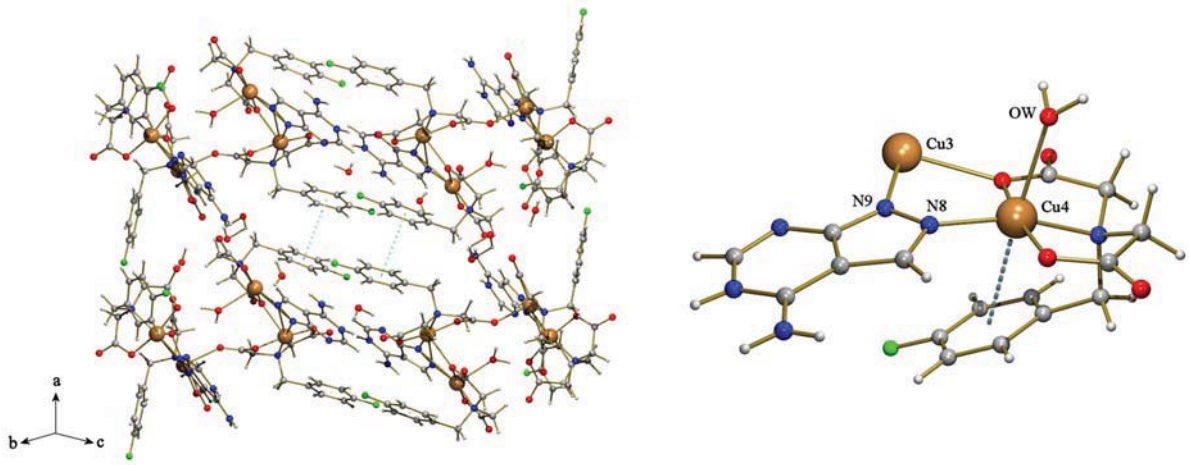


Figure 6. Left: view of unit cell of **2** showing pi,pi-stacking between phenyl groups of neighboring FBIDA ligands; Right: detail of metal-ring interaction within a fragment of the tetranuclear complex (**2**).

Alternatively, other molecular recognition pattern has been described in compound **2** for the H4app ligand. Herein, the ligand uses the H(N1)4app tautomer and display the $\mu_2$-N8,N9 coordination mode. As we have commented previously, this role has been previously reported for H4app and its hydroxo-derivative allopurinol. It should be noted that, although the DFT calculations carried out in this study consider the use of the latter bridging mode, ΔGr values were more favorable to the $\mu_2$-N1,N8 bidentate role. This can be explain considering the difference in energy between the H(N9)4app and H(N1)4app tautomers but the vagaries of compound **2**, i.e. $\mu_2$-N8,N9 can not cooperate with intra-molecular interligand H-bonding interactions. Anyhow, the molecular recognition patterns described for compounds 1 and 2 are in accordance with the assumed N-basicity order of H4app (N9≥N8>N1>N3>>N6), obtained from solution studies, and the previous theoretical calculations (vide supra – see DFT calculations section). Going further on compound **2**, it is noteworthy how non-covalent interactions mainly drive the acyclic non-linear topology of this tetranuclear complex molecule. In this compound, the unit corresponding to Cu4 plays an essential role controlling the nuclearity by means of intra-molecular H-bonds that involve the apical aqua ligand. Besides this, it seems that the topology is further influenced by an unusual contribution of different inter-molecular forces, from which it should be remarked the metal(Cu4)-ring interaction. This latter phenomenon is rather infrequent and of special relevance regarding the interaction of metal ions with biomolecules (i.e. blue copper proteins[32]).

## EPR AND MAGNETIC PROPERTIES

Since compounds **1** and **2** have relevant stacking interactions within their molecular and crystal structures, X and Q band EPR measurements were carried out on powdered samples at several temperatures in the range 5-300 K. In all cases, the spin hamiltonian parameters were estimated by comparison of the experimental spectra with those obtained by a computer simulation program working at the second order of the perturbation theory.

The X-band powder EPR spectrum of 1 has the characteristic shape of Cu(II) sites with rhombic symmetry (Fig. 7). The main g-values are $g_1$ = 2.205, $g_2$ = 2.135 and $g_3$ = 2.048 ($g_{iso}$= 2.129), remaining practically unchanged from room temperature down to 5 K. The calculated G parameter[33] is 2.3, which indicates that the g values obtained from the experiment are not equal to the molecular ones. This fact implies the averaging by exchange coupling of the signal corresponding to magnetically non-equivalent copper sites, as Cu1 and Cu1e (1/2-x, -1/2+y, 1/2-z), connected via hydrogen bonding and separated by 7.8 Å (see Figure S-8.1 in Supporting Information). The EPR line corresponds to a collective resonance when the exchange interaction (J) between copper ions in different lattice sites is larger than the difference between their Zeeman energies (0.3 $cm^{-1}$ at X-band). However, on the Q-band EPR spectrum an additional rhombic signal is observed, with $g'_1$ = 2.269, $g'_2$ = 2.070 and $g'_3$ = 2.048 ($g'_{iso}$= 2.128). Considering that these g-values are molecular (G = 4.7), while the average parameter is practically the same in both signals, it can be concluded that the Q-band spectrum shows the simultaneous presence of collapsed and independent resonances for Cu1 and Cu1e sites. This is a rather uncommon behavior and implies that the condition JCu1-Cu1e>|gCu1-gCu1e|μBH does not hold for any orientation of the magnetic field operating at Q-band.

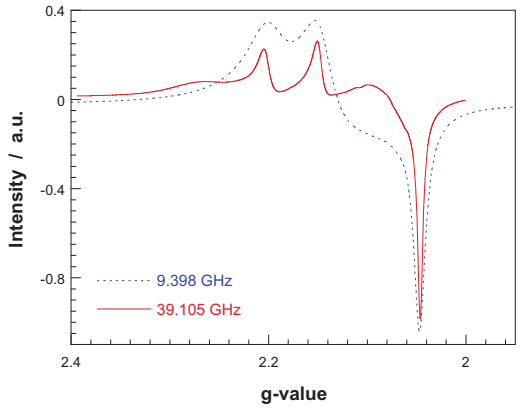


Figure 7. X and Q-band powder EPR spectra of compound 1 registered at r.t.

Only one quasi-isotropic line, with $g_{iso}$=2.13, is observed on the X and Q-band powder EPR spectra of compound **2** registered at room temperature (see

Figure S-8.2 in Supporting Information). The intensity of this signal increases with decreasing temperature, reaching a maximum about 14 K after which it rapidly decreases. Below 20 K, two new satellite bands are observed at about 270 and 375 mT. At the same time, the classical "half-field signal" (ΔMs=2) is also detected. These results indicates that at room temperature EPR spectra are dominated by the characteristics of an S=2 spin state, while a triplet state becomes more important below 20 K. Considering that the two satellite lines correspond to the perpendicular fine structure of the S=1 state, the splitting between them yields the zero-field splitting parameter |D|=52 mT. The g value associated with this doublet is g⊥=2.07. The zero-field interaction within the S=2 state is small and hidden within the experimental line width. It is noteworthy that the observation of a fine structure at low temperatures indicates the absence of appreciable magnetic exchange between tetrameric units.

The thermal variation of the inverse of the magnetic molar susceptibility ($\chi_m^{-1}$) and the $\chi_m$T product ($\mu eff^2 = 8\chi_m T$) for compound 1 is shown in Fig. 8. The effective magnetic moment exhibits a plateau from room temperature to 20 K having a value of 1.8 μB, decreasing to a value of 1.5 μB at 2 K. Above 10 K, the magnetic susceptibility follows a Curie–Weiss law with Cm=0.86 $cm^3Kmol^{-1}$ and θ = -0.7 K. Both, the negative temperature intercept and the decrease of the magnetic effective moment at low temperatures are in agreement with weak antiferromagnetic interactions in the compound. Taking into account the crystal structure the experimental data were fitted to the Bleaney-Bowers[34] expression [Equation 1] for an isotropically coupled pair of S=1/2 ions:

$$\chi m = \frac{Ng^2\beta^2}{kT(3+3\exp(-J/kT)} \qquad [1]$$

where the singlet-triplet energy gap (2J) is defined by the Hamiltonian H = –2J·S1·S2 (S1 = S2 = 1/2); g is the Lande's g factor; N, β and k are the Avogadro's number, the Bohr magneton, and Boltzmann's constant, respectively. The best-fit parameters obtained by minimizing the reliability factor $R = \Sigma[(\chi_m T)\exp - \chi_m T)\text{cal}]^2/\Sigma[(\chi_m T)\exp]^2$ are g = 2.13, J = -0.8 $cm^{-1}$ and R = 6.1x10-5. As shown in Figure 8, calculated curves reproduce satisfactorily the experimental data in the whole investigated temperature range. The low value of the calculated coupling parameter is in good agreement with the long exchange pathway via the H4app ligand.

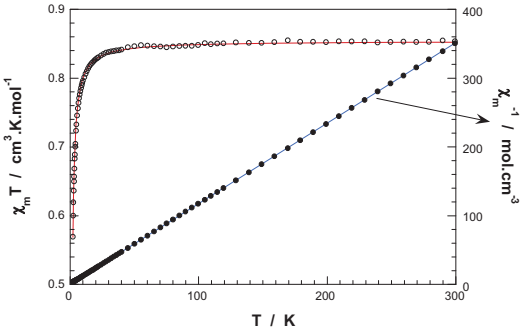


Figure 8. Thermal evolution of the reciprocal magnetic molar susceptibility $\chi_m^{-1}$ and the $\chi_m$T product for compound 1. The solid lines correspond to the best theoretical fits.

The thermal evolutions of both the magnetic molar susceptibility and $\chi_m$T values for compound **2** are shown in Fig. 9. At room temperature, $\chi_m$T is equal to 1.68 $cm^3mol^{-1}K$, a value that is only slightly lower than that expected for a set of four magnetically non-interacting copper(II) ions (ca. 1.70 $cm^3mol^{-1}K$ using the <g> = 2.13 value obtained from the EPR data). Upon cooling, $\chi_m$T continuously decreases, and it practically vanishes at very low temperatures. As the temperature is lowered the susceptibility increases until a maximum of 0.0535 $cm^3mol^{-1}$, which is reached at about 16 K, and then rapidly decreases (0.0035 $cm^3mol^{-1}$ at 3 K). The susceptibility increases below 3 K, probably due to the presence of a small paramagnetic impurity. At high temperature, T ≥ 100 K, the thermal evolution of $\chi_m$ follows the classical Curie–Weiss law, with Weiss temperature θ = −8.5 K and Curie constant Cm = 1.72 $cm^3mol^{-1}K$. These results confirm the prevalence of antiferromagnetic interactions in this compound.

To interpret quantitatively the magnetic data we had analyzed them in terms of the "dipolar coupling" approach for a Cu(II) tetrameric compound. With the numbering scheme used in Figure 2, the Heisenberg spin hamiltonian appropriate for the exchange interaction in this system can be written as:

$H=-2J_1(S1.S2+S3.S4)-2J_2(S2.S3)$

where $J_1$ describes the nearest neighbor interaction between the outer pairs of copper and $J_2$ the central exchange constant. Interactions between non-nearest neighbors or via hydrogen bonds have been neglected to avoid an excessive number of adjustable parameters. The eigenvalues derived from this Hamiltonian[35] were introduced in the van Vleck equation36 to obtain an analytical expression for the magnetic susceptibility. An additional term (ρ) which accounts for uncoupled Cu(II) ions following a simple Curie law, and having the same g factor has been also included [Equation 2]:

$$\chi_m = (1-\rho)\frac{Ng^2\beta^2}{3kT}\frac{\sum_i S_i(S_i+1)(2S_i+1)\exp\left(-\frac{E_i}{kT}\right)}{\sum_i (2S_i+1)\exp\left(-\frac{E_i}{kT}\right)} + 4\rho\frac{Ng^2\beta^2}{4kT} \qquad [2]$$

The best fit to the data where obtained with $J_1$ =-8.9 $cm^{-1}$, $J_2$ = -0.8 $cm^{-1}$, g = 2.14 and ρ=0.007 (R = $2.5x10^{-5}$). The calculated J values implies that the ground state of this cluster is S=0 but two S=1 triplet states are only a few Kelvin over the singlet, in good agreement with the spin triplet signals observed in the EPR spectra at low temperatures.

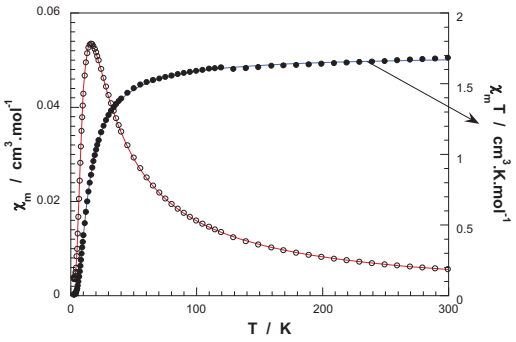


Figure 9. Plots of $\chi_m$ and $\chi_m$T for compound **2**. The solid lines correspond to the best fit to equation 2.

## CONCLUDING REMARKS

The crystallographic and DFT theoretical results presented herein are in good agreement and indicate that the N7/C8 translocation still allows a high versatility in the coordination abilities of H4app compared to adenine. In particular, H4app enables two bridging coordination modes, namely $\mu_2$-N1,N8 and $\mu_2$-N8,N9 for H(N9)4app and H(N1)4app, respectively. In contrast to the metal binding behavior of adenine, our findings suggest that the metal binding to the N1 donor in H4app is favored. In addition, the coordination ability of N8 in H4app should be also remarked. In conclusion, the study of the molecular recognition patterns of this kind of purine-like ligands can provide new insights into the metal binding behavior of larger oligonucleotides in biological systems and, in extend, help to rationalize the design of new promising drugs derived from pyrazolo[3,4-d]pyrimidines.

## ASSOCIATED CONTENT

Supporting Information Available: Additional structural information is provided in S1 to S3 (CCDC 881146 - 881147). Relevant spectral properties and thermal stability information as well as magnetic properties can be found in S4 and S5, respectively. This material is available free of charge via internet at http://pubs.acs.org.

## AUTHOR INFORMATION

### Corresponding Author

* Alicia Domínguez-Martín; e-mail: adominguez@ugr.es; telephone number: +34 958 24 38 53; fax: +34 958 24 62 19.

## ACKNOWLEDGMENT

Financial support from Research Group FQM-283 (Junta de Andalucía), MICINN-Spain (Project MAT2010-15594) and 'Factoría de Cristalización, CONSOLIDER INGENIO-2010' is acknowledged. ADM gratefully acknowledge ME-Spain for a FPU Ph.D contract.

## REFERENCES

(1) (a) Terrón, A.; Fiol, J. J.; García-Raso, A.; Barcelo-Oliver, M.; Moreno, V. *Coord. Chem. Rev.* **2007**, *251*, 1973. (b) Choquesillo-Lazarte, D.; Brandi-Blanco, M. P.; García-Santos, I.; González-Pérez, J. M.; Castiñeiras, A.; Niclós-Gutiérrez, J. *Coord. Chem. Rev.* **2008**, *252*, 1241. (c) Sanz Miguel, P. J.; Amo-Ochoa, P.; Castillo, O.; Houlton, A.; Zamora, F. Metal Complex - DNA interactions; Hadjiliadis, N., Sletten, E., Eds.; Wiley-Blackwell: Chichester, U.K., **2009**; Chapter 4. (d) Lippert, B. Nucleic Acid - Metal Ion Interactions; Hud, N. V., Ed.; RSC Publishing: London, **2009**; Chapter 2.

(2) Patel, D. K.; Domínguez-Martín, A.; Brandi-Blanco, M. P.; Choquesillo-Lazarte, D.; Nurchi, V. M.; Niclós-Gutiérrez, J. *Coord. Chem. Rev.* **2012**, *256*, 193.

(3) (a) Choquesillo-Lazarte, D.; Domínguez-Martín, A.; Matilla-Hernández, A.; Sánchez de Medina Revilla, C; González-Pérez, J. M.; Castiñeiras, A.; Niclós-Gutiérrez, J. *Polyhedron* **2010**, *29*, 170. (b) Patel, D. K.; Choquesillo-Lazarte, D.; Domínguez-Martín, A.; Brandi-Blanco, M.P.; González-Pérez, J. M.; Castiñeiras, A.; Niclós-Gutiérrez, J. *Inorg. Chem.* **2011**, *50*, 10549. (c) Domínguez-Martín, A.; Cho-quesillo-Lazarte, D.; González-Pérez, J. M.; Castiñeiras, A.; Niclós-Gutiérrez, J. *J. Inorg. Biochem.* **2011**, *105*, 1073.

(4) Holla, B. S.; Mahalinga, M.; Karthikeyan, M. S.; Akberali, P. M.; Shetty, N. S.
*Bioorg. Med. Chem.* **2006**, *14*, 2040.
(5) Hasan, A.; Satyanarayana, M.; Mishra, A.; Bhakuni, D. S.; Pratap, R.; Dube, A.; Guru, P. Y. *Nucleos Nucleot Nucleic Acids* **2006**, *25*, 55.
(6) (a) Carraro, F.; Naldini, A.; Pucci, A.; Locatelli, G. A.; Maga, G.; Schenone S.; Bruno, O.; Ranise, A.; Bondavalli, F.; Brullo, C.; Fossa, P.; Menozzi, G.; Mosti, L.; Modugno M.; Tintori, C.; Manetti, F.; Botta M. *J. Med. Chem.* **2006**, *49*, 1549-1561. (b) Franco, L.; Davide, D. F.; Stevens, M. R. PCT Int. Appl. WO2011014239 (A1) **2011**. (c) Indovina, P.; Giorgi, F.; Rizzo, V.; Khadang, B.; Schenone, S.; Di Marzo, D.; Forte, I.M.; Tomei, V.; Mattioli, E.; D'Urso, V.; Grilli, B.; Botta, M:; Giordano, A.; Pentimalli, F. *Oncogene* **2012**, *31*, 929.
(7) Davies, L. P.; Brown, D. J.; Chow, S. C.; Johnston, G. A. R. *Neurosci. Lett.*
**1983**, *41*, 189.
(8) (a) Da Settimo, F.; Primofiore, G.; La Motta, C.; Taliani, S.; Simorini, F.; Marini, A. M.; Mugnaini, L.; Lavecchia, A.; Novellino, E.; Tuscano, D.; Martini, C. *J. Med. Chem.* **2005**, *48*, 5162-5174. (b) Hsieh, J-F.; Wu, S.-H.; Yang, Y.-L.; Choong, K.-F.; Chen, S.-T. *Bioorg. Med. Chem.* **2007**, *15*, 3450-3456.
(9) Nakano, S.; Karimata, H.T.; Kitagawa, Y.; Sugimoto, N. *J. Am. Chem. Soc.* **2009**, *131*, 16881.
(10) (a) Sprang, S.; Scheller, R.; Rohrer, D.; Sundaralingam, M. *J. Am. Chem. Soc.* **1978**, *100*, 2867. (b) Seela, F.; Zulauf, M.; Reuter, H.; Kastner, G. *Acta Crystallogr.* **1999**, *C55*, 1947. (c) Zhang, X.; Budow, S.; Leonard, P.; Eickmeier, H.; Seela, F. *Acta Crystallogr.* **2006**, *C62*, o79. (d) Pasternak, A.; Kierzek, R.; Gdaniec, Z.; Gdaniec, M. *Acta Crystallogr.* **2008**, *C64*, o467.
(11) Dodin, G.; Dreyfus, M.; Bensaude, O.; Dubois J.-E. *J. Am. Chem. Soc.* **1977**, *99*, 7257.
(12) Sheldrick, W. S.; Bell, P.; Hausler, H.-J. *Inorg. Chim. Acta* **1989**, *163*, 181-192.
(13) Bugella-Altamirano, E.; Choquesillo-Lazarte, D.; González-Pérez, J.M.; Sánchez-Moreno, M. J.; Marín-Sánchez, R.; Martín-Ramos, J.D.; Covelo, B.; Carballo, R; . Castiñeiras A.; Niclós-Gutiérrez, J. *Inorg. Chim. Acta*, **2002**, *339*, 160.
(14) BRUKER, SMART and SAINT. Area Detector control and Integration Software, Bruker analytical X-ray instruments Inc., **1997**, Madison, Wisconsin, USA.
(15) BRUKER, APEX2 Software, Bruker AXS Inc., V.2010.11, Madison, Wisconsin, USA.
(16) G.M. Sheldrick, SADABS, Program for Empirical Absorption Correction of Area Detector Data, **2009**, University of Göttingen, Germany.
(17) G.M. Sheldrick, *Acta Crystallogr.*, **2008**, *A64*, 112.
(18) A.L. Spek, PLATON. A Multipurpose Crystallographic Tool, **2010**, Utrecht University, Utrecht, The Netherlands.
(19) C.F. Macrae, I.J. Bruno, J.A. Chisholm, P.R. Edgington, P. McCabe, E. Pidcock, L. Rodriguez-Monge, R. Taylor, J. van de Streek and P.A. Wood, *J. Appl. Cryst.*, **2008**, *41*, 466.
(20) Becke, A. D. *J. Chem. Phys.* **1993**, *98*, 5648.
(21) Gaussian 09, Revision B.01, M. J. Frisch, G. W. Trucks, H. B. Schlegel, G. E. Scuseria, M. A. Robb, J. R. Cheeseman, G. Scalmani, V. Barone, B. Mennucci, G. A. Petersson, H. Nakatsuji, M. Caricato, X. Li, H. P. Hratchian, A. F. Izmaylov, J. Bloino, G. Zheng, J. L. Sonnenberg, M. Hada, M. Ehara, K. Toyota, R. Fukuda, J. Hasegawa, M. Ishida, T. Nakajima, Y. Honda, O. Kitao, H. Nakai, T. Vreven, J. A. Montgomery, Jr., J. E. Peralta, F. Ogliaro, M. Bearpark, J. J. Heyd, E. Brothers, K. N. Kudin, V. N. Staroverov, T. Keith, R. Kobayashi, J. Normand, K. Raghavachari, A. Rendell, J. C. Burant, S. S. Iyengar, J. Tomasi, M. Cossi, N. Rega, J. M. Millam, M. Klene, J. E. Knox, J. B. Cross, V. Bakken, C. Adamo, J. Jaramillo, R. Gomperts, R. E. Stratmann, O. Yazyev, A. J. Austin, R. Cammi, C. Pomelli, J. W. Ochterski, R. L. Martin, K. Morokuma, V. G. Zakrzewski, G. A. Voth, P. Salvador, J. J. Dannenberg, S. Dapprich, A. D. Daniels, O. Farkas, J. B. Foresman, J. V. Ortiz, J. Cioslowski, and D. J. Fox, Gaussian, Inc., Wallingford CT, **2010**.
(22) Hehre, W.J.; Ditchfield R.; Pople, J.A. *J. Chem. Phys.* **1972**, *56*, 2257.
(23) Domínguez-Martín, A.; Choquesillo-Lazarte, D.; Dobado, J. A.; Vidal, I.; González-Pérez, J. M.; Castiñeiras A.; Niclós-Gutiérrez, J. *Dalton Trans.* **2012**, *submitted*.
(24) Miertuš, S.; Scrocco, E.; Tomasi, J.; *Chem. Phys.* **1981**, *55*, 117.
(25) Hänggi, G.; Schmalle, H.; Dubler, E. *J. Chem. Soc. Dalton Trans.* **1993**, 941.
(26) Das, S.; Madhavaiah, C.; Verma, S.; Bharadwaj, P. K. *Inorg. Chim. Acta* **2005**, *358*, 3236.
(27) Janiak, C. *J. Chem. Soc. Dalton Trans.*, **2000**, 3885.
(28) (a) Roitzsch, M.; Lippert, B. *Chem. Commun.* **2005**, 5991; (b) Roitzsch, M.; Lippert, B. *Inorg. Chem.* **2004**, *43*, 5483; (c) Purohit, C.S.; Verma, S. *J. Am. Chem. Soc.* **2007**, *129*, 3488.
(29) Yang, E.-C.; Zhao, H.-K.; Feng, Y.; Zhao, X.-J. *Inorg.Chem.* **2009**, *48*, 3511.
(30) (a) Srivatsan, S. G.; Parvez, M.; Verma, S. *Chem. Eur. J.* **2002**, *8*, 5184; (b) Prajapati, R. K.; Verma, S. *Inorg. Chem.* **2011**, *50*, 3180.
(31) Knobloch, B.; Sigel, R.K.O; Lippert, B.; Sigel, H. *Angew. Chem. Int. Ed.* **2004**, *43*, 3793.
(32) Abdelhamid, R. F.; Obara, Y.; Uchida, Y.; Kohzuma, T.; Dooley, D. M.; Brown, D. E.; Hori H. *J. Biol. Inorg.Chem.* **2007**, *12*, 165.
(33) Hathaway, B.J.; Billing, D. *Coord. Chem. Rev.* **1970**, *5*, 143
(34) Bleaney, B.; Bowers, K.D. *Proc. R. Soc. London, Ser. A*, **1952**, *214*, 451.
(35) Papadopoulos, A.N.; Tangoulis, V.; Raptopoulou, C.P.; Terzis, A.; Kessissoglou, D.P. *Inorg. Chem.* **1996**, *35*, 559.
(36) Van Vleck, J.H. *Theory of Electric and Magnetic Susceptibilities;* Oxford University Press, **19.**

## 3.2. Modulating the metal binding pattern of adenine by selective N-methylation: study of a family of ternary copper(II) iminodiacetate complexes

Draft version of the manuscript to be submitted to *Eur. J. Inorg. Chem.* (2012)


SYNOPSIS

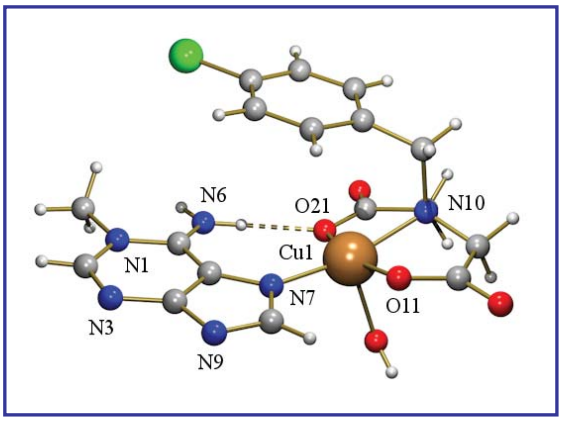


In nine related ternary complexes N1-, N3- or N9-methyladenine binds to copper(II) iminodiacetates via the Cu-N7 bond in cooperation with a N6-H···O intra-molecular interligand interaction (O = coord. carboxylate or apical aqua ligand). In contrast, N7-methyladenine drives the coordination through the minor groove binder N3 and only exhibits the Cu-N3 bond.

RESUMEN

En el presente trabajo se evalúan las consecuencias que tiene la metilación en los dadores N-heterocíclicos de adenina sobre los modos de reconocimiento molecular. Con este propósito, se ha sintetizado y caracterizado estructuralmente una familia de doce compuestos ternarios de cobre(II) estrechamente relacionados: [Cu(CBIDA)(1Meade)$(H_2O)_2$]·$3H_2O$ (**1**), [Cu(IDA)(3Meade)$(H_2O)_2$]·$3H_2O$ (**2**), [Cu(MIDA) (3Meade)$(H_2O)$]·$6H_2O$ (**3**), [Cu(NBzIDA)(3Meade)$(H_2O)_4$]·$2H_2O$ (**4**), {[Cu(CBIDA)(3Meade)]·$H_2O$}$_n$ (**5**), [Cu(MIDA) (7Meade)$(H_2O)$]·$4H_2O$ (**6**), [Cu(IDA)(9Meade)$(H_2O)_2$]·$3H_2O$ (**7**), [Cu(MIDA)(9Meade)$(H_2O)$] ·$2H_2O$ (**8**), {[Cu(EIDA)(9Meade)]·$4H_2O$}$_n$ (**9**), [Cu(NBzIDA)(9Meade)$(H_2O)$]·$4H_2O$ (**10**), [Cu(MEBIDA)(9Meade)$(H_2O)$]·$3H_2O$ (**11**) y [Cu(CBIDA)(9Meade)$(H_2O)$]·$H_2O$ (**12**) (IDA = iminodiacetato y MIDA, EIDA, NBzIDA , MEBIDA y CBIDA = N-metil-, N-etil-, N-bencil-, N-(p-metilbencil) o N-(p-clorobencil)-iminodiacetato, respectivamente). Todos lo compuestos ternario con N1, N3 o N9-metiladenina exhiben un reconocimiento molecular basado en la cooperación del enlace Cu-N7 más una interacción intramolecular interligandos N6-H···O, donde el aceptor O puede ser un oxígeno carboxilato coordinado o un ligando aqua apical (sólo en un

complejo conteniendo IDA como agente quelante). La formación del enlace Cu-N3 sólo se observa cuando se usa 7-metiladenina como ligando. Estos hallazgos son esencialmente racionalizados en función de los modos de coordinación disponibles para cada uno de los ligandos N-metiladenina así como de las preferencias coordinantes por cooperar el enlace Cu-N(xMeade) con una interacción intramolecular de enlace de hidrógeno tipo N-H···O.

# Modulating the metal binding pattern of adenine by selective N-methylation: study of a family of ternary copper(II) iminodiacetate complexes

Alicia Domínguez-Martín[a*], Duane Choquesillo-Lazarte[b], Josefa María González-Pérez[a], Alfonso Castiñeiras[c], Juan Niclós-Gutiérrez[a]

[a] Department of Inorganic Chemistry, Faculty of Pharmacy, Campus Cartuja, University of Granada, E-18071 Granada, Spain.

[b] Laboratorio de Estudios Cristalográficos, IACT-CSIC, Avda. del Conocimiento s/n; E-18100 Armilla (Granada), Spain.

[c] Department of Inorganic Chemistry, Faculty of Pharmacy, University of Santiago de Compostela, E-15782 Santiago de Compostela, Spain.

## ABSTRACT

In order to evaluate the molecular recognition consequences of the N-(heterocyclic)-methyl substitution on adenine, a family of twelve closely related ternary copper(II) iminodiacetate complexes has been synthesized and structurally characterized by single-crystal X-ray crystallography: [Cu(CBIDA)(1Meade)$(H_2O)_2$]·$3H_2O$ (**1**), [Cu(IDA)(3Meade)$(H_2O)_2$]·$3H_2O$ (**2**), [Cu(MIDA)(3Meade)$(H_2O)$]·$6H_2O$ (**3**), [Cu(NBzIDA)(3Meade)$(H_2O)_4$]·$2H_2O$ (**4**), {[Cu(CBIDA)(3Meade)]·$H_2O$}$_2$ (**5**), [Cu(MIDA)(7Meade)$(H_2O)$]·$4H_2O$ (**6**), [Cu(IDA)(9Meade)$(H_2O)_2$]·$3H_2O$ (**7**), [Cu(MIDA)(9Meade)$(H_2O)$]·$2H_2O$ (**8**), {[Cu(EIDA)(9Meade)]·$4H_2O$}$_n$ (**9**), [Cu(NBzIDA)(9Meade)$(H_2O)$]·$4H_2O$ (**10**), [Cu(MEBIDA)(9Meade)$(H_2O)$]·$3H_2O$ (**11**) and [Cu(CBIDA)(9Meade)$(H_2O)$]·$H_2O$ (**12**) (IDA = iminodiacetate ligand and MIDA, EIDA, NBzIDA , MEBIDA and CBIDA = N-methyl-, N-ethyl-, N-benzyl-, N-(p-methylbenzyl) or N-(p-chlorobenzyl)-iminodiacetate ligands, respectively). All the ternary complexes with N1-, N3- or N9-methyladenine as co-ligand exhibit a molecular recognition pattern based on the cooperation of the Cu-N7 bond and a suitable N6-H···O intra-molecular interligand interaction. In these former cases, the O-acceptor involved in H-bonds is a coordinated carboxylate atom or an apical aqua ligand (in one complex that has IDA as chelator). The formation of the Cu-N3 bond is only observed when 7Meade is used as co-ligand. These findings are mainly rationalized on the basis of the metal binding abilities of the different methyl-adenine ligands and the preferences for cooperative molecular recognition patterns: Cu-N(xMeade) bond + N-H···O intra-molecular interligand interaction.

[*] Corresponding author: Department of Inorganic Chemistry, Faculty of Pharmacy, Campus Cartuja, University of Granada, E-18071 Granada, Spain.
Phone: +34958243853, Fax: +34958246219
E-mail address: adominguez@ugr.es

## 1. Introduction

The formation of ternary complexes (MAB) can be understood as a consequence of molecular recognition processes between a binary metal complex MA and a suitable co-ligand B. This general viewpoint is useful for many approaches but overall of great interest concerning many biological processes. In this context, Niclós-Gutiérrez et al. addressed the study of the molecular recognition patterns within ternary copper(II) complexes with iminodiacetate (IDA) or N-R substituted IDA chelators and adenine (Hade). The reactions of this kind of copper(II) chelates and Hade afforded molecular mixed-ligand complexes with essentially different metal binding roles depending the nature of the R group.[1] Thus, for R = alkyl (methyl or ethyl in MIDA or EIDA, respectively) the structure of the compounds [Cu(MIDA or EIDA)(Hade)($H_2O$)]·$H_2O$[1] revealed the formation of the Cu-N7 bond which cooperates with an intra-molecular interligand H-bonding interaction N6-H···O(coordinated carboxylate). In the crystal of these compounds, pairs of complex molecules stacks their Hade ligands by means of a relevant π,π-stacking interactions where the nucleobase ligands fall in an anti-parallel way. In clear contrast, in the crystals of [Cu(NBzIDA, MEBIDA or MOBIDA)(Hade)($H_2O$)]·$H_2O$[1-2] (being the N-R arm = benzyl-, p-methyl-benzyl- or p-methoxy-benzyl-, respectively) the molecular recognition consists of a Cu-N3 bond plus the intra-molecular N9-H···O(coordinated carboxylate) H-bond. In these cases, the aromaticity of the N-R arms in the chelators is expressed building multi-stacked molecular chains by π,π-stacking interactions that involve the aromatic moiety the chelator and the six-membered ring of Hade from the adjacent complex molecule. In the tetranuclear complex [$Cu_4$($\mu_2$-pheida)$_2$(pheida)$_2$($\mu_2$-N3,N7-Hade)$_2$($H_2O$)$_4$]·2$H_2O$ (pheida = N-phenethyl-iminodiacetate ligand), the Cu-N3 and Cu-N7 coordination bonds are reinforced by the corresponding N9-H···O and N6-H···O intra-molecular interligand interactions[1]. In this latter crystal there are not π,π-staking interactions between the aromatic rings of pheida and Hade co-ligands. Interestingly, all these ternary complexes exhibit the most stable tautomer H(N9)ade.

From these results, many questions arise that encourage further structural researches on these sorts of compounds. Probably, the most noticeably aspect is how the non coordinating N-R arms of the chelator is able to influence the molecular recognition pattern between the referred Cu(II) chelates and Hade. Hence, the use of N(heterocylic)-methyladenine derivatives (1Meade, 3Meade, 7Meade or 9Meade – see Scheme I) could be an interesting strategy to prepare closely related ternary complexes that allow us to reach new complementary information about the metal binding behaviour of natural Hade. Therefore, the main aim of this work is to synthesize and structurally characterize ternary mixed-ligand copper(II) complexes with IDA, N-alkyl-IDAs and N-benzyl-IDAs chelators and different N-methyladenines (see Scheme I).

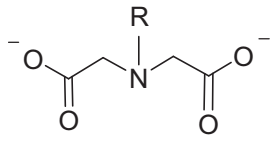

Iminodiacetate-like(2-) anion

R = H (IDA)
R = -$CH_3$ (MIDA)
R = -$CH_2$-$CH_3$ (EIDA)
R = -C-$(CH_3)_3$ (TEBIDA)
R = -$CH_2$-Ph (NBzIDA)
R = -$CH_2$-Ph-$CH_3$ (MEBIDA)
R = -$CH_2$-Ph-Cl (CBIDA)

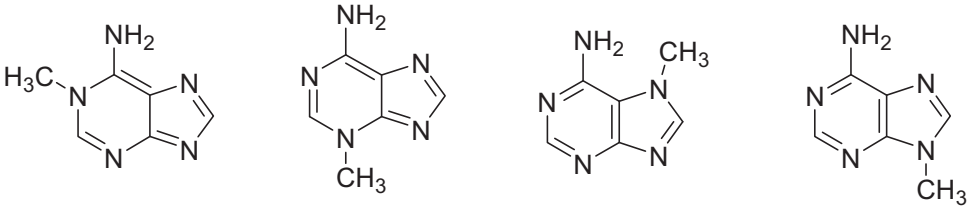

1Meade 3Meade 7Meade 9Meade

Scheme I. Formulas and abbrebiations of the chelating ligands and N-methyladenines used in the present work.

## 2. Experimental

2.1. Materials

Bluish $Cu_2CO_3(OH)_2$ was purchased from Probus. Iminodiacetic acid (IDA), N-methyliminodiacetic acid ($H_2$MIDA), 1-methyladenine (1Meade), 3-methyladenine (3Meade), 7-methyladenine (7Meade) and 9-methyladenine (9Meade) were supplied by Sigma-Aldrich. All reagents were used as received. N-(p-tBu)-, N-benzyl-, N-(p-methylbenzyl)- and N-(p-chlorobenzyl)-iminodiacetic acids ($H_2$TEBIDA, $H_2$NBzIDA, $H_2$MEBIDA and $H_2$CBIDA, respectively) were synthesised in their acid form as reported in refs. [1] and [3].

2.2. Syntheses of novel metal complexes

*[Cu(CBIDA)(1Meade)($H_2O$)$_2$]·3$H_2O$* (**1**). In a Kitasato flask, $Cu_2CO_3(OH)_2$ (0.25 mmol, 0.055 g) was reacted with $H_2$CBIDA acid (0.5 mmol, 0.081 g) in 80 mL of distilled water with heating (50ºC), stirring and moderate vacuum. Once a clear blue solution of the binary chelate was obtained, 1Meade (0.5 mmol, 0.075 g) was added. The solution was left reacting for one hour. Afterwards, it was filtered in a crystallization device (to remove possible un-reacted materials) and stood at r.t. covered with a plastic film to control the evaporation of the solvents. In four months, suitable needle-like blue crystals were collected for X-Ray diffraction (XRD) purposes. Yield ca. 75%. Elemental analysis (%): Calc. for $C_{17}H_{24}ClCuN_6O_7$ (**1**) C 39.09, H 4.38, N 16.09; Found: C 38.75 H 4.02 N 16.27. FT-IR [KBr, $cm^{-1}$]: $\upsilon_{as}(H_2O)$ 3387, $\upsilon_{as}(NH_2)$ and $\upsilon_s(H_2O)$ 3292, $\upsilon_s(NH_2)$ 3123, $\upsilon_{as}(CH_3)$ 2970, $\upsilon_d(CH_3)$ 2851, $\upsilon_{as}(CH_2)$ 2924, $\upsilon_s(CH_2)$ 2828, $\delta(NH_2)$ and $\delta(H_2O)$ overlapped 1624, $\upsilon_{as}(COO)$ 1563, $\upsilon_s(COO)$ 1384, $\pi(C\text{-}H)_{ar}$ (1MeAde) 805, $\pi(C\text{-}H)_{ar}$ (CBIDA) 643. The UV-Vis spectrum shows an asymmetric d-d band with $\lambda_{max}$ at 702 nm ($\nu_{max}$ 14245 $cm^{-1}$). The thermo-gravimetric curve is divided in five steps.

Under air-dry flow, the compound losses almost all the non-coordinated water. Hence, the TG experiment starts with an average formula $[Cu(CBIDA)(1MeAde)(H_2O)]\cdot 0.5H_2O$. In the first step (from 20 to 120 ºC), 0.5 solvent molecule plus the apical aqua ligand are lost (n = 1.5, Calc. 5.455%; Found 6.937%). During the pyrolysis of the organic ligands $H_2O$, $CO_2$, CO, N-oxide gases ($N_2O$, NO and $NO_2$), as well as, peculiarly, isocyanid acid, are evolved. This yields a final CuO residue (640 ºC, Calc. 16.057; Found 18.216%).

*$[Cu(IDA)(3Meade)(H_2O)_2]\cdot 3H_2O$* (**2**). A similar synthetic procedure to that compound (**1**) was followed, using $Cu_2CO_3(OH)_2$ (0.25 mmol, 0.055 g), $H_2$IDA acid (0.5 mmol, 0.066 g) and 3Meade (0.5 mmol, 0.074 g). In four weeks, parallelepiped greenish crystals were isolated from the mother solution and studied by XRD. Also, crystals of the binary chelate $[Cu(IDA)(H_2O)_2]$ and free 3Meade were collected. The nature of these latter crystals was confirmed by FT-IR. Yield ca. 70%. Elemental analysis (%): Calc. for $C_{10}H_{22}CuN_6O_9$ (**2**) C 27.68, H 5.11, N 19.37; Found: C 27.76, H 5.23, N 19.30. FT-IR [KBr, $cm^{-1}$]: $\upsilon_{as}(H_2O)$ 3414, $\upsilon_{as}(NH_2)$ 3302, $\upsilon_s(H_2O)$ and $\upsilon_s(NH_2)$ overlapped 3245, $\upsilon$(N-H) 3144, $\upsilon_{as}(CH_3)$ 2949, $\upsilon_d(CH_3)$ overshadowed, $\upsilon_{as}(CH_2)$ 2943, $\upsilon_s(CH_2)$ 2848, $\delta(NH_2)$ 1660, $\delta(H_2O)$ and $\upsilon_{as}$(COO) overlapped 1615, $\delta$(N-H) 1522, $\upsilon_s$(COO) 1384, $\pi(C\text{-}H)_{ar}$ (3MeAde) 813. The UV-Vis spectrum shows an asymmetric d-d band with $\lambda_{max}$ at 732 nm ($\nu_{max}$ 13661 $cm^{-1}$). The thermo-gravimetric curve is divided in five steps. Under air-dry flow, the compound losses part of the solvent molecules. Hence, the TG experiment starts with an average formula $[Cu(IDA)(3MeAde)(H_2O)_2]\cdot 0.9H_2O$. In the first step (from 30 to 180 ºC), 0.9 water molecules plus the two apical aqua ligands in the 4+1+1 Cu(II) surrounding are lost (n = 2.9, Calc. 13.192%; Found 13.860%). During the pyrolysis of the organic ligands, $H_2O$, $CO_2$, CO, trimethylamine (TMA), $NH_3$, $N_2O$, NO and $NO_2$ gases were evolved, yielding to a CuO residue (530 ºC, Calc. 20.086%; Found 21.837%).

*$[Cu(MIDA)(3Meade)(H_2O)]\cdot 6H_2O$* (**3**). The reaction was performed according to the procedure detailed for compound **2**, using $H_2$MIDA acid (0.5 mmol, 0.074 g) instead of $H_2$IDA acid. After six weeks, suitable parallelepiped blue crystals were collected for XRD purposes. Yield ca. 80-85%. Elemental analysis (%): Calc. for $C_{11}H_{28}CuN_6O_{11}$ (**3**) C 27.30, H 5.83, N 17.37; Found: C 27.42, H 5.79, N 17.30. FT-IR [KBr, $cm^{-1}$]: $\upsilon_{as}(H_2O)$ 3433, $\upsilon_{as}(NH_2)$ 3332, $\upsilon_s(H_2O)$ 3240, $\upsilon_s(NH_2)$ 3118, two types of $\upsilon_{as}(CH_3)$ 3112 and 2968, $\upsilon_d(CH_3)$ overshadowed, $\upsilon_{as}(CH_2)$ 2937, $\upsilon_s(CH_2)$ 2855 , $\delta(NH_2)$ 1668, $\delta(H_2O)$ and $\upsilon_{as}$(COO) overlapped 1618, $\upsilon_s$(COO) 1384, $\pi(C\text{-}H)_{ar}$ (3MeAde) 809. The UV-Vis spectrum shows an asymmetric d-d band with $\lambda_{max}$ at 714 nm ($\nu_{max}$ 14006 $cm^{-1}$). The thermal behaviour of this compound is divided in five steps. Under air-dry flow, the sample loses four solvent molecules, thus the TG experiment starts with an average formula $[Cu(MIDA)(3Meade)(H_2O)]\cdot H_2O$. In the two first steps, the compound only loses water according to the recorded evolved gases from 30 to 175 ºC. Therefore, the first step corresponds to the loss of the non-coordinated water molecule (Calc. 4.794%; Found 4.887%) and the second step corresponds to the loss of the apical aqua ligand (Calc. 4.355%; Found 4.243%). The consecutive pyrolytic steps (from 175 to 490 ºC) yield to a CuO

residue (Calc. 21.165%, Found 22.311%). The evolved gases during the pyrolysis are $H_2O$, $CO_2$, CO, TMA, $NH_3$ and N-oxide gases ($N_2O$, NO and $NO_2$). TMA is typically observed from the pyrolysis of MIDA chelating ligand.

*[Cu(NBzIDA)(3Meade)($H_2O$)]·2$H_2O$* (**4**). The reaction was performed according to the procedure detailed for compound **2**, using $H_2$NBzIDA acid (0.5 mmol, 0.112 g) instead of $H_2$IDA acid. After six weeks, parallelepiped blue crystals appeared, suitable for XRD. Yield of this synthesis is approx. 85%. Elemental analysis (%): Calc. for $C_{17}H_{24}CuN_6O_7$ (**4**) C 41.84, H 4.96, N 17.22; Found: C 41.80, H 5.00, N 17.29. FT-IR [KBr, $cm^{-1}$]: $\upsilon_{as}(H_2O)$ 3425, $\upsilon_{as}(NH_2)$ overshadowed, $\upsilon_s(H_2O)$ 3291, $\upsilon_s(NH_2)$ 3166, $\upsilon_{as}(CH_3)$ 2980, $\upsilon_d(CH_3)$ 2889, $\upsilon_{as}(CH_2)$ 2928, $\upsilon_s(CH_2)$ 2871, $\delta(NH_2)$ and $\delta(H_2O)$ overlapped 1612, $\upsilon_{as}(COO)$ 1595, $\upsilon_s(COO)$ 1384, $\pi(C\text{-}H)_{ar}$ (3Meade) 805, $\pi(C\text{-}H)_{ar}$ (NBzIDA) 712. The UV-Vis spectrum shows an asymmetric d-d band with $\lambda_{max}$ at 737 nm ($\nu_{max}$ 13569 $cm^{-1}$). The thermal behaviour is divided in six steps. Under air-dry flow, the sample loses the non-coordinated water. Afterwards, the sample [Cu(NBzIDA)(3Meade)$(H_2O)_{0.8}$] experiments the loss of weight of the apical aqua ligand (30–125 °C; Calc. 3.215%; Found: 3.550%). Five additional pyrolytic steps produce as evolved gases $H_2O$, $CO_2$, CO (t) N-oxide gases ($N_2O$, NO, $NO_2$) to yield an impure CuO residue at 545 ºC (Calc. 17.743%; Found 19.148%).

*[Cu(CBIDA)(3Meade)($H_2O$)]·2$H_2O$* (**5**). The reaction was performed according to the procedure detailed for compound **2**, using $H_2$CBIDA acid (0.5 mmol, 0.112 g) instead of $H_2$IDA acid. After four weeks, bad shaped blue crystals appeared, not suitable for XRD. Further re-crystallizations in 1:1 water:isopropanol mixtures finally yield to parallelepiped crystals appropriate for XRD purposes. Yield ca. 25%. Elemental analysis (%): Calc. for $C_{17}H_{23}ClCuN_6O_7$ (**5**) C 39.09, H 4.44, N 16.09; Found: C 38.97, H 4.35, N 16.15. FT-IR [KBr, $cm^{-1}$]: $\upsilon_{as}(H_2O)$ 3436, $\upsilon_{as}(NH_2)$ 3336, $\upsilon_s(H_2O)$ 3232, $\upsilon_s(NH_2)$ 3167, $\upsilon_{as}(CH_3)$ 2960, $\upsilon_d(CH_3)$ 2881, $\upsilon_{as}(CH_2)$ 2936, $\upsilon_s(CH_2)$ 2851, $\delta(NH_2)$ 1635, $\delta(H_2O)$ 1611, $\upsilon_{as}(COO)$ 1604, $\upsilon_s(COO)$ 1384, $\pi(C\text{-}H)_{ar}$ (3Meade) 805, $\pi(C\text{-}H)_{ar}$ (CBIDA) 645. UV-Vis and thermo-gravimetric analyses were not performed to compound **5** since it was not possible to have enough pure samples.

*[Cu(MIDA)(7Meade)($H_2O$)·4$H_2O$* (**6**). A similar synthetic procedure to compound **1** was followed using $Cu_2CO_3(OH)_2$ (0.25 mmol, 0.055 g), $H_2$MIDA acid (0.5 mmol, 0.075 g) and 7Meade (0.5 mmol, 0.074 g). In two months, small parallelepiped blue crystals appeared. After several re-crystallizations, the size of the crystals slightly improves and XDR analyses were performed. Yield of this synthesis is approx. 15-20%. Elemental analysis (%): Calc. for $C_{11}H_{24}CuN_6O_9$ (**5**) C 29.50, H 5.40, N 18.79; Found: C 29.64, H 5.32, N 18.60. FT-IR [KBr, $cm^{-1}$]: $\upsilon_{as}(H_2O)$ 3402, $\upsilon_{as}(NH_2)$ 3340, $\upsilon_s(H_2O)$ and $\upsilon_s(NH_2)$ overlapped 3232, $\upsilon_{as}(CH_3)$ 2973, $\upsilon_d(CH_3)$ 2857, $\upsilon_{as}(CH_2)$ 2927, $\upsilon_s(CH_2)$ 2825, $\delta(NH_2)$, $\delta(H_2O)$ and $\upsilon_{as}(COO)$ overlapped 1640, $\upsilon_s(COO)$ 1374, $\pi(C\text{-}H)_{ar}$ (7Meade) 789. UV-Vis and thermogravimetric analyses were not performed to compound **6** since it was not possible to have enough pure samples.

*[Cu(IDA)(9Meade)($H_2O$)$_2$]·3$H_2O$* (**7**). A similar synthetic procedure to compound **1** was followed using $Cu_2CO_3(OH)_2$ (0.25 mmol, 0.055 g), $H_2$IDA acid (0.5 mmol, 0.116 g) and 9Meade (0.5 mmol, 0.074 g). In two weeks, needle-like blue crystals were collected for XRD purposes. Yield is ca. 80-85%. Elemental analysis (%): Calc. for $C_{10}H_{22}CuN_6O_9$ (**6**) C 27.68, H 5.11, N 19.37; Found: C 27.73, H 4.99, N 19.35. FT-IR [KBr, $cm^{-1}$]: $\upsilon_{as}(H_2O)$ 3419, $\upsilon_{as}(NH_2)$ 3337, $\upsilon_s(H_2O)$ and $\upsilon_s(NH_2)$ overlapped 3238, $\upsilon$ (N-H) overshadowed, $\upsilon_{as}(CH_3)$ 2965, $\upsilon_d(CH_3)$ overshadowed, $\upsilon_{as}(CH_2)$ 2934, $\upsilon_s(CH_2)$ 2858, $\delta(NH_2)$ 1653, $\delta(H_2O)$ 1620, $\delta$(N-H) overshadowed, $\upsilon_{as}$(COO) 1599, $\upsilon_s$(COO) 1385, $\pi$(C-H)$_{ar}$ (9MeAde) 791. The UV-Vis spectrum shows an asymmetric d-d band with $\lambda_{max}$ at 713 nm ($\nu_{max}$ 14025 $cm^{-1}$). The thermo-gravimetric curve is divided in five steps. Under air-dry flow, the sample losses nearly all the non-coordinated water molecules. Hence, the starting sample for the TG experiment agree to the formula [Cu(IDA)(9Meade)($H_2O$)$_2$]·0.4$H_2O$. The 0.4 water molecules as well as the two apical aqua ligands, in the 4+1+1 Cu(II) surrounding, are lost during the first step (n = 2.4, Calc. 11.172%; Found 11.661%). Consecutive steps are assigned to the pyrolysis of the organic ligands. FT-IR spectra of the evolved gasses show $H_2O$, $CO_2$, CO, $NH_3$ , TMA(t), as well as N-oxide gases ($N_2O$, NO and $NO_2$). Finally, it yields to a CuO residue at 530 ºC (Calc. 20.553%; Found 21.543%).

*{[Cu(MIDA)(9Meade)($H_2O$)]·2$H_2O$}$_n$* (**8**). The reaction was performed according to the procedure detailed for compound **7**, using $H_2$MIDA acid (0.5 mmol, 0.074 g) instead of $H_2$IDA acid. After six weeks, well-shaped parallelepiped blue crystals appeared, suitable for XRD purposes. Typical yield of this synthesis is ca. 80-85%. Elemental analysis (%): Calc. for $C_{11}H_{20}CuN_6O_7$ (**7**) C 32.08, H 4.89, N 20.41; Found: C 32.12, H 4.96, N 20.36. FT-IR [KBr, $cm^{-1}$]: $\upsilon_{as}(H_2O)$ 3452, $\upsilon_{as}(NH_2)$ 3380, $\upsilon_s(H_2O)$ 3182, $\upsilon_s(NH_2)$ 3136, $\upsilon_{as}(CH_3)$ 2977, $\upsilon_d(CH_3)$ 2861, $\upsilon_{as}(CH_2)$ 2932, $\upsilon_s(CH_2)$ 2859 , $\delta(NH_2)$ and $\delta(H_2O)$ overlapped 1635, $\upsilon_{as}$(COO) 1601, two types of $\upsilon_s$(COO) 1396 and 1384, $\pi$(C-H)$_{ar}$ (9MeAde) 793. The UV-Vis spectrum shows an asymmetric d-d band with $\lambda_{max}$ at 697 nm ($\nu_{max}$ 14347 $cm^{-1}$). The thermal behaviour of this compound is divided in four steps. Under air-dry flow, the sample loses all the solvent molecules and part of the apical aqua ligand, thus the TG experiment starts with an average formula [Cu(MIDA)(9Meade)($H_2O$)$_{0.8}$]. In the first step, the compound loses the rest of the remaining aqua (n = 0.8; Calc. 3.872%, Found 3.520%). Then, consecutive pyrolytic steps (from 170 to 490 ºC) yield to a CuO residue (Calc. 21.370%, Found 22.253%). The evolved gases during the pyrolysis are $H_2O$, $CO_2$, CO, $CH_4$, TMA, $NH_3$ and N-oxide gases ($N_2O$, NO and $NO_2$). TMA is also found in the second step and is typically observed from pyrolysis of MIDA chelating ligand.

*{[Cu(EIDA)(9Meade)]·4$H_2O$}$_n$* (**9**). The reaction was performed according to the procedure detailed for compound **7**, using $H_2$EIDA acid (0.5 mmol, 0.081 g) instead of $H_2$IDA acid. In four months, suitable needle-like blue crystals were collected for XRD purposes. Yield of the synthesis ca. 70-75%. Elemental analysis (%): Calc. for $C_{12}H_{24}CuN_6O_8$ (**8**) C 32.47, H 5.45, N 18.93; Found: C 32.50, H 5.13, N 18.88. FT-IR [KBr, $cm^{-1}$]: $\upsilon_{as}(H_2O)$ 3441, $\upsilon_{as}(NH_2)$ 3356, $\upsilon_s(H_2O)$ and $\upsilon_s(NH_2)$

overlapped 3185, $\upsilon_{as}(CH_3)$ 2981, $\upsilon_{d}(CH_3)$ 2877, $\upsilon_{as}(CH_2)$ 2940, $\upsilon_{s}(CH_2)$ overshadowed , $\delta(NH_2)$ and $\delta(H_2O)$ 1624 overlapped, $\upsilon_{as}(COO)$ 1606, two types of $\upsilon_{s}(COO)$ 1385 and 1394, $\pi(C\text{-}H)_{ar}$ (9Meade) 793. The UV-Vis spectrum shows an asymmetric d-d band with $\lambda_{max}$ at 671 nm ($\nu_{max}$ 14903 $cm^{-1}$). The sample losses nearly 40% of the water content under air-dry flow, thus the starting sample for the thermo-gravimetric experiment agree to the formula $\{[Cu(EIDA)(9Meade)]\cdot 1.5H_2O\}_n$. The remaining non-coordinated water is lost during the first step (30–160 °C; Calc. 6.775%; Found 6.393%). The following pyrolytic steps lead to the decomposition of the sample producing $H_2O$, $CO_2$, CO, $CH_4$, $NH_3$ and N-oxide gases ($N_2O$, NO, $NO_2$) to yield, at 540 ºC, a final CuO residue (Calc. 19.942%; Found 20.723%).

*[Cu(NBzIDA)(9MeAde)($H_2O$)]·4$H_2O$* (**10**). The reaction was performed according to the procedure detailed for compound **7**, using $H_2$NBzIDA acid (0.5 mmol, 0.116 g) instead of $H_2$IDA acid. In two weeks, parallelepiped greenish crystals appeared, suitable for XRD purposes. Typical yield of this synthesis is ca. 90%. Elemental analysis (%): Calc. for $C_{17}H_{28}CuN_6O_9$ (**9**) C 38.97, H 5.39, N 16.04; Found C 38.56, H 5.00, N 16.34. FT-IR [KBr, $cm^{-1}$]: $\upsilon_{as}(H_2O)$ 3389, $\upsilon_{as}(NH_2)$ overshadowed, $\upsilon_{s}(H_2O)$ and $\upsilon_{s}(NH_2)$ overlapped 3197, $\upsilon_{as}(CH_3)$ 2962, $\upsilon_{d}(CH_3)$ 2847, $\upsilon_{as}(CH_2)$ overshadowed, $\upsilon_{s}(CH_2)$ overshadowed, $\delta(NH_2)$ and $\delta(H_2O)$ overlapped 1621, $\upsilon_{as}(COO)$ 1597, $\upsilon_{s}(COO)$ 1384, $\pi(C\text{-}H)_{ar}$ (9Meade) 795, $\pi(C\text{-}H)_{ar}$ (NBzIDA) 716. The UV-Vis spectrum shows an asymmetric d-d band with $\lambda_{max}$ at 748 nm ($\nu_{max}$ 13369 $cm^{-1}$). The thermo-gravimetric curve is divided in four steps. Under air-dry flow, the sample losses part of the solvent molecules, thus the TG experiment starts with an average formula [Cu(NBzIDA)(9Meade)($H_2O$)]·0.9$H_2O$. The 0.9 water molecules as well as the apical aqua ligand, in the 4+1 Cu(II) surrounding, are lost during the first step (n = 1.9, Calc. 7.099%; Found 7.245%). This is in accordance with the recorded evolved gases during such step where only $H_2O$ was identified. In the following pyrolytic steps (from 110 to 545 ºC), the sample is decomposed producing $H_2O$, $CO_2$, CO and N-oxide gases ($N_2O$, NO, $NO_2$) to yield a final CuO residue within the experimental error (Calc. 16.497%; Found 17.888%).

*[Cu(MEBIDA)(9MeAde)($H_2O$)]·3$H_2O$* (**11**). The reaction was performed according to the procedure detailed for compound **7**, using $H_2$MEBIDA acid (0.5 mmol, 0.118 g) instead of $H_2$IDA acid. In three weeks, parallelepiped greenish crystals appeared, suitable for XRD purposes. Yield ca. 90%. Elemental Analysis (%): Calc. for $C_{18}H_{28}CuN_6O_8$ (**10**), C 41.58, H 5.43, N 16.16; Found C 41.64, H 5.40, N 16.05. FT-IR [KBr, $cm^{-1}$]: $\upsilon_{as}(H_2O)$ 3369, $\upsilon_{as}(NH_2)$ overshadowed, $\upsilon_{s}(H_2O)$ and $\upsilon_{s}(NH_2)$ 3184 overlapped, two types of $\upsilon_{as}(CH_3)$ 2981 and 2967, $\upsilon_{d}(CH_3)$ 2860, $\upsilon_{as}(CH_2)$ 2922, $\upsilon_{s}(CH_2)$ overshadowed, $\delta(NH_2)$ and $\delta(H_2O)$ overlapped 1620, $\upsilon_{as}(COO)$ 1597, $\upsilon_{s}(COO)$ 1384, $\pi(C\text{-}H)_{ar}$ (9MeAde) 795, $\pi(C\text{-}H)_{ar}$ (MEBIDA) 807. The UV-Vis spectrum shows an asymmetric d-d band with $\lambda_{max}$ at 738 nm ($\nu_{max}$ 13550 $cm^{-1}$). The thermal behaviour of **2** is divided in five steps. Under air-dry flow, the sample losses almost all the non-coordinated water. Hence the TG experiment starts with an average formula [Cu(MEBIDA)(9Meade)($H_2O$)]·0.7$H_2O$. In the first step, the sample experiments the loss of 1.7 water molecules (Calc. 6.593%; Found 6.390%). Then, consecutive steps

are assigned to the pyrolysis of the organic ligands. FT-IR spectra of the evolved gasses show $H_2O$, $CO_2$, CO, $CH_4$ plus N-oxide gases such as $N_2O$, NO and $NO_2$. Finally, it yields to a CuO residue (550 ºC; Calc. 16.497%; Found 17.888%).

*[Cu(CBIDA)(9Meade)($H_2O$)]·$H_2O$* (**12**). The reaction was performed according to the procedure detailed for compound **7**, using $H_2$CBIDA acid (0.5 mmol, 0.129 g) instead of $H_2$IDA acid. In one month, very thing needle-like crystals appeared, not suitable for XRD purposes. Such solution was filtered several times in an attempt to improve the size of the crystals. After two months, some parallelepiped blue crystals appeared although it was impossible to isolate good quality ones. Therefore, a new strategy of synthesis was followed: to a new 50 mL solution the aforementioned binary chelate [$Cu_2CO_3(OH)_2$ (0.25 mmol, 0.055 g) + $H_2$CBIDA acid (0.5 mmol, 0.129 g)], a 40 mL solution of the base pair 9Meade:Thymine (0.5 mmol, 0.074 g: 0.063 g) was added. The reacting mixture was stirred for 12 hours at room temperature. After one month, good shape parallelepiped crystals were collected for XRD purposes with a yield of 30-35%. One month later, crystals of free thymine, free 9Meade and the above-mentioned needle-like blue crystals appeared. The former free ligands were identified by FT-IR spectroscopy. The two kind of blue crystals (parallelepiped and needle-like) were characterised by elemental analysis, thermo-gravimetry and FT-IR spectroscopy. Moreover, UV-Vis and XRD was only carried out for the parallelepiped blue crystals. (i) Parallelepiped crystals: Elem. Anal. (%) for $C_{17}H_{21}ClCuN_6O_6$ (**11**) Calc. C 40.48, H 4.20, N 16.66; Found C 38.15, H 5.35, N 16.20. FT-IR (KBr) $cm^{-1}$: $\upsilon_{as}(H_2O)$ 3435, $\upsilon_{as}(NH_2)$ 3369, $\upsilon_s(H_2O)$ 3250 (sh), $\upsilon_s(NH_2)$ 3192, $\upsilon_{as}(CH_3)$ 2977, $\upsilon_d(CH_3)$ 2853, $\upsilon_{as}(CH_2)$ 2927, $\upsilon_s(CH_2)$ 2846, $\delta(NH_2)$ and $\delta(H_2O)$ overlapped 1623, $\upsilon_{as}(COO)$ 1596, $\upsilon_s(COO)$ 1385, $\pi(C\text{-}H)_{ar}$ (9Meade) 795, $\pi(C\text{-}H)_{ar}$ (CBIDA) 641. The UV-Vis spectrum shows an asymmetric d-d band with $\upsilon_{max}$ at 14306 $cm^{-1}$. The thermo-gravimetric curve shows four steps. Under dry-air flow, the sample remains stable so that is in the first step when the two water molecules are lost (n = 2, Calc. 7.143%; Found 6.9715), according to the evolved gasses. The three following steps (from 170 ºc to 760 ºC) concern the pyrolysis of the dehydrated compound [Cu(CBIDA)(9MeAde)]. Herein, the $H_2O$, $CO_2$, CO, $CH_4$ and N-oxide gases ($N_2O$, NO, $NO_2$) were identified. A residue of CuO was found at 760 ºC within the experimental error (Calc. 15.770%; Found 14.882%). (ii) Needle-like crystals: Elem. Anal. (%): Calc. for $C_{28}H_{27}Cl_2Cu_2N_7O_8$ (12) Calc. C 34.75, H 4.90, N 10.13; Found C 34.78, H 5.02, N 10.03. These data is in accordance to a formula type $[Cu_2(CBIDA)_2(\mu_2\text{-}9Meade)(H_2O)_2]\cdot 8H_2O$. Considering that the same chromophores would be present in both samples, no relevant differences are found between this and the above described FT-IR. However, it should be noted that those bands related with water are significantly broaden what is in accordance to our proposed model. Likewise, the thermo-gravimetric analysis of the needle-like crystals is also in agreement with higher water content. In this case, the compound would loose the major part of the water content under dry-air flow, starting the TG experiment with a formula $[Cu_2(CBIDA)_2(\mu_2\text{-}9Meade)(H_2O)_2]\cdot 0.5H_2O$. Thus, the first step of the thermo-gravimetric curve agrees to the loss of 2.5 water molecules (from 20 to 160 ºC; n = 2.5 Calc. 5.409%; Found 5.060%). A slightly different decomposition for this compound is evidenced by the

gases evolved during the pyrolysis: $H_2O$, $CO_2$, CO, CHO and N-oxide gases ($N_2O$, NO, $NO_2$). The pyrolysis of the ligand yields to an impure residueo of CuO. Further attempts to crystallize the supposed compound $[Cu_2(CBIDA)_2(\mu_2\text{-}9Meade)(H_2O)_2]\cdot 8H_2O$ have not been successful.

2.3. Crystallographyc methods

Measured crystals were prepared under inert conditions immersed in perfluoropolyether as protecting oil for manipulation. Suitable crystals were mounted on MiTeGen Micromounts™ and these samples were used for data collection. Data were collected with Bruker SMART APEX (**1**-**8**, 293 K), Bruker X8 KappaAPEXII (**9**-**12**, 100 K) diffractometers. The data were processed with APEX2 [4] program and corrected for absorption using SADABS.[5] The structures were solved by direct methods [6], which revealed the position of all non-hydrogen atoms. These atoms were refined on $F^2$ by a full-matrix least-squares procedure using anisotropic displacement parameters.[6] All hydrogen atoms were located in difference Fourier maps and included as fixed contributions riding on attached atoms with isotropic thermal displacement parameters 1.2 times those of the respective atom. Geometric calculations were carried out with PLATON [7] and drawings were produced with PLATON [7] and MERCURY [8]. Crystallographic data for the structural analysis will be deposited with the Cambridge Crystallographic Data Centre. Copies of this information could be obtained free of charge on application to CCDC, 12 Union Road, Cambridge CB2 1EZ, UK (fax: 44 1223 336 033; e-mail: deposit@ccdc.cam.ac.uk or http://www.ccdc.cam.ac.uk).

2.4. Physical measurements

Analytical data were obtained in a Fisons–Carlo Erba EA 1108 elemental micro-analyser. Infrared spectra were recorded by using KBr pellets on a Jasco FT-IR 6300 spectrometer. TG analysis (pyrolysis) of the studied compounds (295–800 ºC) were carried out in air flow (100 mL/ min) by a Shimadzu Thermobalance TGA–DTG–50H instrument, and a series of FT-IR spectra (20–30 per sample) of evolved gasses were recorded for the studied compounds using a coupled FT-IR Nicolet Magma 550 spectrometer. Electronic (diffuse reflectance) spectra were obtained in a Varian Cary-5E spectrophotometer.

## 3. Results and discussions

Compound **1**, $[Cu(CBIDA)(1Meade)(H_2O)_2]\cdot 3H_2O$, consists of a complex molecule and non-coordinated water molecules. The Cu(II) centre is satisfied by three donor atoms from the tridentate chelating ligand CBIDA (N10, O11, O12), in mer-$NO_2$ conformation, the N7 donor of 1Meade and one apical aqua ligand (Fig.1). The metal exhibits a vaguely distorted 4+1 coordination polyhedron, with an Addison parameter of $\tau = 0.04$. The Cu-N7 bond is assisted by an intra-molecular interligand

interaction. The dihedral angle between the mean coordination basal plane and the 1Meade plane is 28.09º.

In the crystal of **1**, adjacent complex molecules are linked by inter-molecular H-bonds using the N6-H(1Meade) exocyclic amino group [N6-H(6A)···O12(non-coord. carboxy, 2.8475(2) Å, 153.2º)]. These 1D chains are further associated by symmetry related H-bonding interactions that involve the apical aqua ligand [O1-H(1A)···O22(non-coord. carboxy, 2.6449(17) Å, 169.7º) and O1-H(1B)···O12(non-coord. carboxy, 2.763(2) Å, 173.9º)], building 2D layers. Finally, inter-molecular interactions such as H-bonds and very weak but massive pi,pi-stacking interactions accomplish the 3D array.

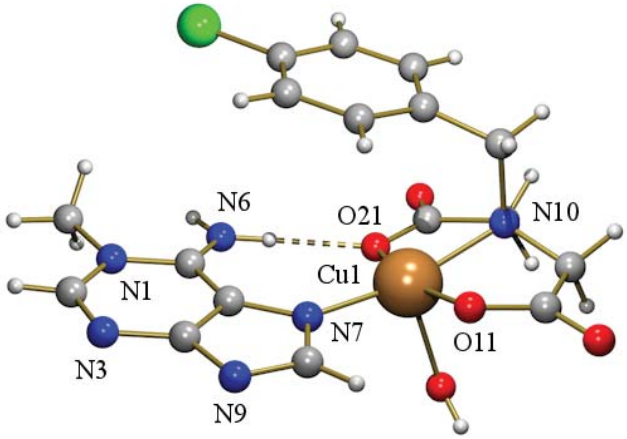


Fig. 1. Complex molecule in the compound $[Cu(CBIDA)(1Meade)(H_2O)_2]\cdot 3H_2O$ (1). Cu-N7 bond 1.972(2) Å, H-bonding interaction: N6-H(6B)···O21(coord. carboxy, 2.801(2) Å, 172.0º).

Compound **2**, $[Cu(IDA)(3Meade)(H_2O)_2]\cdot 3H_2O$**,** consists of one complex molecule and non-coordinated water molecules. The copper(II) atom exhibits a 4+1+1 coordination polyhedron where the four closest donor atoms are supplied by the tridentate-chelating IDA ligand (N10, O11, O12), adopting a mer-$NO_2$ conformation, the N7 atom from 3Meade and two apical aqua ligands. Note that the Cu-N7 bond is reinforced by the intra-molecular interligand N6–H···O21(coord. carboxy, 2.720(6) Å, 162.0º) interaction.

The crystal packing of **2** reveals similarities to compound **1**. Thus, inter-molecular H-bonds, involving the exocyclic amino group [N6-H(6B)...O12(non-coord. carboxy 2.906(6) Å, 148.9º], build ribbons along the b axis (Fig. 2). Additional symmetry related H-bonding interactions achieve corrugated layers where the apical aqua ligand plays a key role [O2-H(2A)···O11(coord. carboxy, 2.839(6) Å, 167.2º and O2-H(2B)···N1 (2.827(6) Å, 162.0º)]. Besides, weak pi,pi-stacking interactions between the 6-membered rings of adjacent 3MeAde ligands help to extra-stabilise the refereed 2D layers. Inter-molecular H-bonding interactions via non-coordinated water molecules lead to the 3D architecture.

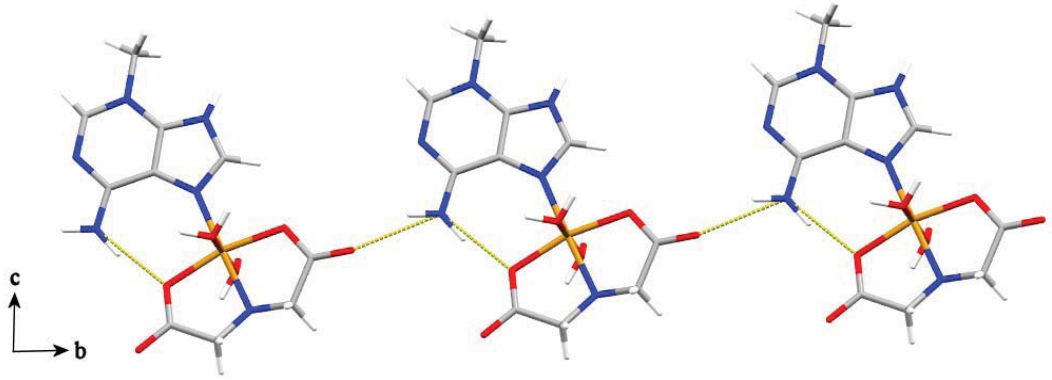


Fig. 2. View of the 1D chains in [Cu(IDA)(3Meade)($H_2O$)$_2$]·3$H_2O$ (**2**) extending along the b axis. Similar interactions are also found in compound **1** and **3**.

Compounds **3** and **4** show the same type of formula: [Cu(IDA-like)(3Meade)($H_2O$)]·n$H_2O$ (where IDA-like = MIDA and n = 6 in **3**; IDA-like = NBzIDA and n = 2 in **4**). Herein, the Cu(II) atoms adopt a nearly regular square-base pyramidal coordination [$\tau$ = 0.05 (**3**) and $\tau$ = 0.075 (**4**)]. In both cases, the basal coordination plane is defined by the tridentate mer-$NO_2$ IDA-like ligand (N10, O11, O21) and the N7(3Meade) donor, while the apical site is occupied by one aqua ligand. Again, the Cu-N7 bond cooperates with an intra-molecular interaction N6–H···O21(coord. carboxy, 2.801(3) Å, 173.2º in **3**; 2.911(3) Å, 149.1º in **4**). The dihedral angle between the basal coordination plane and the 3Meade plane are quite dissimilar, moving from 17.77º in **2** until almost 40º in **4**.

The crystal packing of **3** also resembles compound **2**. 1D chains are built along the b axis by means of inter-molecular interactions that involve the exocyclic amino group [N6-H(6A)...O12(non-coord. carboxy, 2.921(3) Å, 157.6º]. Then, the apical aqua ligand associates, by symmetry related H-bonds, adjacent 1D structures leading to corrugated layers [O1-H(1B)···O11(non-coord. carboxy, 2.957(3) Å, 161.1º and O1-H(1A)...N1 (2.922(3) Å, 176.7º)]. The 3D network is reached thanks to inter-molecular interactions that involve the non-coordinated water molecules. In contrast, the crystal of compound **4** is built is a different manner. In **4**, pairs of complex molecules build staircase ribbons by means of symmetrically related inter-molecular H-bonding interactions [O1-H(1B)···N9 (2.854(3) Å, 174.7º and O1-H(1A)···O22(non-coord. carboxy, 2.768(3) Å, 167.7º)]. Neighbouring ribbons are further associated by pi,pi-stacking interaction between the 5-membered ring of 3Meade and the benzyl moiety of NBzIDA, also building corrugated layers parallel to the ac plane (Fig. 3). In addition, H-bonds that comprise non-coordinated water molecules build the 3D network.

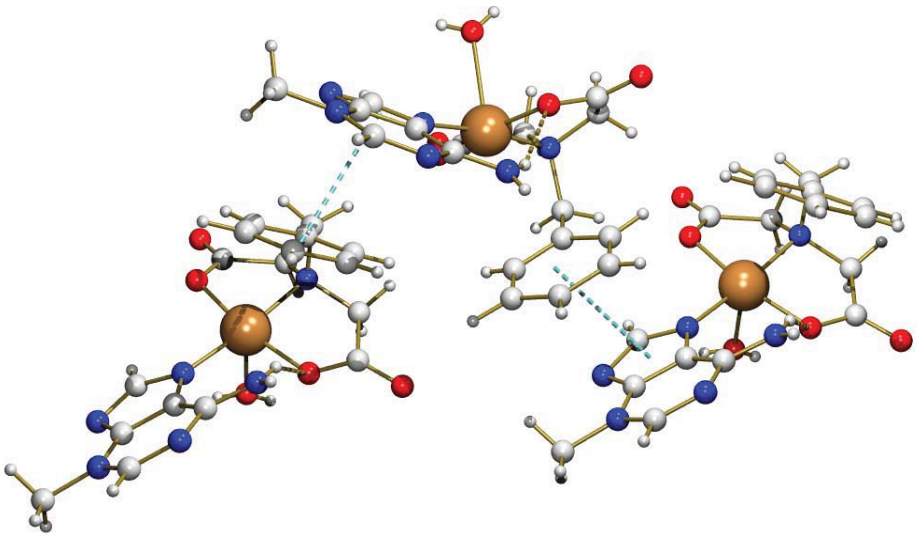

Fig. 3. Detail of pi,pi-stacking interactions that lead to the 2D supramolecular structure in compound **4**.

The molecular nature of compounds **2**-**4** is in contrast to that of compound **5**, which is based on a coordination polymer built by means of the syn–anti carboxylate bridging role of CBIDA ligand, according to the formula $\{[Cu(CBIDA)(3MeAde)]\cdot H_2O\}_n$. Despite this fact, the metal centre in **5** also shows a 4+1 coordination polyhedron where the four closest donor atoms corresponds to the tridentate CBIDA chelating ligand (N10, O11, O21) and the N7 donor of 3MeAde. Thus CBIDA adopts a mer-$NO_2$ conformation. One O-bridging atom from an adjacent carboxylate group occupies the apical position. Once more, the Cu-N7 bond is reinforced by an intra-molecular interligand H-bonding interaction N6–H···O21(coord. carboxy, 2.900(2) Å, 165.0º) (Fig. 4). In this polymer, the distortion in the Cu(II) mean basal plane is rather low, with a τ value of 0.03, while the dihedral angle between the coordination basal plane and the 3Meade plane is evidenced by an angle of 32.20º.

In the crystal of **5**, polymeric chains run along the b axis, connecting to each other by inter-molecular interactions that involve the disordered solvent molecule and pairs of adjacent bases via very weak Watson-Crick H-bonds. These latter interactions build 2D layers which are further associated by hydrophobic interactions comprising the chloride atoms.

Compound **6**, $[Cu(MIDA)(7Meade)(H_2O)\cdot 4H_2O$**,** consists of one complex molecule and non-coordinated water. The metal centre is built by the three donors of the tridentate MIDA chelating ligand (N10, O11, O12), adopting a mer-$NO_2$ conformation, and the N3(7Meade) donor atom. The apical site is occupied by one aqua ligand. It is noteworthy that this molecular recognition pattern does not enable the cooperation of the Cu-N3 bond with an intra-molecular interaction since (i) there is no tautomerizable proton in methyladenines; (ii) the chelators only offers H-acceptors (O-carboxylate) as terminal groups. In this complex, the Cu(II) coordination environment is very close to a square pyramidal coordination, according to the Addison parameter (τ = 0.025).

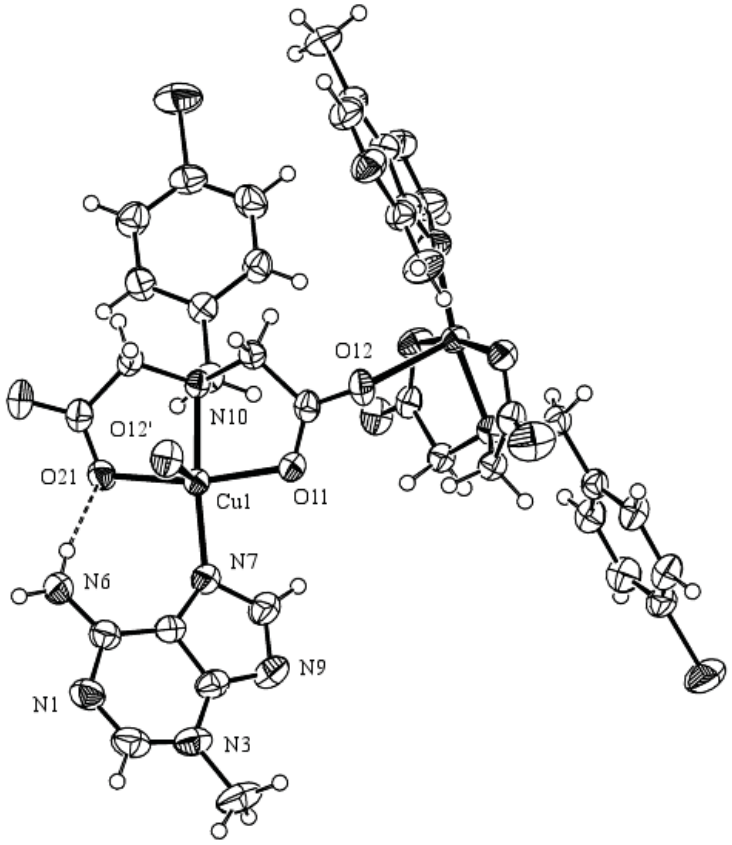


Fig. 4. Ortep view of one polymeric fragment in $\{[Cu(CBIDA)(3MeAde)]\cdot H_2O\}_n$ (**5**). Ellipsoid probability at 50%.

In the complex molecule, the nucleobase 7Meade is nearly perpendicular to the mean basal coordination plane (dihedral angle is almost 83º) what seems significantly influenced by the crystal packing. Indeed, in the crystal, the apical aqua ligand [O1-H(1B)···O12(non-coord. carboxy, 2.764(5) Å, 171.1º)] and the N6-exocyclic amino group is involved in inter-molecular H-bonds building 1D chains along the a axis [N6-H(6A)···O11(coord. carboxy, 2.911(5) Å, 153.9º and N6-H(6B)···O21(coord. carboxy, 2.895(5) Å, 153.7º)]. In addition, very weak but massive pi,pi-stacking interactions connect adjacent 7Meade moieties within the 1D chains (Fig. 5). Inter-molecular H-bonds involving the non-coordinated water molecules complete the 3D framework.

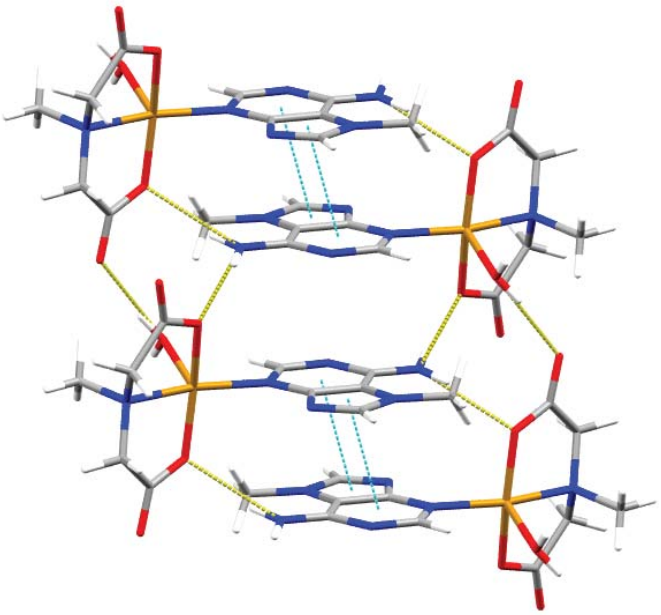

Fig. 5. View in the ac plane of the 1D chains in the compound [Cu(MIDA)(7Meade)($H_2O$)·4$H_2O$ (**6**). H-bonding and pi,pi-stacking interactions that contribute to stabilise the referred 1D structure are depicted.

Compound **7**, [Cu(IDA)(9Meade)($H_2O$)$_2$]·3$H_2O$, consists of a complex molecule and water molecules. In the complex molecule, the Cu(II) atom exhibits a 4+1+1 coordination polyhedron. The metal surrounding is built by three donors (N10, O11, O22) from the mer-$NO_2$ tridentate IDA chelating ligand, the N7 donor from 9MeAde and two aqua ligands placed in the apical sites. The apical coordination distances are quite different [Cu1-O1 2.452(3) Å and Cu1-O2 2.879(4) Å]. Surprisingly, the Cu-N7 bond is not assisted by an intra-molecular H-bond as previously referred from compounds **1-5** but it is involved in inter-molecular interactions. This fact may also contribute to the high value of the dihedral angle between the mean basal coordination plane and the 9MeAde plane (62.67º).

In the crystal, pairs of complex molecules build multi-stacked chains running along the a axis that are extra-stabilised by symmetry related inter-molecular H-bonds that involve one apical aqua ligand as H-donor, [O1-H(1A)···N3 (2.902(5) Å, 168.7º) and O1-H(1B)···O22(non-coord. carboxy, 2.718(5) Å, 169.3º). Adjacent chains are connected via N1-H1···O1 (3.023(5) Å, 160.2º) leading to 2D layers that are further connected by non-coordinated water molecules o achieve the 3D network.

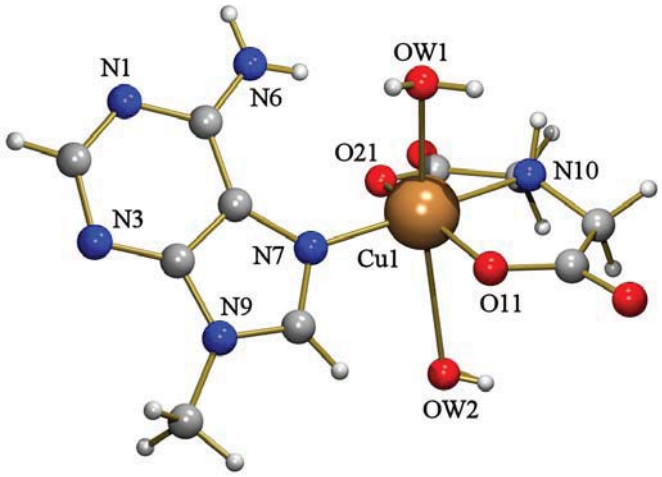


Fig. 6. Complex molecule in $[Cu(IDA)(9Meade)(H_2O)_2]\cdot 3H_2O$ (**7**). Cu-N7 bond 1.975(2) Å.

Compound **8**, $\{[Cu(MIDA)(9Meade)(H_2O)]\cdot 2H_2O\}_n$, is based on a coordination polymer built by the anti-anti role of the carboxylate groups of MIDA. The Cu(II) centre is octahedral. In the Cu(II) basal plane, the four closest donors are supplied by the tridentate chelator MIDA (N10, O11, O12), adopting a mer-$NO_2$ conformation, and by the 9MeAde via N7. Herein, the Cu-N7 is in cooperation with an intra-molecular interligand H-bond N6-H(6A)···O21(coord. carboxy, 2.752(3) Å, 158.5º). This fact favours the coplanarity of the Cu(II) chelate and the nucleobase, being the dihedral angle between the mean basal coordination plane and the 9MeAde plane 5.29º. The apical sites are occupied by one aqua ligand (Cu-O 2.710(2) Å) and one O-bridging atom from a carboxylate group of an adjacent MIDA chelating ligand (Cu-O22 2.4189(2) Å).

In the crystal, the polymeric chains that run parallel to the a axis showing a zig-zag topology. The apical aqua ligand promotes the connection between adjacent polymeric chains by means of inter-molecular H-bonds O1-H(1A)···N1 (2.868(3) Å, 165.6º). Likewise, very weak pi,pi-stacking interactions help to stabilise the 2d layers. Additional H-bonds that involve the non-coordinated water molecules and the apical aqua ligand, finally reach the 3D array.

Compound **9,** $\{[Cu(EIDA)(9Meade)]\cdot 4H_2O\}_{n,}$ is based on a coordination polymer built by the syn-anti role of the carboxylate groups of EIDA. The Cu(II) centre adopts a slightly distorted square-base pyramidal coordination ($\tau = 0.2$). The basal coordination plane is defined by the tridentate mer-$NO_2$ EIDA chelating ligand (N10, O11, O21) and the N7(9MeAde) donor while the apical site is occupied by O-bridging atom from an adjacent carboxylate group. Again, the Cu-N7 bond is reinforced by an intra-molecular interligand interaction N6-H(6A)···O21(coord. carboxy, 2.892(5) Å, 159.8º). In this case, the value of the dihedral angle is a bit higher 24.11º.

In the crystal of **9**, polymeric chains run along the a axis. Adjacent chains connect building zip-like layers by means of pi,pi-stacking interactions. Finally, the 3D network is accomplished by non-coordinated water molecules (Fig. 7).

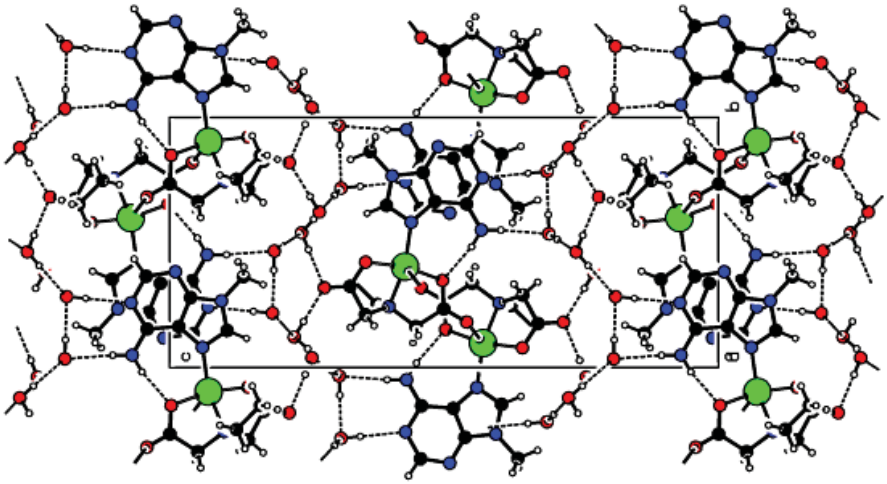

Fig. 7. 3D architecture in the crystal of $\{[Cu(EIDA)(9Meade)]\cdot 4H_2O\}_n$ (**9**). The copper(II) atoms is highlighted in green.

Compound **10,** $[Cu(NBzIDA)(9MeAde)(H_2O)]\cdot 4H_2O$, consists of a complex molecule and non-coordinated water molecules. The metal centre shows a slightly distorted square-pyramidal coordination ($\tau = 0.1$) satisfied by three donors of the chelating ligand NBzIDA (N10, O11 and O12) and by the N7 donor of 9MeAde. Thus, NBzIDA adopts a mer-$NO_2$ confirmation. The apical position is occupied by one aqua ligand. The Cu-N7 is assisted by an intra-molecular interligand H-bonding interaction N6-H(6A)···O21(coord. carboxy, 2.821(3) Å, 172.4º). The dihedral angle, defined by the mean basal coordination plane and the 9MeaAde plane is rather low as expected (17.18º).

In the crystal, multi-stacked chains run along the a axis involving the 5-membered ring of 9Meade and the benzyl moiety of NBzIDA ligand (Fig. 8). These chains are further connected thanks to H-bonds that involve the exocyclic amino group and the apical aqua ligand building 2D layers that extend along the ab plane of the crystal. Further H-bonding interactions complete the 3D structure.

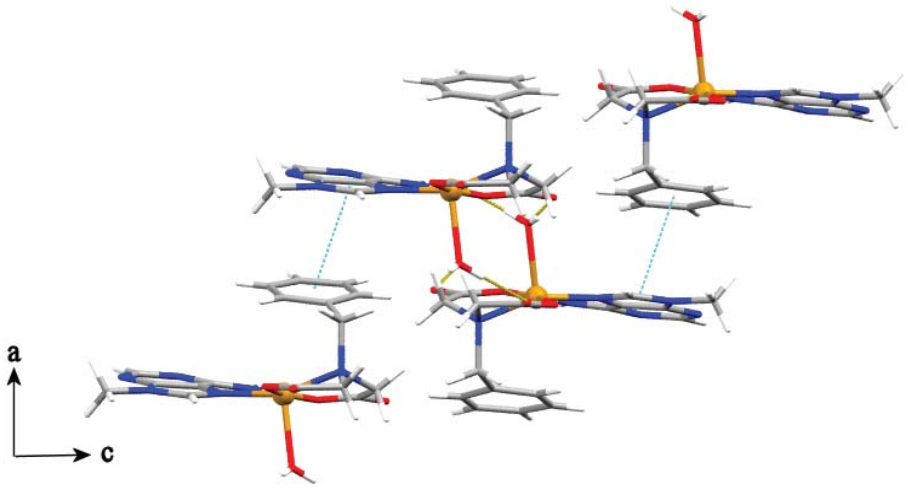


Fig. 8. View in the ac plane of $[Cu(NBzIDA)(9MeAde)(H_2O)]\cdot 4H_2O$ (**10**). The intra-chain pi,pi-stacking interactions are shown.

Compound **11**, [Cu(MEBIDA)(9MeAde)($H_2O$)]·3$H_2O$, consists of a molecular complex plus non-coordinated water molecules. The Cu(II) atom exhibits a 4+1 coordination satisfied by the N10, O11 and O12 donors from the mer-$NO_2$ tridentate MEBIDA chelating ligand and by the N7 atom of 9Meade. The apical site corresponds to one aqua ligand. Again, the Cu-N7 is assisted by an intra-molecular interligand H-bond N6-H(6A)···O21(coord. carboxy, 2.815(2) Å, 169.8º). The Cu(II) surrounding is a bit distorted, with an Addison parameter of $\tau = 0.15$. As previously commented for compound **10**, the dihedral angle is also quite low (15.87º).

In the crystal, multi-stacked chains run along the c axis involving the 5-membered ring of 9MeAde and the aromatic moiety of MEBIDA. These chains are further associated by H-bonds between the exocyclic amino group and O-carboxylate atoms from adjacent units leading to a 2d structure that extend parallel to the bc plane of the crystal and which is reinforced by H-bonding interactions that involve non-coordinated water molecules. Adjacent layers are associated via H-bonds involving aqua ligands and carboxylate group reaching a 3D structure.

Compound **12**, [Cu(CBIDA)(9Meade)($H_2O$)]·$H_2O$ consists of a complex molecule and one solvent molecule. The Cu(II) centre is satisfied by three donor atoms from the tridentate chelating ligand CBIDA (N10, O11, O12), in mer-$NO_2$ conformation, the N7 donor of 9Meade and one apical aqua ligand. The metal exhibits a vaguely distorted 4+1 coordination polyhedron, with an Addison parameter of $\tau = 0.075$. The Cu-N7 bond is assisted by an intra-molecular interligand interaction N6-H(6A)···O21(coord. carboxy, 2.782 Å, 167.6º). The dihedral angle between the mean coordination basal plane and the 9Meade plane is 39.54º.

In the crystal, complex molecules build staircase 2D ribbons by means of alternating H-bonding interactions that involve the apical aqua ligand [O1-H(1B)···O22(non-coord. carboxy, 2.701(2) Å, 166.4º)] and the N6 and N1 donors of the adenine moiety in an Watson-Crick-like interaction [N6-H(6B)···N1 (3.036(2) Å, 173.21º)] (Fig. 9). The non-coordinated water molecule also contributes in the stabilization of this 2D structure. Hydrophobic interactions connect adjacent ribbons to build the 3D network.

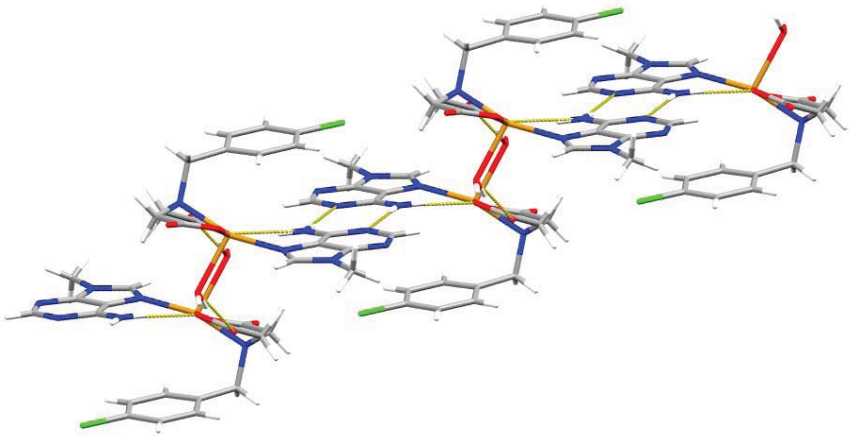

Fig. 9. Detail of the ribbons built in [Cu(CBIDA)(9Meade)($H_2O$)]·$H_2O$ (**12**). The contribution of the non-coordinated water molecule is omitted for clarity reason.

## 3. Concluding remarks

The use of N1, N3 and N9-methyladenines in ternary with copper(II)-iminodiacetate chelates, highlights the metal binding mode Cu-N7 + N6-H···O. These finding suggest that the latter molecular recognition patterns are highly influenced by the facts that, in the referred N-methyladenines, (i) N7 is less sterically hindered that N1, N3 or N9 regarding coordination of metal ions and (ii) the possibility of assisting the Cu-N bond with the corresponding H-bond. The only way to prevent the formation of the Cu-N7 bond in the studied compounds is the use of 7Meade. In the ternary complex Cu(IDA-like)(7Meade), the metal ion binds 7Meade via the minor groove binder N3. This pattern does not allow any kind of reinforcement since no tautomerizable proton is available. The reasons why this particular complex prefers to coordinate the N-ligand by N3 instead of N9 remains quite unclear.

## References

[1] E. Bugella-Altamirano, D. Choquesillo-Lazarte, J.M. González-Pérez, M.J. Sánchez-Moreno, R. Marín-Sánchez, J.D. Martín-Ramos, B. Covelo, R. Carballo, A. Castiñeiras, J. Niclós-Gutiérrez. Inorg. Chim. Acta 339 (2002) 160.

[2] M.J. Sánchez Moreno, D. Choquesillo-Lazarte, J.M. González-Pérez, R. Carballo, A. Castiñeiras, J. Niclós-Gutiérrez, Inorg. Chem. Commun. 5 (2002) 800.

[3] P. X. Rojas-González, Duane Choquesillo-Lazarte, J. M. González-Pérez, S.A. Ruíz-García, R. Carballo, A. Castiñeiras, J. Niclós-Gutiérrez, Polyhedron 22 (2003) 1027.

[4] BRUKER, APEX2 Software, Bruker AXS Inc., V2010.11, Madison, Wisconsin, USA, 2010.

[5] G.M. Sheldrick, SADABS, Program for Empirical Absorption Correction of Area Detector Data, University of Göttingen, Germany, 2009.

[6] G.M. Sheldrick, Acta Crystallogr. A64 (2008) 112.

[7] A.L. Spek, PLATON. A Multipurpose Crystallographic Tool, Utrecht University, Utrecht, The Netherlands, 2010.

[8] C.F. Macrae, I.J. Bruno, J.A. Chisholm, P.R. Edgington, P. McCabe, E. Pidcock, L. Rodriguez-Monge, R. Taylor, J. van de Streek and P.A. Wood, J. Appl. Cryst. 41 (2008) 466.

# CHAPTER 4:

Studies concerning synthetic nucleosides

## 4.1. Metal ion binding patterns of acyclovir: Molecular recognition between this antiviral agent and copper(II) chelates with iminodiacetate or glycylglycinate

Article published in *J. Inorg. Biochem*. 105 (2011) 616-623

### SYNOPSIS

Glycylglycinate-Cu(II) chelate and acyclovir recognize each other by the Cu-N7(acv) bond and the intra-molecular interaction (glygly) N-H···O6(acv). Such interligand interaction cannot be built in the complex Cu(iminodiacetate)-acv because IDA ligand does not offer suitable terminal H-donor groups.

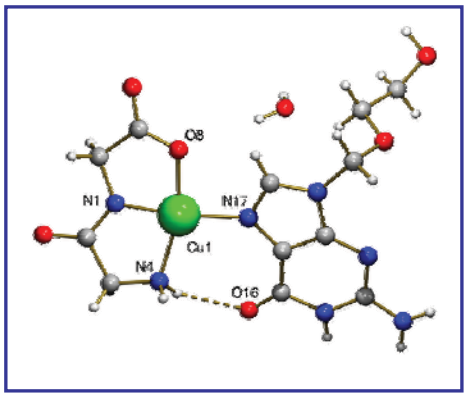


### RESUMEN

Con el propósito de ahondar en los modos de unión a metales de aciclovir (acv), los compuestos $\{[Cu(IDA)(acv)]\cdot 2MeOH\}_n$ (**1**) y $[Cu(glygly)(acv)]\cdot H_2O$ (**2**) han sido sintetizados e investigados mediante cristalografía de Rayos-X, así como otras técnicas espectrales y térmicas. Dichos compuestos han sido elegidos bajo el supuesto que los ligandos quelantes iminodiacetato (IDA) y glicilglicinato (glygly) pueden unirse al cobre(II) adoptando una conformación *mer*-tridentada, aportando dos grupos carboxilatos terminales como aceptor de hidrógenos (IDA) o un grupo carboxylato aceptor de hidrógeno y un grupo amino primario como dador de hidrógenos (glygly). El principal objetivo de este trabajo es esclarecer si el grupo amino presente en glygly puede participar en interacciones de enlace de hidrógeno intra-moleculares interligando para reforzar el enlace Cu-N7 (acv). Nuestros resultados se discuten en el contexto de una revisión actualizada y crítica de información estructural relacionada. Desde el punto de vista del reconocimiento molecular, la estructura **1** muestra que el reconocimiento quelato-nucleósido sólo involucra al enlace de coordinación Cu-N7(acv). Por el contrario, el complejo número **2** muestra el enlace Cu-N7(acv) reforzado por un enlace de hidrógeno (glygly)N–H···O6(acv, 2.961(3) Å, 140.5°).

# Structural insights on the molecular recognition patterns between $N^6$-substituted adenines and N-(aryl-methyl)iminodiacetate copper(II) chelates

Alicia Domínguez-Martín[a*], Ángel García-Raso[b], Catalina Cabot[c], Duane Choquesillo-Lazarte[d], Inmaculada Pérez-Toro[a], Antonio Matilla-Hernández[a], Alfonso Castiñeiras[e], Juan Niclós-Gutiérrez[a]

[a] Department of Inorganic Chemistry, Faculty of Pharmacy, Campus Cartuja, University of Granada, E-18071 Granada, Spain.
[b] Department of Chemistry, Group of Bioinorganic and Bioorganic Chemistry, University of Illes Balears, E-07122 Palma, Spain.
[c] Department of Biology, Group of Bioinorganic and Bioorganic Chemistry, University of Illes Balears, E-07122 Palma, Spain.
[d] Laboratorio de Estudios Cristalográficos, IACT, CSIC-Universidad de Granada, Av. de las Palmeras 4, E-18100 Armilla, Granada, Spain.
[e] Department of Inorganic Chemistry, Faculty of Pharmacy, University of Santiago de Compostela, E-15782 Santiago de Compostela, Spain.

ABSTRACT

For a better understanding of the metal binding pattern of $N^6$-substituted adenines, six novel ternary Cu(II) complexes have structurally characterized by single crystal X-ray diffraction. [Cu(NBzIDA)(HCy5ade)($H_2O$)]·$H_2O$ (**1**), [Cu(NBzIDA)(HCy6ade)($H_2O$)]·$H_2O$ (**2**), [Cu(FurIDA)(HCy6ade)($H_2O$)]·$H_2O$ (**3**), [Cu(MEBIDA)(HBAP)($H_2O$)]·$H_2O$ (**4**), [Cu(FurDA)(HBAP)]$_n$ (**5**) and {[Cu(NBzIDA)(HdimAP)]·$H_2O$}$_n$ (**6**). In these compounds: (i) the IDA-like chelators are N-substituted iminodiacetates with a non-coordinating aryl-methyl pendant arm (benzyl in NBzIDA, p-tolyl in MEBIDA and furfuryl in FurIDA), and (ii) the adenine derivatives have as $N^6$-substituents a N-benzyl (HBAP, a plant cytokinin), or a N-cycloalkyl (HCy5ade or HCy6ade) arm or two N-methyl groups (HdimAP). Irrespective of the molecular (**1**-**4**) or polymeric (**5**-**6**) nature of the studied compounds, the Cu(II) centre exhibits a type 4+1 coordination where the tridentate IDA-like chelators adopt a *mer*-conformation. In **1**-**5** the $N^6$-R-adenines use their most stable tautomer H(N9)ade-like, and molecular recognition consists of the cooperation of the Cu-N3(purine) bond and the intra-molecular interligand N9-H···O(coordinated carboxy) interaction. In contrast, $N^6$,$N^6$-dimethyl-adenine shows the rare tautomer H(N3)dimAP in **6**, so that the molecular recognition with the Cu(NBzIDA) chelate consist of the Cu-N9 bond and the N3-H···O intra-molecular interligand interaction. On the other hand, contrastingly to the cytokinin activity found in the free ligands HBAP, HCy5ade and HCy6ade, the corresponding Cu(II) ternary complexes did not show any activity.

* Corresponding author: Department of Inorganic Chemistry, Faculty of Pharmacy, Campus Cartuja, University of Granada, E-18071 Granada, Spain. Phone: +34958243853, Fax: +34958246219.
E-mail address: adominguez@ugr.es

## 1. Introduction

After the discovery of the antitumoral pro-drug Cisplatin by B. Rosenberg in the 1960s [1], a large number of research groups have been focused on the field of metal-nucleic acid complexes. Indeed, during the last decades, much effort has been made to rationalize the metal binding modes of nucleobases, nucleosides and nucleotides, and/or their derivatives, with transition metal ions [2-6]. This is based on the idea that the in-depth study of the chemistry of this kind of ligands, including non-covalent interactions, will allow us to better understand the biochemical processes within biological systems and therefore to build up novel bio-mimetic systems with therapeutic interest. In particular, our research group has been devoted to the study of the metal binding patterns of adenine (Hade), which has proved to behave as a fairly versatile ligand in its neutral form, where proton tautomerism phenomena enhance the possibilities of diverse molecular recognition patterns, but also in its different anionic and cationic forms [5]. For instance, neutral adenine is able to recognize several Cu(II)-iminodiacetate-like chelates in different ways. Thus, Cu(N-alkyl-IDA) chelates bind Hade by the Cu–N7 bond reinforced by a N6–H···O interaction while Cu(NBzIDA) and Cu(MEBIDA) chelates bind Hade via N3 and such coordination bond is in cooperation with the N9–H···O interaction [7]. Notably, the reaction of Cu(NBzIDA) chelate and the complementary base-pair adenine:thymine yields the binuclear compound $[Cu_2(NBzIDA)_2(H_2O)_2(\mu_2\text{-N7,N9-Hade})]\cdot 3H_2O$. In this latter compound, adenine exhibits the rare tautomer H(N3)ade and the Cu–N7 and Cu–N9 bonds are assisted by the N6–H···O and N3–H···O interactions, respectively [8].

For a long time, the research on N-substituted adenines has been a topic of great interest. In this context, a huge number of structures have been reported for N9-blocked adenine-like ligands because of their similarities with the building blocks of nucleic acids. Likewise, the study of N1, N3 and N7-(heterocyclic) substituted adenines has also been addressed. However, the chemistry of $N^6$-substituted adenines was rather unexplored until the discovery of their presence in plant physiology [9] where these compounds are included in the family of plant hormones called cytokinins [10]. The main difference between these $N^6$- and the rest of N-heterocyclic substituted adenines is that substitutions in the exocyclic amino group still allow proton tautomerism in the adenine moiety, and this fact may contribute to a higher versatile coordination. In this context, an increasing number of papers has been published in the past years related either to their physiological role in plants or to their metal binding properties. In particular, this latter approach is mostly based on the potential use of metal complexes having $N^6$-substituted adenine ligands with therapeutic purposes [11-13]. Nevertheless, future works are still needed to fully understand, at molecular level, the biochemistry of these molecules.

According to the aforementioned panorama, we have synthesized and structurally characterized novel ternary Cu(II) complexes with iminodiacetate-like chelators and different $N^6$-substituted adenines (Scheme 1). The aim of this work is to rationalize the molecular recognition patterns between such $N^6$-substituted adenines and copper(II) chelates where the tridentate chelator used (1) is unable to block the

four closest coordination sites of the metal ion and (2) offers O-coordinated atoms as H-acceptor in intra-molecular interligand interactions. Note that the substituents of both chelating and $N^6$-R-adenine ligands are closely related (see scheme 1). The novel compounds have been also investigated by spectral and thermal methods. Moreover, as the ligand 6-benzyladenine (HBAP) is a natural cytokinin we compare, in the present paper, its activity with two related $N^6$-cycloalkyladenine derivatives, as well as the effect of Cu(II) coordination using the *Amaranthus* bioassay.

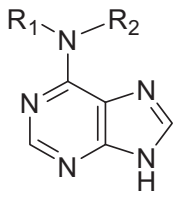

$R_1$,$R_2$ = $CH_3$ (HdiMAP)
$R_1$ = cyclopentyl, $R_2$ = H (HCy5ade)
$R_1$ = cyclohexyl, $R_2$ = H (HCy6ade)
$R_1$ = benzyl, $R_2$ = H (HBAP)
$R_1$ = $-CH_2$  , $R_2$ = H (HKin)

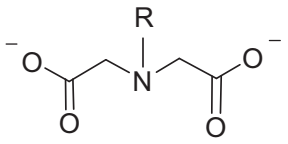

R = $-CH_2$-Ph (NBzIDA)
R = $-CH_2$-Ph-$CH_3$ (MEBIDA)
R = $-CH_2$  (FurIDA)

Scheme 1. Formulas of the $N^6$-substituted adenines and chelating ligands used in this work.

## 2. Experimental

2.1. Materials

Bluish $Cu_2CO_3(OH)_2$ was purchased from Probus. N-Methyliminodiacetic acid ($H_2$MIDA), 6-(dimethylamino)purine (HdimAP), 6-(benzylamino)purine (HBAP), 6-(furfuryl)adenine (kinetine, Hkin) and thymine (Hthy) were supplied by Sigma-Aldrich. All reagents were used as received. N-benzyl- and N-(p-methylbenzyl)iminodiacetic acids ($H_2$NBzIDA and $H_2$MEBIDA, respectively) were synthesized in the acid form as reported in ref. [7]. N-Furfuryl-iminodiacetic acid ($H_2$FurIDA) was synthesized in the acid form according to an adapted procedure derived from that reported by Irving and da Silva et al. [14] and the aforementioned synthesis [7]. It should be noted that the pure ligand in its acid form ($H_2$FurIDA) is rather difficult to isolate whereas the monopotassium salt (KHFurIDA) crystallizes easily at neutral pH from the mother liquors of the synthesis. Further purifications can be performed by re-crystallization. Likewise, pure white samples of free $H_2$FurIDA acid can be obtained, at the expense of lower yields, by passing a concentrated aqueous solution of the monopotassium salt through an ion exchange column (by concentration under reduced pressure of the aqueous eluates with pH < 4 and slow evaporation of the resulting aqueous solution). $N^6$-cyclohexyladenine (HCy6ade) and $N^6$-cyclopentyladenine (HCy5ade) were synthesised *de novo* by F. M. Albertí Aguiló et al. [15].

2.2. Syntheses of novel metal complexes

2.2.1. *Synthesis of [Cu(NBzIDA)(HCy5ade)($H_2O$)]·$H_2O$ (**1**)*

A blue solution of N-benzyliminodiacetate copper(II) chelate was prepared by reaction of $Cu_2CO_3(OH)_2$ (0.03 mmol, 0.006 g) and $H_2$NBzIDA acid (0.06 mmol, 0.013 g) in 10 mL of water, heating (50 ºC) and stirring under

moderate vacuum. Once the reaction of the binary chelate was completed, the solution was cooled down at room temperature. Then, an aqueous solution (10 mL) of the complementary base pair HCy5ade/Hthy (0.06 mmol, 0.012 g/0.008 g, respectively) was added over the binary chelate solution and let reacts. After one hour, the reacting mixture was filtered on a crystallization device. Evaporation of the solvent was controlled with the aid of a plastic film. In three weeks, blue needle-like crystals suitable for X-Ray Diffraction (XRD) purposes appeared. One month later, colourless crystals were collected and identified as free thymine (Hthy) by FT-IR spectroscopy. Yield of this synthesis is ca. 85%. Elemental analysis (%): Calc. for $C_{21}H_{28}CuN_6O_6$ (**1**): C 48.08, H 5.29, N 16.18; Found: C 48.13, H 5.39, N 16.04. FT-IR (KBr, $cm^{-1}$) $\nu_{as}(H_2O)$ 3418, $\nu_s(H_2O)$ 3220, $\nu(N^6\text{-}H)$ 3235, $\nu$(N-H) 3119, $\nu_{as}(CH_2)$ 2947, $\nu_s(CH_2)$ 2850, $\delta(H_2O)$ 1629, $\nu_{as}$(COO) 1598, $\delta(N^6\text{-}H)$ 1539, $\delta$(N-H) 1498, $\nu_s$(COO) 1384, $\pi(C\text{-}H)_{ar}$ 709. The UV/Vis spectrum shows an asymmetric d-d band with $\lambda_{max}$ at 682 nm ($\nu_{max}$ 14663 $cm^{-1}$).

2.2.2. *Synthesis of [Cu(NBzIDA)(HCy6ade)($H_2O$)]·$H_2O$ (**2**)*

A synthetic procedure similar to that of compound **1** was followed, using $Cu_2CO_3(OH)_2$ (0.06 mmol, 0.013 g), $H_2$NBzIDA acid (0.125 mmol, 0.028 g) and the complementary base pair HCy6ade/Hthy (0.125 mmol, 0.027 g/0.016 g, respectively) in 30 mL of water. After one hour stirring, a micro-suspension was still observed within the reacting mixture what was indicative of the incomplete reaction of the adenine-like ligand. At the expense of lower yields, we decided to filter the solution. The crystallization device was allowed to stand at room temperature covered with a plastic film to control the evaporation of the solvent. Five days later, blue needle-like crystals suitable for XRD purposes were collected. After three weeks, colourless crystals appeared which were identified as free Hthy by FT-IR spectroscopy. Yield is ca. 65-70%. Elemental analysis (%): Calc. for $C_{22}H_{30}CuN_6O_6$ (**2**): C 49.15, H 5.33, N 15.49; Found: C 49.11, H 5.62, N 15.62. FT-IR (KBr, $cm^{-1}$) $\nu_{as}(H_2O)$ 3426, $\nu_s(H_2O)$ 3233, $\nu(N^6\text{-}H)$ 3227, $\nu$(N-H) 3123, $\nu_{as}(CH_2)$ 2941, $\nu_s(CH_2)$ 2855, $\delta(H_2O)$ 1637, $\nu_{as}$(COO) 1606, $\delta(N^6\text{-}H)$ 1541, $\delta$(N-H) 1496, $\nu_s$(COO) 1384, $\pi(C\text{-}H)_{ar}$ 707. The UV/Vis spectrum shows an asymmetric d-d band with $\lambda_{max}$ at 677 nm ($\nu_{max}$ 14771 $cm^{-1}$).

2.2.3. *Synthesis of [Cu(FurIDA)(HCy6ade)($H_2O$)]·$H_2O$ (**3**)*

A blue solution of N-furfuryl-iminodiacetate copper(II) chelate was prepared by reaction of $Cu_2CO_3(OH)_2$ (0.06 mmol, 0.013 g) and $H_2$FurIDA acid (0.125 mmol, 0.026 g) in 15 mL of water, heating (50 ºC) and stirring under moderate vacuum. In this case, HCy6ade was directly added to the mother blue solution of the binary chelate (0.125 mmol, 0.027 g). However, a micro-suspension stood again after one hour of stirring and heating (25 ºC). Then, the solution was filtered on a crystallization device at the expense of lower yields. The evaporation of the solvent was controlled with the aid of a plastic film. In ten days, blue parallelepiped crystals were collected for XRD studies. Yield of this synthesis is ca. 55-65%. Elemental analysis (%): Calc. for $C_{20}H_{28}CuN_6O_7$ (**3**): C 45.38, H 5.22, N 16.06; Found: C 45.50, H 5.34, N 15.92. FT-IR (KBr, $cm^{-1}$) $\nu_{as}(H_2O)$ 3415, $\nu_s(H_2O)$ 3285, $\nu(N^6\text{-}H)$ 3229, $\nu$(N-H) 3123, $\nu_{as}(CH_2)$ 2936, $\nu_s(CH_2)$ 2856, $\delta(H_2O)$ and $\nu_{as}$(COO) overlapped 1637, $\delta(N^6\text{-}H)$ 1541, $\delta$(N-H) 1497, $\nu_s$(COO) 1384, $\pi(C\text{-}H)_{ar}$ 640. The UV/Vis spectrum shows an

asymmetric d-d band with $\lambda_{max}$ at 683 nm ($\nu_{max}$ 14641 $cm^{-1}$).

2.2.4. *Synthesis of [Cu(MEBIDA)(HBAP)(H₂O)]·H₂O (**4**)*

A synthetic procedure similar to that of compound **3** was followed, using $Cu_2CO_3(OH)_2$ (0.25 mmol, 0.055 g), $H_2$MEBIDA acid (0.5 mmol, 0.118 g) and HBAP (0.5 mmol, 0.113 g) in 90 mL of water. The ligand HBAP did not seem to be soluble in the binary chelate liquors, then 20 mL of isopropanol were added. After one hour stirring, the reaction was completed and the solution was filtered on a crystallization device covered by a plastic film. The solution dried off yielding only an amorphous blue product. Such residue was dissolved in 25mL of acetonitrile and again covered with a plastic to control evaporation. One month later, blue prismatic crystals were collected, suitable for XRD purposes. Yield ca. 75%. Elemental analysis (%): Calc. for $C_{24}H_{28}CuN_6O_6$ (**4**): C 51.57, H 5.09, N 14.92; Found: C 51.47, H 5.04, N 15.01. FT-IR (KBr, $cm^{-1}$) $\nu_{as}(H_2O)$ 3423, $\nu_s(H_2O)$ 3266, $\nu(N^6\text{-}H)$ 3212, $\nu$(N-H) 3150, two types of $\nu_{as}(CH_2)$ 2940 and 2923, $\nu_s(CH_2)$ 2857, $\delta(H_2O)$ 1635, $\nu_{as}$(COO) 1611, $\delta(N^6\text{-}H)$ 1545, $\delta$(N-H) 1496, $\nu_s$(COO) 1391, $\pi(C\text{-}H)_{ar}$(HBAP) 705 and 644, $\pi(C\text{-}H)_{ar}$(MEBIDA) 752. The UV/Vis spectrum shows an asymmetric d-d band with $\lambda_{max}$ at 678 nm ($\nu_{max}$ 14749 $cm_{-1}$).

2.2.5. *Synthesis of [Cu(FurIDA)(HBAP)]$_n$ (**5**)*

A synthetic procedure similar to that of compound **3** was followed, using $Cu_2CO_3(OH)_2$ (0.25 mmol, 0.055 g), $H_2$FurIDA acid (0.5 mmol, 0.111 g) and HBAP (0.5 mmol, 0.113 g) in 100 mL of a 1:1 water:methanol mixture. After half an hour stirring and soft heating (25 ºC), the reaction was completed and the solution was filtered on a crystallization device, covered by a plastic film to control the evaporation of the solvents. One month later, blue needle-like crystals were collected suitable for XRD purposes. Yield of this synthesis is ca. 70%. Elemental analysis (%): Calc. for $C_{21}H_{19}CuN_6O_5$ (**5**): C 50.51, H 3.80, N 16.93; Found: C 50.55, H 3.84, N 16.85. FT-IR (KBr, $cm^{-1}$) $\nu_{as}(H_2O)$ 3433, $\nu_s(H_2O)$ 3265, $\nu(N^6\text{-}H)$ 3206, $\nu$(N-H) 3150, $\nu_{as}(CH_2)$ 2924, $\nu_s(CH_2)$ 2855, $\delta(H_2O)$ 1637, $\nu_{as}$(COO) 1616, $\delta(N^6\text{-}H)$ 1546, $\delta$(N-H) 1497, two types of $\nu_s$(COO) 1382 and 1374, $\pi(C\text{-}H)_{ar}$ (HBAP) 703 and 644, $\pi(C\text{-}H)_{ar}$ (FurIDA) 598. The UV/Vis spectrum shows an asymmetric d-d band with $\lambda_{max}$ at 683 nm ($\nu_{max}$ 14641 $cm^{-1}$).

2.2.6. *Synthesis of {[Cu(NBzIDA)(HdimAP)]·H₂O}$_n$ (**6**)*

A synthetic procedure similar to that of compound **3** was followed, using $Cu_2CO_3(OH)_2$ (0.25 mmol, 0.055 g), $H_2$NBzIDA acid (0.5 mmol, 0.116 g) and HdimAP (0.5 mmol, 0.082 g) in 80 mL of water. The reaction progressed rapidly without problems and the resulting solution was filtered on a crystallization device and left evaporates at r.t. controlled by the aid of a plastic film. Approximately two months later, blue crystals appeared. Nonetheless, such crystals were not suitable for XRD. Further re-crystallizations in isopropanol were carried out. After five months, well-shaped crystals appeared, suitable for XRD purposes. Yield of this synthesis is ca. 25%. Elemental analysis (%): Calc. for $C_{18}H_{22}CuN_6O_5$ (**6**): C 46.33, H 4.92, N 18.21; Found: C 46.40, H 4.76, N 18.04. $\nu_{as}(H_2O)$ 3433, $\nu_s(H_2O)$ 3251, $\nu$(N-H) 3161, two types of $\nu_{as}(CH_3)$ 2978 and 2960, $\nu_{as}(CH_2)$ 2930, $\nu_d(CH_3)$ 2870, $\nu_s(CH_2)$ 2855, $\delta(H_2O)$ 1613, $\nu_{as}$(COO) 1594, $\delta$(N-H) 1492, $\delta(CH_2)$ 1451, $\delta_{as}(CH_3)$ 1443, $\delta_s(CH_3)$ 1430, $\nu_s$(COO) 1384, $\pi(C\text{-}H)_{ar}$ (NBzIDA) 755, $\pi(C\text{-}H)_{ar}$ (HdimAP)

711. The UV/Vis spectrum shows an asymmetric d-d band with $\lambda_{max}$ at 688 nm ($\nu_{max}$ 14535 $cm^{-1}$).

*2.2.7. Synthesis of a related Cu(II) compound with $N^6$-furfuryl-adenine.*

A synthetic procedure similar to that of compound **3** was followed, using $Cu_2CO_3(OH)_2$ (0.25 mmol, 0.055 g), $H_2$NBzIDA acid (0.5 mmol, 0.116 g) and Hkin (0.5 mmol, 0.107 g) in 80 mL of water. The ligand Hkin did not seem to be soluble in the binary chelate liquors, then 20 mL of isopropanol were added dropwise until a clear blue solution was obtained. After one hour stirring, the solution was filtered on a crystallization device and covered by a plastic film. After two weeks, very thin needle-like crystals were collected although they were not valid for XRD purposes. Crystallization on gel medium was performed to improve the size and the quality of the crystals, as described herein: H7deaA (0.02 mmol, 0.0027 g) was added as a solid powder to a vial. Afterwards, 2 mL of an 0.5% agar solution of Cu(NBzIDA) 0.01M was added to the same vial, stirring the solution in a water bath (gentle heating) until the reaction took place. Then, the solution, properly capped, was left gel at room temperature. The vial stood at room temperature where larger crystals appeared within four weeks. However, neither these latter crystals provide good quality XRD data.

2.3. Crystallography

Measured crystals were prepared under inert conditions immersed in perfluoropolyether as protecting oil for manipulation. Suitable crystals were mounted on MiTeGen Micromounts™ and these samples were used for data collection. Data were collected with Bruker SMART APEX (**2** and **3**, 293 K), Bruker X8 KappaAPEXII (**4** and **5**, 100 K) diffractometers, whereas those of **1** and **6** were collected at the ESRF SYNCHROTRON BM16 beamline (Grenoble, France). The data were processed with APEX2 (**2 - 5**) [16] and HKL2000 (**1**,**6**) [17] programs and corrected for absorption using SADABS [18]. The structures were solved by direct methods [19], which revealed the position of all non-hydrogen atoms. These atoms were refined on $F^2$ by a full-matrix least-squares procedure using anisotropic displacement parameters [19]. All hydrogen atoms were located in difference Fourier maps and included as fixed contributions riding on attached atoms with isotropic thermal displacement parameters 1.2 times those of the respective atom. Geometric calculations were carried out with PLATON [20] and drawings were produced with PLATON [20] and MERCURY [21]. Additional crystal data and more information about the X-ray structural analyses are shown in Supplementary material S1 to S7. Crystallographic data for the structural analysis have been deposited with the Cambridge Crystallographic Data Centre, CCDC No. 906728 – 906733 from 1 to 6, respectively. Copies of this information may be obtained free of charge on application to CCDC, 12 Union Road, Cambridge CB2 1EZ, UK (fax: 44 1223 336 033; e-mail: deposit@ccdc.cam.ac.uk or http://www.ccdc.cam.ac.uk).

2.4. *Amaranthus betacyanin* bioassay

This bioassay was performed according to Biddington et al. [22] with the following modifications: *Amaranthus caudatus L.* seeds were germinated in Petri dishes with distilled water, in the dark, at 28 ºC. In 7 days, ten cotyledons were cut at the hypocotyls level under dim green light (in order to avoid activation of

betacyanin) and placed in a new Petri dish filled with 5mL of treatment solution. Cytokinin-like mother solutions (200 μM) were prepared by dissolving the corresponding compounds (**1**-**4**) in a total volume of 10 mL of 100 μM KCl + 0.4 gL-1 Tyr. Moreover, a mother solution of $N^6$-benzyl-aminopurine (HBAP) was prepared in the same conditions to be used as internal reference. From the mother solutions, curves of dilutions were carried out leading to different treatment solutions at 200, 50, 12.5, 3.125, 0.78, 0.195, 0.048 and 0.012 μM, respectively. After incubation of HBAP and the studied compounds, at 28 ºC for 20 h, the cotyledons were placed in an Eppendorf tube with 1mL of distilled water. Betacyanin was extracted by three freeze–thaw cycles with liquid $N_2$ (-70 ºC) and sonication during 10 minutes. After centrifugation at 10,000g, the supernatant was recovered and the betacyanin content was calculated by the difference in optical densities at 542 and 620 nm [23]. This procedure was repeated three times in order to ensure reproducibility of the bioassays.

2.5. Physical measurements

Analytical data were obtained in a Fisons–Carlo Erba EA 1108 elemental micro-analyser. Infrared spectra were recorded by using KBr pellets on a Jasco FT-IR 6300 spectrometer. TG analysis (pyrolysis) of the studied compounds (295–800 ºC) were carried out in air flow (100 mL/ min) by a Shimadzu Thermobalance TGA–DTG–50H instrument, and a series of FT-IR spectra (20–30 per sample) of evolved gasses were recorded for the studied compounds using a coupled FT-IR Nicolet Magma 550 spectrometer. Electronic (diffuse reflectance) spectra were obtained in a Varian Cary-5E spectrophotometer.

## 3. Results and discussion

3.1. Syntheses of the novel mixed-ligand copper(II) complexes.

All the syntheses were carried out according to the procedure previously reported by our research group [8-24]. This consists of a two-step reaction. First, the metal chelate is obtained by stoichiometric reaction of the appropriate chelating agent in its acid form and basic copper(II) carbonate. This reaction yields $CO_2$ as main by-product, easily removable by stirring, heating and moderate vacuum, thus avoiding the presence of undesired by-products (i.e. alkaline inorganic salts) that could interfere in the crystallization process. Afterwards, the binary compound reacts with the corresponding purine-like ligand (alone) or with the appropriate base pair. The use of complementary base pair Hade:Hthy in this kind of syntheses within ternary complexes was first introduced by us [8]. Our observations suggest that the use of appropriate base pairs, instead of the purine-like base alone, yields to more efficient incorporation of such latter ligand [24].

3.2. Molecular and crystal structure of $[Cu(NBzIDA)(HCy5ade)(H_2O)]\cdot H_2O$ (**1**)

Compound **1** consists of a complex molecule and one solvent molecule. In the complex, the copper(II) atom exhibits a 4+1 coordination polyhedron where the four closest donor atoms correspond to the tridentate NBzIDA chelating ligand (N10, O11, O21) and the N3(purine-like) donor of HCy5ade. Thus, NBzIDA ligand adopts a mer-$NO_2$ conformation. The apical coordination site is occupied by one aqua ligand.

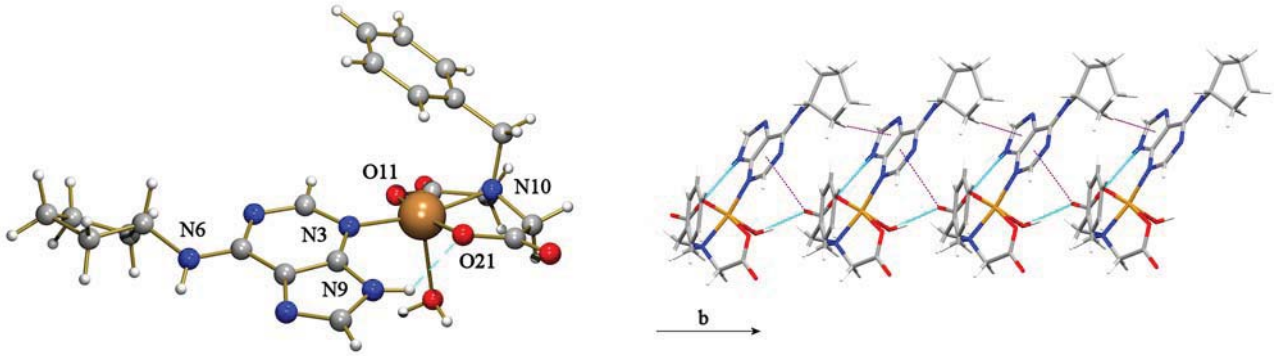


Figure 1. Left: Molecular structure of [Cu(NBzIDA)(HCy5ade)($H_2O$)]·$H_2O$ (**1**). Only one of the two disordered positions for the cyclopentyl moiety is depicted for clarity. Bond distances (Å): Cu1-O1 2.2966(11), Cu1-N10 2.0058(12), Cu1-O11 1.9381(11), Cu1-O21 1.9683(10), Cu1-N3 1.9849(12). Right: View of the H-bonded 1D chain through the b axis highlighting the C-H···π and Y-X···π interactions in purple.

HCy5ade shows its most stable tautomer H(N9)Cy5ade what allows the cooperation of the Cu-N3 bond with an intra-molecular interligand H-bond [N9-H···O21(coord. carboxy, 2.724(2) Å, 131.9º) – Fig. 1, left]. Note that, in the crystal, the cyclopentyl moiety is disordered over two positions with an occupancy factor of 0.61/0.39. In this complex, the Cu(II) coordination environment is close to an elongated square-based pyramid, with a negligible basal distortion according to the estimated value of the Addison parameter τ = 0.02 [25].

In the crystal of **1**, the complex molecules build 1D chains along the b axis by H-bonding interactions that involve the apical aqua ligands [O1-H1B···O22(non-coord. carboxy, 2.731(2) Å, 170.3º) – Fig. 1, right]. Moreover, inter-molecular C-H···π interactions between two disordered positions of the cyclopentyl moiety and the imidazole ring of HCy5ade stabilize the 1D chains [C65A-H65A···Cg, 2.71 Å, C-H···Cg 163º; C62B-H62D···Cg, 2.91 Å, 134º]. In addition, C22-O22···Cg interactions, involving the six-membered ring of HCy5ade, are identified within the 1D chains (see Table S7.1.). The polymeric chains are cross-linked by inter-molecular H-bonding interactions that comprise the non-coordinated water molecule, as donor and acceptor, and the Hoogstein face (N6 and N7 atoms) of the HCy5ade ligand (see Table S1.3.) giving rise to 2D layers. Hydrophobic forces accomplish the 3D array.

### 3.3. Molecular and crystal structure of [Cu(NBzIDA)(HCy6ade)($H_2O$)]·$H_2O$ (**2**)

Compound **2** consists of a molecular complex and one non-coordinated water molecule. The copper(II) atom is penta-coordinated, type 4+1. The NBzIDA chelator acts as a tridenate ligand, occupying three of the four closest sites around the metal centre (N10, O11, O21), in a mer-$NO_2$ conformation. Moreover, the Cu(II) coordination is satisfied by the N3(purine-like) donor from HCy6ade (in basal position) and one apical aqua ligand (Fig. 2, left). In this compound, the Addison parameter (τ = 0.01) reveals an almost regular square-based pyramidal coordination. Again, the Cu-N3 bond cooperates with an intra-molecular interligand H-bonding interaction N9-H···O21(coord. carboxy, 2.736(4) Å, 131.8º), thus showing the ligand its most stable tautomer H(N9). Note that the cyclohexyl moiety is

disordered over two positions with an occupancy factor of 0.75/0.25.

Compounds **1** and **2** display rather similar crystal packing (Fig. 2, right). The main difference between both crystals concerns the intra-chain C-H···π interaction that in **2** involves the cyclohexyl moiety of HCy6ade and the 5-membered ring of an adjacent HCy6ade ligand [C62A-H62A···Cg, 2.56 Å, 148º]. Besides this latter interaction, additional very weak intermolecular C-H···π interactions between the same cyclohexyl moiety and the 6-membered ring of HCy6ade ligand could also be considered (see Table S2.3. and Table S7.2.).

3.4. Molecular and crystal structure of [Cu(FurIDA)(HCy6ade)($H_2O$)]·$H_2O$ (**3**)

Compound **3** comprises one ternary complex molecule and one solvent molecule. Once more, the metal exhibits a slightly distorted square-based pyramidal coordination, type 4+1 (Addison parameter τ = 0.015), built by the N10, O11, and O21 donors of the tridentate FurIDA chelator (in mer-$NO_2$ conformation) and the N3 donor of the ligand HCy6ade.The apical position is occupied by one aqua ligand (Fig. 3). The apical position is occupied by an aqua ligand. Note that the furfuryl ring is disordered over two positions with an occupancy factor of 0.57/0.43. This molecular recognition pattern uses the most stable tautomer H(N9)Cy6ade, that can reinforce the Cu-N3 bond with an intra-molecular interligand H-bonding interaction N9-H···O21(coord. carboxylate, 2.742(4) Å, 130.7º).

Crystals of compounds **2** and **3** display nearly the same crystal packing. Indeed, N-benzyl and N-furfuryl pendant arms of the IDA chelating group play similar roles. This finding can be explained by the non-coordinating role of the O-heterocyclic atom, which is involved in the aromaticity of the furane ring, along with the similar steric hindrance caused by the furfuryl- and benzyl- substituents. In the crystal of **3**, two C-H···π interactions can also be considered (Fig. 4). The strongest interaction involves the cyclohexyl moiety of HCy6ade and the imidazole ring of an adjacent HCy6ade ligand [C62-H62A···Cg, 2.61 Å, 140º]. The other is defined by the cyclohexyl moiety of HCy6ade and the pyrimidine ring of HCy6ade [C63-H63B···Cg, 2.78 Å, 136º] (see Table S3.3. and Table S7.3.).

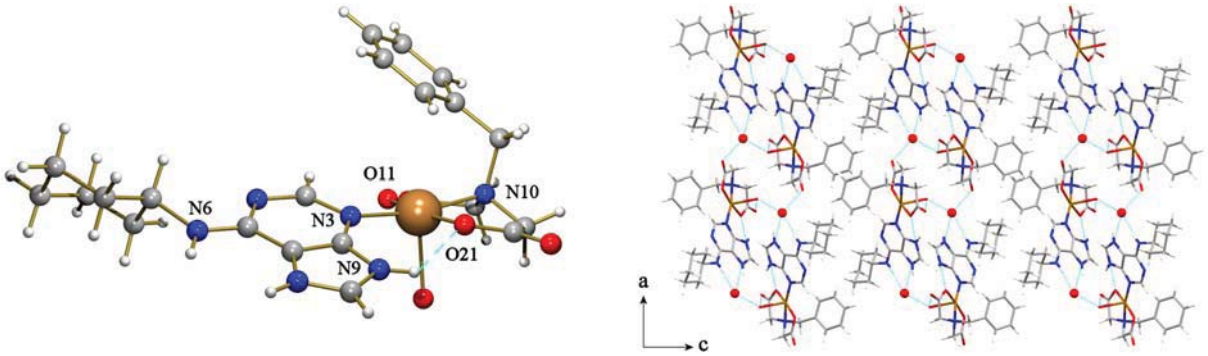


Figure 2. Left: Molecular structure of [Cu(NBzIDA)(HCy6ade)($H_2O$)]·$H_2O$ (**2**). Only one of the two disordered positions for the cyclohexyl moiety is depicted for clarity. Bond distances (Å): Cu1-O1 2.306(2), Cu1-O11 1.935(2), Cu1-O21 1.970(2), Cu1-N10 2.003(3), Cu1-N3 1.988(3). Right: 3D network of compound **2** in the ac plane.

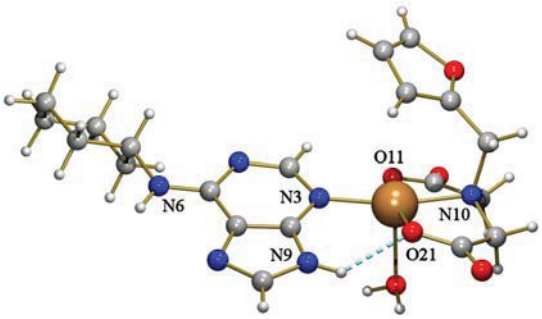


Figure 3. Left: Molecular structure of [Cu(FurIDA)(HCy6ade)($H_2O$)]·$H_2O$ (**3**). Only one of the two disordered positions is depicted for the furfuryl arm for clarity reasons. Bond distances (Å): Cu1-O1 2.301(2), Cu1-O11 1.943(2), Cu1-O21 1.970(2), Cu1-N10 2.006(3), Cu1-N3 1.978(3).

3.5. Molecular and crystal structure of [Cu(MEBIDA)(HBAP)($H_2O$)]·$H_2O$ (**4**)

The crystal of **4** also consists of a complex molecule and one non-coordinated water molecule. The copper(II) atom shows a 4+1 coordination polyhedron. The four closest Cu(II) donor atoms are supplied by the tridentate-chelating MEBIDA ligand (N10, O11 and O21), adopting a mer-$NO_2$ conformation, and the N3 donor of H(N9)BAP (Fig. 5, left). One aqua ligand occupies the apical site. Once again, the stability of the ternary complex is reinforced by the intra-molecular interligand interaction N9–H···O21(coord. carboxy, 2.648(2) Å, 137.5º). Herein, the basal distortion of the coordination polyhedron is remarkably higher (τ = 0.20) than in the above-referred complex molecules **1**-**3**. This fact can be attributed to the implication of the N9-H group in a bifurcated H-bonding interaction, involving the latter referred intra-molecular interligand interaction and the N9-H···O2(W, 2.962(2) Å, 128.7º) H-bond. Indeed, the dihedral angle between the plane of the purine moiety in HBAP and the mean basal coordination plane of the complex molecule in **4** (39.74º) is also higher compared to that of compounds **1**-**3** (~ 23º).

In the crystal of **4**, complex molecules build multi-stacked chains along the c axis by means of intermolecular π,π-stacking interactions between the 6-membered ring of the HCy6ade ligand and the aromatic moiety of the MEBIDA ligandappertaining to an adjacent molecule within the chain [Cg···Cg 3.541 Å, α = 6.56º, β = 9.75º, γ = 15.14º (Fig. 5, right)]. Besides, the aromatic moiety of MEBIDA ligand seems to involved in weak metal···π interactions within the complex molecules [Cu···Cg 3.753 Å, β = 43.21º].

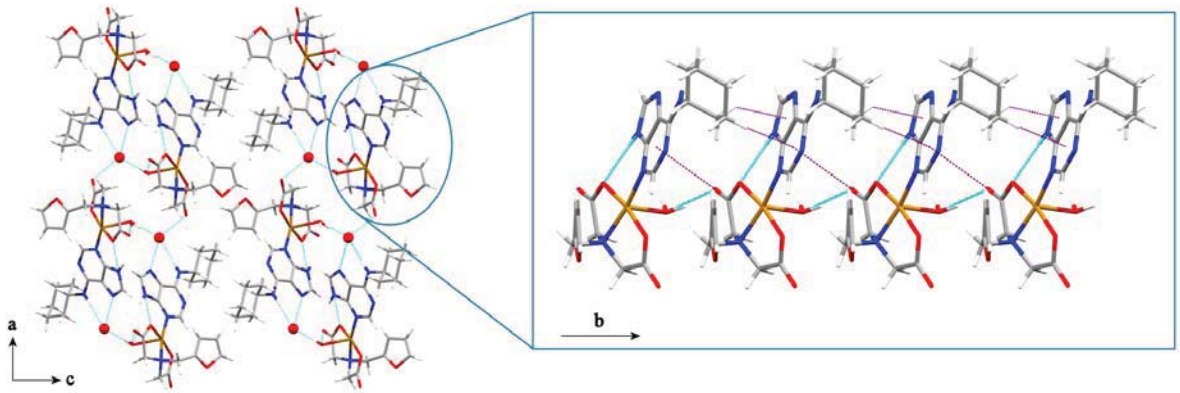


Figure 4. View in the ac plane of the 3D architecture of [Cu(FurIDA)(HCy6ade)($H_2O$)] ·$H_2O$ (**3**) with a detail of the 1D chain highlighting the C-H···π and Y-X···π interactions in purple.

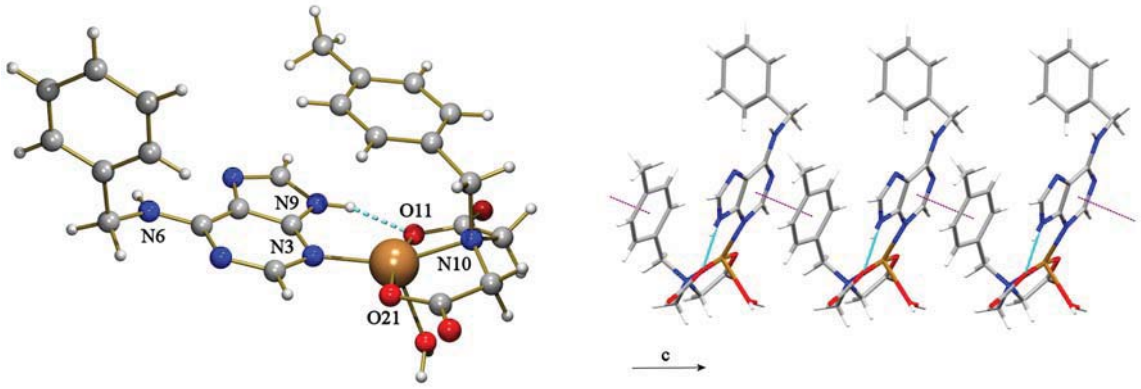


Figure 5. Left: Molecular structure of [Cu(MEBIDA)(HBAP)($H_2O$)]·$H_2O$ (**4**). Bond distances (Å): Cu1-O11 1.9485(14), Cu1-O21 1.9524(14), Cu1-N3 1.9963(17), Cu1-N10 2.0203(17), Cu1-O1 2.2249(15). Right: Detail of multi-stacked 1D chains along the c axis.

Pairs of 1D chains are linked by symmetry related inter-molecular H-bonding interactions between the Hoogstein faces of two adjacent HBAP nucleobases [N6-H6···N7(HBAP, 2.981(2) Å, 164.0º)], building layers parallel to the ab plane that extra-stabilized by inter-molecular C-H···π interactions (see Table S7.4.). The 2D structure is further connected by H-bonds that involve the apical aqua ligand and solvent molecules giving rise to the 3D framework (see Table S4.3.).

### 3.6. Crystal structure of [Cu(FurIDA)(HBAP)]$_n$ (**5**)

The crystal of compound **5** is based on a coordination polymer built by the syn-anti bridging carboxylate group of FurIDA ligand. The metal exhibits a square-based pyramidal coordination, type 4+1. The N10, O11, and O21 donors of the tridentate mer-$NO_2$ FurIDA chelator and the N3 atom from HBAP satisfy the basal coordination plane. The apical position is occupied by the bridging O-atom from a carboxylate group of an adjacent FurIDA (Fig. 6, left). It is documented that the ligand N,N-bis(picolyl)furfurylamine (BPFur) acts as tripodal tetradentate chelator in [Cu(BPFur)Cl]$ClO_4$ [26] where the O-furfuryl donor weakly binds the metal centre [Cu-O 2.750(3) Å]. However, in compound **5** the O-furfuryl atom should not be considered as a donor atom for the copper(II) center since the corresponding Cu-O distance [Cu-O 2.951(3) Å] is according to a simple contact, close to the sum of Van der Waals radii are Cu (1.40 Å) and O (1.50 Å). The molecular recognition pattern between the Cu(FurIDA) chelate and the HBAP ligand is featured by the cooperative role of the Cu-N3 bond and the intra-molecular interligand N9-H···O21(coord. carboxy, 2.811(3) Å, 129.9º) H-bonding interaction.It is remarkably that the N9-H group also participates in an inter-molecular H-bond with nearly the same strength [N9-H···O11(coord. carboxy, 2.816(3) Å, 128.5º)]. This bifurcated interaction is the main responsible of the dihedral angle (32.86º) between the mean basal coordination plane and the purine moiety plane of HBAP. The trans-angles of the basal planes are quite similar so that the Addison parameter has a value close to τ = 0.01, as previously described for compounds **1** – **3**. Note that compounds **1**-**4** have similar molecular topology whereas compound **5** builds a polymer.

In the crystal of **5**, polymeric chains run along the c axis. Adjacent 1D chains are further associated by means of symmetry related H-bonds between the Hoogstein faces of two adjacent HBAP nucleobases [N6-H6···N7(HBAP, 3.000(3) Å, 156.4º)] building 2D layers where the ligands HBAP run along the $2_1$ screw axes parallel to the bc plane (Fig. 6, right). Hydrophobic forces connect neighbouring layers to generate the 3D architecture. Despite both FurIDA and HBAP ligands have aromatic moieties, no stacking interactions have been observed in this compound.

3.7. Crystal structure of {[Cu(NBzIDA)(HdimAP)]·$H_2O$}$_n$ (**6**)

The crystal of compound **6** consists of polymeric chains that extend along the b axis and non-coordinated water. The copper(II) atom exhibits a nearly regular square-based pyramidal coordination (Addison parameter $\tau$ = 0.004), type 4+1, where the four closest donor atoms correspond to the tridentate NBzIDA chelating ligand (N10, O11, O21) and the N9(purine-like) donor of HdimAP. Thus, the NBzIDA ligand adopts a mer-$NO_2$ conformation. The apical donor is the O22 atom from the bridging carboxylate group of an adjacent NBzIDA ligand (Fig. 7, left). It is noteworthy that the dissociable proton in the HdimAP moiety is shifted to the N3 donor, showing the rare tautomer H(N3)dimAP. This tautomer allows to assist the bond Cu-N9 with an intramolecular interligand H-bonding interaction N3-H···O11(coord. carboxy, 2.728 Å, 133.9º). Note that this molecular recognition pattern is just the opposite of that referred for compounds **1**-**5**.

In the crystal of **6**, 1D polymeric chains extend throughout the b axis running along $2_1$ screw axes. These latter chains connect each other building layers by means of H-bonding interactions that involve the solvent.

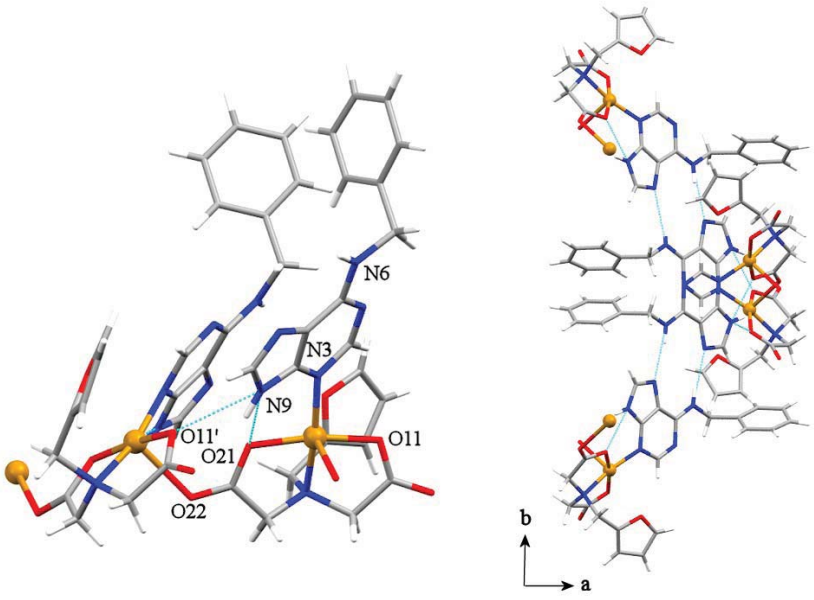


Figure 6. Left: Molecular structure of [Cu(FurIDA)(HBAP)]$_n$ (**5**). Bond distances (Å): Cu1-O21 1.930(2), Cu1-O11 1.941(2), Cu1-N3 1.987(2), Cu1-N10 2.010(2), Cu1-O22(#1) 2.376(2); (#1 x,-y+3/2,z-1/2). Right: View in the ba plane of one layer where adjacent chains connect by Hoogstein faces of HBAP ligands.

In addition, the N3-H group is also involved in a weak intermolecular H-bond [N3-H···O1(W, 3.035(8) Å, 137.6º)] that help to stabilize the 2D structure (see Table S6.3.). Finally, hydrophobic interactions lead to the 3D architecture (Fig. 7, right). No stacking interactions are observed in this compound.

3.8. Molecular recognition between the $N^6$-substituted adenines and copper(II)-iminodiacetate chelates and closely related mixed-ligand metal complexes.

The M-N3 + N9-H···O metal binding pattern has been previously described for adenine (Hade) [5] as well as other related $N^6$-substituted adenine ligands such as HdimAP [27-29] or HBAP [30]. In particular, those complexes containing Hade as ligand were published by our research group and comprises Cu(II)-NBzIDA-like chelates [5,7,8]. In particular, the mononuclear complex [Cu(NBzIDA)(Hade)($H_2O$)]·$H_2O$ [7] shows the same formula and metal binding pattern. However, they are not isotype crystals since, therein, crystal packing was highly influenced by π,π-stacking interactions between the aromatic moieties of Hade and NBzIDA. Among those reported compounds having N6-subsitutued adenines, it should be remarked a very recent paper concerning the crystal structure of [Cu($\mu_2$-1,4-BDC)(HBAP)$_2$($H_2O$)]$_n$ [30] (1,4-BDC = benzene-1,4-dicarboxylate(2-) anion), where each HBAP ligand recognizes the 1D-polymeric matrix Cu($\mu_2$-1,4-BDC)($H_2O$) by means of the M-N3 bond plus the N9-H···O(coord. carboxy) H-bonding interaction. Likewise, a search in the CSD restricted for neutral monodentate HdimAP ligand, with any metal ion, reveals only 4 hits [UFIDAP ($Ru^{III}$) [27], VABQOE ($Re^{III}$) [28], VABQUB ($Re^{IV}$) [28], VAZLOX ($Rh^{I}$) [29], in which HdimAP displays its most stable tautomer H(N9) and the molecular recognition consists of a coordination bond M-N3 + N9-H···Cl intra-molecular interligand H-bond. This former pattern is similar to that showed previously in compounds **1**-**5** but also to those containing adenine-like ligands (vide supra).

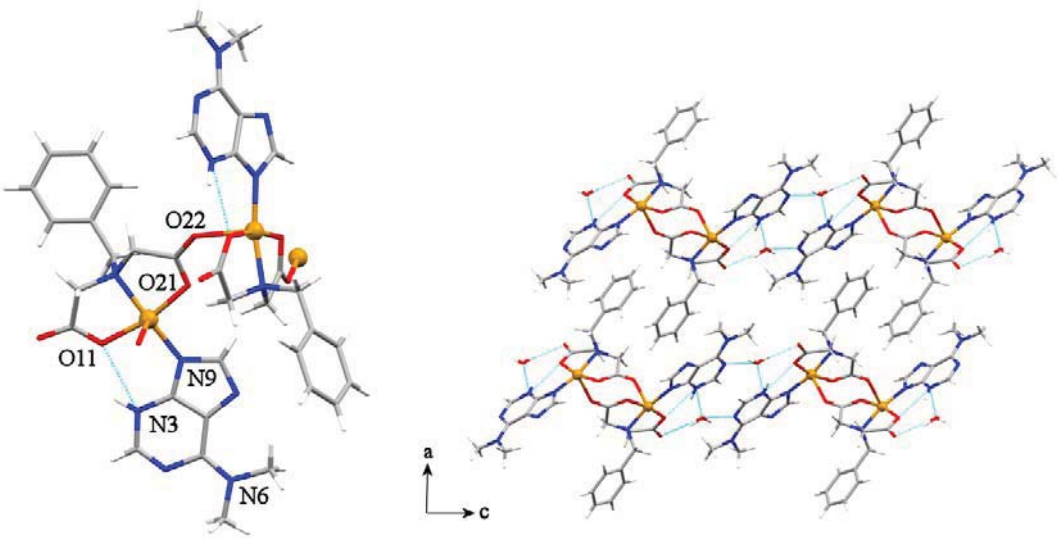


Figure 7. Left: Molecular structure of {[Cu(NBzIDA)(HdimAP)]·$H_2O$}$_n$ (**6**). Bond distances (Å): Cu1-N10 2.007(5), Cu1-O21 1.950(4), Cu1-O11 1.953(4), Cu1-N9 1.949(5), Cu1-O22(#1) 2.379(4); (#1 -x+2,y-1/2,-z+1/2). Right: 3D architecture in the ac plane of compound **6**.

Therefore, the recognition pattern N9 + N3-H···O reported for compound **6** in this work is unprecedented for the HdimAP ligand. Nonetheless, the molecular reasons of this particular metal binding still remain quite unclear. In fact, a clear relationship could not be identified between the metal binding patterns displayed by HdimAP and the molecular/polymeric nature or the metal HSAB Pearson character of the reposted compounds. Furthermore, the rare tautomer H(N3)purine-like has never been described for purine-like ligands within mononuclear complexes. On the other hand, the H(N3) tautomer has been reported only twice regarding ternary binuclear compounds where adenine and 2,6-diaminopurine (Hdap) act as bridging ligands according to the formula: $[Cu_2(NBzIDA)_2(\mu_2\text{-}N7,N9\text{-}H(N3)ade)(H_2O)_2]\cdot 3H_2O$ [8] and $[Zn_2(\mu_3\text{-benzene-1,4-dicarboxylate})(\mu_2\text{-}N7,N9\text{-}H(N3)dap]_n$ or $\{[Zn_2(\mu_4\text{-benzene-1,3,5-tricarboxylate})(\mu_2\text{-hydroxo})(\mu_2\text{-}N7,N9\text{-}H(N3)dap]\cdot H_2O\}_n$ [31].

3.9. Cytokinin activity

The cytokinin activity of HBAP, HCy5ade and HCy6ade ligands is shown in Fig 8 – see also Table in S8. On the other hand, the *Amaranthus betacyanin* bioassay did not show any cytokinin activity for the tested Cu(II) complexes in the studied range of concentrations (**1**-**4**). The lack of activity of Cu(II)-HBAP-like complexes could be explained considering the stability of the Cu-adenine bond which do not permit the correct interaction with cytokinin receptors. To our knowledge, the N3, N9 moiety of the purine ring needs to be exposure in order to interact with the cytokinin receptors [32] and therefore, it would be necessary the release of alkylaminopurine moiety.

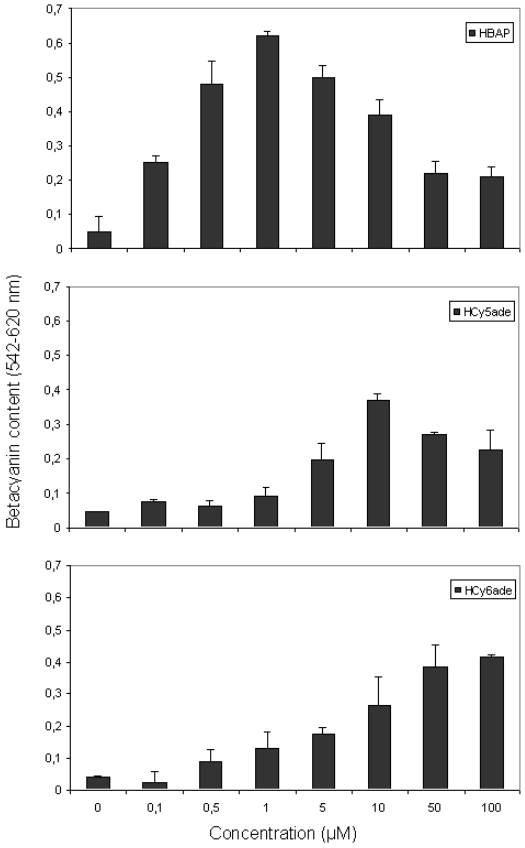


Figure 8. Dose-response curves from 0.1 to 100 μM of HBAP, HCy5ade and HCyC6ade ligands in the *Amaranthus* betacyanin bioassay.

Furthermore, no copper(II) toxicity is observed in the studied plants what would have been indicative of the dissociation of the ternary complexes.

## 4. Concluding remarks

The molecular recognition patterns presented in this work highlight the role of N3 in those complexes containing $N^6$-monosubstituted adenine derivatives. Besides this feature, compounds **1**-**5** also have in common that they all have a $N^6$-ring substituent (aliphatic **1-3** or aromatic **4-5**).

Despite their molecular (**1**-**4**) or polymeric nature (**5**), in all the latter compounds the Cu–N3 bond is reinforced by an intra-molecular interligand H-bonding interaction N9-H···O. In contrast, in the polymer of compound **6**, the

disubstituted ligand HdimAP exhibits the molecular recognition pattern Cu-N9 + N3-H···O. It is remarkable that this metal binding pattern has not been reported before for this ligand or any neutral adenine-like ligand acting as monodentate.

In terms of nucleic acids, or their building blocks, the N3 donor (located in the minor groove of DNA) is generally disfavoured in comparison with the N7 donor, which is more accessible due to its location in the major groove of DNA. Moreover, N7 is more basic than N3 and this is consistent with their metal binding behaviour. According to B. Lippert and H. Sigel et al., the alkylation of the exocyclic amino group has a relatively minor effect on the N-basicity order of the Hade (N9>N1>N7>N3>>N6). Nevertheless, the presence of bulky substituents in the $N^6$-exocyclic amino group of purines hinders in a relevant way the N1 and N7 sites, driving the coordination through the minor groove binder N3. This metal binding behaviour is in accordance with the reported compounds **1-5** but also has previously been described for 9-methyl-dimAP [33]. Although most of the interactions between metal ions and nucleic acids are described in the major groove, interactions within the minor groove of DNA should not be underestimated. Indeed, the minor groove is a relevant hydrogen acceptor group that could interact with enzymes, proteins or other active molecules and/or metal complexes [34-35]. Therefore the interaction between different organic compounds and/or metal complexes with the N3(purine-like) donor is a topic of increasing interest and encourage further researches regarding the rational design of new biomimetic systems with biological and/or pharmaceutical applications. Indeed, Travnicek et al. have already reported studies with ternary metal complexes and $N^6$-subsituted adenines that show potential in vitro antitumoral activity [36-37].

## Acknowledgements

Financial support from Research Group FQM-283 (Junta de Andalucía) and MICINN-Spain (Project MAT2010-15594) is acknowledged. The project 'Factoría de Cristalización, CONSOLIDER INGENIO-2010' provided X-ray structural facilities for this work. Financial support from ERDF Funds and Junta de Andalucía to acquire the FT-IR spectrophotometer Jasco 6300 is acknowledged. ADM gratefully acknowledges ME-Spain for a FPU Ph.D Contract.

## Appendix A. Supplementary data

Additional crystal data and structural information for 1 -6 (S1-S6), analysis of π,π-stacking interactions and C-H···π (S7) and data about the *Amaranthus* bioassay (S8) are provided. For further information about the spectral properties (FT-IR and UV-Vis) or Thermal analyses (TGA) carried out to all the reported compounds, please contact with the corresponding author. Supplementary data to this article can be found online at doi: /jinorgbio 20xx.mm.qqq.

## References

[1] B. Rosenberg, L. Van Camp, T. Krigas, Nature 205 (1965) 698-699.

[2] H. Sigel *Pure Appl. Chem.* 76 (2004) 1869–1886

[3] A. Terrón, J.J Fiol, A. García-Raso, M. Barceló-Oliver, V. Moreno, *Coord. Chem. Rev.* 251 (2007) 1973–1986.

[4] B. Lippert, in: N. V. Hud (Ed.), *Nucleic Acid - Metal Ion Interactions*, RSC Publishing, 2009, Chap. 2.

[5] D. K Patel, A. Domínguez-Martín, M.P. Brandi-Blanco, D. Choquesillo-Lazarte, V.M. Nurchi, J. Niclós-Gutiérrez, *Coord. Chem. Rev.* 256 (2012)

193-211.

[6] A. Sigel, H. Sigel, R.K.O. Sigel, *Interplay between Metal ions and Nucleic Acids* – Metal Ions in Life Science vol.10., Springer, the Netherlands, 2012.

[7] E. Bugella-Altamirano, D. Choquesillo-Lazarte, J.M. González-Pérez, M.J.Sánchez-Moreno, R. Marín-Sánchez, J.D. Martín-Ramos, B. Covelo, R. Carballo, A. Castiñeiras, J. Niclós-Gutiérrez, *Inorg. Chim. Acta* 339 (2002) 160–170.

[8] P.X. Rojas-González, A. Castiñeiras, J. M. González-Pérez, D. Choquesillo-Lazarte, J. Niclós-Gutiérrez, *Inorg. Chem.* 41 (2002) 6190-6192.

[9] C.O. Miller, F. Shoog, M.H. Von Saltza, M. Strong, *J. Am. Chem. Soc.* 77 (1955) 1329-1334.

[10] H. Sakakibara, *Annu. Rev. Plant. Physiol.*, 57 (2006) 431-449.

[11] L. Szucova, Z. Travnicek, M. Zatloukal, I. Popa, *Bioorg. Med. Chem.* 14 (2006) 479-491.

[12] P. Starha, Z. Travnicek, I. Popa, *J. Inorg. Biochem.* 103 (2009) 978-988.

[13] J. Vicha, G. Demo, R. Marek, Inorg. Chem. 51 (2012) 1371-1379.

[14] H. Irving, J. J. R. F. da Silva, *J. Chem. Soc.* (1963) 1144–1148.

[15] Francisca M. Albertí Aguiló, Ph.D. Thesis; University of Palma de Mallorca, Spain, 2008.

[16] BRUKER, APEX2 Software, Bruker AXS Inc., V2010.11, Madison, Wisconsin, USA, 2010.

[17] Z. Otwinowski, W. Minor, in: C.W. Carter, Jr. and R. M. Sweet (Eds.), *Methods in Enzymology*, vol. 276, part A, Academic Press, 1997, pp. 307-326.

[18] G.M. Sheldrick, SADABS, Program for Empirical Absorption Correction of Area Detector Data, University of Gӧttingen, Germany, 2009.

[19] G.M. Sheldrick, *Acta Crystallogr.* A64 (2008) 112.

[20] A.L. Spek, PLATON. A Multipurpose Crystallographic Tool, Utrecht University, Utrecht, The Netherlands, 2010.

[21] C.F. Macrae, I.J. Bruno, J.A. Chisholm, P.R. Edgington, P. McCabe, E. Pidcock, L. Rodriguez-Monge, R. Taylor, J. van de Streek and P.A. Wood, *J. Appl. Cryst.* 41 (2008) 466.

[22] N. L. Biddington, T. H. Thomas, *Planta* 111 (1973) 183-186.

[23] C. Bigot, *Compt. Rend. Acad. Sci.* 266 (1958) 349.

[24] A. Domínguez-Martín, D. Choquesillo-Lazarte, J. M. González-Pérez, A. Castiñeiras, J. Niclós-Gutiérrez, *J. Inorg. Biochem.* 105 (2011) 1073-1080.

[25] A. W. Addison, T. N. Rao, J. Reedijk, J. Van Rijn and G. C. Verschoor, *J. Chem. Soc., Dalton Trans.* (1984) 1349-1356.

[26] Y. Kani, S. Ohba, S. Ito, Y.Nishida, *Acta Crystallogr.* C56 (2000), e233.

[27] B. Cebrian-Losantos, E. Reisner, C.R. Kowol, A. Roller, S. Schova, V. B. Arion, B. K. Keppler, *Inorg. Chem.* 47 (2008) 6513-6523.

[28] C. Pearson, A.L. Beauchamp, *Inorg. Chem.* 37 (1998) 1242-1248.

[29] W. S. Sheldrick, B. Gunther, *J. Organomet. Chem.* 375 (1989) 233-243.

[30] W.-B. Li, *Acta Crystallogr.* E67 (2011) m1249.

[31] E.-C. Yang, Y.-N. Chan, H. Liu, Z.-C. Wang, X.-J. Zhao, *Cryst. Growth Des.*, 9 (2009) 4933-4944.

[32] J. Pas , M. von Grotthuss, L.S. Wyrwicz, L. Rychlewski, J. Barciszewski, FEBS Letters 576 (2004) 287-290.

[33] C. Meiser, B. Song, E. Freisinger, M. Peilert, H. Sigel, B. Lippert *Chem. Eur. J.* 3 (1997) 388-398.

[34] A. V. Vargiu, A. Magistrato, *Inorg. Chem.* 51 (2012) 2046−2057.

[35] R.Guddneppanavar, U.Bierbach, *Anti-Cancer agents in Medicinal Chemistry* 7 (2007) 125-138.

[36] Z. Travnicek, I. Popa, M. Cajan, R. Herchel, J. Marek, *Polyhedron* 26 (2007) 5271-5282.

[37] A. Klanicova, Z. Travnicek, J. Vanco, I. Popa, Z. Sindelar, *Polyhedron* 29 (2010) 2582-2589.

## 4.2. Intrinsic Acid-Base Properties of a Hexa-2'-deoxynucleoside Pentaphosphate, d(ApGpGpCpCpT). Neighboring Effects and Isomeric Equilibria

Article accepted in *Chem.-Eur. J.* (2012)

RESUMEN

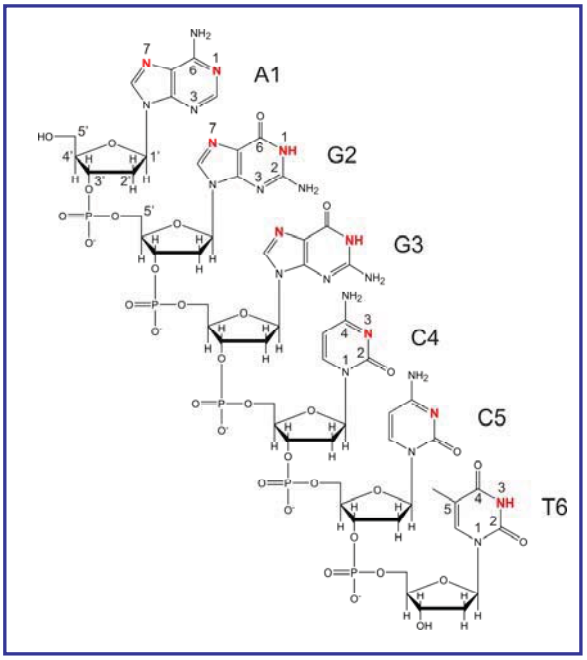


Las propiedades ácido-base intrínsecas del hexa-2'-desoxinucleosido pentafosfato, d(ApGpGpCpCpT) [= (A1·G2·G3·C4·C5·T6) = $(HNPP)^{5-}$] han sido determinadas mediante experimentos de Resonancia Magnética Nuclear de protón ($^1$H-RMN). Los valores de p$K_a$ de los residuos de los nucleósidos individuales: adenosina(A), guanosina (G), citidina (C) y timidina (T) fueron medidos en agua bajo condiciones de hebra sencilla (10% $D_2O$, 47°C, I = 0.1 M, $NaClO_4$). Estos resultados cuantifican la liberación de $H^+$ desde las dos unidades $(N7)H^+$ (G·G), las dos unidades $(N3)H^+$ (C·C), y la unidad $(N1)H^+$ (A), así como de las dos posiciones (N1)H (G·G) y la posición (N3)H (T). Basándonos en medidas de 2'-desoxinucleosidos a 25° y 47°C, los correspondientes valores de p$K_a$ fueron calculados en agua a 25ºC y I = 0.1M. En la hebra sencilla se forman interacciones de apilamiento entre las nucleobases A1 y G2, así como también, con gran probabilidad, entre G2 y G3. En HNPP, se observan tres grupos de p$K_a$, e.g., el que abarca los valores de p$K_a$ 2.44, 2.97 y 3.71 de $G2(N7)H^+$, $G3(N7)H^+$ y $A1(N1)H^+$ respectivamente, con regiones de amortiguamiento solapadas. La población de tautómeros ha sido estimada, dadndo la para pérdida de un solo protón desde la especie totalmente protonada $H_5(HNPP)^{\pm}$, los tautómeros (G2)N7, (G3)N7, y (A1)N1 con un grado de formación alrededor del 74, 22 y 4%, respectivamente. La distribución de tautómeros revela rutas tanto para donar como aceptar protones a una velocidad que se espera rápida y que ocurra prácticamente "sin costes". Los ocho valores de p$K_a$ para $H_5(HNPP)^{\pm}$ están comparados con los datos

disponibles para nucleósidos y nucleótidos individuales. Los resultados muestran que los residuos nucleosídicos están en parte afectados de manera diferente dependiendo del nucleósidos vecino. Además, la constantes de acidez intrínsecas para un derivado de ARN r(A1·G2·G3·C4·C5·U6), donde U = uridina, han sido calculadas. Finalmente, el efecto de los iones metálicos en los valores de pKa de las correspondientes unidades se discute de manera breve ya que, de esta forma, las reacciones de desprotonación pueden ser fácilmente trasladadas al rango de pH fisiológico.

# Intrinsic Acid-Base Properties of a Hexa-2'-deoxynucleoside Pentaphosphate, d(ApGpGpCpCpT). Neighboring Effects and Isomeric Equilibria

Alicia Domínguez-Martín,[a,b] Silke Johannsen,[a], Astrid Sigel,[c] Bert P. Operschall,[c] Bin Song,[c,d] Helmut Sigel,[c] Andrzej Okruszek,[e] Josefa María González-Pérez,[b] Juan Niclós-Gutiérrez,[b] and Roland K. O. Sigel*[a]

[a] A. Domínguez-Martín, Dr. S. Johannsen, Prof. Dr. R. K. O. Sigel Institute of Inorganic Chemistry, University of Zürich Winterthurerstrasse 190, 8057 Zürich (Switzerland)
Fax: (+41)44-635-6802
E-mail: roland.sigel@aci.uzh.ch

[b] A. Domínguez-Martín, Prof. Dr. J. M. González-Pérez, Prof. Dr. J. Niclós-Gutiérrez Department of Inorganic Chemistry, Faculty of Pharmacy, University of Granada, Campus Cartuja, 18071 Granada (Spain)

[c] A. Sigel, Dipl.-Ing. B. P. Operschall, Dr. B. Song, Prof. Dr. H. Sigel Department of Chemistry, Inorganic Chemistry, University of Basel Spitalstrasse 51, 4056 Basel (Switzerland)

[d] Dr. B. Song
Vertex Pharmaceuticals Inc.,
130 Waverly Street, Cambridge, MA 02139 (USA)

[e] Prof. Dr. A. Okruszek
Department of Bioorganic Chemistry, Centre of Molecular & Macromolecular Studies Polish Academy of Sciences, 90-363 Lódz (Poland)
and Institute of Technical Biochemistry, Faculty of Biotechnology & Food Sciences Lódz University of Technology, 90-924 Lódz (Poland)

Supporting information for this article is available on the WWW under http://dx.doi.org/...

**Abstract:** The intrinsic acid-base properties of the hexa-2'-deoxynucleoside pentaphosphate, d(ApGpGpCpCpT) [= (A1·G2·G3·C4·C5·T6) = $(HNPP)^{5-}$] have been determined via $^{1}H$ NMR shift experiments. The p*K*a values of the individual sites of the adenosine (A), guanosine (G), cytidine (C), and thymidine (T) residues were measured in water under single strand conditions (10% $D_2O$, 47°C, $I$ = 0.1 M, $NaClO_4$). These results quantify the release of $H^+$ from the two $(N7)H^+$ (G·G), the two $(N3)H^+$ (C·C), and the $(N1)H^+$ (A) units, as well as from the two (N1)H (G·G) and the (N3)H (T) sites. Based on measurements with 2'-deoxynucleosides at 25° and 47°C, they were transferred to p*K*a values valid in water at 25°C and $I$ = 0.1 M. Intramolecular stacks between the nucleobases A1 and G2 as well as most likely also between G2 and G3 are formed. For HNPP three p*K*a clusters occur, e.g., encompassing the p*K*a values of 2.44, 2.97, and 3.71 of $G2(N7)H^+$, $G3(N7)H^+$, and $A1(N1)H^+$, respectively, with overlapping buffer regions. The tautomer populations were estimated, giving for the release of a single proton from 5-fold protonated $H5(HNPP)^{\pm}$, the tautomers (G2)N7, (G3)N7, and (A1)N1 with formation degrees of about 74, 22, and 4%, respectively. Tautomer distributions reveal pathways for proton-donating as well as for proton-accepting reactions both being expected to be fast and to occur practically at no "costs". The eight p*K*a values for $H_5(HNPP)^{\pm}$ are compared with data for nucleosides and nucleotides, revealing that the nucleoside residues are in part affected very differently by their neighbors. In addition, the intrinsic acidity constants for the RNA derivative r(A1·G2·G3·C4·C5·U6), where U = uridine, were calculated. Finally, the effect of metal ions on the p*K*a values of nucleobase sites is shortly discussed because in this way deprotonation reactions can easily be shifted to the physiological pH range.

**Keywords:** acidity · basicity · DNA · metal ions · RNA · tautomerism

## 1. Introduction

Both types of nucleic acids, DNA and RNA, consist overwhelmingly of only four different nucleobase residues which are linked to each other via the phosphate sugar backbone. Despite this very limited number of building blocks, the information storage in these nucleic acids is tremendous including the genetic code, the expression of proteins, etc.[1] The selectivity of information transfer like transcription and translation is determined by the order of the nucleobase residues which itself affects not only internal hydrogen bonding and stacking interactions but also the protonation and deprotonation reactions of the nucleobases. Naturally, the indicated acid-base properties have a strong impact on the metal ion-binding properties[2,3] of nucleic acids and these are closely interwoven with their reactivity.[4,6]

It follows that the acid-base properties are of fundamental relevance for understanding the functioning of nucleic acids, yet the available information on neighboring effects is very scarce,[7,8] though p$K_a$ shifts in the order of 2 log units are known.[9] Therefore, we decided to investigate an oligonucleotide by $^1$H NMR shift measurements and to determine the intrinsic acid-base properties of the various nucleobases using the hexanucleoside pentaphosphate, d(ApGpGpCpCpT), shown in Figure 1.[10]

There were several reasons for selecting this oligonucleoside phosphate: (i) Oligo-2'-deoxynucleoside phosphates are more stable, that is, less hydrolysis-sensitive, than their RNA counterparts; (ii) the *cis*-$(NH_3)_2Pt^{2+}$ complex of the compound seen in Figure 1 had previously been studied[11,12] and therefore we expected that interesting comparisons might become possible; and (iii) the effect of the ribose *versus* the 2'-deoxyribose residue on the acid-base properties of nucleotides is known[13,14] allowing us to make sophisticated estimates also for the intrinsic acidity constants of the corresponding RNA oligonucleoside phosphate.

The hexa-2'-deoxynucleoside pentaphosphate $(HNPP)^{5-}$ of Figure 1 may also be abbreviated as dApdGpdGpdCpdCpdT or d(ApGpGpCpCpT) following conventional rules. However, for the present it is more convenient to write simply A1·G2·G3·C4·C5·T6 as is indicated in Figure 1. In this way the position of a given nucleoside within the hexanucleoside pentaphosphate is immediately evident facilitating comparisons.

Because A1·G2·G3·C4·C5·T6 is self-complementary and forms a double helix[12] at room temperature and an ionic strength ($I$) of 0.1 M, the experiments were carried out at 320 K where the oligo exists overwhelmingly in the single-stranded form and thus the

protons are not involved in helix-hydrogen bonding. The resulting acidity constants are compared with those of the individual nucleosides also measured at 320 K (= 47°C) and 298 K (= 25°C) as well as those of the corresponding nucleotides taken from the literature. These comparisons, including measurements with buffers, allow further to correct for the solvent (water containing 10% $D_2O$) and the temperature effects (47°C) and to present the intrinsic acidity constants of A1·G2·G3·C4·C5·T6 also for 25°C and $I$ = 0.1 M ($NaClO_4$).

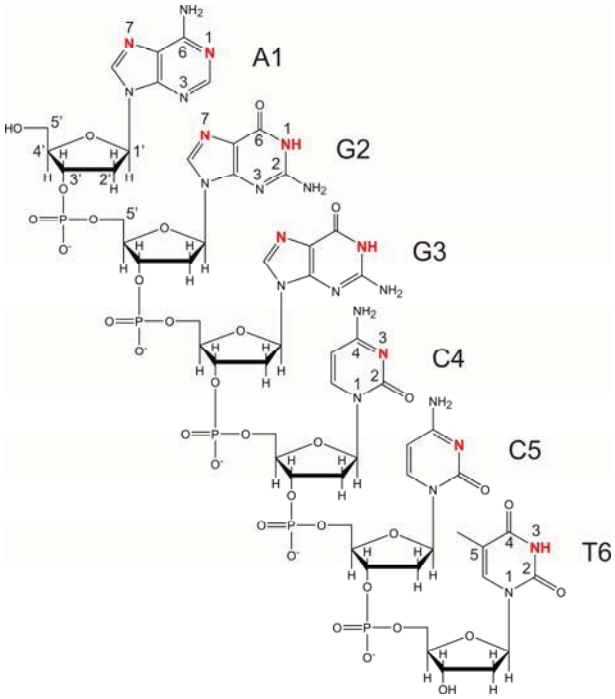


Figure 1. Chemical structure of the hexa-2'-deoxynucleoside pentaphosphate, $d(ApGpGpCpCpT)^{5-}$, also abbreviated as $(HNPP)^{5-}$ or A1·G2·G3·C4·C5·T6 (with charges only given where needed). The nine sites, whose acid-base equilibria are discussed here are shown in red (for details about $A1(N7)H^+$ see Ref. [10]).

## 2. Results and Discussion

**2.1. Conditions for the formation of single strands:** The self-complementary hexanucleoside A1·G2·G3·C4·C5·T6 forms at room temperature a double helix.[12] Therefore, we determined the melting temperature ($T_m$) by measuring the UV absorption at 260 nm in dependence on the temperature (Figure 2, blue curve). Similarly, a corresponding plot of the molar ellipticity at 280 nm, based on CD spectra taken in the range of 200 to 320 nm in dependence on temperature (see Supporting Information; Figure S1), furnished a further value for $T_m$ (red curve). In total four determinations were made, i.e., three by UV absorption at 260

nm, namely heating ($T_m$ 38.8°C), cooling (36.0°C; Figure 2) and $A_{260}$ from the CD measurement (36.9°C), as well as one CD experiment at 280 nm (molar ellipticity; $T_m$ = 32.7°C; Figure 2). The overall result of these four values provides $T_m$ = 36.1 ± 2.5 (2) as measured in aqueous solutions of 1.5·10–4 M $(HNPP)^{5-}$ (Figure 2) at pH 6.5. This value agrees with the previous result, $T_m$ = 37 ± 2°C, which was determined, also by UV-absorption spectroscopy at 260 nm, in 1.6·10–5 M solution in $D_2O$ at pD 7.8.[12] The somewhat different pH values of the experiments do not have any influence on the result because in this pH range no acid-base reaction occurs with $(HNPP)^{5-}$ (see Section 2.8). The different concentrations employed, i.e., $1.5 \cdot 10^{-4}$ M versus $1.6 \cdot 10^{-5}$ M, apparently also do not have any significant effect on Tm, though at a 30 times higher concentration, i.e., $4.5 \cdot 10^{-3}$ M, $T_m$ is increased as measured by $^1H$ NMR.[12]

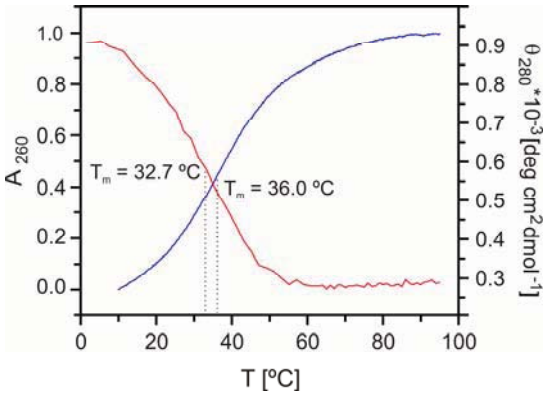


Figure 2. *Red curve*: Plot of molar ellipticity at 280 nm *versus* temperature (see also Figure S1). *Blue curve*: Plot of the normalized UV absorption at 260 nm versus temperature ($\varepsilon = 5.51 \cdot 10^4$ $M^{-1}$ $cm^{-1}$ at 10ºC; $\varepsilon = 6.13 \cdot 10^4$ $M^{-1}$ $cm^{-1}$ at 95ºC). – All measurements were carried out with 0.15 mM $(HNPP)^{5-}$ in 0.1 M $NaClO_4$ at pH = 6.5.

The acid-base properties of the hexanucleoside were thus studied at 320 K (= 47°C; *vide infra*) for the following reasons: the purine-H8 exchange is increasingly facilitated the higher the temperature and most important, it was our aim to measure the p$K_a$ values at the lowest temperature possible at which the single strand strongly dominates. Indeed, this is the case at 320 K, as is seen from the results given in Figure 3: The [$^1H$, $^1H$]-NOESY measurements presented in the upper part (A) refer to 281 K (= 8°C) and here the sequential walk can be followed proving that the double helix strongly predominates. In contrast, in the lower part (B) of Figure 3 the dipolar proton couplings have mostly disappeared, indicating that at 320 K (= 47°C) an undefined structure is present as it is the case for a single strand. Moreover, the hydrodynamic radius as determined by DOSY (Diffusion-Ordered SpectroscopY) experiments, decreases from 1.17 ± 0.02 (2 σ) nm at 8°C to 1.03 ± 0.02 (2 σ)

nm at 47°C confirming that the particle is getting smaller and that at a d(ApGpGpCpCpT) concentration of $1.5 \cdot 10^{-4}$ M the single-stranded species dominates. This conclusion is verified by the simplifying assumption that both species exist in a first approximation in a spherical form; then one may calculate their volume according to $4\pi r^3/3$ and obtains at 8°C for the double helix 6.71 $nm^3$ and at 47°C for the single strand the much smaller volume of 4.58 $nm^3$.

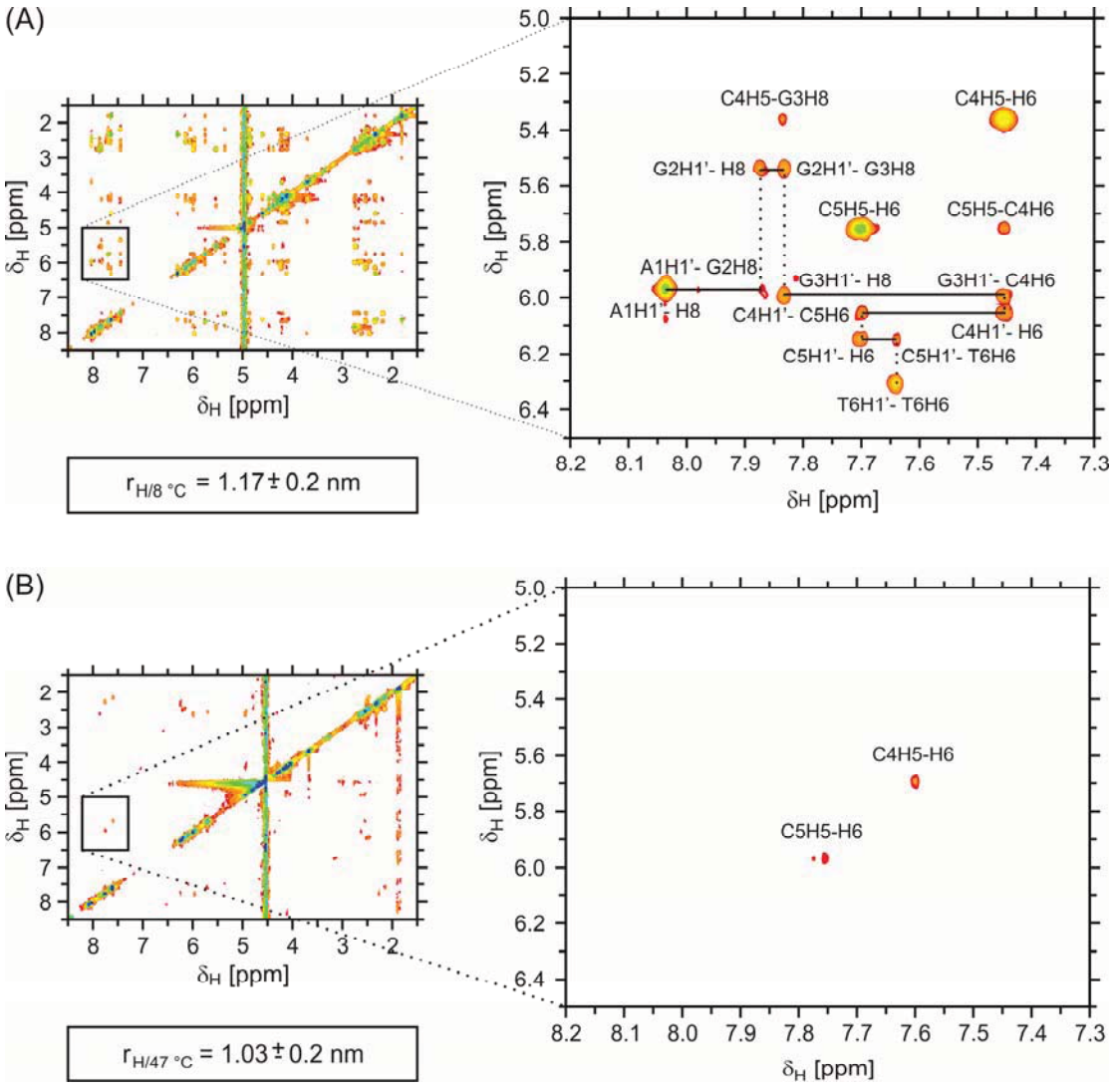


Figure 3. [$^1$H,$^1$H]-NOESY spectra of the *duplex* [d(ApGpGpCpCpT)]$_2$ at 281 K (8°C) (**A**) and of the *single strand* d(ApGpGpCpCpT) at 320 K (47°C) (**B**). The appropriate hydrodynamic radii calculated from DOSY experiments are provided below the spectra. Magnified sections of the sequential walk region are depicted on the right. In **A** the sequential walk can be followed through the entire sequence proving a double helical structure at 8°C. At 47°C (**B**) only two intra-residue correlations are visible indicating a single strand formation. The measurements were performed with 0.15 mM solutions of $(HNPP)^{5-}$ in 100% D2O ($I$ = 0.1 M, $NaClO_4$; pD = 6.3).

**2.2. Definitions of the acid-base equilibria**: The hexa-2'-deoxynucleoside pentaphosphate $(HNPP)^{5-}$ (Figure 1) carries a charge of minus five because each of the five phosphodiester bridges has a charge of minus one. This species may be 5-fold protonated, namely at N1 of A1 (N7 of A1 is not of relevance because p*K*a/(N7)H ca. –1.5),[10] twice at N7 each of G2 and G3, and also twice at N3 each of C4 and C5 (cf. the structure in Figure 1). We define this protonated species as $H_5(HNPP)^{\pm}$. On the other hand, the two (N1)H sites of G2 and G3 as well as (N3)H of T6 may be deprotonated each. Thus, after deprotonation of these three, initially uncharged (N)H sites, we obtain $(HNPP - 3H)^{8-}$. The deprotonation reactions of the mentioned examples are indicated in Equilibria (1) to (3). All the other acidity constants are defined analogously:

$$H_5(HNPP)^{\pm} \rightleftharpoons H_4(HNPP)^{-} + H^{+} \quad (1a)$$

$$K^{H}_{H_5(HNPP)} = [H_4(HNPP)^{-}][H^{+}]/[H_5(HNPP)^{\pm}] \quad (1b)$$

$$(HNPP)^{5-} \rightleftharpoons (HNPP - H)^{6-} + H^{+} \quad (2a)$$

$$K^{H}_{(HNPP)} = [(HNPP - H)^{6-}][H^{+}]/[(HNPP)^{5-}] \quad (2b)$$

$$(HNPP - 2H)^{7-} \rightleftharpoons (HNPP - 3H)^{8-} + H^{+} \quad (3a)$$

$$K^{H}_{(HNPP - 2H)} = [(HNPP - 3H)^{8-}][H^{+}]/[(HNPP - 2H)^{7-}] \quad (3b)$$

Please note, that, e.g., $(HNPP - H)^{6-}$, should be read as "HNPP *minus* H". Furthermore, in the present context it needs to be added that the affinity of monoprotonated phosphate monoesters, $(RO)(HO)P(O)_2^{-}$ , or of phosphodiester bridges, $(RO)2P(O)_2^{-}$ , for protons is very low. In fact, if protonation is enforced in such species $H^{+}$ is released with p*K*a ca. 1.[15-17] This means, this reaction is not of relevance for the present study which encompasses pH values above 2.

For comparison also the acid-base properties of several nucleosides had to be quantified (Sections 2.3 and 2.9) or taken from the literature.[18-22] These nucleosides encompass monoprotonated $H(Ns)^{+}$ species, e.g., adenosine (Ado) being protonated at N1 giving $H(Ado)^{+}$, as well as species which have lost a proton from their nucleobase, $(Ns - H)^{-}$, like from (N1)H of guanosine (Guo) giving $(Guo - H)^{-}$. These equilibria are expressed

in Equations (4) and (5):

$$H(Ns)^+ \rightleftharpoons Ns + H^+ \quad (4a)$$

$$K^H_{H(Ns)} = [Ns][H^+]/[H(Ns)^+] \quad (4b)$$

$$Ns \rightleftharpoons (Ns - H)^- + H^+ \quad (5a)$$

$$K^H_{Ns} = [(Ns - H)^-][H^+]/[Ns] \quad (5b)$$

The corresponding equilibria for nucleoside monophosphates ($NMP^{2-}$), like for $H2(GMP)^{\pm}$ or $H_2(dGMP)^{\pm}$ which carry a proton each at N7 and the $PO_3^{2-}$ residue and lose one from their (N1)H site, are given in Equations (6) to (8) (see also Section 2.10):

$$H_2(NMP)^{\pm} \rightleftharpoons H(NMP)^- + H^+ \quad (6a)$$

$$K^H_{H_2(NMP)} = [H(NMP)^-][H^+]/[H_2(NMP)^{\pm}] \quad (6b)$$

$$H(NMP)^- \rightleftharpoons NMP^{2-} + H^+ \quad (7a)$$

$$K^H_{H(NMP)} = [NMP^{2-}][H^+]/[H(NMP)^-] \quad (7b)$$

$$NMP^{2-} \rightleftharpoons (NMP - H)^{3-} + H^+ \quad (8a)$$

$$K^H_{NMP} = [(NMP - H)^{3-}][H^+]/[NMP^{2-}] \quad (8b)$$

In the calculations of the acidity constants for the above equilibria (for details see 4. Experimental Section), the direct pH-meter readings were used and these quantify the $H^+$ activity and not the $H^+$ concentration. Hence, the presented constants are so-called practical constants,[19] also known as mixed or Brønsted constants,[19,23,24] which include activity and concentration terms. However, these values can easily be transferred into concentration constants.[24]

**2.3. Summary of some experimental hurdles:** The pH meter was calibrated with buffers; the calibration was checked after the measurements: The average drift was very small [±(0.007 ± 0.005) pH unit] and ignored (see Supporting Information).

The measurements were carried out in water containing 10% $D_2O$ ($I$ = 0.1 M, $NaClO_4$) for technical reasons (see 4. Experimental Section). The isotope effect[25] is small, i.e., 0.01 ± 0.007 pH unit, but it was considered in the final evaluations (see Supporting Information).

More important, the temperature effect between NMR measurements at 25°C and 47°C also had to be determined. Since it is difficult to adjust a desired pH value in an NMR tube at 47°C by using a glass rod and dotting with $HClO_4$ and/or NaOH, we adjusted the desired pH at 25°C and measured then the NMR spectra at 47°C. Because one expects that a pH determined in a solution at 25°C differs somewhat from that of the same solution if measured again at 47°C, we used the monoprotonated nucleosides cytidine (Cyd) and guanosine (Guo) as probes and measured the p$K$a values for $H(Cyd)^+$ and $H(Guo)^+$ in water containing 10% D2O at 25°C (i.e., at the same temperature for the pH meter and the NMR instrument). The experiments with $H(Guo)^+$ and $H(Cyd)^+$ are shown in Figure 4 and S2, respectively. Next, we repeated the experiments by adjusting the pH at 25°C but carrying out the NMR-shift measurements at 47°C. Moreover, both types of experiments were also carried out in $D_2O$. All the relevant p$K_a$ values are listed in Table S1 of the Supporting Information.

If one calculates now the difference, $\Delta pK_a$, between the $pK_{a/25}$ value valid for 25°C and the one determined at 47°C (with the solution pH adjusted at 25°C) and plots these data (see Table S1), that is, $\Delta pK_a$ (y-axis) *versus* $pK_{a/47}$ (x-axis), one obtains a straight line (see Figure S3), the parameters of which are given in Equation (9):

$$Y = m \cdot x + b \tag{9a}$$

$$\Delta pK_a = -(0.0330 \pm 0.0017) \cdot pK_{a/47} + (0.2266 \pm 0.0104) \tag{9b}$$

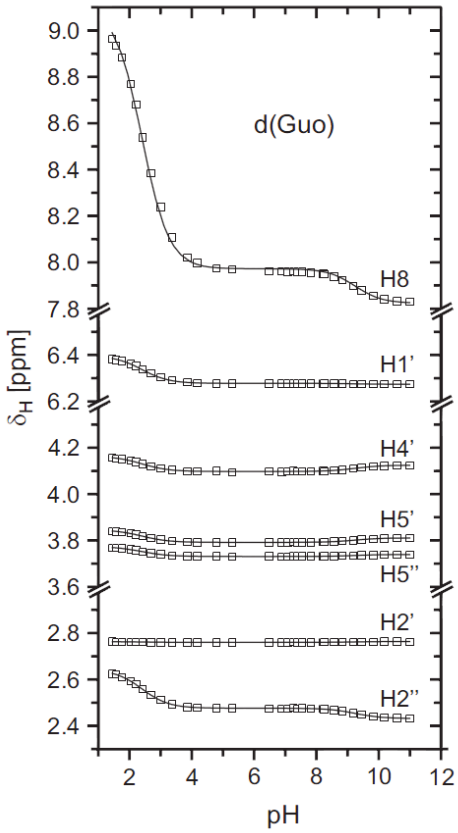


Figure 4. Variation of the chemical shift $\delta_H$ (in ppm) for the proton of 2'-deoxyguanosine (0.5 mM) in dependence on pH as measured in an aqueous solution containing 10% $D_2O$ at 25°C (both, pH-meter and Bruker 500 MHz spectrometer) and $I$ = 0.1 M ($NaClO_4$; see also Experimental Section). The solid curves are the calculated best fits of the experimental data using the final results (from two experiments), i.e., $pK^{H}_{H(dGuo)}$ = 2.40 ± 0.14 and $pK^{H}_{dGuo}$ H = 9.24 ± 0.03 (see also Table S1 of the Supporting Information).

The error limit within the $pK_{a/47}$ range from about 2 to 10 amounts to ±0.04 (3□) for $\Delta pK_a$. The value calculated for $\Delta pK_a$ needs to be added to the apparent acidity constant, $pK_{a/47}$, measured at 47°C to obtain the acidity constant, $pK_{a/25}$, valid for 25°C. The corrections are not dramatic, though, e.g., for the "extreme" $pK_a$ values of 2.5 and 9.5 they amount to $\Delta pK_a$ = 0.14 ± 0.04 and –0.09 ± 0.04, respectively. The mentioned two $pK_a$ values correspond roughly to a Guo residue. The $\Delta pK_a$ corrections have opposite signs because the first $H^+$ is removed from the positively charged $(N7)H^+$ site, whereas the second one originates from the neutral (N1)H unit. To conclude, application of Equation (9) to the $pK_{a/47}$ values measured for the nucleobases of A1·G2·G3·C4·C5·T6 leads to the acidity constants of the single-stranded hexanucleoside valid for 25°C in aqueous solution containing 10% $D_2O$ ($I$ = 0.1 M, $NaClO_4$) (see Section 2.8).

**2.4. Evaluation procedure of the $^1$H NMR shift measurements in water containing 10% $D_2O$ at 320 K**: At 47°C and a concentration of 0.15 mM, the hexanucleoside pentaphosphate d(ApGpGpCpCpT) (Figure 1) exists overwhelmingly in the single-stranded form (Figure 3). Under these conditions the acid-base equilibria of Section 2.2 can occur and consequently, the $^1$H NMR chemical shifts of the various nucleoside protons vary with pH (see Figure 5).

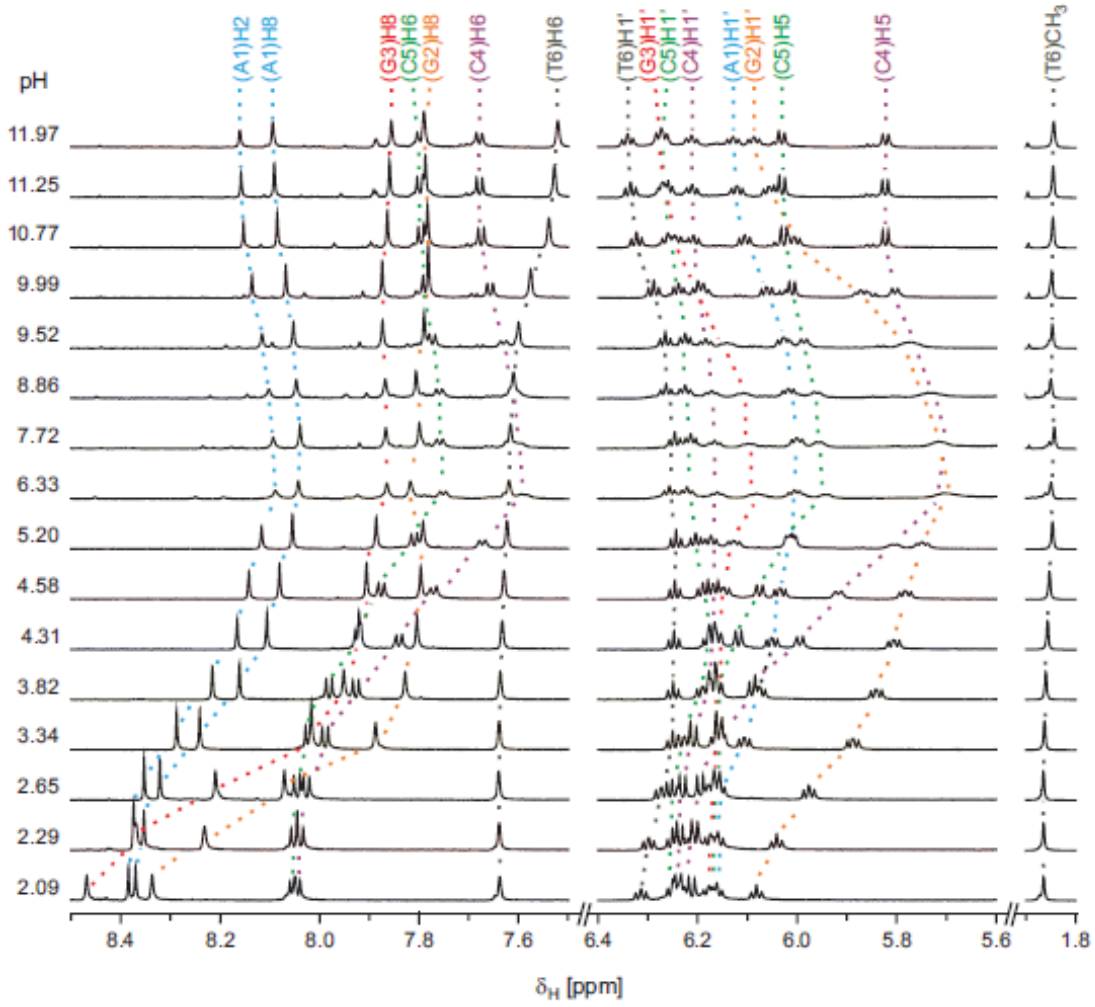


Figure 5. Shown is the pH dependence of the $^1$H NMR spectra (Bruker 700MHz spectrometer)of 0.15 mM hexamer, that is of A1·G2·G3·C4·C5·T6 at 320 K (= 47°C) in water containing 10% $D_2O$ and $I$ = 0.1 M ($NaClO_4$). **Left**: Aromatic protons of the nucleobase residues. **Middle**: H1' of the ribose moieties as well as of H5 of C4 and C5. **Right**: CH3 protons at carbon(5) of T6.

To obtain the acidity constant of a given site in a nucleobase residue we plotted the measured chemical shifts of the various protons in dependence on pH. For the evaluation of a given (de)protonation site, the protons of the nucleoside residue in question as well as those of its next two neighbors were taken into account. This means, the p$K_a$ value for the (N1)$H^+$ site of the adenosine residue of A1 was determined via the weighted mean by taking into account not only the chemical shifts of H2, H8, and H1' of the Ado residue but also by considering the chemical shifts of other protons which showed a significant pH dependence, that is, in the present case H1' of G2 [see Table 1; note, H8 of G2 was not used because in this case the effect of the (N7)$H^+$ site is very large (see Figure 7, *vide infra*)]. Correspondingly, for measuring the p$K_a$ of the (N1)H site of G2 we also considered the chemical shifts of A1 and G3, etc., by fitting the chemical shift changes to two p$K_a$ values (see Table 1).

A view on the individual p$K_a$ values obtained for a given site (Table 1) shows that the neighboring nucleoside residues sometimes feel a somewhat lower but sometimes also higher p$K_a$ value. A typical example for this behavior is (N1)H of G3, the deprotonation of which is reflected at G2 and also at C4. Of course, one could argue against this kind of evaluation and state that only the chemical shift(s) observed for a given nucleoside residue should be used: For example, this would give for G2 based on experiment 1 p$K_a$ = 10.30 ± 0.08 (Table 1, column 3; the values are now rounded) and for G3 p$K_a$ = 10.10 ± 0.09; from experiment 2 p$K_a$ = 10.28 ±0.12 follows for G2 and p$K_a$ = 10.08 ± 0.11 for G3. These values differ somewhat from the weighted mean given in column 5 of Table 1, which are for the two (N1)H sites of G2 and G3 p$K_a$ =10.18 ± 0.04 and 9.99 ± 0.11, respectively, though within the error limits the values still overlap. More important, the difference in acidity between the two (N1)H sites is about 0.2 p$K$ unit in all instances. Overall, we are convinced that the weighted means, which include the p$K_a$ values from the neighboring nucleoside residues, describe the situation best.

As indicated, two independent experiments were carried out. From the individual results (Table 1, columns 3 and 4) the weighted means were calculated (Table 1, column 5; the arithmetic mean is given for comparison). The errors of the results obtained for the individual protons vary considerably, also between the two series, though those for experiment 1 are commonly a bit smaller (there were more data points in this case). The weighted means are therefore considered as the best possible result. Indeed, if one considers the difference in the chemical shifts between the protonated and the deprotonated species (see also Figure 5) it is clear that if this difference is small the error in p$K_a$ is expected to be

large and *vice versa*. In the next step we checked if the determined p*K*a values could be fitted in a satisfactory manner to the shifts of the protons of the nucleoside residues considered. Indeed, this is the case as is seen from the examples shown in Figure 6.

Table 1. Individual acidity constants as determined by $^1$H NMR shift experiments at 47°C ($I$ = 0.1 M, $NaClO_4$) in water containing 10% $D_2O$ for the (N1)$H^+$ and (N3)$H^+$ sites of the adenine and cytosine residues, respectively (see Figure 1), as well as for the (N1)H and (N3)H sites for the guanine and thymine residues, respectively. For the evaluation of the two independent experiments (Exp. 1 and Exp. 2) always the chemical shifts of the protons of a given nucleoside (Ns) residue as well as those of its next neighbors were considered.[a]

| Ns residue | Proton | p$K_a$ (Exp. 1) | p$K_a$ (Exp. 2) | p$K_{a/av}$ weighted mean (arith. mean) |
|---|---|---|---|---|
| A1 | (A1)H2 | 3.695 ± 0.024 | 3.604 ± 0.043 | 3.614 ± 0.044 (3.544 ± 0.061) |
| | (A1)H8 | 3.612 ± 0.023 | 3.451 ± 0.044 | |
| | (A1)H1' | 3.609 ± 0.059 | 3.614 ± 0.060 | |
| | (G2)H1' | 3.617 ± 0.073 | 3.148 ± 0.098 | |
| G2 | (A1)H2 | 10.041 ± 0.147 | 9.940 ± 0.265 | 10.184 ± 0.038 (10.159 ± 0.037) |
| | (A1)H8 | 10.206 ± 0.201 | 10.215 ± 0.402 | |
| | (A1)H1' | 10.253 ± 0.115 | 10.179 ± 0.102 | |
| | (G2)H1' | 10.299 ± 0.081 | 10.277 ± 0.119 | |
| | (G3)H1' | 10.095 ± 0.095 | 10.082 ± 0.106 | |
| G3 | (G2)H1' | 10.299 ± 0.081 | 10.277 ± 0.119 | 9.989 ± 0.113 (9.914 ± 0.115) |
| | (G3)H1' | 10.095 ± 0.092 | 10.082 ± 0.106 | |
| | (C4)H5 | 9.604 ± 0.092 | 9.458 ± 0.146 | |
| | (C4)H6 | 9.896 ± 0.123 | 9.603 ± 0.181 | |
| C4 | (G3)H1' | 4.112 ± 0.124 | 4.245 ± 0.128 | 4.404 ± 0.048 (4.402 ± 0.066) |
| | (C4)H5 | 4.384 ± 0.022 | 4.397 ± 0.028 | |
| | (C4)H6 | 4.345 ± 0.020 | 4.353 ± 0.027 | |
| | (C5)H5 | 4.628 ± 0.043 | 4.869 ± 0.031 | |
| | (C5)H6 | 4.343 ± 0.016 | 4.345 ± 0.030 | |
| C5 | (C4)H5 | 4.384 ± 0.022 | 4.397 ± 0.028 | 4.411 ± 0.051 (4.467 ± 0.054) |
| | (C4)H6 | 4.345 ± 0.020 | 4.353 ± 0.027 | |
| | (C5)H5 | 4.628 ± 0.043 | 4.869 ± 0.031 | |
| | (C5)H6 | 4.343 ± 0.016 | 4.345 ± 0.030 | |
| | (T6)H6 | 4.479 ± 0.039 | 4.526 ± 0.099 | |
| T6 | (T6)H6 | 10.199 ± 0.015 | 10.118 ± 0.034 | 10.170 ± 0.092 (9.949 ± 0.094) |
| | (T6)H1' | 10.212 ± 0.040 | 10.124 ± 0.076 | |
| | (C5)H5 | 9.833 ± 0.138 | 9.486 ± 0.100 | |
| | (C5)H6 | 9.946 ± 0.144 | 9.671 ± 0.268 | |

[a] For the values of the (N7)$H^+$ units in G2 and G3 see text in Section 2.5.

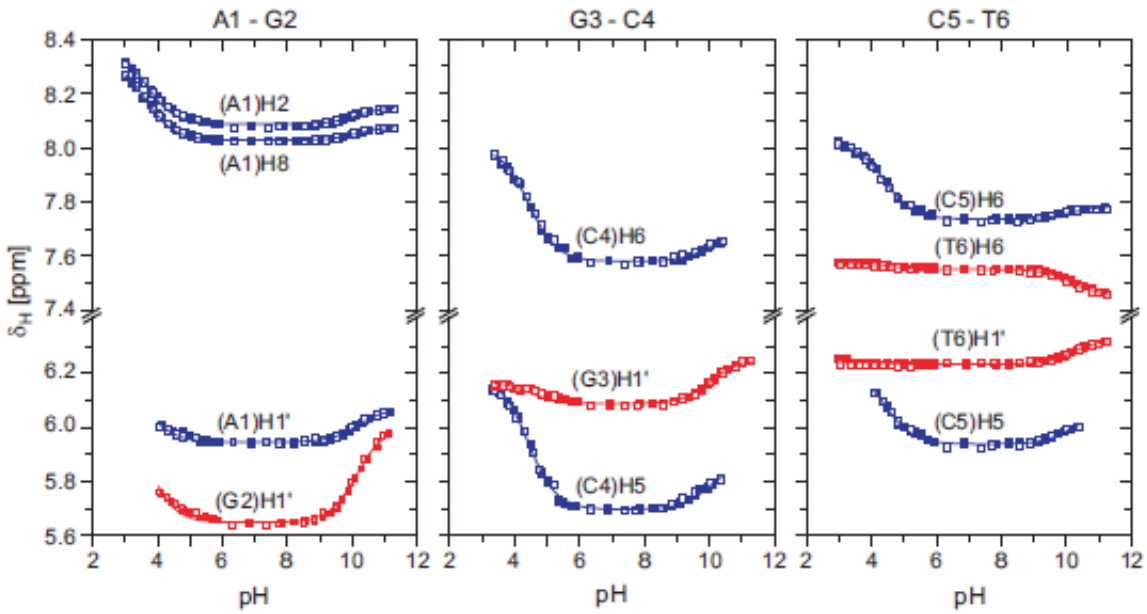


Figure 6. Preliminary fits of the chemical shifts $\delta_H$ for several protons of the hexamer A1·G2·G3·C4·C5·T6 in dependence on pH by using the results summarized in Table 1, this means, e.g., for A1-G2 (left in the figure) only the p$K_a$ values of 3.614 and 10.184 were used for the fitting procedure (see also text). The NMR measurements were made twice (open and solid data points; see also Table 1, columns 3 and 4) in water containing 10% $D_2O$ ($I$ = 0.1 M, $NaClO_4$) at 47°C (= 320 K); the probes had prior been adjusted at 25°C to the desired pH.

**2.5. Estimation of the acidity of the (N7)H$^+$ sites in G2 and G3:** In the way described in Section 2.4 we determined the acidity constants for the N1 sites of the purine derivatives and for the N3 sites of the pyrimidines, which amounts in total to six acidity constants (Table 1). The corresponding values for the two (N7)H$^+$ units of G2 and G3 could not be determined by such a simple fit because the chemical shift for the fully protonated species is not well enough defined, aside from the fact that five variables are involved, i.e., two p$K$a values and three limiting shifts. Furthermore, to adjust a pH of about 1 is not advisable because then the phosphodiester bridge will also be protonated, as the p$K_a$ of (RO)2P(O)(OH) is about 1 (Section 2.2).[15-17]

Therefore, we kept the mentioned six acidity constants fixed and fitted the experimental data again by allowing for the variation of two more p$K_a$ values, that is, in total eight acidity constants were considered. A fitting procedure with only seven acidity constants was also possible by using p$K_a$ = 2.5 to 2.6 but the fits were less satisfying. Therefore, we used the eight- p$K_a$ procedure which gave for the two (N7)H$^+$ sites of G2 and G3 p$K_{a/G2(N7)H}$ = 2.3 ±

0.2 and p$K_{a/G3(N7)H}$ = 2.85 ± 0.2, respectively, whereby the error limits are estimated. These two p$K$a values also agree well with the situation seen in the pH-stack plot shown in Figure 5.

The given site attribution is at this point tentative (see also Section 2.7) but it is supported by the plots seen in Figure 7: A comparison of the chemical shifts of (G2)H8 and (G3)H8 in dependence on pH indicates that the "equivalence" point for (G2)H8 is located at a somewhat lower pH than the one of (G3)H8. This tentative reasoning is also supported by the following electrostatic consideration: The $H_5(HNPP)^{\pm}$ species [Eq. (1)] contains three positively charged sites in a row, that is, A1(N1)$H^+$, G2(N7)$H^+$, and G3(N7)$H^+$. Hence, if (N7)$H^+$ of G2 is deprotonated, the charge repulsion at the two other sites will decrease. Because the guanine residue of G2 is now neutral, stacking interactions with the still positively charged purine sites of A1 and G3 may take place, as it is known to occur between partly charged purines.[26-27] However, it is also evident that the buffer ranges of the two p$K$a values overlap. Clearly, this problem deserves further considerations (see Section 2.11).

To conclude, it is satisfying to observe that application of the eight determined p$K$a values for $H5(HNPP)^{\pm}$, i.e., the six values listed in Table 1 plus p$K_{a/G2(N7)H}$ = 2.3 and p$K$a/G3(N7)H = 2.85, to the measured chemical shifts for all six nucleoside residues of A1·G2·G3·C4·C5·T6 (Figure 1) leads throughout to excellent fits as is borne out from Figure 7.

**2.6. Determination of the limiting chemical shifts of the various species:** From the results discussed so far it is evident that in the pH range from about 2 to 12 there are in total eight N sites in the hexanucleoside pentaphosphate $(HNPP)^{5-}$ which can initially be protonated or which carry already a proton, giving thus rise to eight deprotonation reactions [Eqs. (1) – (3)]. This means, the nine species $H_5(HNPP)^{\pm}$, $H_4(HNPP)^{-}$, $H_3(HNPP)^{2-}$, $H_2(HNPP)^{3-}$, $H(HNPP)^{4-}$, $(HNPP)^{5-}$, $(HNPP - H)^{6-}$, $(HNPP - 2H)^{7-}$, and $(HNPP - 3H)^{8-}$ [see Eqs. (1) to (3)] have different protonation degrees. It is now possible to attribute a limiting chemical shift to each of these species (cf. also Figure 7). To facilitate matters we rename the species by neglecting charges but by indicating the total number of removable protons present, e.g., $H_8NP$, $H_7NP$, ... $H_2NP$, HNP, and NP (NP = nucleoside phosphate), where the last abbreviation refers to $[A1·(G2 - H)·(G3 - H)·C4·C5·(T6 - H)]^{8-}$.

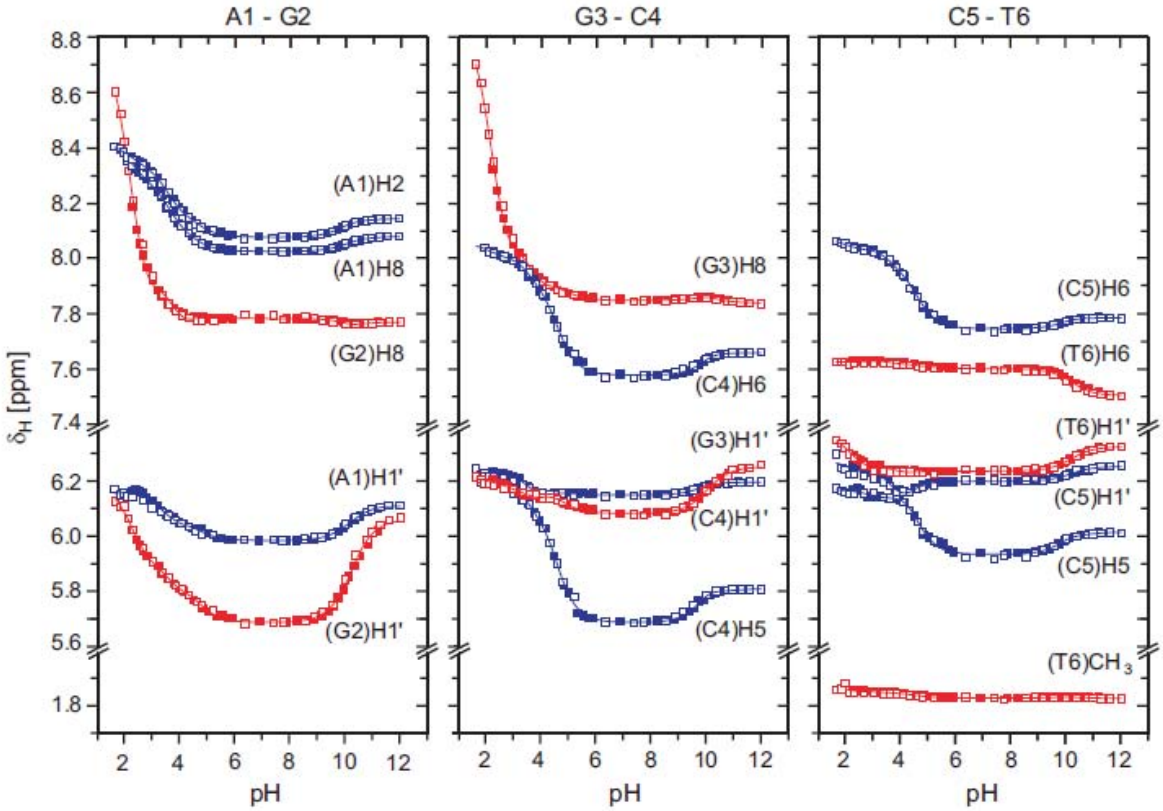


Figure 7. Variation of the $^1$H NMR chemical shift $\delta_H$ (see also Figure 5) for the aromatic-ring and 2'-deoxyribose-residue protons H1' of the hexamer A1·G2·G3·C4·C5·T6 in dependence on pH. The experiment was performed twice (open and closed data points). The solid curves are the calculated best fits of all the experimental data by using the 6 p$K_a$ values listed in Table 1 (column 5) as well as the two (N7)H$^+$ acidity constants (2.3 and 2.85) of G2 and G3 (see also text and for the experimental conditions the legend of Figure 6).

This procedure also facilitates the definitions of shift differences, e.g., [Eqs. (10) and (11)]:

$$\Delta\delta_{8,7} = \delta(H_8NP) - \delta(H_7NP) \quad (10a)$$

$$= \delta[H_5(HNPP)^{\pm}] - \delta[H_4(HNPP)^{-}] \quad (10b)$$

to

$$\Delta\delta_{1,0} = \delta(HNP) - \delta(NP) \quad (11a)$$

$$= \delta[(HNPP - 2H)^{7-}] - \delta[(HNPP - 3H)^{8-}] \quad (11b)$$

Because two such successive species are always interlinked by an acidity constant (p$K$a), we write in addition Equations (12) and (13) by giving the corresponding p$K$a value from Table 1 (column 5; rounded to two digits) (see also Section 2.5) as a subscript to $\Delta\delta$:

$$\Delta\delta_{8,7} = \Delta\delta_{2.3} \tag{12}$$

to

$$\Delta\delta_{1,0} = \Delta\delta_{10.18} \tag{13}$$

The chemical shifts $\delta(H_8NP)$ to $\delta(NP)$ for the species $H_5(HNPP)^{\pm}$ through $(HNPP - 3H)^{8-}$ are listed in Table S2 of the Supporting Information. To facilitate the overview we provide on top of each column not only, e.g., $\delta(H_8NP)$, but give as a link also $\delta[H_5(HNPP)]$ and indicate further from which site of the species the proton will mainly be removed. In this context it needs to be emphasized that, e.g., the analytical species $H_2(HNPP)^{3-}$ is actually a mixture of several isomers including especially $C4(N3)H^+$ and $C5(N3)H^+$ because both $(N3)H^+$ sites in the dCyd residues of C4 and C5 have practically identical p$K_a$ values, i.e., 4.40 and 4.41 (Table 1, column 5). Consequently, the chemical shift $\delta(H_5NP) = \delta[H_2(HNPP)^{3-}]$ listed in Table S2 is a combination of all the chemical shifts of the various isomers involved. This fact makes interpretations difficult. There are more such "isomeric" cases with very similar p$K_a$ values as is seen from Table 1 (see also Sections 2.11, 2.12, and 2.13). Of course, the indicated difficulties also hold for shift differences like $\Delta\delta_{5,4} = \Delta\delta_{4.40}$ (see below).

However, quite generally one may state that the removal of a proton, i.e., of a positive charge, should enhance the electron density at nearby sites, leading to a better shielding of the protons at these sites and thus to upfield shifts, that is, to smaller ppm values. From the shift data in Table S2 as well as in Figures 6 and 7 it is evident that matters are rather complicated because both up- and downfield shifts are observed with an increasing deprotonation degree.

**2.7. Considerations of chemical shift differences and some connected conclusions**: A better overview on the complicated situation indicated in Section 2.6 is obtained if one considers the shift differences defined in Equations (10) to (13). Of course, if a given proton "feels" the effect of a deprotonation reaction, this will depend on the proton

considered and in a first approximation on the distance from the deprotonation site. To facilitate the interpretations further, we printed in Table 2 those Δδ values in bold which are far beyond the error limits (about 8σ or more). If the chemical shift differences, Δδ, are smaller or close to the error limit (2σ), i.e., close to zero, they are given in parentheses because an interpretation is difficult or not meaningful. For the observation of a Δδ value close to zero one may offer two explanations: (i) The distance between the observed proton and the deprotonation site is large; (ii) two opposing effects occur which largely compensate each other.

A comparison of the shift differences $\Delta\delta_{8,7}$ that occur with p$K_a$ = 2.3, which is largely attributed to G2(N7)$H^+$, reveals that the protons H2 and H8 of A1 are considerably more affected than it is the case for p$K_a$ = 2.85 attributed mainly to G3(N7)$H^+$ (see also Section 2.5). This indicates that p$K_a$ = 2.3 quantifies indeed to a large part the deprotonation reaction of (N7)$H^+$ in G2. In accord herewith is also that the overall shift changes connected with p$K_a$ = 2.3 are somewhat larger for G2 than for G3. These observations agree with the conclusion of Section 2.5 as well as with the stack formation between the purine residues of A1 and G2: Once the guanine residue is neutral it is well suited for stack formation with the still positively charged adenine residue.[26-28] Furthermore, it is known that AG stacks are somewhat more stable than GG ones.[29] The deprotonation occurring with p$K_a$ = 2.85 affects the $\Delta\delta_{7,6}$ values for H8 of G2 and G3 in the form of downfield shifts to the same extent within the error limits. This is expected if some GG stacks are formed.

Deprotonation of (N1)$H^+$ of A1, which occurs with p$K_a$ = 3.61 (Table 1), leads to upfield shifts for H2, H8, and H1' ($\Delta\delta_{6,5}$) of A1, as expected. The $\Delta\delta_{6,5}$ values for H8 of G2 and G3 are affected by this reaction to the same extent but H1' of G2 shifts more than twice as much as H1' of G3, again indicating that a reorganization of the single strand occurs and that the AG stack is somewhat preferred over the GG stack. Interestingly, also C4 which is separated from A1 by G2 and G3 still feels something of the (N1)$H^+$ deprotonation of A1, possibly because the rearrangement of the strand allows now stacking between the guanine of G3 and the cytosine of C4. Such distance effects have been observed before.[8] Interestingly, deprotonation of the (N3)$H^+$ unit of C4 gives rise to downfield shifts throughout, whereas the same reaction of C5 (p$K_a$ ca. 4.4 for both) leads to upfield shifts as expected (see also footnote [a] of Table 2 as well as Sections 2.6 and 2.12). The analogous pattern is observed for the deprotonation reaction of (N1)H in G3 (p$K_a$ = 9.99) and T6/G2 (p$K_a$ = 10.17 and 10.18; Table 1).

Table 2. Chemical shift differences Δδ in ppm [Eqs. (10) to (13)] resulting from the increasing deprotonation of the single-stranded d(A1·G2·G3·C4·C5·T6) species in water containing 10% $D_2O$ (47°C, see legend of Figure 6; $I$ = 0.1 M, $NaClO_4$).[a]

| | | G2 | G3 | A1 | C4/C5 | C5/C4 | G3 | T6/G2 | G2/T6 |
|---|---|---|---|---|---|---|---|---|---|
| Ns | H | $\Delta\delta_{2,3}$ | $\Delta\delta_{2,85}$ | $\Delta\delta_{3,61}$ | $\Delta\delta_{4,40}$ | $\Delta\delta_{4,41}$ | $\Delta\delta_{9,99}$ | $\Delta\delta_{10,17}$ | $\Delta\delta_{10,18}$ |
| | | $\Delta\delta_{8,7}$ | $\Delta\delta_{7,6}$ | $\Delta\delta_{6,5}$ | $\Delta\delta_{5,4}$ | $\Delta\delta_{4,3}$ | $\Delta\delta_{3,2}$ | $\delta_{2,1}$ | $\delta_{1,0}$ |
| A1 | H8 | **0.179** ± 0.016 | –0.030 ± 0.021 | **0.220** ± 0.021 | –0.051 ± 0.023 | **0.094** ± 0.018 | –0.043 ± 0.018 | (0.024 ± 0.028) | –0.035 ± 0.022 |
| | H2 | **0.107** ± 0.018 | (–0.024 ± 0.023) | **0.224** ± 0.023 | –0.090 ± 0.026 | **0.128** ± 0.020 | –0.073 ± 0.020 | (0.039 ± 0.031) | –0.033 ± 0.024 |
| | H1' | (–0.023 ± 0.030) | 0.058 ± 0.037 | 0.122 ± 0.037 | –0.089 ± 0.040 | 0.110 ± 0.030 | –0.090 ± 0.030 | (0.062 ± 0.048) | –0.098 ± 0.038 |
| G2 | H8 | **1.195** ± 0.059 | **–0.409** ± 0.075 | **0.335** ± 0.076 | –0.133 ± 0.084 | (0.044 ± 0.064) | (0.023 ± 0.064) | (0.014 ± 0.106) | (–0.024 ± 0.086) |
| | H1' | **0.335** ± 0.041 | (–0.068 ± 0.052) | 0.189 ± 0.054 | –0.143 ± 0.058 | **0.197** ± 0.044 | **–0.240** ± 0.044 | 0.195 ± 0.074 | **–0.327** ± 0.061 |
| G3 | H8 | **1.109** ± 0.047 | **–0.350** ± 0.061 | **0.345** ± 0.061 | –0.200 ± 0.065 | 0.155 ± 0.050 | (–0.027 ± 0.052) | (0.012 ± 0.086) | (0.024 ± 0.069) |
| | H1' | (0.035 ± 0.028) | (0.006 ± 0.035) | 0.074 ± 0.037 | –0.133 ± 0.040 | **0.150** ± 0.030 | **–0.149** ± 0.032 | 0.099 ± 0.053 | –0.120 ± 0.043 |
| C4 | H6 | 0.084 ± 0.032 | –0.059 ± 0.041 | **0.207** ± 0.042 | –0.119 ± 0.045 | **0.371** ± 0.034 | –0.094 ± 0.034 | (0.027 ± 0.057) | (–0.015 ± 0.047) |
| | H5 | (0.042 ± 0.038) | (–0.039 ± 0.050) | **0.223** ± 0.051 | –0.134 ± 0.055 | **0.439** ± 0.042 | **–0.196** ± 0.042 | 0.127 ± 0.070 | (–0.053 ± 0.057) |
| | H1' | (0.018 ± 0.023) | (–0.022 ± 0.030) | **0.140** ± 0.031 | –0.096 ± 0.034 | 0.046 ± 0.026 | –0.063 ± 0.026 | (0.033 ± 0.043) | (–0.017 ± 0.035) |
| C5 | H6 | 0.071 ± 0.027 | –0.065 ± 0.034 | **0.160** ± 0.034 | –0.085 ± 0.037 | **0.246** ± 0.028 | –0.047 ± 0.028 | (0.019 ± 0.047) | (–0.012 ± 0.039) |
| | H5 | (0.006 ± 0.037) | (0.028 ± 0.047) | (0.000 ± 0.048) | (–0.044 ± 0.052) | **0.245** ± 0.040 | –0.106 ± 0.040 | (0.070 ± 0.067) | (–0.045 ± 0.055) |
| | H1' | 0.085 ± 0.043 | –0.082 ± 0.055 | 0.186 ± 0.057 | –0.092 ± 0.061 | (–0.014 ± 0.046) | (–0.040 ± 0.046) | (0.028 ± 0.077) | (–0.043 ± 0.063) |
| T6 | H6 | (0.003 ± 0.021) | (–0.017 ± 0.025) | (0.033 ± 0.025) | (–0.027 ± 0.027) | 0.032 ± 0.020 | 0.059 ± 0.022 | (–0.039 ± 0.036) | 0.078 ± 0.029 |
| | $(CH_3)5$ | (0.028 ± 0.021) | (–0.018 ± 0.025) | (0.019 ± 0.027) | (–0.009 ± 0.031) | (0.019 ± 0.024) | (–0.006 ± 0.024) | (0.001 ± 0.042) | (0.006 ± 0.035) |
| | H1' | **0.169** ± 0.019 | –0.068 ± 0.024 | 0.056 ± 0.025 | (–0.019 ± 0.027) | (0.001 ± 0.020) | –0.058 ± 0.022 | (0.040 ± 0.036) | –0.070 ± 0.029 |

[a] The shift differences Δδ were calculated from the chemical shift data listed in Table S2. Positive Δδ values indicate an upfield shift and negative Δδ values a downfield shift as follows also from Equations (10) to (13). The error limits correspond to twice the standard deviation (2σ); they were calculated according to the error propagation after Gauss based on the errors listed in Table S2. Those values with an error limit of the same size, i.e., 2σ or slightly above, are listed in parentheses (see text in Section 2.7). Those values which are clearly much larger than their error limit are printed in bold. Finally, on the very top of each column the nucleoside residue is given to which Δδ mostly refers, i.e., the difference between the protonated and deprotonated state.

T6, which is far away from most nucleoside residues (Figure 1), is only little affected. Of course, its deprotonation at (N3)H affects the shifts of (T6)H6 and (T6)H1' leading to shielding (upfield) and deshielding (downfield), respectively. The significant downfield shift of –0.327 ppm observed for G2(H1') upon deprotonation of G2(N1)H/T6(N3)H indicates that the single strand changes its conformation upon formation of $(HNPP - 3H)^{8-}$. Of interest is here also the remarkable upfield shift observed for (T6)H1' upon deprotonation of $G2(N7)H^{+}$. In fact, overall it appears that the single strand of the hexanucleoside pentaphosphate is very flexible.

**2.8. Intrinsic acidity constants in water for the various (N)H sites in the single-stranded DNA derivative d(A1·G2·G3·C4·C5·T6) at 25°C:** At this point it needs to be recalled that the $^{1}$NMR shift experiments had to be carried out at 47°C (Section 2.1) to be able to measure the acid-base properties of the single-stranded hexanucleoside pentaphosphate (Figure 1). However, for practical reasons the pH in the NMR tubes for these experiments at 47°C had to be adjusted at 25°C. This discrepancy in temperature was quantified for the pH (p*K*) range of about 2 to 12 by measurements with dGuo and dCyd. In these instances, both the pH-meter and the NMR instrument could be used at 25°C (and the NMR spectrometer at 47°C as well), and thus Equation (9) was obtained which allows now to transfer the 47°C data to those valid for 25°C. In addition, the isotope effect due to the change of the solvent from water to water containing 10% $D_2O$ was also quantified (Section 2.3 and Supporting Information).

Hence, application of the mentioned two corrections to the results summarized in column 5 of Table 1 (see also Section 2.5) allowed now to calculate the intrinsic acidity constants of single-stranded d(A1·G2·G3·C4·C5·T6) valid for water at 25°C and $I$ = 0.1 M ($NaClO_4$). These final results are summarized in column 6 of Table 3.

A view on the results of Table 3 reveals that several of the p$K_a$ values are very close together as was already indicated in Sections 2.6 and 2.7. The result of this is that isomeric equilibria exist between species which have the same protonation degree. In the case of C4 and C5, where in both instances for $(N3)H^{+}$ p$K_a$ ca. 4.3 holds, it is evident that the two isomers each occur with a formation degree of about 50% (see also Section 2.12).

Table 3. Intrinsic acidity constants of the various (N)H sites in single-stranded d(A1·G2·G3·C4·C5·T6) (see Figure 1) valid for aqueous solution at 25°C and $I$ = 0.1 M ($NaClO_4$).

| Ns residue | (N)H | p$K_a$ for 47°C[a] (pH meter: 25°C) in $H_2O$ with 10% $D_2O$ | $\Delta$p$K_a$[c] correction for 25°C | p$K_a$ valid[d] for 25°C in 10% $D_2O$ | p$K_a$ valid[e] for 25°C in $H_2O$ |
|---|---|---|---|---|---|
| A1 | $(N1)H^+$ | 3.614 ± 0.044 | 0.107 ± 0.036 | 3.721 ± 0.057 | 3.71 ± 0.07 |
| G2 | $(N7)H^+$ | 2.3 ± 0.2[b] | 0.151 ± 0.036 | 2.451 ± 0.203 | 2.44 ± 0.21 |
| | (N1)H | 10.184 ± 0.038 | –0.109 ± 0.036 | 10.075 ± 0.052 | 10.07 ± 0.06 |
| G3 | $(N7)H^+$ | 2.85 ± 0.2[b] | 0.133 ± 0.036 | 2.983 ± 0.203 | 2.97 ± 0.21 |
| | (N1)H | 9.989 ± 0.113 | –0.103 ± 0.036 | 9.886 ± 0.119 | 9.88 ± 0.13 |
| C4 | $(N3)H^+$ | 4.404 ± 0.048 | 0.081 ± 0.036 | 4.323 ± 0.060 | 4.31 ± 0.07 |
| C5 | $(N3)H^+$ | 4.411 ± 0.051 | 0.081 ± 0.036 | 4.330 ± 0.062 | 4.32 ± 0.07 |
| T6 | (N3)H | 10.170 ± 0.092 | 0.109 ± 0.036 | 10.061 ± 0.099 | 10.05 ± 0.11 |

[a] Values taken from column 5 in Table 1. [b] From Section 2.5. [c] Calculated with Equation (9); see also text in Section 2.3 and Figure 3S in the Supporting Information. [d] The values in the two columns at the left were added together and the error limits were calculated according to the error propagation after Gauss. [e] As described in the second paragraph of Section 2.3 and the corresponding Supporting Information, there is a small isotope effect of 0.01 ± 0.007 pH (p$K$) units between water and water containing 10% $D_2O$. Therefore, from the values listed in column 5 above 0. 01 was deducted and 0.007 was added to the error limits; all values were rounded to two digits after the decimal point.

Interestingly, G2(N1)H is with p$K_a$ = 10.07 (Table 3) by about 0.2 p$K$ units more basic than the same unit in G3 (p$K_a$ = 9.88), probably because the guanine residue in G2 stacks with the adenine residue of A1. However, the (N3)H site of T6 has also a p$K_a$ value of 10.05 which is very close to that of G2 and therefore, tautomeric forms must exist here as well. In Section 2.13 some of the equilibria involved in this tautomerism will be considered more in detail.

**2.9. Acid-base properties of 2'-deoxycytidine and 2'-deoxyguanosine:** There were two main reasons to measure the acidity constants of these two monoprotonated deoxynucleosides: (i) To be able to carry out the temperature correction (47°C versus 25°C) as described in Section 2.3 and as defined in Equation (9), and (ii) to see if these

pKa values determined by $^1$H NMR shift experiments agree with the acidity constants available in the literature, which were to the largest part determined by potentiometric pH titrations. This latter point (ii), if positive, is an important back-up for the validity of our results listed in Table 3 (column to the right).

The p$K_a$ values were measured in water containing 10% $D_2O$, as this corresponds to the solvent used for the measurements with d(A1·G2·G3·C4·C5·T6), and also repeated in 100% $D_2O$. Both results can be transferred to H2O as solvent (25°C; $I$ = 0.1 M, $NaClO_4$) by applying the small correction (–0.01 p$K$ unit) described in Section 2.3 for 10% $D_2O$. For 100% $D_2O$ Equation (14), as provided by Martin,[25] was employed:

$$pK_a(H_2O) = (pK_a(D_2O) - 0.45)/1.015 \quad (14)$$

Evidently, for $H(dCyd)^+$ we determined the acidity constant as defined by Equation (4) and for $H(dGuo)^+$ those as defined by Equations (4) and (5). The results are listed in Table 4.

Table 4. Negative logarithms of the acidity constants, p$K_a$, as determined by $^1$H NMR shift experiments (see Figures 4 and S2) for 2'-deoxycytidine (dCyd) and 2'-deoxyguanosine in various $D_2O$ solvents (25°C; $I$ = 0.1 M, $NaClO_4$).[a]

| dNs | (N)H[b] | % $D_2O$ | p$K_a$ as measured | p$K_a$ valid for $H_2O$ |
|---|---|---|---|---|
| $H(dCyd)^+$ | $(N3)H^+$ | 10 | 4.39 ± 0.05 | 4.38 ± 0.06[c] |
| | $(N3)H^+$ | 100 | 4.98 ± 0.07 | 4.46 ± 0.10[d] |
| $H(dGuo)^+$ | $(N7)H^+$ | 10 | 2.40 ± 0.14 | 2.39 ± 0.15[c] |
| | $(N7)H^+$ | 100 | 2.89 ± 0.04 | 2.40 ± 0.10[d] |
| dGuo | (N1)H | 10 | 9.24 ± 0.03 | 9.23 ± 0.04[c] |
| | (N1)H | 100 | 9.73 ± 0.02 | 9.14 ± 0.10[d] |

[a] So-called practical (or mixed) constants are listed;[18] see also Table 1S and text in Section 2.2. [b] Site at which deprotonation occurs. [c] The isotope effect between solutions containing 10% $D_2O$ and those consisting of $H_2O$ only amounted to –0.01 ± 0.07 by going from 10% $D_2O$ to $H_2O$ (Section 2.3). This value was deducted from the one given at the left and the error limit was enlarged by 0.01. [d] This constant is calculated from the value listed at the left by application of Equation (14). The error limit (±0.10) is an estimate and was generously taken to cover any uncertainties possibly connected with the transformation.

For the p$K_a$ of $H(dCyd)^+$ we are aware of only two literature values, i.e., 4.30 ± 0.10[24] and 4.33 ± 0.06 (which is based on $pK^H_{H(Cyd)}$ plus 0.13 ± 0.04;[11] see Table S3); both values agree within the error limits with 4.38 ± 0.06 and 4.46 ± 0.10 as listed in Table 4 (column 5, top). The two values determined now for $pK^H_{H(dGuo)}$ = 2.39 ± 0.15 and 2.40 ± 0.10 agree also well with the average of 5 values from the literature, i.e., 2.30 ± 0.04 (see Table S3). Finally, the average of 5 literature values for $pK^H_{(dGuo)}$ = 9.25 ± 0.02 (Table S3) is in excellent agreement with the value given in Table 4, i.e., 9.23 ± 0.04, and both values also agree with 9.14 ± 0.10 (within the error limits) as it results from 100% $D_2O$ as solvent. To conclude, the agreement of the acidity constants listed in Table 4 with those of the literature (see Table S3) validates further our results obtained for aqueous solution of the nucleoside residues of single-stranded d(A1·G2·G3·C4·C5·T6) (Table 3, column 6).

**2.10. Comparison of the acid-base properties of the 2'-deoxynucleoside residues of d(A1·G2·G3·C4·C5·T6) with those of the corresponding and individual nucleosides, and the effect of the phosphate group in nucleoside monophosphates:** To allow a comparison of the $pK_a$ values due to the nucleoside residues of single-stranded d(A1·G2·G3·C4·C5·T6) with those of the corresponding free nucleosides, we listed these values again in column 3 of Table 5 but this time in the order of their increasing basicity. In column 5 the corresponding $pK_a$ values for the free nucleosides are listed.[47–52] For $H(dAdo)^+$ and dThd the averages of 4 and 7 values from the literature, respectively, are given (for details see Table S3 of the Supporting Information). In the case of $H(dCyd)^+$ and $H(dGuo)^+$ (entries 1, 2, 6, and 8; column 5) we re-calculated the average values listed in Table S3 by including now also our own results from Table 4. These averages are now based on 3 and 6 independent determinations, respectively.

The $\Delta pK_a$ values given in column 4 of Table 5 are the differences between the p$K_a$ values valid for the nucleoside residues of d(A1·G2·G3·C4·C5·T6) (column 3) and the corresponding ones for the individual nucleosides (column 5). The results are at a first superficial glance rather surprising because (i) no evident systematic trend is recognizable, and (ii) the $\Delta pK_a$ values vary between about 0 and 0.8 meaning that the higher basicity of values for the HNPP-nucleoside residues cannot simply be explained by the effects of the negatively charged phosphodiester bridges (Figure 1).

Table 5. Comparison of the acid-base properties of the 2'-deoxynucleoside (dNs) residues in the single-stranded d(A1·G2·G3·C4·C5·T6) species (= HNPP; Figure 1) with those of the corresponding nucleosides ($H(dNs)^+$/dNs) [Eqs. (4), (5)], together with the resulting $\Delta pK_a$ values. For further comparisons also some acidity constants of protonated 2'-deoxynucleoside monophosphates ($2'dNMP^{2-}$) [Eqs. (6), (8)] are listed (aqueous solution; 25C; $I$ = 0.1 M)[a]

| No. | dNs residue / $H(dNs)^+$ or $(dNs)$[b] | $pK_a$ of HNPP | $\Delta pK_{a/HNPP/dNs}$[c] | $pK^H_{H(dNs)}$ or $pK^H_{(dNs)}$ [d] | $pK^H_{H_2(2'd5'NMP)}$ or $pK^H_{H(2'd5'NMP)}$ [e] | $pK^H_{H_2(2'd3'NMP)}$ or $pK^H_{H(2'd3'NMP)}$ |
|---|---|---|---|---|---|---|
| 1 | G2(N7)$H^+$/$H(dGuo)^+$ | 2.44 ± 0.21 | 0.13 ± 0.22 | 2.31 ± 0.05 | 2.69 ± 0.03 | 2.29 ± 0.04[f] |
| 2 | G3(N7)$H^+$/$H(dGuo)^+$ | 2.97 ± 0.21 | 0.66 ± 0.22 | 2.31 ± 0.05 | | |
| 3 | A1(N1)$H^+$/$H(dAdo)^+$ | 3.71 ± 0.07 | –0.06 ± 0.08 | 3.77 ± 0.04 | 3.97 ± 0.02 | 3.83 ± 0.05[g] |
| 4 | C4(N3)$H^+$/$H(dCyd)^+$ | 4.31 ± 0.07 | –0.03 ± 0.10 | 4.34 ± 0.07 | 4.46 ± 0.01 | 4.37 ± 0.06[h] |
| 5 | C5(N3)$H^+$/$H(dCyd)^+$ | 4.32 ± 0.07 | 0.02 ± 0.10 | 4.34 ± 0.07 | | |
| 6 | G3(N1)H/(dGuo) | 9.88 ± 0.13 | 0.63 ± 0.13 | 9.25 ± 0.02 | 9.56 ± 0.02 | 9.45 ± 0.02[f] |
| 7 | T6(N3)H/(dThd) | 10.05 ± 0.11 | 0.34 ± 0.13 | 9.71 ± 0.07 | 9.90 ± 0.03 | |
| 8 | G2(N1)H/(dGuo) | 10.07 ± 0.06 | 0.82 ± 0.06 | 9.25 ± 0.02 | | |

[a] Throughout so-called practical (or mixed) constants are listed;[18] see text in Section 2.2. The values in the second column, including their errors, are from column 6 of Table 3. The error limits in columns 3 to 6 refer to 3σ; the errors of derived values were calculated according to the error propagation after Gauss. [b] The constants listed in columns 6 and 7 refer to the corresponding 2'-deoxynucleoside 5'- or 3'-monophosphate. [c] The difference $\Delta pK_{a/HNNP/dNs}$ follows from the values to the left (column 3) *minus* those at the right (column 5). [d] These acidity constants are the averages of the values collected from the literature (see Table S3). In the case of $H(dCyd)^+$ and $H(dGuo)^+$ our own results (Table 4) are now also included into the average. [e] These values are abstracted from Table 1 in Ref. [11]. [f] From Ref. [45]. [g] This value is based on the reasonable[11] assumption that $pK^H_{H_2(5'AMP)} - pK^H_{H_2(3'AMP)} = pK^H_{H_2(2'd5'AMP)} - pK^H_{H_2(2'd3'AMP)}$ = (3.84 ± 0.02)[38] – (3.70 ± 0.04)[47] = (3.97 ± 0.02)[e] – $pK^H_{H_2(2'd3'AMP)}$; hence, $pK^H_{H_2(2'd3'AMP)}$ = (3.97 ± 0.02) – (3.84 ± 0.02) + (3.70 ± 0.04) = 3.83 ± 0.05. [h] In analogy to footnote [g] it follows: $pK^H_{H_2(2'd3'CMP)} = pK^H_{H_2(2'd5'CMP)} - pK^H_{H_2(5'CMP)} + pK^H_{H_2(3'CMP)}$ = (4.46 ± 0.01)[48] – (4.33 ± 0.04)[49] + (4.24 ± 0.04) = 4.37 ± 0.06. The constant $pK^H_{H_2(3'CMP)}$ = 4.24 is from Ref. [50]; it needs to be noted that the results given in Ref. [50] are identical with our own previous determinations,[49,51] i.e., $pK^H_{H_2(5'AMP)}$ = 3.84 ± 0.02 and $pK^H_{H_2(5'CMP)}$ = 4.33 ± 0.04.

The latter point has led us to include in Table 5 also values for $H_2(dNMP)^{\pm}$ (entries 1, 3, 4) and $H(dNMP)^-$ (entries 6, 7) species, which carry one proton at the phosphate group [Eq. (7)]; this is released only with p$K_a$ about 6.2.[41,53] This means, the species with a monoprotonated but negatively charged phosphate group simulate to some extent the situation of the also negatively charged phosphodiester bridges present in d(A1·G2·G3·C4·C5·T6) (Figure 1). From the data in columns 6 and 7 it follows that the $2'd5'NMP^{2-}$ species are in all four cases (where values are available; entries 1, 3, 4, and 6) somewhat more basic than their $2'd3'NMP^{2-}$ isomers. Considering that in d(A1·G2·G3·C4·C5·T6) the phosphate bridges are located at the 3' and 5' positions of the 2'-deoxyribose residue, it is interesting to observe that the p$K_a$ values of the $H_2(2'd3'NMP)^{\pm}$ species (entries 1, 3, and 4; column 7) are within the error limits identical to those of the $H(dNs)^+$ ones (column 5). Consequently, the ribose residue shields the negative charge of the $PO_3H^-$ group at the 3' position so well that no remarkable influence on the $(N7)H^+$ (entry 1; dGuo), the $(N1)H^+$ (entry 3; dAdo) or $(N3)H^+$ (entry 4; dCyd) units occurs. Of course, for $2'd5'TMP^{2-}$ this is different because here the phosphate group has lost the proton and is thus 2-fold negatively charged, hence, $pK^{H}_{(2'd3'TMP)} > pK^{H}_{(dThd)}$.

Having said the above regarding $H_2(2'd3'NMP)^{\pm}$, it is no surprise to see that the p$K_a$ values for the terminal $A1(N1)H^+$ having only a 3'-phosphate linkage and those of $H(dAdo)^+$ as well as $H_2(2'd3'AMP)^{\pm}$ are identical within their error limits (see row of entry 3). The fact that the same observation holds for $C4(N3)H^+$ and $C5(N3)H^+$ (rows in entries 4 and 5) means that the $P(O)_2(O)^-_2$ bridge does also not lead to a charge effect in these instances; this is also understandable because in the *anti* conformation $(N3)H^+$ of the cytosine ring is turned away from the phosphate group (Figure 1). The p$K_a$ equality of the mentioned three series of data is very comforting because it is further support for the quality of our d(A1·G2·G3·C4·C5·T6) data.

Overall we are now left with the higher basicities of the N7 sites in G2 and G3 of HNPP (entries 1, 2) compared with those of Guo and $H(2'd3'GMP)^-$. Indeed, these increased basicities, especially the one of G3, cannot be explained by simple charge effects as a comparison of p$K_a$ = 2.97 ± 0.26 of $G3(N7)H^+$ (Table 5; entry 3, column 3) with p$K_a$ = 2.91

± 0.07 of $H_2(dGDP)^{2-/+}$ shows;[11] note, the 5'-diphosphate group in $H_2(dGDP)^{2-/+}$ carries two negative charges! Most likely there are two reasons for the increased basicity: (i) Stacking interactions as discussed in Section 2.7, and (ii) "macrochelate" formation of the $(N7)H^+$ with the 5'-phosphate group *via* and including hydrogen bonding with (C6)O (see Figure 1), as it was proposed for xanthosinate 5'-monophosphate.[53] In accord with this latter point is also the higher basicity of $H(2'd5'GMP)^-$ ($pK_a = 2.69 \pm 0.03$) compared with that of $H(2'd3'GMP)^-$ ($pK_a = 2.29 \pm 0.04$; Table 5). Furthermore, the inhibited deprotonation of the G2(N1)H and G3(N1)H sites, if compared with the related values listed in columns 5 to 7 of Table 5 (row 6 and 8), may possibly be explained as well by the mentioned points (i) and (ii). On the other hand, it is clear that the various conformations which the hexanucleoside pentaphosphate can adopt, affect the acid-base properties as well; this is borne out from $pK_a = 10.05 \pm 0.11$ for T6(N3)H, if compared with 9.71 ± 0.07 [Eq. (5)] and 9.90 ± 0.03 [Eq. (8)] of dThd and $2'd5'TMP^{2-}$, respectively.

### 2.11. Tautomeric distributions for the release of a single proton from one of the A1(N1)H$^+$, G2(N7)H$^+$ or G3(N7)H$^+$ sites of fully protonated $H_5(HNPP)^{\pm}$:

The dominating species of the hexanucleoside pentaphosphate in the neutral pH range is $d(A1{\cdot}G2{\cdot}G3{\cdot}C4{\cdot}C5{\cdot}T6)^{5-}$, in which all nucleoside residues are uncharged; the five negative charges result from the five phosphodiester bridges. This species can accept five protons as discussed in Section 2.2 and is then represented by $H_5(HNPP)^{\pm}$; for the release of one proton Equilibrium (1) holds. The problem now is that the $pK_a$ values of 2.44, 2.97, and 3.71 for the G2(N7)H$^+$, G3(N7)H$^+$, and A1(N1)H$^+$ sites, respectively, are relatively close together (Table 5, column 3). Certainly, one expects that largely the G2(N7)H$^+$ site is deprotonated because this site has the lowest $pK_a$ value. However, the buffer ranges of all three sites clearly overlap and therefore tautomeric equilibria between these three sites are expected upon the release of a single proton. The next site, i.e., C4(N3)H$^+$ is with $pK_a = 4.31$ nearly 2 p$K$ units more basic (compared with $pK_a = 2.44$) and thus not of real relevance for the indicated tautomerism. The question thus is: To which extent is the first proton removed not only from the G2(N7)H$^+$ site, but also from G3(N7)H$^+$ and A1(N1)H$^+$? Therefore, we attempt now to calculate the population of the G2(N7), G3(N7), and A1(N1) tautomers after removal of a *single* proton from $H_5(HNPP)^{\pm}$.

For the quantification of such a tautomeric situation so-called micro acidity constants are needed.[10] These microconstants describe the release of a single proton from one of the G2(N7)$H^+$, G3(N7)$H^+$, and A1(N1)$H^+$ sites under conditions where the other two sites remain protonated. Such microconstants are not easily accessible[10] and are for the present situation not known (but see below). In any case, the corresponding three micro acidity constants are for $H_5(HNPP)^{\pm}$ defined in Equations (15) – (17), where for reasons of readability the charges are partly omitted:

$$k^{G2(N7)}_{H_5(HNPP)} = ([G2(N7)][H^+]/[H_5(HNPP)^{\pm}] \quad (15)$$

$$k^{G3(N7)}_{H_5(HNPP)} = ([G3(N7)][H^+]/[H_5(HNPP)^{\pm}] \quad (16)$$

$$k^{A1(N7)}_{H_5(HNPP)} = ([A1(N1)][H^+]/[H_5(HNPP)^{\pm}] \quad (17)$$

These microconstants allow now to define the tautomeric ratios given in Equations (18) and (19),

$$R_{T/G2,G3} = \frac{[G2(N7)]}{[G3(N7)]} = \frac{k^{G2(N7)}_{H_5(HNPP)}}{k^{G3(N7)}_{H_5(HNPP)}} \quad (18)$$

$$R_{T/G3,A1} = \frac{[G3(N7)]}{[A1(N1)]} = \frac{k^{G3(N7)}_{H_5(HNPP)}}{k^{A1(N1)}_{H_5(HNPP)}} \quad (19)$$

and they provide also the following definition:

$$\frac{[H_4(HNPP)^-][H^+]}{[H_5(HNPP)^{\pm}]} = \frac{([G2(N7)] + [G3(N7)] + [A1(N1)])[H^+]}{[H_5(HNPP)^{\pm}]} \quad (20)$$

From Equation (20) follows Equation (21),

$$[H_4(HNPP)^-]_{tot} = [G2(N7)] + [G3(N7)] + [A1(N1)] = 1 \quad (21)$$

where $[H_4(HNPP)^-]_{tot}$ corresponds to the total molar fraction, which equals 1.

Insertion of Equations (18) and (19) into (21) allows calculation of the molar fraction of the G3(N7) tautomer [Eqs. (22a) and (22b)]:

$$\frac{k^{\mathrm{G2(N7)}}_{\mathrm{H5(HNPP)}}}{k^{\mathrm{G3(N7)}}_{\mathrm{H5(HNPP)}}}[\mathrm{G3(N7)}] + [\mathrm{G3(N7)}] + [\mathrm{G3(N7)}]\frac{k^{\mathrm{A1(N1)}}_{\mathrm{H5(HNPP)}}}{k^{\mathrm{G3(N7)}}_{\mathrm{H5(HNPP)}}} = 1 \qquad (22a)$$

$$[\mathrm{G3(N7)}]\left(\frac{k^{\mathrm{G2(N7)}}_{\mathrm{H5(HNPP)}}}{k^{\mathrm{G3(N7)}}_{\mathrm{H5(HNPP)}}} + 1 + \frac{k^{\mathrm{A1(N1)}}_{\mathrm{H5(HNPP)}}}{k^{\mathrm{G3(N7)}}_{\mathrm{H5(HNPP)}}}\right) = 1 \qquad (22b)$$

Since electrostatic interactions within HNPP do not seem to be of a dramatic order (see Section 2.10), we tentatively assumptione that the microconstants correspond in a first approximation to the intrinsic macroconstants which were measured for the various sites (Tables 3 and 5). Hence, Equations (23) to (25) hold, where the two constants are set equal:

$$k^{\mathrm{G2(N7)}}_{\mathrm{H5(HNPP)}} = K^{\mathrm{H}}_{\mathrm{H5(HNPP)}} = 10^{-2.44} \qquad (23)$$

$$k^{\mathrm{G3(N7)}}_{\mathrm{H5(HNPP)}} = K^{\mathrm{H}}_{\mathrm{H4(HNPP)}} = 10^{-2.97}\,(10^{-2.67};\, 10^{-3.27}) \qquad (24)$$

$$k^{\mathrm{A1(N1)}}_{\mathrm{H5(HNPP)}} = K^{\mathrm{H}}_{\mathrm{H3(HNPP)}} = 10^{-3.71}\,(10^{-3.41};\, 10^{-4.01}) \qquad (25)$$

Indeed, Equation (23) describes the situation certainly quite well because deprotonation of $\mathrm{G2(N7)H^+}$ will occur largely under conditions where the other two sites still carry their proton and therefore the micro and macro acidity constants will be quite similar. However, the equality fixed in Equations (24) and (25) is certainly less true; to provide a feeling for the errors involved, we carried out the calculations also with the values given in parentheses, where first 0.3 p*K* unit were added and next 0.3 p*K* unit were deducted. We feel that within these boundaries the situations should be well described.

Application of the macroconstants from Equations (23) – (25) to Equation (22b) gives Equation (26),

$$[\mathrm{G3(N7)}]\left(\frac{10^{-2.44}}{10^{-2.97}} + 1 + \frac{10^{-3.71}}{10^{-2.97}}\right) = 1 \qquad (26)$$

and the resulting molar fraction for the G3(N7) tautomer is provided in Equation (27):

$$[\mathrm{G3(N7)}] = 0.2187987 \qquad (27)$$

From the result in Equation (27) and its application to Equations (18) and (19) one obtains the

tautomeric molar fractions for the deprotonated G2(N7) and A1(N1) forms [Eqs. (28) and (29)]:

$$R_{T/G2,G3} = \frac{[G2(N7)]}{[G3(N7)]} = \frac{[10^{-2.44}]}{[10^{-2.97}]} = 10^{0.53} = \frac{[G2(N7)]}{0.2187987} \quad (28a)$$

$$[G2(N7)] = 0.7413865 \quad (28b)$$

$$R_{T/G3,A1} = \frac{[G2(N7)]}{[A1(N1)]} = \frac{[10^{-2.97}]}{[10^{-3.71}]} = 10^{0.74} = \frac{0.2187987}{[A1(N1)]} \quad (29a)$$

$$[A1(N1)] = 0.0398148 \quad (29b)$$

From the molar fractions given in Equations (27), (28b), and (29b) follow the percentages of the tautomers present in an aqueous solution of monodeprotonated $H_5(HNPP)^{\pm}$, i.e.,

G2(N7) = 74.14%

G3(N7) = 21.88%

A1(N1) = 3.98%

which sum up to 100% for the $H_4(HNPP)^{-}$ species.

Repetition of the calculations with the values given in parentheses in Equations (24) and (25) [the value of Equation (23) remains unaltered for the reasons described] leads to the following percentages:

G2(N7) = (58.96; 85.12)%

G3(N7) = (34.72; 12.59)%

A1(N1) = (6.32; 2.29)%

If one summarizes these individual results, one obtains for the percentages of the three tautomers, which have lost *one* proton at *one* nucleobase residue (the other two sites still being protonated), the following overall results:

G2(N7) = 74 ± 15%

G3(N7) = 22 ± 12%

A1(N1) = 4 ± 2%

To conclude, despite all shortcomings of the described evaluation due to the missing micro acidity constants, it is clear that the populations of all three tautomers are significant. Since protonation/deprotonation reactions are fast, the three species are of course in rapid equilibrium with each other.

2.12. Tautomeric populations of the A1(N1)$H^+$, C4(N3)$H^+$, and C5(N3)$H^+$ sites in H(HNPP)$^{4-}$, where only a single protonation site is left: In the preceding Section 2.11 we have considered the release of a single proton from all the protonated sites and we have seen that even the tautomer with the N1 site of A1 occurs with a formation degree of about 4%; hence, this site can act as a proton acceptor and due to its linkage to G2(N7) as well as G3(N7) the proton can be rapidly "transported" away. Now we consider the "opposite" situation: In $(HNPP)^{5-}$ all nucleobase residues are uncharged (Figure 1) and this species dominates evidently in the physiological pH range of about 6–8 (see Table 5). However, if one proton is added to form H$(HNPP)^{4-}$, where does it bind? This question is of relevance because the corresponding site(s) can act as proton donors. The most basic site in $(HNPP)^{5-}$ is N3 of C5, though the properties of C4(N3) and A1(N1) are also very similar or at least not very different, respectively, meaning that the proton has several choices where it may bind and therefore tautomers must form.

The following reasonings are closely related[10] to those described in Section 2.11. Again, at first, the relevant micro acidity constants need to be defined; this is done in Equations (30) to (32) (charges are partially omitted):

$$k^{(\mathrm{HNPP})}_{\mathrm{C5(N3)H}} = \frac{[(\mathrm{HNPP})^{5-}][\mathrm{H}^+]}{[\mathrm{C5(N3)H}]} = K^{\mathrm{H}}_{\mathrm{H(HNPP)}} = 10^{-4.32} \qquad (30)$$

$$k^{(\mathrm{HNPP})}_{\mathrm{C4(N3)H}} = \frac{[(\mathrm{HNPP})^{5-}][\mathrm{H}^+]}{[\mathrm{C4(N3)H}]} = K^{\mathrm{H}}_{\mathrm{H_2(HNPP)}} = 10^{-4.31} \qquad (31)$$

$$k^{(\mathrm{HNPP})}_{\mathrm{A1(N1)H}} = \frac{[(\mathrm{HNPP})^{5-}][\mathrm{H}^+]}{[\mathrm{A1(N1)H}]} = K^{\mathrm{H}}_{\mathrm{H_3(HNPP)}} = 10^{-3.71} \qquad (32)$$

Now the ratios of the tautomers can also be formulated [Eqs. (33) and (34)] and Equation (35) be defined:

$$R_{\mathrm{T/C5,C4}} = \frac{[\mathrm{C5(N3)H}^+]}{[\mathrm{C4(N3)H}^+]} = \frac{k^{(\mathrm{HNPP})}_{\mathrm{C4(N3)H}}}{k^{(\mathrm{HNPP})}_{\mathrm{C5(N3)H}}} \qquad (33)$$

$$R_{T/C4,A1} = \frac{[C4(N3)H^+]}{[A1(N1)H^+]} = \frac{k^{(HNPP)}_{A1(N1)H}}{k^{(HNPP)}_{C4(N3)H}} \quad (34)$$

$$\frac{[H(HNPP)^{4-}]}{[(HNPP)^{5-}][H^+]} = \frac{([C5(N3)H] + [C4(N3)H] + [A1(N1)])[H]}{[(HNPP)^{5-}][H^+]} \quad (35)$$

From Equation (35) follows Equation (36), where $[H(HNPP)^{4-}]_{tot}$ corresponds to the total molar fraction which equals 1:

$$[H(HNPP)^{4-}]_{tot} = [C5(N3)H] + [C4(N3)H] + [A1(N1)H] = 1 \quad (36)$$

Insertion of Equations (33) and (34) into (36) allows calculation of the molar fraction of the $C4(N3)H^+$ tautomer [Eq. (37)]:

$$\frac{k^{(HNPP)}_{C4(N3)H}}{k^{(HNPP)}_{C5(N3)H}}[C4(N3)H] + [C4(N3)H] + [C4(N3)H]\frac{k^{(HNPP)}_{C4(N3)H}}{k^{(HNPP)}_{A1(N1)H}} = 1 \quad (37a)$$

$$[C4(N3)H]\left(\frac{k^{(HNPP)}_{C4(N3)H}}{k^{(HNPP)}_{C5(N3)H}} + 1 + \frac{k^{(HNPP)}_{C4(N3)H}}{k^{(HNPP)}_{A1(N1)H}}\right) = 1 \quad (37b)$$

In Section 2.10 we have seen that the p$K$a values of the $A1(N1)H^+$, $C4(N3)H^+$, and $C5(N3)H^+$ sites are within the error limits equal to the values of the corresponding protonated 2'- deoxynucleosides as well as to those of their 3'-monophosphates (see Table 5). Consequently, neither the phosphodiester bridges, nor the neighboring 2'-deoxynucleoside residues, nor their protonation degree affect the acid-base properties of the mentioned sites in HNPP remarkably and therefore the measured intrinsic (macro)constants correspond in these cases directly to the micro acidity constants. This equality is already expressed in Equations (30) to (32). Application of these constants to Equation (37b) gives Equation (38) as well as the molar fraction for the $C4(N3)H^+$ tautomer [Eq. (39)]:

$$[C4(N3)H]\left(\frac{10^{-4.31}}{10^{-4.32}} + 1 + \frac{10^{-4.31}}{10^{-3.71}}\right) = 1 \quad (38)$$

$$[C4(N3)H] = 1/(10^{0.01} + 1 + 10^{-0.60}) = 0.43996606 \quad (39)$$

From the results in Equation (39) and its application to Equations (33) and (34) one obtains the molar fractions of the other two tautomers:

$$R_{T/C5,C4} = \frac{[C5(N3)H^+]}{[C4(N3)H^+]} = \frac{[10^{-4.31}]}{[10^{-4.32}]} = 10^{0.01} = \frac{[C5(N3)H^+]}{0.43996606} \qquad (29a)$$

$$[C5(N3)H^+] = 0.4499016$$

$$R_{T/C4,A1} = \frac{[C4(N3)H^+]}{[A1(N1)H^+]} = \frac{[10^{-3.71}]}{[10^{-4.31}]} = 10^{0.60} = \frac{0.43996606}{[A1(N1)H^+]} \qquad (29a)$$

$$[A1(N1)H^+] = 0.1104378$$

From the molar fractions given above follow the percentages of the tautomers present in aqueous solution of monoprotonated $(HNPP)^{5-}$, i.e., of $H(HNPP)^{4-}$, in which the proton has three deoxynucleoside residues as choices for being bound. That is:

$C5(N3)H^+ = 45\%$

$C4(N3)H^+ = 44\%$

$A1(N1)H^+ = 11\%$

Either site can evidently act as a proton donor and it will then immediately be recharged from the other sites, as such proton transfer reactions are fast.

**2.13. Further p$K_a$ clusters that warrant an evaluation:** There occurs one more p$K_a$ cluster in d(A1·G2·G3·C4·C5·T6) which encompasses the p$K_a$ values of the G3(N1)H, T6(N3)H, and G2(N1)H sites which amount to 9.88, 10.05, and 10.07, respectively (see Table 5, column 3). Again, these p$K_a$ values are so close to each other that tautomeric equilibria must occur.

Also in these cases no micro acidity constants are available but evaluations analogous to those described in Sections 2.11 and 2.12 are possible and are provided in the Supporting Information.

The questions to be asked are:

(i) From which sites and to what extent is the first proton released from the neutral nucleobases in $(HNPP)^{5-}$? What are the percentages of $G3(N1)^-$, $T6(N3)^-$, and $G2(N1)^-$?

The answer is:

$G3(N1)^-$ = 43 ± 17%

$T6(N3)^-$ = 29 ± 8%

$G2(N1)^-$ = 28 ± 8%

(ii) Or one may ask: Which are the tautomeric populations in the $(HNPP - 2H)^{7-}$ [Eq. (3)] species? What are the percentages of the G3(N1)H, T6(N3)H, and G2(N1)H sites still carrying a proton under conditions where in total only a *single* proton can be released from the last (N)H site in a neutral nucleobase residue (cf. Figure 1), i.e., the one of the $(HNPP - 2H)^{7-}$ species? For this case one obtains:

G2(N1)H = 38 ± 7%

T6(N3)H = 37 ± 7%

G3(N1)H = 25 ± 13%

One should note that in case (i) the anionic deprotonated form of the tautomers is given, which all together provide the total amount of $(HNPP - H)^{6-}$ present. Clearly, here we have a series of proton acceptors. This contrasts with case (ii), where the percentages of the final hydrogen-donor sites are listed. However, in both cases the populations of the isomers/tautomers are considerable and the possible transport of a proton-hole or of a proton along a pathway is evident. These results, including those of Sections 2.11 and 2.12, are surely of a general nature and hold for any type of nucleic acid.

**2.14. A short appraisal of metal ion coordination to the DNA derivative d(A1·G2·G3·C4·C5·T6):** An important question with regard to biological systems is: To what extent are acid-base properties of such an oligonucleo(s/t)ide, as studied now, affected by the coordination of metal ions? Since *Cisplatin*, *cis*-$(NH_3)_2PtCl_2$, is an important anticancer drug,[55-57] which is believed to act via a DNA adduct,[58] many studies exist which deal especially with the coordination of *cis*-$(NH_3)_2Pt^{2+}$ to nucleobase derivatives.[16]

In this context Lippard et al.[11,12] have studied the intrastrand adduct of *cis*-$(NH_3)_2Pt^{2+}$, in which $Pt^{2+}$ is coordinated to G2(N7) and G3(N7) of $(HNPP)^{5-}$. We tried to evaluate their NMR chemical shift data (Figure 7 in Ref. [12]) via a curve-fitting procedure as done before with other literature data (e.g., [59]). Indeed, the overall p$K_a$ of the (N1)H sites equals 7.75 ± 0.3 for the single-stranded $(HNPP)^{5-}$, the adduct having the formula

[*cis*-$(NH_3)_2$Pt(HNPP –2H,G2*N7*,G3*N7*)]$^{5-}$. That this $Pt^{2+}$ complex is single-stranded has already previously been shown by Caradona and Lippard.[12] Because a further evaluation of the ligand data from Ref[12] leads to p$K_a$ values similar to ours (despite the helix) (Tables 3, 5), we assume that in the literature data[12] the isotope effect ($D_2O$ *versus* $H_2O$ as solvent) had already been considered. Comparison of the above value with the average p$K_a$ measured now for G2(N1)H and G3(N1)H, i.e., p$K_{a/av}$ = 9.98 ± 0.19 (2σ) [as follows from 9.88 ± 0.13 and 10.07 ± 0.06; Table 5], gives on average an acidification of $\Delta pK_a$ = 2.2 ± 0.4. Unfortunately, a big caveat needs to be made here because the measurements of the $Pt^{2+}$ adduct were done at 70°C (and in 0.1 M phosphate buffer) [12] whereas our values refer to 25°C (*I* = 0.1 M, $NaClO_4$) (Table 3). Hence, the given $\Delta pK_a$ is most likely an overestimate, but still it proves that the G2(N7)/G3(N7)-coordinated *cis*-$(NH_3)_2Pt^{2+}$ acidifies the G2(N1)H/G3(N1)H sites.

In previous studies[39,59] of simple guanine derivatives it was shown that (N7)-coordinated divalent metal ions acidify (N1)H sites in the following decreasing order:[40] $Cu^{2+}$ ($\Delta pK_a$ = 2.2 ± 0.3) > $Ni^{2+}$ (1.7 ± 0.15) > $Pt^{2+}$ (1.4 ± 0.1) ~ $Pd^{2+}$ (1.4). Into this picture fit also data obtained for the dinucleoside monophosphates d(GpG)$^-$ and (GpG)$^{\cdot-}$:[40] For example, the formation of the M[d(GpG – H)] complex gives rise, in the case of $Ni^{2+}$, to $\Delta pK_{a/Ni}$ = 1.97 ± 0.25, and for $Cd^{2+}$ to $\Delta pK_{a/Cd}$ = 1.81 ± 0.31; for Cd(GpG – H) $\Delta pK_{a/Cd}$ = 1.84 ± 0.04 was observed. [40]

The acidity constants for the (N1)H deprotonations of (GpG)$^-$ are p$K_{a/1}$ = 9.34 ± 0.07 and p$K_{a/2}$ = 10.38 ± 0.10, and for d(GpG)$^-$ p$K_{a/1}$ = 9.37 ± 0.03 and 10.39 ± 0.07.[40,60] The average acidity constants are thus p$K_{a/av/GpG}$ = 9.86 and p$K_{a/av/d(GpG)}$ = 9.88, both being very similar and within the error limits actually identical to the above mentioned average observed for G2(N1)H and G3(N1)H: i.e., 9.98 ± 0.19. Hence, one may consider in a first approximation the dinucleoside monophosphates (GpG)$^-$ and d(GpG)$^-$ as reasonable mimics for the corresponding unit in d(A1·G2·G3·C4·C5·T6)$^{5-}$, even though the p$K_{a/1}$ and p$K_{a/2}$ values of (GpG)$^-$ and d(GpG)$^-$ are somewhat further apart than those of G2(N1)H and G3(N1)H. The reason for this is that most likely the intramolecular guanine-guanine stacking[60] in d(GpG)$^{\cdot-}$ is somewhat more pronounced than the corresponding one in d(A1·G2·G3·C4·C5·T6)$^{5-}$, where the adenine-guanine stacks are somewhat more stable than the guanine-guanine ones [29] (see also Section 2.7), as indeed is expected.[27,61]

Furthermore, it should be noted that from the previous and already indicated results[37,55] for the $Ni^{2+}$ and $Cd^{2+}$ complexes of (GpG)$^-$ and d(GpG)$^-$, that is, $pK^{H}_{M(GpG)}$ equals ca. 7.5,

it follows from the *Stability Ruler* of Martin[61] that at least for $Zn^{2+}$ the acidification is so strong that the physiological pH range is reached. In fact, even with $Mg^{2+}$, where $pK^{H}_{M(GpG)}$ is ca. 8.3,[37] this is also to some extent the case: At pH 7.5 about 15% of $Mg(GpG)^{+}$ exist in the (N1)-deprotonated Mg(GpG – H) form. The biological relevance is obvious and the reasonings certainly also hold for the hexa-2'-deoxynucleoside pentaphosphate considered in this study.

**2.15. Derived acid-base properties for the RNA derivative r(A1·G2·G3·C4·C5·U6):** Because ribozyme reactions include proton transfers and perturbed $pK_a$ values have been shown to occur in ribozymes,[9,63-66] we are making now a sophisticated attempt to transfer the accumulated information for the hexa-2'-deoxynucleoside pentaphosphate to the corresponding ribosyl derivative, that is, to r(A1·G2·G3·C4·C5·U6) [U = uridine residue]. To be able to achieve this aim, it is necessary to quantify, as exactly as possible, the effect on the acid-base properties resulting from the substitution of the hydrogen at C2' of the pentose residue by an OH group. To this end we collected the p*K*a values assembled in Tables 6 and S4.

In entries 1 to 4 of Table 6 the $pK_a$ values for 2'-deoxyadenosine (dAdo) and also for adenosine (Ado) are listed, as well as for the corresponding mono-, di-, and triphosphates. Surprisingly, all the $\Delta pK_a$ values as defined by Equation (40),

$$\Delta pK_{a(dN/rN)} = pK_{a/deoxyribose} - pK_{a/ribose} \qquad (40)$$

are within their error limits identical, and this despite the fact that the first pair in its deprotonated form (entry 1) has no charges, whereas the pair of entry 4 carries a monoprotonated triphosphate residue with a charge of 3–. Moreover, even a switch of the phosphate residue from C5' to C3' does not affect the difference (Table S4). The average $\Delta pK_{a(dN/rN)}$ for the adenine derivatives of Table 6 amounts to 0.13 ± 0.05 (3σ) and the one of Table S4 to 0.14 ± 0.02. Hence, neither the charge of the phosphate residues nor their position at the (2'-deoxy)ribosyl residue (5' *versus* 3') affects the $\Delta pK_{a(dN/rN)}$ value. The same conclusion holds for all the other entries of Tables 6 and S4: The 2'-deoxy compounds are always somewhat more basic than their ribose relatives.

Table 6. Comparison of the negative logarithms of the acidity constants, p$K_a$ [Eqs. (4) to (6) and (8)], valid for aqueous solutions of some (2'-deoxy)nucleosides [(d)Ns and (r)Ns] and their corresponding 5'-phosphates, together with the resulting $\Delta pK_a$ differences (25°C; $I$ = 0.1 M)[a]

| No. | Acid dN/rN | p$K_a$ of the sites (N1)H$^+$/(N7)H$^+$ or (N1)H/(N3)H[b] | $\Delta pK_{a(dN/rN)}$ |
|---|---|---|---|
| 1 | H(dAdo)$^+$/H(Ado)$^+$ | 3.77 ± 0.04/3.62 ± 0.04 | 0.15 ± 0.06 |
| 2 | $H_2$(dAMP)$^{\pm}$/$H_2$(AMP)$^{\pm}$ | 3.97 ± 0.02/3.84 ± 0.02 | 0.13 ± 0.03 |
| 3 | $H_2$(dADP)$^-$/$H_2$(ADP)$^-$ | 4.00 ± 0.03/3.92 ± 0.02 | 0.08 ± 0.04 |
| 4 | $H_2$(dATP)$^{2-}$/$H_2$(ATP)$^{2-}$ | 4.14 ± 0.02/4.00 ± 0.01 | 0.14 ± 0.03 |
| 5 | H(dGuo)$^+$/H(Guo)$^+$ | 2.31 ± 0.05/2.12 ± 0.04 | 0.19 ± 0.06 |
| 6 | $H_2$(dGMP)$^{\pm}$/$H_2$(GMP)$^{\pm}$ | 2.69 ± 0.03/2.48 ± 0.04 | 0.21 ± 0.05 |
| 7 | $H_2$(dGDP)$^-$/$H_2$(GDP)$^-$ | 2.91 ± 0.07/2.67 ± 0.02 | 0.24 ± 0.07 |
| 8 | $H_2$(dGTP)$^{2-}$/$H_2$(GTP)$^{2-}$ | 3.16 ± 0.05/2.94 ± 0.02 | 0.22 ± 0.05 |
| 9 | dGuo/Guo | 9.25 ± 0.02/9.22 ± 0.02 | 0.03 ± 0.03 |
| 10 | dGMP$^{2-}$/GMP$^{2-}$ | 9.56 ± 0.02/9.49 ± 0.02 | 0.07 ± 0.03 |
| 11 | dGDP$^{3-}$/GDP$^{3-}$ | 9.64 ± 0.04/9.56 ± 0.03 | 0.08 ± 0.03 |
| 12 | dGTP$^{4-}$/GTP$^{4-}$ | 9.66 ± 0.04/9.57 ± 0.02 | 0.09 ± 0.04 |
| 13 | dThd/– | 9.71 ± 0.07/ – | 0.52 ± 0.07 |
| 14 | –/Urd | – /9.19 ± 0.02 | |
| 15 | dTMP$^{2-}$/ – | 9.90 ± 0.03/ – | 0.45 ± 0.04 |
| 16 | – /UMP$^{2-}$ | – /9.45 ± 0.02 | |
| 17 | dTDP$^{3-}$/ – | 9.93 ± 0.02/ – | 0.46 ± 0.03 |
| 18 | – /UDP$^{3-}$ | – /9.47 ± 0.02 | |
| 19 | dTTP$^{4-}$/ – | 10.08 ± 0.05/ – | 0.51 ± 0.05 |
| 20 | – /UTP$^{4-}$ | – /9.57 ± 0.02 | |

[a] Error limits (3σ); see also footnote [a] of Table 2. The values in entries 1, 5, 9, 13, and 14 are from Table S4; those in entries 2–4, 6–8, 10–12, and 15–20 are from Ref. [11]. [b] The site (N1)H$^+$ occurs in H(Ado)$^+$, etc.; (N7)H$^+$ in H(Guo)$^+$, etc.; (N1)H in Guo, etc.; and (N3)H in dThd, etc., and in Urd, etc. (for the structures of the nucleoside residues see also Figure 1).

This observation has been made before,[13,14,71] and the different $\Delta pK_{a(dN/rN)}$ values observed for (d)Ado(N1)$H^+$, (d)Guo(N7)$H^+$, (d)Guo(N1)H, and (d)Cyd(N3)$H^+$, etc., have been discussed.[13] It should be noted that for the cytosine derivatives only information about the H(dCyd)$^+$/H(Cyd)$^+$, $[H_2(2'd5'CMP)]^{\pm}/[H_2(5'CMP)]^{\pm}$, and $[H_2(2'd3'CMP)]^{\pm}/[H_2(3'CMP)]^{\pm}$ pairs exists (see Table S4). Similarly, for the thymine residues only values for the dThd family are available and for the related uracil moiety only those for Urd derivatives exist (Table 6, entries 13–20)[13] (see also below).

Because the $\Delta pK_{a(dN/rN)}$ values do not experience any charge effects and are also independent of the location of the phosphate substituent at the (2'-deoxy)ribose residue, there is no reason why this principle should not also hold for an oligonucleo(s/t)ide phosphate. Therefore, we have averaged the $\Delta pK_{a(dN/rN)}$ [Eq. (40)] values of Tables 6 and S4, always for the nucleobase considered, and these values are now listed in column 3 of Table 7.

Table 7. Estimation of the intrinsic acidity constants of the various (N)H sites in the single-stranded RNA derivative, r(A1·G2·G3·C4·C5·U6). These acidity constants are based on those of the corresponding 2'-deoxy derivative by application of Equation (40) (aqueous solution; 25°C; $I$ = 0.1 M)[a]

| No. | (d)ribose Ns residue | $\Delta pK_{a(dN/rN)}$ | p$K_a$ of d(HNPP) | p$K_a$ of r(HNPP) |
|---|---|---|---|---|
| 1 | G2(N7)$H^+$ | 0.21 ± 0.04 | 2.44 ± 0.21 | 2.23 ± 0.21 |
| 2 | G3(N7)$H^+$ | 0.21 ± 0.04 | 2.97 ± 0.21 | 2.76 ± 0.21 |
| 3 | A1(N1)$H^+$ | 0.13 ± 0.04 | 3.71 ± 0.07 | 3.58 ± 0.08 |
| 4 | C4(N3)$H^+$ | 0.13 ± 0.03 | 4.31 ± 0.07 | 4.18 ± 0.08 |
| 5 | C5(N3)$H^+$ | 0.13 ± 0.03 | 4.32 ± 0.07 | 4.19 ± 0.08 |
| 6 | G3(N1)H | 0.07 ± 0.04 | 9.88 ± 0.13 | 9.81 ± 0.14 |
| 7a | T6(N3)H | 0.49 ± 0.05 | 10.05 ± 0.11 | – |
| 7b | U6(N3)H | | – | 9.56 ± 0.12 |
| 8 | G2(N1)H | 0.07 ± 0.04 | 10.07 ± 0.06 | 10.00 ± 0.07 |

[a] For the error propagation see footnote [d] of Table 3. The values in the fourth column are from Table 5 (column 3). The values in the third column are based on Equation (40); they are the arithmetic means (with 3s) of the $\Delta pK_a$ values listed in Tables 6 and S4 (see also text in Section 4).

Because the 2'-deoxyribose derivatives are more basic than the ribose ones, the $\Delta pK_{a(dN/rN)}$ values in column 3 need to be deducted from the acidity constants determined for the various nucleobase residues in d(A1·G2·G3·C4·C5·T6). These latter values are taken from Table 3 (or Table 5) and are listed again in column 4 of Table 7. Because in RNA the thymidine (dThd) residue of DNA is replaced by an uridine (Urd) residue, which differs at C5 (see Figure 1) by a $CH_3$ *versus* a H substituent, the relatively large difference of 0.49 ± 0.05 p*K* units (entry 7 of Table 7) needs to be taken into account. The value of 0.49 contains both (i) the substituent effect at C5 ($CH_3$ *versus* H), as well as (ii) the substituent effect at C2' (H *versus* OH). The results obtained in the described way for the RNA derivative r(HNPP) are summarized in column 5 of Table 7.

## 3. Conclusions and Outlook

During the course of this study we have seen that in the hexanucleoside pentaphosphate $d(A1{\cdot}G2{\cdot}G3{\cdot}C4{\cdot}C5{\cdot}T6)^{5-}$, a DNA derivative, intramolecular stacking between the purine residues occurs. This affects the $pK_a$ values of certain of the involved residues. Some 2'- deoxynucleoside residues show the same acid-base properties like their individual "monomeric" 2'-deoxynucleosides, but other residues differ significantly in their properties (see Section 2.10). It is thus obvious that a certain fold created by stacking and/or hydrogen bonding in such an oligonucleo(s/t)ide may result in unexpected properties.

The evaluation of the tautomeric equilibria (Sections 2.11 to 2.13) and the quantification of several of their tautomer populations indicate that a proton-donor or a proton-acceptor site can switch from one place to another without affecting the overall formation degree of the protonic status of the species. Evidently, this leads to the creation of pathways for the transport of protons over distances at a low cost. For reactivities of nucleic acids, including ribozymes,[2,9,63-67] and DNAzymes,[68-70] this is certainly of relevance. Furthermore, this also holds for the influence of metal ions on the acid-base properties of nucleic acids as indicated in Section 2.14: Metal ion coordination allows easily $pK_a$ shifts into the physiological pH region.

Even though not directly measured, the $pK_a$ values listed in column 5 of Table 7 (Section 2.15) for the RNA derivative r(A1·G2·G3·C4·C5·U6) should prove helpful in many kinds of comparisons. This includes $pK_a$ shifts due to metal ion coordination (Section 2.14)

and here, e.g., Urd is favored compared to dThd if the physiological pH range should be reached.[46] Of course, any experimental or theoretical confirmation of the derived values for the ribose-HNPP is desirable. However, even more needed are now studies dealing with the metal ion-binding properties of such short nucleic acids because these results would be highly relevant for studies on ribozymes[2-6,64,72-74] and DNAzymes.[68-70,75,76]

## 4. Experimental Section

**Materials:** The deuterated reagents $D_2O$ (99.998%), NaOD (40% in $D_2O$; 99.9% D) and $DNO_3$ (65% in $D_2O$; 99.5% D) were purchased from Armar Chemicals (Doettlingen, Switzerland). The buffer solutions used (pH 4.00, 7.00, 9.00) were based on standard reference material (SRM) of the US National Institute of Science and Technology (NIST) and were from Metrohm AG (Herisau, Switzerland). Further, also standardized buffers (pH 2.00, 3.00, 4.62) were obtained from Carl Roth, Karlsruhe, Germany, (pH 9.21) from Mettler-Toledo, Schwerzenbach, Switzerland, and (pH 10.01) from Hanna Instruments, Woonsocket, USA. The 2'-deoxynucleosides dCyd and dGuo were obtained from Acros Organics (Geel, Belgium) and were used without further purification. All other chemicals were at least puriss p.a. and purchased either from Fluka-Sigma-Aldrich (Buchs, Switzerland) or Brunschwig Chemie (Amsterdam, The Netherlands).

**Synthesis of $(HNPP)^{5-}$:** The hexanucleo(s/t)ide $(HNPP)^{5-}$ was synthesized by standard phosphoramidite chemistry on a 50 μmol scale.[77,78] After deprotection with 30% aqueous ammonia (10 hours at 55°C) the crude hexanucleoside pentaphosphate was purified by ion-exchange chromatography on DEAE Sephadex A-25 (elution with a linear gradient of triethylammonium bicarbonate from 0.2 to 1.0 M). The purified oligonucleotide was transformed into the penta-$Na^+$ salt by passing its aqueous solution through a Dowex 50Wx8 ($Na^+$ form) column and lyophilized to give the final product as a white solid in 59% yield. The purity was confirmed by $^{31}P$ NMR ($D_2O$) showing four signals with the chemical shifts –0.381, –0.575, – 0.636, and –0.656 ppm, the most upfield one being of double intensity. The MALDI TOF mass spectrum (negative ions) gave m/z = 1792 (calculated MW 1794.29 for the free acid). The $^{31}P$ NMR spectra were recorded on a Bruker AC200 spectrometer (200.113 MHz for 1 H) with standard proton decoupling and referenced to 85% H3PO4 (as an external standard). The MALDI TOF mass spectra were recorded with a

Voyager-Elite spectrometer in the negative mode. The HNPP synthesis was performed with an automatic ABI 394 DNA Synthesizer.

For the NMR experiments, the oligonucleotide was desalted using NAP$^{TM}$-10 columns from GE Healthcare (Otelfingen, Switzerland), lyophilized and resuspended in either 90% $H_2O$/10% $D_2O$ or 100% $D_2O$, with 0.1 M $NaClO_4$. The DNA concentration was determined using an extinction coefficient at 260 nm ($\varepsilon_{260}$, 25°C) of 56200 $M^{-1}cm^{-1}$which was estimated with the help of the nearest-neighbor approximation.[79]

**UV-melting curves:** UV-melting curves of $(HNPP)^{5-}$ were recorded on a Cary 100 Scan UV-VIS (Varian Inc., Palo Alto, USA) connected to a circulating temperature controller with a total volume of 350 mL, a path length of 1 mm, and 0.15 mM $(HNPP)^{5-}$ in 0.1 M $NaClO_4$ at pH 6.5. The solution was covered carefully with paraffin oil and heated from 1 to 95°C in 0.5ºC/min steps. The absorption was recorded every 0.2ºC at 260 nm during two heating and two cooling cycles. The first cooling and the second heating curve were used to determine the $T_m$ value, which was obtained from the inflexion point (see Section 2.1 and Figure 2).

**CD measurements:** Temperature-dependent circular dichroism (CD) spectra of $(HNPP)^{5-}$ (0.15 mM in 0.1 M $NaClO_4$ at pH 6.5) were recorded on a J-810 spectrapolarimeter (Jasco Inc., Japan) using a 1 mm QS cuvette with a total volume of 350 mL. Absorption and CD spectra (see Section 2.1) were recorded every 2ºC from 1°C to 63°C and every 1ºC from 64°C to 95°C (see Figure S1 in the Supporting Information). Each measurement was repeated twice at a scan speed of 100 nm/min from 350 to 200 nm.

**NMR spectroscopy of HNPP:** NMR spectra were recorded either on a Bruker AV700 MHz spectrometer equipped with a TXI z-gradient CryoProbe® or on a Bruker AV2-500 MHz spectrometer equipped with a QNP z-gradient CryoProbe® in 5-mm Shigemi NMR tubes with 350 mL sample volume. NMR spectra of 0.15 mM $(HNPP)^{5-}$ were acquired in 100% D2O containing 100 mM NaClO4 at pD 6.3. [$^1$H, $^1$H]-NOESY spectra at 8°C and 47°C (see Figure 3) were recorded with presaturation water suppression and a mixing time of 250 ms. DOSY (diffusion ordered spectroscopy) spectra were measured with the standard Bruker pulse program ledbpgp2s_es, which applies stimulated echoes using bipolar gradient

pulses for diffusion. The diffusion time (Δ), the gradient length (δ) and the recovery delay after gradient pulses were set on 350 ms, 2.4 ms, 200 ms respectively, while the gradient strength was incremented from 14.4 to 45.7 G/cm in 32 steps. The NMR data were processed with TOPSPIN 2.1.

The resonances of the aromatic, H5, H1', and $CH_3$ protons (see the three parts of Figure 5) were assigned based on the [$^1$H, $^1$H]-NOESY spectrum (Figure 3) of the duplex form of $((HNPP)^{5-})_2$, i.e., $[d(ApGpGpCpCpT)]_2$, at 8ºC ($D_2O$, pD = 6.3). Our duplex assignments agree with those published in Ref. [12]. To obtain the resonance assignment under single strand conditions at 47°C, the NOESY based assignment was transferred to the 1D $^1$H NMR spectrum at 8°C and then followed in 1D temperature dependence experiments up to 47°C. The chemical shift of each proton was then followed in a pH-dependent manner (see Section 4.6). In cases of resonance overlap, all possible assignments were checked by plotting the change of the chemical shifts *versus* pH and the one following the chemical shift trend best was used. Line broadening of resonances is observed close to the neutral pH range (Figure 5), where the nucleobase residues are uncharged (Table 5, column 3), the reason for the broadening being unknown (possibly due to intrinsic dynamics of the single strand). Nevertheless, chemical shifts could still be assigned with good accuracy as seen, e.g., in Figures 6 and 7.

**$^1$H NMR shift experiments of nucleosides and HNPP:** $^1$H NMR spectra of dCyd (0.5 mM) and dGuo (0.5 mM) in 100% $D_2O$ and 10% $D_2O$/90% $H_2O$ in dependence on pD were recorded at 25°C and 47°C and $I$ = 0.1 M ($NaClO_4$) using the center peak of the tetramethylammonium ion (TMA) triplet as internal reference. All measured chemical shifts were converted to the 3-(trimethylsilyl)propane-1-sulfonic acid sodium salt (DSS, also known as sodium 2,2-dimethyl-2-silapentane-5-sulfonate) reference by adding 3.173 ppm in 100% $D_2O$ or 3.153 ppm in 10% $D_2O$/90% $H_2O$. The value for 100% $D_2O$ is well in agreement with the previously published value of 3.174.[32,80] $^1$H NMR spectra of $(HNPP)^{5-}$ (0.15 mM) in 10% $D_2O$/90% $H_2O$ in dependence on pH were measured at 47°C and $I$ = 0.1 M ($NaClO_4$) using TMA (10% $D_2O$/90% $H_2O$, δ = 3.153 ppm) as external standard.

The pH (or pD) was adjusted by adding concentrated $DNO_3$ or NaOD solutions (see Section 4.1). The pH (pD) was measured with a Hamilton Minitrode glass electrode (Hamilton AG, Bonaduz, Switzerland) connected to a Metrohm 605 digital pH meter (Metrohm AG, Herisau, Switzerland). The buffer solutions at pH 4.00, 7.00, and 9.00

mentioned above were used to calibrate the instrument. The pD values of the solutions were obtained by adding 0.40 to the pH meter reading.[81,82] The experimental data were analyzed by means of the Newton-Gauss nonlinear least-squares method. Results were obtained with the aid of a computer-based curve- fitting program using the general equation published previously (see also Section 2.4).[32,83-85] The $pK_a(H_2O)$ values for $H_2O$ solutions were calculated from the $pK_a(D_2O)$ values valid in $D_2O$ according to Equation (14).[25]

As indicated above, the direct pH-meter readings were used in the calculations of the acidity constants (Section 2.2); that is, these constants, determined at $I$ = 0.1 M ($NaClO_4$), are so- called practical, mixed or Brønsted constants.[24] They may be converted into the corresponding concentration constants by subtracting 0.03 ± 0.02 from the listed $pK_a$ values[24] (see also Table S3, footnote [h]); this conversion term contains both the junction potential of the glass electrode and the hydrogen ion activity.[23,24]

**Acknowledgments**

We thank Joachim Schnabl for his help with the NIST and IUPAC data bases. Financial support from the Swiss National Science Foundation (R.K.O.S.), the European Research Council (ERC Starting Grant to R.K.O.S.), the Universities of Zürich (R.K.O.S.), Granada (J.M.G.-P. & J.N.-G.), and Basel (H.S.), as well as the Polish Academy of Sciences and the Lódz University of Technology (A.O.) are gratefully acknowledged. Also gratefully acknowledged is the fellowship received by A.D.-M. from the Ministerio de Educación, Spain (FPU Program), as well as the Marie Heim-Vögtlin fellowship administered by the Swiss National Science Foundation and received by S.J..

REFERENCES

[1] W. Saenger, *Principles of Nucleic Acid Structure*, Springer, New York, **1984**, pp. 1–556.

[2] R. K. O. Sigel, A. M. Pyle, *Chem. Rev.* **2007**, *107*, 97–113.

[3] R. K. O. Sigel, H. Sigel, *Acc. Chem. Res.* **2010**, *43*, 974–984.

[4] J. Schnabl, R. K. O. Sigel, *Curr. Opinion Chem. Biol.* **2010**, *14*, 269–275.

[5] R. K. O. Sigel, S. Gallo, *Chimia* **2010**, *64*, 126–131.

[6] E. Freisinger, R. K. O. Sigel, *Coord. Chem. Rev.* **2007**, *251*, 1834–1851.

[7] E. T. Kool, *Annu. Rev. Biophys. Biomol. Struct.* **2001**, *30*, 1–22.

[8] P. Acharya, S. Acharya, P. Cheruku, N. V. Amirkhanov, A. Földesi, J. Chattopadhyaya, *J. Am. Chem. Soc.* **2003**, *125*, 9948–9961.

[9] B. Gong, J.-H. Chen, E. Chase, D. M. Chadalavada, R. Yajima, B. L. Golden, P. C. Bevilacqua, P. R. Carey *J. Am. Chem. Soc.* **2007**, *129*, 13335-13342.

[10] L. E. Kapinos. B. P. Operschall, E. Larsen, H. Sigel, *Chem. Eur. J.* **2011**, *17*, 8156–8164.

[11] J. P. Caradonna, S. J. Lippard, M. J. Gait, M. Singh, *J. Am. Chem. Soc.* **1982**, *104*, 5793– 5795.

[12] J. P. Caradonna, S. J. Lippard, *Inorg. Chem.* **1988**, *27*, 1454–1466.

[13] A. Mucha, B. Knobloch, M. Jeżowska-Bojczuk, H. Kozłowski, R. K. O. Sigel, *Chem. Eur. J.* **2008**, *14*, 6663–6671.

[14] P. Acharya, P. Cheruku, S. Chatterjee, S. Acharya, J. Chattopadhyaya, *J. Am. Chem. Soc.* **2004**, *126*, 2862–2869.

[15] B. Knobloch, D. Suliga, A. Okruszek, R. K. O. Sigel, *Chem. Eur. J.* **2005**, *11*, 4163–4170.

[16] B. Lippert, *Prog. Inorg. Chem.* **2005**, *54*, 385–447.

[17] A. Fernández-Botello, R. Griesser, A. Holý, V. Moreno, H. Sigel, *Inorg. Chem.* **2005**, *44*, 5104–5117.

[18] *Stability Constants of Metal Ion Complexes*, Suppl. No 1 (Compiled by L. G. Sillén and A. E. Martell), Spec. Publ. No. 25, The Chemical Society, London, UK, **1971**.

[19] A. E. Martell, R. M. Smith, *Critical Stability Constants*, Vol. 1, *Amino Acids*, Plenum Press, New York & London, **1974**, see Introduction.

[20] A. E. Martell, R. M. Smith, *Critical Stability Constants*, Vol. 2, *Amines*, Plenum Press, New York & London, **1975**.

[21] *NIST Critically Selected Stability Constants of Metal Complexes*, Reference Database 46, Version 8.0 (data collected and selected by R. M. Smith and A. E. Martell), US Departement of Commerce, National Institute of Standards and Technology, Gaithersburg, MD, USA, **2004**.

[22] *IUPAC Stability Constants Database*, Release 6, Version 5.83 (compiled by L. D. Pettit and H. K. J. Powell), Academic Software; Timble, Otley, West Yorkshire, UK, **2008**; see also L. D. Pettit, G. Pettit, *Pure Appl. Chem.* **2009**, *81*, 1585-1590.

[23] H. M. Irving, M. G. Miles, L. D. Pettit, *Analyt. Chim. Acta* **1967**, *38*, 475–488.

[24] H. Sigel, A. D. Zuberbühler, O. Yamauchi, *Anal. Chim. Acta* **1991**, *255*, 63–72.

[25] R. B. Martin, *Science* **1963**, *139*, 1198–1203.

[26] N. A. Corfù, A. Sigel, B. P. Operschall, H. Sigel, *J. Indian Chem. Soc.* **2011**, *88*, 1093– 1115 (Sir A. P. Chandra Ray issue).

[27] N. A. Corfù, H. Sigel, *Eur. J. Biochem.* **1991**, *199*, 659–669.

[28] J. Gu, G. Liang, Y. Xie, H. F. Schaefer, III, *Chem. Eur. J.* **2012**, *18*, 5232–5238.

[29] S. Jafilan, L. Klein, C. Hyun, J. Florián, *J. Phys. Chem. B* **2012**, *116*, 3613–3618.

[30] M. Rawitscher, J. M. Sturtevant, *J. Am. Chem. Soc.* **1960**, *82*, 3739–3740.

[31] H. Reinert, R. Weiss, *Hoppe-Seyler's Z. Physiol. Chem.* **1969**, *350*, 1321–1326.

[32] R. Tribolet, H. Sigel, *Eur. J. Biochem.* **1987**, *163*, 353–363.

[33] C. P. Da Costa, H. Sigel, *Inorg. Chem.* **2000**, *39*, 5985–5993.

[34] T. Vojtylová, D. Dospivová, O. Třísková, I. Pilařová, P. Lubal, M. Farková, L. Trnková,P. Táborský, *Chem. Papers* **2009**, *63*, 731–737.

[35] R. B. Martin, *Fed. Proc.* **1961**, *20*, Suppl. 10, 54–57, see [18].

[36] Y. Kinjo, R. Tribolet, N. A. Corfù, H. Sigel, *Inorg.Chem.* **1989**, *28*, 1480–1489.

[37] Y. Kinjo, L.-n. Ji, N. A. Corfù, H. Sigel, *Inorg. Chem.* **1992**, *31*, 5588–5596.

[38] H. Sigel, B. Song, G. Oswald, B. Lippert, *Chem. Eur. J.* **1998**, *4*, 1053–1060.

[39] B. Song, J. Zhao, R. Griesser, C. Meiser, H. Sigel, B. Lippert, *Chem. Eur. J.* **1999**, *5*, 2374–2387.

[40] C. P. Da Costa, H. Sigel, *Inorg. Chem.* **2003**, *42*, 3475–3482.

[41] H. Sigel, S. S. Massoud, N. A. Corfù, *J. Am. Chem. Soc.* **1994**, *116*, 2958–2971.

[42] M.-C. Lim, *J. Inorg. Nucl. Chem.* **1981**, *43*, 221–223.

[43] R. M'Boungou, M. Petit-Ramel, G. Thomas-David, G. Perichet, B. Pouyet, *Can. J. Chem.* **1987**, *65*, 1479–1484.

[44] M. Shionoya, E. Kimura, M. Shiro, *J. Am. Chem. Soc.* **1993**, *115*, 6730–6737.

[45] C. F. Moreno-Luque, E. Freisinger, B. Costisella, R. Griesser, J. Ochocki, B. Lippert, H. Sigel, *J. Chem. Soc., Perkin Trans. 2* **2001**, 2005–2011.

[46] B. Knobloch, W. Linert, H. Sigel, *Proc. Natl. Acad. Sci. USA* **2005**, *102*, 7459–7464.

[47] B. Knobloch, H. Sigel, A. Okruszek, R. K. O. Sigel, *Org. Biomol. Chem.* **2006**, *4*, 1085– 1090.

[48] S. S. Massoud, H. Sigel, *Eur. J. Biochem.* **1989**, *179*, 451–458.

[49] B. Song, G. Feldmann, M. Bastian, B. Lippert, H. Sigel, *Inorg. Chim. Acta* **1995**, *235*, 99–109.

[50] S. S. Massoud, H. Sigel, *Inorg. Chem.* **1988**, *27*, 1447–1453.

[51] N. Ogasawara, Y. Inoue, *J. Am. Chem. Soc.* **1976**, *98*, 7048–7053.

[52] H. Sigel, S. S. Massoud, R. Tribolet, *J. Am. Chem. Soc.* **1988**, *110*, 6857–6865.

[53] R. K. O. Sigel, M. Skilandat, A. Sigel, B. P. Operschall, H. Sigel, *Met. Ions Life Sci.* **2013**, *11*, in press.

[54] H. Sigel, B. P. Operschall, R. Griesser, *Chem. Soc. Rev*. **2009**, *38*, 2465–2494.

[55] K. R. Barnes, S. J. Lippard, *Met. Ions Biol. Syst*. **2004**, *42*, 143–177.

[56] a) M. A. Jakupec, M. Galanski, B. K. Keppler, *Met. Ions Biol. Syst.* **2004**, *42*, 179–208; b) A. Ummat, O. Rechkoblit, R. Jain, J. R. Choudhury, R. E. Johnson, T. D. Silverstein,

A. Buku, S. Lone, L. Prakash, A. K. Aggarwal, *Nat. Struct. Mol. Biol*. **2012**, *19*, 628-632.

[57] a) J. Reedijk, *Proc. Natl. Acad. Sci. USA* **2003**, *100*, 3611-3616; b) J. Reedijk, *Metallomics* **2012**, *4*, 628-632.

[58] *Cisplatin: Chemistry and Biochemistry of a Leading Anticancer Drug* (Ed.: B. Lippert), VCH, Zürich,; Wiley-VCH, Weinheim, **1999**, pp 1–563.

[59] R. Griesser, G. Kampf, L. E. Kapinos, S. Komeda, B. Lippert, J. Reedijk, H. Sigel, *Inorg. Chem.* **2003**, *42*, 32–41.

[60] B. Knobloch, A. Okruszek, H. Sigel, *Inorg. Chem.* **2008**, *47*, 2641–2648.

[61] N. A. Corfù, R. Tribolet, H. Sigel, *Eur. J. Biochem.* **1990**, *191*, 721–735.

[62] a) R. B. Martin, *Met. Ions Biol. Syst.* **1986**, *20*, 21–65; b) R. B. Martin in *Molecular Biology and Biotechnology* (Ed.: R. A. Meyers), VCH Publishers, New York, **1995**, pp 83–86; c) R. B. Martin in *Encyclopedia of Molecular Biology and Molecular Medicine*, *Vol. 1* (Ed.: R. A. Meyers), VCH Publishers, Weinheim, **1996**, pp 125–134.

[63] a) J.-H. Chen, R. Yajima, D. M. Chadalavada, E. Chase, P. C. Bevilacqua, B. L. Golden, *Biochemistry* **2010**, *49*, 6508-6518; b) A. L. Cerrone-Szakal, N. A. Siegfried, P. C. Bevilacqua, *J. Am. Chem. Soc.* **2008**, *130*, 14504-14520.

[64] A. Huppler, L. J. Nikstad, A. M. Allmann, D. A. Brow, S. E. Butcher, *Nature Struct. Biol.* **2002**, *9*, 431-435.

[65] M. D. Smith, R. Mehdizadeh, J. E. Olive, R. A. Collins, *RNA* **2008**, *14*, 1942-1949.

[66] A. E. Johnson-Buck, S. E. McDowell, N. G. Walter, *Met. Ions Life Sci.* **2011**, *9*, 175-196.

[67] R. K. O. Sigel, H. Sigel, *Met. Ions Life Sci.* **2007**, *2*, 109–180.

[68] T. Lan, Y. Lu, *Met. Ions Life Sci.* **2012**, *10*, 217–248.

# CONCLUSIONS AND OUTLOOK / CONCLUSIONES

Reviews concerning the available structural contributions about metal complexes with adenine or adenine-like ligands (deaza-adenines, adenina isomers, aza-adenines, etc.) reveal a very unbalanced panorama that basically can be summarised as a fairly versatile metal binding behaviour for the natural nucleobase adenine and a very limited information about other related N-ligands. This is true for all the reported ligands except for 7-azaindole and, with less extend for purine. On this basis, this research work aimed to provide new structural results about the molecular recognition patterns of adenine-like ligands through the study of mixed-ligand ternary copper(II) complexes with derivatives of the iminodicatete chelator. Likewise, This Ph.D, Thesis includes one study about the intrinsic acid-base properties of a hexa-2'-deoxinucleoside pentaphosphate.

The referred contributions incluyes original results that lead to the following CONCLUSIONS:

A) Regarding deaza-adenine ligands.

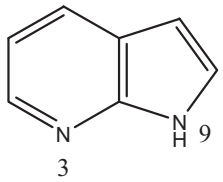


1. *7-Azaindole (*H7azain) uses its most stable tautomer (H(N9)7azain) to coordinate to different Cu(II) iminodiacetates. Thus, the molecular recognition pattern consists of the Cu-N3 coordination bond in cooperation with the intra-molecular interligand interaction N9-H···O(coord. carboxy). This behaviour is observed in nearly all the reported complexes in literature for H7azain with very few exceptions.

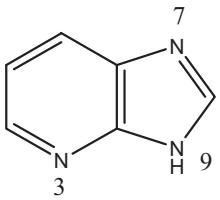


2. The molecular recognition between *4-azabencimidazole* (H4abim) and chelates type Cu(IDA) or Cu($H_2$EDTA) – derived from the ethylendiaminotetraacetic acid – represents the formation of a single coordination bond (Cu-N7 or Cu-N9, respectively). In the studied complexes, the ligand exhibits the two most stable tautomers: H(N9)4abim and H(N7)4abim, respectively. The use of the H(N7)4abim tautomer is unprecedented in literature. Since the

tautomerizable /dissociable proton remains in the imidazolic moiety, and the referred chalets only supply O-acceptor in their terminal endings, the Cu-N7 and Cu-N9 can not be reinforced by appropriate intra-molecular H-bonds type N-H···O.

The presence of the H(N3)4abim tautomer does not have structural support. This is in agreement to the relative sequence of basicity of this N-ligand N9 > N7 >> N3.

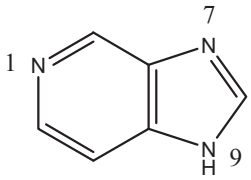


3. Two investigated complexes with *5-azabencimidazole* (H5abim) are dinuclear and shows, with Cu(IDA)-like chelating ligands, the bidentate bridging mode $\mu_2$-N7,N9, as the H(N1)5abim tautomer. The molecular skeleton of this N-ligand makes impossible the cooperation of the coordination bonds N7,N9 with intra-molecular H-bonds.

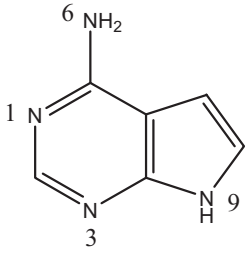


4. The absence of the N7 donor in *7-deaza-adenine* (H7deaA) enhances the coordination abilities of the N1 donor within the adenine moiety. Nevertheless, three mononuclear complexes reveal that this N-ligand has a clear preference for recognizing Cu(IDA) chelates by the formation of Cu-N3 bonds assisted by the N9-H···O intra-molecular interaction.

The use of the Cu(MIDA) chelate shows the unprecedentes bridging role $\mu_2$-N1,N3 for H7deaA. The presence of the most stable tautomer H(N9)7deaA, allow to reinforce the two coordination bonds by the corresponding intra-molecular interligand interactions N6-H···O y N9-H···O, respectively.

B) Regarding adenine isomers.

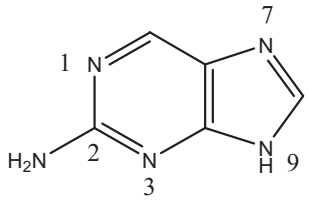


5. The shift of the exocyclcic amino group from C6 (in adenine) to C2 leads to the ligand *2-aminopurine* (H2AP). This fact introduces significant changes in the metal binding behaviour of this nucleobase. Thus, the metal binding versatility shown by adenine with Cu(IDA)-like chelates is reduced to a single molecular recognition pattern in H2AP. It consists of the formation of the Cu-N7 bond showing the most stable tautomer H(N9)2AP. This latter pattern can nor cooperate with intra-molecular H-bonds type N-H···O (coord. carboxy).

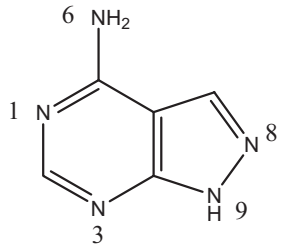


6. The shift of the N7 and C8 atoms in adenina leads to the ligand *4-aminopyrazolo[3,4-d]pirimidine* (H4app). As already reported from H7deaA, the available structural information suggests the increase of the enhancement of the coordination abilities of the N1 donor in the absence of N7. The molecular recognition patterns $\mu_2$-N1,N8-H(N9)4app and $\mu_2$-N8,N9-H(N1)4app (in di- or tetra-nuclear complexes, respectively), reveals the influence of the tautomerism phenomena, in contrast to that observed for H2AP. In this complexes, the Cu-N(H4app) bonds act in cooperation with the corresponding intra-molecular interactions when possible.

Particularly noteworthy, under the supramolecular viewpoint, is the acyclcic, non-lineal, topology of the tetranuclear complex of H4app. In this complex, hydrogen bonds established between the apical aqua ligand of one terminal metal (Cu4) and the O-carboxylate acceptors from two chelating ligands that appertain to other metal centres (Cu1 y Cu2), play a crucial role.

C) Relativas a N-derivados de adenina.

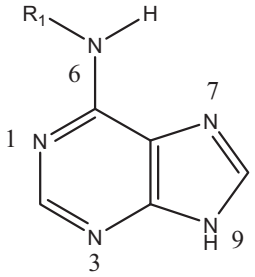


7. The molecular recognition pattern between *N6-monosubstituted adenines* and copper(II) N-(aryl-methyl)-iminodiacetates always consists of a Cu-N3 bond plus the intra-molecular interligand interaction N9-H···O(coord. carboxy).

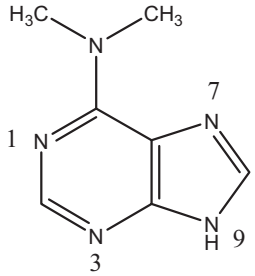


In clear contrast, the chelate Cu(II) N-benzyliminodiacetate recognizes the H(N3)dimAP tautomer by means of the Cu-N9 bond and the intra-molecular interaction N3-H···O(coord. carboxy). The presence of this tautomer is fairly rare in adenine-like ligands. The reasons why *N6-dimethyladenine* (HdimAP) uses this tautomer are not fully understood.

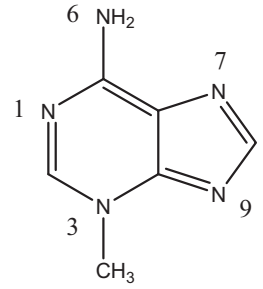


8. The use of *N-methyl-adenines*, with methyl substituent in one of the N-heterocyclic donors, and Cu(II)IDA-like chelates generally leads to the formation of the Cu-N7 bond, assisted by the intra-molecular interligand H-bond N6-H···O(coord. carboxy), except for 7-metiladenine that coordinates via N3, without any possibility of reinforcement.

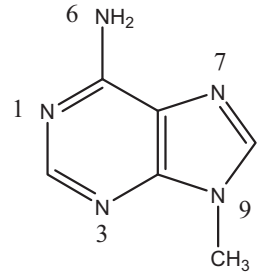


The ligands *3-methyladenine* (3Meade) and *9-methyladenine* (9Meade) bind different copper(II) iminodiacetate chelates by means of the Cu-N7 bond. This molecular recognition pattern is clearly influenced by the facts that: (i) N7 is less sterically hindered that N1, N3 or N9 regarding coordination of metal ions and (ii) the possibility of assisting the Cu-N bond with the corresponding H-bond (N-H···O).

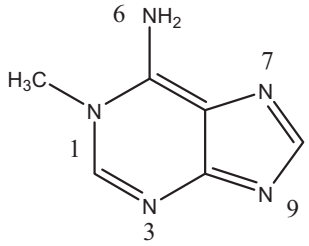


Also, the methylation over N1 leads to the molecular recognition between *1-methyladenine* (1Meade) and the Cu(CBIDA) chelate by means of the Cu-N7 bond and the interaction N6-H···O. In this case, the preference is essentially related to the impossibility of the Cu-N3 or Cu-N9 bonds to cooperate with intra-molecular H-bonds type N-H···O (coord. carboxy).

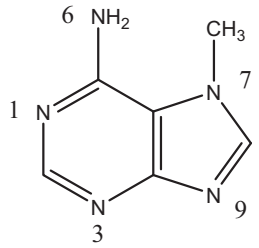


The metal binding pattern shown by *7-methyladenine* (7Meade) via N3 instead of N1, can be explained due to the steric hindrance imposed by the –(6)$NH_2$ group. However, why N9 is not involve in coordination remains quite unclear.

D) Regarding synthetic nucleosides.

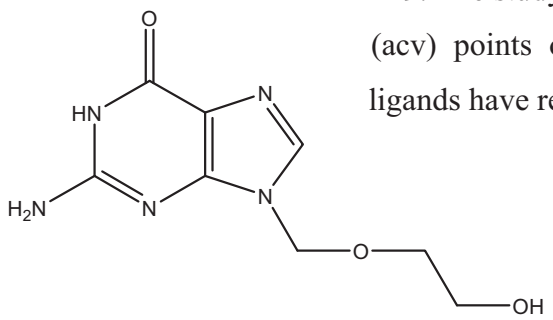


9. The study of ternary copper(II) complexes with *acyclovir* (acv) points out that he selection of appropriate chelating ligands have relevant consequences in molecular recognition.

Therefore, the substitution of an IDA chelating ligand, that only offers O-aceptors for H-bonding interactions, by glycylglycynate (glygly), that also supplies one terminal amino group terminal, allow to reach different molecular recognition patterns. The compound Cu(glygly)(acv) shows the Cu-N7(acv) coordination bond plus the intra-molecular interaction (glygly)N-H···O6(acv). This latter H-bond is not possible in the molecular recognition between the Cu(IDA) chelate and acv.

10. The study of the p$K_a$ values of the residues within a DNA derivative revealed changes in the acid-base properties of some of its ‘monomers’, in comparison to the corresponding isolated nucleosides and nucleotides. This fact is essentially related to supramolecular processes in the single strand such as π,π-stacking interactions between adjacent nucleobases. Likewise, the isomeric equilibria were evaluated what revealed the creation of pathways for the transport of protons over distances at a low cost. These findings shed light on the not-fully-understood catalytic role of nucleic acids and holds for the influence of metal ions on the acid-base properties of nucleic acids.

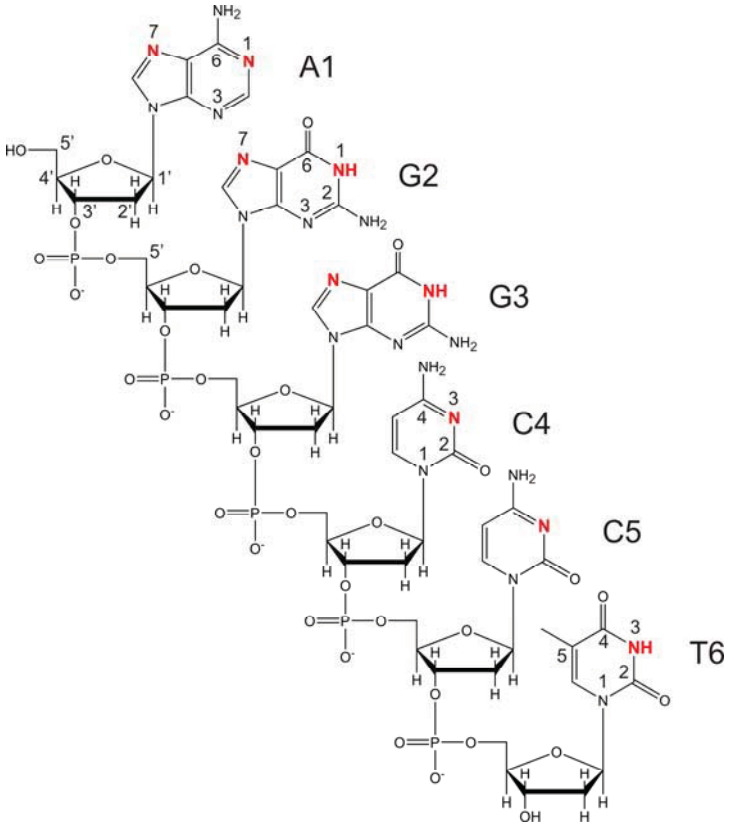

Revisiones de las aportaciones estructurales sobre complejos metálicos conteniendo adenina o ligandos nitrogenados análogos (deaza-adeninas, isómeros de adenina o aza-adeninas) revelan un panorama muy desigual que, en pocas palabras, consiste en un comportamiento extremadamente versátil para la nucleobase natural y un conocimiento muy limitado del comportamiento de otros heterociclos relacionados, con la salvedad de 7-azaindol y, en menor extensión, de purina. Sobre esta base, el presente trabajo de investigación se planteó como objetivo general realizar nuevas aportaciones estructurales sobre ligandos análogos de adenina, a través del estudio de complejos de cobre(II) con mezclas de ligandos conteniendo, las más de las veces, un quelante tipo iminodiacetato. Asimismo, la Tesis doctoral incluye un estudio de las propiedades acido-base de un hexa-2'-desoxinucleósido pentafostafo.

Las referidas aportaciones contienen resultados originales que conducen a las siguientes CONCLUSIONES:

A) Relativas a deaza-adeninas.

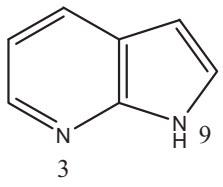


1. *7-Azaindol (*H7azain) usa su tautómero más estable (H(N9)7azain) para coordinarse a iminodiacetatos de cobre(II), de manera que el reconocimiento molecular quelato-H7azain consiste en la formación del enlace Cu-N3, en cooperación con la interacción intramolecular interligandos N9-H···O(carboxilato coordinado). Este comportamiento se observa, con muy pocas excepciones, en los complejos de H7azain aportados en la bibliografía.

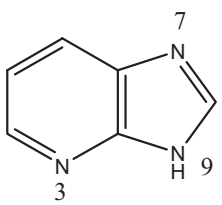


2. El reconocimiento entre *4-azabencimidazol* (H4abim) con quelatos tipo Cu(IDA) o con Cu($H_2$EDTA) – derivado del ácido etilendiaminotetraacético – representa sólo la formación de un enlace coordinado (Cu-N7 o Cu-N9, respectivamente). Asimismo, los compuestos estudiados muestran sus tautómeros más estables: H(N9)4abim y H(N7)4abim, respectivamente. El uso del tautómero

H(N7)4abim como ligando carece de antecedentes estructurales. Dado que el protón disociable permanece en el anillo imidazólico, y que los referidos quelatos de cobre(II) sólo ofrecen átomos O-carboxilato como aceptores, los enlaces Cu-N9 y Cu-N7 no pueden ser reforzados por una interacción interligandos de tipo enlace de hidrógeno.

La existencia del tautómero H(N3)4abim carece, por el momento, de soporte estructural, como reflejo de la secuencia de basicidad N9 > N7 >> N3.

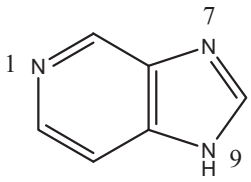


3. Los dos compuestos investigados con *5-azabencimidazol* (H5abim) son dinucleares y muestran, con quelatos tipo Cu(IDA), el modo de coordinación puente $\mu_2$-N7,N9, en forma del tautómero H(N1)5abim. El esqueleto molecular de este ligando nitrogenado hace imposible la cooperación de los enlaces coordinados con puentes de hidrógeno intramoleculares interligandos.

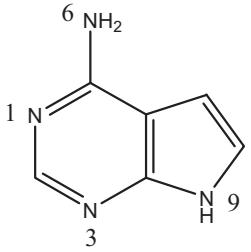


4. La ausencia de dador N7 en *7-deaza-adenina* (H7deaA) promociona las posibilidades de N1 como átomo dador. No obstante, tres compuestos mononucleares revelan que este ligando nitrogenado tiene una clara preferencia por reconocerse con quelatos tipo Cu(IDA) mediante el enlace Cu-N3 reforzado por una interacción intramolecular interligandos N9-H···O.

El reconocimiento con el quelato Cu(MIDA) implica a H7deaA como ligando puente $\mu_2$-N1,N3, sin precedentes en bibliografía. La presencia del tautómero más estable H(N9)7deaA, posibilita la cooperación de los enlaces Cu-N1 y Cu-N3 con las correspondientes interacciones intramoleculares interligandos N6-H···O y N9-H···O, respectivamente.

B) Relativas a isómeros de adenina.

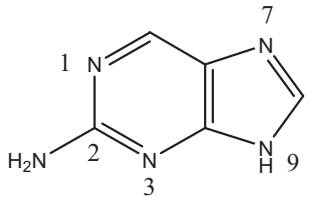


5. La transposición del grupo amino exocíclico de adenina desde C6 a C2 lleva al ligando *2-aminopurina* (H2AP). Este hecho introduce drásticos cambios en el comportamiento de esta base nitrogenada. Así, la versatilidad del reconocimiento molecular entre adenina y quelatos tipo Cu(IDA) se reduce a un único modo de coordinación para H2AP, consistente en la formación del enlace Cu-N7 con el tautómero más estable H(N9)2AP. Este modo carece de la posibilidad de refuerzo por una interacción intramolecular interligandos tipo N-H···O (carboxilato coordinado).

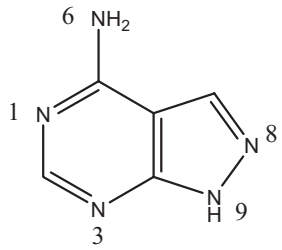


6. La translocación de N7 y C8 en adenina resulta en el ligando *4-aminopirazolo[3,4- d]pirimidina* (H4app). Aquí, al igual que para el ligando H7deaA, los datos disponibles realzan las posibilidades coordinantes del dador N1 ante la ausencia de dador N7. Los modos de coordinación establecidos, $\mu_2$-N1,N8-H(N9)4app y $\mu_2$-N8,N9-H(N1)4app (en complejos di- o tetra-nucleares, respectivamente), reflejan también la implicación de la tautomería, en contra de lo observado para H2AP. En estos modos de coordinación de H4app actúan en cooperación de interacciones intramolecular interligandos siempre que es posible.

De particular interés, bajo el punto de vista supramolecular, es la topología acíclica, no lineal, del complejo tetranuclear de H4app. En este compuesto, enlaces de hidrógeno, establecidos por el ligando aqua apical del centro metálico terminal (Cu4) y aceptores O-carboxilato pertenecientes a los quelates de otros centros metálicos (Cu1 y Cu2), desempeñan un papel crucial.

C) Relativas a N-derivados de adenina.

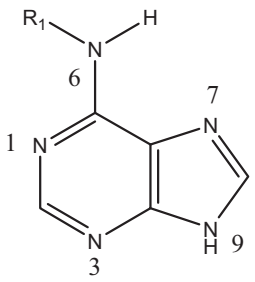


7. El reconocimiento molecular entre derivados *N6-monosustituidos de adenina* y N-(aril-metil)-iminodiacetatos de cobre(II) consiste, sin excepción, en la formación del enlace coordinado Cu-N3 y de la interacción intramolecular interligando N9-H···O(carboxilato coordinado).

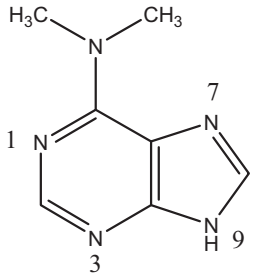


En claro contraste, el quelato N-benciliminodiacetato de cobre(II) se reconoce con el tautómero H(N3)dimAP mediante el enlace Cu-N9 y la interacción intramolecular interligandos N3-H···O(carboxilato coordinado). La presencia de este tautómero es muy inusual en ligandos tipo adenina. Las razones por las cuales *N6-dimetiladenina* (HdimAP) usa este tautómero no son bien comprendidas.

8. El uso de *N-metil-adeninas*, con sustituyentes en cada uno de los nitrógenos heterocíclicos, y quelatos tipo Cu(IDA) conduce, en general, a la formación del enlace Cu-N7, con la cooperación del la interacción intramolecular interligandos N6-H···O(carboxilato coordinado), excepto con 7-metiladenina que coordina por N3, sin posibilidad de refuerzo.

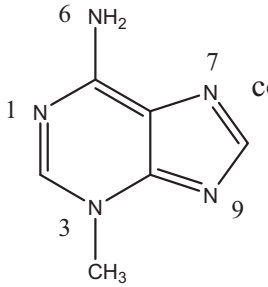


Los ligandos *3-metiladenina* (3Meade) y *9-metiladenina* (9Meade) se reconocen con diferentes quelatos de iminodiacetato de cobre(II) a través del enlace Cu-N7. Este modo de reconocimiento molecular está claramente influenciado por: (i) el hecho de que el dador N7 sufre con menor intensidad que N1 el factor estérico de $-(6)NH_2$; (ii) la posibilidad de cooperación del enlace Cu-N7 con una interacción intramolecular N6-H···O. En esta interacción, el átomo O-aceptor es de tipo carboxilato coordinado en todos los casos, excepto cuando el quelante es el

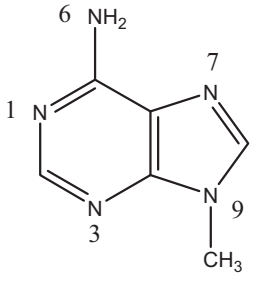

propio IDA, donde el aceptor es el átomo del ligando aqua apical.

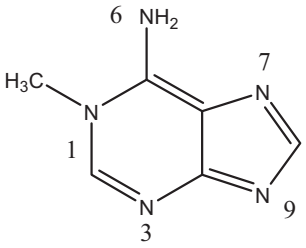


También la metilación de adenina en N1 conduce al reconocimiento de *1-metiladenina* (1Meade), con el quelato Cu(CBIDA), mediante del enlace Cu-N7 más la interacción N6-H···O. En este caso, la preferencia es explicada, esencialmente, dada la imposibilidad de cooperación de los enlaces Cu-N9 o Cu-N3 con una interacción intramolecular interligandos tipo N-H···O(carboxilato coordinado).

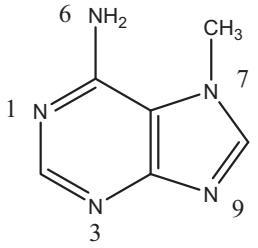


La preferencia de *7-metiladenina* por el dador N3, en lugar de N1, se explica por el factor estérico impuesto por –(6)$NH_2$. Sin embargo, la pasividad de N9 permanece poco clara.

D) Relativas a nucleósidos de síntesis.

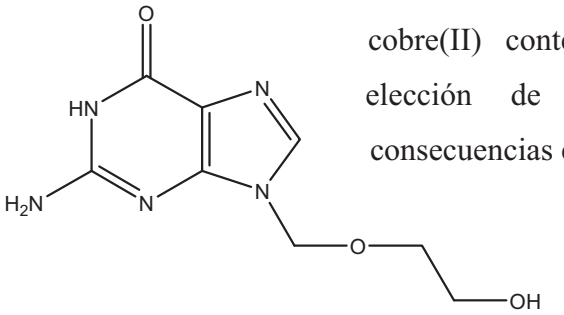


9. Del estudio las estructuras de los complejos ternarios de cobre(II) conteniendo *aciclovir* (acv) se deduce que la elección de quelantes apropiados tiene importantes consecuencias en la expresión del reconocimiento molecular

Así, la sustitución de un quelante tipo iminodiacetato (IDA), que sólo puede por ofrecer O-aceptores para interacciones de enlace de hidrógeno intramoleculares, por glicilglicinato (glygly), con un grupo amino primario terminal, lleva a diferentes modos de reconocimiento molecular. El compuesto Cu(glygly)(acv) muestra el enlace coordinado Cu-N7(acv) acompañado de la interacción intramolecular interligando (glygly)N-H···O6(acv). La referida interacción por enlace de hidrógeno no es posible en el

reconocimiento entre el quelato Cu(IDA) y acv, por lo que resulta limitada a la formación del enlace Cu-N7(acv).

10. El estudio de los valores de p$K_a$ de un derivado de ADN revelaron cambios en las propiedades ácido-base de algunos de sus "monómeros", en comparación con los correspondientes nucleósidos y nucleótidos aislados. Este hecho está ligando, fundamentalmente, a fenómenos supramoleculares que acontecen en la hebra sencilla, por ejemplo, interacciones de apilamiento entre nucleobases contiguas. Asimismo, los efectos derivados de los equilibrios tautoméricos dentro de la hebra permiten la formación de rutas capaces de transportar protones a larga distancia y a bajo coste. Este hallazgo arroja un poco de luz sobre la incomprendida reactividad de los ácidos nucleicos, así como de la influencia de los iones metálicos en las propiedades ácido-base de los ácidos nucleicos.

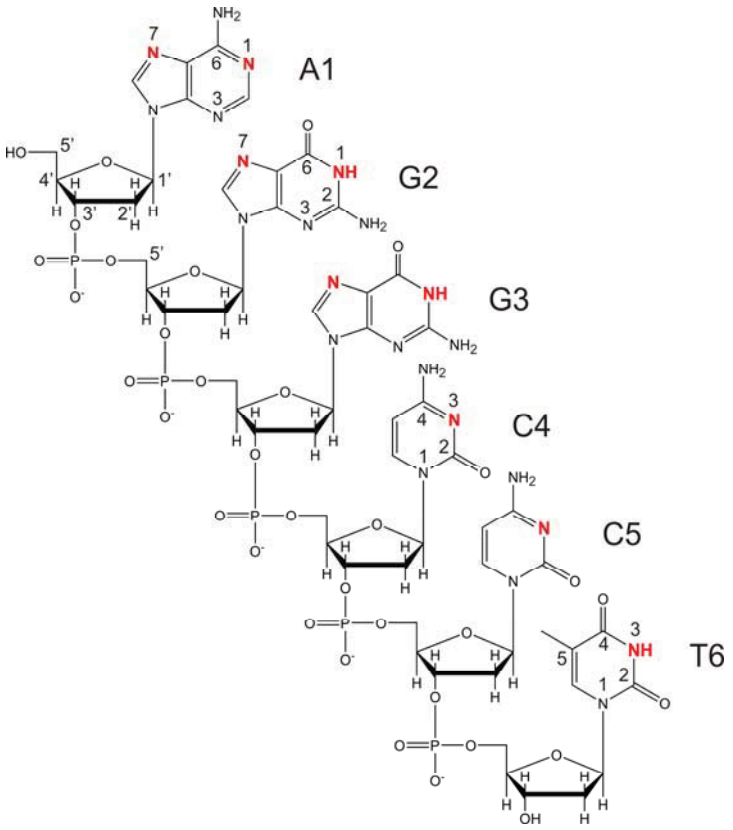

## *Curriculum Vitae*

**Personal data**

| | |
|---|---|
| Family name | Domínguez Martín |
| Fisrt name | Alicia |
| Date and Place of Birth | 26/11/1985, Marbella (Málaga), Spain |
| Nationality | Spanish |
| Marital status | Married |
| Languages | Spanish (mother language) |
| | English (fluent) |
| | French (basic) |

**Education**

| | |
|---|---|
| 09/1991 – 06/1997 | Primary school, in MR. Bocanegra, Marbella |
| 09/1997 – 06/2001 | Secondary school, in M.R. Bocanegra, Marbella |
| 09/2001 – 06/2003 | High school , in I.E.S. Rio Verde, Marbella |
| 09/2003 - 09/2008 | Studies of Pharmacy at University of Granada, Spain. |
| 10/2008 – 10/2009 | Master degree on "Drug Development "at University of Granada, Spain. |
| 10/2009 – to date | Ph.D. Thesis at the University of Granada, Spain. |
| December 2012 | Dissertation at the University of Granada, Spain |
| | Subject: *Molecular Recognition between Copper(II)-iminodiacetates and purine-like ligands or synthetic nucleosides* |

**Research fellowships and internships**

| | |
|---|---|
| 09/2006 – 06/2007 | Collaboration on Universitary Research, at Department of Inorganic Chemistry, University of Granada. |
| 09/2007 – 06/2008 | Student assistant in Collaboration on Universitary Research, at Department of Inorganic Chemistry, University of Granada. |
| 09/2008 – 09/2009 | Fellowship from the Spanish Ministry of Education for Master Degree Studies. |
| 09/2009 – to date | FPU Program Fellowship from the Spanish Ministry of Education for Ph.D. Studies. |

**Scientific Teaching Experience**

| | |
|---|---|
| 03/2012 – 05/2012 | Teaching assistant in the aboratoty Course in Inorganic Chemistry for Pharmaceutical students at the University of Granada, Spain. |

**Courses**

I Workshop *Introduction to Crystal structure Resolution by X-Ray Determination*
Royal society of Spanish Chemistry (RSEQ), 15-17 July 2009 (25 hours)

*Internacional School of Crystallization 2009: Foods, Drugs and Agrochemicals*
Consejo Superior de Investigaciones Científicas (CSIC), 25-29 May 2009 (40 hours)

*Crystal structure Resolution by X-Ray Determination*
Consejo Superior de Investigaciones Científicas (CSIC), April 2009 (80 hours)

*Practical course of Mnova - NMR*
Nuclear Magnetic Resonante Unit at Centro de Instrumentación Científica (CIC), Universidad de Granada, 7-11 March 2011 (10 hours)

*Combined practical and lecture course on Chemistry of Metals in Biological systems*
Federation of European Biochemical Societies (FEBS), 15-22 May 2011 (42 hours)

*Course on Caracterization Techniques used in Bioinorganic Chemistry.*
Spanish Association of Nioinirganic Chemistry (AEBIN), 14-18 July 2010 (40 hours)

**Publications derived from the Ph.D. Thesis**

*1. Looking 7-azaindole as 1,6,7-trideazaadenine for Metal-complex Formation: Structure of [Cu(IDA)(H7azain)]n.*

A. Domínguez-Martín, D. Choquesillo-Lazarte, C. Sánchez de Medina-Revilla, J.M. González-Pérez, A. Castiñeiras, J. Niclós-Gutiérrez. in Henryk Kozlowski (Ed), *EUROBIC9 Medimond International Proceedings.* Wroclaw (Poland) September **2008**. ISBN 978-88-7587-463-6(volume), ISBN 978-88-7587-464-3(cd-rom)

*2. Restricting the versatile metal-binding behaviour of adenine by using deaza-purine ligands in mixed-ligand copper(II) complexes*

D. Choquesillo-Lazarte, A. Domínguez-Martín, A. Matilla-Hernández, C. Sánchez de Medina-Revilla, J. M. González-Pérez, A. Castiñeiras, J. Niclós-Gutiérrez, *Polyhedron,* **2010***, 62,* 170-177

*3. Metal ion binding patterns of acyclovir: Molecular recognition between this antiviral agent and copper(II) chelates with iminodiacetate or glycylglycinate*

M.P. Brandi-Blanco, D. Choquesillo-Lazarte, A. Domínguez-Martín, J. M. González-Pérez, A. Castiñeiras, J. Niclós-Gutiérrez, *J. Inorg. Biochem.,* **2011***, 105,* 616-623.

*4. Molecular recognition patterns of 2-aminopurine versus adenine: a view through ternary copper(II) complexes*

A. Domínguez-Martín, D. Choquesillo-Lazarte, J. M. González-Pérez, A. Castiñeiras, J. Niclós-Gutiérrez, *J. Inorg. Biochem.,* **2011***, 105,* 1073-1080.

*5. Metal ion binding modes of hypoxanthine and xanthine versus the versatile behaviour of adenine*

D. K. Patel, A. Dominguez-Martin, M. P. Brandi-Blanco, D. Choquesillo-Lazarte, V.M- Nurchi, J. Niclos-Gutierrez, *Coord. Chem. Rev.*, **2012**, *256*, 193-211.

*6. Structural consequences of the N7 and C8 translocation on the metal binding behavior of adenine*

A. Domínguez-Martín, D. Choquesillo-Lazarte, J. A. Dobado, H. Martínez-García, L. Lezama, J. M. González-Pérez, A. Castiñeiras, J. Niclós-Gutiérrez, *submitted to Inorg. Chem*., under revision **(**2012**)**

*7. Intrinsic Acid-Base Properties of a Hexa-2'-deoxynucleoside Pentaphosphate, d(ApGpGpCpCpT). Neighboring Effects and Isomeric Equilibria*

A. Domínguez-Martín, S. Johannsen, A. Sigel, B. P. Operschall, B. Song, H. Sigel, A.Okruszek, J. M. González-Pérez, J. Niclós-Gutiérrez, R. K. O. Sigel, *submitted to Chem.-Eur.J.*, under revision **(**2012**)**

*8. From 7-azaindole to adenine: molecular recognition aspects on mixed-ligand Cu(II) complexes with deaza-adenine ligands*

A. Domínguez-Martín, D. Choquesillo-Lazarte, J. A. Dobado, I. Vidal, L. Lezama, J. M. González-Pérez, A. Castiñeiras, J. Niclós-Gutiérrez, *submitted to Dalton Trans.*, under revision **(**2012**)**

*9. Structural insights on the molecular recognition patterns between $N^6$-substituted adenines and N-(aryl-methyl)iminodiacetate copper(II) chelates*

A. Domínguez-Martín, A. García-Raso, C. Cabot, D. Choquesillo-Lazarte, I. Pérez-Toro, A. Matilla-Hernández, A. Castiñeiras, Juan Niclós-Gutiérrez, *submitted to J. Inorg. Biochem.,* under revision **(**2012**)**

*10. Unravelling the versatile metal binding modes of adenine: Looking at the recognition roles of deaza- and aza-adenines in mixed-ligand metal complexes*

A. Domínguez Martín, M.P. Brandi-Blanco, A. Matilla-Hernández, V. M. Nurchi, J. M. González-Pérez, A. Cartiñeiras, J. Niclós-Gutiérrez, *submitted to Coord. Chem. Rev.,* under revision **(**2012**)**

**Other publications**

*Synthesis, crystal structure and properties of three different derivatives of the bis[di(2 pyridil)methanediol]copper(II) cation, $[Cu(bpmd)_2]^{2+}$*

C. Sánchez de Medina-Revilla, A. Domínguez-Martín, D. Choquesillo-Lazarte, J. M.González-Pérez, C. Valenzuela-Calahorro, A. Castiñeiras, I. García-Santos, J. Niclós-Gutiérrez, *J.Coord. Chem.* **2009***, 62,* 120-129

*Nickel(II) derivatives of N-benzyliminodiacetate(2-) ligands, with and without imidazole: synthesis, crystal structures and properties*

D.K. Patel, D. Choquesillo-Lazarte, J.M. González-Pérez, A. Domínguez Martín, A. Matilla-Hernandez, A. Castiñeiras, J. Niclós-Gutiérrez, *Polyhedron,* **2010***, 29,* 683-690.

*Iron(III) and aluminum(III) complexes with hydroxypyrone ligands aimed to design kojic acid derivatives with new perspectives*

V. M. Nurchi, G. Crisponi, J. I. Lachowicz, S. Murgia, T. Pivetta, M. Remelli, A. Rescigno, J Niclós-Gutíerrez, J. M. González-Pérez, A. Domínguez Martín, A. Castiñeiras, Z. Szewczuk, *J. Inorg. Biochem.* **2010,** *104,* 560-566.

*Kojic acid derivatives as powerful chelators for iron(III) and aluminium(III)*

V.M. Nurchi, J.I. Lachowicz, G. Crisponi, S. Murgia, M. Arca, A. Pintus, P. Gans, J. Niclós-Gutiérrez, A. Dominguez-Martin, A. Castiñeiras, M. Remelli, Z. Szewczuk, T. Lis, *Dalton Trans*., **2011**, *40*, 5984-5998.

*Isotype 1D polymers of cobalt(II) or zinc(II) constructed with square-planar tetraaqua-metal(2+) units and the bis-zwitterionic form of the $\mu_2$-O,O'-trans-1,4-dihydrogen-cyclohenane-diaminotetraacetate(2-) ligand.*

H. El Bakkali, D. Choquesillo-Lazarte, A. Domínguez-Martín, M. P. Brandi-Blanco, A. Castiñeiras, J. Niclós-Gutiérrez, *Polyhedron* **2012**, 31, 463-471.

**Conference Contributions**

• INTERNATIONAL MEETINGS

*1. A tri-copper(ii) complex cation with dipyridylanime and N-(1-adamantyl)iminodiacetate(2-) ligands"* – Poster P-15.

A. Castiñeiras, C. Sánchez de Medina Revilla, A. Domínguez Martín, D. Choquesillo Lazarte, J. M. González Pérez, J. Niclós Gutiérrez.

XVIII Italian-Spanish Congress on Thernodynamics of metal Complexes and XXXIV Annual Congreso of the Gruppo di Termodinamica dei Complessi (ISMEC'07), Calgliary (Italy), 05-09 June 2007

*2. Three novel compounds having the bis(di-2(2-pyridyl)methanediol)copper(II) cation* – **Oral Commun. O-19.**

A. Domínguez Martín, C. Sánchez de Medina Revilla, E. Bugella Altamirano, A. Castiñeiras, D. Choquesillo Lazarte, C. Alarcón Payer, R. Fernández Piñar, J. M. González Pérez, J. Niclós Gutiérrez.

XIX Spanish-Italian Congress on Thernodynamics of metal Complexes and XXXV Annual Congreso of the Gruppo di Termodinamica dei Complessi (SIMEC'08), Baeza (Spain), 9-13 June 2008

*3. Looking 7-azaindole as 1,6,7-trideazaadenine for metal-complex formation: structure of [Cu(IDA)(H7azain)]n* - Poster P-39

A. Domínguez Martín, D. Choquesillo Lazarte, C. Sánchez de Medina Revilla, J. M. González Pérez, A. Castiñeiras, J. Niclós Gutiérrez.

9th European Biological Inorganic Chemistry Conference (EUROBIC9), Wroclaw (Poland), 02-06 September 2008

*4. Coordinating mode of H7azaindole in ternary copper(II) complexes* – **Oral Commun. OC-5**

A. Domínguez Martín, D. Choquesillo Lazarte, J. M. González Pérez, A. Matilla Hernández, A. Castiñeiras, J. Niclós Gutiérrez

XX Italian-Spanish Congress on Thernodynamics of metal Complexes and XXXVI Annual Congreso of the Gruppo di Termodinamica dei Complessi (ISMEC'09), Pisa (Italy), 07-11 June 2009

*5. Copper(II) bis-chelates with the HL(1-) form of N-substituted-iminodiacetic acids ($H_2L$)* - Poster P-40

A. Domínguez Martín, A. Castiñeiras, A. Matilla-Hernández, D. Choquesillo Lazarte, E. Bugella-Altamirano, J. Niclós Gutiérrez.

International Symposium on Metal Complexes (ISMEC2010), Bilbao (Spain), 7-11 June 2010

*6. Structural evidences of molecular recognition: a deepen view through N-methylated adenine complexes* **-** Poster P-52

A. Domínguez Martín, J. M. González-Pérez, A. Castiñeiras, D. Choquesillo Lazarte, M.Teresa Fernández-Martínez, J. Niclós Gutiérrez.

10th European Biological Inorganic Chemistry Conference (EUROBIC10), Thessaloniki (Greece), 22-26 June 2010

*7. Mixed-ligands copper(II) complexes with iminodiacetate and 2,6-diaminopurine showing different molecular recognition patterns* - Poster P-174

A. Domínguez Martín, M. P. Brandi-Blanco, D. Choquesillo Lazarte, A. Castiñeiras, A. Matilla-Hernández, J. Niclós Gutiérrez.

10th European Biological Inorganic Chemistry Conference (EUROBIC10), Thessaloniki (Greece), 22-26 June 2010

*8. New insights into molecular recognition: coordination abilities of 9-methyladenine* - **Young Researchers Lectures L-34**

A. Domínguez Martín, A. Matilla-Hernández, D. Choquesillo Lazarte, A. Castiñeiras, H. El-Bakkali , J. Niclós Gutiérrez.

XI International Symposium on Inorganic Biochemistry, Kudowa Zdrój (Poland), 4-8 September 2010

*9. Assymetric tetranuclear mixed-ligand copper(II) complex with 4-aminopyrazolo[3,4-d]pyrimidine ligand* - **Oral Commun.O-14.**

A. Domínguez-Martín, D. Choquesillo-Lazarte, E. Bugella-Altamirano, J. M. González-Pérez, A. Castiñeiras, J. Niclós-Gutiérrez

International Symposium on Metal Complexes (ISMEC2011), Giardini Naxos, Sicilia (Italia), 13-16 June 2011

*10. Copper(II) binding modes of 2,6-diaminopurine involving the coordination of its different N-exocyclic amino groups* - Poster 22

M. P. Brandi-Blanco, A. Domínguez-Martín, D. Choquesillo-Lazarte, J. M. González-Pérez, A. Castiñeiras, J. Niclós-Gutiérrez

5th EuCheMS Conference on NITROGEN LIGANDS, Granada, 4-8 September 2011

*11. Aryl-metal chelate ring pi,pi,-stacking interaction in three ternary copper(II) complexes with aromatic pi,pi-diimine ligands* - Poster 38

A. Domínguez-Martín, H. El Bakkali, I. García-Santos, D.e Choquesillo-Lazarte, J. M. González-Pérez, A. Castiñeiras, J. Niclós-Gutiérrez

5th EuCheMS Conference on NITROGEN LIGANDS, Granada, 4-8 September 2011

*12. Molecular and polymeric forms within the crystals of two copper(II) complexes having N-benzyl-iminodiacetate-like chelators and purine as co-ligands* – Poster 92

A. Matilla-Hernández, A. Domínguez-Martín, M. P. Brandi-Blanco, D. Choquesillo-Lazarte, J. M. González-Pérez, A. Castiñeiras, J. Niclós-Gutiérrez

5th EuCheMS Conference on NITROGEN LIGANDS, Granada, 4-8 September 2011

*13. Intrinsic $pK_a$ Values within a DNA Oligonucleotide: The Basis for Acid-Base Catalysis in DNAzymes and Ribozymes* - Poster 25

A.Dominguez-Martin, S. Johannsen, R.K.O. Sigel

International Symposium on Applied Bioinorganic Chemistry – ISABC11, Barcelona (Spain), 2-5 December 2011.

*14. Molecular Recognition Patterns in Ternary Copper(II) Complexes with Deaza-Adenine and Amino-polycarboxylate Ligands* - Oral Communication O-41.

A. Domínguez-Martín, D. Choquesillo-Lazarte, J.A. Dobado, I. Vidal, J. M. González-Pérez, A. Castiñeiras, J. Niclós-Gutiérrez

International Symposium on Metal Complexes (ISMEC2012), Lisbon (Portugal) 18-22 June 2012

*15. Novel Cu(II)-iminodiacetate complexes with cytokinin derivatives: Synthesis, Molecular recognition and biological properties* - Oral Communication O-8.

A. Domínguez-Martín, A. García-Raso, C. Cabot, D. Choquesillo-Lazarte I. Pérez-Toro, A. Matilla-Hernández, J.M. González-Pérez, A. Castiñeiras, J. Niclós-Gutiérrez.

11th European Biological Inorganic Chemistry Conference (EUROBIC11), Granada (Spain), 12-16 September 2012

*16. Molecular recognition in ternary complexes derived from (N-furfuryl-iminodiacetate)copper(II) chelate and N6-substituted-adenines as co-ligands* - Poster P-168

I. Pérez-Toro, A. Domínguez-Martín, A. García-Raso, M.P. Brandi-Blanco, J.M. González-Pérez, A. Castiñeiras, J. Niclós-Gutiérrez.

11th European Biological Inorganic Chemistry Conference (EUROBIC11), Granada (Spain), 12-16 September 2012

*17. First insights on the metal binding patterns of 2,6-dicloropurine: Its role as co-ligand in two novel Cu(II) ternary compounds.* – Poster P-74

A. Domínguez-Martín, M.E. García-Rubiño, D. Choquesillo-Lazarte, J.M. Campos, D.K. Patel, A. Castiñeiras, J. Niclós-Gutiérrez.

11th European Biological Inorganic Chemistry Conference (EUROBIC11), Granada (Spain), 12-16 September 2012

*18. First copper(II) complex with 8-aminoquinoline: Structure of $[Cu(MIDA)(H8AQ)(H_2O)]\cdot 3H_2O$* – Poster 150

R. Navarrete-Casas, A. Domínguez-Martín, D. Choquesillo-Lazarte, A. Castiñeiras, M.T. Fernández-Martínez, J.M. González-Pérez, J.Niclós-Gutiérrez.

11th European Biological Inorganic Chemistry Conference (EUROBIC11), Granada (Spain), 12-16 September 2012

• NACIONAL MEETINGS (SPAIN)

*1. Estudio estructutural comparado de $[Cu(N\text{-}p\text{-}ClBZIDA)(Hade)(H_2O)]\cdot H_2O$ [1] y $\{[Cu(N\text{-}(p\text{-}ClBZIDA)(3MAde)]\cdot H_2O\}_n$ [2]* - Poster P-19

A. Domínguez Martín, M. M. Benavides Jiménez, C. Alarcón Payer, D. Choquesillo Lazarte, A. Castiñeiras, J. M. González Pérez, J. Niclós Gutiérrez.

V Reunión Nacional de Bioinorgánica, Santiago de Compostela, 16-19 September 2007

*2. Reconocimiento molecular entre 2,6-diaminopurina y el quelato Cu(ODA) en el cristal de [Cu(ODA)(Hdap)($H_2O$)]·2$H_2O$ [ODA = oxidiacetato(2-)]* **-** Poster P-41

A. Domínguez Martín, C. Alarcón Payer, D. Choquesillo Lazarte, A. Castiñeiras, J. M. González Pérez, J. Niclós Gutiérrez.

XIII Reunión Científica Plenaria de Química Inorgánica y VII Reunión Científica Plenaria de Química en Estado Sólido (QIES-08), Almuñécar ,Granada, 16-19 September 2008

*3. Reconocimiento molecular entre 2-aminopurina (H2apur) y diversos iminodiacetatos de cobre(II)) [N-R-IDA con R = H, metilo o bencilo]* **- Oral Commun. O-10**

A. Domínguez Martín, D. Choquesillo Lazarte, J. M. González Pérez, R. Navarrete Casas, A. Castiñeiras, J. Niclós Gutiérrez.

VI Reunión Nacional de Bioinorgánica, Mallorca, 15-18 July 2009

*4. Síntesis, estructura y propiedades del compuesto ternario de cobre(II), N-benciliminodiacetato y 4-azabencimidazol, Cu(NBzIDA)(H4abim)]$_n$* **-** Poster P-48

A. Domínguez Martín, D. Choquesillo Lazarte, C. Sánchez de Medina Revilla, J. M. González Pérez, A. Castiñeiras, A. G. Sicilia Zafra, J. Niclós Gutiérrez.

VI Reunión Nacional de Bioinorgánica, Mallorca, 15-18 July 2009

*5. Reconocimiento molecular entre el quelato $Cu^{II}$(NBzIDA) Y 2-aminopiridina* **-** Poster P-5

A. Domínguez Martín, D. Choquesillo Lazarte, J. M. González Pérez, A. Matilla, A. Castiñeiras, J. Niclós Gutiérrez.

VI Simposium de Jóvenes Investigadores (RSEQ), Granada, 22-25 November 2009

*6. Correlación en compuestos ternarios entre la conformación del quelante tipo iminodiacetato y el reconocimiento con hipoxantina* – **Oral Commun. OC-5**

A. Domínguez-Martín, M. P. Brandi-Blanco, D. K. Patel, D. Choquesillo-Lazarte, J. M. González-Pérez, A. Castiñeiras, J. Niclós-Gutiérrez.

VII Reunión Nacional de Bioinorgánica, Águilas, Murcia, 3-6 July 2011

*7. Consecuencias de la N7-metilación de adenina en complejos ternarios de cobre(II) con N-metil-iminodiacetato como quelante* – Poster P-17

A. Domínguez-Martín, M.P. Brandi-Blanco, D. Choquesillo-Lazarte, J. M. González-Pérez, A. Castiñeiras, J. Niclós-Gutiérrez.

VII Reunión Nacional de Bioinorgánica, Águilas, Murcia, 3-6 July 2011

*8. Inducción de la coordinación del dador N1(purina) en compuestos modelo* – Poster 10

A. Domínguez-Martín, D. Choquesillo-Lazarte, A. Matilla, J. M. González-Pérez, A. Castiñeiras, J. Niclós-Gutiérrez.

VII Reunión Nacional de Bioinorgánica, Águilas, Murcia, 3-6 July 2011

**Experience in organizing Scientific events**

1. Meeting for the consolidation of the European Project ref: FP7-226306-2).

London 27 Mayo 2008

2. Member of the Local Organizing Committee in the Nacional Conference QIES'08: XIII Reunión Científica Plenaria de Química Inorgánica y VII Reunión Científica Plenaria de Química

en Estado Sólido.

Almuñecar (Granada), 16-19 September 2008.

3. Member of the Local Organizing Committee in the International Conference EUROBIC11: 11th European Biological Inorganic Chemistry Conference.

Granada, 12-16 September 2012.

**Stays in Foreign countries**

1. Faculty of Pharmacy and Universitary Hospital of Tucson (Arizona, EEUU)

ISPF (Internacional Pharmaceutical Students' Federation) Student Exchange Program in Clinical Pharmacy

Intership: 6 weeks ; July-August 2007.

2. Institute of Inorganic Chemistry, University of Zürich (Switzerland)

Research project: *Intrinsic $pK_a$ Values within a DNA Oligonucleotide: The Basis for Acid-Base Catalysis in DNAzymes and Ribozymes*

Pre-doctoral stay: 16 weeks ; September-December 2011.

**Projects**

1. CO2SolStock-Biobased geological CO2 storage (ref:FP7-226306-2) – *EU funding.*

Participants: Biomin-Greenloop, , University of Lausanne, University T.U. Delft, University of Edinburgh. Number of participants: 24

Predoctoral contract: from April 1st 2009 until July 31st 2009

2. Reconocimiento molecular entre diversos iminodiacetatos de cobre(II) (mononucleares y dinucleares) y una selección de purinas o bases nitrogenadas relacionadas, así como de nucleósidos de síntesis – *University of Granada funding*.

Participants: University of Granada. Number of participants: 8

From 01/01/2009 to 31/12/2009

3. Nuevos materiales y estrategias para la integración de las nuevas tecnologías de la comunicación en la impartición de las asignaturas del Departamento de Química Inorgánica en la titulación de Farmacia (Código: 10-13)- *University of Granada funding*.

Participants: University of Granada. Number of participants: 8

From 29/10/2010 to 30/10/2011

4. Materiales cristalinos microporosos basados en polímeros de coordinación de los lantánidos con carboxilatos. Síntesis, propiedades y aplicaciones potenciales – *Spanish Ministry of Science and Innovation funding.*

Participants: University of Santiago de Compostela, University of Granada. Number of participants: 5

From 01/10/2010 to 01/10/2012